Revised & Enlarged Edition

NUCLEAR PHYSICS

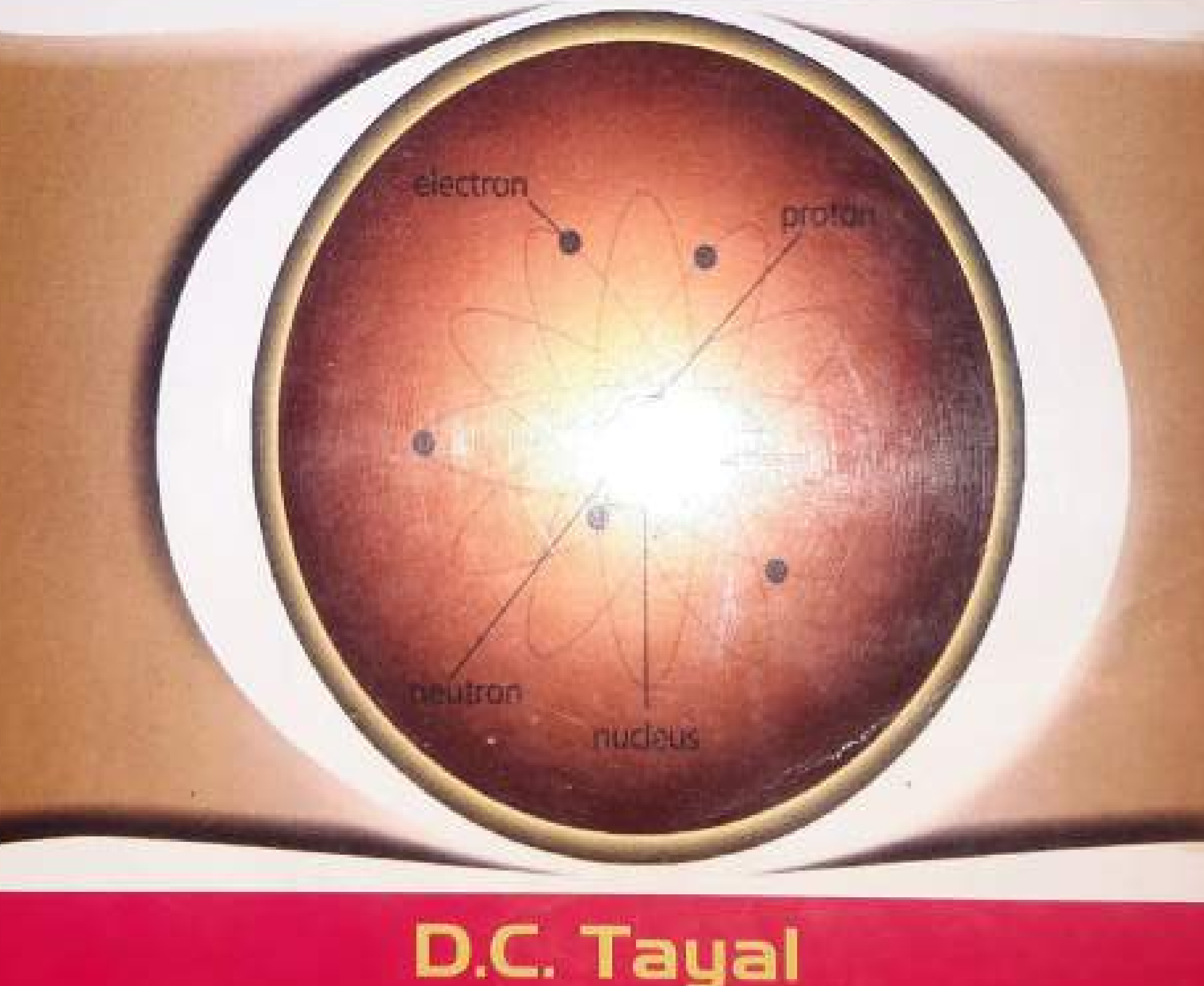
electron
proton
neutron
nucleus

D.C. Tayal

Himalaya Publishing House
ISO 9001:2015 CERTIFIED

NUCLEAR PHYSICS

(For M.Sc. and B.E. Students of all Indian Universities)

D.C. TAYAL
M.Phil., Ph.D.
Head, Department of Physics,
N.R.E.C. College, Khurja - 203131.

Himalaya Publishing House
ISO 9001:2015 CERTIFIED

CONTENTS

Sem 3

Chapter *Pages*

1. **General Properties of Atomic Nucleus** 1

Introduction, Scattering of α-particles, (*Rutherford's Scattering Formula and its Experimental Verification*), Nuclear size and its determination (*e.g. Mesonic X-rays, Electron scattering*). Mass Spectroscopy (*Basic Components, Mattauch, Bainbridge and Jordan, Nier, Doublet Method, Mass synchrometer*), Theories of Nuclear Composition (*Proton-Neutron, etc.*), Binding Energy, Semi-empirical Mass Formula (*nuclear stability*), Quantum Numbers for Individual Nucleons, Independence of atomic and Nuclear Properties, Quantum Properties of Nuclear States. Nuclear Magnetic Dipole Moment (*with various determination methods*), Electric Multipole Moment, Electric Quadrupole Moment, Potential well, A Brief Summary, Exercises, Short Answer Questions, Problems, Questions, References.

2. **Radioactivity and Isotopes** 62

Introduction, Fundamental Laws of Radioactivity, Radioactive Equilibrium, Radioactive Branching, Dosimetry, Induced Radioactivity by Nuclear Bombardment, Mixture of Activities, Radio-isotope Therapy, Statistical Fluctuations (*Binominal, Poission, and Normal distributions*), Measurement of decay constants, Radioactive Dating (*Age of earth*), Natural Radioactive Series, Isotopes (*separation and uses*), A Brief Summary, Exercises, Short Answer Questions, Problems, Questions, References.

3. **Interactions of Nuclear Radiations with Matter** 99

Introduction, Interaction of Charged Particles with Matter, Stopping Power of Heavy Charged Particles, Delta Rays, Energy loss of heavy ions, Range and Straggling, Stopping Power and Range for Electrons, Cerenkov Radiation, Synchrotron Radiation, Absorption of Gamma rays (*Thomson, Rayleigh and Delbruck Scatterings, Photoelectric effect, Compton effect, Pair production*), A Brief Summary, Exercises, Short Answer Questions, Problems, Questions, References.

4. **Detection and Measurement of Nuclear Radiations** 129

Introduction, Ionization Chamber (*Pocket Dosimeter*), Semiconductor Detectors (*Diffused junction, Surface barrier and Lithium drifted junction-Ge(Li), HP-Ge*), Regions of multiplicative operation, Proportional Counter, Geiger Muller Counter (*Quenching of discharge*). Scintillation Counters (*Photomultiplier tube, Scintillators, Pulse Formation, Resolving Power*), Cerenkov Counters, Cloud Chamber (*Diffused Cloud Chamber*), Bubble Chamber, Spark Chamber, Nuclear Emulsions, List of common nuclear detectors, Differentiating and Integrating Circuits, Nuclear Instrument Modules (*Bins, Amplifiers, Discriminators and Single Channel Analysers, Multichannel Analysers*), Nuclear Spectrometers/Counting Systems (*Compton Suppression Spectrometer, GDA*), Coincidence Teachniques, Particle Identification System, A Brief Summary, Exercises, Short Answer Questions. Problems, Questions, References.

Chapter Pages

5. **Alpha-Particles** 185

Introduction. Determination of q/M for the α-particle (*Rutherford & Royd's experiment*) Range of α-particles (*Bragg Curve*). Energy of α-Particles. Range-Velocity-Energy-Half Life Relations (*Geiger Nuttal Law*). Alpha Decay Energy-Mass Number, Alpha-Particle Spectra. Gamow's Theory of α-decay (*Decay Probability, Hindrance Factors, Spontaneous Nuclear Distegration*). Advances in the theory of alpha-decay, A Brief Summary, Exercises, Short Answer Questions. Problems, Questions, References.

Beta-Decay 209

Introduction. Beta--Spectroscopy (*Flat-type and lens-type spectrometers*). The Neutrino, Energy-Half life Relationships. Fermi theory of β-decay, (*Kurie Plots, Mass of neutrino, Life-time of β-decay*). Classification of Beta Transitions (*Selection rules for allowed and forbidden transitions*). General Theory of β-decay, Electron Capture, Violation of Parity Conservation in β-decay. Helicity (*Helicity of electron and of neutrino*), Double Beta Decay, A Brief Summary, Exercises, Short Answer Questions, Problems, Questions, References.

7. **Gamma-Radiation** 251

Introduction. Measurement of gamma ray energies (*Crystal spectrometer, Absorption measurement, Secondary Electron Methods, Photodisintegration Method*), Multipole Radiations (*Theory and Selection Rules, Decay Constants, Reduced Transition Probability*). Internal Conversion. Internal pair creation, Nuclear Isomerism, Coulomb Excitation, Angular Distribution and Directional correlation in γ-emission, Measurements of Lifetimes of Nuclear States (*Electronic Timing Methods, Doppler Shift Techniques, Indirect Methods*), Nuclear Resonance Fuorescence, Mossbauer Effect, A Brief Summary, Exercises, Short Answer questions. Problems, Questions, References.

8. **Nuclear Forces** 301

Introduction. Deuteron (*Properties, No excited S-states, Excited States of the Deuteron*) Neutron-Proton Scattering at Low Energies (*Scattering length, Phase shift Analysis, Spin dependence, Coherent scattering*), Shape Independent Effective Range Theory of *n-p*-scattering (*Determination of scattering length and effective range*), Proton-Proton Scattering at Low Energies. Effective Range Theory of $p-p$ scattering, Neutron-Neutron Scattering, Similarities between (*nn*) and (*pp*) forces, Non-Central forces (*Experimental evidence for the existence of non-central forces, General form of this force, its properties, Ground state of the deuteron, Magnetic moment, Electric Quadrupole moment, n-p scattering below 10 MeV, Photo disintegration*), Saturation of Nuclear Forces (*Exchange forces, Isotopic Spin Formalism*), High energy *n-p* and *p-p* scattering, Polarization and Scattering parameters. Meson theory of exchange forces, Phase Shifts and Nucleon-nucleon scattering data, One Boson Exchange Potential, A Brief Summary, Exercises, Short Answer Questions, Problems, Questions, References.

9. **Nuclear Models** 355

Introduction. Fermi gas model, Liquid drop model, Shell model (*Magic numbers*), Extreme Single Particle model (*Square well of infinite depth, Harmonic Oscillator Potential, Spin-Orbit Potential*), *Single Particle Model, Individual Particle Model, Predictions of shell model*. Collective Nuclear Model, Unified Model (*Deformed Shell Model, Nilsson Model*), Superconductivity Model, A Brief Summary, Exercises, Short Answer Questions, Problems, Questions, References.

10. **Nuclear Reactions** 401

Types of Nuclear Reactions, Conservation Laws, Nuclear Reaction Kinematics, Nuclear Transmutations, Charged Particle Reaction Spectroscopy, Neutron Spectroscopy, Nuclear

Chapter *Pages*

Cross-section, Classical Analysis of Cross Section, Partial Wave Analysis of Reaction Cross Section, Thick Target Yield, Requirements for a Reaction, Reaction Mechanism, General Features of Reaction Cross-sections, Inverse Reaction, Principle of Detailed Balance, Compound Nucleus, Compound Nucleus Reactions, Disintegration of a Compound Nucleus, Hauser-Feshbach Theory, Continuum Theory of Nuclear Reaction, Resonance Cross-sections (*Breit Wigner Dispersion formula*), Optical Model, Different Stages of a Nuclear Reaction, Statistical Theory of Nuclear Reactions, Direct Reactions (*Stripping reactions, Pickup reactions*), Stripping Reactions and the Shell model, Giant Resonances, Heavy Ion Reactions, Nuclear Shock waves, A Brief Summary, Exercises, Short Answer Questions, Problems, Questions, References.

11. Particle Accelerators 463

Introduction, Ion Sources, Heavy Ion Sources, Polarized Ion Sources, Electrostatic Accelerators (*Cockcroft-Walton, Van de Graaff, Tandem, Pelletron, Resonance transformers*), Low Energy Circular Accelerators : Cyclotron fixed frequency, Betatron, Principle of Phase Stability, Linear Accelerators (*Drift Tube, Wave Guide*), Synchrotrons (*Synchrocyclotron, Electron synchrotron, Proton synchrotron-Cosmotron*), Microtrons, Alternating Gradient (*Strong Focusing*) Accelerators, Isochronous Cyclotrons (*AVF or Sector Cyclotrons*), Storage Rings (*Electron-Positron Storage rings, ISR, Proton-antiproton Storage rings*), Heavy Ion Accelerators (*Electron Ring Accelerator*), Indian Accelerators, A Brief Summary, Excercises, Short Answer Questions, Problems, Questions, References.

12. Neutrons 543

Discovery, Neutron Sources, Neutron Collimators, Basic Properties of Neutron (*Mass, Charge, Statistics, Decay, Half life, Wave properties, Magnetic moment*), Classification of Neutrons as to Energy, Neutron Detection (*Slow, Intermediate, Fast, Ultra-High Energy and Threshold Detectors*), Neutron Spectrometer, Slowing down of Neutrons (*Energy loss, Scattering angles in L-and C.M. system, Average Energy loss per collision, Transport mean free path, Logarithmic energy decrement, Slowing down power and Moderating ratio, Slowing down Density, Slowing down time*), Energy Distribution of Thermal Neutrons, Neutron Diffusion (*Current density, leakage rate, Thermal neutron diffusion, The exponential pile, Fermi age equation*), Neutron Velocity Selector (*Crystal Spectrometer, Mechanical selector, Time of flight, Velocity selector*), A Brief Summary, Exercises, Short Answer Questions, Problems, Questions, References.

13. Nuclear Fission and Fusion 578

Nuclear fission, Types of Fission, Distribution of fission products, Neutron Emission in Fission, Fissile and Fertile materials, Spontaneous fission, Deformation of liquid drop : Bohr and Wheeler's Theory, Quantum effects. Fission Product Radioactivity, Nuclear Fusion and Thermo Nuclear Reactions, Controlled Thermonuclear Reactions (*Hydrogen bomb, Fusion reactor, Different methods for the production of fusion reactions*), A Brief Summary, Exercises, Short Answer Questions, Problems, Questions, References.

14. The Artificial Elements 606

Transuranic Elements, Experimental Methods to detect & identify transactinide nuclei, Production and properties (From Z = 93 to Z = 110), Super Heavy Nuclei, Missing Elements in the Periodic Table (*Technetium, Promethium, Francium, Astatine*), References.

15. Nuclear Fission Reactors 626

Need for Nuclear Power, Nuclear Chain Reaction (*Four Factor Formula*). The Critical Size of a Reactor (*Reactor buckling, Non-leakage factors, Effects of reflectors*), General Aspects of Reactor Design, Classification of Reactors : Research Reactors (*Graphite-Moderated,* *Water Boiler, Swimming Pool-Apsara, Light Water moderated. Heavy Water moderated—Cirus, Zerlina, Purnima, Dhurva*), Production Reactors, Power Reactors (*Pressurized water, Boiling water—Tarapur, Heavy water moderated—RAPS, MAPS, NAPS, KAIGA, KKAPP, Organic moderated, Gas cooled, Sodium Graphite, Liquid fuel, Fast Breeder Reactor—FBTR, PFBR*), Peaceful Nuclear Explosions, Hydrogen Bomb, Nuclear Power Production in India, A Brief Summary, Exercises, Short Answers Questions, Problems, References.

16. Chemical & Biological Effects of Radiations 658

Radiation, Radiation Monitoring & Dosimeters, Physical effects of Radiation, Chemical Effects of Radiation (*Radiation effects on Water and Aqueous solutions, on Polymers*), Nuclear Agriculture (*Food Irradiation, Control of Insects, New Varieties of Plants*), Biological Effects of Radiation, Somatic and Genetic Effects, Radio-nuclides, Radio Isotopes in India, Tracer Techniques in Medical Science, Nuclear Energy and Social Development—DAE, Exercises, Problems, References.

17. Cosmic Rays 674

Introduction, Secondary Cosmic Rays, Geomagnetic effects (*at low and high altitudes*), Interpretation of Geomagnetic Effects, Absorption of Cosmic Rays, Showers (*Theory of electron showers*), Cosmic ray Primaries, High Energy Nuclear Interactions, Extensive Air Showers, Origin of Cosmic rays, References.

18. Elementary Particles 692

Introduction, Classification of Elementary Particles, Fundamental Interactions (*Gravitational, Electromagnetic, Strong, Weak*), Conservation laws, Invariance under charge, parity, C.P., time and CPT, Electron and Positron, Proton and antiproton, Neutron and Antineutron, Neutrino and Antineutrino, Graviton, Photon and Gluon, Mesons : Muons, Tauons, Pions, *K*-mesons, η-meson, Hyperons : Λ-, Σ, Ξ, Ω-hyperons, Hypernuclei, Resonance States, Elementary Particle Symmetries, Quarks, Isospin of Quarks, Quark Wavefunctions of Pseudoscalar Mesons, of Baryons, Magnetic Dipole Moment of the Baryon Octet, Quantum Chromodynamics, Electroweak Interaction Theory, Grand Unification Theories, Heavy Quark Effective Theory, Cosmology and Particle Physics, Electromagnetic Structure of Nucleons, A Brief Summary, Exercises, Short Answer Questions, Problems, Questions, References.

Appendix A—Physical Constants in S.I. Units. 774

Appendix B—Stable Nuclides of the Elements. 775

Index 778

1

GENERAL PROPERTIES OF ATOMIC NUCLEUS

1.1 INTRODUCTION

The four element theory, *i.e.*, all matter was composed of four elements namely fire, earth, air and water, was widely accepted not only by ancient Hindu thinkers (*Chhat, jal, pawak, gagan, samera*), but also by Greeks. At the beginning of the nineteenth century (1808) John Dalton on experimental grounds first assumed that atoms were the smallest part of the element identical in mass, while different elements had atoms of different masses. In 1815, Prout suggested that the atoms of all elements were made up of atoms of hydrogen. This hypothesis was soon discarded by more accurate atomic weight measurements. Goldstein and Crookes discovered cathode rays, given the name *electron* by J.J. Thomson. Since the atom is electrically neutral under normal conditions and the atoms of radioactive element are transformed into atoms of another element by emitting negatively or positively charged particles, hence it was said that atoms were made up of equal number of positive and negative charges. Two important questions then arose : (1) How many electrons were there in an atom? and (2) how were the electrons and positive charges arranged in it? The scattering of *X*-rays showed that the number of electrons in an atom of the lighter elements was equal to about half the atomic weight, except that in the atom of hydrogen. Thomson assumed the atom as consisted of a sphere of positive electricity of uniform density throughout of which was distributed an equal and opposite charge in the form of electrons. Thomson's theory came into conflict with the experiments of Rutherford and his collaborators on the scattering of α-particles.

1.2 SCATTERING OF ALPHA PARTICLES

In 1906, E. Rutherford observed diffused traces on a photographic plate, when alpha particles from a radioactive source after penetrating from a thin sheet of metal fell on it. This diffuseness was called scattering. It was assumed as due to the interaction of α-particles with the atoms of the metal sheet. In 1908, E. Rutherford and H. Geiger carried out experiments to count α-particles with Geiger's gas counter. Geiger studied the small angle of scattering and found nothing very unexpected. H. Geiger and E. Marsden in 1909 performed experiments on the scattering of alpha particles by thin metal films. They observed that almost all the alpha particles passed straight and some were scattered through large angles even greater then 90°. In view of J.J. Thomson's model of the atom it appeared possible that alpha particle scattering might be due to encounters with electrons. But *Rutherford said, "Remembering that the mass, momentum and kinetic energy of the alpha particle are very large compared with the corresponding values for the electron...it does not seem possible... that an alpha particle can be deflected through a large angle by a close approach to an electron."* He therefore concluded that the atom did not consist of a uniform sphere of positive electrification as supposed by Thomson, but that the positive charge was concentrated in a small region at the centre of the atom, which he later (1912) called the *nucleus*.

In developing the theory of α-scattering by atomic nuclei, Rutherford assumed that both the nucleus and α-particle behaved as point charges, Coulomb's law was valid for such small distances, Newtonian mechanics was applicable and the nucleus was considered so heavy that its motion during the impact was not considerable.

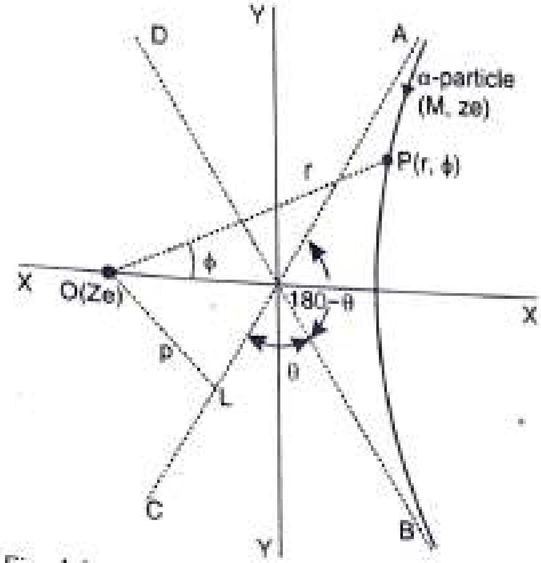

Fig. 1.1. Scattering of an α-particle by Rutherford nuclear atom.

Let us consider a nucleus of charge Ze at point O and α-particle of mass M and charge ze approaching it along AC with an initial velocity v_0. The force of repulsion between these two charges

$$F = Zze^2/4\pi\varepsilon_0 r^2, \qquad \ldots(1)$$

where r is the distance of the α-particle from the nucleus. The α-particle is deflected from its original direction of motion by this force of repulsion and its actual path is a conic section, Fig. 1.1.

To derive the expression for the path of the alpha particle, let us assume that P be the position of an α-particle at any instant t and (r, ϕ) be its polar co-ordinates with nucleus as the pole, the acceleration a may be resolved into two components, one along the radius, a_r, and other transverse to it, a_ϕ. Since force of repulsion F acts along the radius vector and there is no force transverse to the radius vector, hence we have

$$a_r = \frac{d^2r}{dt^2} - r\left(\frac{d\phi}{dt}\right)^2 = \frac{F}{M} = \frac{Zze^2}{4\pi\varepsilon_0 Mr^2} = \frac{J}{r^2}, \qquad \ldots(2)$$

where $J = Zze^2/4\pi\varepsilon_0 M$

and

$$a_\phi = \frac{1}{r}\frac{d}{dt}\left(r^2\frac{d\phi}{dt}\right) = 0,$$

or

$$r^2 d\phi/dt = \text{constant } K. \qquad \ldots(3)$$

To change the independent variable t to ϕ, let us assume $u = 1/r$.

$$\therefore \quad \frac{dr}{d\phi} = -\frac{1}{u^2}\frac{du}{d\phi} \text{ and } \frac{dr}{dt} = \frac{dr}{d\phi}\cdot\frac{d\phi}{dt} = -K\frac{du}{d\phi}.$$

Similarly $d^2r/dt^2 = -K^2u^2(d^2u/d\phi^2)$. $\qquad \ldots(4)$

Substituting values of dr/dt and d^2r/dt^2 in Eq. (2), we get $\qquad \ldots(5)$

$$\frac{d^2u}{d\phi^2} + u = -\frac{J}{K^2}.$$

Since J/K^2 is constant, hence this equation can be written as $\qquad \ldots(6)$

$$\frac{d^2}{d\phi^2}\left(u + \frac{J}{K^2}\right) = -\left(u + \frac{J}{K^2}\right).$$

This is the differential equation with solution

$$u + J/K^2 = A\cos(\phi - \delta),$$

where A and δ are the constants of integration.

By proper choice of the axes, the phase angle δ can be set equal to zero. Further by setting $A = (J/K^2)\,\varepsilon$, we have

$$u = \frac{1}{r} = -\frac{J}{K^2}(1 - \varepsilon\cos\phi). \qquad \ldots(7)$$

This is one form of the equation of a conic section in polar co-ordinates (r, ϕ) with eccentricity ε, which may be determined by the help of the principle of conservation of energy. If v be the velocity of an α-particle at point P on its path, then its potential and kinetic energies will be $Zze^2/4\pi\varepsilon_0 r$ and $\frac{1}{2}Mv^2$ respectively. From the principle of conservation of energy, we thus have

$$\tfrac{1}{2}Mv_0^2 = \tfrac{1}{2}Mv^2 + \frac{Zze^2}{4\pi\varepsilon_0 r} = \tfrac{1}{2}Mv^2 + \frac{JM}{r}, \qquad \text{...(8)}$$

or

$$v_0^2 = v^2 + 2J/r.$$

Since

$$v^2 = (dr/dt)^2 + r^2(d\phi/dt)^2 = [(dr/d\phi)^2 + r^2]\,(d\phi/dt)^2$$

$$= (J^2/K^2)\,(1 + \varepsilon^2 - 2\varepsilon\cos\phi).$$

∴

$$v_0^2 = \frac{J^2}{K^2}[1+\varepsilon^2 - 2\varepsilon\cos\phi] - \frac{2J^2}{K^2}[1-\varepsilon\cos\phi].$$

or

$$\varepsilon = \sqrt{[1 + (Kv_0/J)^2]}. \qquad \text{...(9)}$$

By conservation of angular momentum $Mr^2 d\phi/dt = MK = Mv_0 p$, where p is the distance from the nucleus to AC, called the *impact parameter*.

∴

$$\varepsilon = \sqrt{[1+(4\pi\varepsilon_0 Mv_0^2 p/Zze^2)^2]}. \qquad \text{...(10)}$$

Since $\varepsilon > 1$, hence the conic is a hyperbola with the nucleus at the focus outside the branch of the curve AB. The asymptotes AC and DB represent the initial and final directions of the α-particle. The angle θ between the asymptotes is the angle through which particle has been deflected and is called the *angle of scattering*.

The equation of hyperbola in rectangular coordinates is given by

$$x^2/a^2 - y^2/b^2 = 1.$$

The equations of its asymptotes are $y = \pm\,(b/a)x$.

Slope of these asymptotes $b/a = \tan\psi = \tan[(180 - \theta)/2] = \cot(\theta/2)$.

For hyperbola, $b^2/a^2 = \varepsilon^2 - 1$, therefore $\varepsilon^2 - 1 = \cot^2(\theta/2)$

Using Eqn. (10), we have $\cot(\theta/2) = 4\pi\varepsilon_0 Mv_0^2 p/Zze^2$,

or

$$p = (Zze^2/4\pi\varepsilon_0 Mv_0^2)\cot(\theta/2). \qquad \text{...(11)}$$

With the help of this equation the fraction of α-particles scattered through an angle lying between θ and $\theta + d\theta$ can be calculated. For this let a beam of α-particles is incident perpendicularly on a thin foil of material of thickness t, containing n atoms per unit volume and *of small thickness so that the particles pass through it without any significant change in velocity*. Let us imagine a circle of radius p drawn around each nucleus, then the area occupied by all such circles in a unit area of foil is $\pi p^2 nt$. Since every α-particle that comes within a distance p of a nucleus is deflected through an angle equal to or greater than θ, hence the probability of such deflection or the fraction of the total number of α-particles that is deflected through an angle equal to or greater than θ is given by

$$f = \pi p^2 nt/1 = \pi nt[Zze^2/4\pi\varepsilon_0 Mv_0^2]^2\cot^2(\theta/2). \qquad \text{...(12)}$$

The probability that the original direction of motion of an α-particle that would fall between the radii p and $p + dp$ is given by

$$df = 2\pi\, ntp\, dp.$$

This will be equal to the probability that an α-particle would be deflected through an angle lying between θ and $\theta + d\theta$. Therefore

$$df = -\pi nt[Zze^2/4\pi\varepsilon_0 Mv_0^2]^2\cot(\theta/2)\operatorname{cosec}^2(\theta/2)d\theta.$$

In the experiments made to test the theory, the scattering was determined by counting the number of α-particles (from radon source R) incident perpendicularly on a constant area dS of a fluorescent (ZnS)

screen S after passing through a thin foil F, as shown in Fig. 1.2. The α-particles scattered through an angle lying between θ and θ + $d\theta$ will travel in between the cones of semivertex angles θ + $d\theta$ and θ.

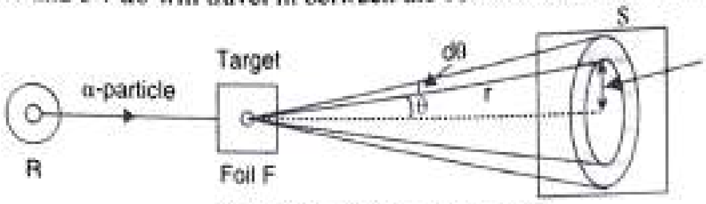

Fig. 1.2. Scattering of α-particle.

The area dA on the screen at which these scattered α-particles fall is given as

$$dA = 2\pi(r\sin\theta)r\,d\theta.$$

If Q is the total number of α-particles incident on the foil and N the number striking area dS of the screen. Then we have $N/Q = (df/dA)dS$. Therefore

$$\frac{N}{Q} = \frac{\frac{1}{2}\pi nt\,dS[Zze^2/4\pi\varepsilon_0 Mv_0^2]^2\sin\theta\operatorname{cosec}^4(\theta/2)\,d\theta}{2\pi r\sin\theta\, r\,d\theta}$$

or

$$N = Qnt\frac{dS}{4r^2}\left(\frac{Zze^2}{4\pi\varepsilon_0 Mv_0^2}\right)^2\operatorname{cosec}^4(\theta/2). \qquad \ldots(13)$$

This is the famous *Rutherford's scattering formula.*

Experimental Verification—The experimental arrangement used by Geiger and Marsden consisted of a cylindrical metal box fixed to a graduated circular platform which could be rotated about a vertical axis in the plane of the foil by means of the ground conical joint J. The box was closed air tight at the top by a ground glass plate P and evacuated through the tube T. The collimated beam of α-particles emerged from a radon source R placed in a block B, after passing through diaphragm D, was scattered by the foil F. The scattered α-particles were detected by the scintillations produced in the small fluorescent screen dS mounted in front of the objective of a low power microscope M. Block and foil were mounted independently on the box, so that the microscope and screen could be rotated along with the box. In this way they were able to detect the α-particles scattered over a wide range of angles from 5° to 150°. For observations at small angles a much weaker source is necessary. The results obtained may be summarised as follows :

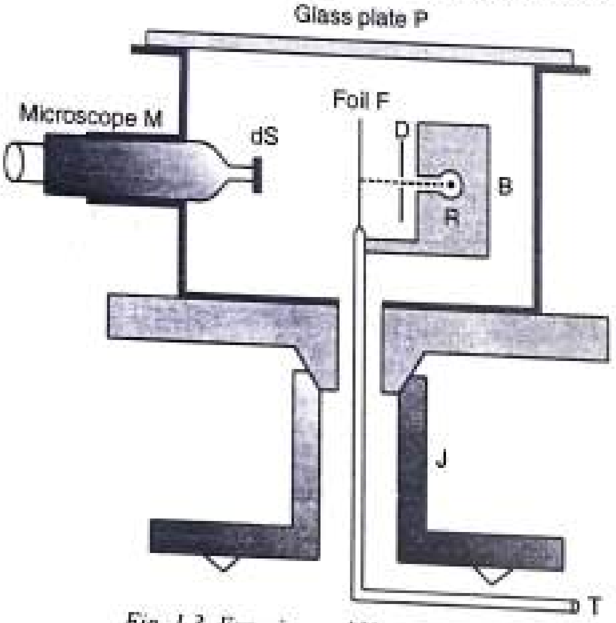

Fig. 1.3. Experimental Verification.

(a) Angular distribution of α-particles scattered by thin foil—Geiger and Marsden placed the microscope M at different angles and counted the number of particles striking the screen in each case, Fig. 1.4. They found that $N \propto 1/\sin^4(\theta/2)$, or $N\sin^4(\theta/2)$ = constant.

(b) Dependence of the scattering on the thickness of the foil—The foils of different thicknesses and also of different materials were used. The number of particles scattered per minute, N, through an constant angle 45° were noted. Graphs were drawn between number of particles and thickness for different materials as shown in Fig. 1.5. The straight lines show that for any one element $N \propto t$.

(c) Dependence of the scattering on the velocity of α-particles—The velocity of α-particles was changed by placing absorbing screen of mica between source and scattering foil. The velocities of α-particles were

determined first by finding the range R of the particles in air and then applying Geiger's law $R \propto v_0^{3/2}$. Thus it was found that $Nv_0^4 = \text{constant}$.

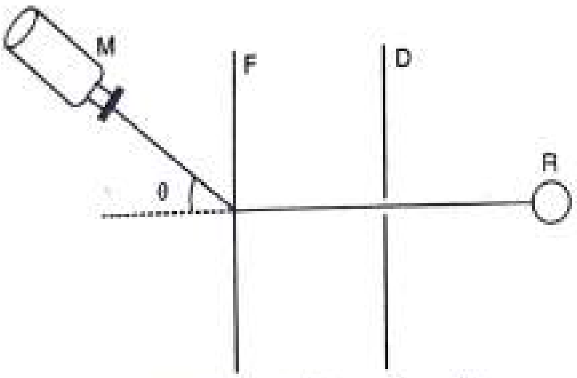

Fig. 1.4. Angular distribution of α-particles scattered by a thin foil.

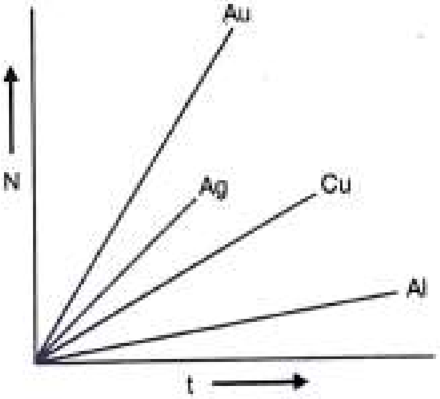

Fig. 1.5. Dependence of scattering on the thickness.

(d) Dependence of the scattering on the nuclear charge—In 1920, Chadwick determined the atomic number from scattering experiment. The apparatus consisted of a scattering foil AA' in the form of an annular ring, source of α-particles R, thick lead screen L to cut completely the direct beam RS, and screen S or the detector so placed that $RA = AS$.

Let ω_1 and ω_2 be the solid angles subtended at R by the inner and the outer edges of the foil AA' respectively. The solid angle subtended by an elementary annular ring at R

$$d\Omega = 2\pi \sin(\theta/2)\, d(\theta/2).$$

∴ Number of particles falling per second on the elementary ring

$$= \frac{2\pi \sin(\theta/2)\, d(\theta/2)}{4\pi} Q.$$

where Q is the number of particles emitted by the source per sec.

∴ Number of particles scattered to unit area of the screen placed normally to RS

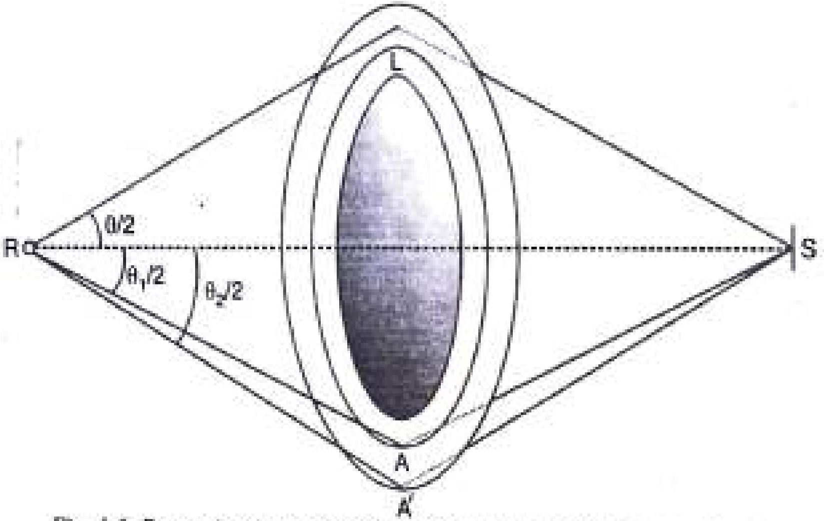

Fig. 1.6. Determination of atomic number from scattering experiment.

$$= \frac{2\pi}{4\pi} Q \sin(\theta/2)\, d(\theta/2) \frac{nt(Zze^2)^2 \operatorname{cosec}^4(\theta/2)}{4r^2 (4\pi\varepsilon_0 Mv_0^2)^2}.$$

Total number of α-particles scattered from an annular ring AA'

$$= \int_{\theta_1/2}^{\theta_2/2} \frac{Qnt(Zze^2)^2 \operatorname{cosec}^3(\theta/2)\, d(\theta/2)}{8r^2 (4\pi\varepsilon_0 Mv_0^2)^2}$$

$$= \frac{Qnt(Zze^2)^2}{16r^2 (4\pi\varepsilon_0 Mv_0^2)^2} \left[\log \tan\frac{\theta_2}{4} - \log\tan\frac{\theta_1}{4}\right] + \left(\cot\frac{\theta_1}{2} \operatorname{cosec}\frac{\theta_1}{2} - \cot\frac{\theta_2}{2} \operatorname{cosec}\frac{\theta_2}{2}\right) \quad \ldots(14)$$

The number of α-particles falling directly per sec per unit area on the screen was $Q/4\pi(RS)^2$. Thus Ze was obtained. Knowing the value of e, the values of Z for different scatterers were obtained. Chadwick showed that the value of Z for *Cu*, *Ag* and *Pt* was 29.3, 46.3 and 77.4 respectively. These were very close to the atomic numbers 29, 47 and 78.

Applications : The α-particle scattering theory may be used to calculate the distance of closest approach of the α-particle to the nucleus, which will be smallest, known as *critical distance*, when the scattering angle θ is greatest and particles go back to their initial path. At the point of *closest approach the kinetic energy decreases to zero and particle has only Coulomb's potential energy.*

$$\therefore \qquad Zze^2/4\pi\varepsilon_0\, b \;=\; \tfrac{1}{2}Mv_0^2 \text{ or } b = 2Zze^2/4\pi\varepsilon_0 M v_0^2. \qquad \ldots(15)$$

where b is the *critical distance*. Considering the process of scattering as a type of collision between two particles, the distance of closest approach gives an upper limit to the size of the nucleus. The condition for normal scattering is $2Zze^2/4\pi\varepsilon_0\; Mv_0^2 > b$. If the collision of the α-particle and the light nucleus takes place within the critical distance considerable deviation from normal scattering may be expected to occur. This is known as *inelastic collision*, where the part of the kinetic energy is spent in producing transformations in the internal structure of the nucleus. As a result of inelastic collision we have the phenomenon of *anomalous scattering* of α-particle. Experimentally it has been observed that for the fastest α-particles ($v_0 = 2 \times 10^7$ *m/sec*), the scattering is normal for all elements heavier than copper ($Z = 29$). For *Au*, *Ag* and *Cu*, b was found to be 3.2, 2 and 1.2×10^{-14} *m* respectively.

Based on the theory of scattering of α-particles, *Rutherford proposed that the positive charge and most of the mass of the atom is concentrated in a very small central core, called the nucleus*. Since the atom as a whole is electrically neutral, the negatively charged electrons must be distributed in space round the nucleus to balance its positive charge. These extra nuclear electrons can not be stationary, if it is so they will be gradually attracted by the nucleus till ultimately they fall into it. To have a stable atom, the surrounding electrons are supposed to be moving about the nucleus in closed orbits so that the electrostatic force is balanced by centrifugal force. This model of atom was most strongly in conflict with the classical theory of electro-magnetism. The conflict was resolved by Niels Bohr in 1913, who applied with remarkable success the quantum theory to the Rutherford nuclear atom with revolving electrons in stationary orbits.

1.3 NUCLEAR SIZE

In 1919, Rutherford found that the deviation from pure Coulomb's scattering, *anomalous scattering*, was observable when α-particles were scattered by the lightest elements. In these light elements, the closest distance of approach was of the order of 5×10^{-15} *m*. The distance of closest approach at which anomalous scattering begins was identified as the first measure of the *nuclear radius*.

It is evident from experiments that the nucleus is composed of protons and neutrons only, known as *nucleons*. The shape of the nucleus is taken spherical, because for a given volume this shape possesses the least surface area and thus provides maximum short range binding forces between the nucleons in the nucleus. Small asymmetries of the distribution of negative charge are present in some nuclei as these nuclei exhibit high electric quadrupole moments. In most nuclei the ellipticity is only of the order of one per cent, thus we may suppose that protons are uniformly distributed inside the spherical nucleus.

There is an experimental evidence that nuclear density ρ remains approximately constant over most of the nuclear volume and then decreases rapidly to zero. This means that the nuclear volume is approximately proportional to the number of nucleons, *i.e.*, mass number A.

$$\text{Thus} \qquad V \;=\; \tfrac{4}{3}\pi R^3 \propto A, \text{ or nuclear radius } R \propto A^{1/3},$$

$$\therefore \qquad R \;=\; R_0 A^{1/3}, \qquad \ldots(16)$$

where R_0 is the *nuclear unit radius*. Thus our purpose is to find R_0.

The methods of measuring nuclear radius are divided into two main categories. One group of methods is based on the study of the range of nuclear forces, the nucleus is probed by a *nucleon or light nucleus*. Other group of methods studies the electric field and charge distribution of the nucleus, the nucleus is probed by *electron* or *muon*.

1. Nuclear Force Methods

(a) Lifetime of α-Emitters. In 1928 Gamow and Gurney and Condon gave wave mechanical treatment for the problem of α-decay (will be discussed in chapter 5). The half life for radioactive decay $t_{1/2}$ is related with the disintegration probability λ as

$$t_{1/2} = \log_e 2/\lambda = 0.693/\lambda,$$

where λ is the product of an internal disintegration probability λ_0 (decay constant without barrier) and a barrier transmission coefficient $e^{-\gamma}$ *i.e.*,

$$\lambda = \lambda_0 e^{-\gamma}.$$

Here λ_0 can be defined as the product of the probability of existence of α-particle in the nucleus (0.1 to 1) and the rate of hitting the barrier (v_{inside}/R). The exponent γ depends on nuclear radius R and changes λ much strongly as

$$\lambda = \lambda_0 e^{-(a-bR_0^{1/2})}. \qquad \dots(17)$$

Using experimental data, λ_0 and R_0 can be calculated. The average value of the nuclear unit radius R_0, found from α-decay experiments, is

$$R_0 = 1.48 \times 10^{-15}\,meter = 1.48\,fermi.$$

Blatt and Weisskopf have pointed out that the correct radius R_A of the daughter product will always be smaller than the effective radius R, because of the finite size (radius R_α) of the α-particle. If r_α is a semi-empirical radius correction for the α-particle, the radius R can be expressed as

$$R = R_A + r_\alpha. \qquad \dots(18)$$

The value $r_\alpha = 1.2 \times 10^{-15} m$ has been taken as reasonable, as it gives good agreement with observations. Using $R = (1.5 \pm 0.1) \times 10^{-15} A^{1/3}$, the corrected nuclear unit radius

$$R_{0A} = (1.3 \pm 0.1) \times 10^{-15}\,m.$$

(b) Anomalous Scattering of α-particles. The classical collision diameter, the distance of closest approach $b = 2Zze^2/4\pi\varepsilon_0 Mv^2$ was the first measure of the nuclear radius R. Pollard suggested $R_0 = 1.4$ to $1.5 \times 10^{-15}\,m$. With the correction for finite size of α-particle, the corrected value of R_{0A} for the target nuclei was found to be $(1.3 \pm 0.1) \times 10^{-15}\,m$.

(c) Attenuation of fast Neutrons. As neutrons possess no charge. A fast neutron passes easily through bulk matter and the target cross section can be expected to be the geometrical cross section πR^2. Using neutron size as $\bar{\lambda}$, one can estimate the cross section for a direct encounter as

$$\sigma_{absorption} = \pi(R + \bar{\lambda})^2.$$

Considering the neutron beam as a plane wave, the each nucleus will cast a shadow. The amount of energy diffracted is equal to that absorbed by the opaque sphere. For the fast neutrons with $\bar{\lambda} << R$, this diffraction corresponds to a small angle elastic scattering and the scattering cross section is the same as the absorption cross section (will be discussed in chapter 10), *i.e.*,

$$\sigma_{sc} = \sigma_{abs} = \pi(R + \bar{\lambda})^2.$$

$\therefore$ Total nuclear cross section $\sigma_t = 2\pi(R + \bar{\lambda})^2. \qquad \dots(19)$

It is about twice the effective geometrical area of the nucleus. Using the measured values of σ_t, we get nuclear unit radii in the domain of $(1.4 \pm 0.1) \times 10^{-15}\,m$.

(d) Nuclear Reactions by Charged Particles. Using Bohr's compound nucleus model of nuclear reactions, we can calculate nuclear radius. If the target nucleus X is bombarded by the charged particle x, a compound nucleus $(X + x)$ is formed. The compound nucleus dissociates in a large number of ways. If the partial level width is Γ_y, which is proportional to the probability of emission of the particle y from the compound nucleus, then the total level width $\Gamma = \Sigma\Gamma_y$. The cross section for such a reaction $(X + x \rightarrow C^* \rightarrow Y + y)$ is

$$\sigma(x, y) = [\sigma_C(x)](\Gamma_y/\Gamma).$$

The classical cross section for the forming of the compound nucleus is $\sigma_C(x) = \pi a^2$, where a is a largest value of the impact parameter. If the effective nuclear radius $R' = R + \bar{\lambda}$, then we have

$$\sigma_C = \pi a^2 = \pi(R + \bar{\lambda})^2(1 - U/T). \qquad \dots(20)$$

where $U = Zze^2/4\pi\varepsilon_0(R + ƛ)$ and the K.E. of the incident particle $T = \hbar^2/2Mƛ^2$ in the C.M. system of coordinates.

σ_C is small but finite for bombarding energies T for below the Coulomb barrier height $B = Zze^2/4\pi\varepsilon_0 R$. It increases very rapidly with T and approaches asymptotically a maximum value πR^2, when $T >> B$.

The available experimental data for σ_C suggest the nuclear unit radius near the domain of $R_0 = (1.4 \pm 0.1) \times 10^{-15} m$.

Angular distributions for the elastic scattering of protons in the energy range 5–300 *MeV*, using optical model analysis for the nuclear reactions, suggest $R_0 = 1.33 \times 10^{-15} m$.

2. Electromagnetic Methods :

(a) Mesonic X-rays—The bombardment of nuclei by high energy particles or photons can evoke the emission of π^+ or π^- mesons from the target nuclei. These π^+ mesons (pions) are repelled by nuclei and decay into μ^+-mesons (muons) as

$$\pi^+ \rightarrow \mu^+ + \nu \, (\tau = 0.02 \, \mu \, sec.). \qquad ...(21)$$

μ^+-mesons also decay into positrons as

$$\mu^+ \rightarrow e^+ + \bar{\nu} + \nu \, (\tau = 2.15 \mu \, sec.). \qquad ...(22)$$

where ν and $\bar{\nu}$ represent a neutrino and antineutrino respectively.

The negative μ-mesons are also produced in a similar manner. μ-meson has a mass value $m_\mu = 207 \, m_e$ where m_e is the mass of the electron. It has the same spin and charge as an electron and thus behaves like a heavy electron.

Mesons traversing in matter loss energy by excitation and ionization processes. When they reach thermal energies, μ^--mesons [*not* μ^+ *mesons*] may be captured into Bohr type orbits. As all the mesonic atomic states are unoccupied, the μ^--meson will fall to states of lower energy, first by means of non-radiative transitions (*by collisions and by Auger electrons*) and then by radiative transitions. In the last few orbit transitions *X*-rays are radiated. The time for a negative muon to slow down from about 2keV and be captured into 1*s* atomic orbit has been estimated to be about 10^{-13} sec in graphite, which is much smaller than the life time (2×10^{-6} *sec*) of the muon. Thus so many mesons may be capable of forming *mesonic-atoms*.

Since for an one-electron atom, the radius r and energy E of the stationary states, assuming nucleus as point charge, are given by

$$r_n = n^2 h^2 \varepsilon_0 / \pi m_e Z e^2, \qquad ...(23)$$

and

$$E_n = -m_e Z^2 e^4 / 8 n^2 h^2 \varepsilon_0^2. \qquad ...(24)$$

Therefore the analogous result for a mesonic atom is given by

$$r_n(\mu^-) = a_0 n^2 m_e / Z m_\mu, \qquad ...(25)$$

where a_0 = ground state radius of the hydrogen atom = 5.29×10^{-11} *m*.

Thus the radii of the Bohr orbits for μ^--meson are m_e/m_μ times smaller than that for the electron and the μ-meson in its lowest atomic state (*K–shell*) spends a large fraction of its time inside the nucleus. It should therefore be possible to use μ-mesonic atoms to determine the nuclear size.

As clear from Eq. (24), the difference in the energy levels of the muonic atom are larger than the corresponding electronic orbits. The wavelengths of the emitting electromagnetic radiation are therefore in *X*-ray range. Measurement of the energies of the *X*-rays obtained from μ^--mesons while jumping from one orbit to the other was first made by Fitch and Rainwater in 1953, using a *negative* meson beam of well defined momentum as a nuclear probe. π-mesons from a cyclotron decayed into μ^--particles, which were then allowed to enter a block of the material under investigation. As π-mesons have a very strong interaction with nucleons hence are not useful for measuring nuclear radii. Thus to absorb these the beam was allowed to pass through a piece of Cu (3" thick). *X*-rays produced in the absorber were detected with a scintillation counter

[*NaI(Tl) crystal*]. Absorbers of different atomic numbers, ranging from Z = 13 to Z = 83 were used. The most probable transition would be a $2p \rightarrow 1s$ transition giving rise to a characteristic line. A typical *X*-ray spectrum from µ-mesonic atom of titanium is shown in Fig. 1.7(*a*). In this spectrum we have characteristic line at 0.955 MeV.

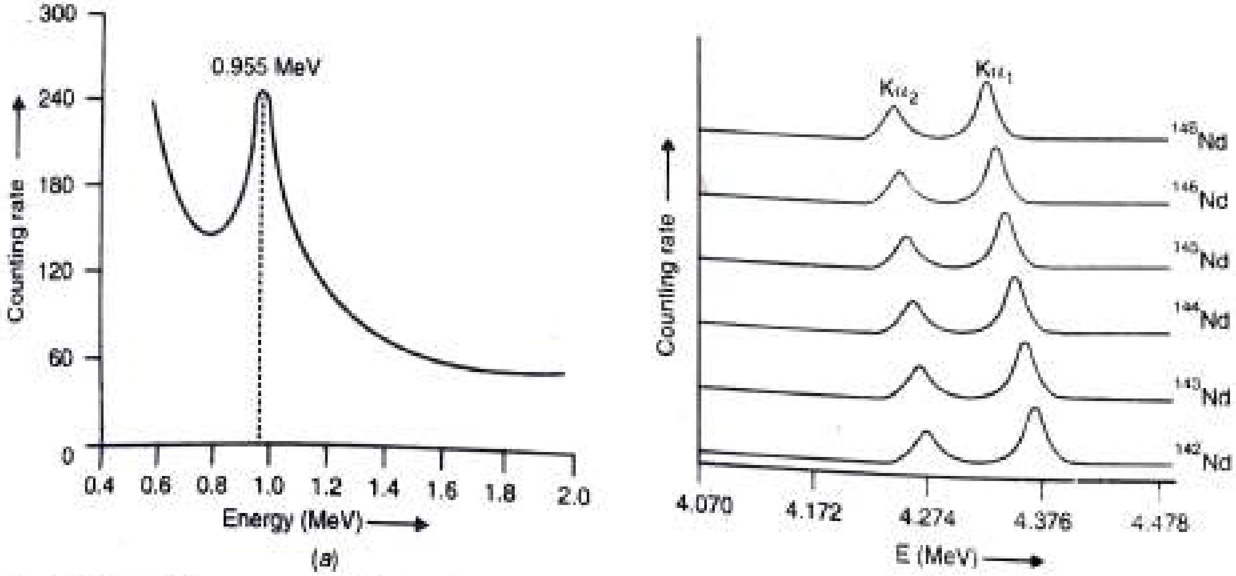

(*a*)

(*b*)

Fig. 1.7. Muonic K X-ray spectrum (a) from Ti using NaI scintillation detector, (b) from Nd isotopes using Ge (Li) detector

The availability of Ge(Li) detectors has improved the accuracy of such measurements and made possible to resolve the K_{α_1} and K_{α_2} lines, which are from $2p_{1/2} \rightarrow 1s_{1/2}$ and $2p_{3/2} \rightarrow 1s_{1/2}$ muonic transitions respectively, Fig. 1.7 (*b*). This figure shows the isotope shift in muonic atoms. The isotope shifts also give information on the nuclear charge distribution. K_{α_1} energy slightly exceeds the K_{α_2} energy.

In Pb, the radius of the µ-mesonic *K*-shell for a point nucleus, obtained from relation (23), would be about $3.1 \times 10^{-15} m$, while that of *L*-shell $12 \times 10^{-15} m$. Thus we see that the value of the radius of *K*-shell is smaller than the radius of ^{208}Pb of 7.1 *fm* as estimated from $R = R_0 A^{1/3}$, using $R_0 = 1.2 fm$. The energy of a muon in a 1*s* orbit around the nucleus of a lead, using relation (24), is 19MeV. Using Sommerfeld theory, we obtain

$$E_{nl} = E_n \left[1 + \left(\frac{\alpha Z}{n} \right)^2 \left(\frac{n}{|k|} - \frac{3}{4} \right) \right] \qquad \ldots(26)$$

where $\alpha = e^2/4\pi\varepsilon_0 \hbar c = 1/137$, $|k| = l + 1$ for $j = l + 1/2$ and $|k| = l$ for $j = l - 1/2$. The transition energy between $2p_{3/2}$ and $1s_{1/2}$ states would thus be 16.4 MeV. This is greater than the observed energy 6.02 MeV of the electromagnetic radiation. This difference is due to the finite size of the nucleus. For the 1*s* state in *Pb*-mesonic atom, the muon spends about 50% of its time inside the nuclear volume, the Coulomb field acting on the muon is reduced (similar to the gravitational intensity, which decreases inside the earth). The reduction in the Coulomb force reduces the binding of the muonic states and all the energy levels are raised. This effect is most pronounced for 1*s* orbit.

The change in the Coulomb interaction energy due to the finite nuclear size is obtained by the first order perturbation theory and is given by

$$\Delta E = \int_0^\infty |\psi|^2 [V(r) - Ze^2/4\pi\varepsilon_0 r] d^3 r. \qquad \ldots(27)$$

where $V(r)$ and $Ze^2/4\pi\varepsilon_0 r$ are the potentials due to the finite nucleus and the point nucleus respectively. The charge distribution may be assumed as

$$\int_0^\infty \rho(r) 4\pi r^2 dr = Ze. \qquad \ldots(28)$$

For light elements the shift in the energy of the *K*-shell is small and is approximately proportional to R^2Z^4, where $R = R_0 A^{1/3}$. The shift is greatest for 1*s* level, much less for the $2p_{1/2}$ level and still smaller for $2p_{3/2}$ level.

The energies of the bound states can be calculated if we solve the relativistic wave equation (Dirac equation) for the muon-nucleus system by using a potential that corresponds to the electrical charge distribution in the nucleus. Such calculations are complicated, so that the experimental results may be compared with the theoretical calculations based on different assumed nuclear radii. The observed energies and the energies calculated on the basis of a point nucleus are listed in Table 1.1. The best estimated value of R_0 which fits the observed *X*-rays are given in the last column. The value of R_0, determined by this process is 1.20 ± 0.03 fermi, assuming the distribution of charge to be homogeneous with in the nucleus. The differences from the values given by Eq. (24) provide a measure of the charge distribution in the nucleus, discussed in references (5 & 7).

Table 1.1. Mesonic *X*-rays : $2p_{3/2} \rightarrow 1s_{1/2}$ transitions

Element	*(Z)*	*Calculated energy (point nucleus, MeV)*	*Observed X-ray energy (MeV)*	*"Best fit" value of R_0 (fermi)*
Al	*13*	*0.363*	*0.35*	—
Si	*14*	*0.421*	*0.41*	—
Ti	*22*	*1.045*	*0.955*	*1.17*
Cu	*29*	*1.826*	*1.55*	*1.21*
Zn	*30*	*1.954*	*1.6*	—
Sb	*51*	*5.83*	*3.5*	*1.22*
Hg	*80*	*15.51*	*5.8*	—
Pb	*82*	*16.41*	*6.02*	*1.17*
Bi	*83*	*16.88*	*6.0*	—

(b) Electron Scattering—In recent years, the scattering of high energy electrons from the nucleon and from nuclei has provided important information about the size of the nucleus. The amount of information depends on the magnitude of the de-Broglie wavelength of the incident electrons compared with the radius of the scattering nucleus. When these lengths are of the same order, *electron scattering by the nuclear charge is closely analogous to electron diffraction (at wavelength ~ 0.1Å) by the electron charge distribution of an atom. For highly relativistic electrons.*

$$E = T + m_0c^2 \simeq T \simeq cp.$$

∴ de-Broglie wavelength $\lambda = h/p = hc/E.$

This relation shows that the de-Broglie wavelenth associated with the electron of energy 100 *MeV* or higher is of the order of a few fermis. For highly relativistic electrons ($E = cp$) electron-nucleus collision process can be treated as a process similar to photon-electron Compton collision. The energy of the recoiling nucleus E_n when the incident electron of energy E is scattered through an angle θ is given by

$$E_n = \frac{E^2}{Mc^2} \cdot \frac{1-\cos\theta}{1+(E/Mc^2)(1-\cos\theta)}, \quad \text{..(29)}$$

where M is the mass of the nucleus.

Outstanding accelerators of the travelling wave type have been built at Standford University. A 600 *MeV* linear electron accelerator has been responsible for much of our knowledge of nuclear charge distribution. Hofstadter used this machine and performed a series of electron scattering experiments. Beams of energy upto 550 *MeV* were used for work on the lightest nuclei, while for most of the heavier nuclei energies between 100 and 190 *MeV* were used. The different groups of scattered electrons were resolved using a semicircular magnetic momentum analyser. The Stanford analyser for 550 *MeV* electrons has a magnetic spectrometer of central radius of curvature 3ft and a total weight of 30 tons. Electron beam from linear accelerator is deflected by magnets M_1 and M_2. Electrons scattered by the target are focussed on to a detector by magnet.

The targets used are often in the form of thin metal foil (*e.g.*, gold 0.002" thick). Sometimes gas targets (hydrogen or helium) at high pressure (2000 lb per in^2) are used. The experimental arrangement is shown in Fig. 1.8. The intensity of scattered electrons is obtained as a function of the scattering angle by rotating the spectrometer with respect to the target position.

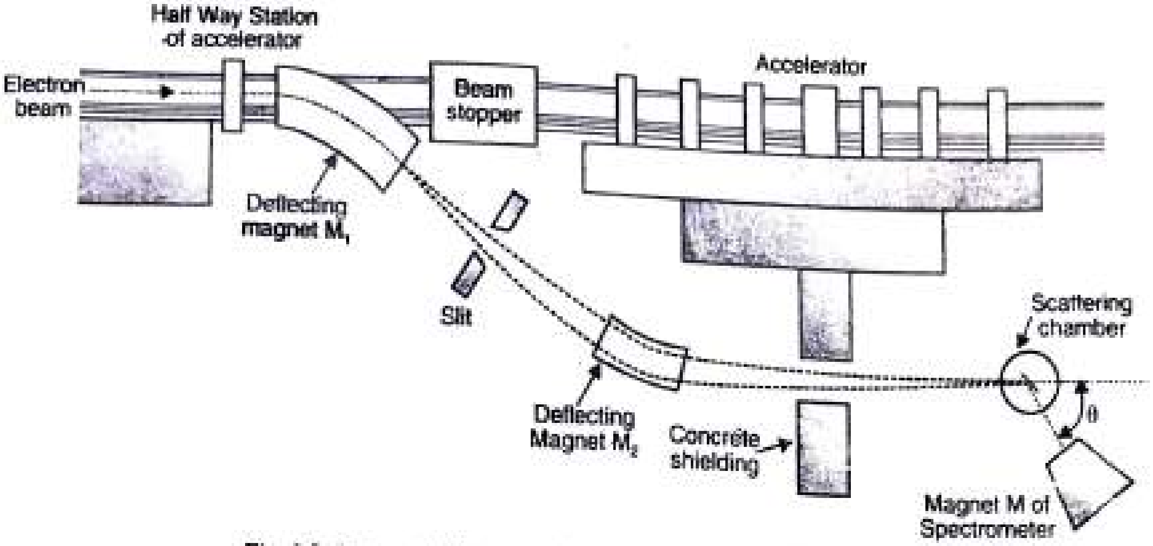

Fig. 1.8. Systematic diagram of the electron scattering experiment.

The observed elastic scattering of high energy electrons is compared with theoretical results. The scattering at different energies and angles is expressed in terms of the differential scattering cross-section $\sigma(\theta)$. If a collimated beam of I electrons crosses unit area of a thin target containing N nuclei per unit volume, then the number of electrons scattered through an angle θ into an elementary solid angle $d\Omega$ per unit time is given by the relation

$$n_\theta = \sigma(\theta) I d\Omega, \qquad \ldots(30)$$

where $d\Omega = 2\pi \sin\theta\, d\theta$. For elastic scattering of an electron of velocity βc, from a point nucleus (charge Ze) of zero spin, Mott obtained the following formula for the differential cross-section.

$$\sigma_M(\theta) = \left(\frac{Ze^2}{8\pi\varepsilon_0 m_e c^2}\right)^2 \left(\frac{1-\beta^2}{\beta^4}\right)\frac{1}{\sin^4\frac{1}{2}\theta}\left(1-\beta^2\sin^2\frac{\theta}{2}\right). \qquad \ldots(31)$$

In the non-relativistic limit, we have $E = m_e c^2$ and the kinetic energy of the incident electron becomes $p^2/2m_e$ and the Mott formula reduces to the Rutherford formula.

For high energy electrons β is very close to unity and we can write

$$\beta^4 = 1 \text{ and } E = m_e c^2/\sqrt{(1-\beta^2)}.$$

$$\therefore \qquad \sigma_M(\theta) = \left(\frac{Ze^2}{8\pi\varepsilon_0 E}\right)^2 \frac{\cos^2(\theta/2)}{\sin^4(\theta/2)}. \qquad \ldots(32)$$

This formula is derived by a Born approximation and it describes the scattering of the electron waves by the Coulomb potential of the point nucleus in terms of plane waves. This formula is valid for light nuclei but is seriously in error for heavy nuclei. This is because the wavefront of the electron wave train is distorted by the strong Coulomb field in the vicinity of the nucleus. The observed scattering of high energy electrons by a nucleus of finite size is less than that of predicted for a point nucleus. This can be obtained by multiplying the Mott formula by a new factor, known as charge form factor, as

$$\sigma_S(\theta) = \sigma_M(\theta)|F|^2, \qquad \ldots(33)$$

The form factor F is an integral of the charge density times the phase factor over the nuclear volume. It is written in terms of the momentum $\hbar q$ transferred to the nucleus in the scattering.

$$F = F(q) = \int_0^\infty \rho(r) e^{i\mathbf{q}\cdot\mathbf{r}} d\tau. \quad \text{...(34)}$$

The nuclear charge density distribution $\rho(r)$ is defined in terms of the ground state wave function of a nucleus $\psi(r)$, as

$$\rho(r) = Z|\psi(r)|^2. \quad \text{...(35)}$$

It is taken that the nuclear wave function $\psi(r)$ is normalized to unity and the charge density is normalized to Z, the number of protons in the nucleus.

In the non-relativistic limit, the momentum transfer hq from the electron to the nucleus is defined as

$$hq = \mathbf{p}_f - \mathbf{p}_i. \quad \text{...(36)}$$

where $\mathbf{p}_i$ and $\mathbf{p}_f$ are the momentum vectors of electron before and after the scattering respectively. For elastic collision

$$p_i = p_f \text{ and } hq = 2p_i \sin \tfrac{1}{2}\theta$$

or

$$q = \frac{4\pi}{\lambda}\sin\frac{\theta}{2} \qquad \left(\because p_i = \frac{E}{c} = \frac{h}{\lambda}\right)$$

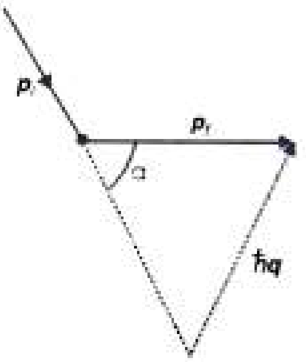

Fig. 1.9. Momentum Transfer diagram.

For nuclear size studies, we are mainly interested in the radial dependence of the density and thus can take an averge over the angular distribution. The charge form factor F may thus the expressed in the radial form as

$$F = \int_0^\infty \rho(r)\frac{\sin qr}{qr} 4\pi r^2 dr = \frac{4\pi}{q}\int_0^\infty \rho(r)\sin(qr) r dr. \quad \text{...(37)}$$

It is a function of q^2, it is due to this reason $F(q)$ is sometimes written as $F(q^2)$.

The two typical angular distributions for electrons scattered elastically by gold are shown in Fig. 1.10. The intensity falls off very rapidly for increasing angle θ. It decreases with the increase of energy E.

F is nearly equal to unity for low energies and small scattering angles and is much smaller than unity for higher energies and large scattering angles. Thus explains the experimental results.

The model of the nuclear charge distribution which is the best fit to the experimental scattering observations for nuclei over a wide range of mass number (heavy nuclei) is known as the Fermi model and is represented by the equation

$$\rho(r) = \frac{\rho_0}{1 + e^{(r-c)/z}}. \quad \text{...(38)}$$

where ρ_0 is the density at small values of r and c is the distance from the centre of the nucleus to the point where $\rho(r)$ has fallen to half its central value. It is called mean electromagnetic radius of the nucleus. z is the *diffuseness*, related to the thickness of the surface region. It is defined as $t = 4z \log_e 3$, where t is called *skin thickness*. Hofstadter *et al.* defined the thickness t as the distance between points on the fall away of $\rho(r)$ corresponding to $\rho(r)$ equal to 90% and 10% of the central density ρ_0.

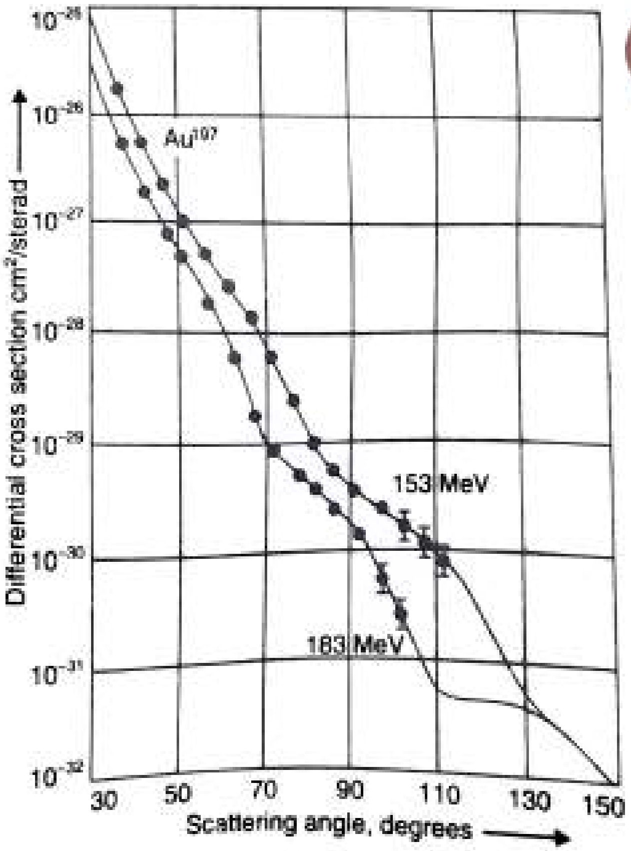

Fig. 1.10. Angular distributions for electrons by gold.

Typical charge distributions found in some nuclides are shown in Fig. 1.12. The central parts of all these nuclei show the same charge density. The experimental results indicate that

$$t = (2.4 \pm 0.3) \times 10^{-15}\, m$$

and

$$c = (1.07 \pm 0.02)\, A^{1/3} \times 10^{-15} m.$$

When the charge density is non-uniform, the nuclear charge radius is the root of mean square radius, which is defined as

$$\overline{r^2} = \frac{\int_0^\infty r^2\, 4\pi r^2\, \rho(r)\, dr}{\int_0 4\pi r^2\, \rho(r)\, dr}. \quad \ldots(39)$$

The electron scattering determinations of nuclear radii over a wide range of mass number A, agree with formula $R = R_0 A^{1/3}$, where R is the root mean square radius and $R_0 = 1.32$ fermi for $A < 50$ and 1.21 fermi for $A > 50$.

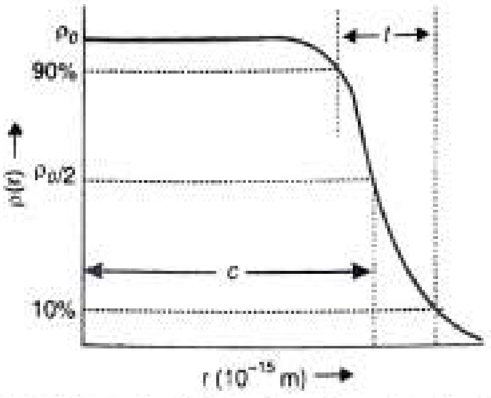

Fig. 1.11. Fermi model of nuclear charge distribution.

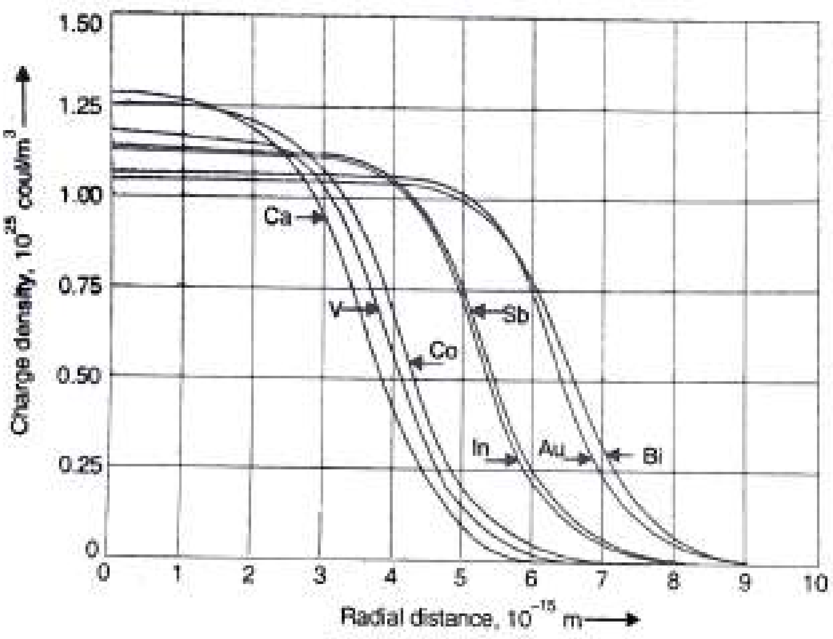

Fig. 1.12. Charge density distribution.

The better description of the observed density is provided by a modified Fermi form with an additional parameter ω, known as three parameter (c, z, ω) Fermi form,

$$\rho_{3pF}(r) = \rho_0 \frac{1 + \omega (r/c)^2}{1 + e^{(r-c)/z}}. \quad \ldots(40)$$

Other form is the three parameter Gaussian, given by

$$\rho_{3pG}(r) = \rho_0 \frac{1 + \omega (r/c)^2}{1 + e^{(r^2-c^2)/z^2}} \quad \ldots(41)$$

Harmonic oscillator model form is also used.

$$\rho_{HO}(r) = \rho_0 [1 + z(r/c)^2] e^{-(r/c)^2}. \quad \ldots(42)$$

The charge density distributions for various nuclei using these forms are tabulated in *Atomic Data and Nucl. Data Tables 36, 495 (1987).*

(c) Coulomb energies of Mirror Nuclei—There exists many light unstable nuclei in which Z differs from N by unity. Among these there are pairs which consist of the same odd number of nucleons, say $(2Z+1)=A$, but one of them has Z protons and $(Z+1)$ neutrons, while the other $(Z+1)$ protons and Z neutrons. Such nuclei are called *mirror nuclei*. The few examples are :

$$({}_1^3H, {}_2^3He);({}_3^7Li, {}_4^7Be);({}_6^{13}C, {}_7^{13}N);({}_{19}^{39}K, {}_{20}^{39}Ca).$$

If the odd nucleon changes from a proton to a neutron by positron emission, then total number of nucleons remains unchanged.

$${}_7^{13}N \rightarrow {}_6^{13}C + e^+ + \nu.$$

Assuming that the charge is uniformly distributed in the nuclear spherical volume of radius R, the Coulomb potential energy due to the nuclear charge

$$E_c = \tfrac{3}{5}(Z^2e^2/4\pi\varepsilon_0 R).$$

The difference in the electrostatic energies between the nuclei differing by one unit in Z is thus given by

$$\Delta E_c = \frac{3}{5}\frac{e^2}{4\pi\varepsilon_0 R}\left[Z^2-(Z\pm1)^2\right] = \frac{3}{5}\frac{(2Z\pm1)e^2}{4\pi\varepsilon_0 R}. \qquad \ldots(43)$$

Hence the maximum positron energy, when the daughter nucleus is formed in the ground state, is given by

$$E_{\beta^+} = \tfrac{3}{5}[(2Z-1)e^2/4\pi\varepsilon_0 R] - m_0c^2 - (m_n - m_p)c^2 - \Delta B_{nuc},$$

where m_0c^2 is the rest mass energy of the positron absorbed in creating it, $(m_n - m_p)c^2$ the energy absorbed in transforming a proton of mass m_p into a neutron of mass m_n and ΔB_{nuc} is the difference between the nuclear binding energies in the pair of mirror nuclei. Since $m_0c^2 = 0.51\ MeV$, $(m_n - m_p)c^2 = 1.29\ MeV$ and $A = 2Z-1$, hence

$$\begin{aligned} E_{\beta^+} &= \frac{3}{5}\frac{Ae^2}{4\pi\varepsilon_0 R_0 A^{1/3}} - 0.51\ MeV - 1.29\ MeV - \Delta B_{nuc} \\ &= \frac{3}{5}\frac{e^2A^{2/3}}{4\pi\varepsilon_0 R_0} - 1.80\ MeV - \Delta B_{nuc}. \end{aligned} \qquad \ldots(44)$$

If the positron energy of the unstable members of the mirror nuclides is plotted against $A^{2/3}$, we get a straight line. The slope of the line $\frac{3}{5}e^2/4\pi\varepsilon_0 R_0$ is a measure of the nuclear unit radius R_0. Its value comes out to be about 1.45 fermi which is about 20% higher than that from electron scattering method. This discrepancy was avoided after considering Pauli's principle, which reduces effectively the probability of finding two protons close together and hence reduces Coulomb energy. The values of R_0 for several nuclei measured in this way are given below :

Nucleus	${}^{11}B$	${}^{12}C$	${}^{13}N$	${}^{17}O$	${}^{19}F$	${}^{21}Ne$	${}^{22}Na$	${}^{25}Mg$	${}^{27}Al$
R_0(fermi)	1.28	1.34	1.31	1.26	1.26	1.25	1.22	1.23	1.20

Excluding the first three values of R_0, the mean value for remaining mirror nuclei is given by $R_0 = 1.23 \pm 0.03$ fermi.

(d) Isotope Shift—The optical spectroscopy gives sufficiently accurate measurement of the effect, known as *isotope shift*, due to the finite size of nuclei and provides information about the distribution of charge with in the nuclei. It shows the influence of neutrons in charge distributions experimentally. If the charge distribution is independent of neutrons in the nucleus, we expect the isotopic shift for different isotopes to be negligible. The shifts are found small but not zero. For a point nucleus, the potential $V(r)$ is simply a Coulomb potential, having a value $Ze/4\pi\varepsilon_0 r$. For a finite nucleus, above relation is valid for $r > R$, where R is the nuclear radius. If the nuclear charge is distributed uniformly throughout the nuclear volume, then potential

$$V_i(r) = \frac{Ze}{4\pi\varepsilon_0 R}\left[\frac{3}{2}-\frac{1}{2}\left(\frac{r}{R}\right)^2\right] \qquad r \le R \qquad \ldots(45)$$

The energy of the electronic state depends upon the energy of the atomic electron in the nuclear Coulomb potential. The *s*-electrons have a finite probability of being inside the nuclear radius. If $\psi^2(r)$ is the probability density of the electron being at a distance r from the centre of the nucleus, the potential energy of this electron in the central field $V(r)$ is given by

$$U(r) = e\int_0^\infty \psi^2(r)V(r)4\pi r^2\,dr.$$

Hence the decrease of the atomic binding energy of an *s*-electron can be obtained for the volume charged nuclear model as

$$\Delta W = e\int_0^R \psi^2(r)\,[V_v(r) - V(r)]\,4\pi r^2\,dr. \qquad \ldots(46)$$

For the elements having two or more stable isotopes, which have even mass numbers, certain lines in the emission spectra of these elements are found to consist of a number of closely spaced components. These do not split further because the nuclear moments are zero valued. The isotope shift is a measure of the difference $\Delta W_1 - \Delta W_2$. The finite value of this difference represents that the protons in the nuclei of both isotopes move in regions of different sizes.

Brix and Kopfermann compared the observed and theoretical values of the isotope shifts for $R_0 = 1.5$ fermi and 1.1 fermi. The data corresponding to the latter are found to be in agreement.

1.4 MASS SPECTROSCOPY

Since one gram-atom of any substance contains N atoms, hence mass of one atom = atomic weight/N. This was a rough method. Instruments of moderate precision can be used to measure mass numbers, to determine the relative abundance of isotopes or to produce separated isotopes. Instruments in which we use a photographic plate and obtain the series of lines (called the mass spectrum) are known as *mass spectrographs*. Those in which an electric or a magnetic field is adjusted to make each part of the spectrum in turn to fall on a fixed detecting slit and measured electrically are called *mass spectrometers*.

The accurate determination of atomic masses began in 1919 with the invention of the mass spectrography by F.W. Aston. Modern instruments are based on the mass doublet technique in which the quantity actually determined is the difference in mass between two ions of the same mass number but having slightly different masses. Several novel *"time of flight"* instruments have been introduced. In these instruments the time needed for ions to describe a number of revolutions in a uniform magnetic field is proportional to the mass of the ions. A different approach to the problem of mass differences is through the energy measurements in nuclear reactions.

Mass spectroscopy plays an important role in nuclear physics because differences in masses between neighbouring nuclides reflect differences in binding energies of the last nucleons. This is of great interest and can be used for predicting disintegration and reaction energies. Another important application of mass spectrometry is the determination of the relative abundances of isotopes in a mixture. Knowledge of the masses of middle weight and heavy nuclei is important particularly in the theories of nuclear forces and nuclear structure.

(A) Basic Components of Mass Spectroscopes :

(1) Ion Source—All mass spectroscopes start with an ion source, where the ions are produced either by electron bombardment of gases or by heating the suitably coated filaments. For accurate isotopic abundance ratios, great care is necessary in the selection and operation of the ion source.

Positive ions of alkali metals (*Li, Na, K, Cs*) may be obtained by heating certain of their minerals. Ions of materials such as *Pt, Au, U,* etc., may be obtained by passing an oscillating spark discharge between the electrodes containing such materials. Positive ions of many elements and molecules may be obtained by taking such a gas at low pressure in the high voltage discharge tube. Positive ions of the materials, which can be put in gaseous or vapour form, may be produced by bombarding the gas at low pressure with low voltage electrons (≤ 100 *eV*).

The ions emerging from the ion source have three characteristics : *(a)* the ionic charge ne may be an integral multiple of e, *(b)* the ions may have a wide range of energy, momentum and masses, and *(c)* they may move in a diverging beam.

(2) Energy Filters—The ions of charge $q(= ne)$ from the ion source are given nearly the same energy by accelerating them through a potential difference V_0 chosen so large that neV_0 is much greater than the initial ion energies. This method is suitable for a low voltage ion source. The ions emerging from exit slit B have all nearly the same energy given by the relation

$$\tfrac{1}{2}Mv^2 = neV_0. \qquad ...(47)$$

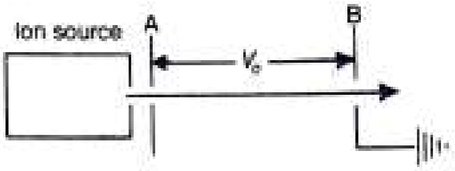

Fig. 1.13. Energy Filter.

Due to this reason, the arrangement is called the *energy filter.*

The *electrostatic cylindrical energy filter* is its improved form. As shown in Fig. 1.14, it consists of pair of cylindrical plates A and B. The plate separation is d and the potential difference between the plates is V. If the speed of the ions is too great, they will not be affected by the radial electric field and will collide with plate B. If the speed is very small, the ions will collide with plate A. The ions can move along the central ray of radius of curvature R_e only, when the speed is such that it satisfies the relation

$$neE = neV/d = Mv^2/R_e$$

or

$$\tfrac{1}{2}Mv^2 = \frac{neVR_e}{2d}. \qquad ...(48)$$

Thus we see that the filter selects ions of one definite K.E. The emerging beam is made up of several speed components, one for each mass. For the ions entering the filter with the correct energy but inclined at a small angle α to the direction of the central ray, Hughes and Rajansky showed that approximate direction focusing takes place if the angular aperture POQ of the cylinder is chosen to be $\pi/\sqrt{2}$(1 = 127° 17′). This is a form of direction focusing. The emerging ions will have lateral displacement $4\alpha^2R_e/3$.

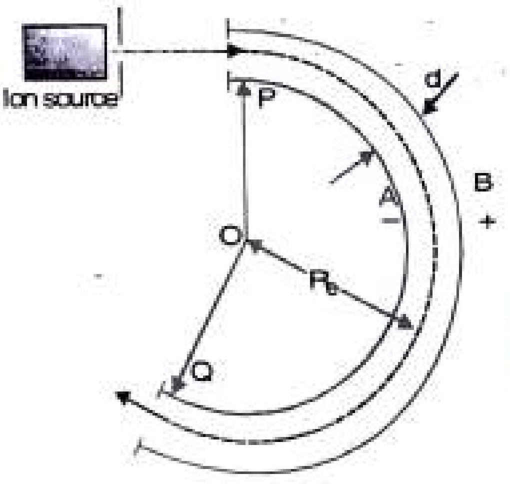

Fig. 1.14. Cylinderical electrostatic energy filter.

(3) Momentum Filters—The ions emerging from the energy filter all have the same kinetic energy, but ions of different masses will have different momenta. To focus ions of same mass, the beam emerging from the exist slit of the energy filter is passed through a sectorial magnetic field. For the optimum space focusing the entrance slit S_1, the apex O of the boundaries of the magnet and the exist slit S_2 all must lie on the same straight line, Fig. 1.15. Ions entering the magnetic field of flux density B follow a circular path with centre O, radius R_m and normal to the magnetic field.

$$\therefore \qquad Bnev = Mv^2/R_m \text{ or } Mv = B\,R_m\,ne. \qquad ...(49)$$

The central ray leaves the magnetic field normal to the field boundary. The particles of the same momentum, but making an angle ± α with the central ray, are brought to focus at A which lies closer to O than the point B where the central ray crosses the straight line $S_1\,OS_2$. Here we see that this device has a dispersion characteristic also. It is a momentum dispersion if ions of various masses are considered. The dotted line in figure shows the trajectory of a central ray particle having slightly greater momentum.

For the rays having the same momentum, the lateral spread (*aberration*) is the distance between A and B along the width of slit S_2 and from the simple geometry of the Fig. 1.15 can be written as

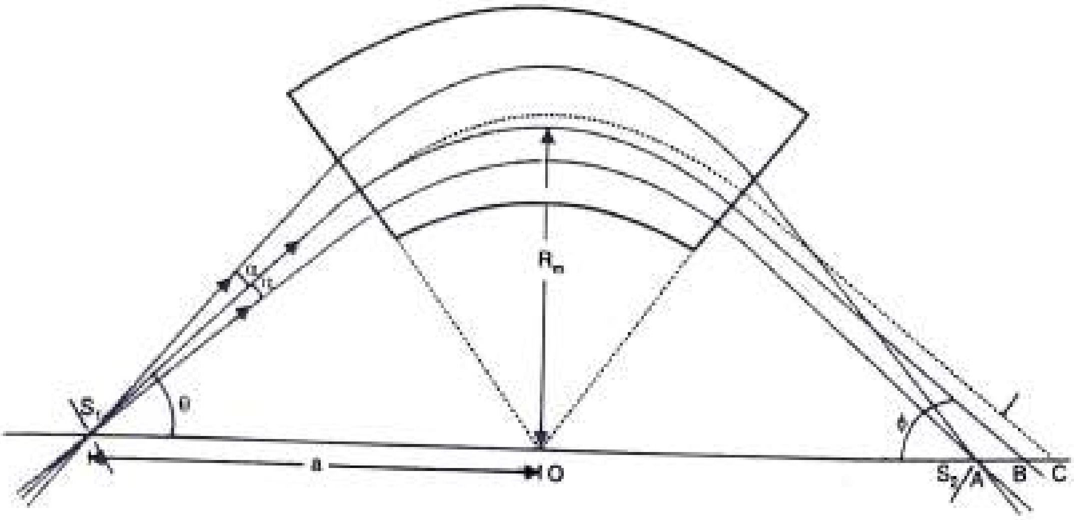

Fig. 1.15. Momentum filter.

$$S = \frac{a\alpha^2}{2}\left(\frac{\sin^2\theta}{\sin\phi} + \frac{\sin^2\phi}{\sin\theta}\right). \qquad \ldots(50)$$

where $a = S_1O$ and θ and ϕ are the angles which the central ray makes with the line S_1OS_2 before and after emerging the magnetic field respectively. For a symmetrical sector type magnet $\theta = \phi$ and we have

$$S = a\alpha^2 \sin\theta = \alpha^2 R_m. \qquad \ldots(51)$$

If we consider the initial central ray as made up of two momenta groups say Mv and $Mv + \Delta\,(Mv)$. These rays do not fall at the same point. The lateral velocity dispersion is the distance along the width of the slit S_2 corresponding to the distance between B and C, the points where the central ray joins the line S_1OS_2, is given by

$$D = a\frac{\Delta(Mv)}{Mv}\left(\frac{\sin\theta}{\sin\phi}\right)(\sin\theta + \sin\phi). \qquad \ldots(52)$$

For a symmetrical sector type of magnet, we have

$$D = 2(a\sin\theta)\,\Delta(Mv)/Mv = 2R_m\,\Delta(Mv)/Mv.$$

Relations (51) and (52) show that S and D are independent of magnet angle and vary directly as R_m.

If the charged particle passes through a sector magnet or electrostatic deflector with central radius R_0 and deflection angle ϕ, its motion inside the field can be written as

$$y = y_0 \sin(kx + \alpha),$$

where k is the wave number for median plane focussing. k for magnetic and electrostatic sectors can be given by the relations

$$k_m = \sqrt{1-n}\,/\,R_0 \text{ and } k_e = \sqrt{2}\,/\,R_0. \qquad \ldots(53)$$

where n is regarded as a constant.

If the object is at a distance d_0 on the left and the image is at a distance d_i on the right of the sector (magnetic or electrostatic), and the origin is assumed at the left end of the sector, then at

$$x = 0,\ y = d_0\,(dy/dx).$$

$$\therefore \qquad \tan\alpha = kd_0. \qquad \ldots(54)$$

At the exit boundary of the sector, we have

$$y = -d_i\,(dy/dx) \text{ at } x = R_0\phi.$$

$$\therefore \qquad \tan(k\,R_0\phi + \alpha) = -kd_i. \qquad \ldots(55)$$

Combining Eqns (54) and (55), we get

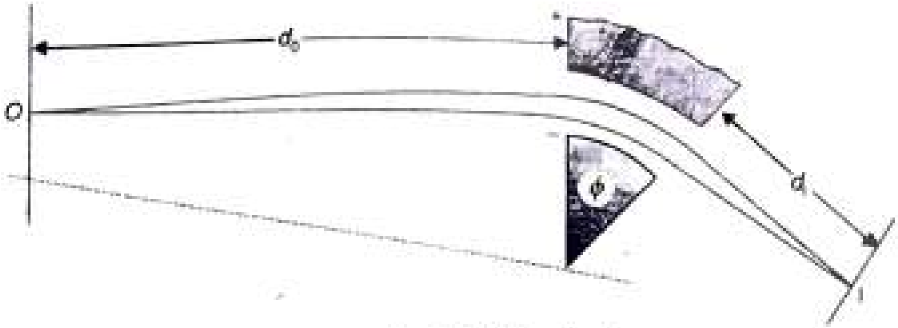

Fig. 1.16. Generalized cylinderical condenser.

$$\frac{1}{d_0+h}+\frac{1}{d_i+h} = \frac{1}{f}, \qquad \text{...(56)}$$

where $$h = \frac{\tan(kR_0\phi/2)}{k} \text{ and } f = \frac{1}{k\sin kR_0\phi}.$$

Eq. (56) shows that the electric or magnetic sector acts as a lens with principal planes located at a distance h from the ends and with focal length f.

For a very narrow sector $\phi \to 0$ and $h \to 0$, hence Eq. (56) reduces to

$$1/d_0 + 1/d_i = 1/f. \qquad \text{...(57)}$$

This is same as lens formula for thin lenses.

Thus we see the exact analogy between the motion of ions in electric and magnetic fields and the behaviour of light in lenses and prisms. Each of the sectors of Figs. 1.15 and 1.16 behaves like a combination of a cylinderical lens (for focusing) and a prism (for dispersion).

(4) Velocity Filters—If electrostatic and magnetic fields are simultaneously applied ⊥ to each other and adjusted such that the force due to one is balanced by the force due to other, then we have

$$neE = Bnev \text{ or } v = E/B. \qquad \text{...(58)}$$

Thus the outgoing particles have same velocity irrespective of their masses and charges.

(5) Angular Velocity Filter—When a charged particle moves in a normal uniform magnetic field B along the circular path of radius R, its angular velocity is given by

$$\omega = v/R = Bne/M. \qquad \text{...(59)}$$

The particles of same specific charge ne/M will thus traverse circular paths in the same period of time. This is the well known relation for the cyclotron resonance frequency. The cyclotron may thus be used as a mass spectrometer. The same has been used by Alvarez and Corneg (1939) for proving the existence of the stable isotope ^3He in atmospheric and commercial helium.

(B) **Double-focusing Mass Spectrograph**—F.W. Aston 1919, first introduced the idea of velocity focusing in a mass spectrograph. His first instrument could separate isotopes with a mass difference of about 1%. During the period 1935-1940, several instruments were designed using directional focusing as well as velocity focusing (*i.e.*, double focusing), which had much better resolving power and accuracy both.

(a) Mattauch Mass Spectrograph—Mattauch in 1936 built a double focusing instrument, shown in Fig. 1.17. A very large mass spectrum can be recorded on the photographic plate simultaneously. This instrument has 31°50′ electric deflection, followed by 90° magnetic deflection. The object slit is so placed with respect to the electrostatic deflector and the pd applied to it is so chosen that the ions emerge in parallel beams from the sector. The direction of the emerging beam varies with the ion-speed, this sector is thus a collimater with a speed dispersion characteristic. The wide slit accepts a certain part of the beam and the magnetic field focuses the parallel beam on a photographic plate, placed in the magnetic field. The radius of curvature and angular deflection in the magnetic field are designed to give a velocity dispersion of focal length which

exactly cancels that of the electrostatic deflector. Thus both direction and velocity focusing can occur. For the central ray, both the conditions ($Ee = Mv^2/R_e$, and $Mv = BeR_m$) must apply simultaneously. For a charge ne, we get

$$M = B^2R_m^2ne/ER_e = B^2R_m^2ned/VR_e, \qquad \ldots(60)$$

where V is the potential difference between the two plates, separated by a distance d, of the electrostatic sector. Putting $x + x_0 = R_m\sqrt{(2)}$, gives

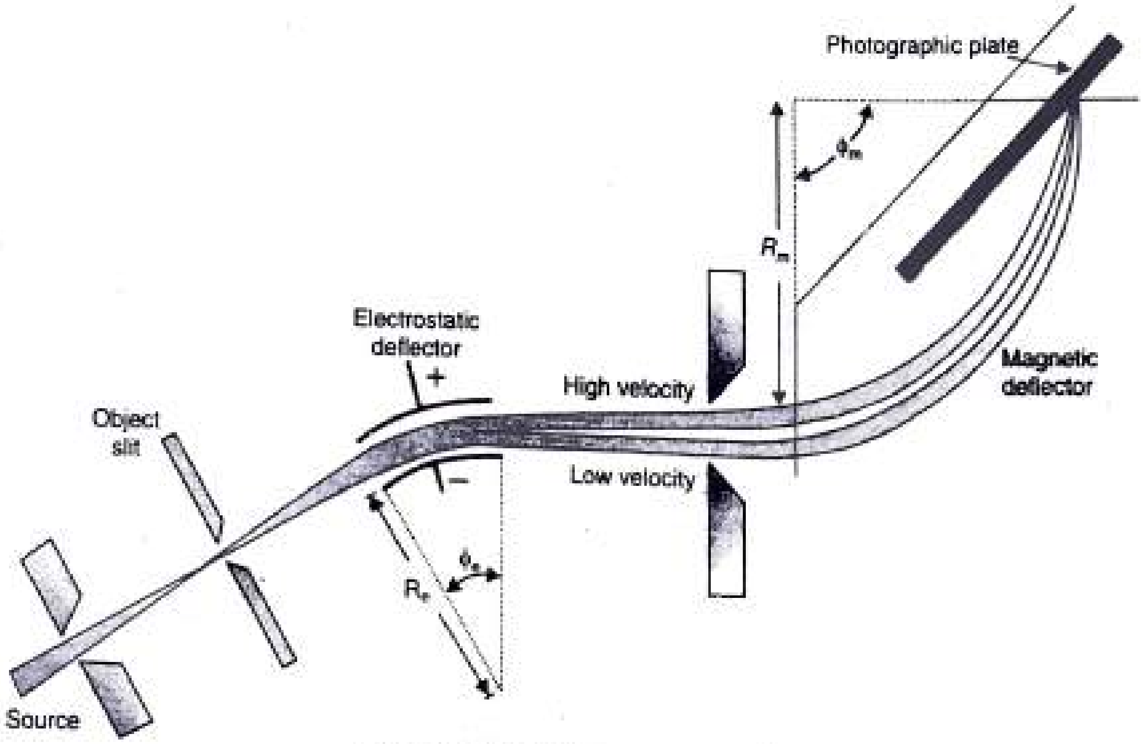

Fig. 1.17. Mattauch mass spectrograph.

$$M = B^2ne\,d\,(x + x_0)^2/2VR_e. \qquad \ldots(61)$$

Here x is the distance along the plate from a fiduciary mark, x_0 is the distance of this mark from the point at which the central ray enters the magnetic field. The dispersion coefficient can be measured empirically for various regions of the plate by recording the spectra of a sequence of ions whose mass differences are known. This instrument is double focusing for all masses and a very large mass spectrum can be recorded on the photographic plate simultaneously.

(b) Bainbridge and Jordan Mass-Spectrograph—It is one of the best double focusing mass spectrographs, called after the name of inventors K.T. Bainbridge and E.B. Jordan who invented it in 1936. It is the modified and improved form of Bainbridge spectrograph in which only the velocity focusing is used. The systematic diagram, illustrating the main components of the instrument is shown in Fig. 1.18. When the 127°-electrostatic analyzer is employed, the resulting velocity dispersion can be just annulled by a momentum filter if the total magnetic sector angle is 60°. The stray field at the edge of the magnet can be corrected by cutting the edges of the poles by about 1.6 gap widths. These two filters have been so arranged that the combination possesses the further advantage of linear mass scale.

Ions are produced in a high voltage (20 kV) low current discharge tube with a fairly broad energy spread. They emerge into a cylindrical electrostatic energy filter . maintained at a good high vacuum pressure 10^{-6} mm of Hg. It consists of a pair of cylindrical plates of radius of curvature 25 cm. The ions emerging from the energy filter E are then analysed by the magnetic filter M into different mass species. Each component is focused as a line trace on the photographic plate P. The exist slit of the energy filter, the apex of the magnet and the photographic plate P are collinear.

After an exposure to the ion beam the plate is developed and the positions of lines on the plate are observed with a traveling microscope. By measuring ΔM, the width of the spectral line produced on the plate by ions of mass M, the mass resolving power δ (= $M/\Delta M$) of the mass spectrograph can be calculated. The Bainbridge-Jordan instrument, with R approximately equal to 25 cm for each filter, has a resolving power of the order of 10^4. This corresponds to the separation on the photographic plate of about 5 mm between spectral lines produced by ions differing in mass by 1 per cent.

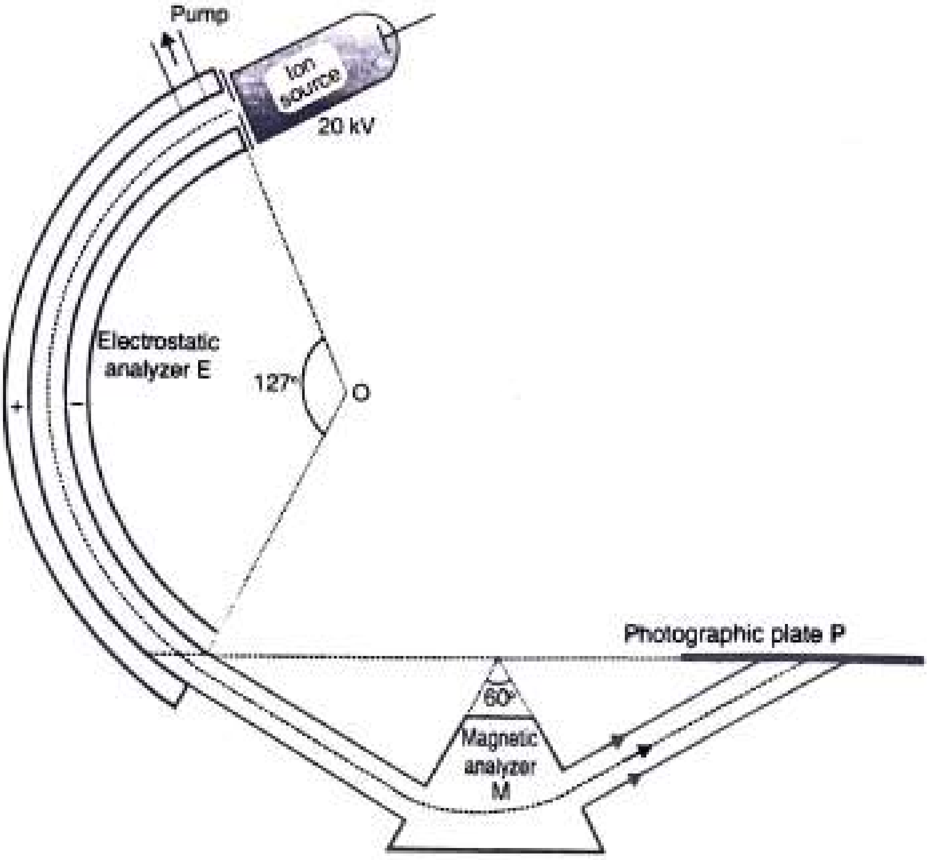

Fig. 1.18. Bainbridge and Jordan mass spectrograph.

This instrument can measure atomic masses very accurately as it has following advantages :

(i) The mass displacement scale across the photographic plate is very nearly linear; *(ii)* No attempt is made to deduce the mass of an ion from the electron optics of the spectrograph; *(iii)* The position of one spectral line is carefully compared with the positions of known mass reference lines; *(iv)* Once the dispersion factor $\Delta M/\Delta x$ across the detector is known, M is determined from the measurement of the line spacing Δx; *(v)* It has a resolving power of the order of 10^4 and *(vi)* The simultaneous focusing of velocity and direction enables the use of beams diverging in direction to a much greater extent than possible in the other type of apparatuses and results in higher intensities.

Because of the limited and nonlinear contrast scale of a photographic emulsion, this instrument is less desirable for the measurement of isotopic abundance ratios.

(C) Double-focusing Mass Spectrometer—During sixties, mass spectrometry has advanced rapidly. One of the most useful instruments was that of A.O. Nier and T.R. Roberts, designed in 1951 at the University of Minnesota. It has extremely high resolving power and sensitivity and is especially designed for searching rare isotopes and measuring relative abundances. It now can measure masses to an accuracy of about one part in a million. The accuracy is increased by increasing the size of the apparatus and by using an ingenious form of electrical recording.

Positive ions are formed in the ion source by the electron bombardment of the gas under investigation. The ions are accelerated through a potential difference of 40 *kV* and are focused on the fine slit S_1, which is about 0.0008 cm wide. This acceleration is equivalent to an energy filter of the type shown in Fig. 1.13. The second slit S_2, 0.02 cm wide limits the angular divergence of the ion beam entering the 90° electrostatic energy filter. The energy filter has a pair of cylindrical plates placed 2 cm apart with a radius of curvature of the order of 50 cm. A symmetric potential of the order of 3 *kV* is applied to the plates. This filter will deflect and focus the ions in such a way that ions of the same energy will converge toward the same point on the slit S_3 (0.4 cm wide). The ions are again directionally focused by the magnetic filter such that ions of the same momentum passing through the same point at S_3 will converge toward a point at slit S_4 (0.0008 cm wide). The dimensions of the filters and the slit distances are chosen so that the second velocity dispersion cancels the first but the total mass dispersion is non zero. A mass spectrum is therefore produced at S_4. The lateral position of the impact of a given ion at S_4 is dependent only on the mass of the ion and practically independent of velocity and the direction of the ion through slit S_1. Equations (48) and (49) show that the only ions which can be transmitted successively through both filters must have the specific charge

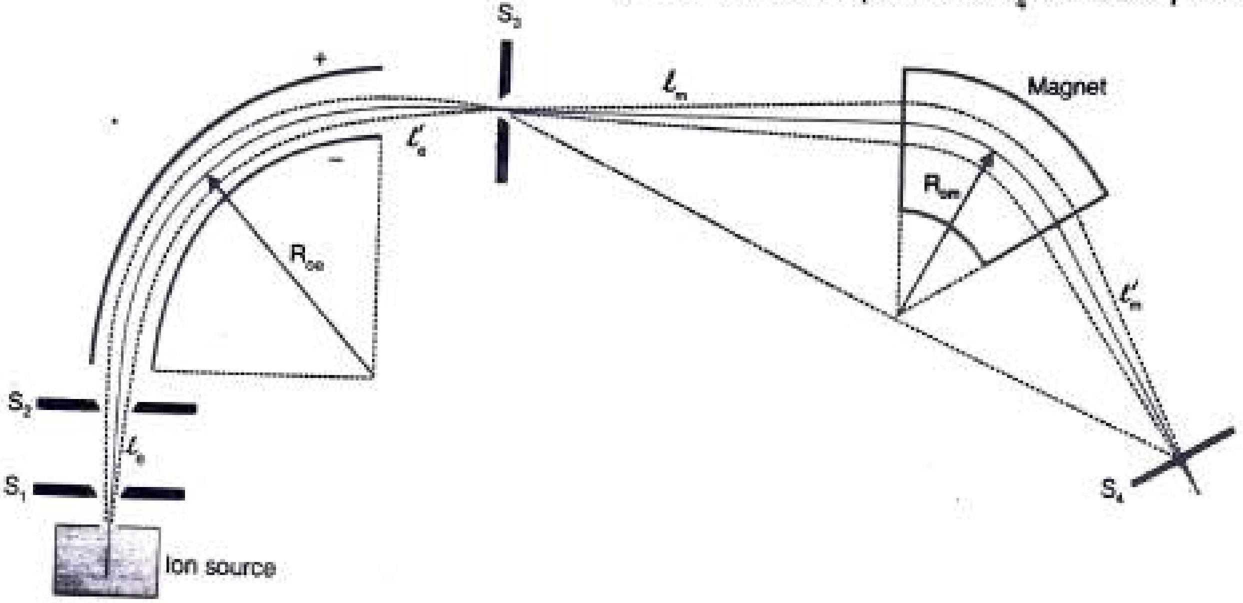

Fig. 1.19. Nier and Robert's Mass Spectrometer.

$$\frac{ne}{M} = \frac{R_e V/d}{R_m^2 B^2} = K.\frac{V}{B^2}, \qquad \ldots(62)$$

where *K* is a constant for any particular slit arrangement.

The mass spectrum of descrete values of *ne/M* can therefore be obtained by changing *V*, or *B*, or both. In order to avoid uncertainties due to hysteresis in the magnet, generally *B* is kept constant and mass spectrum is obtained by varying the potential applied to the electrostatic filter. Simultaneously the accelerating potential at the ion source exit is varied proportionately. Both potentials being obtained from a common potential divider. The transmitted ion current will generally be in the domain of 10^{-12} amp or less and can be measured accurately with an electrometer or an electron multiplier tube. The isotope abundances are closely proportional to the magnitude of the peaks of the positive ion current.

The electrostatic deflector is a sector of a cylinderical capacitor. The central ray of the diverging beam enters and leaves the magnetic sector normal to the field boundary. Calculations for electrostatic or magnetic sector deflector indicate that a beam diverging from a point at a distance *l* from the field boundary converges at point at a distance *l′* from the exit field boundary. These distances are related as

$$\frac{1}{l+(1/k)\tan(kR_0\phi/2)} + \frac{1}{l'+(1/k)\tan(kR_0\phi/2)} = k\sin kR_0\phi, \qquad \ldots(63)$$

where ϕ is the sector angle, R_0 is the orbit radius for the central ray, the wave number $k = \sqrt{2}/R_0$ for electrostatic deflector and $k = 1/R_0$ for magnetic deflector. This equation is similar to the optical lens equation $1/v + 1/u = 1/f$. The comparison shows that the focal length f of the device is equal to

$$f = 1/k \sin kR_0\phi. \qquad \text{...(64)}$$

Numerical parameters for the Nier and Robert's spectrometer

$$\phi_e = 90^\circ \qquad \phi_m = 60^\circ$$
$$R_{0e} = 18.87\ cm. \qquad R_{0m} = 15.24\ cm.$$
$$l_e = l'_e = 6.61\ cm. \qquad l_m = 34.77\ cm, l_m' = 20.73\ cm.$$

satisfy the lens equation for both sectors. It shows that particles diverging from slit S_1 will be directionally focused on slit S_3 by the electrostatic lens and then again directionally focused on slit S_4 by the magnetic lens. Thus we see that particles of different velocities will be focused from slit S_1 to slit S_4. It can be shown that the total magnetic dispersion of this spectrometer is given by the relation

$$D(M) = 0.133\ (\Delta M/M)\ \text{meter}.$$

As the width of slit S_4 is 0.0008 cm, hence the maximum possible value of dispersion which can be detected will be 0.0008 cm.

Thus resolving power of this spectrometer is given by

$$R.P. = (\Delta M/M) = D(M)/0.133 = 8 \times 10^{-6}/0.133 = 6 \times 10^{-5}. \qquad \text{...(65)}$$

(D) Doublet Method of Mass Spectroscopy—Atomic masses are now measured by chemists as well as by physicists on a new scale. The symbol for this new unified mass unit is m_u or u only which is equal to the twelfth part of the mass of the ^{12}C atom, whereas the symbol for the earlier unit based on the ^{16}O scale was *amu*. The mass of any ion can be calculated by calibrating first the mass spectroscope with ^{12}C ion. Although the mass spectroscopes discussed upto this time have a very good resolution. For a much higher accuracy *doublet method* is used. In this method a very small difference between two masses which have about the same intensity and the same integral value of ne/M is obtained. In the mass spectroscope both ions are produced simultaneously in the ion source and are focused as two nearly lines on the plate.

A number of important fundamental mass doublets are of great practical value. For example, consider the three doublet measurement.

$$M/ne = 16 : (^{12}C^1H_4)^+ — (^{16}O)^+ = a = 36381.5 \pm 0.9\ \mu u$$
$$M/ne = 48 : (^{12}C_4)^+ — (^{32}S^{16}O)^+ = b = 33016.4 \pm 1.3\ \mu u$$
$$M/ne = 32 : (^{16}O_2)^+ — (^{32}S)^+ = c = 17754.3 \pm 0.9\ \mu u.$$

Solving these equations and substituting the mass value $^{12}C = 12$, we obtain the masses of the three unknowns :

$$^1H = 1 + \tfrac{1}{12}(3a + c - b) = 1.0078235\,u$$
$$^{16}O = 16 - \tfrac{1}{3}(b - c) = 15.9949126\ u$$
$$^{32}S = 32 - \tfrac{1}{3}(c + 2b) = 31.9720719\,u$$

Similarly by the study of following doublet the masses of ^1H, ^2H and ^{16}O can be determined with reference to $^{12}C = 12$.

$$M/ne = 2 : (^1H_2)^+ - (^2H_1)^+ = a = 1.54825 \pm 0.001\ m\,u$$
$$M/ne = 6 : (^2H_3)^+ - (^{12}C_1)^{++} = b = 42.3065 \pm 0.004\ m\,u$$
$$M/ne = 16 : (^{12}C_1^1H_4)^+ - (^{16}O_1)^+ = c = 36.38594 \pm 0.0002\,m\,u.$$

Solving these relations, we get

$$^1H = 1 + \tfrac{1}{6}(3a + b) = 1.0078252\,u$$
$$^2H = 2 + (b/3) = 2.0141022\ u$$
$$^{16}O = 16 - \tfrac{1}{3}(3c - 2b - 6a) = 15.9949149\,u.$$

According to the theory of error the total error or uncertainty is equal to the square root of the sum of the squares of the combinations of the individual measurements. This gives the uncertainty in the mass of ^{16}O as.

$$= \frac{1}{3}\sqrt{[(6\Delta a)^2 + (2\Delta b)^2 + (3\Delta c)^2]} = 3.34\,\mu u.$$

In this way, the masses ^1H, ^2H, ^{16}O, ^{32}S have been determined with sufficient accuracy to warrant their use as secondary standard of mass.

The masses of heavy nuclei may be measured by comparing multiply charged ions of the heavy elements with singly charged light ions, since both will have same value of M/ne. Dempster used doublet $(^{16}O)^+ - (^{48}Ti)^{+++}$ and $(^{50}Ti)^+ - (^{197}Au)^{++++}$. In the Nier spectrometer, two nearby mass lines are brought to focus to the detector slit in rapid succession by changing accelerating potential and the potential on the electrostatic filter simultaneously. In this instrument the output from the detector is displayed on an oscilloscope so that the two lines can be visually compared. A typical example of a mass doublet measured with Nier spectrometer is

$$C_{12}H_{16} - {}^{160}Gd = 198.05 \pm 0.09\ m\,u.$$

Using the number obtained for the hydrogen mass we get for the mass of gadolinium :

$$Gd^{160} = 144 + 16 \times 1.0078235 - 0.19805 = 159.92713\ u.$$

Nier used an ingenious form of electrical recording in which the mass spectra of the components of a doublet are superimposed on the screen of a C.R.O. It is done by adjusting the resistance. When two doublet peaks are superimposed the mass difference ΔM is obtained in terms of resistances and the mass of the lighter component.

One source of confusion in mass spectroscopy is connected with the existence of the ^{13}C atom. One can obtain a molecule of the same mass number by replacing a ^{12}C atom and a hydrogen atom with a ^{13}C atom in a hydro-carbon molecule. At high mass numbers, these two ions are so close in mass that they are very hard to resolve. Now-a-days we have mass spectrometers with a resolving power sufficiently high to separate the ^{13}C atom from the main peak.

Professor Nier's group and others have also improved the technique to use the mass spectrometer for determining the mass differences between isotopes of the same element. Since the difference of the masses are of the order of one mass unit or more, therefore the accuracy obtained in these measurements is not so high as for the true mass doublets. In the case of Zr-isotopes

$$^{92}Zr - {}^{91}Zr = 0.9993972u \pm 11.7\ \mu\,u.$$

(E) **Mass Synchrometer**—Goudsmit in 1948 has suggested a novel type of mass spectroscope based upon two facts :—

(a) An ion projected normally in a uniform magnetic field will move in a circle. (b) The time of revolution ($T = 2\pi M/neB$) *is independent of the speed of the ion and for a given charge it depends only upon the mass.* The period of the revolution and hence the mass can be measured by pulsing the ion source and noting the elapsed time until the ions reach the detector. The time of flight method depends also on the fact that the direction focusing takes place for a 360° deflection. The ion source and the detector cannot occupy the same position. If direction of magnetic field is vertical, then it is necessary to place one on top of the other. The ions then travel in helixes. In the original instrument, the ions were emitted in pulses from an ion source and the flight time for certain number of spirals was measured electronically.

L.G. Smith and coworkers in 1956 has modified and improved the above mentioned instrument. The principle of operation is different in that a multiple of the cyclotron frequency is measured rather than the flight time. This spectrometer employs electrical recording with the mass doublet components brought into sharp coincidence on an oscilloscope screen. In this case frequency is the circuit parameter which is adjusted to produce synchronism rather than the resistance.

Schematic diagram of the mass synchrometer is shown in Fig. 1.20. Ions are produced in the ion source by electron bombardment of the gas to be ionized. After acceleration the ions pass through the narrow slit S_1 with a kinetic energy of 25 keV. A uniform magnetic field of flux density B (0 to 0.7 Tesla) acting ⊥ to the plane of the figure, deflects the ions into a circular trajectory. The ions with a selected momentum $mv = ne\,BR$ will pass through slit S_2, S_3 and S_4. The two outer slits S_2 and S_4 are earthed and a radiofrequency alternating potential is applied to this modulator slit S_3, where the ions are given an impulse by radiofrequency potential. The sign and magnitude of the impulse depend on the phase of the oscillations of the electric field at the moment the ions pass. The ions receiving *a + ve* impulse travel with a larger radius of curvature and arrive at S_1 with *a + ve* displacement. Other ions receiving *a – ve* impulse travel with a smaller radius of curvature and arrive at S_1 with *a* – ve displacement. If the phase of radiofrequency field is such that ions entering modulator slit S_3 receive *a – ve* impulse of right amount to enable these ions to pass through the fine slit S_5. After a further half revolution they again enter the modulator slit system and again experience another change in momentum. If the frequency of oscillation of the r.f. voltage at position S_3 is a multiple of the cyclotron frequency ($f_c = neB/2\pi M$) of the ions, the ions receive the same impulse as the first time ($\Delta_2 = \Delta_1$). After a third passage through the modulator slit the ions again have received the same reduction in momentum and after another one half turn enter the detector, Faraday cup, mounted behind the slit S_7.

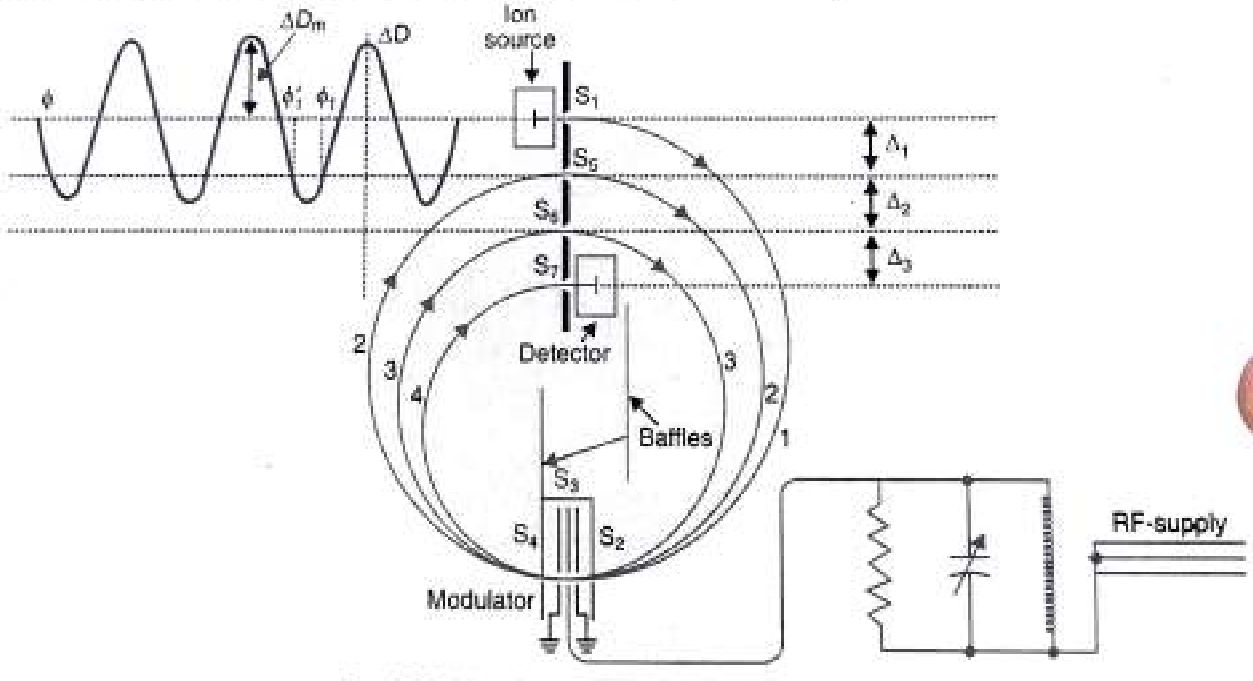

Fig. 1.20. Mass Synchrometer (Schematic diagram).

The frequency of r.f. voltage at S_3 is an integer multiple of f_c, *i.e.*, $f_0 = nf_c$. In a typical mass determination we have $f_0 \sim 15 Mc/s$ for $n \sim 100$. On account of this large value of n a slight change in the cyclotron frequency of the ion will be detected as a comparatively large change in phase. As $f_c \propto 1/M$, hence an ion having mass slightly different from the resonant mass will fall out of phase and be stopped by either slit S_6 or S_7. In this way we can use the instrument as a spectrometer. The diameter of the outer ion orbit is 11 inches and of last orbit is about 9 inches.

The difference in mass ΔM of the component of a doublet is determined in terms of the frequency difference Δf of the signal required to superimpose the signal peaks on the screen of an oscilloscope. An alternating voltage of resonant frequency f (for one of the doublet components) is applied to the modulator slits. The other doublet component corresponding to the resonant frequency $f + \Delta f$ is displayed on the other alternate sweeps of the saw tooth (sinusoidal) voltage. The resonant frequency difference Δf of two mass components is determined with the help of stable variable audio frequency oscillator. This oscillator can be set at any frequency between 20 and 20,000 *c/s*. It locks the frequency difference of two r.f. oscillators at a frequency Δf equal to the frequency of the audio oscillator. The outputs of the two r.f. oscillators are fed alternately to a mixer, which is fed also with the output of a thrid r.f. oscillator. The output signal from the mixer is alternately of frequency f and frequency $f + \Delta f$. After passing through frequency multiplier the output the is applied to the modulator slits.

After knowing the value of Δf, the ΔM is obtained by either of the relations

$$\frac{\Delta f}{f_2} = \frac{\Delta M}{M_1}, \frac{\Delta f}{f_1} = \frac{\Delta M}{M_2}, \qquad \ldots(66)$$

where f_1 corresponds to the resonant frequency of ions of mass M_1 and similarly for f_2 and M_2.

The mass synchrometer is capable of covering a range of mass number from 2 to 250. Its resolving power is about 1 part in 20,000 and a few tenths of a micromass unit can be claimed by using doublet method.

1.5 THEORIES OF NUCLEAR COMPOSITION

Rutherford's nuclear theory based on the scattering of α-particles suggested the nucleus to be of compact structure. Natural radio-activity suggested that though the nucleus is compact, it is capable of emitting several particles, *e.g.*, α-and β-particles and γ-rays. The study of α-and γ-ray spectra suggested discrete levels in the nucleus, while β-ray spectrum suggested a new particle neutrino. Researches in artificial transmutation of elements show that α-particles, p, n, e^- and e^+ are present in the nucleus some how or the other. Cosmic rays studies predict us another particle 'meson' inside it. Some of the well established properties of atomic nuclei are :

(i) All nuclei are positively charged and the magnitude of the electric charge is an integral multiple (Z) of the proton charge e.

(ii) More than 99.9 per cent of the mass of an atom is concentrated inside the tiny volume of the nucleus.

(iii) Nuclei are spherical or nearly spherical in shape having radius R given by $R = R_0 A^{1/3}$.

(iv) The striking correlation between R and A suggests that there is a universal density for nuclear matter.

$$\text{Density } \rho = \frac{\text{Mass}}{\text{Volume}} = \frac{A \times 1.66 \times 10^{-27}}{\frac{4}{3}\pi (1.2 \times 10^{-15})^3 A} = 10^{17} \text{ kg/meter}^3.$$

$$\therefore \qquad \text{Number of nucleons/c.c.} = \frac{\text{Density}}{\text{Mass of a nucleon}} = \frac{10^{17}}{1.66 \times 10^{-27}} = 10^{44} \text{ nucleons/meter}^3.$$

(v) The nucleus is a tightly bound system of the nucleons with a large potential energy.

Several theories of nuclear composition were put forward.

1. Proton-Electron Theory. Prout suggested that all atomic weights were whole numbers and hence could be assumed as the integral multiple of the atomic weight of hydrogen. The slight change from the whole number was explained by the presence of two or more isotopes. This hydrogen theory confirmed the presence of protons inside the atom. Since electrons were known to be emitted from some nuclei, it was natural to believe in the beginning that the electrons were the constituents of all nuclei. To account for the mass of the nucleus whose atomic weight was nearly equal to the integer A, it was necessary to assume that nucleus would consist A protons. But if this was the case the charge on the nucleus would be A, not equal to the atomic number Z. To remove this difficulty it was assumed that in addition to A protons the atomic nuclei would contain $(A - Z)$ electrons. These would contribute a negligible amount to the mass of nucleus but would make the charge $+ Z$ as required.

This theory could explain the emission of α-and β-particles. Presence of electrons in the nucleus showed that under the appropriate condition, β-particle or electron might be ejected and two electrons could combine with four protons to form α-particle before emitting. This theory led to a number of contradictions with experiments. Few of them are given below :

(a) Finite size—Since electrons are the spherical charges of finite dimensions, hence for the heavy nucleus it is difficult to have several electrons inside.

(b) Spin consideration—As electron and proton each has spin $\frac{1}{2}(h/2\pi)$, hence the nucleus must have integral spin if it contains an even number and half integral spin if it contains an odd number of particles (protons + electrons) in the nucleus. But experimentally it has been found that spin depends on the mass number A of the nucleus and is zero or an integer for A even and is an odd half integral for A odd. The band

spectra of $^{14}_{7}N$ gave the value of nuclear angular momentum I as 1, which showed that this nucleus must contain odd number $(2A - Z)$ of fermions and thus contradicted the proton-electron theory.

(c) Statistics—From band spectra and Raman spectra the statistics of the $^{14}_{7}N$ was found to be Bose Einstein. This was in disagreement with the proton-electron theory which suggested Fermi-Dirac statistics for $(2A - Z)$ odd fermions in $^{14}_{7}N$.

(d) Magnetic moment consideration—Since the nucleus is electrically charged and the rotation of charged particles gives rise to a magnetic moment. The magnetic moment $(eh/4\pi m)$ of a proton is nearly 1837 times less than that of an electron. The magnetic moments of all nuclei are small in comparison with the magnetic moment of an electron. This shows that electron is not the constituent of the nucleus.

(e) Wave mechanical consideration—According to the Heisenberg's uncertainty principle $\Delta x . \Delta p \sim \hbar$. Suppose that the principle is applied to an electron in the nucleus. The uncertainty in position $\Delta x = 10^{-14} m$, as an electron is confined to a sphere of diameter $10^{-14} m$. Thus the uncertainty in the momentum

$$\Delta p \sim 10^{-34}/10^{-14} (= 10^{-20} \text{ Joule sec/meter}).$$

It is now assumed that the momentum p of the electron is same as just found for the uncertainty Δp. Hence total energy of the electron is given by

$$E^2 = p^2c^2 + m_0^2c^4 = 9 \times 10^{-24} + 6.72 \times 10^{-27}$$

or

$$E \sim 3 \times 10^{-12} \text{ joule or } 18.7\ MeV.$$

According to this result a free electron confined within the nucleus would have a K.E. of the order of 19 *MeV*. Further experimentally, electrons emitted by radioactive nuclei have never been found to have kinetic energies greater than about 4 *MeV*. This large discrepancy show that nuclei cannot contain free electrons.

(f) Compton wavelength—Several theoretical considerations suggest that a bound fundamental particle cannot be localised in the region smaller than its Compton wavelength λ_C $(= h/mc)$.

Compton wavelength of electron $= 6.626 \times 10^{-34}/9.1094 \times 10^{-31} \times 3 \times 10^{8} = 242 \times 10^{-14} m \sim 250$ (*Nuclear diameter*).

This excludes the possibility of keeping the electrons inside the nucleus.

(g) β-decay—The dual β-decay (β^- & β^+) exhibited in many nuclides could not be explained with this theory. The annihilation, would occur if e^- and e^+ were inside the nucleus.

(h) Electron-neutrino pairs—Fermi's interpretation of β-decay in terms of the emission of an electron neutrino-pair can not be explained with electron-proton theory.

2. Proton-Neutron Theory—The experimental discovery of the neutron led Heisenberg in 1932 to suggest that the nuclei might be composed of protons and neutrons rather than of protons and electrons. Thus for an atom $^{A}_{Z}X$, the nucleus contains Z protons and $(A - Z)$ neutrons. The total number of particles inside the nucleus $= A$, the atomic number. This nucleus is surrounded by Z electrons to make the atom electrically neutral. This theory avoids the failure of proton-electron theory.

(a) Finite Size—As the neutrons have nearly the same mass as that of protons and total number of nucleons are same as that of atomic number, hence the nucleus can have neutrons in it.

(b) Spin Consideration—As both the proton and neutron have same spin quantum number $\frac{1}{2}$. Hence according to the quantum theory, the resultant spin of A nucleons will be an integral or half integral multiple of $h/2\pi$ according as A is even or odd. This is in agreement with all the experimental observations.

(c) Statistics—As the neutrons and protons are both fermions with spin $\frac{1}{2}$, their combination will agree with observations.

(d) Magnetic Moment Consideration—The values for both the proton and neutron are consistent with those measured for many different nuclei.

(e) Wave Mechanical Consideration—It is assumed, as in the case of the electron, that the momentum is of the order of uncertainty in the momentum $\sim (h/\Delta x)$. Hence the total energy of the proton is given by

$$E^2 = p^2c^2 + m^2c^4 = (10^{-20})^2 \times (3 \times 10^8)^2 + (1.6726 \times 10^{-27})^2 (3 \times 10^8)^4$$

or

$$E = 940\ MeV.$$

This value is slightly greater than rest enery of proton which is 938 *MeV*. Hence the K.E. of neutron or proton in the nucleus is of the order of few *MeV* and it should be possible for a free neutron or proton to be contained in the nucleus.

(f) Compton Wavelength—Compton wavelength of neutron is given by

$$\lambda_C = h/mc = 6.626 \times 10^{34}/1.67 \times 10^{-27} \times 3 \times 10^8 = 0.14 \text{ (Nuclear diameter)}.$$

Thus the protons and neutrons can be squarized into nuclear volume.

(g) β-decay—The β-ray emission from some nuclei can be suggested as follows : The electron does not pre-exist in the nucleus but is formed at the time of emission as indicated by the equation

$$n \to p + e^- + \bar{\nu}.$$

β^+—decay is due to the reaction $p \to n + e^+ + \nu$.

(h) Nuclear Reactions—Many nuclear reactions, *e.g.*, (p, γ), (γ, p), (n, γ), (γ, n), (p, n), involve only the addition or subtraction of one proton or one neutron or an interchange of proton and neutron. The interpretation of these reactions require neutron-proton model of nuclear constitution.

(i) Pions—The binding forces between nucleons are due to the exchange of π-mesons between protons and neutrons. The nuclear multiple moments of the nuclei are very well explained with the help of mesonic current in nuclei.

3. Neutron-Positron Theory—Jean Parrin proposed neutron-positron theory by saying that atomic nuclei were built up with neutron and positron only. Though this theory goes deeper into the structure of atomic nuclei, still met with the same difficulties with which proton-electron theory came across. The positron emission is likewise due to the converse process

$$p \to n + e^+.$$

4. Anti Proton-Neutron—This theory has been suggested by Gamow, Klin, etc. It can be shown that the relation between the negative protons and ordinary protons is not quite analogous to that between positrons and electrons in Dirac's theory. When a neutron transforms itself into antiproton, a positron will be emitted ($n \to p^- + e^+$). A antiproton may be conceived to be formed by a neutron and electron ($p^- \to n + e^-$). Antiproton like positrons, can not exist free for long with in the ordinary material as they will be immediately attracted and absorbed by nearest + vely charged nucleus. A energy of over 4000 *MeV* would be required to create a pair of proton and antiproton.

At last we may say that the neutron-proton model is still the accepted one.

1.6 BINDING ENERGY

It might at first be supposed that the mass of an atom should be the sum of the masses of its constituent particles, *i.e.*, electrons, protons and neutrons. But the mass of any permanently stable atom is found to be less than the sum of the masses of its constituents. Aston called the decrease in the mass or loss of mass upon coalescence of the elementary constituents the *mass defect*, now generally called *mass deficiency*. This can be explained as under :

The nucleons that hold the stable nucleus are held together by strong attractive forces, and therefore work must be done in separating them from each other until they are very large distance apart. In other words *energy must be supplied to the nucleus to separate it into the individual constituents*, and the total energy of the constituents when at a very large distance apart is greater than when they form the nucleus. For convenience the masses of atoms rather than the masses of nuclei are used in all calculations. This causes no difficulty, except that the binding energy of the atomic electrons should also be considered. For simplicity, we usually omit it. The principle of equivalence of mass and energy confirms the idea that the amount of energy required to break up the atom into its constituents is equivalent to the *mass deficiency*. It can also be defined as the amount of mass which would be converted into energy if a particular atom is to be assembled from its constituents. The energy equivalent of mass difference or mass *deficiency* is a measure of binding energy of the atom. *It is analogous to the heat of formation of a chemical compound.*

The constituents of the atom are consequently Z protons and Z electrons, which are equivalent in mass to Z hydrogen atoms, and $(A - Z)$ neutrons and their total mass is $ZM_H + (A - Z)\, M_n$, where M_H and M_n represent the masses of the hydrogen atom and of the neutron respectively. If ${}^A_Z M$ is isotropic atomic mass of an atom, then we can write, *mass difference or mass deficiency*

$$\Delta M = ZM_H + (A-Z)M_n - {}^A_Z M. \qquad \ldots(67)$$

As the binding energy is a measure of the energy equivalent of mass defect, hence we can write *binding energy*

$$E_B = \Delta Mc^2 = [ZM_H + (A-Z)M_n - {}^A_Z M]c^2. \qquad \ldots(68)$$

Since the state of infinite separation of nucleons is taken to be zero level of energy hence the total energy of the nucleus is just $-E_B$, or simply written as $-B$.

The binding energy may either be expressed in *u* or converted into *MeV* as *one atomic mass unit.*

$$u = \frac{\text{mass of } {}^{12}C \text{ atom}}{12} = \frac{1 kg}{N_A} = \frac{1}{6.0221367(36) \times 10^{26}}$$
$$= 1.6605402(10) \times 10^{-27} \text{ kg}$$

It is equivalent to 931.49432(28) *MeV*.

Aston, in 1927 expressed the deviations of the masses from mass numbers in the form of a packing fraction for each nuclide, given by

Packing fraction $\quad f = ({}^A_Z M - A)/A.$

$$\therefore \quad {}^A_Z M/A = 1 + f. \qquad \ldots(69)$$

To minimise confusion with mass defect, $({}^A_Z M - A)$ can be called the *mass excess.*

The binding energy per nucleon in terms of mass unit *u*

$$\bar{B} = \frac{B}{A} = \frac{Z}{A} M_H + \left(1 - \frac{Z}{A}\right) M_n - \frac{{}^A_Z M}{A}$$
$$= \frac{Z}{A}[M_H - M_n] + M_n - (1 + f) = -\frac{Z}{A}[0.0008397] + 0.0086649 - f. \qquad \ldots(70)$$

Thus the binding energy per nucleon is maximum when f is minimum. In the intermediate region of atomic weights f is negative, hence the $\bar{B}$ is greater and the nuclei are more stable. For the nuclides from ${}^{40}Ca$ to ${}^{120}Sn$, Z/A varies between 0.50 and 0.42 with the mean value 0.46. In this region the average value of $f = \approx -6 \times 10^{-4}$ *u*/nucleon, hence the value of $\bar{B} = 0.009\, u = 8.5$ *MeV*/nucleon.

The work necessary to separate a proton, neutron, deuteron or alpha particle from a nucleus is called the *separation energy S*. Conversely, this energy is released when the nucleus captures such a particle. The separation energy is expressed in terms of binding energies of these nuclei, such as

$$S_n = [M(A-1, Z) + M_n - M(A, Z)]c^2 = B(A, Z) - B(A-1, Z)$$
$$S_\alpha = B(A, Z) - B(A-4, Z-2) - B(4, 2).$$

The separation energy of nucleus is analogous to the heat of vaporization of solids or liquids. The average binding energy per molecule, called the latent heat of vaporisation is of the order of *eV*, while the average nuclear binding energy is of the order of *MeV*.

Variation of binding energy with mass number—A graph for the binding energies of the nuclei, expressed in *MeV*, against the mass number *A* is a curve (roughly straight line), which shows that to a first approximation the binding energy increases practically linearly with the mass number. Fig. 1.21 shows the binding energy per nucleon $\bar{B}\,(= B/A)$, plotted against the mass number *A*. The graph gives us following results—

(a) With the exception of ^4He, ^8Be, ^{12}C and ^{16}O, the values fall on or in proximity to a single curve. The binding energies of some of the lighter nuclides, such as ^1H, ^2He and ^3He are very low, but over a very considerable range of mass numbers, the binding energy per nucleon is close to 8 *MeV*.

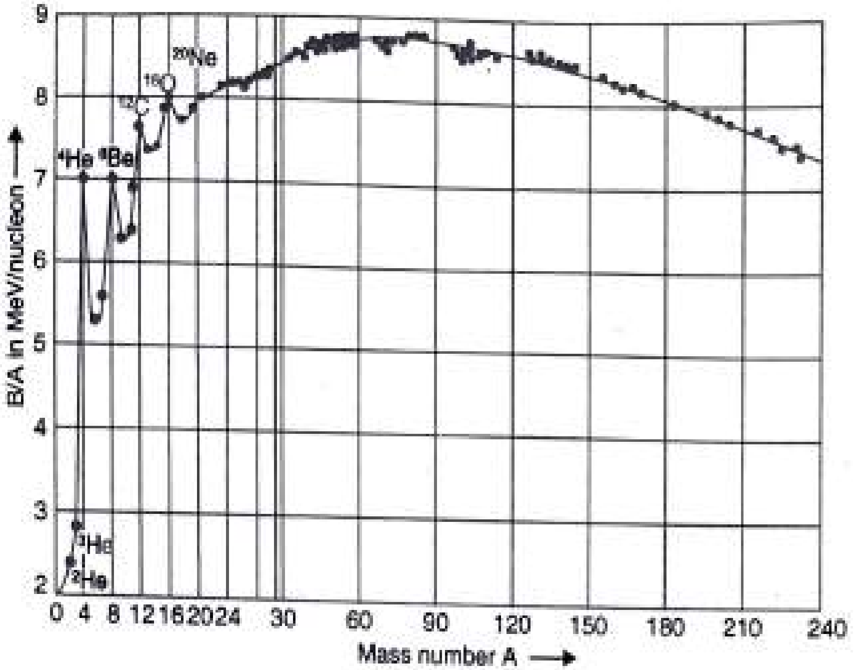

Fig. 1.21. Variation of binding energy per nucleon with the mass number.

(b) The positive value of *B/A* for all values of *A* shows the stability of the nucleus. This shows that there will be attractive nuclear forces between these constituents with in the nuclear volume. As nuclei do not collapse, these forces must become repulsive for very close distances of approach of the nuclear particles.

(c) The values of *B/A* vary in an erratic manner from nucleus to nucleus for the very light nuclides. There is a rapid increase in the value of *B/A* for light nuclei with a notable peaks at $A = 4n$ (^4He, ^8Be, ^{12}C, ^{16}O, ^{20}Ne, ^{24}Mg). This reflects the peculiar stability of the α-particle structure. This great stability is mainly a consequence of the pairing off of the two protons and two neutrons with opposite spins.

(d) Above $A \sim 20$, the binding energy per nucleon *B/A* is remarkably constant (upto ~ 10%). This must reflect an important property of nuclear forces. If the nucleons *A* inside the nucleus interacted with all the remaining $(A-1)$ nucleons with the same strength one would expect *B* to increase as $A(A-1)$ or approximately as A^2 for heavy nuclei. Agreement with observations is obtained if it is postulated that the nuclear constituents interact with only a limited number of their neighbours or the *nuclear forces are saturated.*

(e) The curve indicates that *B/A* increases to a maximum of about 8.8 *MeV* per nucleon around mass number 56 and then decreases slowly to about 7.6 *MeV* per nucleon at $A = 238$. This explains the energy release in the fusion of light elements and in splitting (fission) of a heavy element.

(f) Discontinuities were observed by several workers at *Z* or *N* equal to the magic number in the curve *B/A* vs. *A*. Duckword *et al.* reported at $^{140}_{58}$Ce, Nier at Z or $N = 20$ and 28 and at $Z = 50$, and Demster at doubly magic $^{208}_{82}$Pb.

Separation Energy for one nucleon—The energy required to remove one neutron from the nucleus, called the *removal* or *separation energy* of a neutron, is expressed as

$$S_n(Z, N) = [M(Z, N-1) + M_n - M(Z, N)]c^2$$

In terms of binding energy *B*, it is expressed as

$$S_n(Z, N) = B(Z, N) - B(Z, N-1) = B_n(Z, N), \qquad \ldots(71)$$

where $B_n(Z, N)$ is the binding energy of the last neutron of the atom $^A_Z X$.

In the analogous way, the proton separation energy or the binding energy of the last proton is given by

$$\begin{aligned} S_p(Z, N) &= [M(Z-1, N) + M_p - M(Z, N]c^2. \\ &= B(Z, N) - B(Z-1, N) = B_n(Z, N) \end{aligned} \qquad \ldots(72)$$

Because of the saturation property of nuclear force, the values of $S_n(Z, N)$ are larger for even N than the corresponding values for nearby odd N-nuclei. It means that in odd-N nuclides the final neutron is lightly bound. There is a complete similarity in the variation of $S_p(Z, N)$. The separation energies for protons and neutrons are greater for even Z or N than for odd Z or N. This is due to attractive forces between pairs of nucleons with opposite spins, occupying the same level. The pairing energy for neutrons may be defined as

$$P_n(Z, N) = \tfrac{1}{2}[S_n(even - N) - S_n(odd - N)]. \qquad \ldots(73)$$

Similarly we have the proton pairing energies. The close similarities between S_n and S_p, P_n and P_p suggest that the forces between nucleons are charge independent.

1.7 SEMI-EMPIRICAL MASS FORMULA

The mass M of a neutral atom whose nucleus contains Z protons and $(A - Z)$ neutrons is given by

$$^{A}_{Z}M = ZM_p + (A-Z)M_n + ZM_e - B = ZM_H + (A-Z)M_n - B, \qquad \ldots(74)$$

where B (sometimes written as E_B) is the binding energy, may be regarded as being made up of a number of terms, each of which represents some general characteristics of nuclei. Von Weizsacker in 1935 obtained a formula, known as *semi-empirical mass formula*, for expressing the atomic mass of a nuclide, in terms of a series of binding energy terms, which are free from complicated calculations based on shell structure and nucleon-nucleon interactions. It is of great importance in nuclear stability problems. We shall now proceed term by term with the assumptions : *(i)* The nucleus is like a drop of incompressible fluid, *(ii)* The forces between the nucleons are spin independent and charge independent and *(iii)* They have short range character.

(a) Volume binding energy—The neutrons and protons are held together by short range attractive forces. These forces reduce the mass of the nucleus below that of its constituents by an amount proportional to the number of nucleons A Since the volume of the nucleus is proportional to A, hence this term may be regarded as a *volume binding energy* often called *exchange energy*, and is given by

$$B_v = a_v A, \qquad \ldots($$

where a_v is a proportionality constant and the subscript v is for volume.

(b) Surface binding energy—Some nucleons are nearer to the surface so that they interact with few nucleons. Thus the binding energy B_v is reduced by an amount proportional to the surface area of the nucleus of radius R. For light nuclei nearly all the nucleons are at the surface, while for heavy nuclei about half the nucleons are at the surface. Thus the main binding energy must be corrected by a disruptive term, propotional to the surface area, known as *surface energy*. The surface energy is analogous to the surface tension of a liquid, although it is generally a larger quantity than the latter. It is therefore proportional to R^2 or $A^{2/3}$,

or

$$B_s = -a_s A^{2/3},$$

where a_s is the proportionality constant and the subscript s is for surface. ...(76)

(c) Coulomb Energy—The only long range force in the nuclei is the Coulomb repulsion between protons. The Coulomb repulsion term is equal to the potential energy of Z protons packed together in a spherically symmetric assembly of mean radius $R = R_0 A^{1/3}$ and of uniform charge density $\rho_c = Ze/\frac{4}{3}\pi R_0^3 A$.

The electrostatic energy is simply the work done against electrostatic forces in assembling such a sphere. Let dq be the charge on the shell of thickness dr on the sphere of radius r.

$$dq = \rho_c \times 4\pi r^2 dr = (3Ze/R_0^3 A) r^2 dr.$$

Hence the work in bringing this charge dq from infinity to r against the charge on the sphere of radius r is

$$\frac{3Ze}{R_0^3 A} \cdot r^2 dr \times \frac{\frac{4}{3}\pi r^3 \rho_c}{4\pi\varepsilon_0 r} = \frac{3Z^2 e^2}{4\pi\varepsilon_0 R_0^6 A^2} \cdot r^4 dr.$$

Integrating from 0 to $R (= R_0 A^{1/3})$ we have work done against Coulomb repulsion or the loss of binding energy B_c due to the disruptive Coulomb energy.

∴
$$B_c = -\frac{3}{5}\frac{Z^2e^2}{4\pi\varepsilon_0 R_0 A^{1/3}} = -a_c\frac{Z^2}{A^{1/3}}, \qquad \ldots(77)$$

where a_c is a constant and the subscript c is for Coulomb.

(d) Asymmetry Energy—Study of number of neutrons (N) and protons (Z) of stable nuclei shows that for nuclei with $Z + N$ upto 18, $N - Z = 0$ or $+ 1$, with the exception of hydrogen and ^3_2He, there is a sharp tendency for neutrons and protons to pair up. As $(Z + N)$ increases, nuclear forces do not increase much, but repulsion increases with charge. So proton increases in number less rapidly than neutrons, thus heavy nuclei have more neutrons than protons. A simple theory of this asymmetry is shown in schematic diagram of nuclear energy levels near the highest filled levels separated by the same energy Δ. Keeping $(N + Z)$ constant, if we remove a proton from level 3 and add a neutron to level 4, $N - Z$ becomes 2 and the energy has increased or B has decreased by an amount Δ. Transferation of two nucleons in this way increases the energy by an amount 4 Δ (Δ for the first and 3 Δ for the second). We thus find as a generalization of this process that the transfer of $(N - Z)/2$ nucleons decreases the binding energy by an amount $-\Delta(N - Z)^2/4$. Since Δ decreases as A increases, hence decrease in binding energy due to asymmetry

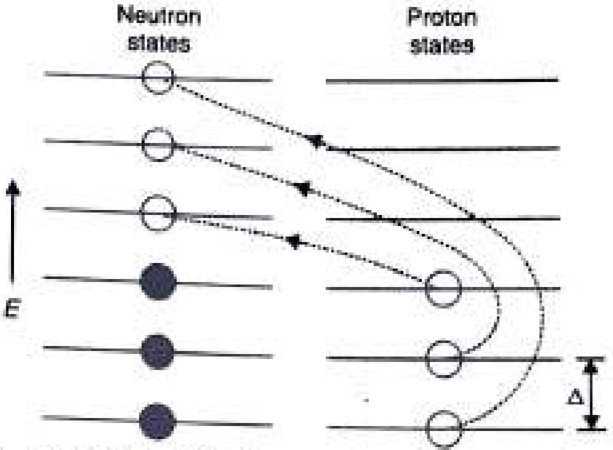

Fig. 1.22. Schematic diagram of nuclear energy levels near the highest filled level.

$$B_{as} = -a_a\frac{(N-Z)^2}{A} = -a_a\frac{(A-2Z)^2}{A},$$

where a_a is a constant and subscript a is for asymmetry.

(e) Pairing Energy—The nuclides with even numbers of protons and neutrons are the most abundant and most stable. Nuclei with odd numbers of both neutrons and protons are the least stable, while nuclei for which either proton or neutron number is odd are intermediate in stability. To take account of this pairing effect an additional term is used. Conventionally this term is taken as zero for odd-A, $-\delta$ for odd-odd and $+\delta$ for even-even nuclides. On the basis of more detailed analysis, we have $\delta = a_p/A^{-3/4}$, where a_p is the *pairing energy constant*. Hence we have

$$B_p = 0 \text{ for } A \text{ odd, } Z \text{ even and } N \text{ odd or } Z \text{ odd and } Z \text{ even,}$$
$$B_p = a_p/A^{3/4}, \text{ for } A \text{ even, } Z \text{ even and } N \text{ even,}$$
$$B_p = -a_p/A^{3/4}, \text{ for } A \text{ even, } Z \text{ odd and } N \text{ odd.}$$

(f) Magicity energy—When a shell is filled by having either the number of neutrons or the number of protons equal to one of the numbers 2, 8, 20, 28, 50, 82, or 126, which are known as magic numbers, a small local maximum in B as a function of A occurs.

∴
$$B_m = a_m A,$$

where a_m is known as *coefficient of magicity*.

Collecting together the different stability or mass correction terms we can write Weizsacker's semi-empirical mass formula as :

$$^A_Z M = ZM_H + (A-Z)M_n - a_v A + a_s A^{2/3} + a_c Z^2 A^{-1/3} + a_a (A-2Z)^2 A^{-1} \mp a_p A^{-3/4}. \qquad \ldots(79)$$

This mass formula does not include closed shell effects or the magicity energy term. Experimentally it was observed that the mass of any isobar having Z or N equal to any magic number lies about 1 or 2MeV below the value predicted by the mass formula. So we have to add this term to avoid the discontinuities in masses at the magic numbers.

The five constants of the semi-empirical mass formula can be evaluated from five masses of five nuclear reactions. When inserted in mass formula, they should give other masses. A good representative set proposed by Fermi in *MeV* is

a_v	a_s	a_c	a_a	a_p
14.0	13.0	0.583	19.3	33.5

The contribution of the various terms to B_{ave} is shown in Fig. 1.23. The initial rise of B/A with A, obtained empirically in Fig. 1.21, is mainly due to the decreasing importance of surface energy as A increases. At still larger A, the importance of the Coulomb energy becomes dominant causing a maximum at $A \sim 60$ and a subsequent decline at larger A. The semi-empirical mass formula matches the observed binding energies with in about 1% beyond $A = 40$. The discrepancies occur in neighbourhood of magic nuclei, having Z or N equal to 28, 50, 82 or 126. Mozer proposed a formula for odd A using a least-squares analysis of atomic masses.

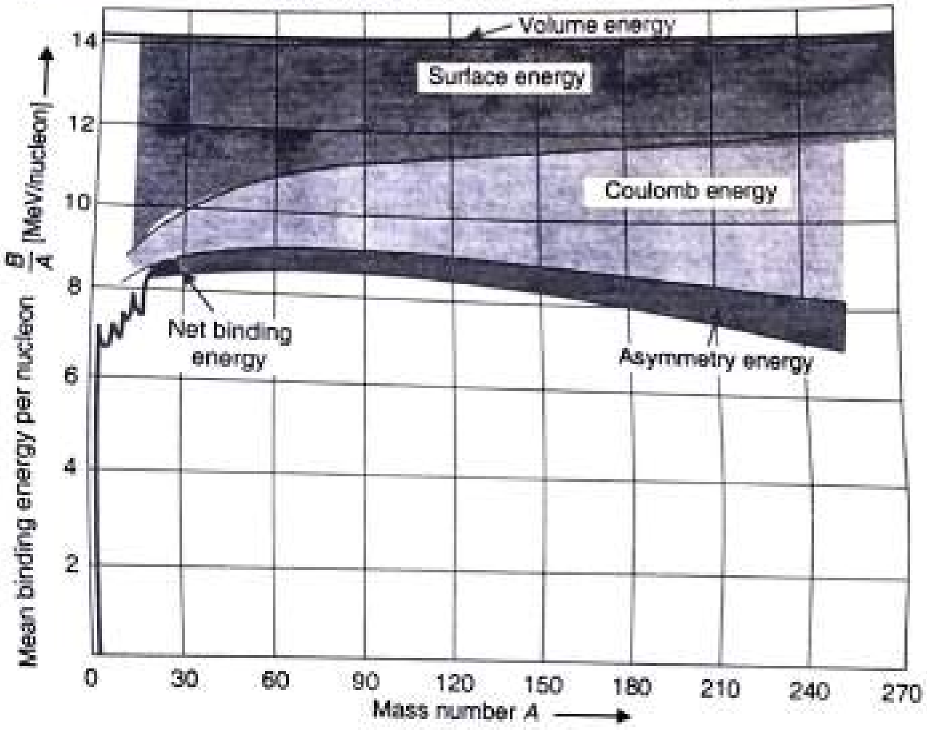

Fig. 1.23. Contribution of Various terms.

$$ {}^{A}_{Z}M = ZM_H + (A-Z)M_n - a_vA + a_sA^{2/3} + a_cZ(Z-1)A^{-1/3} + a_a(A-2Z)^2A^{-1} + S(Z, A) + D(Z, A), $$

where S and D are the shell effect energy and the nuclear deformation energy terms respectively. Mozer found coefficients as :

a_v	a_s	a_c	a_a
15.29	15.76	0.69	22.63

Applications of the Semi-empirical Mass Formula

(1) Coulomb Radius—As obtained in Eq. (77) the Coulomb energy constant $a_c = \frac{3}{5}e^2/4\pi\varepsilon_0R_0$. Substituting the value of a_c as 0.69 *MeV*, we get $R_0 = 1.25$ fermi. This is in excellent agreement with the values obtained by other methods.

(2) Radius for mirror nuclei—The mass difference for mirror nuclei, using Eq. (79), is given by

$$ \Delta M = {}^{A}_{Z}M - {}^{A}_{A-Z}M = (A-2Z)\,[M_n - M_H - a_cA^{2/3}]. $$

Hence the difference in respective binding energies

$$\Delta B = B(Z, A) - B(A - Z, A) = a_c A^{2/3} (A - 2Z).$$

Thus ΔB for mirror nuclei gives a value of a_c and hence of R_0.

(3) Fission Process—When a ${}^{235}U$ nucleus captures a neutron, it decays into a pair of nuclides by a fission process. We shall discuss it in chapter 13.

(4) Alpha-Decay—The total energy liberated in α-decay is

$$\begin{aligned} Q_\alpha &= ({}^{A}_{Z}M - {}^{A-4}_{Z-2}M - {}^{4}_{2}M)c^2. \\ &= B(\alpha) + B(Z-2, A-4) - B(Z, A) = B(\alpha) + \Delta B. \end{aligned}$$

The finite difference $B(Z-2, A-4) - B(Z, A)$ can be well approximated by the corresponding derivatives with $dZ = -2$ and $dA = -4$. Thus we have

$$\Delta B = -2\partial B/\partial Z - 4\partial B/\partial A.$$

Using semi-empirical mass formula for B and experimental value of $B(\alpha)$ as 28.3 MeV, we get

$$Q_\alpha = 28.3 - 4a_v + \tfrac{8}{3}a_s A^{-1/3} + 4a_c Z A^{-1/3}(1 - Z/3A) - 4a_a(1 - 2Z/A)^2.$$

Numerical substitution gives + *ve* values of Q_α for $A \geq 150$, which are therefore α-unstable.

(5) The Behaviour of Isobars in β-decay—Most of the unstable nuclides are natural β-emitters. The stability of β-emitting isobars can be predicted from the mass formula.

For odd-A isobars, $a_p = 0$ and mass M is a quadratic function of Z, hence M versus Z curve is a parabola. The isobar, for which the binding energy is greatest showing maximum stability, is at or near the bottom of the curve. All isobars whose binding energies are less than that of the stable one will lie on the two arms of the curve. All these isobars decay into stable isobars either by β^--emission ($Z < Z_0$), or by β^+ emission and electron capture ($Z > Z_0$). The curve between ${}^{A}_{Z}M$ and Z for $A = 65$ along with the decay processes is shown in Fig. 1.24*(a)*. Electron capture process is indicated by ε in the figure. Isobars to the left of the stable one have fewer protons than the stable one and decay by electron emission.

$${}^{65}_{27}Co \xrightarrow{\beta^-} {}^{65}_{28}Ni \xrightarrow{\beta^-} {}^{65}_{29}Cu\,(Stable)$$

Isobars which lie to the right of the lowest point contain an excess of protons and decay by positron emission or by K-capture, or by both.

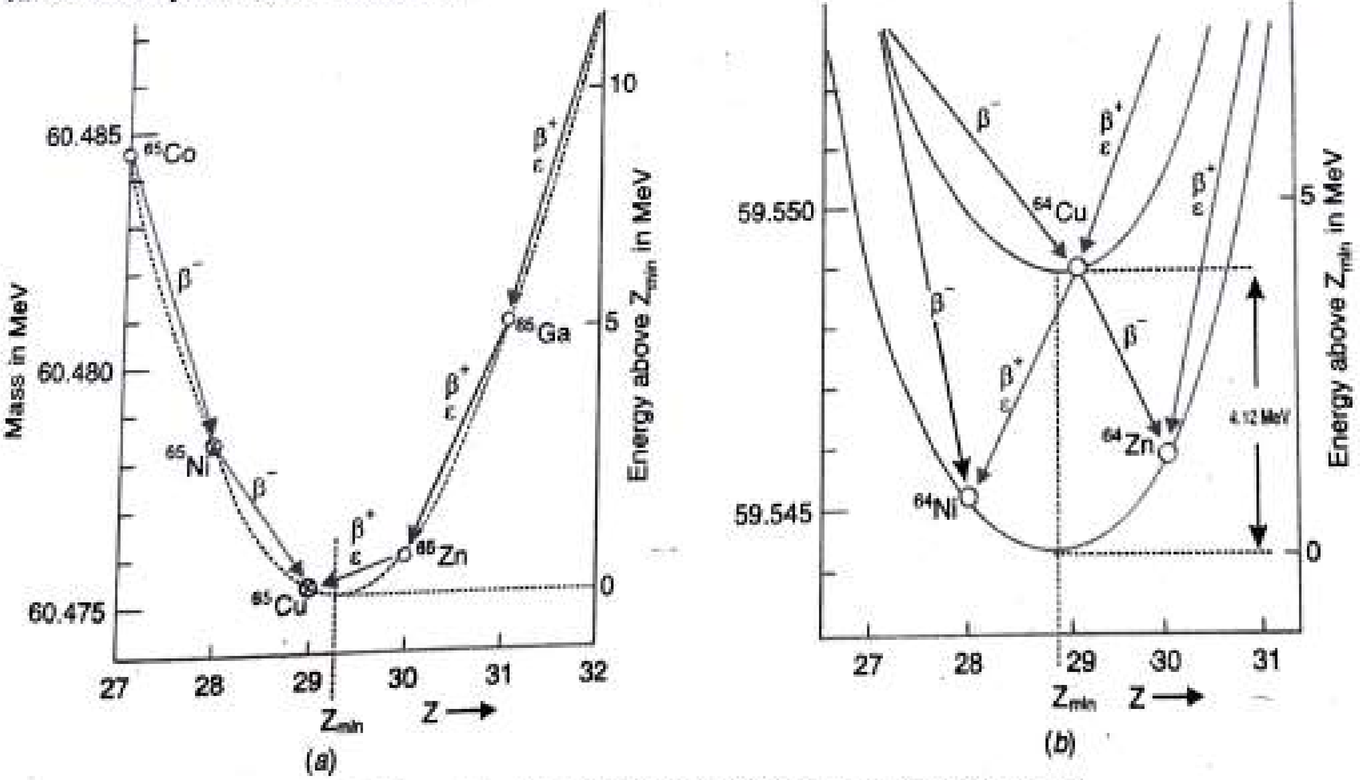

Fig. 1.24. Schematic plots of M versus Z for (a) odd A and (b) for even A.

$$^{65}_{32}Ge \xrightarrow{\beta^+} {}^{65}_{31}Ga \xrightarrow{\beta^+} {}^{65}_{30}Zn \xrightarrow{\beta^+} {}^{65}_{29}Cu(Stable).$$

The situation for even A is more complicated as the last term of semi-empirical mass formula is positive for even Z-even N and negative for odd Z-odd N nuclides. Hence there are two parabolas, the upper one for Z and N both odd and the lower one for Z and N both even. The curve for even N-even Z-nuclides shows that two isobars with Z-values differing by two units lie cose to the bottom of the lower curve and constitute stable isobaric pairs. All other isobars decay into stable isobars either by β^- emission or by β^+ emission. The isobar at the bottom of the odd Z-odd N curve decays either by positron or by electron emission.

Equation of the Mass Parabolas for Constant A—We can arrange the semi-empirical mass formula as follows :

$$\begin{aligned} {}^{A}_{Z}M &= Z(M_H - M_n) + A\,M_n - a_v A + a_s A^{2/3} + a_c Z^2 A^{-1/3} + a_a A - a_a 4Z + a_a 4Z^2 A^{-1} \mp a_p A^{-3/4} \\ &= \alpha A + \beta Z + \gamma Z^2 - (\pm\,\delta), \end{aligned} \quad \ldots(80)$$

where $\alpha = M_n - (a_v - a_a - a_s/A^{1/3})$, $\beta = -4a_a - (M_n - M_H)$.

and
$$\gamma = \left(4\frac{a_a}{A} + \frac{a_c}{A^{1/3}}\right) = 4\frac{a_a}{A}\left(1 + \frac{A^{2/3}}{4a_a/a_c}\right) \text{ and } \delta = \frac{a_p}{A^{3/4}}.$$

For constant A, Eq. (80) represents a parabola. It is also clear from this relation that α is nearly dependent of A, β is independent of A and γ varies approximately inversely with A. The most stable isobar will have the smallest mass on the parabola, Z_0 value for the same can be obtained as follows :

$$(\partial M/\partial Z)_{A\,=\,constant} = \beta + 2\gamma Z_0 = 0$$

or
$$Z_{stable} = Z_0 = -\beta/2\gamma. \quad \ldots(81)$$

For odd A

$\delta = 0$ and the mass of the hypothetical most stable isobar is

$${}^{A}_{Z_0}M = \alpha A - 2\gamma Z_0 Z_0 + \gamma Z_0^2 = \alpha A - \gamma Z_0^2 \quad \ldots(82)$$

and
$${}^{A}_{Z}M = \alpha A - 2\gamma Z_0 Z + \gamma Z^2. \quad \ldots(83)$$

Eliminating αA from these relations, we have

$${}^{A}_{Z}M - {}^{A}_{Z_0}M = \gamma[Z^2 - 2Z_0 Z + Z_0^2] = \gamma[Z - Z_0]^2. \quad \ldots(84)$$

This relation contains only the coefficient γ and is helpful in calculating the transition energies in the reactions where Z changes at constant A.

Q-value of reaction in which $Z \to (Z+1)$, at constant A, such as the case of β^--decay, (p, n) and $(d, 2n)$ reactions is given by

$$\begin{aligned} Q &= {}^{A}_{Z}M - {}^{A}_{Z+1}M = \gamma[(Z - Z_0)^2 - (Z + 1 - Z_0)^2] \\ &= 2\gamma[Z_0 - Z - \tfrac{1}{2}]. \end{aligned} \quad \ldots(85)$$

Similarly the Q-value of reactions in which $Z \to (Z-1)$, at constant A, such as (n, p), electron capture and β^+—decay, is given by

$$\begin{aligned} Q &= {}^{A}_{Z}M - {}^{A}_{Z-1}M = \gamma[(Z - Z_0)^2 - (Z - 1 - Z_0)^2] \\ &= 2\gamma[Z - Z_0 - \tfrac{1}{2}]. \end{aligned} \quad \ldots(86)$$

Both can be summarized as

$$Q_{\beta\mp} = {}^{A}_{Z}M - {}^{A}_{Z\pm 1}M = 2\gamma[\pm(Z_0 - Z) - \tfrac{1}{2}]. \quad \ldots(87)$$

Thus for any odd A, two measured Q-values are sufficient for the determination of Z_0 and γ. For example, the β-decay schemes of ${}^{131}_{52}Te$ and ${}^{131}_{53}I$, having Q values 2.16 ± 0.1 & $0.97 \pm 0.01\ MeV$ respectively, give $Z_0 = 54.3 \pm 0.1$ and $\gamma = 0.60 \pm 0.05\ MeV$.

For even A

$\delta \neq 0$ and the mass of the hypothetical most stable isobar is

$${}^{A}_{Z_0}M = \alpha A - \gamma Z_0^2 \mp \delta. \quad \ldots(88)$$

This relation shows that there are two possible most stable isobars one corresponds to + δ and other corresponds to – δ, δ is + *ve* for even *Z*-even *N* and is – *ve* for odd *Z*—odd *N* nuclei, hence we have to take negative sign for the mass of the most stable isobar. For even *A*, we thus have

$$ {}^{A}_{Z}M - {}^{A}_{Z_0}M = \gamma(Z - Z_0)^2 + \begin{Bmatrix} 2\delta \text{ for odd–}Z \\ 0 \text{ for even–}Z \end{Bmatrix} \qquad \ldots(89) $$

Q-value of reactions in which $Z \to (Z \pm 1)$, at constant *A*, is

$$ Q = {}^{A}_{Z}M - {}^{A}_{Z\pm 1}M = 2\gamma\left[\pm(Z_0 - Z) - \tfrac{1}{2}\right] + \begin{bmatrix} +2\delta \text{ for odd–}Z \\ -2\delta \text{for even–}Z \end{bmatrix} \qquad \ldots(90) $$

Here + sign in $\pm (Z_0 - Z)$ is with $Z \to (Z + 1)$, *i.e.*, for β^-—decay, (*p*, *n*) and (*d*, 2*n*) reactions, and the – sign corresponds to $Z \to (Z - 1)$ transitions, such as β^+ decay, (*n*, *p*) reactions, etc.

Evaluation of Energy Coefficients—The five empirical coefficients (a_v, a_s, a_c, a_a and a_p) can be evaluated by comparison of Eq. (79) with data on the masses of stable nuclides or energies of nuclear reactions. These will then serve to predict hundreds of other masses and reactions. The semi-empirical formula with these coefficients gives an extremely good average values over a wide range of *A*. The method of least squares adjustment to mass data for β-stable nuclides is used for the determination of four energy coefficients (a_v, a_s, a_c and a_a).

These coefficients were also determined as follows :

Using $R_0 = 1.45 \pm 0.05$ fermi for $10 < A < 240$, the

Coulomb coefficient
$$ a_c = \frac{3}{5}\frac{e^2}{4\pi\varepsilon_0 R_0} = 0.595 \pm 0.02\, MeV. \qquad \ldots(91) $$

The asymmetry energy term is evaluated with the data for most stable isobar. *Z* is called nuclear charge Z_0. Thus by setting $(\partial M/\partial Z)_{A = const} = 0$ for odd *A*, we get

$$ 2a_c Z_0/A^{1/3} - 4a_a(A - 2Z_0)/A = M_n - M_H, $$

or

$$ \frac{a_a}{a_c} = \frac{1}{2}\left(\frac{Z_0 A^{2/3}}{A - 2Z_0}\right) - \left(\frac{A}{A - 2Z_0}\right)\frac{M_n - M_H}{4a_c}. \qquad \ldots(92) $$

Using the value of a_c as 0.595 *MeV*, we get $(M_n - M_H)/4a_c = 0.33$.

The second term of Eq. (92) acts as a correction of about 5% for heavy nuclides to 10% for light nuclides. Thus the asymmetry energy coefficient a_a is obtained by direct calculation from *Z* and *A* of stable odd nuclides using Eq. (92). The average value of $a_a/a_c = 32 \pm 1$ gives $a_a = 19.0 \pm 0.9 MeV$.

The comparison of experimental value of *B/A* using Eq. (70) and theoretical value of *B/A* using Eq. (79) for masses of ^{65}Cu and ^{127}I gave $a_v = 14.28\, MeV$ and $a_s = 13.6\, MeV$.

1.8 QUANTUM NUMBERS FOR INDIVIDUAL NUCLEONS

The state of body as determined by the quantities as energy, momentum and angular momentum is defined by its wave function. The solution of the wave equation for the system is characterized by the parameters termed as quantum numbers. Because of many apparent similarities between atomic and nuclear affairs, it seems logical to adopt same nomenclature for these numbers as used in atomic physics.

***(a)* Principle quantum number (*n*)**—Each bound individual particle has been associated with its principle quantum number *n*, which can take on positive integral values 1, 2, 3, ... In the strong central field, the first order term for the total energy of the state is determined by *n*, as

$$ E = E_{kin} + E_{pot} = -\frac{1}{2}\frac{Ze^2}{4\pi\varepsilon_0 r} = -\frac{1}{n^2}\frac{Z^2 e^4 m}{2(4\pi\varepsilon_0)^2\hbar^2}. $$

This is not true for the noncoulomb fields in which the nuclear particles are bound.

Sommerfeld modified the Bohr's model and suggested azimuthal quantum numebr n_ϕ and radial quantum number n_r, as given by

$$ n = n_\phi + n_r, $$

***(b)* Orbital quantum number (*l*)**—The original azimuthal quantum number n_ϕ is now replaced by the orbital quantum number l, as the former was for the radial oscillation of the electron through the nucleus. It can take on positive integral values 0, 1, 2…, $(n-1)$, corresponding to orbital angular momenta $\hbar\sqrt{[l(l+1)]}$. Individual values of l are designated by the letter sequence s, p, d, f … The orbital magnetic quantum number m_l, is the component of l in a specified direction, applied magnetic field direction termed the quantization direction and usually taken as the z-axis. It can take on $(2l+1)$ possible values such as $l, (l-1) \ldots 1, 0, -1, -2, \ldots\ldots, -(l-1), -l$.

***(c)* Radial quantum number (n_r)**—In the solution of the radial wave equation for the non-Coulomb field potential, we get n_r. This represents the number of nodes at $r > 0$ in the radial wave function and can take on positive integral values 1, 2, 3....., n.

***(d)* Spin quantum number (*s*)**—The intrinsic angular momentum of a particle is termed the spin and represented by a quantum number s. This has a magnitude $\hbar[s(s+1)]^{1/2} \cdot s = \frac{1}{2}$ for all elementary particles which follow Fermi Dirac statistics and which obey the Pauli exclusion principle. s has integral values (0, 1, …) for particles described by Bose-Einstein statistics to which the Pauli principle does not apply.

The magnetic spin quantum number m_s is the component of s in a specified direction, applied magnetic field direction. It can take on $(2s+1)$ possible values such as $s, (s-1), \ldots 1, 0, -1, \ldots, -(s-1), -s$. For particles with $s = 0$, $m_s = 0$; with $s = \frac{1}{2}$, $m_s = +\frac{1}{2}$ and $-\frac{1}{2}$, corresponding to parallel and antiparallel alignments with respect to the z-direction.

***(e)* Total angular momentum quantum number (*j*)**—The total angular momentum of a nucleon is the vector sum of its orbital and its spin angular momenta and is represented by a quantum number j.

$$\mathbf{j} = \mathbf{l} + \mathbf{s}.$$

The total angular momentum has magnitude $\hbar\ [j(j+1)]^{1/2}$. For fermions $s = \frac{1}{2}$ and l is an integer, hence j can take on the values $\frac{1}{2}, \frac{3}{2}, \frac{5}{2}, \ldots$

The magnetic total angular momentum quantum number m_j is the component of j in the quantization direction. It can take on $(2j+1)$ possible values such as $j, j-1, \ldots \frac{1}{2}, -\frac{1}{2}, \ldots, -(j-1), -j$.

***(f)* Isospin quantum number (*T*)**—Neutrons and protons are similar in all respects except charge. On this basis, Heisenberg suggested these particles as just different manifestations of the same inherent particle, the *nucleon*. To describe their quantum state, quantum number used was termed the *isotopic spin quantum number* by Wigner. It is because of the similarity to the spin quantum numbers s and m_s, although it is not strictly an angular momentum as spin is. As the neutron and proton have similar masses, hence it was renamed *isobaric spin*. Now a days it is generally named as *isospin* or *T-spin*.

Isospin quantum number is a useful and an important quantum number that is conserved in nuclear transformations. As the states with spin s have multiplicity $(2s+1)$, for $s = 1/2$ we have a doublet $(m_s = -1/2, +1/2)$ and for $s = 1$ we have a triplet $(m_s = -1, 0, +1)$. In an analogous manner, a nucleon is assigned an isospin of 1/2 and in an electromagnetic field two charge states with isospin components of 1/2 and −1/2 can be distinguished as the proton and neutron respectively. The isospin is a vector in a three dimensional space, called isospin space, which has no relation to physical space. The component that is measured is said to be T_3, or T_z, the component of T in the direction of the third axis in isospin space.

Intrinsic spin is a property not of nucleons but also of complex nuclei and of the wide variety of particles and states known in high energy physics.

***(g)* Parity**—Parity is a property of the wavefunction describing a quantum mechanical system and is of great importance in atomic and nuclear physics. The parity of a system of elementary particles, atoms or molecules is a fundamental property of its motion. It is constant for an isolated system and can change if radiation or a particle enters or leaves the system. The nuclear parity may change if the emitted or absorbed particles or quanta have odd total parity. Non-quantum theories are always invariant under reflection of coordinates. Invariance under reflection requires that all terms of equation must have the same behaviour under reflection. The reflection symmetry principle is equivalent to the statement that the parity of a closed system cannot change. This symmetry property is called the *parity* and said to be even (*or* +) for even functions and odd (*or* –) for odd functions.

$$\psi(x, y, z, s) = \psi(-x, -y, -z, s) \qquad \textit{even or + parity}$$

$$\psi(x, y, z, s) = -\psi(-x, -y, -z, s) \qquad \textit{odd or − parity.}$$

Here the sign of s remains unchanged under space inversion $\mathbf{r} \to -\mathbf{r}$. The interchange of the vectors $\mathbf{r}$ and $-\mathbf{r}$ is equivalent to replacing the spherical coordinates r, θ and ϕ by r, $\pi - \theta$ and $\pi + \phi$. As the wave function describing many particles can be written as a product of individual particle wavefunctions, hence parity of a whole system is the product of the parities of the individual particles. Parity is also conserved in nuclear processes as the conservation of charge and of angular momentum. However, since the publication of Lee and Yang experiment, several experiments have demonstrated that parity is not conserved in certain processes, specially in weak interactions. The parity of a nuclear state is often indicated by a superscript + or − on the angular momentum I.

Wavefunction symmetries depend upon the values of the orbital angular momentum quantum number l. It can be shown that the spatial part of ψ does not change sign on reflection of the particle, if l is even and it does change sign if l is odd. Hence the parity of a motion with an even value of l is even, or +, while odd value of l gives odd, or − parity. The parity of the particle is the product of the parity of the angular momentum state and intrinsic parity of the particle. From the properties of simple system it has been found experimentally that the instrinsic parity of the electron, proton, neutron, neutrino, muon is even. In contrast, the π meson is found to have odd intrinsic parity. Photon is found to have either value depending upon mode of generation. The parity of photon will depend upon the value of l and also upon whether its origin was electric or magnetic.

$$E \text{ parity} = (-1)^l \text{ and } M \text{ pariy} = -(-1)^l. \qquad \ldots(93)$$

The parity of a given nuclear level is determined by the odd or even number of nucleons in the nucleus and will be discussed in the chapter of *'Nuclear Models.'*

***(h)* Quantum Statistics**—Quantum statistics is applied to particles which are theoretically and practically indistinguishable. It arises from the symmetry properties of wave functions. The wave functions for a system of two or more identical particles may be divided into two symmetry classes : *(i)* symmetric and *(ii)* anti-symmetric. Correspondingly the particles are said to obey Fermi-Dirac and Bose-Einstein statistics.

(a) Fermi-Dirac Statistics—If the wavefunction is anti-symmetric (changes sign) under the exchange of the coordinates (three space coordinates and one spin) of two equal particles, the particles are said to obey Fermi-Dirac statistics, *i.e.*,

$$\psi(x_1, y_1, z_1; x_2, y_2, y_2;; \ldots x_i, y_i, z_i : \ldots; x_j, y_j, z_j; \ldots; s)$$

$$= -\psi(x_1, y_1, z_1 : x_2, y_2, z_2 : \ldots x_j, y_j, z_j; \ldots x_i, y_i, z_i; \ldots; s)$$

If the two equal particles have same coordinates, the wave-function will thus be zero. It means that the two particles can never be found at the same place. Thus Pauli exclusion principle holds for Fermi Dirac particles. Actually two identical particles are never found at a distance small compared to $\lambda\!\!\!^{-}$. It is the case when the particles are in the same spin, as two identical particles of opposite spins are considered different. The particles, *e.g.*, electron, proton, neutron, muons and neutrinos, obey Fermi-Dirac statistics, are known as *fermions*. These are associated with half integral spins.

(b) Bose-Einstein statistics—If the wavefunction is symmetric (does not change sign) under the exchange of the coordinates (including spin) of two indentical particles, the particles are said to obey Bose-Einstein statistics. These particles do not obey Pauli-exclusion principle, *i.e.*, two or more identical particles may be in the same quantum state. These are named bosons, and have integral spin. The examples are photons, pions, α-particles and deuterons.

1.9 INDEPENDENCE OF ATOMIC AND NUCLEAR PROPERTIES

Except the nuclear charge, all the other properties of the nucleus are almost irrelevant to the behaviour of the electrons. The electrons have almost no influence on the nucleus. The situation is same as for the earth and its satellites. On account of this decoupling of nuclei and electrons, the nuclear and atomic properties are largely decoupled. All properties of matter can thus be identified as either primarily atomic or primarily nuclear, but not both. The electrons account for all of the physical and chemical properties of the elements. The nucleus is the source of the mass of an atom, its position in the periodic table and its radioactivity, if any.

The nuclear binding energies are about one million times greater than atomic binding energies and the energy changes in nuclear quantum transitions are also about one million times greater than the energy changes of the atomic transitions. This difference in energy scales arises from the difference in mass of nucleons and electrons and the difference in size of these two systems.

The particle states of motion fill in a somewhat different order in nuclei than in atoms. This is due to two sources: *(i)* The shapes of the potential energy curves are different in these cases and *(ii)* Strong spin-orbit coupling of nucleons in the nucleus and a weak spin orbit coupling in atoms. The potential well of the nucleus is of short range in contrast with the long range of the Coulomb potential.

For the long range potential the spacing of energy levels tends to zero as the zero of energy (dissociation energy is approached while for short range the level spacing is much more uniform.

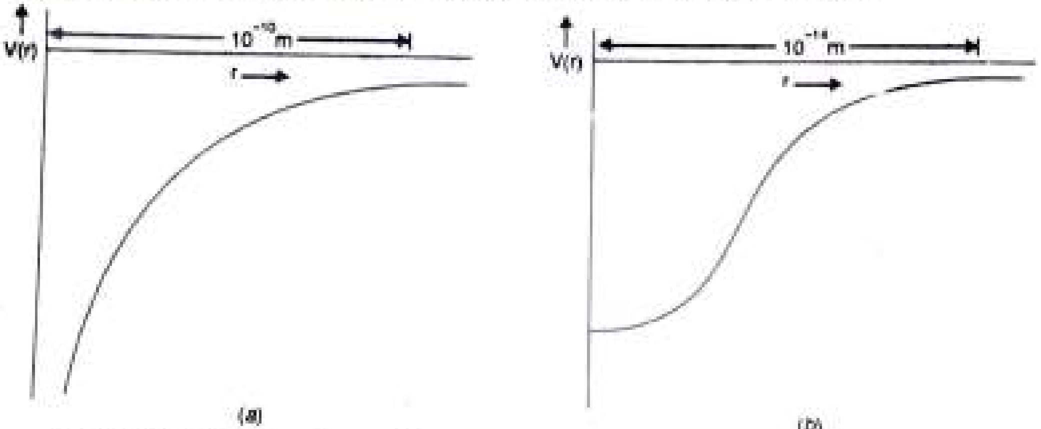

Fig. 1.25. Comparison of potential energy curves for (a) atomic and (b) nuclear cases.

1.10 QUANTUM PROPERTIES OF NUCLEAR STATES

(a) Nuclear Energy Levels—Similar to the discrete energy states of the electrons in an atom, the nucleons comprising a nucleus have possible-energy states given by Heisenberg principle.

$$H_n \psi_n = E_n \psi_n \qquad \ldots(94)$$

Here Schrodinger wave function ψ_n depends upon spatial coordinates and also spin and isospin quantum numbers. The ground state possesses latent energy, in the form of potential energy which is normalized to zero. Excitation energies of the higher levels are referred to the zero energy of the ground level. γ-rays of discrete values are emitted by the de-excitation of the nucleus to its ground state. Levels are said to be *virtual*, if they can dissociate with the emission of a particle and *bound* if not. The energy level diagram represents excitation energy, nuclear spin *I*, parity π, lifetime τ and isospin *T*.

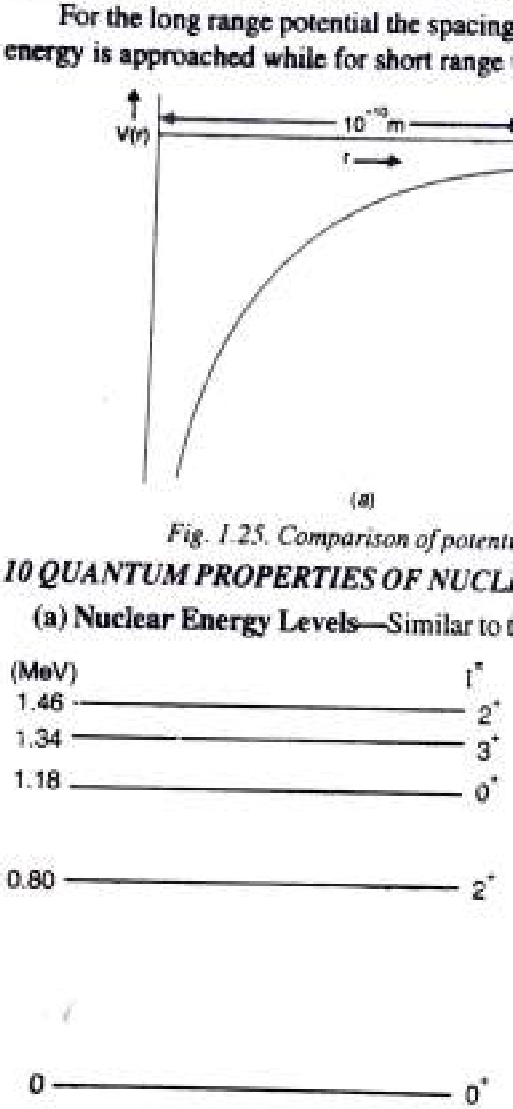

Fig. 1.26. Level Scheme of Pb-206.

(b) Nuclear Angular Momentum—In 1924, W. Pauli, while explaining hyperfine structure of spectral lines, suggested that certain atomic nuclei may possess an intrinsic angular momentum as well as a magnetic moment. The nuclear angular momentum can be deduced from the measurement of multiplicity and relative spacing of the spectral lines.

It has been found that the neutron and the proton possess an intrinsic angular momentum, commonly referred to as its spin, of magnitude $\frac{1}{2}\hbar$ just as the electron does. Since nuclei are built up of nucleons (neutrons and protons), each possesses an angular momentum, which consists of both orbital angular momentum due to the motion about the centre of the nucleus and intrinsic spin angular momentum of $\frac{1}{2}\hbar$ due to the spinning about its axis per nucleon. The total angular momentum of a particular nuclear state is the resultant of the individual momenta of the constituent nucleons. Corresponding to total angular momentum quantum number I, the absolute magnitude of total angular momentum is $\hbar\ [I(I+1)]^{1/2}$. The value of I depends on the type of interaction between the nucleons.

LS-Coupling—In this case the spin-orbit interaction is negligible and there is a collective interaction of orbital and intrinsic momenta, *i.e.*,

$$\mathbf{I} = \mathbf{L}+\mathbf{S}, \text{ where } L = \sum_i l_i \text{ and } S = \sum_i s_i. \qquad ...(95)$$

For $L = 0, 1, 2, 3...$, we have levels S, P, D, F ... For each value of L there are $(2S+1)$ possible separated energy levels. The multiplicity $(2S+1)$ is written as a superscript before the letter representing L and the value of I as subscript. Hence for $L = 1$ and $S = 1/2$, we have levels ${}^2P_{3/2}$ and ${}^2P_{1/2}$, the spin doublet.

j-j-Coupling—In this case the orbital and spin momenta of each individual nucleon are strongly coupled. I is the vector sum of the individual j values. Hence

$$I = \sum_i \mathbf{j}_i, \text{ where } \mathbf{j}_i = l_i + s_i. \qquad ...(96)$$

This type of coupling is called strong spin-orbit coupling. If s-nucleon $(l = 0, j = 1/2)$ couples with p-nucleon $(l = 1, j = 3/2, 1/2)$, we have $I = 0, 1, 1$ *or* 2.

These two coupling schemes are the extreme forms. One can employ intermediate coupling schemes of varying degrees of complexity. The total angular momentum of a nucleus is usually called as *nuclear spin*. It is an unfortunate terminology for the angular momentum, because spin is generally used for intrinsic angular momentum of elementary particles. Experimentally it is found that all nuclei have relatively low spin in their ground states. The spins of the excited states may differ from the spin of the ground state by integral multiples of $\hbar$. The term "spin of the nucleus," without any specification, always refers to the ground state. It has been found that all even-even nuclei have a spin $I = 0$ in the ground state. Odd-odd nuclei all have integral nuclear spin, other than zero. All odd-even nuclei have half integral nuclear spins lying between $\hbar/2$ to $11\,\hbar/2$.

Total angular momentum vector **I** can be oriented in space with respect to a given axis in $(2I+1)$ directions. The component along the axis in any of the states has the magnitude $m\hbar$, where m is the magnetic quantum number, having values from I to $-I$, as $I, (I-1), (I-2)..., -(I-1), -I$. Thus the largest value of m is I.

(c) Pariy—Nuclear parity is the product of the parities of the nuclear constituents. As will be discussed in the chapter of nuclear models, for even Z-even N nuclei, ground states have positive parity $(I^\pi = 0^+)$. The parity of odd A nuclei is given by $(-1)^l$, where l is the orbital angular momentum of the unpaired nucleon. Odd-odd nuclei have a parity $(-1)^{l_n+l_p}$. Few exceptions to this rule require explanation. In general the parity of the system of n particles is given by Σl_n. Parity is even if this sum is *positive* and is odd if the sum is *negative*.

(d) Isospin—For a given nucleus, the value of T_3 or T_z is just the minus one half of the neutron excess.

$$T_3 = -\tfrac{1}{2}(N-Z) = -\tfrac{1}{2}(A-2Z). \qquad ...(97)$$

In a set of isobars of given A, a member X will have an isospin $T_{z\,\max}$ largest among the set. For this $T = T_{z\,\max} = \frac{1}{2}(Z_X - N_X)$, having $(2T+1)$ states. These states are corresponding to different T_z and hence to different charges $(Z = A/2 + T_z)$. The isobars ${}^{14}C$, ${}^{14}N$, ${}^{14}O$ have $T_z = -1, 0$ and $+1$ respectively. The mirror nuclei ${}^3H$ and ${}^3He$ have $T = \frac{1}{2}$ in their ground state. Isospin assignments to excited nuclear levels can be established through reaction or scattering studies.

(e) Statistics—It can be seen experimentally that ${}^1H$, ${}^7Li$, ${}^{19}F$, ${}^{23}Na$, ${}^{31}P$, ${}^{35}Cl$ obey the Fermi-Dirac statistics. In general, all nuclei of odd mass numbers obey the Fermi-Dirac statistics. ${}^2H$, ${}^4He$, ${}^{12}C$, ${}^{14}N$, ${}^{16}O$, ${}^{32}S$ are known to obey Bose-Einstein statistics. In general, the photons and all nuclei of even mass number follow Bose-Einstein statistics.

1.11 NUCLEAR MAGNETIC DIPOLE MOMENT

Any charged particle moving in a closed path produces a magnetic field, which at large distances acts as due to magnetic dipole located at the current loop. The protons inside the nucleus are in orbital motion and therefore produce electric currents which produce nuclear magnetic field. Each nucleon possesses an intrinsic magnetic moment which is parallel to its spin and is probably caused by the spinning of the nucleon. A spinning positive charge produces a magnetic field whose *N*-pole direction is parallel to the direction of spin. The magnetic moment is defined as positive in this case.

If a particle having a charge q and mass m circulates about a force centre with a frequency, ν, the equivalent current $i = q\nu$. From Kepler's law of areas, the area swept $d\mathbf{A}$ in time dt by the particle is related with its angular momentum $\boldsymbol{l}$ as

$$d\mathbf{A}/dt = \tfrac{1}{2} l/m = \text{constant.}$$

On integration over one period T, we get

$$\mathbf{A} = \tfrac{1}{2} T\, l/m.$$

The magnetic moment of a ring of current around an area of magnitude A is called *orbital magnetic dipole moment* and is given by

$$\boldsymbol{\mu}_l = i\mathbf{A} = (q\nu)\left(\frac{Tl}{2m}\right) = \frac{q}{2m} l. \qquad ...(98)$$

Thus $\boldsymbol{\mu}_l$ and l are proportional to each other. This relation is also valid in quantum mechanics. However, since the particles (electron, proton and neutron) possess a spin in addition to orbital angular momentum, experimentally it is found that the spin is also the source of a magnetic moment. Using $q = e$ and a dimensionless correction factor g_s, we can write Eq. (98) for the spin magnetic dipole moment as

$$\boldsymbol{\mu}_s = g_s (e/2m)\mathbf{s}. \qquad ...(99)$$

The factor g_s is different for the electron, proton and neutron. Similarly, we introduce a factor g_l for the orbital angular momentum and have

$$\boldsymbol{\mu}_l = g_l (e/2m)\boldsymbol{l}. \qquad ...(100)$$

The total magnetic dipole moment $\boldsymbol{\mu}$ is given as :

$$\boldsymbol{\mu} = \boldsymbol{\mu}_s + \boldsymbol{\mu}_l = (e/2m)\,[g_s \mathbf{s} + g_l \boldsymbol{l}]. \qquad ...(101)$$

For the nucleus of mass number A, magnetic dipole moment, called nuclear magnetic moment

$$\boldsymbol{\mu} = \frac{e}{2m}\left[\sum_{k=1}^{A} g_s\, s_k + \sum_{k=1}^{Z} g_l\, l_k\right] \qquad ...(102)$$

Since total angular momentum of the nucleus

$$\boldsymbol{I} = \sum_{k=1}^{Z} l_k + \sum_{k=1}^{A} s_k. \qquad ...(103)$$

$$\therefore\quad \boldsymbol{\mu} = g_I (e/2m)\boldsymbol{I} = g_I (e\hbar/2m)\boldsymbol{I}/\hbar, \qquad ...(104)$$

where g_I is the *gyromagnetic ratio* (g-factor) of the nucleus. It is the dimensionless ratio of the magnetic moment μ in terms of $eh/2m$ to the angular momentum I in terms of h. If I is measured in terms of $\hbar$, it is called angular momentum quantum number. Using quantum mechanics we have $[l(l+1)]^{1/2}$ and $[s(s+1)]^{1/2}$ instead of l and s respectively, we thus get

$$g_I = \frac{1}{2}(g_l + g_s) + \frac{1}{2}(g_l - g_s)\frac{l(l+1) - s(s+1)}{I(I+1)}. \qquad ...(105)$$

The magnetic dipole moment is measured in terms of nuclear magneton, defined as

$$\begin{aligned}\mu_N &= eh/2m_p = 5.05079 \times 10^{-27}\ A.m^2 \\ &= 3.15245 \times 10^{-8}\ eV - m^2/\text{weber}.\end{aligned} \qquad ...(106)$$

It is 1836 times smaller than the Bohr magneton μ_B on account of a factor $m_e/m_p = 1/1836$. In units of nuclear magneton μ_N

$$g_l = \begin{cases} 1 \textit{ for a proton} \\ 0 \textit{ for a neutron,} \end{cases} \qquad g_s = \begin{cases} 5.585 \textit{ for a proton} \\ -3.826 \textit{ for a neutron} \end{cases}$$

The magnetic moment of even-odd and odd-even nuclei is due to only a single (unpaired) nucleon. If the odd nucleon is a proton $g_l = 1$, $g_s = g_p = 5.585$ and if it is a neutron $g_l = 0$, $g_s = g_n = -3.826$. In this case $s = ½$ and $I = l + ½$ or $l - ½$.

For a odd A-nucleus, we may write Eq. (104) as

$$\mu = I\left[g_l \pm \frac{g_s - g_l}{2l+1}\right] \qquad \text{for } I = l \pm \tfrac{1}{2}. \qquad \ldots(107)$$

There are considerable number of methods which are used to determine nuclear spins and magnetic moments. We shall here limit ourselves to the following important ones :

(a) Analysis of the hyperfine structure in atomic spectra—The interaction of spin-orbit coupling splits the atomic levels and gives us the fine structure in the spectrum. In the same way these splitted levels split further by **J** – **I** coupling and leads to *hyperfine structure* in the spectral lines. The total angular momentum F for the atom results from a vector sum of the nuclear angular momentum $\boldsymbol{I}$ with numerical value $\sqrt{I(I+1)}\,\hbar$ and the electronic angular momentum $\boldsymbol{J}$ with numerical value $\sqrt{J(J+1)}\,\hbar$ as shown in Fig. 1.27. *(a)*. Thus we have

$$\mathbf{F} = \mathbf{I} + \mathbf{J}. \qquad \ldots(108)$$

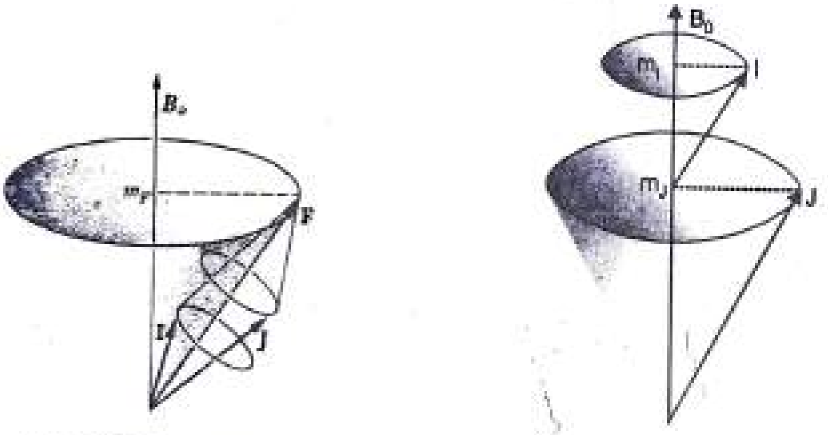

Fig. 1.27. Vector diagram showing the coupling and decoupling of I and J.

F is known as the hyperfine quantum number and $F\hbar$ gives the total angular momentum of the atom. Since each of the numbers can be integer or half integer, F is also an integer or half integer having values $J + I, J + I - 1, \ldots, |J - I|$. According to the usual rules of addition of quantum vectors the no. of values of F, *i.e.*, the number of hyperfine levels or states or the multiplicity for given values of I and J is $(2I + 1)$ if $I < J$ and $(2J + 1)$ if $I > J$. From the number of lines in a spectroscopic hypermultiplet, the nuclear spin I can be determined under suitable conditions.

The magnetic field is produced by the atomic electrons at the nucleus. The nuclei have very small magnetic dipole moments. The magnetic interaction energy between them is given by

$$W = -(\mu_I \cdot B_J) = -\mu_I B_J \cos(\boldsymbol{I}, \boldsymbol{J}).$$

Since $\boldsymbol{B}_J$ is parallel to $\boldsymbol{J}$ and $\mu_I = g_I I$ in μ_N, therefore above equation may be written as

$$W = a\, IJ \cos(\boldsymbol{I}, \boldsymbol{J}).$$

This energy produces hyperfine structure splitting of atomic levels. Here a is called coupling constant. If E_0 is the quantum energy, then the energy of the state is given by

$$E_F = E_0 + a' \, [J(J+1)]^{1/2} \, [I(I+1)]^{1/2} \cos(\boldsymbol{I}, \boldsymbol{J}).$$

Using the law of cosines for the combination of two vectors $\boldsymbol{I}$ and $\boldsymbol{J}$, we get

$$\begin{aligned} E_F - E_0 &= \tfrac{1}{2} a' [F(F+1) - I(I+1) - J(J+1)] \\ &= \tfrac{1}{2} h \, \Delta\nu_0 \, [F(F+1) - I(I+1) - J(J+1)] \end{aligned}$$

where $\Delta\nu_0$ is also called the hyperfine *separation constant*. The energy spacing between states with the same J, the same I, but different F values, is known as *hfs* splitting and is given by

$$E_F - E_{F-1} = h \, \Delta\nu_0 \, F. \qquad \text{...(109)}$$

Thus from the relative spacing of the hyperfine levels F and $F - 1$, I can be determined. The magnetic moment can be calculated from the magnitude of the splitting, provided that the nuclear spin is known. The nuclear magnetic moments of ^{209}Bi and ^{23}Na determined by this method were +4.080 and +2.217 nuclear magneton respectively.

The hyperfine structure splitting may also arise from the coupling between quadrupole moment of the nucleus and the gradient of the electric field produced by the electrons. This is usually smaller. This electric quadrupole hyperfine structure can be seen by X-ray spectra of muonic atoms.

Effect of external magnetic field on Hyperfine structure—If an external magnetic field $\boldsymbol{B}_0$ is applied to the atom, Zeeman effects occur in hyperfine structure. It is due to both the internal magnetic field $\boldsymbol{B}_J$ and the applied field $\boldsymbol{B}_0$.

If the applied field $\boldsymbol{B}_0$ is very small, the coupling between $\boldsymbol{I}$ and $\boldsymbol{J}$ persists and the resultant vector $\boldsymbol{F}$ will precess about the direction of $\boldsymbol{B}_0$, as shown in Fig. 1.27. The each hyperfine level F is broken up into $2F + 1$ magnetic substates (m_F), where $m_F = F, F - 1, F - 2 \ldots, -(F - 1), -F$. This is the *Zeeman effect* of hyperfine structure. The interaction energy

$$W = a \, I \, J \cos(\boldsymbol{I}, \boldsymbol{J}) - m_F \, g_F \, \mu_B \, B_0, \qquad \text{...(110)}$$

where g_F is a factor of the order of g_J, the atomic Lande-factor (which is often negative) defined in terms of the Bohr magneton μ_B. The energy difference between adjacent magnetic substates is approximately $\mu_J \, B_0/F$.

When the external magnetic field $\boldsymbol{B}_0$ is increased, the frequency of precession of $\mathbf{F}$ about $\boldsymbol{B}_0$ increases. Because of the small value of μ_I, the coupling between $\boldsymbol{I}$ and $\boldsymbol{J}$ is weak and the frequency of their precession about $\boldsymbol{F}$ is small. At sufficiently large value of $\boldsymbol{B}_0$, the frequency of precession of $\boldsymbol{F}$ about $\boldsymbol{B}_0$ exceeds that of $\boldsymbol{I}$ and $\boldsymbol{J}$ about $\boldsymbol{F}$. Thus the decoupling of the $\boldsymbol{I}$ and $\boldsymbol{J}$ takes place and these two vectors precess independently about the field direction, as shown in Fig. 1.27*(b)*. Each becomes space quantized independently in the direction of $\boldsymbol{E}_0$ with independent magnetic quantum numbers m_I and m_J. This is called *Paschen – Back effect*. The interaction energy

$$W = a \, m_I \, m_J - m_I \, g_I \, \mu_N \, B_0 - m_J \, g_J \, \mu_B \, B_0, \qquad \text{...(111)}$$

where the first term measures the interaction between nuclear and atomic moments μ_I and μ_J and the other two terms give the energy of these moments individually in the external field. The second term is however negligible.

Each level of a given m_J splits into $2I + 1$ substates corresponding to $m_I = I, I - 1, \ldots -(I - 1), -I$. *This number is same for all terms in an atom.* The spectroscopic diagram of the splitting of a $2S_{1/2}$ atomic state due to a nuclear angular momentum $I = 1$ caused by internal fields (hyperfine structure), a very weak field and weak field is as shown in Fig. 1.28. For $2S_{1/2}$ level, $L = 0$, $S = 1/2$, $J = 1/2$. The hyperfine structure by internal fields only (zero field) has two levels corresponding to $F = 3/2$ and $F = 1/2$, using relation $\boldsymbol{F} = \boldsymbol{I} + \boldsymbol{J}$. At very weak fields, the substates are in terms of F and m_F. At weak fields, the states are determined in terms of I and its components m_I, and J and its components m_J. At very high magnetic fields, the quantum number J will also be broken up into its components S and L.

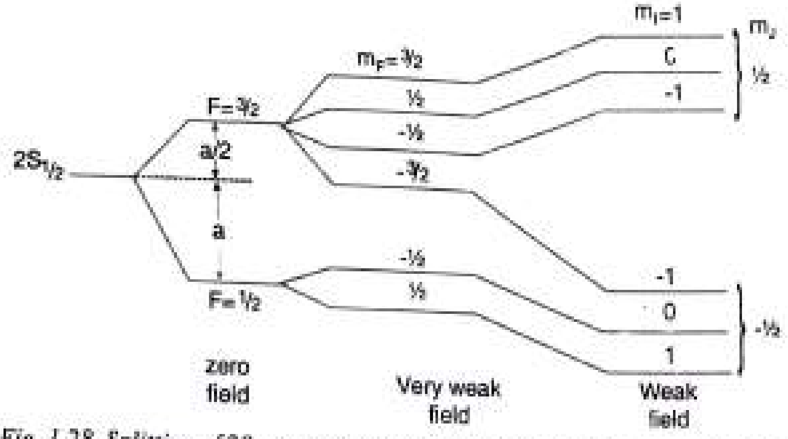

Fig. 1.28. Splitting of $2S_{1/2}$ atomic state with nuclear angular momentum $I = 1$.

Breit and Rabi in 1931 deduced formula for the hyperfine splitting, Zeeman splitting and Paschen Back splitting, which has been supported by experiments on nuclear effects in optical spectroscopy.

(b) Study of alternating intensities in band spectra—An important means of measuring nuclear spin has been to study the band spectra of homonuclear diatomic molecules, such as H_2. The wave functions may be symmetric or anti-symmetric in their nuclear spins. A gas of homonuclear diatomic molecules essentially consists of molecules of two types : *(i) Ortho-molecules* whose combined nuclear spin wave functions are symmetrical in the two nuclei. *(ii) Para-molecules* whose nuclear spin wave functions are anti-symmetric. The symmetric spin states are allowed only if the rotational quantum number is even for Bose statistics or odd for Fermi statistics and the antisymmetric spin states are allowed for alternate possibilities for the quantum number.

If there was no nuclear spin, the statistical weight of any rotational level for which the total angular momentum is J would be $(2J + I)$. But the presence of nuclear spin changes the statistical weights of the levels of different extent in the symmetrical and antisymmetrical cases. Let $g_s(2J + 1)$ and $g_a(2J + 1)$ be the statistical weights of the levels in the symmetric and anti-symmetric cases respectively. Theoretical considerations show that the ratio of the weight factors g_a/g_s is $(1 + I)/I$ when the nuclei obey Fermi statistics and is $I/(1 + I)$ when the nuclei obey Bose statistics.

Intensity of a level depends upon the weight factor. Transitions can take place between a strong and a weak level. This gives rise to the alternative strong and weak lines actually observed. The ratio of the intensities of the successive lines is equal to $(1 + I)/I$ regardless of which type of statistics is obeyed by the nuclei in a homonuclear diatomic molecule. The intensities of the successive lines in the band spectra of homonuclear diatomic molecules, preferably in the Raman effect, are measured accurately. Hence the nuclear spin can be determined. This method gives no information about the nuclear magnetic moment. For example the observed value of this ratio is 2.8 in case of the moleculer band spectrum of $^3He - {}^3He$. For $I = 1/2$, the expected value of this raito is 3 and for $I = 3/2$, it is 1.67. Therefore there is little doubt that the angular momentum I of ^3He is $1/2$.

This method can be applied when the nuclear spin is small. In the case of heavy elements the separation of individual lines becomes small and thus makes measurements impossible.

(c) Molecular Beam Resonance Method—The existence of magnetic moments of atoms was beautifully demonstrated by Stern and Gerlach in 1922. A well defined beam of neutral silver atoms was directed into the region of an inhomogeneous magnetic field. The beam splitted on account of the interaction between the magnetic moment of the atom with the inhomogeneous field. Frisch and Stern in 1933 were able to make the first measurements of the proton moment by the similar type of molecular beam apparatus.

Rabi and coworkers in 1939, introduced a very powerful extension of the Stern and Gerlach technique. This method is *called molecular beam magnetic resonance method*, as it works on the application of the nuclear magnetic resonance principle. When a nucleus of the magetic moment μ is placed in a magnetic field *B*, it will precess with a Larmor angular frequency ω_L about the direction of magnetic field, given by

$$\omega_L = \mu B/Ih. \quad \text{...(112)}$$

It is independent of the orientation of the magnetic moment with respect to the *B*-direction and is therefore same for any of the $2I + 1$ orientations of angular momentum quantum number *I*, allowed quantum mechanically.

A narrow stream of neutral atoms or molecules from the source oven *O* passes successively through three magnets *A*, *C* and *B*. The *A*-magnet and the *B*-magnet are both inhomogeneous field magnets with the same direction of the magnetic field **B**, but with opposite field gradients *dB/dz*. The *C*-magnet is a homogeneous field magnet. In the Rabi's original apparatus a single hairpin loop was placed inside the gap of the poles of magnet *C* and connected to a radio frequency (*RF*) generator. A schematic diagram of the apparatus is shown in Fig. 1.29. A very small fraction of these molecules will pass through the collimating slit *S* and reaches the detector at *D*. In the absence of an inhomogeneous magnetic deflecting fields, *OSD* is the path of direct beam of molecules. Inhomogeneous fields produced by specially designed magnets *A* and *B* are in the same direction, but their gradients, *dB/dz* are in opposite directions and are so adjusted that the beam is refocused. The deflection produced by each magnetic field depends upon the velocity of the molecule which is the function of temperature. In the region of homogeneous field *B* due to a magnet *C* there is a high frequency alternating magnetic field produced by sending a current in opposite directions through two parallel wires *W* placed between the pole faces of the magnet *C*. When a molecule of magnetic moment μ enters the region, it will precess about *B* with the frequency ν.

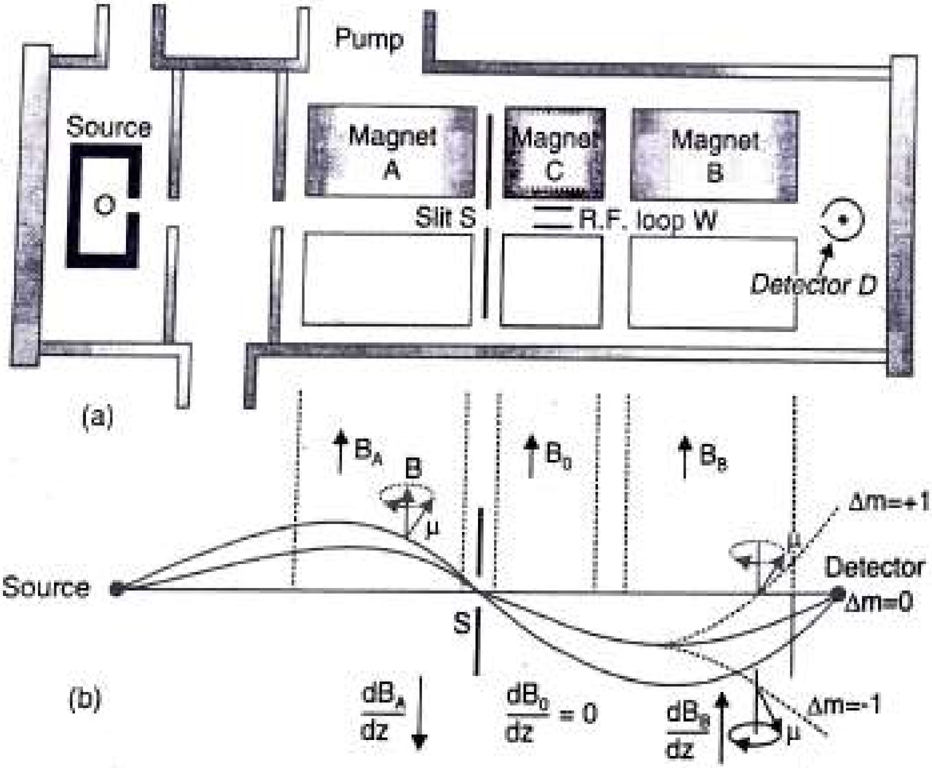

Fig. 1.29. Schematic diagram of the apparatus used in the molecular beam experiment.

If *B* reaches a value for which the Larmor frequency ν_L of the molecules is equal to the frequency *f* of the oscillating field, resonance sets in, producing a large increase or decrease in the angle between **μ** and **B**. Thus at resonance the molecules are no more refocused at *D* by the field due to *C* and we observe a decrease in intensity at the detector. If the beam intensity is plotted as a function of the magnetic field strength *B* produced by the magnet *C* at a constant frequency of the alternating field, the resonance value is the minimum value of curve.

Since $\mu = gI\mu_N = g(e\hbar/2m)I$. ...(113)

$$\therefore \quad g = \frac{2m\mu}{eI\hbar} = \frac{2m}{e}\frac{\omega}{B} = \frac{4\pi m}{e}\frac{f}{B}. \qquad ...(114)$$

This equation gives g factor for the particular nucleus. If its nuclear spin quantum number I is known, then

$$\mu = gI. \qquad ...(115)$$

In the case of ^7Li nucleus $I = 3/2$, measured value of $g = 2.1688$. Hence its magnetic moment = 3.2532 nuclear magnetons.

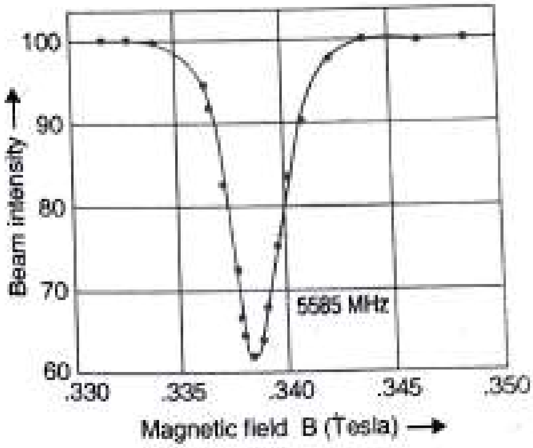

Fig. 1.30. Curve showing the occurrence of magnetic resonance for ^7Li.

(d) Nuclear induction and resonance absorption spectra—Block, Hansen and Packard, in 1946 introduced a modification in the magnetic resonance spectra method. They measured the induced emf., or some effect due to the induced emf., produced by a change in the orientation of the nuclear magnetic moments in a sample (liquid or solid).

In this nuclear induction experiment, a sample of a suitable diamagnetic material (*e.g.*, water) is placed between the poles of an electromagnet that provides steady magnetic field $B_z = B_0$. An inducing coil surrounds the same in $y - z$ plane to provide an oscillating field $B_x = 2B \cos \omega t$. This field is equivalent to two oppositely rotating fields of flux density B applied in $x - y$ plane and allowed to rotate with angular velocity ω. The field rotating in the direction opposite to that of the precession about B_0 may be disregarded. To detect the reorientation of the rotating magnetization a pickup coil also called receiver coil with its axis in the y-direction (*i.e.*, prepedicular to both B_0 and B) is used. The output (induced emf.) produced in the pickup coil is amplified and fed as the y-deflection on an oscilloscope. The field B_0 is modulated by a small $50 Hz$ field so that the resultant magnetic field sweeps through the resonance value $B_0 = \omega/\gamma_I$, where γ_I is the nuclear gyromagnetic ratio $(= \mu_I/I\hbar)$. The $50\ Hz$ modulation provides the time base for the oscilloscope, Fig. 1.31.

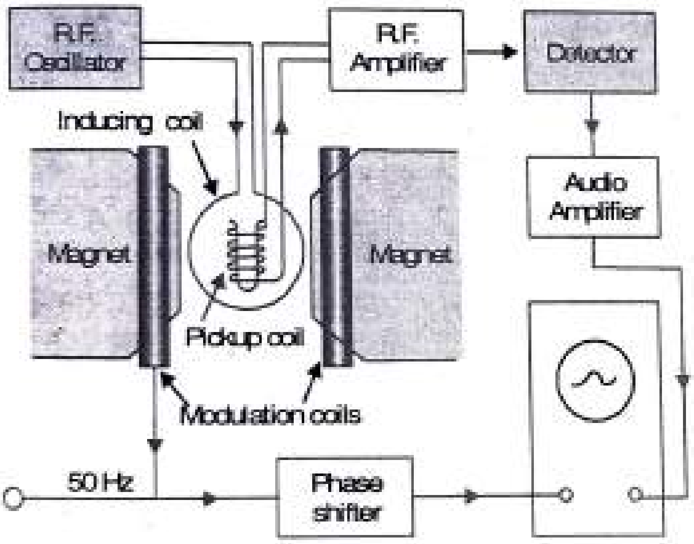

Fig. 1.31. Nuclear Induction Apparatus of F. Block et al.

Due to the constant magnetic field B_0 nuclear magnet precesses about the z-axis with the Larmor precessional frequency v. Due to the change in magnetic flux produced by the magnetization of the sample in y-direction, the emf is induced in the pickup coil. The closer the alternating magnetic field frequency is to the Larmor precession frequency of the nuclei, the greater will be the change in induced emf. Thus the output signal on the oscilloscope gives the Larmor precession frequency and therefore the nuclear gyromagnetic ratio. The shape of the signal depends on the relaxation time for the protons used and on the internal fields in the specimen. In the original experiment *a* sample of about 1.5 cm^3 volume was used and about millivolt signals were obtained on a 10 turn receiver coil with a frequency of 7.765 MHz and resonance field of 0.1826 T.

Nuclear Magnetic resonance absorption method was developed by Purcell, Torrey and Pound in 1948. In this experiment, the sample forms part of a resonant circuit and the transmission of radiofrequency power through the circuit is measured as a function of steady magnetic field B_0 applied to the sample. The radiofrequency oscillatory field B is developed by the circuit at right angles to B_0. At the nuclear resonance field, the Q-value of the resonant circuit is lowered due to the extra absorption of power by the precessing nuclei and a sharp change in the output power is detected.

In the original experiment, they put a piece of paraffin about $850 cm^3$ into a resonant cavity and placed the resonator in *a* strong magnetic field. The resonant frequency was 29.8 MHz. The output of the resonator was balanced against a signal derived from the input in a bridge circuit, so that the resonant absorption could be clearly displayed. By a 50 Hz modulation the field B_0 was varied through the nuclear resonance value of 0.7100 T, a 50 per cent change in output power was observed.

These methods measure nuclear gyromagnetic ratios. If I is known, then μ_I may be obtained in the absolute units. If I is not known, the nuclear g-factor is obtained using the relation $g_I = \gamma_I(2m_p/e) = \gamma_I(\hbar/\mu_N)$. The spin I may be found from resonance experiment itself if there are internal electric fields which produce fine structure of $2I$ lines instead of a single resonance frequency. The sign of μ may be obtained with the induction method if rotating field is applied from two coils with their axes set at 90°.

(e) Analysis of microwave spectra—A very powerful tool for nuclear spin determination is microwave spectroscopy. Many transitions, particularly between rotational states of heavy molecules occur in the microwave region. Analysis of such hyperfine structure in microwave spectra offers a direct means of estimating the spins and magnetic moments of nuclei.

In the *gaseous absorption spectroscopy*, the observations are made of the variation of the absorption coefficient of gas in a cell with the frequency of the incident radiation. The structure visible in the absorption near the frequency of rotational transition is a hyperfine effect. The hyperfine structure is not directly due to the nuclear magnetic moment. Molecular magnetic fields are small, the nuclear spins however orient in the normal way in the internal field. The energy splitting arises because of the interaction of the nuclear electric quadrupole moment with the molecular electric field gradient. The number of hyperfine states is directly determined by the nuclear spin as the axis of the quadrupole moment is fixed with respect to the nuclear spin axis. The spacing is not determined by the nuclear magnetic moment. If the molecular field can be calculated one may find electric quadrupole moment. This technique does not extend much above a frequency of 3×10^{11} Hz and the lighter molecules having rotational frequencies lying in the infra red region can not be studied. Nuclear spins for ^{10}B, ^{33}S, ^{35}Cl and several other nuclei using suitable molecules mainly consisting atoms with spin zero nuclei have been determined by this method.

Microwave spectroscopy can be used for nuclear mass determination as a high precession method, as distinct rotational absorption lines are observed for each isotopic species. It is also possible to observe the Zeeman splitting of the hyperfine lines of a given rotational transition.

In the *electron paramagnetic resonance absorption* spectroscopy, the nuclear spin I is found by counting the absorption peaks and the nuclear moment μ_I is obtained from the spacing between them if the internal field can be calculated. This method has been widely used for investigations of the solid state. Many paramagnetic ions in crystalline solids behave as if their magnetic effect is due to a single electron spin. If their nuclei have a spin I, a hyperfine splitting occurs due to the interaction between nuclear and electronic moments. In an external field B_0, each of two levels $m_s = \pm 1/2$, is split into $2I + 1$ hyperfine levels. Because of the small interaction of the nuclear moment with the microwave field, the microwave absorption takes place between the substates with the same value of m_I at a frequency $\nu_e \approx 2\mu_B B_0/h$. The $2I + 1$ absorption peaks are found as the field B_0 is increased. The apparatus used by Van Wieringen is shown in Fig. 1.32. Here K is a klystron which generates *a* microwave of constant frequency in the wave guide G. The specimen S is placed in a resonant cavity C mounted between the pole pieces of a magnet M. The signal reflected from C is fed to the detector D with a directional coupler R. The signal level is controlled by the wave meter W and attenuator A. Magnetic field B_0 is varied and the detector output is recorded at a fixed frequency.

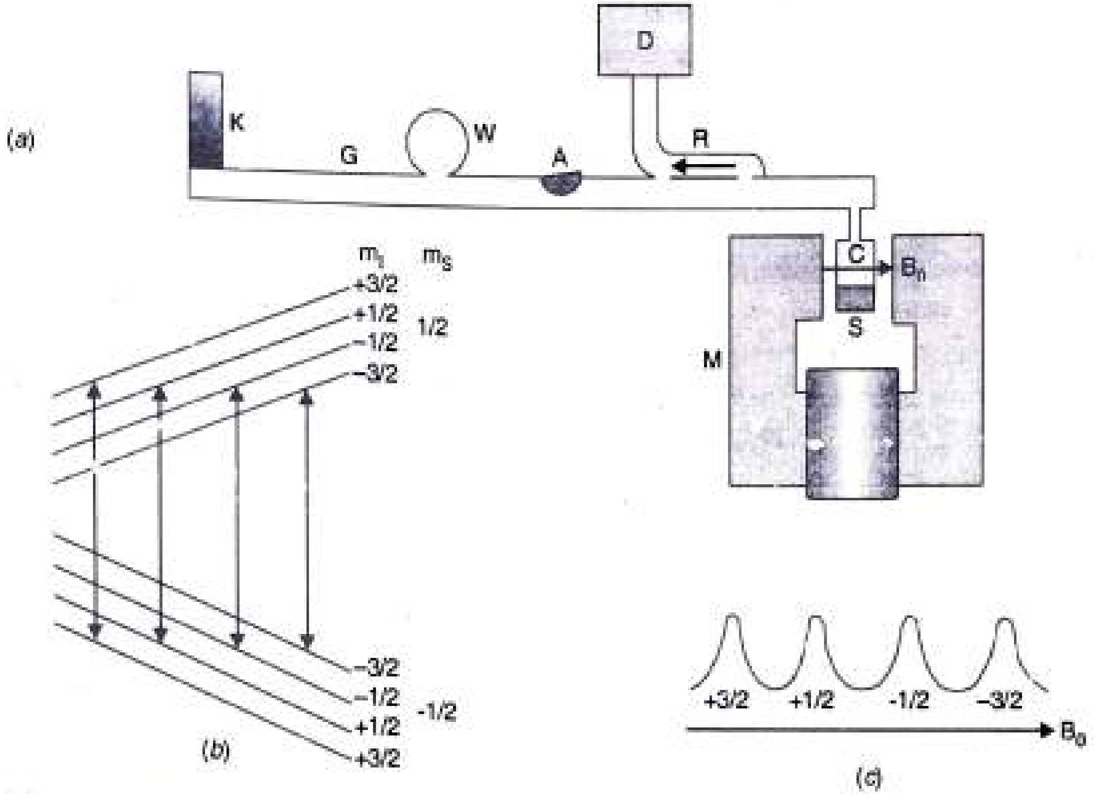

Fig. 1.32. (a) Paramagnetic resonance absorption apparatus, (b) Energy levels with spin $S = 1/2$ and nuclear spin $I = 3/2$ in a field B_0 and (c) absorption lines corresponding to $\Delta m_I = 0$.

1.12 ELECTRIC MULTIPOLE MOMENT

We now consider how the internal distribution of nuclear charge contributes to the effective moments. We place a nucleus having a charge density $\rho(\boldsymbol{r})$ with its charge center at the origin. As the nucleus is surrounded by its orbital electrons hence an electrostatic potential φ which originates from these electrons produces an electrostatic interaction energy, resulting from the interaction between φ and ρ. This energy is defined as

$$U = \int_{\tau} \rho(\boldsymbol{r})\varphi(\boldsymbol{r})\,d\tau. \qquad \ldots(116)$$

where $d\tau$ represents a small volume element. To express this energy in terms of the electric moments of the distribution, we expand the potential in a Taylor's series about the origin or the center of charge, as

$$\varphi(\boldsymbol{r}) = \varphi(x,y,z) = \varphi_0 + \left[\left(\frac{\partial\varphi}{\partial x}\right)_0 x + \left(\frac{\partial\varphi}{\partial y}\right)_0 y + \left(\frac{\partial\varphi}{\partial z}\right)_0 z\right] + \left[\frac{1}{2}\left(\frac{\partial^2\varphi}{\partial x^2}\right)_0 x^2 + \frac{1}{2}\left(\frac{\partial^2\varphi}{\partial y^2}\right)_0 y^2 + \frac{1}{2}\left(\frac{\partial^2\varphi}{\partial z^2}\right)_0 z^2 \right.$$
$$\left. + \left(\frac{\partial^2\varphi}{\partial x\partial y}\right)_0 xy + \left(\frac{\partial^2\varphi}{\partial x\partial z}\right)_0 xz + \left(\frac{\partial^2\varphi}{\partial y\partial z}\right)_0 yz\right] + \ldots$$

where the subscript zero means that the quantity is evaluated at the origin.

In the tensor form, above equation may be written as

$$\varphi(\boldsymbol{r}) = \varphi_0 + x_i\left(\frac{\partial\varphi}{\partial x_i}\right)_0 + \frac{1}{2}x_i x_j\left(\frac{\partial^2\varphi}{\partial x_i\partial x_j}\right)_0 + \ldots = \varphi_0 + \boldsymbol{r}\cdot(\nabla\varphi)_0 + \frac{1}{6}(r^2\delta_{ij} + q_{ij})\left(\frac{\partial^2\varphi}{\partial x_i\,\partial x_j}\right)_0 + \ldots \qquad \ldots(117)$$

where

$$q_{ij} = 3x_i x_j - r^2\delta_{ij}. \qquad \ldots(118)$$

Inserting this value of $\varphi(\boldsymbol{r})$ in Eq. (116), we get

$$U = \varphi_0\int\rho(\boldsymbol{r})d\tau + (\nabla\varphi)_0\cdot\int\boldsymbol{r}\rho(\boldsymbol{r})d\tau + \frac{1}{6}\left(\frac{\partial^2\varphi}{\partial x_i\,\partial x_j}\right)_0\int(r^2\delta_{ij} + q_{ij})\rho(\boldsymbol{r})d\tau + \ldots \qquad \ldots(119)$$

Using the relations

$$E = -\nabla\varphi, \quad q = \int \rho(\boldsymbol{r})d\tau = Ze,$$

$$\boldsymbol{p} = \int \boldsymbol{r}\rho(\boldsymbol{r})d\tau, \quad Q_{ij} = \int \rho(\boldsymbol{r})\,(3x_i x_j - \delta_{ij} r^2)d\tau, \qquad \text{...(120)}$$

we get

$$U = q\varphi_0 - \boldsymbol{p}\cdot\boldsymbol{E}_0 - \tfrac{1}{6}Q_{ij}(\partial E_j/\partial x_i)_0 + \tfrac{1}{6}\nabla^2\varphi_0 \int r^2\rho(\boldsymbol{r})d\tau + \ldots, \qquad \text{...(121)}$$

where the symbols $\boldsymbol{E}$, q, $\boldsymbol{p}$, and Q_{ij} stand for electric field, total nuclear charge, electric dipole vector and electric quadrupole tensor respectively.

The first term simply gives the interaction of a point charge (monopole). The second term gives the energy of an electric dipole. The third term gives the energy of the electric quadrupole. The fourth term, which is basically a part of third term is known as energy associated with the isotope shift of atomic spectra and given by the relation

$$U_{is} = \tfrac{1}{6}\nabla^2\varphi_0 \int r^2\,\rho(\boldsymbol{r})d\tau. \qquad \text{...(122)}$$

If the potential $\phi(\boldsymbol{r})$ is due to an external applied electric field only, then according to Laplace's equation $\nabla^2\phi = 0$ and we have $U_{is} = 0$ and the interaction energy is given by

$$U = q\varphi_0 - \boldsymbol{p}\cdot\boldsymbol{E}_0 - \tfrac{1}{6}Q_{ij}(\partial E_j/\partial x_i)_0 + \ldots \qquad \text{...(123)}$$

The right hand side terms correspond to nuclear monopole, dipole, quadrupole, octupole and higher electric multipoles. The higher order terms of the charge distribution are important when the net charge q is zero and the dipole term also vanishes.

1.13. ELECTRIC QUADRUPOLE MOMENT

A quadrupole may be generated by two identical dipoles, one of which is displaced and inverted. It was shown in the previous section that the nuclear charge distribution can be described by a series of terms consisting of the total charge (mono-pole), the electric dipole moment, the electric quadrupole moment, the electric octupole moment, etc. The nuclear electric quadrupole moment is a measure of the lowest order of deviation of the nuclear charge distribution from a spherical shape. If the charge distribution has spherical symmetry, all moments as defined by Eq. (120) vanish. If there is axial symmetry with respect to oz or z-axis, the dipole moment vanishes but the quadrupole moment

$$Q_{zz} = \Sigma e_i\,(3z_i^2 - r_i^2) \qquad \text{...(124)}$$

is finite. The intrinsic quadrupole moment of the nucleus with respect to axial symmetry is given by

$$Q_0 = \int \rho(3z^2 - r^2)d\tau, \qquad \text{...(125)}$$

where $\rho d\tau$ is the charge within the volume element $d\tau$. In nuclear physics, it is customary to remove the dimensions of charge and we thus define the quadrupole moment as

$$Q = \frac{1}{e}\int(3z^2 - r^2)\rho d\tau. \qquad \text{...(126)}$$

This relation shows that $Q = 0$ for a spherically symmetric charge distribution $(<x^2> = <y^2> = <z^2> = \frac{1}{3}r^2)$. The Q is +*ve* when $3z^2 > r^2$ and the charge distribution is stretched in the z-direction (*prolate*-spheroid or egg shaped). In an oblate or discus like spheroid (pumpkin shaped) distribution $3z^2 < r^2$ and Q is –*ve*. Since the expression is divided by the electronic charge, the dimension of the quadrupole moment is that of an area. As it is very small, hence in nuclear physics it is measured in *barns* (1 barn = $10^{-28}\ m^2$).

In semi-classical calculations, one must consider the fact that the nuclear symmetry axis is not the *space fixed z-axis* but I-axis can be regarded as a symmetry axis. According to quantum mechanics the angular momentum vector I^* can never line up in any given direction say that of an external field, but always precess around it at some angle. The magnitude of I^* is $[I(I+1)]^{1/2}\hbar$ and the maximum projected value is $I\hbar$. Thus the smallest possible value of β is given by (assuming $I > 0$) the relation

$$\cos \beta = I/\sqrt{[I(I+1)]}. \qquad \text{...(127)}$$

Nuclear quadrupole moments are defined not to the body axis of the charge distribution (z'-direction) but to the precession axis (z-direction). The I^* is along z'-direction and $I\hbar$ is along z-direction.

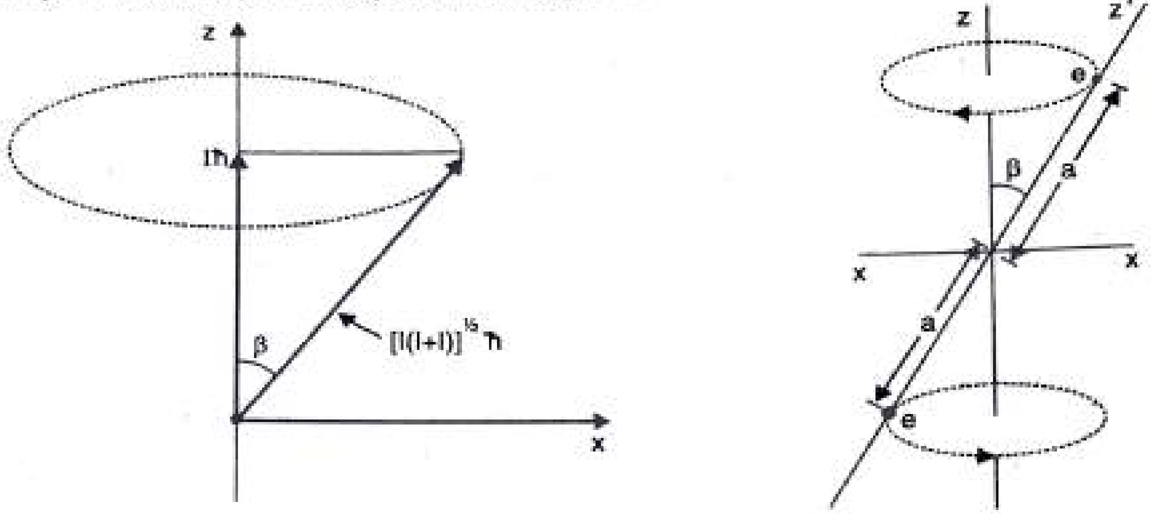

Fig. 1.33. Electric Quadrupole Moment.

For the charge distribution of Fig. 1.33*(b)*, the result of applying Eq. (126) to the z'-axis is

$$Q'_0 = (3a^2 - a^2)e + (3a^2 - a^2)e = 4e\,a^2.$$

Applying it to the z-axis, we get

$$Q_0 = 2ea^2(3\cos^2\beta - 1) = \tfrac{1}{2}Q'_0\,(3\cos^2\beta - 1)$$

$$\therefore \qquad Q_0 = \tfrac{1}{2}\frac{2I-1}{I+1}Q'_0 = \tfrac{1}{2}\frac{2I-1}{I+1}\int(3z'^2 - r^2)\rho\,d\tau. \qquad \text{...(128)}$$

Thus nuclei which have $I = 0$ and 1/2 can exhibit no quadrupole moment Q and hence smallest value of angular momentum I for which Q does not vanish is one.

Let us assume that the nuclei are uniformly charged ellipsoids of rotation with the semi-axis a along the axis of symmetry and the semi axis b ⊥ to the symmetry axis. Let us further suppose that $a = R(1 + \epsilon)$ and $b = R(1 - \tfrac{1}{2}\epsilon)$, where ϵ is a distortion parameter (the deviation from the average in the direction of symmetry axis $\Delta R/R$). These assumptions ensure that the volume of the distorted sphere is equal to the undistorted sphere. Thus for such an ellipsoid, with charge Ze, we have

$$Q = Z(3z^2 - r^2)_{av} = \tfrac{2}{5}Z(a^2 - b^2) = \tfrac{6}{5}ZR^2\epsilon. \qquad \text{...(129)}$$

From observations of Q, we see that the distortions of nuclei from the perfect sphere are relatively small.

In a quantum mechanical definition, the charge density ρ is replaced by the probability density $|\Psi|^2$ and the Eq. (128) thus reduces to

$$Q = \tfrac{1}{2}\frac{2I-1}{I+1}\int\Psi^*(r)(3z'^2 - r^2)\Psi(r)\,d\tau. \qquad \text{...(130)}$$

From the Nuclear Data 5,443 (1969), the largest positive quadrupole moment is 8×10^{-28} m^2 for ^{176}Lu and the largest negative quadrupole moment is -3×10^{-28} m^2 for ^{233}Pa. The fact that the deuteron possesses a small quadrupole moment (2.73×10^{-31} m^2) is an important to the basic nature of nuclear forces. The study of quadrupole moment gives an idea about nuclear closed shells and helps in the study of nuclear models.

The quadrupole moments of nuclear ground states may be detected through their interaction with electric field gradients. Observations of various effects due to the interaction result in values of the *quadrupole* *coupling*, which is the product of the Q and the electric field gradient. The coupling measurements have been made from optical hyperfine spectra, microwave spectroscopy and paramagnetic resonance spectroscopy. Q have also been measured from the "isotope shift."

1.14 POTENTIAL WELL

Let us plot the potential binding energy of the nucleon versus the distance from the other nucleon or from the centre of the nucleus. This is done in Fig. 1.34 *(a)* for a proton-neutron-pair, in Fig. *(b)* for a proton-proton pair, in Fig. *(c)* for a nucleus and neutron and in Fig. *(d)* for a nucleus and proton. They are seen to be very similar except that the proton-neutron potential has no positive contribution as has the proton-proton potential due to the Coulomb repulsion between the two protons. For a neutron inside the nucleus, energy is negative since forces are attractive. The shape of the curve has suggested the name of *sink* or *well* of potential to describe this phenomenon. The phenomenon is different for the interaction potential between nuclei and protons or other charged particles such as α-particles. Outside the nucleus there remains only the Coulomb repulsion, whose potential is represented by an hyperbola. The inner sides of the well extend much higher than before and are connected in an unknown way with the Coulomb hyperbolas. The various shapes of the potential well are discussed in the chapters on *Nuclear Forces and Nuclear Models.*

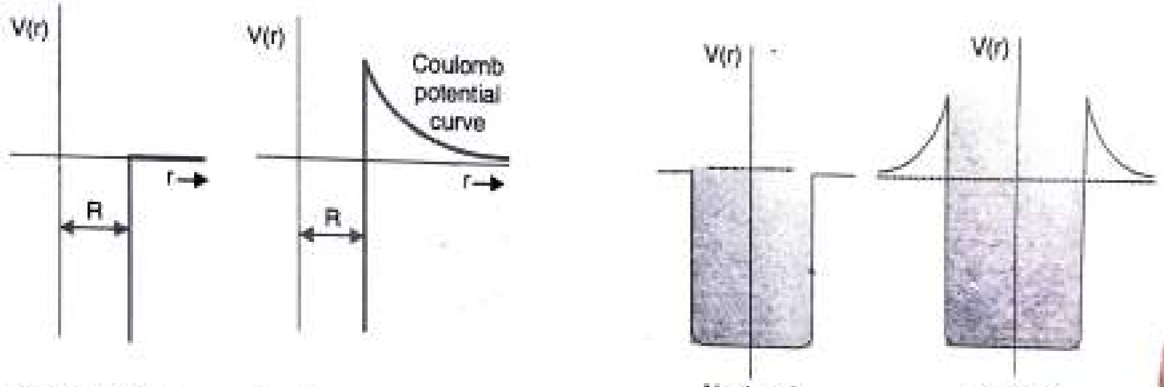

Proton-neutron
(*a*)

Proton-proton
(*b*)

Neutron in Nucleus
(*c*)

Proton in Nucleus
(*d*)

Fig. 1.34. Potential wells in various cases.

A Brief Summary

The *nucleus* is the heavy central core of the atom, with roughly same density (~ 10^{13} times that of the solid matter). A cubic inch of nuclear material would weigh about 1 billion tons. It is consisted of neutrons and protons, also called nucleons. The total number of nucleons is called mass number A, because it is very close to the atomic weight (mass) of atom.

The *spin* and *symmetry* character of nuclei composed to protons and neutrons are in agreement with the measurements. For nuclei with A-even and Z-odd, the spin and symmetry character disagree with the measurements if nuclei are composed of protons and electrons.

The measurements of electron scattering provide information about the *nuclear charge distribution, i.e.*, the distribution of protons in the nucleus. These measurements showed that the charge density of nuclei is constant in the nuclear interior and falls fairly rapidly to zero at the nuclear surface. The radius, the distance at which density has one half its interior value, increases slowly with increasing the mass number A. The charge density in the interior decreases slowly with increasing A. The mass density in the interior is approximately the same for all nuclei.

The mass of an atom was measured in terms of the mass of one ^{16}O atom and symbol used was amu (1 atomic mass unit = 1/16 of the mass of one oxygen atom). Now the measurements are made in terms of 1/12 of the rest mass of one $^{12}_{6}C$ atom and represented by the symbol u. Mass spectrometers/spectrographs are used for measuring the mass of the atom accurately and to provide accurate determinations of the relative abundance of the various isotopes. In the mass spectrograph, a photographic plate is used to obtain the series of lines, while in mass spectrometer each part of the spectrum is allowed to fall on a fixed detecting slit and measured electrically. The ion source, energy filter, momentum filter and detector (or a photographic plate) are the essential components of the mass spectrometers. It has been observed that the mass of an atom is always smaller than the mass of the constituent parts. This difference of mass is called mass deficiency or mass loss. The energy equivalent to this mass (ΔM) is called the binding energy of the nucleus. It is the energy required to dissociate the constituents of the nucleus. The binding energy of the nucleus divided by the number of nucleons it contains is found roughly constant for most of the nuclei, especially in the middle A region and is about 8 *MeV*. This property shows that the nuclear forces are saturated, similar to the saturation of molecular forces in covalent bonding, but without any link in their origins. For small Z, the stable nuclei have $Z = N$. This shows that the nuclear forces operate symmetrically on neutrons and protons or the nuclear forces are charge independent. For large Z, the stable nuclei tend to have $Z < N$, due to the Coulomb repulsions between protons. A comparison of binding energies for light and heavy nuclei shows that it is easy for the light nuclei to fuse and for the heavy nuclei to disintegrate (fission reaction).

The nuclei have magnetic dipole moments, which arise from the intrinsic magnetic dipole moments of the protons and neutrons in the nuclei and from the currents circulating in the nuclei due to the motion of the protons. Nuclei with A and Z both even have magnetic dipole moment zero. The total nuclear angular momentum quantum number I, usually called the nuclear spin is an integer for nuclei of even A, with $I = 0$ if Z is also even, and is a half integer for nuclei of odd A. The nuclei with integral spin quantum number I (nuclei of even A) are of the symmetric type (bosons), while nuclei with half integral (nuclei of odd A) are of the antisymmetric type (fermions). It is not true that the magnetic dipole moment is entirely due to the single odd nucleon and all the other nucleons are paired off with total angular momenta and magnetic dipole moments that cancel strictly.

Many nuclei are not precisely spherical in shape, but are in the shape of an ellipsoid. The departure of the nuclear charge distribution from spherical symmetry is specified by the nuclear quadrupole moment Q. The ellipsoidal charge distribution is elongated in the direction of its symmetry axis for $Q > 0$ or (positive). Q becomes more positive with the increase of elongation. For $Q < 0$ (or negative), the ellipsoidal charge distribution is flattened in the direction of its symmetry axis. For nuclei spin $I \geq 1$, the hyperfine splitting measurements show that Q may be positive or negative. For nuclei with $I =$ 0 or 1/2, no departures from spherical shape are observed and therefore $Q = 0$. It is because the nuclei with no nuclear spin ($I = 0$) do not have any particular orientaton in space. The nuclei must then have all possible orientations in space and the averaged over a sample containing many nonspherical nuclei, the nuclei would appear to be spherical. For $I = 1/2$, there are only two possible orientations of the nuclear shapes relative to the direction defined by any electric field applied to the nuclei. Since both give the same energy of interaction between this field and the electric quadrupole moments. On the average the hyperfine splitting is zero and thus no evidence of quadrupole moments can be observed. The nuclei in the region of the rare earth elements, the largest values of Q are found.

The difference between the experimental values of μ_p and μ_n and the theoretical values can be explained by assigning a definite structure to the nucleons.

EXERCISES

Example 1. *What is the distance of closest approach of a 2 MeV proton to a gold nucleus? How does this distance compare with those for a deuteron and an α-particle of the same energy?*

The distance of closest approach b is that distance from the nucleus at which the total energy of incident particle is equal to the potential energy and is given by

$$\tfrac{1}{2}MV_0^2 = Zze^2/4\pi\varepsilon_0 b \text{ or } b = 2Zze^2/4\pi\varepsilon_0 MV_0^2.$$

Here $\tfrac{1}{2}MV_0^2 = K.E.$ of proton $= 2MeV = 2 \times 1.60218 \times 10^{-13}$ joule,

$Z = 79$, $z = 1$, $e = 1.60218 \times 10^{-19}$ coulomb, $4\pi\varepsilon_0 = 1/9 \times 10^9$

$$\therefore \quad b = 2 \times 79 \times 1 \times (1.60218 \times 10^{-19})^2 \times 9 \times 10^9/2 \times 2 \times 1.60218 \times 10^{-13}$$

$$= 5.69575 \times 10^{-14} \text{ meter.}$$

This distance b is same for deuteron of the same energy as charge ze on the deuteron is same as that of proton.

Since the charge on the α-particle is double that of on the proton, hence $b = 1.13915 \times 10^{-13}$ meter.

Example 2. *The measured nuclear spin and symmetry character of nitrogen with Z = 7 and A = 14 are 1, symmetric. Show that these measured values disagree with the assumption that nuclei contain A protons and A − Z electrons.*

If the nucleus contains 14 protons and 7 electrons, it contains an odd number of particles, 14 + 7 = 21. All these particles have half integral intrinsic spin angular momentum quantum numbers. The rule of combination gives that the total angular momentum quantum number or the spin will be half integral, which is in disagreement with the measurements.

The symmetry character of a nucleus containing an odd number of antisymmetric particles must be antisymmetric, *i.e.*, $(-1)^{odd} = -1$ or antisymmetric. This is again in disagreement with the measurements. (*i.e.*, symmetric nucleus).

If the nucleus contains 7 neutrons and 7 protons, the total number of particles will be 7 + 7 = 14 (even). Since the neutrons have half integral intrinsic spin angular momentum quantum number and symmetry character as protons. Thus the total spin of even particles will be integral and the nucleus will be of the symmetric type. Both these predictions are in agreement with the measurements.

Example 3. *If an electron is confined within a nucleus whose diameter is 10^{-14} m, estimate its minimum kinetic energy and the Coulomb energy.*

Prove that the electrons are not the nuclear binding blocks.

One half of the de Broglie wavelength of the minimum energy electron would fit into the diameter of the nucleus. Thus the electron's momentum would be of the order of magnitude

$$p = \frac{h}{\lambda} = \frac{6.6262 \times 10^{-34}}{2 \times 10^{-14}} = 3.3131 \times 10^{-20} \text{ Joule sec./m} = 62\ MeV/c.$$

The corresponding kinetic energy

$$K.E. = \sqrt{p^2c^2 + E_0^2} - E_0 = \sqrt{(62\ MeV)^2 + (0.511\ MeV)^2} - 0.511\ MeV$$
$$= 61.49\ MeV.$$

Since $R = R_0 A^{1/3}$, therefore

$$A = \left(\frac{R}{R_o}\right)^3 = \left(\frac{0.5 \times 10^{-14}}{1.4 \times 10^{-15}}\right)^3 = 46. \text{ and } Z = A/2 = 23.$$

The Coulomb energy per electron

$$E_C = -\frac{Ze^2}{4\pi\varepsilon_0 R} = -\frac{9 \times 10^9 \times (1.60218 \times 10^{-19})^2}{0.5 \times 10^{-14}}$$
$$= -1.0627 \times 10^{-12} \text{ Joule} = -6.633\ MeV.$$

This is negligible compared to the 61.49 *MeV*. The electrons emitted from nuclei have K.E. of a few MeV, and not the predicted value of = 54 *MeV*. There results show that the electrons are not the nuclear binding blocks.

Example 4. *Electrons of kinetic energy 500 MeV are scattered from a target of nuclei into a diffraction pattern that has minima with an average separation of θ = 30°. Find the charge distribution radius r′ of the target nuclei.*

$$\text{The electron momentum } p = \frac{E}{c} = \frac{K}{c} = \frac{500\ MeV}{3 \times 10^8\ m/sec} = \frac{500 \times 1.60218 \times 10^{-13}}{3 \times 10^8} \text{ Joule sec/m.}$$
$$= 2.67 \times 10^{-19} \text{ Joule sec/m.}$$

∴ The de Broglie wavelength associated with these electrons

$$\lambda = \frac{h}{p} = \frac{6.6262 \times 10^{-34}}{2.67 \times 10^{-19}} = 2.48 \times 10^{-15}\ m.$$

From the theory of diffraction, we have

$$r' = \frac{\lambda}{\theta} = \frac{2.48 \times 10^{-15}}{30\pi/180} = 4.74 \times 10^{-15} m = 4.74\ fm.$$

Example 5. *Chlorine-33 decays by positron emission with a maximum energy of 4.3 MeV. Calculate the radius of the nucleus from this.*

The decay scheme is

$$^{33}_{17}Cl \rightarrow {}^{33}_{16}S + {}^{0}_{-1}e + \nu + E_\beta .$$

When the positron emits with a maximum energy, the neutrino energy will be zero and the daughter nucleus ^{33}S will be formed in the ground state.

$$\therefore \qquad E_\beta = \frac{3}{5}\frac{e^2A^{2/3}}{4\pi\varepsilon_0 R_0} - 1.80\ MeV = 4.3\ MeV.$$

$$\text{or} \qquad \frac{3}{5}\frac{e^2A^{2/3}}{4\pi\varepsilon_0 R_0} = 6.1\ MeV = 6.1 \times 1.60218 \times 10^{-13}\ \text{joule}$$

$$\text{or} \qquad R_0 = \frac{3}{5}\frac{e^2A^{2/3}}{4\pi\varepsilon_0 \times 6.1 \times 1.60218 \times 10^{-13}} = \frac{3}{5}\frac{(1.60218\times 10^{-19})^2(33)^{2/3}\times 9\times 10^9}{6.1\times 1.60218\times 10^{-13}}$$

$$= 1.4592 \times 10^{-15}\ \text{meter.}$$

$$\therefore \qquad R = R_0A^{1/3} = 1.4592 \times 10^{-15} \times 33^{1/3} = 4.68 \times 10^{-15} m.$$

Example 6. *In a mass spectrometer, a single charged + ve ion is accelerated through a potential difference of 1000 volts. It then travels through a uniform magnetic field for which B = 1000 gauss and is deflected into a circular path of 18.2 cm in radius. What is (a) the speed of the ion? (b) the mass of the ion, in gms and u? and (c) the mass number of the ion?*

In passing through accelerator, the positive ions carrying a charge ne, acquire kinetic energy, given by the relation $\frac{1}{2}\ Mv^2 = neV$.

If R is the radius of curvature of the circular path of the ion when travels through a uniform magnetic field B, then $Mv^2/R = B\ nev$. From these relations, we have

$$v = \frac{2V}{RB} = \frac{2\times 1000}{18.2\times 10^{-2}\times 1000\times 10^{-4}} = 1.099\times 10^5\ \text{meter/sec.}$$

$$\text{Hence mass of the ion } M = \frac{2neV}{v^2} = \frac{2\times 1\times 1.60218\times 10^{-19}\times 1000}{(1.099\times 10^5)^2}$$

$$= 2.653 \times 10^{-26}\ kg. = 15.98\ u.$$

$\therefore$ Mass number of the ion = 16.

Example 7. *In a Bainbridge mass spectrograph singly ionized atoms of neon-20 pass into the deflection chamber with a velocity of 10^5 m/sec. If they are deflected by a magnetic field of flux density 0.08 tesla, calculate the radius of their path and where neon-22 ions would fall if they had the same initial velocity.*

For an ion moving in a magnetic field B with velocity v along a circular path of radius R, we have a relation

$$Mv^2/R = B\ nev \text{ or } R = Mv/Bne.$$

$$\text{For neon-20,} \qquad R = \frac{20\times 1.66054\times 10^{-27}\times 10^5}{0.08\times 1\times 1.60218\times 10^{-19}} = 0.259 m.$$

For the ions with the same velocity and charge, in the same magnetic field, radius of the path followed $R \propto M$. Hence for neon-22

$$R = \left(\frac{22}{20}\right) \times \text{radius of the path for the neon-20} = 0.285\ m.$$

Example 8. *From the mass spectroscopic doublets,*

$$^{12}C^{16}O_2 - {}^{12}C\,{}^{32}S = a = 17.78 \times 10^{-3}\ amu.$$

$$^{12}C_3\,{}^1H_8 - {}^{12}C^{16}O_2 = b = 72.97 \times 10^{-3}\ amu.$$

$$^{12}C_6\,{}^1H_4 - {}^{12}C^{32}S_2 = c = 87.33 \times 10^{-3}\ amu.$$

Determine the mass of hydrogen which is obtained from this group of doublets.

From the above set of measurements one can determine the masses of hydrogen, carbon and sulphur, which are all regarded as standards. For solving, above relations can be written as

$$C + 2O - C - S = a \quad \text{or} \quad 2O - S = a, \qquad \text{...}(i)$$

$$3C + 8H - C - 2O = b \quad \text{or} \quad 2C - 2O + 8H = b, \qquad \text{...}(ii)$$

$$6C + 4H - C - 2S = c, \quad \text{or} \quad 5C + 4H - 2S = c. \qquad \text{...}(iii)$$

Since the doublet measurements are in *amu*, the unit of mass in which the mass of ^{16}O isotope is assumed 16, hence we have to solve above relations in such a way that H comes in terms of O and doublet separations a, b, c. After solving we get

$$32H - 2O = 4a + 5b - 2c \quad or \quad H = 1 + \tfrac{1}{32}(4a + 5b - 2c).$$

Substituting values, we get $H = 1.008166$ *amu*.

If the doublet measurements are given in u, we should solve the equations in terms of C and the doublet separations a, b and c, as the mass of ^{12}C isotope is assumed 12 in this unit of mass.

$$\therefore \quad H = 1 + \tfrac{1}{12}(2a + 2b - c) = 1.004884\ u.$$

Example 9. *In Smith's mass synchrometer, Ag⁺ ions of mass 106.9 u circulate in a magnetic field of 6500 gauss. They succeed in reaching the detector when the radio frequency is 11.21 Mc/s. The distance between the slits S_1 and S_2 is 27.94 cm. The difference in the inter slit distances $S_1 - S_2$ and $S_4 - S_5$ is 1.692 cm. Calculate the K.E. of the ions entering and leaving the modulator.*

Angular velocity ω of the charged ions circulating in a magnetic field B in a orbit of radius R is given by $\omega = Be/M$.

Its linear velocity $v = \omega R = BeR/M$, therefore K.E. $= \frac{1}{2} M\,[BeR/M]^2 = B^2e^2R^2/2M$.

Radius of orbit of ions entering slit $S_2 = R = \frac{1}{2}$ distance $S_1S_2 = 13.97\ cm$.

$$\therefore \quad K.E. = \frac{(0.65)^2\,(1.60218 \times 10^{-19})^2\,(0.1397)^2}{2 \times 106.9 \times 1.66054 \times 10^{-27}}\ \text{joule} = 3721\ eV.$$

At the time of leaving the modulator

$$R = \tfrac{1}{2}\ \text{distance}\ S_4\,S_5 = \tfrac{1}{2} \times (27.94 - 1.692) = 13.124\ cm.$$

$$\therefore \text{K.E. of ions leaving the slit}\ S_4 = \frac{(0.65)^2(1.60218 \times 10^{-9})^2\,(0.13124)^2}{2 \times 106.9 \times 1.66054 \times 10^{-27}} = 3284\ eV.$$

Example 10. *Examine the possibilities of isomeric transition between nuclei $^{7}_{4}Be$ and $^{7}_{3}Li$.*

The isotopic masses of these nuclei are

$$^{7}_{3}Li = 7.0116004\ u \text{ and } ^{7}_{4}Be = 7.016929\ u.$$

We know that for a β^--decay to be possible

$$^{A}_{Z}M >\, ^{A}_{Z+1}M + {}^{0}_{-1}e \ \text{(Nuclear masses)}.$$

By adding z electron masses to both sides, the nuclear masses are changed into isotopic masses and the same condition appears now as

$$^{A}_{Z}M >\, ^{A}_{Z+1}M \ \text{(Atomic masses)}.$$

Since mass of $^{7}_{3}Li$ < mass of $^{7}_{4}Be$, hence β^--decay is not possible.

We know that for a β^+-decay to be possible

$$^{A}_{Z}M >\, ^{A}_{Z-1}M + {}^{0}_{+1}e \ \text{(Nuclear masses)}.$$

By adding Z-electron masses to both sides, the nuclear masses are changed into isotopic masses and the same condition appears as

$${}^{A}_{Z}M > {}^{A}_{Z-1}M + 2\,{}^{0}_{+1}e \text{ (Atomic masses).}$$

Since the mass difference between given isotopes is 0.000925 u = 0.862 MeV, which is less than the energy equivalent of two electron masses, *i.e.*, 1.022 MeV, hence no β^+-decay is possible.

The atomic binding energy of the *K*-electron in the ${}^7Be$-atom, however, is considerably less than the available energy 0.862 MeV, hence *K*-capture is energetically possible.

Example 11. *Calculate the binding energies of the following isobars and their binding energies per nucleon :*

$${}^{64}_{28}Ni = 63.927958\, u,\ {}^{64}_{29}Cu = 63.929759\, u.$$

Which of these would you expect to be β-active and how would it decay? Why?

(*a*) Since mass of neutron M_n = 1.008665 u and M_H = 1.007825 u, hence for ${}^{64}_{28}Ni$,

$$NM_n + ZM_H = 36 \times 1.008665 + 28 \times 1.007825 = 64.53104\, u$$

$$\therefore \quad \Delta M = 64.53104 - 63.927958 = 0.6030825\, u.$$

Hence binding energy = 559.306 MeV and binding energy per nucleon is 8.739 MeV.

Similarly for ${}^{64}_{29}Cu$,

$$NM_n + ZM_H = 35 \times 1.008665 + 29 \times 1.007825 = 64.53020\, u$$

$$\therefore \quad \Delta M = 64.53020 - 63.929759 = 0.600441\, u.$$

Hence binding energy = 559.306 MeV and binding energy per nucleon is 8.739 MeV.

(*b*) These isobars are β^- emitters, *i.e.*,

$${}^{64}_{28}Ni \rightarrow {}^{64}_{29}Cu + \beta^- \text{ and } {}^{64}_{29}Cu \rightarrow {}^{64}_{30}Zn + \beta^-,$$

if the mass of the final isotope is less than of the corresponding initial isotope, *i.e.*, if ${}^{A}_{Z}M > {}^{A}_{Z+1}M$. Since mass of ${}^{64}Cu$ is greater than that of ${}^{64}Ni$ and ${}^{64}Zn$, hence ${}^{64}Ni$ is not a β^--emitter but ${}^{64}Cu$ is a β^--emitter.

These isobars are β^+-emitters, if ${}^{A}_{Z}M > {}_{Z-1}^{A}M + 2\,{}_{+1}e^0$.

Since $M({}^{64}Cu) - M({}^{64}Ni) = 0.00181\, u = 1.6776\, MeV$ is greater than the mass of two electrons, hence Cu^{64} is also a β^+-emitter.

Example 12. *Find the energy release, if two ${}^2_1H$ nuclei can fuse together to form ${}^4_2He$ nucleus, the binding energy per nucleon of ${}^2H$ and ${}^4He$ is 1.1 MeV and 7.0 MeV respectively.*

Since number of nucleons in ${}^4_2He$ nucleus is 4, hence B.E. for ${}^4_2He$ = 28.0 MeV, similarly B.E. for ${}^2H$ nucleus (combination of one proton and one neutron) = 2.2 MeV.

Mass of ${}^4_2He$ nucleus = 2 [Mass of proton] + 2 [Mass of neutron] – 28.0 MeV.

Mass of ${}^2_1H$ nucleus = (Mass of proton) + [Mass of neutron) – 2.2 MeV.

In fusion reaction energy released ΔE = 2 [Mass of ${}^2_1H$] – [Mass of ${}^4_2He$]

$$= 2\,[M_p + M_n - 2.2] - [2M_p + 2M_n - 28.0] = 23.6\, MeV$$

Example 13. *For what elements should stable isobars exist for (a) A = 97 and (b) A = 80?*

Semi-empirical mass formula for a ${}^A_ZX$-atom is

$${}^{A}_{Z}M = M_n(A - Z) + M_H Z - a_v A + a_s A^{2/3} + a_c Z(Z-1)A^{-1/3} + a_a (A - 2Z)^2 A^{-1} \pm a_p A^{-3/4}.$$

Substituting values of constants in terms of *MeV*, we have

$${}^{A}_{Z}M = 939.6\,(A-Z) + 938.8Z - 14.0A + 13.0A^{2/3} + 0.583\,Z(Z-1)A^{-1/3} + 19.3\,(A-2Z)^2A^{-1} \pm 33.5\,A^{-3/4}$$

For a most stable isobar

$$(\partial M/\partial Z)_{Z=Z_A} = -0.8 + 0.583\,(2Z_A - 1)A^{-1/3} - 77.2\,(A - 2Z_A)A^{-1} = 0$$

or

$$Z_A = \frac{78.0 + 0.583\,A^{-1/3}}{154.4 + 1.166\,A^{2/3}}A.$$

For odd value of A, there should be only one stable isobar, the neighbouring isobars are unstable and decay to stable isobar. For $A = 97$

$$Z_A = \frac{78.0 + 0.583 \times (97)^{-1/3}}{154.4 + 1.166\,(97)^{2/3}}(97) = 42.33.$$

Hence the most stable isobar is ${}^{97}_{42}Mo$.

By similar calculations for $A = 80$, we get $Z_A = 35.32$. Hence the most stable isobar will be ${}^{80}_{35}Br$. It is the case of Z-odd, N-odd. It has been discussed in theory that for even-A values, we get two parabolas due to the term $\pm a_p A^{-3/4}$. The odd Z values are associated with upper and even Z-values with lower. The possible stable isobars with even Z values are ${}^{80}_{34}Se$ and ${}^{80}_{36}Kr$.

Example 14. *For $A = 50$, the known masses are : ${}^{50}_{21}Sc$, ${}^{50}_{22}Ti$, ${}^{50}_{23}V$, ${}^{50}_{24}Cr$ and ${}^{50}_{25}Mn$ are 49.951730 u, 49.944786 u, 49.947164 u, 49.946055 u and 49.954215 u respectively. From these data estimate the constant related with the strength of the pairing term in the semiempirical mass formula.*

Semi-empirical mass formula for the ${}^{A}_{Z}X$ atoms is

$${}^{A}_{Z}M = M_n(A-Z) + M_HZ - a_vA + a_sA^{2/3} + a_cZ(Z-1)A^{-1/3} + a_a(A-2Z)^2A^{-1} \mp a_pA^{-3/4}$$

Substituting the values given, we have.,

$${}^{50}_{21}M = 49.951730 = M_n(50-21) + M_H(21) - 50a_v + 50^{2/3}a_s + 21\times 20\times 50^{-1/3}a_c + (8^2/50)a_a \mp a_p50^{-3/4}$$

$${}^{50}_{22}M = 49.944786 = M_n(50-22) + 22M_H - 50a_v + 50^{2/3}a_s + 22\times 21\times 50^{-1/3}a_c + (6^2/50)a_a \mp a_p50^{-3/4}$$

$${}^{50}_{23}M = 49.947164 = M_n(50-23) + 23M_H - 50a_v + 50^{2/3}a_s + 23\times 22\times 50^{-1/3}a_c + (4^2/50)a_a \mp a_p50^{-3/4}$$

$${}^{50}_{24}M = 49.946055 = M_n(50-24) + 24M_H - 50a_v + 50^{2/3}a_s + 24\times 23\times 50^{-1/3}a_c + (2^2/50)a_a \mp a_p50^{-3/4}$$

$${}^{50}_{25}M = 49.954215 = M_n(50-25) + 25M_H - 50a_v + 50^{2/3}a_s + 25\times 24\times 50^{-1/3}a_c + 0 \mp 50^{-3/4}a_p.$$

Solving these equations by taking third difference

$$\begin{aligned}{}^{50}_{24}M - 3\,{}^{50}_{23}M + 3\,{}^{50}_{22}M - {}^{50}_{21}M &= M_n[26-81+84-29] + M_H[24-69+66-21] + a_c[24\times 23 - 3\times 23\times 22\\ &\quad + 3\times 22\times 21 - 21\times 20] + a_a(4 - 3\times 16 + 3\times 36 - 64)\,50 - 8\times 50^{-3/4}a_p\end{aligned}$$

$$0.946055 - 3(0.947164) + 3(0.944786) - 0.951730 = -8\times 50^{-3/4}a_p$$

or

$$a_p = (50^{3/4}/8)\,(0.0128094) = 0.030107\,u = 28.09\,MeV$$

If we take another third difference, we get

$${}^{50}_{25}M - 3\,{}^{50}_{24}M + 3\,{}^{50}_{23}M - {}^{50}_{22}M = 8\times 50^{-3/4}a_p$$

$\therefore$

$$a_p = (50^{3/4}/8)\,(0.012756\,u) = 0.02998\,u = 27.93\,MeV.$$

These two estimates for a_p are seen to be very close together.

Example 15. *Prove that the masses of a set of isobars that are members of the same isospin multiplet can be written as*

$$M = a + bT_z + cT_Z^2,$$

where a, b, c are constants and T_z is the operator for the Z-component of the *isotopic spin.* How large must the isospin be in order to test it experimentally ?

Members of the same isospin multiplet have the same spin-parity. Their mass differences are determined by the Coulomb energies and the neutron proton mass difference. Thus for a mass number A, neutron number N, we have

$$A = Z + N = 2Z - (Z - N) = 2Z - 2T_z \text{ or } Z = \tfrac{1}{2}(A + 2T_Z)$$

$$\therefore \quad M = \frac{3}{5}\frac{e^2Z^2}{4\pi\varepsilon_0 R} + (m_p - m_n)T_Z + M_0$$

$$= \frac{3}{5}\frac{e^2}{4\pi\varepsilon_0 R}\left(\frac{A}{2} + T_Z\right)^2 + (m_p - m_n)T_Z + M_0$$

$$= \frac{3}{5}\frac{e^2}{4\pi\varepsilon_0 R}T_Z^2 + \left(\frac{3}{5}\cdot\frac{e^2A}{4\pi\varepsilon_0 R} + m_p - m_n\right)T_Z + \left(M_0 + \frac{3}{5}\cdot\frac{e^2}{4\pi\varepsilon_0 R}\cdot\frac{A^2}{4}\right)$$

$$= a + bT_z + cT_Z^2.$$

Here the quadratic term is due to the Coulomb energy, while the linear terms arise from the Coulomb energy and the neutron-proton mass difference.

There are three constants a, b and c in the above relation. Hence to find their values three independent linear equations are needed. As there are $(2T + 1)$ multiplets of an isospin T. The minimum value of T required to test the formula experimentally is 1.

Example 16. *Show that the classical cross-section for elastic scattering of point particles from an infinitely massive sphere (hard sphere) of radius R is isotropic.*

In classical mechanics, in elastic scattering of a point particle from a fixed surface, the emergent angle equals the incident angle. Thus for the incident angle ϕ, the particle is deflected by an angle $\theta = 2\phi$. As the impact parameter $b = R\sin\phi$, the differential scattering cross section is

$$\frac{d\sigma}{d\Omega} = \frac{2\pi b\,db}{2\pi\sin\theta\,d\theta} = \frac{R^2\sin\phi\cos\phi\,d\phi}{4\sin\phi\cos\phi\,d\phi} = \frac{R^2}{4}$$

which is independent of ϕ, showing that the scattering is isotropic.

Example 17. *Given a deformed nucleus of the shape of an ellipsoid, with the major axis 10% longer than the minor axis. Compute the electric potential at the first Bohr radius. What accuracy is expected if the nucleus is treated as a point charge ? Make reasonable estimate without integration process.*

Let the charge distribution in the nucleus is uniform, ellipsoidal and axially symmetric. The electric dipole moment of the nucleus is thus zero, and the potential at a distance r is given by

$$V = V_p + V_Q = \frac{q}{4\pi\varepsilon_0 r} + \frac{qQ}{4\pi\varepsilon_0 r^3},$$

where the first term is the potential produced by the nucleus as a point charge and the second term is due to the electric quadrupole moment of the nucleus. Here for the ellipsoid nucleus, the major axis $a = (1 + \in)R$ and the minor axis $b = (1 - \in/2)R$, where $\in$ is the deformation parameter and R is the nuclear radius.

Since $a/b = 1.1$, therefore $(1 + \in)/(1 - \tfrac{1}{2}\in) = 1.1$ or $\in = 0.2/3$.

$\therefore$ Electric quadrupole moment $Q = \tfrac{2}{5}(a^2 - b^2) = \tfrac{1.22}{15}R^2$

For a medium nucleus, let $A = 125$, for which $R = 1.2\,A^{1/3} = 6$ fermi

$$\therefore \quad \frac{V_Q}{V_p} = \frac{Q}{r^2} = \frac{1.22R^2}{15r^2} = \frac{1.22(6\times10^{-15})^2}{15(0.53\times10^{-10})^2} = 10^{-9}.$$

Here r = first Bohr radius = $0.53 \times 10^{-10}\ m$.

Thus the relative error in the potential if we treat the nucleus as a point is about 10^{-9} at the first Bohr orbit.

Example 18. *Calculate the energy levels of a nucleus whose spin quantum number is I in a magnetic field* **B**. *Using the selection rule $\Delta m_j = \pm 1$, evaluate the angular frequency of an electromagnetic quantum which will induce the system to jump from one orientation to another.*

If a nucleus is put into a magnetic field B, then the couple with which the field acts on the magnetic moment makes the angular momentum vector to precess about the direction of the field, just like the top. The energy of the motion, also known as interaction energy, is given by

$$U = \mu\cdot\boldsymbol{B} = g_I \mu_N \boldsymbol{I}\cdot\boldsymbol{B},$$

where μ_N, the nuclear magneton = $\mu_0 e\hbar/2m_p = 3.152 \times 10^{-8}\ eV - m^2$/weber.

Since $\boldsymbol{I}\cdot\boldsymbol{B} = m_I B$, where m_I is the magnetic quantum number, having values lying between $-I$ to I (*i.e.*, $-I \le m_I \le I$).

$\therefore$

$$U = g_I(\mu_0 e\hbar/2m_p)\, m_I B.$$

In a magnetic field a given energy is thus split up into levels with separation

$$h\nu = g_I(\mu_0 e\hbar/2m_p)B,$$

$\therefore$ Larmor frequency $\nu_L = g_I(\mu_0 e/4\pi m_p)B$.

Example 19. *Evaluate the maximum energy shift that can be observed for a body whose quadrupole moment is Q.*

If the nucleus is under the influence of the potential, then we have an interaction energy

$$U = \int \varphi(r)\rho(r)\,d\tau,$$

where ρ is the proton density in the nucleus.

We can expand the electric potential φ, the quadrupole interaction energy

$$\Delta U_2 = \tfrac{1}{4}(\partial^2\varphi/(\partial z^2)_0 \int (3z^2 - r^2)\,\rho\, d\tau = \tfrac{1}{4}eQ(\partial^2\varphi/\partial z^2)_0,$$

where Q is the quadrupole moment. The energy shift is maximum, when the nuclear symmetry axis is I-axis. Hence the Q to the precession axis is

$$Q_{pr} = \frac{1}{2}\frac{2I-I}{I+1}Q_{intrinsic}.$$

$\therefore$ Maximum energy shift for a body of intrinsic quadrupole moment Q is

$$(\Delta U_2)_{max} = \frac{1}{8}eQ\left(\frac{\partial^2\varphi}{\partial z^2}\right)_0 \frac{2I-1}{I+1}.$$

Example 20. *Find the value of the quadrupole moment of a system in which a proton is circling a spherical nucleus of equal values of Z and N.*

As spheroid is having zero quadrupole moment and $<x^2> = <y^2> = <z^2> = \frac{1}{3}r^2$. As the proton is circling in $x-y$ plane, hence change will be in $x-y$ plane or the distribution of charge is of oblate shape and thus the quadrupole moment is negative.

Example 21. *The quadrupole moment for ${}^{155}_{64}Gd$ is 130 fm^2. Show that the ${}^{155}Gd$ nucleus is almost spherical.*

The electric quadrupole moment of a nuclear charge distribution which is symmetric about the z-axis is given by

$$Q = \frac{1}{e}\int (3z^2 - r^2)\,\rho(x,y,z)\,dx\,dy\,dz.$$

For the uniformly charged ellipsoid of revolution defined by the equation

$$\frac{x^2+y^2}{a^2} + \frac{z^2}{b^2} = 1,$$

the electric quadrupole moment reduces to

$$Q = \tfrac{2}{5}Z(b^2 - a^2),$$

where Ze is the total nuclear charge.

If the average nuclear radius is taken to be $R_0^3 = a^2 b$ (as the volume of the ellipsoid is $\frac{4}{3}\pi a^2 b$) and $b = R_0 + \delta R_0$, then for $\delta R_0 << R_0$,

$$a^2 = \frac{R_0^3}{R_0 + \delta R_0} = R_0^2\left(1+\frac{\delta R_0}{R_0}\right)^{-1} = R_0^2\left(1-\frac{\delta R_0}{R_0}\right)$$

$$\therefore \quad b^2 - a^2 = R_0^2\left(1+\frac{\delta R_0}{R_0}\right)^2 - R_0^2\left(1-\frac{\delta R_0}{R_0}\right) = R_0^2\left[1+2\frac{\delta R_0}{R_0}+\left(\frac{\delta R_0}{R_0}\right)^2 - 1 + \frac{\delta R_0}{R_0}\right]$$

$$= 3R_0^2\,(\delta R_0/R_0).$$

Hence $Q = \dfrac{2}{5}Z.3R_0^2\,\dfrac{\delta R_0}{R_0} = \dfrac{6Z}{5}R_0^2\,\dfrac{\delta R_0}{R_0}$.

In the present problem $Q = 130\,fm^2$ and $R_0 = (1.4\,fm)A^{1/3}$

$$\therefore \quad \frac{\delta R_0}{R_0} = \frac{5Q}{6ZR_0^2} = \frac{5\times 130\,fm^2}{6\times 64\,(1.4\,fm)^2\cdot(155)^{2/3}}$$
$$= 0.0299.$$

This shows that the deviation from sphericity for $^{155}_{64}Gd$ is only 2.99% of the average radius. therefore the ^{155}Gd nucleus may be assumed as almost spherical.

Oral Questions

1. *To study the nuclear size, shape and density distribution, the electrons, protons and neutrons are employed as probes. What are the criteria in selecting the probe? Can we use photons as probes?*

   (The basic criterion for selecting probes is that the de Broglie wavelength of the probe must be less than or equal to the size of the object being studied. Thus for the effective study of the nuclear charge distribution we require $\lambda << 2R$. For a medium nucleus $d = 2R \simeq 10^{-14} m$. We thus require electrons of energy

   $E \simeq pc = (h/2R)c = (6.6260755 \times 10^{-34}/10^{-14}) \times 3 \times 10^8 = 1.988 \times 10^{-12}$ *Joule* $= 12.4$ *MeV*.

   Thus high energy electrons ($\simeq$ 100 *MeV*) are a suitable probe to study the nuclear electromagnetic radius and charge distribution because electrons do not take part in strong interactions. The protons can be used to study the nuclear structure as the proton beams of high flux and suitable parameters are readily available. Its disadvantage is that both electromagnetic and strong interactions are present in proton-neutron scattering and the results are complex to analyse. Neutrons as a probe are in principle better than protons. Experimentally it is much more difficult to generate high energy neutrons and measurements are also more difficult. The use of photons as probe is not practicable, as the high energy photons used to interact with nuclei would show a hadron-like character and complicate the problem.

2. Which experiment may be called the foundation stone for the Nuclear Physics?

   (Rutherford's α-particle scattering experiment)

3. The nucleus is assumed spherical - why?

4. Determine the stable nucleus that has a radius 1/3 of ^{189}Os.
5. Determine the possible states of a deuteron if its angular momentum quantum number is 1.
6. Evaluate the nuclear magneton in units of J/T. What is the ratio with the Bohr magneton?
7. All nuclei have an electric monopole moment. Some have an electric quadrupole moment. Why would we not expect electric dipole moments for nuclei?
8. Nuclei have magnetic dipole moments. Why do they not have magnetic monopole moment?
9. Why are the most stable nuclei found in the region near $A = 60$?
10. What is the simplest distribution of point charges that has an electric quadrupole moment?
11. A positive electric point charge is surrounded by a concentric circular ring of negative charge of total magnitude equal to that of the point charge. Is the system an electric monopole, dipole, quadrupole or octopole?
12. To penetrate the Coulomb barrier of a light nucleus, a proton must have a minimum energy of the order of (a) *keV*, (b) *MeV*; (c) *GeV*.

Problems

1. An α-particle of energy 5 *MeV* is scattered through 180° by a uranium nucleus. Calculate the distance of closest approach between the nucleus and the α-particle. $(5.3 \times 10^{-14} m)$
2. 9 *MeV* α-particles are incident normally upon aluminium foil 1.0 μ*m* thick. A fraction 1 in 10^4 was scattered through an angle of 60° and detected by a scintillation counter of area 25 mm^2 at a distance of 50 *mm*. Calculate the atomic number of aluminium, given its specific gravity 2.7. (13)
3. Show that a nucleon which is confined to a region of the order of 10^{-15} meter must have a velocity of the order of 6×10^7 *m/sec* and a K.E. of the order of 20 *MeV*.
4. In a crossed magnetic and electric field velocity filter, find the magnetic field necessary to filter 20 *keV* singly charged ^{40}Ar ions if the electric field is 10^5 volts/meter. (0.3226 tesla)
5. Singly ionized magnesium atoms enter a Bainbridge mass spectrograph with a velocity of 4×10^5 m/sec. Calculate the radii of the paths followed by the three most abundant isotopes of masses 24, 25 and 26, when the magnetic flux density is 0.5 tesla. (32.5 cm, 31.3 cm, 30 cm).
6. A uniform magnetic field is used as a momentum filter for a high energy filter. A slit system is adjusted to allow the particles having a radius of curvature ρ. The magnetic field B is first adjusted for α-particles of energy 5.3 *MeV*. The magnetic field is raised to 2.3 B and deuterons are allowed to pass into the filter. What is the energy of the deuterons transmitted by the filter. (14.0 *MeV*).
7. How much energy will be released by the synthesis of 1 gm of ^4He from neutrons and protons?, from two deuterons, from one triton and one proton? (28.297, 23.847, 19.823 *MeV*)
8. Calculate the binding energies for the mirror nuclei ^{39}K and ^{39}Ca from the semi-empirical binding energy equation. What do you infer from these energies about the relative stabilities.

   (327.3 *MeV*, 320.6 *MeV*. Latter unstable and radioactive)
9. Determine the mass difference between two mirror nuclei which have N and Z differing by one unit and the same odd value of A. $[M_p - M_n + a_c A^{2/3}]$
10. $^{27}_{14}Si$ and $^{27}_{13}Al$ are mirror nuclei having identical ground states except for charge. If their mass difference is 6 *MeV*, estimate their radius, neglecting the proton-neutron mass difference. (3.88 *fm*)
11. Both nuclei $^{14}_{7}N$ and $^{12}_{6}C$ have isospin $T = 0$ for the ground state. The lowest $T = 1$ state has an excitation energy of 2.3 *MeV* in the case of $^{14}_{7}N$ and about 15.0 *MeV* in the case of $^{12}_{6}C$. Why is there such a marked difference?
12. The greatest binding energy per nucleon occurs near ^{56}Fe and is much less for ^{238}U. Explain this in terms of the semiempirical nuclear binding theory.
13. Uranium nucleus breaks up spontaneously into two roughly equal parts. Estimate the reduction in electrostatic energy of the nuclei. How is it related with the total change in energy. (.64 *MeV*)
14. A nucleus of mass 240 is broken up into four nuclei each of mass 60. How much energy is released? If the nucleus of mass 60 is formed by the fusing together of three nuclei each of mass 20. Calculate the energy released, if any. Explain why it is not the same as in the earlier case. (288 *MeV*, 42 *MeV*)
15. Our sun has a mass of 1.98×10^{30} kg, and a radius of 7.4×10^5 km. Assume the mass to suddenly shrink until it attains nuclear density, what would be in the radius of the new sun? How much energy would be available from 1 gm of solar material falling from the old radius to the new? $(1.48 \times 10^4 m,\ 8.93 \times 10^{12}$ *joules*)

16. For what elements should stable isobars exist for (*a*) $A = 169$ and (*b*) $A = 110$? $({}^{169}_{69}Tm;\ {}^{110}_{46}Pd,\ {}^{110}_{48}Cd)$

17. Using semi-empirical mass formula, find the most stable isobar for a nucleus having $A = 43$. Given Coulomb energy coefficient $a_3 = 0.583\ MeV$ and asymmetry energy coefficient $a_4 = 19.3\ MeV$. $({}^{40}_{20}Ca)$

18. Assuming a proton to be a sphere of radius of $1.5 \times 10^{-15}\ m$ and of uniform density and to have an actual angular momentum of $\hbar\sqrt{s(s+1)}$, compute the angular velocity in revolutions per second and the peripheral speed at the equator of the proton. $(\omega = 0.96 \times 10^{23}$ rev/sec, 0.91×10^{8} m/sec)

19. Calculate the electric quadrupole moment of a charge of magnitude Ze distributed over a ring of radius R and with axis along (*a*) the z-axis, and (*b*) the x-axis.

20. The electric quadrupole moment of ${}^{165}_{67}Ho$ is 300 fm^2, $R_0 = (1.4\ fm) \times A^{1/3}$, find $\delta R_0/R_0$. (6.33%)

REFERENCES

1. Blatt, J.M. and V.F. Weisskopf, ''*Theoretical Nuclear Physics*'', Wiley, New York, 1952.
2. Blin-Stoyle, R.J., ''*Theories of Nuclear Moments*'', Oxford University Press, 1957.
3. Breit, G. and I.I., Rabi, *Phys, Rev.*, **38**, 2082L (1931).
4. Burcham, W.E., ''*Nuclear Physics an Introduction*'' Longman Group Limited, London, 1973.
5. Condon, E.U. and H. Odishaw, ''*Handbook of Physics*'', McGraw-Hill Book Co., 1967.
6. Devons, S., and I. Duerdoth, *Adv. Nucl. Phys.*, **2**, 295 (1969).
7. Elton, L.R.B., ''*Nuclear Sizes*'', Oxford University Press, 1961.
8. Enge, A, Harald, ''*Introduction to Nuclear Physics*'', Addison Wesley, 1966.
9. Evans, Robley D., ''*The Atomic Nucleus*'', McGraw-Hill Book Co., 1955.
10. Fitch, V.L. and J. Rainwater, *Phys. Rev.*, **92**, 789 (1953).
11. Gordy, W., W.V. Smith and R. Trambanulo, ''*Microwave Spectroscopy*'', John Wiley & Sons, Inc., New York, 1953.
12. Hahn, B., D.G. Ravenhall, and R. Hofstadter, *Phys. Rev.*, **101**, 1131 (1956).
13. Hans, H.S., ''*Nuclear Physics*'', New Age International (P) Limited Publishers, New Delhi, 2001.
14. Hofstadter, R., ''*Nuclear and Nucleon Structure*,'' Benjamin, New York, 1963.
15. Kopferman, H., ''*Nuclear Moments*'', Academic Press, 1958.
16. Marmier, Pierre and Eric Sheldon, ''*Physics of Nuclei & Particles*,'' Vol. I, Academic Press, 1969.
17. Nier, A.O., K.S. Quisenberry and T.T. Scolman, *Phy. Rev.*, **102**, 1071 (1956).
18. Nier, A.O. and T.R. Roberts, *Phys. Rev.*, **81**, 507, (1951).
19. Preston, M.A., ''*Physics of the Nucleus*,'' Addison Wesley, Reading, Mass., 1962.
20. Ramsey, N.F., ''*Experimental Nuclear Physics*,'' Vol. I, Wiley, New York, 1953.
21. Rutherford, E., *Phil., Mag.* **21**, 669 (1911); **37**, 537 (1919).
22. Smith, C.M.S., ''*A Text Book of Nuclear Physics*'', Pergamon Press, 1966.
23. Smith, K.F. and P.J., Unsworth, ''*Molecular Beam Spectroscopy*,'' Sci. Progr., **53**, 45 (1965).
24. Smith, L.G. and C.C. Damm, *Rev. Sci. Instr.*, **27**, 638 (1956).
25. Weizsacker Von, C.F. ''*Z. Physik*,'' **96**, 431 (1935).
26. Wong, Samual S.M., ''*Introductory Nuclear Physics*'', Prentice-Hall of India, 1996.
27. Wu, C.S. and L. Wilets, *Ann. Rev. Nuci. Sci.*, **19**, 527 (1969).

6

BETA-DECAY

6.1 INTRODUCTION

The portion of the radiation, emitted from a radioactive source, that was strongly deflected by perpendicular magnetic field was termed *beta-radiation*. There are three modes of beta radioactivity : *negatron* (β^-) *emission, positron* (β^+) *emission and orbital electron capture. Negatron emission is much more common than the other decay processes.* Beta rays are easily distinguished from α-particles by their considerably greater range in matter. When a radio-element emits a β^--particle, the product has the same mass number as the parent, but its atomic number is greater by one unit. Similarly when a positron is emitted the mass number is still unchanged but the atomic number of product is now one unit less than that of the parent. When the ratio of neutrons to protons is low, another type of decay known as *orbital electron capture process* has been found to occur. In this process instead of a proton being converted into a neutron with an emission of a positron, electron from the first (usually) or any other atomic quantum level is captured by the nucleus which combines immediately with a proton to form a neutron. The product of this type would have the same mass number as its parent but its atomic number would be one unit lower as in the case of positron emission.

$$\beta^- \text{-process} \rightarrow {}^{A}_{Z}Mc^2 = {}_{Z+1}^{\;\;A}M^+c^2 \text{(positive ion)} + m_0c^2 + Q_{\beta^-}$$

$$\beta^+ \text{-process} \rightarrow {}^{A}_{Z}Mc^2 = {}_{Z-1}^{\;\;A}M^-c^2 \text{ (negative ion)} + m_0c^2 + Q_{\beta^+}$$

$$EC\text{-process} \rightarrow {}^{A}_{Z}Mc^2 = {}_{Z-1}^{\;\;A}M^*c^2 \text{(neutral but excited)} + Q_{EC}.$$

The β^--process increases the nuclear charge by one unit with number of atomic electrons unchanged. If B be the binding energy of the last atomic electron, then we have

$${}^{A}_{Z+1}Mc^2 = {}_{Z+1}^{\;\;A}M^+c^2 + m_0c^2 - B.$$

$$\therefore \quad Q_{\beta^-} = {}^{A}_{Z}Mc^2 - {}_{Z+1}^{\;\;A}Mc^2 - B. \qquad \text{...(1)}$$

The β^+-process decreases the nuclear charge by one unit. The rest energy of the negative ion formed is given by

$${}_{Z-1}^{\;\;A}M^-c^2 = {}_{Z-1}^{\;\;A}Mc^2 + m_0c^2 - B.$$

$$\therefore \quad Q_{\beta^+} = {}^{A}_{Z}Mc^2 - {}_{Z-1}^{\;\;A}Mc^2 - 2m_0c^2 + B. \qquad \text{...(2)}$$

The Q-value of EC-process is similarly written as

$$Q_{EC} = {}^{A}_{Z}Mc^2 - {}_{Z-1}^{\;\;A}Mc^2 - E_B + B, \qquad \text{...(3)}$$

where E_B is the ionization/binding energy of the atomic captured electron.

We have showed in chapter 1 that the hypothesis concerning the existence of electrons inside the nucleus is not in accord with the experimental facts. Now question arises how do we acquire beta-decay with the hypothesis that nuclei contain only neutrons and protons? A solution is to imagine that the electrons are created at the time of emission similar to the photons from excited atoms. The three modes of beta radioactivity can be shown by the following reactions

$$_0n^1 \rightarrow {}_{+1}p^1 + {}_{-1}e^0 \qquad \textit{(Negatron emission)}$$

$$_{+1}p^1 \rightarrow {}_0n^1 + {}_{+1}e^0 \qquad \textit{(Positron emission)}$$

$$_{+1}p^1 + {}_{-1}e^0 \rightarrow {}_0n^1 \qquad \textit{(Orbital electron capture)}$$

The above equations emphasize that *the proton and neutron can be treated as different states of single particle, known as nucleon, and the electrons play a photons like role.*

6.2 BETA-SPECTROSCOPY

The energies of β-rays emitted by radioactive substances are measured by means of a β-ray spectrometer. The kinetic energies of the negatrons and positrons in beta decay cover a continuous range from zero upto a maximum value, which is the characteristic of the beta active isotope. The maximum kinetic energy E_0 corresponds closely to that expected from the exact rest mass energies of the parent and daughter atoms. There is a possibility of the daughter nucleus being created in an excited state, which might decay subsequently by γ-emisson. Rutherford suggested that part of γ-radiation is absorbed by the outer electrons of the same atom and as a result of this the secondary β-ray electrons are ejected. The electron is ejected with kinetic energy $h\nu - E_K$, $h\nu - E_L$ ... , where E_K, E_L ... are the binding energies of the electrons in the *K*, *L*, ... shells respectively and $h\nu$ the energy difference between the two nuclear states. The process is called internal conversion by analogy with the ordinary photoelectric conversion of the energy. In this way in addition to continuous primary spectrum several sharp lines are sometimes seen on the plate at positions characteristic of the radioactive substance. These lines form a line spectrum, observed for many, but not for all β-emitters. The continuous electron spectrum from ^{137}Cs is shown in Fig. 6.1. On the right are the *K* and *L* conversion lines corresponding to an isomeric transition in ^{137}Ba, the product of the ^{137}Cs beta decay.

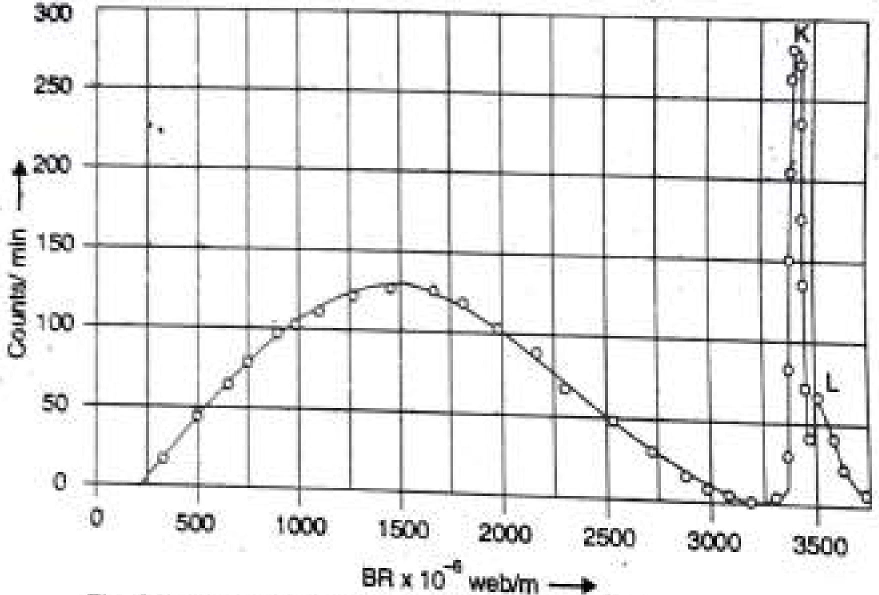

Fig. 6.1. Beta particle spectrum of ^{137}Cs showing the line spectrum.

A typical β-ray spectrum of *RaE* is shown in Fig. 6.2. This type of spectrum shows that β-rays have a maximum energy E_{max} below which there is a continuous spectrum with average energy usually less than half the maximum. Every continuous β-spectrum has a definite maximum, the height and position of which depend on the nucleus emitting the particles. There is also a definite upper limit or end point of energy for β-particles emitted by the nucleus, which is different for different β-emitting nuclides. Due to uncertainty of measurements of the low energy particles, the shape of the curve at low energy end is not known correctly. The maximum kinetic energy varies over a wide range throughout the list of beta unstable nuclei, smallest 18 keV for tritium and largest 13 MeV for isotope ^{12}B.

Early measurements of the energies of beta particles were performed with the use of aluminium or other absorbers. The value of the thickness of absorber needed to cut off the count completely give information about the maximum energy in the beta spectrum. Some excellent work in beta spectroscopy has been done with three types of particle counters, the *proportional gas counter, the solid state counter and the scintillation counter*. If the counter volume is large enough so that most of the beta particles are stopped in the counter material, the pulse height spectrum is a good representation of the energy spectrum. Sometimes range measurements are made by observing the photographs of electron tracks in *cloud chambers or in nuclear emulsion plates*.

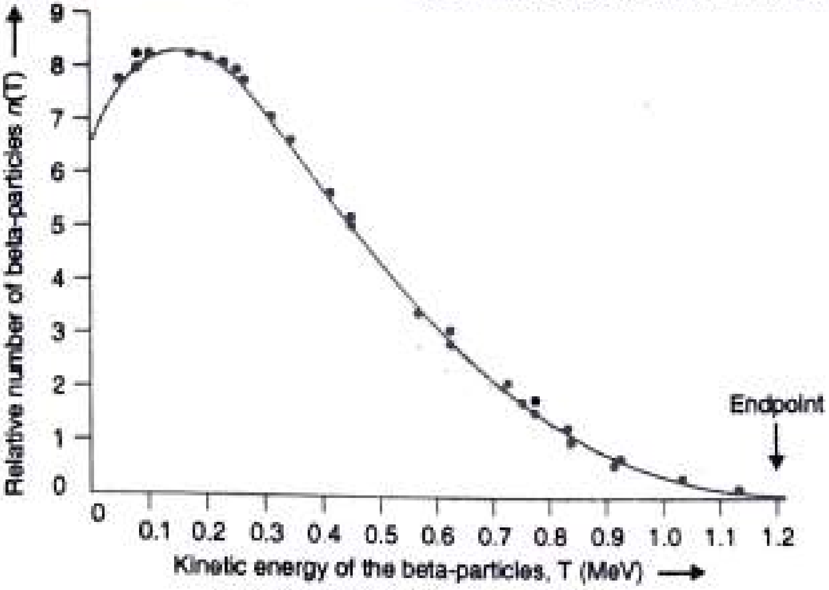

Fig. 6.2. Beta-particle spectrum of RaE.

Undoubtedly the most exact methods of measuring β-ray spectra utilize deflection of the particles in magnetic fields. The two basic requirements of a β-ray spectrometer are *high collection efficiency at the detector and high energy resolution* . The former is particularly important for sources of low specific activity. The spectrometers may be classified into magnetic and electric spectrometers, the first group being by far in greater use. The magnetic spectrometers or spectrographs consist of the source, a focusing magnet providing the focusing field and a detector. The electron paths are confined by baffles with appropriate slits, so that only electrons leaving the source within a certain solid angle Ω will be transmitted. Spectrometers are usually classified as *transverse*, in which the principal component of the bending magnetic field remains perpendicular to the electron trajectories, or *longitudinal*, in which the principal component of the focusing field remains nearly parallel to the electron trajectories. The former type is sometimes called *flat type or prismoidal focus*, whereas the latter is called *helical* or *axial* or *lens focusing*. In both types the field may be either long or short. In a *short focusing field* the field does not extend all the way to the source and detector and the trajectories near source and exit slit are nearly straight. Whereas in a *long focusing field* the field extends over the entire length of the electron trajectories which are curved.

The transverse homogeneous field focuses electrons in only one plane, whereas the longitudinal field is space focusing. These two focusing systems correspond in optics to cylindrical and spherical lenses respectively. The transverse field is called *single focusing*, if it forms a line image of a point source and is called *double focusing* if it forms a point image. The images are not perfect lines or points. If the spread of the image is proportional to the square of the angle of divergence at the source (ϕ_0^2 in Fig. 6.3), it is known as *first order focus*. If it is proportional to ϕ_0^4 , it is called the *third order focus*. No focusing is possible if it is proportional to ϕ_0. Single focusing spectrometers with long transverse field have been built with both first and third order focus. Double focusing fields usually provide third order focus in one direction and first order in the other (ϕ and ψ). Both arrangements are available also with short and with long longitudinal fields.

A particle of charge e, traveling with speed v in a plane perpendicular to a uniform magnetic field B experiences a force normal to the plane containing v and B and describes a circular path of radius R, such that

$$Bev = mv^2/R \quad \text{or} \quad p = mv = BRe,$$

where m is relativistic mass of the particle given by $m = m_0\sqrt{1 - v^2/c^2}$. If R can be measured, one can find p in terms of B. Thus we have

$$p = KB., \qquad \ldots(4)$$

where K is a constant.This equation holds for magnetic β-ray spectrometers of all types. The constant K can be found for a particular instrument. Momentum is directly determined by a magnetic spectrum. To convert momentum distribution of electrons $n(p)\,dp$, the number of electrons in the narrow momentum range p to $p + dp$, into an energy distribution $n(E)\,dE$, we use the formula for non-relativistic particles.

$$E = p^2/2m \quad \text{or} \quad dE = p\,dp/m.$$

Hence the relation $n(p)\,dp = n(E)\,dE$ becomes

$$n(E) = n(p)\,m/p. \qquad \ldots(5)$$

In a magnetic spectrometer the finite width of the slit in front of the detector corresponds to the acceptance of electrons with a small range in R. For a constant field the momentum spread dp of the electrons entering the detector is given by

$$dp = Be\,dR.$$

The detector is usually kept in a fixed position and electrons of different energy are selected by varying B. To obtain the number of counts for equal momentum $n(p)$, the observed number of counts must be divided by p, or a quantity proportional to it, *e.g.*, B.

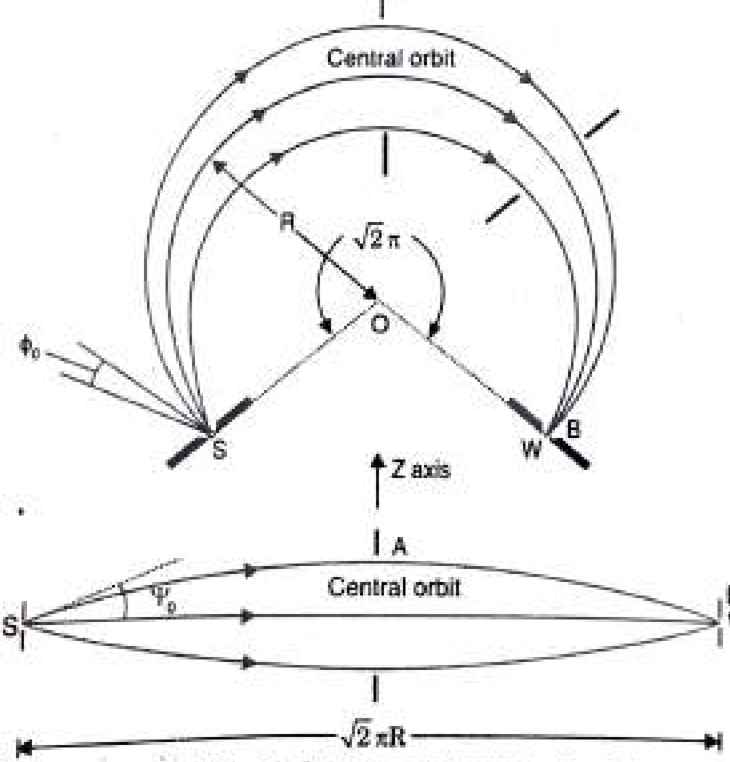

Fig. 6.3. Double focusing spectrometer principle.

1. Flat-type Spectrometers. Many workers have analysed the transverse spectrometers with *(a)* homogeneous fields, *(b)* non-uniform fields, using first order single focusing, third order single focusing, double focusing with short or long fields. According to Kerst and Serber (1941), the charged particles circulating in a transverse magnetic field, which decreases gradually with radial distance, execute simple harmonic oscillations in the median plane $z = 0$ and in the vertical z-direction. Using cylindrical co-ordinates (r, θ, z), the plane of symmetry of the magnetic field is the plane $z = 0$. Here $B_z = B_0$, $B_r = 0$ and $B_\theta = 0$. The z-component of the magnetic field is chosen so that it decreases with increasing r in the vicinity of the central ray at $r = R$, according to the relation

$$B_z = B_0(R/r)^n, \qquad \ldots(6)$$

where n is a constant and B_0 is the value of B on a circular orbit of radius R from the z-axis, defined as the central orbit. The source S and the detector W are both located on this central orbit. The gradient of B is

$$\partial B_z/\partial r = nB_z/r,$$

for an electron trajectory close to the central orbit. If an electron leaves the source in this plane at right angles to R, it will travel in a circle which we may call the reference circle. If it strikes nothing, it will travel around this circle at an angular rate ω_0 given by

$$\omega_0 = v/R = B_0 e/m, \qquad ...(7)$$

where m is the relativistic mass. The electrons emitted from the source but diverging from the central orbit will experience horizontal and vertical forces directed towards the central orbit and of magnitude proportional to the distance from the central orbit. Hence electron will oscillate, the angular frequencies of oscillations in the radial direction and in the z-direction are given by

$$\omega_r = \omega_0 \sqrt{(1-n)} \text{ and } \omega_z = \omega_0 \sqrt{n}. \qquad ...(8)$$

For focusing we want to arrange it so that when the electron has completed one half of a radial oscillation it will also just have completed one half of a z-oscillation and thus will be back on the reference circle. This means that

$$n = \tfrac{1}{2} \text{ and } \omega_r = \omega_z = \omega_0/\sqrt{2}. \qquad ...(9)$$

This condition, once fixed, holds for all initial directions of emission provided initial direction of electron does not make a large angle with the tangent to the reference circle. The above relation indicates that the focusing will occur not at 180°, but at an angle of $\sqrt{2}\pi = 254° \, 33'$. Thus the rays leaving S at small values of angle ϕ_0 and ψ_0 should be sharply focused at W, if the point source S and detector slit B subtend an angle at O of $254° \, 33'$. Particles with higher momenta will be focused at a point outside R and particles with lower momenta at a point inside R. A momentum spectrum of the particles, therefore, appears at position W.

Here we have considered only a simple first order theory of focusing. Several approximations were applied in the derivation of the formula and it was found that the theory was good only for small angles of divergence of the rays from the central orbit. For large angles of divergence, the image will be distorted. The limit of this solid angle depends on the resolving power of the instrument. The resolving power also depends on the area of the source and the area of the detector slit. A closer study of these problems indicates that for a desired momentum resolving power $R.P. = p/\Delta p$. It can also be defined as

$$R.P. = \frac{s}{4R} + \frac{w}{4R} - \frac{h^2}{32R^2} - \frac{\phi^2}{3}, \qquad ...(10)$$

where s is the source width, w the width of the detector slit, h the source height in z-direction and ϕ_0 the angle restricted by the aperture A of Fig. 6.3. The spread due to ψ_0 is negligible.

The principles required for double focusing were well known before they were applied to beta spectroscopy. The focusing of charged particle trajectories has been studied in great detail in connection with particle accelerators. The first precision spectrometer of large radius of curvature (R = 50cm) was designed by Hedgran, Seigbahn and Svartholm soon after the double focusing principle was established. A rotating coil system was developed for the continuous field measurements in this spectrometer. The luminosity of the instrument has recently been substantially improved by Bergkvist by adding two electrostatic correctors, one for the influence of the source width and one for the spherical aberration. Seigbahn designed an iron free double focusing instrument to increase the resolution. It consists of two concentric coils with radii 24 and 36 cm and height 48.7 cm. The iron free spectrographs have the advantage that they are free from hysteresis effects and are therefore more accurate.

2. Lens-type spectrometers. The focusing action of short and long coils has been known for a long time. H. Busch was, however, the first to point out the close analogy between ordinary light and electron optics, when dealing with these magnetic lenses. Longitudinal type homogeneous field spectrometer operates on the same principle as a magnetic lens, familiar from electron microscopes, television tubes, etc. This type of spectrometer, first suggested by Kapitza has been further developed by Witcher in 1941 and by Du Mond in 1949 among others. Principle of operation of this type of spectrometer is shown in Fig. 6.4. For calculating the electron orbits in this instrument, we use a cylindrical co-ordinate system with the z-direction along the axis of the instrument and the direction of the magnetic induction B. We consider a particle emitted, from source, with a velocity v in the direction making an angle α with the axis. Its component along the z-axis is unaffected by the magnetic field. Thus the equation of motion in the z-direction is given by

$$z = v_z t = v t \cos \alpha. \qquad \dots(11)$$

The motion is circular in the r-ϕ plane, with a period T having a value $2\pi/\omega$, where ω (= eB/m) is the cyclotron frequency for the particle in the field B.

Distance L, traveled in the z-direction by the particle when it turns to the axis after the period T, is given by the relation

$$L = Tv \cos \alpha = (2\pi m/eB)\, v \cos \alpha. \qquad \dots(12)$$

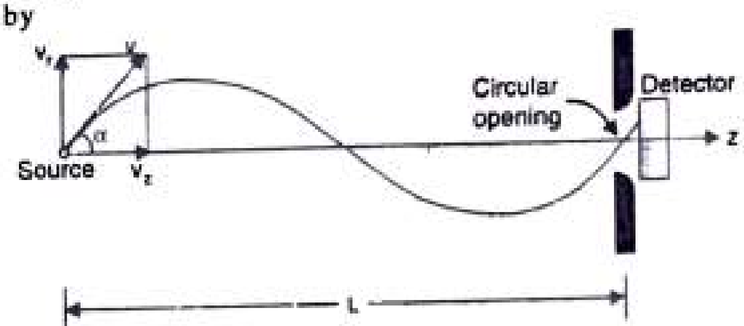

Fig. 6.4. Principle of operation of the longitudinal type homogeneous field spectrometer (single focusing).

If the detector is placed on the axis at this distance from the source, the relationship between p and B is given by

$$LB = (2\pi m v/e) \cos \alpha = (2\pi/e)\, p \cos \alpha. \qquad \dots(13)$$

This indicates that there is a linear relationship between the magnetic induction and the momentum of the particle, but the constant of proportionality depends on the angle α. The spectrometer is, therefore, not double focusing. The above equation is completely independent of ϕ because of the cylindrical symmetry. For limiting value of the range of α, a ring shaped aperture can be used. This can be improved to *double focusing* by using a ring shaped counter slit that is not located immediately adjacent to the counter, but placed as shown in Fig. 6.5. This shows that two particles having different values of α, but having a same momentum can both pass through the narrow energy defining slit. The position at which this energy defining slit should be placed can be found by describing the particle orbit in the rz plane as $r = f(z, \alpha, p)$ and putting $\partial f(z, \alpha, p)/\partial \alpha = 0$. This yields with the use of above equation

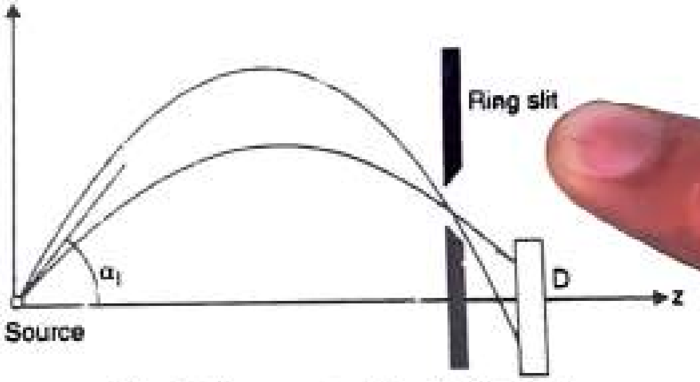

Fig. 6.5. Spectrometer (double focusing).

$$\tan (\pi z_1/L) = -(\pi z_1/L) \tan^2 \alpha_1, \qquad \dots(14)$$

where z_1 is the distance of the position of ring shaped slit from the source. From Fig. 6.5, we see that *to collect all particles passing through the ring slit the detector D must be larger then that for single focusing spectrometer.*

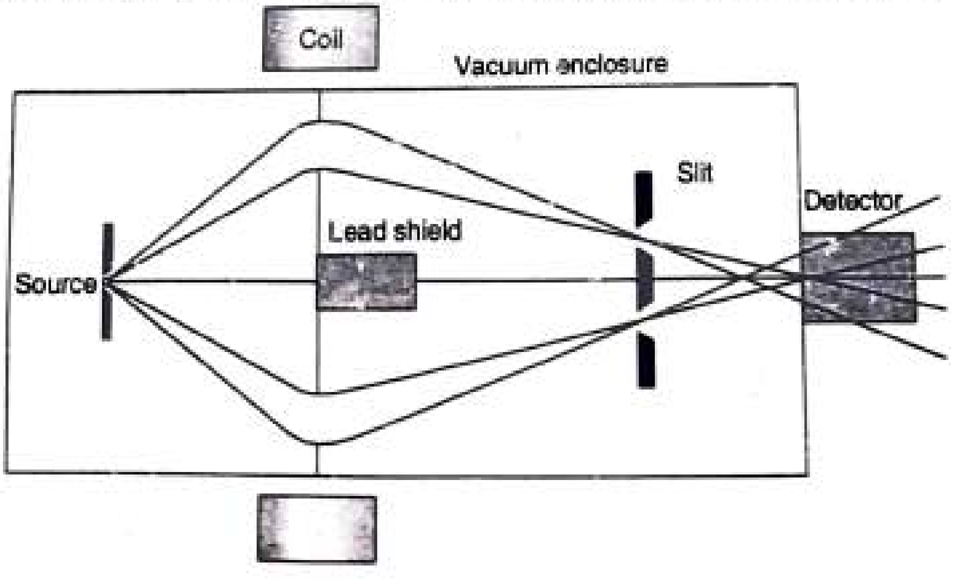

Fig. 6.6. Short lens beta spectrometer.

The *short lens beta spectrometer* is the another example of a lens-type spectrometer. The construction and working principles are somewhat similar to the homogeneous field longitudinal type of spectrometer. It has the advantage of greater accessibility to the source and detector areas. It has a focusing magnetic field extending over a relatively short length of the instrument. The field is usually produced by current carrying coils wrapped round the central regions of the instrument. These spectrometers must be very carefully oriented so that the magnetic field has cylindrical symmetry about the line joining the source and detector. The approximate expression for the focal length of a short magnetic lens for electrons of momentum *BRe* as obtained from elementary electron optics is given by

$$f = 8(BR)^2 / a B_0^2 \pi, \qquad \ldots(15)$$

where B_0 is the axial field at the centre of the lens coil and a is the half width of the axial distribution.

6.3 THE NEUTRINO

The continuous energy distribution of electrons in β-decay proved to be a great puzzle, although the maximum energy of the distribution corresponds to that expected from the mass difference of the parent and the daughter. There is also an apparent failure to conserve linear and angular momentum in β-decay. The emitted electron does not usually travel in a direction opposite to that of the product nucleus. In the process $^{14}C \rightarrow {}^{14}N + \beta^-$, the nuclear angular momenta of ^{14}C and ^{14}N are found to be 0 and 1 respectively. As the electron has an intrinsic spin of ½, therefore, the angular momentum cannot be conserved during the transition. As far as the statistics are concerned, $^{14}N + \beta^-$ is a fermion and ^{14}C is a boson.

All these difficulties were eliminated by Pauli in 1933 by assuming the existence of an additional particle. This hypothetical particle is called a *neutrino* (little neutral one). To preserve not only the principle of energy conservation but also the principle of conservation of electric charge and of angular momentum and the rules governing statistics, we must ascribe certain properties to the neutrino. *(i)* Charge is already conserved by the disintegration electron in β decay hence *the neutrino has zero charge*. *(ii)* In β-decay the parent and the daughter nuclei always have the same mass number. This requires that both have the same statistics and that their nuclear angular momenta may differ only by zero or an integer multiple of $h/2\pi$. As the β-ray electron has Fermi-Dirac statistics and a spin of $\frac{1}{2}\hbar$, the neutrino *must also have Fermi-Dirac statistics* and an intrinsic spin of $\frac{1}{2}\hbar$ in order to conserve statistics and angular momentum. *(iii)* Since the neutrino has a spin $\frac{1}{2}$, it is therefore expected to obey the Dirac theory and in addition to a neutrino, an *anti-particle*, called *anti-neutrino*, should also exist. *(iv)* Just as electron is generic term used for positrons and negative electrons, *neutrino is a term often used generically for a neutrino or an antineutrino*. The neutrino and antineutrino are represented as ν and $\bar{\nu}$ respectively. The particle anti-particle relation assigns to the antineutrino the same mass, spin, charge and magnitude of magnetic moment as those of the neutrino. In all processes where a neutrino is emitted, an antineutrino can be absorbed with the same result and vice versa. As neutrinos have zero charge. Now question arises whether there are in fact two different neutrinos. A positive answer to this question seems to have been given by the requirements of a *doubly beta particle decay*. If ν and $\bar{\nu}$ are not identical, the double beta decay must be accompanied by the emission of two antineutrinos. The two particles in the neutrino pair cannot differ in charge, but it appears that they do differ in the relative directions of their spin vectors. *In the neutrino the spin and angular momentum vectors are oppositely directed and in the antineutrino these vectors are aligned together*. This property gives to the neutrino a *handedness* introducing a fundamental asymmetry in its behaviour.

Since a matter anti-matter pair is formed whenever energy is converted into mass, hence in a conversion of a nuclear neutron to a proton, the negative electron (a member of the matter) should accompany antineutrino (antimatter). Similarly neutrino is emitted with β^+ emission and orbital electron capture. Thus three types of β-decay are :

β^--decay- $\quad n \rightarrow p + e^- + \bar{\nu}$

β^+-decay- $\quad p \rightarrow n + e^+ + \nu$

EC-process- $p + e^- \rightarrow n + \nu$. ...(16)

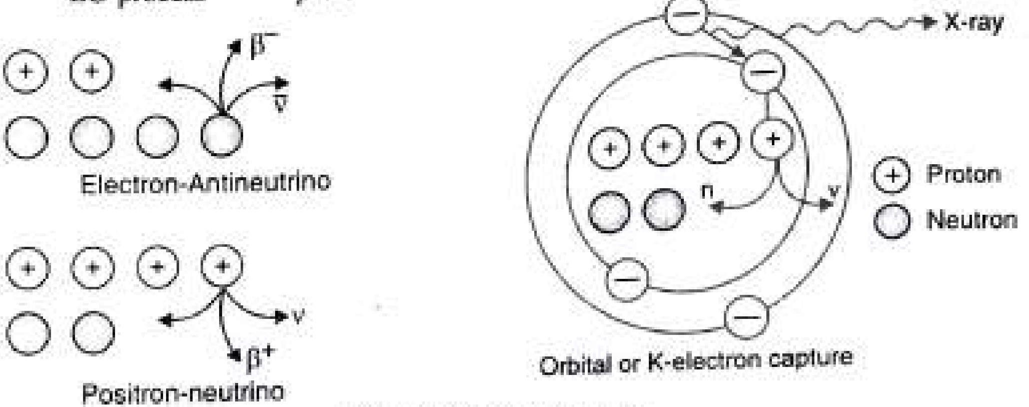

Fig. 6.7. Beta-decay process.

The electron, neutrino and product nucleus share among them the energy, momentum and angular momentum available from the nuclear transitions. The β-particle gets maximum energy when the neutrino is emitted with zero momentum.

Two general procedures have been used to provide positive evidence for the supposition that neutrinos accompany beta-decay.

Indirect Method—In this method the neutrino energy can be determined in two ways. First by measuring the electron energy and subtracting it from the total energy available and second by measuring the momentum of an electron and of recoiling residual nucleus and using conservation of momentum to obtain the neutrino momentum and energy. Unfortunately this method requires measurement of both the nuclear recoil energy and its direction with respect to the electron momentum. Because of the small recoil energy both of these are very difficult measurements. In 1952, a more satisfactory method has been employed in which the recoil nucleus from *K*-electron capture is observed. Since the captured *K*-electron has negligible momentum, the momentum of the recoil nucleus will be equal to that of the neutrino.

$$p_{re} = p_\nu \, (= E_\nu/c)$$

Hence the total recoil energy

$$E_{re} = p_{re}^2/2M = (E_\nu/c)^2/2M, \qquad ...(17)$$

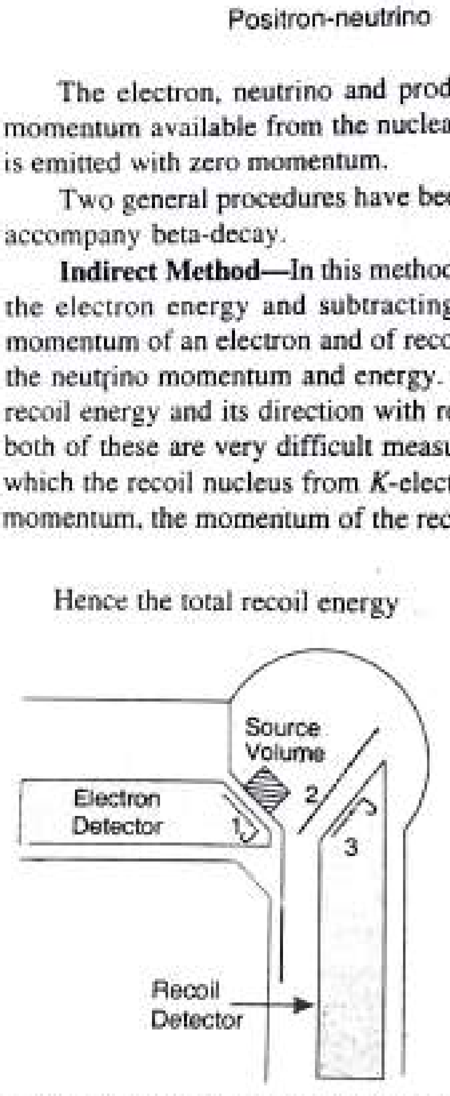

Fig. 6.8. The neutrino recoil apparatus by Rodeback and Allen.

where E_ν is the neutrino energy, c is the velocity of light and of neutrino, and M is the mass of recoiling nucleus. If E_0 is the total energy liberated during *K*-capture, then $E_\nu = E_0 - E_{re} = E_0$ and we have

$$E_{re} = E_0^2/2Mc^2. \qquad ...(18)$$

Devis in 1952 investigated *K*-capture in the reaction

$$^{7}_{4}Be + e_K^- \rightarrow {}^{7}_{3}Li + \nu_e + 0.864 \text{ MeV} \qquad ...(19)$$

The Eq. (18) gives E_{re} for the *Li*-nucleus as 57.3 eV. The interpretation of his data was affected by the complication that when a molecule breaks up, it is difficult to establish which fragment of molecule acquires the charge by which its recoil energy is determined experimentally. Later studies have used ^8Li and ^{24}Na. Since the rare gases are monatomic, Rodeback and Allen studied *K*-capture process with ^{37}Ar.

$$^{37}_{18}Ar + e_K^- \rightarrow {}^{37}_{17}Cl + \nu_e + 0.814 \text{MeV}. \qquad ...(20)$$

The recoil energy E_{re} = 9.6 eV. The apparatus used for measuring the velocity of the recoiling nucleus is sketched in Fig. 6.8. The chamber was kept at a low pressure of 10^{-5} mm of *Hg*, the effective volume of the argon source is indicated by a shaded region. The Auger electrons traveled to grid 1 into the electron detector, which is an Allen type multiplier. The recoil ^{37}Cl ions are accelerated between grid 2(V = 0) and grid 3(V = – 4500V) and detected by a multiplier. The time of flight of the recoil ions was measured by a 20 channel delayed coincidence circuit. A sharp peak in excellent agreement with that expected on the basis of the conservation of linear momentum between the neutrino and the recoil nucleus was observed. The maximum time of flight, *i.e.*, time spent by an ion in travelling the maximum distance (6 cm) was ~ 7.5 μsec. The time of flight is shortened by ~ 1.4 μsec for threefold charged ions. Thus a maximum time of flight obtained was 8.9 ± 0.9 μsec. This corresponds to a neutrino momentum of 0.8 ± 0.1 MeV/*c*, in good agreement with the *Q*-value 815 ± 2 keV for the $^{37}Cl\ (p,\ n)\ ^{37}Ar$ reaction or the $^{37}Ar - ^{37}Cl$ mass difference of 0.814 MeV.

Two interesting investigations of ^{37}Ar recoils have been performed where not only the recoil energy but also the charge spectrum of the recoils have been studied. In the investigation by the Kofoed-Hansen and Nielson an integral recoil spectrometer using crossed electric and magnetic fields was used. The spectrometer is called integral type as it gives integrals over the charge spectrum. The radioactive gas was distributed uniformly between the two plates of a capacitor and the currents to these plates of recoils and secondary electrons (mainly from Auger effect) were measured when different electic and magnetic fields were applied across the gas region. The recoil energy and the charge distribution were obtained from the currents. The recoil momentum times *c* was obtained to be 812 ± 8 keV, in agreement with the expected value of 814 keV.

In the Snell and Pleasonton's recoil spectrometer, the deflection was carried out in separate magnetic and electric spectrometers. It yielded differential spectra as regards both energy and charge. The apparatus used is shown in Fig. 6.9. In this apparatus, the source is defined by means of differential pumping. Strong pumping is applied between the narrow exit from the source volume and the narrow exit from the deflection magnet and between the latter and the entrance to the detector. These pumps lead into a purification and recirculation system. The detector volume is also pumped down with high speed pumps. The energy and charge of the recoil atoms are measured by separate magnetic and electric deflection. The recoil energy is found to be 9.63 ± 0.06 eV in very good agreement with the predicted value 9.65 ± 0.05 eV. The charge spectrum of recoil ions was obtained showing charges upto 7e.

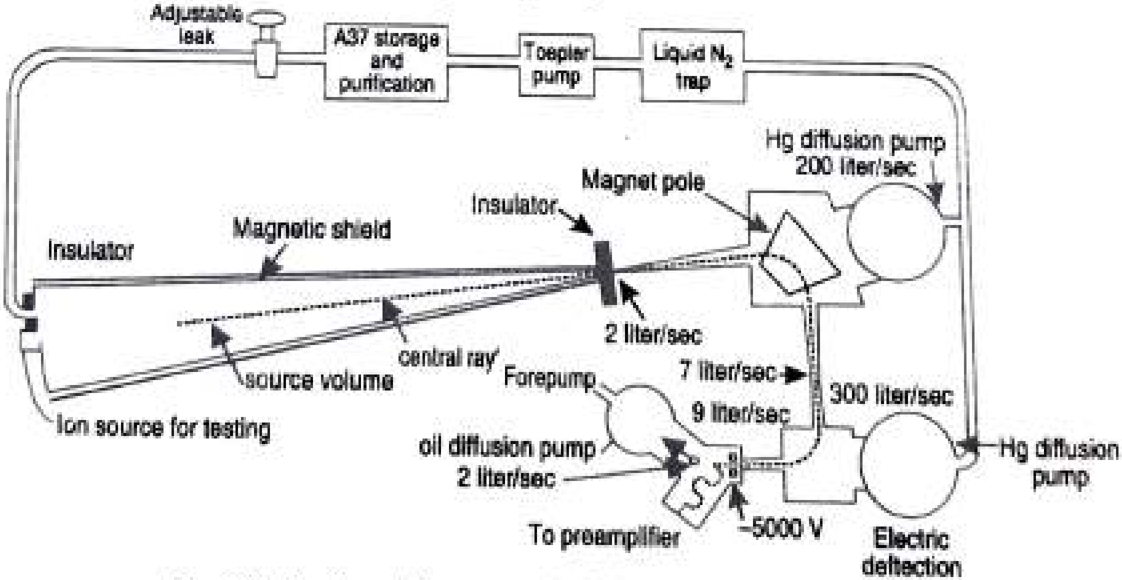
Adjustable leak
A37 storage and purification
Toepler pump
Liquid N_2 trap
Hg diffusion pump 200 liter/sec
Magnet pole
Insulator
Magnetic shield
Insulator
2 liter/sec
central ray
source volume
Forepump
7 liter/sec
9 liter/sec
300 liter/sec
Ion source for testing
oil diffusion pump 2 liter/sec
Hg diffusion pump
To preamplifier
-5000 V
Electric deflection

Fig. 6.9. Snell and Pleasonton's differential recoil spectrometer.

Direct Method— Theoretical calculations indicate that the probability of the interaction of anti-neutrino with proton is very small. Thus for the detection of this rare interaction, number of antineutrinos must be extremely large. Experiments were performed at several places in United States, near the nuclear reactors. Reines and Cowan reported their results in 1957, which were subsequently refined by Nezrick and Reines in 1966 in accuracy as improved techniques became available. Antineutrinos from a powerful reactor entered a liquid scintillator of volume 1.4 × 10³ litres (1.83 *m* × 1.32*m* × 0.56*m*), and were absorbed by the hydrogen of the organic scintillator solution due to the process

$$p+\bar{\nu} = n+\beta^{+}-1800\ \text{keV}. \qquad \ldots(21)$$

For the antineutrinos of energy above the threshold, sequence of two light pulses were produced. The first was due to the passage of the fast positrons through the scintillator and the second was due to the neutron absorbed in the scintillator, as follows :

Within the extremely short time (10^{-9} sec), the positron is slowed down and combined with an atomic electron. The two simultaneous annihilation γ-photons each of energy 0.511 MeV, and traversing in opposite directions produced the first pulse. The neutron produced was slowed down by multiple collisions in the scintillator and was finally captured in a cadmium nucleus present in the scintillator in the form of cadmium propionate within about 10 μsec. of its production. The neutron capture process produced a photon spectrum of total energy of about 9.1 MeV per capture, which was detected by the liquid scintillator. The positron and neutron pulses were detected in delayed coincidence and the difference between the counting rate with the reactor on or off was taken to find the true antineutrino absorption events. From the true counting rate of 36 ± 4 counts/hour, the cross section for the inverse β-decay was found to be $(11 \pm 2.6) \times 10^{-48} m^2$. This is in fine agreement with the theoretically expected value of $(10.7 \pm 0.7) \times 10^{-48} m^2$. The magnetic moment of the antineutrino was shown to be less than 10^{-9} μ_B.

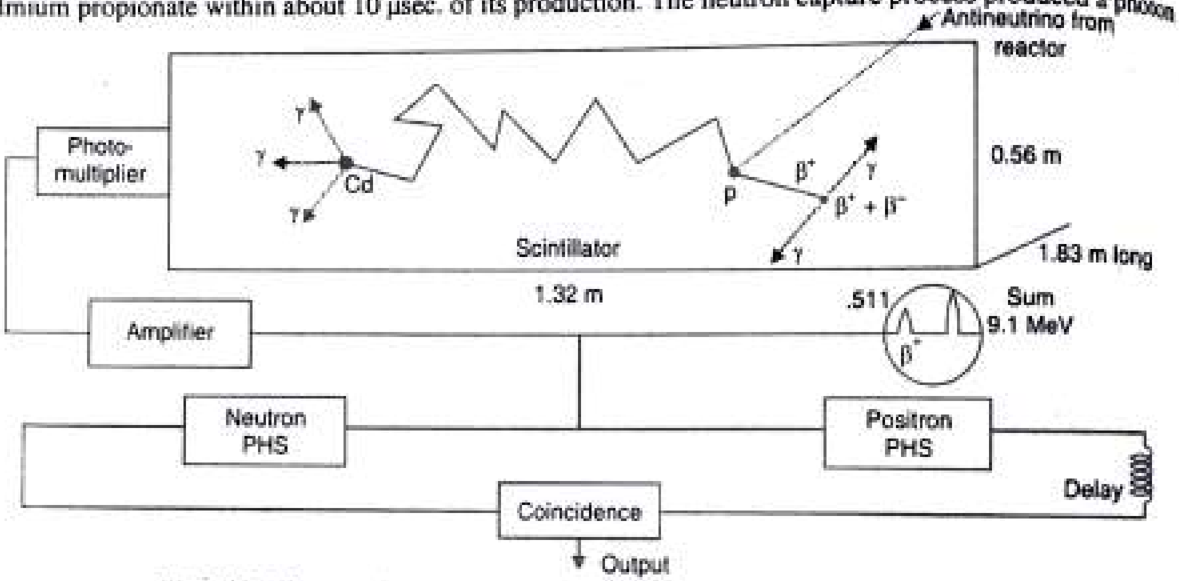

Fig. 6.10. Schematic diagram of apparatus with electronics for neutrino detection.

6.4 ENERGY HALF-LIFE RELATIONSHIPS

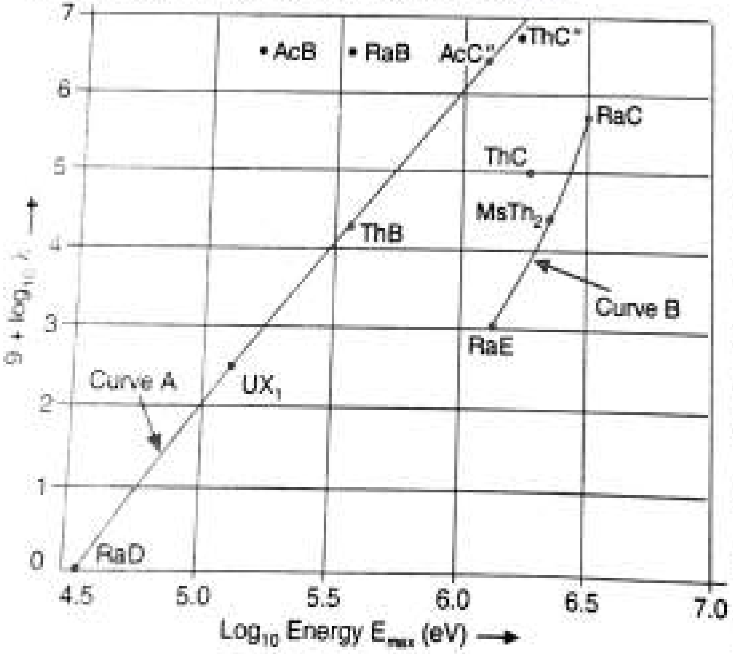

Fig. 6.11. Sargent curves.

In 1933, B.W. Sargent found that when log λ was plotted against log E_{max} for the naturally occurring β-emitters, most of the points fell on or near two straight lines, as depicted in Fig. 6.11. These lines, called *Sargent diagram* (or *curves*), represent empirical rules, analogous of the Geiger-Nuttall law in α-decay. The two curves do not correspond each to one radioactive series. For a given value of E_{max}, the upper curve gives a value of λ, which is about 100 times greater than corresponding value on the lower curve. The transitions in the short lived group are said to be *allowed*, the longer half-lives come from *forbidden transitions*, hence the *upper curve represents allowed transitions and the lower curve the forbidden transitions*. The transitions are now said to be first, second, ... or n-forbidden. As in α-decay, hindered would be better term than forbidden, but the latter is now firmly established.

The degree of forbiddenness affects the shape of the β-particle spectrum as well as the half-life of the transitions. The forbidden transitions show a greater number of low energy particles than are seen in an allowed transitions, but in many cases the differences are not great.

Most of the beta decay cases obey the Gamow-Teller rules and some follow the Fermi rules. A few nuclei appear to require a mixture of two sets of rules. Favoured transitions are found only in light nuclei, $A < 44$. In most of these cases, parent and daughter are mirror nuclei. Favoured transitions occur in a very small group of three member isobars, each case consisting of a parent made up of two nucleons more than a core of even N, even Z. For example ${}^{18}_{9}F \rightarrow {}^{18}_{8}O + \beta^{+}$.

6.5 FERMI THEORY OF BETA DECAY

The measured half-lives for β-decay vary from 10^{-3} sec to 10^{16} years. The large half lives of β-radioactive nuclei are against the existence of electrons in the nucleus. Various types of β-decay can be classified by the orbital angular momentum carried out by electron and neutrino and by the parity change in process. The decays may be classified as *Gamow-Teller-decays* (intrinsic spins of the electron and neutrino parallel) and *Fermi-decays* (spins anti-parallel). For zero orbital angular momentum carried off (*allowed transitions*) the decay constant increases roughly as the *fifth power* of the decay energy. To explain these effects the Italian Physicist Enrico Fermi, in 1934, formulated a successful theory of beta decay based on Pauli's neutrino hypothesis. This theory is based on the following assumptions :

(1) The light particles, the electron and neutrino are created by the transformation of a neutron into a proton in a nucleus, or vice versa.

(2) The energy remains conserved in the decay process, the available energy being shared among the electron and the neutrino. Due to the larger mass, product nucleus does not receive K.E.

(3) The neutrino has rest mass zero, or very small mass compared to that of the electron.

(4) The β-decay process is analogous to the emission of electromagnetic radiation by an atom, with the ***electron-neutrino*** field acting in place of the electromagnetic field. The nucleons are the source of light particles (e^{-}, $\bar{\nu}$; e^{+}, ν) similar to the charge as the source of photons.

(5) Electron-neutrino field is weak in contrast to the short range strong interaction which exist between the nucleons bound in the nucleus.

(6) Time dependent perturbation theory is a very good approximation because of the smallness of coupling constants (or exceptionally weak nature of the interaction).

(7) No nuclear parity change occurs and higher order terms in R/λ can be neglected.

(8) As nucleons' move with velocities of only ~ $c/10$ in nuclei, calculations can be made with non-relativistic nuclear wave functions.

Using Dirac's expression for the transition probability per unit time of an atomic system to emit photon, using time dependent perturbation theory, the probability that an electron of momentum between p_e and $p_e + dp_e$ is emitted per unit time may be written as

$$P(p_e)\,dp_e = \frac{2\pi}{\hbar}|H_{if}|^2 \frac{dN}{dE_0} \qquad \ldots(22)$$

where dN/dE_0 is the number of quantum mechanical states of the final system per unit energy interval and H_{if} the ***matrix element of potential or interaction*** relating the initial and final states, and causing the transitions. The former, known as statistical factor, determines the shape of the β-spectrum and the latter relates the electron and neutrino emission to the associated transformation.

Interaction Matrix Element—It is defined as

$$H_{if} = \int \Psi_f^{*} H \Psi_i \, d\tau, \qquad \ldots(23)$$

where Ψ_f and Ψ_i respectively are the wave functions of the system in its final state and in its initial state. H is the Hamiltonian operator that describes the weak interaction between the two states and $d\tau$ is the volume element.

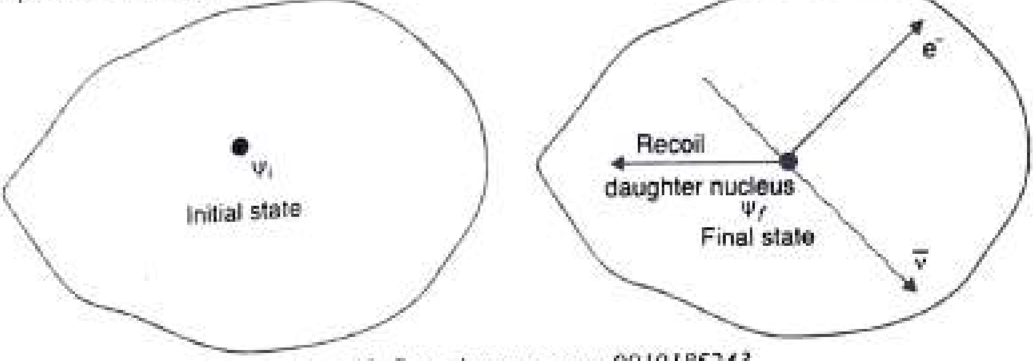

Fig. 6.12. Beta-decay process.9910185243

For the negatron decay $n \rightarrow p + {}_{-1}e^0 + \bar{\nu}$, we have

$$\Psi_i = \psi\,(\text{parent nucleus}) = \psi_I$$

and

$$\Psi_f = \psi\,(\text{daughter nucleus})\,\psi\,(\text{electron})\,\psi\,(\text{antineutrino}) = \psi_f\psi_e\psi_{\bar{\nu}}, \qquad \ldots(24)$$

We do not know the form of interaction operator H, but Fermi suggested a new constant, called as *Fermi coupling constant denoted by g*, (also represented by β in some books) which determines the strength of the β-interaction. This universal constant g has the value 0.9×10^{-4} *MeV fm*^{3} and is analogous to the electron charge e in the photon decay theory. Its character resembles that of the gravitational constant of the fine structure constant when expressed in dimensionless terms. Moreover, the emission of a neutrino and the absorption of an anti-neutrino of opposite momentum are equivalent and we may replace $\psi^*_{\bar{\nu}}$ by ψ_ν to make the equations more symmetrical. Thus the matrix element is written as

$$H_{\text{if}} = g\int\left[\psi^*_f\psi^*_e\psi_\nu\right]M\,\psi_i\,d\tau. \qquad \ldots(25)$$

where M is a dimensionless matrix element, which is an operator.

Since the neutrino interacts very weakly with nucleons, it is reasonable to assume the neutrino waves undistorted by the nuclear potential and may be taken as plane waves with the propagation constant $k = p_\nu/\hbar$, as

$$\psi_\nu = V^{-1/2}\exp.[-(i/\hbar)\boldsymbol{p}_\nu.\boldsymbol{r}] \qquad \ldots(26)$$

For light nuclei and electrons with kinetic energy $T_e > 200$ keV, the effect of Coulomb field of the nucleus upon the ejected electrons may be ignored and the electron waves may be taken as plane waves. Thus we have

$$\psi_e = V^{-1/2}\exp.[(i/\hbar)\boldsymbol{p}_e.\boldsymbol{r}] \qquad \ldots(27)$$

Here V is the whole volume in which we enclose the system for normalization purposes. $\boldsymbol{p}_\nu$ and $\boldsymbol{p}_e$ are the momenta of the neutrino and electron respectively and $\boldsymbol{r}$ is the position co-ordinate. Here we have neglected the spins, as the magnitudes of wave functions ψ_ν and ψ_e at the position of the nucleus are certainly much larger for S-wave neutrinos and electrons than for these particles with larger orbital angular momenta.

Thus matrix element becomes

$$H_{\text{if}} = g\int\psi^*_f\,\frac{1}{V}\left\{\exp.\left[-\frac{1}{\hbar}(\boldsymbol{p}_e + \boldsymbol{p}_\nu).\boldsymbol{r}\right]\right\}M\,\psi_i\,d\tau. \qquad \ldots(28)$$

The exponential factor can be expanded as a power series about the origin $\boldsymbol{r} = 0$, thus we have

$$\exp.\left[-\frac{i}{\hbar}(\boldsymbol{p}_e + \boldsymbol{p}_\nu)\cdot\boldsymbol{r}\right] = 1 - \frac{i}{\hbar}(\boldsymbol{p}_e + \boldsymbol{p}_\nu)\cdot\boldsymbol{r} - \frac{1}{2\hbar^2}\left[(\boldsymbol{p}_e + \boldsymbol{p}_\nu)\cdot\boldsymbol{r}\right]^2 + \ldots$$

Since the nuclear wave functions have appreciable values only in region of the order of nuclear dimensions, the significant values of r are no greater than the nuclear radius R. If p_e and p_ν are both of the order of magnitude $m_e c$, as is usually the case, the exponent will be of the order of $2m_e c R/\hbar = 1/50$. This small value suggests that we need to retain only the highest term, unity, in the power series. When this term is inserted into Eq. (28), the matrix element is non-vanishing and is no longer dependent upon the energies or momenta of the light particles. This gives us the allowed transitions. Matrix element of forbidden transitions will be energy dependent as they contain terms of the form $(\boldsymbol{p}_e + \boldsymbol{p}_\nu) \cdot \boldsymbol{r}$. Thus for allowed transitions, Eq (28) can be written as

$$H_{\text{if}} = \frac{g}{V}\int \psi_f^* M \psi_i \, d\tau = \frac{g}{V}|M_{\text{if}}|, \qquad \ldots(29)$$

where $|M_{\text{if}}|$ is the overlap integral or the *nuclear matrix element* of the final and initial wave functions of the nucleus. This can only be computed in a few cases where the structure of the nuclei is reasonably well known.

Statistical factor (Final state density) dN/dE_0—The statistical factor indicates the density of possible final states in the phase space of the electron-neutrino field. This can be derived with the help of the Heisenberg uncertainty relation. The position and momentum of electron or neutrino can be represented by a point in phase space, *the space containing three spatial and three momentum dimensions*. The uncertainty principle prevents us from representing a moving particle by a single vector. This is because such a representation would amount to specifying both the position and the momentum exactly. Thus in the 6-dimensional phase space defind by (x, y, z, p_x, p_y, p_z), the state of a particle can not be defined to a greater precision than that indicated by the volume element, also called cell. Since

$$\Delta x \cdot \Delta y \cdot \Delta z \cdot \Delta p_x \cdot \Delta p_y \cdot \Delta p_z \approx h^3.$$

Thus the state of a system cannot be specified more closely than by saying that the tip of the vector representing it lies in one of these cells. The states available to a free particle are distributed uniformly in phase space with a density h^{-3}. Thus the number of states of a particle restricted to a spatial volume V and whose momentum lies between the limits p and $p + dp$, without any regard to the direction in which the particle is moving, is given by

$$dN = V \times 4\pi p^2 \, dp/h^3.$$

The number of states corresponding to the apearance in volume V of the electron with the momentum in the range p_e to $p_e + dp_e$ is therefore given by

$$dN_e = 4\pi V p_e^{\,2} \, dp_e/h^3$$

Since the neutrino hardly interacts with its surroundings and may therefore be considered as a free particle once it is created. The number of states of neutrino with the momentum in the range p_ν to $p_\nu + dp_\nu$ is similarly written as

$$dN_\nu = 4\pi V p_\nu^2 \, dp_\nu / h^3.$$

As electron and neutrino are independent of one another, hence the number of states available to them jointly is given by

$$dN = (4\pi V p_e^2 \, dp_e/h^3)(4\pi V p_\nu^2 \, dp_\nu/h^3).$$

This denotes the number of accessible states in the phase space of the electron-neutrino field. The number of states per unit energy interval is

$$\frac{dN}{dE_0} = \frac{16\pi^2 V^2}{h^6} p_e^2 p_\nu^2 \, dp_e \frac{dp_\nu}{dE_0}. \qquad \ldots(30)$$

Since the total available energy, the overall decay energy E_0, is shared between the electron and the neutrino, therefore

$$E_0 = E_e + E_\nu. \qquad \ldots(31)$$

We have ignored variations of end point energy due to small differences in the recoil energy of the daughter nucleus. Thus for a fixed electron energy E_e, we have

$$dE_0 = dE_\nu. \qquad \ldots(32)$$

The momenta p_e and p_ν are related to the electron and neutrino energy respectively by the equations $E_e^2 = p_e^2 c^2 + m_e^2 c^4$ and $E_\nu = cp_\nu$. (Assuming zero rest mass) ...(33)

$$\therefore \quad dE_\nu = c\,dp_\nu. \qquad \ldots(34)$$

Using Eqs. (31), (32), (33) and (34) in Eq. (30), we have

$$\frac{dN}{dE_0} = \frac{16\pi^2 V^2}{h^6} p_e^2 \left(\frac{E_0 - E_e}{c}\right)^2 dp_e \frac{1}{c}.$$

Inserting this statistical factor and H_{if} from Eq. (29) into Eq. (22) we get the probability

$$\begin{aligned} P(p_e)\,dp_e &= \frac{2\pi g^2}{\hbar V^2}|M_{if}|^2 \cdot \frac{16\pi^2 V^2}{c^3 h^6} p_e^2 (E_0 - E_e)^2\, dp_e. \\ &= \frac{g^2 |M_{if}|^2}{2\pi^3 c^3 \hbar^7} (E_0 - E_e)^2\; p_e^2 dp_e. \qquad \ldots(35) \end{aligned}$$

Coulomb Correction. In the derivation of above relation no account has been taken of the Coulomb interaction which can be neglected only for the lightest nuclei ($Z < 10$) and sufficiently high electron energies. If this restriction is relaxed the plane wave for the emitted electrons must be replaced by a distorted Coulomb wave function. This can be taken into account by multiplying $|\psi_e|^2$ with a factor sometimes called *Coulomb factor*, $F(Z, E_e)$, also called *Fermi function*. It is the ratio of the electron density at the daughter nucleus to the density at infinity, *i.e.*

$$F(Z, E_e) = |\psi_e(0)^2_{coulomb} / |\psi_e(0)|^2_{free}.$$

$F(Z, E_e)$ is fairly complicated. In a non-relativistic approximation, it has the value

$$F(Z, E_e) = 2\pi\,\eta/(1 - e^{-2\pi\eta}), \qquad \ldots(36)$$

where $\eta = Ze^2/4\pi\varepsilon_0\ \hbar v$ for electrons, $\eta = -\,Ze^2/4\pi\varepsilon_0\ \hbar v$ for positrons, Z the atomic number of the product nucleus and v being the velocity of electron at a great distance from the nucleus. $F_{(Z, E_e)} \geq 1$ for β^- emission and is ≤ 1 for β *emission*. When consideration is given to this effect, equation (35) becomes

$$P(p_e)\,dp_e = \frac{g^2 |M_{if}|^2}{2\pi^3 c^3 \hbar^7} F(Z, E_e)(E_0 - E_e)^2\, p_e^2\, dp_e = C^2 F(Z, E_e)(E_0 - E_e)^2\, p_e^2\, dp_e, \qquad \ldots(37)$$

where

$$C = g|M_{if}|(2\pi^3 c^3 \hbar^7)^{-1/2}. \qquad \ldots(38)$$

We can transform this into probability per unit time that the kinetic energy of the emitted electron lies in the range T_e to $T_e + dT_e$. Using the relations

$$\begin{aligned} E_e &= T_e + m_e c^2 \text{ and } E_e^2 = p_e^2 c^2 + m_e^2 c^4, \text{ we get} \\ 2E_e\,dE_e &= 2p_e\,dp_e c^2 \text{ or } p_e\,dp_e = c^{-2}(T_e + m_e c^2)\,dT_e. \\ E_0 - E_e &= T_0 - T_e \text{ and } p_e^2 c^2 = [(T_e + m_e c^2)^2 - m_e^2 c^4] \text{ or } p_e = c^{-1}[T_e^2 + 2m_e c^2 T_e]^{1/2} \\ \therefore \quad P(T_e)dT_e &= \frac{g^2 |M_{if}|^2}{2\pi^3 c^6 \hbar^7} F(Z, T_e)(T_0 - T_e)^2 (T_e^2 + 2m_e c^2 T_e)^{1/2} (T_e + m_e c^2)\,dT_e. \qquad \ldots(39) \end{aligned}$$

Relation (39) may be written in terms of the reduced momentum $p = p_e/m_e c$ and reduced energy $w = E_e/m_e c^2$, as

$$\begin{aligned} P(p)dp &= \frac{g^2 |M_{if}|^2}{2\pi^3 c^3 \hbar^7} F(Z, w)(w_0 - w)^2 m_e^2 c^4 p^2 m_e^2 c^2 m_e c\,dp \\ &= \frac{G^2}{2\pi^3}|M_{if}|^2 F(Z, w)(w_0 - w)^2 p^2 dp \qquad \ldots(40) \end{aligned}$$

where

$$G^2 = (m_e^5 c^4/\hbar^7)g^2.$$

Since

$$p = \frac{p_e}{m_e c} = \frac{(E_e^2 - m_e^2 c^4)^{1/2}}{m_e c} = (w^2 - 1)^{1/2}, \text{ and } p\ dp = wdw$$

$$\therefore \quad P(w)dw = (G^2/2\pi^3)\,|M_{if}|^2\, F(Z, w)\,(w^2 - 1)^{1/2}\, w(w_0 - w)^2 dw. \qquad \ldots(41)$$

The behaviour of β-spectrum at very low electron or positron energies can be obtained directly from above relation. The Coulomb correction enhances the probability of electron emission and decreases the probability of positron emission, especially at low energies. The Coulomb force loses its effect on the spectrum shape at high energies and spectrum approaches that computed without the Coulomb correction. This can be explained in the following way : The Coulomb field accelerates the positive electron and decelerates the negative electron. Hence the positron spectrum has fewer slow particles and electron spectrum has more slow particles, than they would have in the absence of the Coulomb correction.

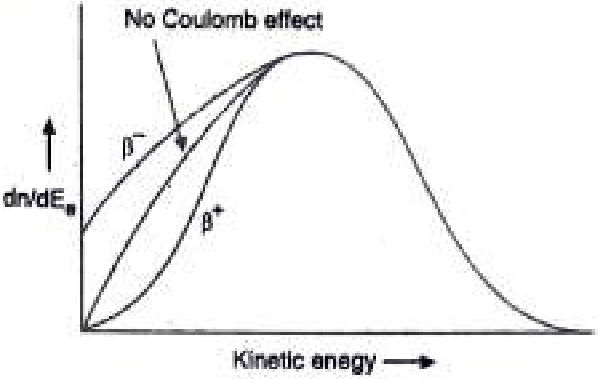

Fig. 6.13. Theoretical β-energy spectrum (Fermi theory).

Classically, no positron will be expected to emerge below the barrier energy $Ze^2/4\pi\varepsilon_0 R$. The actual spectrum does contain some low energy positrons, as a result of the tunnel effect. The relation for low energy β^+-emission is identical to that for α-decay,

$$F(Z, E_e) = -\frac{2\pi Ze^2}{4\pi\varepsilon_0\hbar v}\frac{1}{1-e^{2\pi Ze^2/4\pi\varepsilon_0\hbar v}} = \frac{Ze^2}{2\varepsilon_0\hbar v}e^{-Ze^2/2\varepsilon_0\hbar v}. \qquad \text{...(42)}$$

Screening by Atomic Electrons. In addition to the nuclear Coulomb effect the electrostatic potential of the atomic electrons affects the shape of the β-spectra. Reitz has tabulated and found corrections from 1.5 to 400 keV. This effect reduces the probability of β-emission by about 2% for a 50 keV β^--ray at $Z \sim 50$. The correction increases as Z increases or as β^--ray energy decreases. This effect is more important for β^+-ray as it reduces the height and thickness of the potential barrier. The probability of β^+-emission is increased by about 37% at $Z \sim 50$ for a 50 keV β^+-rays. Thus the atomic electrons exert very little effect on β^--spectra but affect considerably the emission of low energy (< 100 keV) β^+-rays, especially in heavy elements.

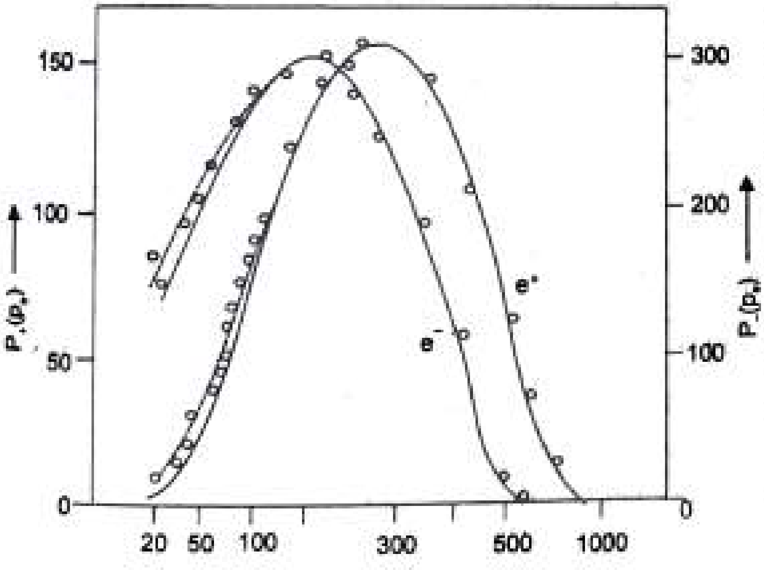

Fig. 6.14. Momentum spectra of ⁶⁴Cu electrons and positrons.

Allowed Spectra, β^+/β^- Ratio. Assuming the screening by atomic electrons as negligible, the ratio of positron to electron decay can be obtained by obtained by Eq. (40) for the same momentum interval p_e and $p_e + dp_e$ as

$$\frac{P_+(p_e)dp_e}{P_-(p_e)dp_e} = \frac{|M_{if}|_+^2 F_+(Z, E_e)(E_0 - E_e)_+^2}{|M_{if}|_-^2 F_-(Z, E_e)(E_0 - E_e)_-^2}$$

This ratio is dominated by the exponential term in $F(Z, E_e)$ while all other energy dependent terms nearly cancel, hence

$$\frac{P_+(p_e)}{P_-(p_e)} = const\frac{e^{-(Z-1)e^2/2\varepsilon_0\hbar v}}{e^{(Z+1)e^2/2\varepsilon_0\hbar v}} = \text{const}.\, e^{-Ze^2/\varepsilon_0\hbar v}.$$

Wu and Albert, using ^{64}Cu source, found that experimental and theoretical curves between log $[P_+(p_e)/P_-(p_e)]$ and $Ze^2/\varepsilon_0\hbar v$ were in excellent agreement. The slight variations at energies below about 50 keV, as shown in Fig. 6.14, are possibly due to instrumental error. *This was the best test for the Fermi theory in the light of β-ray spectra.*

Kurie Plots. A more convenient way of plotting the experimental results and checking with the theory was suggested in 1936 by Kurie. Equation (40) can be written as

$$\sqrt{[P(p_e)/F(Z,E_e)p_e^2]} = C(E_0 - E_e) = C(T_0 - T_e). \qquad ...(44)$$

where T_0 and T_e are kinetic energies of the β-particles. A plot of the function on the left hand side of above equation against T_e should be a straight line intersecting the energy axis at T_0. This graph is known as *Kurie plot*. This provides a good means of determining the maximum energy of the β-spectrum. Maximum energies of electron and positron, obtained by Kurie plots are 571 and 657 keV respectively for β-rays emitted from ^{64}Cu.

Many of the early Kurie plots were non-linear at low electron energies. The deviations at the low energy side are probably instrumental, caused by electron scattering and source due to the energy loss in the source material. If we take into account a relativistic mass correction term for the neutrino, then we see that Fermi plot near the end point energy is not a straight line but turns sharply to intersect the energy axis at a point smaller than the value for zero mass neutrino.

Mass of the Neutrino. The rest mass of neutrino can be measured with the help of Fermi-theory. The total disintegration energy in terms of the neutrino rest mass energy is given by

$$E_0 = E_e + E_\nu + m_\nu c^2. \qquad ...(45)$$

$\therefore$ Maximum β-particle energy $E_{\max} < E_0$.

Using relativistic energy-momentum relation

$$p_\nu = \frac{1}{c}[E_\nu(E_\nu + 2m_\nu c^2]^{1/2}, \qquad ...(46)$$

The probability distribution is given by

$$P(p_e)dp_e = C^2 F(Z,E_e)p_e^2[E_0 - E_e][(E_0 - E_e)^2 - (m_\nu c^2)^2]^{1/2} \qquad ...(47)$$

This reduces to equation (37) for $m_\nu = 0$. A great many experiments have been carried on the β-spectrum. Langer and Moffat compared the precision measurements at the high energy end of the ^3H spectrum taken with a high resolution magnetic spectrometer with Kurie plots drawn for $m_\nu = 0, 0.25, 0.5, 1.0$ *keV*. The data are consistent with a neutrino rest mass of zero and set an upper limit of 0.25 keV for a possible rest energy, Fig. 6.15. It is about 0.05% of the electron rest mass and can thus be assumed as zero. Lubimov, *et al* estimated the best fit value for neutrino mass as 37eV. These results are inconsistent with the experimental values, discussed earlier.

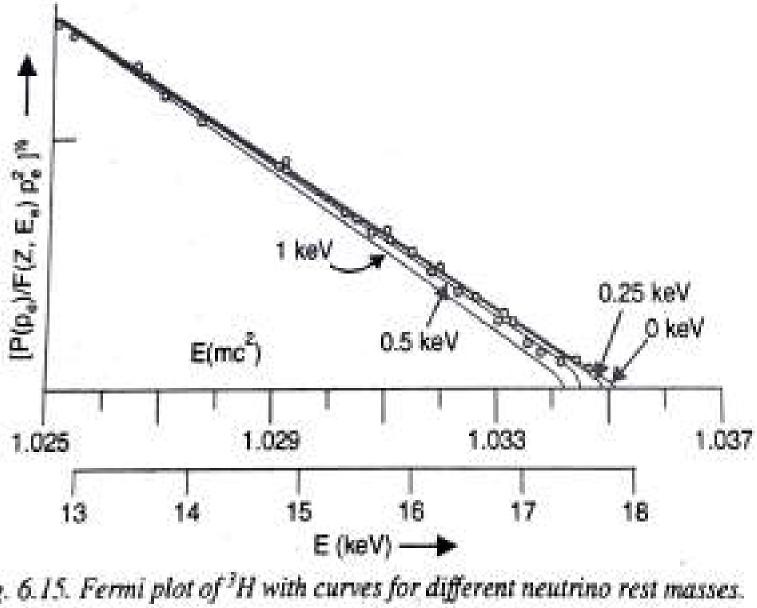

Fig. 6.15. Fermi plot of ^3H with curves for different neutrino rest masses.

Life time of β-decay. Equation (37) gives the probability per second for the emission of an electron with the momentum p_e and $p_e + dp_e$. The total probability per second λ, for beta disintegration can be computed from this by integrating over all values of the electron momentum from 0 to $p_{\max}$.

$$\lambda = \frac{\log_e 2}{t_{1/2}} = \int_0^{p_{\max}} P(p_e)dp_e$$

$$= \frac{g^2|M_{if}|^2 m_e^5 c^4}{2\pi^3 \hbar^7} \int_0^{p_{\max}} F(Z,w)(p_e^2)(w_0 - w)^2 dp_e = \frac{g^2|M_{if}|^2 m_e^5 c^4}{2\pi^3 \hbar^7} f \qquad ...(48)$$

If $E_0 >> m_ec^2$ or $p_{\max} >> m_ec$ and $F(Z, E_e) \sim 1$, f varies roughly as E_0^5. This E_0^5 dependence connecting λ and E_0 was first noticed by Sargent in 1933, and is known as the *fifth power law* and is obeyed in some cases, particularly by the positron spectra of light nuclei. For heavy nuclei the distortion due to the Coulomb field is more effective and there is no simple analytical expression for f. The *comparative half life* of a beta unstable nuclide is defined as $ft_{1/2}$, usually written as ft. The product ft depends solely upon the nuclear matrix element, as

$$ft = \frac{2\pi^3\hbar^7 \log_e 2}{g^2 m_e^5 c^4 |M_{if}|^2} = \frac{0.693\tau_0}{|M_{if}|^2}, \qquad \ldots(49)$$

where τ_0 is a new natural constant, known as *universal β-decay time constant*. The substitution of numerical values gives τ_0 = 7000 sec.

$$\therefore \qquad ft = 5000/|M_{if}|^2. \qquad \ldots(50)$$

This equation shows that the comparative half-life is proportional to the inverse square of the matrix element, which depends on the nuclear structure. It is expressed in sec and covers a very wide range of values (10^3 to 10^{23} sec.). It has been therefore found more convenient to use its logarithm, *i.e.*, log ft. The greater the value of ft, the longer is comparative half-life and smaller the probability of the radioactive change.

6.6 CLASSIFICATION OF BETA TRANSITIONS (SELECTION RULES)

The β-decay life-times fell into two categories, accordingly transitions are broadly divided into those which are allowed and those which are forbidden. These transitions are governed by certain selection rules. The above theory is applicable when the electron and neutrino carry away no orbital angular momentum while leaving nucleus. In fact, if electron and neutrino are emitted with their intrinsic spins antiparallel (*singlet state*), the change in nuclear spin ΔI must be strictly zero, if these are emitted with their spins parallel (*triplet state*), ΔI may be + 1, 0, or − 1 (but no $I_i = 0$ to $I_f = 0$), where subscripts i and f refer to the initial and final nuclear states. The former selection rule was one originally proposed by Fermi, the latter was subsequently suggested by *Gamow and Teller*. In both types of allowed transitions orbital angular momentum and parity are left unchanged. The interactions that give rise to Fermi and Gamow Teller selection rules are different. Experiment shows that the allowed transitions of the type $\Delta I = 1$, obeying $G - T$ selection rule, are forbidden by F-selection rule, as in the decay

$$\begin{array}{llll} {}^{6}_{2}He \rightarrow {}^{6}_{3}Li + \beta^{-} + \bar{\nu} & (0^+ \rightarrow 1^+) & \log ft = 2.77 \\ {}^{14}_{6}C \rightarrow {}^{14}_{7}N + \beta^{-} + \bar{\nu} & (0^+ \rightarrow 1^+) & \log ft = 3.62 \\ {}^{75}_{32}Ge \rightarrow {}^{75}_{33}As + \beta^{-} + \bar{\nu} & (1/2^- \rightarrow 3/2^-) & \log ft = 5.0 \end{array}$$

There are also allowed transitions of the 0 → 0 type that are allowed by F-selection rules but forbidden by $G - T$ selection rules, *e.g.*,

$${}^{14}_{8}O \rightarrow {}^{14}_{7}N^* + \beta^+ + \nu. \qquad (0^+ \rightarrow 0^+) \qquad \log ft = 3.487$$

The ground state of ${}^{14}_{7}N$ has a spin 1, however 2.31 MeV excited state ${}^{14}_{7}N^*$ has a spin O.

$$\begin{array}{llll} {}^{26}_{13}Al \rightarrow {}^{26}_{12}Mg + \beta^+ + \nu & (0^+ \rightarrow 0^+) & \log ft = 3.48 \\ {}^{34}_{17}Cl \rightarrow {}^{34}_{16}S + \beta^+ + \nu & (0^+ \rightarrow 0^+) & \log ft = 3.49 \\ {}^{50}_{25}Mn \rightarrow {}^{50}_{24}Cr + \beta^+ + \nu & (0^+ \rightarrow 0^+) & \log ft = 3.13 \\ {}^{54}_{27}Co \rightarrow {}^{54}_{26}Fe + \beta^+ + \nu & (0^+ \rightarrow 0^+) & \log ft = 3.13 \end{array}$$

However, many transitions are allowed by both selection rules. This is always possible in the allowed decays in which $I_i = I_f \neq 0$. The examples are

$$\begin{array}{llll} {}^{1}_{0}n \rightarrow p + \beta^- + \bar{\nu} & (1/2^+ \rightarrow 1/2^+) & \log ft = 3.074 \\ {}^{3}_{1}H \rightarrow {}^{2}_{3}He + \beta^- + \bar{\nu} & (1/2^+ \rightarrow 1/2^+) & \log ft = 3.05 \end{array}$$

$$
\begin{array}{lll}
{}^{35}_{16}S \rightarrow {}^{35}_{17}Cl + \beta^- + \bar{\nu} & (3/2^+ \rightarrow 3/2^+) & \log ft = 5.0 \\
{}^{17}_{9}F \rightarrow {}^{17}_{8}O + \beta^+ + \nu & (5/2^+ \rightarrow 5/2^+) & \log ft = 3.4 \\
{}^{7}_{4}Be \rightarrow {}^{7}_{3}Li + \beta^+ + \nu & (3/2^+ \rightarrow 3/2^+) & \log ft = 3.36
\end{array}
$$

These allowed transitions are further classified as *favoured* (*super allowed*) and *unfavoured* (*allowed*) *transitions*. The allowed transition is said to be favoured if the nucleon which changes its charge remains in the same level, it is unfavoured if the nucleon changes its level. Most of the allowed β-transitions are unfavoured. For the β^--decay, the change of a neutron into a proton without the change of level would increase the total energy of the nucleus and would, therefore, not lead to a spontaneous decay. For the β^+-decay, the surplus of neutrons makes the allowed transitions unfavoured. There are few exceptions, *e.g.*,

$$
{}^{3}_{1}H \rightarrow {}^{3}_{2}He,\ {}^{6}_{2}He \rightarrow {}^{6}_{3}Li,\ {}_{6}C^{11} \rightarrow {}^{11}_{5}B \quad \text{and} \quad {}^{18}_{9}F \rightarrow {}^{18}_{8}O.
$$

The conditions for super-allowed transitions are same as that for unfavoured or allowed transitions. The matrix element is also energy independent. The main different between the two cases is that the unfavoured or simply allowed transitions are not between mirror nuclei.

In the case of super-allowed transitions, the decay probability is very high and log *ft* is very low. The mirror nuclei, from *C* – 11 to *Ti* – 43, have their half lives ranging from 1230 sec to 0.6 sec and the corresponding E_{max} values are 0.99 MeV to about 5 MeV. The values of log *ft* are thus very close together.

Table 6.1. *Nuclear decay in mirror nuclei*

Nuclear decay	*Transition*	$t_{1/2}$/sec	E_{max}/MeV	*log ft*
${}^{11}_{6}C \rightarrow {}^{11}_{5}B + \beta^+$	$3/2^- \rightarrow 3/2^-$	1230	0.99	3.6
${}^{19}_{10}Ne \rightarrow {}^{19}_{9}F + \beta^+$	$1/2^+ \rightarrow 1/2^+$	20.3	2.18	3.4
${}^{27}_{14}Si \rightarrow {}^{27}_{13}Al + \beta^+$	$5/2^+ \rightarrow 5/2^+$	4.9	3.64	3.7
${}^{34}_{17}Cl \rightarrow {}^{34}_{16}S + \beta^+$	$0^+ \rightarrow 0^+$	1.53	4.50	3.493
${}^{35}_{18}Ar \rightarrow {}^{35}_{17}Cl + \beta^+$	$3/2^+ \rightarrow 3/2^+$	1.88	4.4	3.7
${}^{41}_{21}Sc \rightarrow {}^{41}_{20}Ar + \beta^+$	$7/2^- \rightarrow 7/2^-$	0.87	4.94	3.6
$n \rightarrow p + \beta^-$	$1/2^+ \rightarrow 1/2^+$	11.7 *m*	0.782	3.074
${}^{3}_{1}H \rightarrow {}^{3}_{2}He + \beta^-$	$1/2^+ \rightarrow 1/2^+$	12.46*y*	0.019	3.05
${}^{6}_{2}He \rightarrow {}^{6}_{3}Li + \beta^-$	$0^+ \rightarrow 1^+$	0.813	3.50	2.77

Let us now consider what happens when the transition from initial to final nucleus does not take place by the emission of *S*-wave electron and neutrino. Because of the finite size of the nucleus, the electron and neutrino emission with orbital angular momenta other than zero is also possible. The magnitudes of the wave functions ψ_e & ψ_ν for *p*-wave, *d*-wave, etc., over the nuclear volume decrease rapidly with increasing orbital angular momentum. β-transitions with angular momentum, carried off by the two light particles together, $l_\beta = 1, 2, 3$, etc., are classified as first, second, third etc., *forbidden transitions*.

If l_β is odd, initial and final nuclei must have opposite parities (*parity changes in these transitions*); for even l_β values the initial and final nuclei must have same parity (*no change in parity*). Furthermore, as in allowed transitions, the emission of leptons (electron and neutrino) in the singlet state (Fermi-selection rule) requires $\Delta I \leq l_\beta$, whereas triplet-state (*G–T* selection rule) emission requires $\Delta I \leq l_\beta + 1$. Thus selection rules for forbidden transitions are :

First forbidden—For these transitions $l_\beta = 1$ and parity changes.

Fermi-selection rules : $\Delta I = \pm 1, 0$ (except $0 \rightarrow 0$).

Gamow Teller rules : $\Delta I = \pm 2, \pm 1, 0$ (except $0 \rightarrow 0, \frac{1}{2} \rightarrow \frac{1}{2}, 0 \leftrightarrow 1$)

The examples are :

$^{39}_{18}Ar \rightarrow ^{39}_{19}K + \beta^-$	$(7/2^- \rightarrow 3/2^+)$	*GT.*	log $ft = 9.03$
$^{14}_{6}C \rightarrow ^{14}_{7}N + \beta^-$	$0 \rightarrow 1$	*F*	log $ft = 9.0$
$^{38}_{17}Cl \rightarrow ^{38}_{18}Ar + \beta^-$	$(2^- \rightarrow 2^+)$	*F + GT mixed*	log $ft = 8.15$
$^{139}_{56}Ba \rightarrow ^{139}_{57}La + \beta^-$	$(7/2^- \rightarrow 7/2^+)$	*F + GT mixed*	log $ft = 6.7$
$^{143}_{59}Pr \rightarrow ^{143}_{60}Nd + \beta^-$	$(7/2^+ \rightarrow 7/2^-)$	*F + GT mixed*	log $ft = 7.6$
$^{147}_{61}Pm \rightarrow ^{147}_{62}Sm + \beta^-$	$(7/2^+ \rightarrow 7/2^-)$	*F + GT mixed*	log $ft = 7.6$
$^{85}_{36}Kr \rightarrow ^{85}_{37}Rb + \beta^-$	$(9/2 \rightarrow 5/2)$	*GT.*	log $ft = 7.0$
$^{89}_{38}Sr \rightarrow ^{89}_{39}Y + \beta^-$	$(5/2^+ \rightarrow 1/2^-)$	*GT.*	log $ft = 8.5$
$^{137}_{55}Cs \rightarrow ^{136}_{56}Ba^* + \beta^-$	$(7/2^+ \rightarrow 11/2^-)$	*GT.*	log $ft = 9.6$

Second forbidden. For these transitions $l_\beta = 2$ and no change in parity.

Fermi-selection rules : $\Delta I = \pm 2, \pm 1$ (except $0 \leftrightarrow 1$)

Gamow Teller rules : $\Delta I = \pm 3, \pm 2,$ (except $0 \leftrightarrow 2$)

The examples are :

$^{137}_{55}Cs \rightarrow ^{137}_{56}Ba + \beta^-$	$(7/2^+ \rightarrow 3/2^+)$	*F + GT mixed*	log $ft = 12.2$
$^{10}_{4}Be \rightarrow ^{10}_{5}B + \beta^-$	$(0^+ \rightarrow 3^+)$	*GT.*	log $ft = 12.08$
$^{22}_{11}Na \rightarrow ^{22}_{10}Ne + \beta^+$	$(3^+ \rightarrow 0^+)$	*GT.*	log $ft = 11.9$

Similarly for third, fourth and so on forbidden we have :

Third forbidden : $^{87}_{37}Rb \rightarrow ^{87}_{38}Sr + \beta^-$ $(3/2^- \rightarrow 9/2^+)$ *F + GT*, change in parity, log $ft = 17.6$

$^{40}_{19}K \rightarrow ^{40}_{20}Ca + \beta^-$ $(4^- \rightarrow 0^+)$ *GT*, change in parity, log $ft = 15.60$

Fourth forbidden : $^{115}_{49}In \rightarrow ^{115}_{50}Sn + \beta^-$ $(9/2^+ \rightarrow 1/2^+)$ no change in parity, *F + GT*, log $ft = 23.02$

l^{th} forbidden : Fermi-selection rules $\Delta I = \pm l, \pm (l-1)$

G.T. selection rules $\Delta I = \pm l, \pm (l+1)$

Parity changes for l odd and does not change for l even.

The allowed and forbidden nature of the transitions is often determined from the ft value, which depends upon the atomic number, the end point energy and half-life period, ft values threw light on nuclear matrix elements, as it varies inversely as the square of the matrix element. The total distribution of ft values, from the compilation of G.E. Gleit *et al.*, shows that one cannot easily divide them into clearly separated groups, but the additional information gained from shell model considerations or from emipirical spin determinations has made it possible to group corresponding to different orders of forbiddenness. The reason for the large ft-values in forbidden β-decays comes from the fact that, with $l > 0$, the emission of β-particles is inhibited due to angular momentum barrier. This results in a reduction in the nuclear transition matrix element and hence an increase in the ft-values. The larger the value of l, the larger will be the effect and the ft-value. The nuclear matrix element M_{if} is very large (~ 1) for mirror nuclei as the initial and final state nuclear wave functions are very similar and the overlapping is nearly complete. In the allowed transitions, the overlap in the wave functions is far less and the matrix element is reduced.

The smallest values of ft are found for a group of light nuclei for which log ft = 2.7 to 3.7. The transformations of this group are described as *favoured allowed or super-allowed transitions*. Another group of nuclides is found for which log ft = 4.4 to 5.8. The transformations are described as *normal (or unfavoured) allowed transitions*. The first forbidden transitions have ft about 1000 times bigger. The rough classification into categories according to ft value is shown in **Table 6.2**.

Table 6.2. Classification of β-Transitions.

$\log_{10} ft = 2.7 - 3.7$	Super-allowed
$\log_{10} ft = 4 - 6$	allowed
$\log_{10} ft = 6 - 10$	for first forbidden
$\log_{10} ft = 10 - 14$	for second forbidden
$\log_{10} ft = 14 - 17$	for third forbidden
$\log_{10} ft = 17 - 24$	for fourth forbidden

To obtain ft values from measured decay energies and half-lives, it is convenient to use either the extensive graphs of log f verses E_0 and Z published by Feenberg and Trigg or the monograph of ft, half-life and E given by Moszkowski. One can use approximate expressions :

$$\log_{10} f_{\beta-} = 4.0 \log_{10} E_0 + 0.78 + 0.02Z - 0.005(Z-1) \log_{10} E_0$$
$$\log_{10} f_{\beta+} = 4.0 \log_{10} E_0 + 0.79 + 0.007\,Z - 0.009\,(Z+1)\,(\log_{10} E_0/3)^2,$$

where E_0 is the K.E. in MeV and Z is the atomic number of the product nuclide.

6.7 GENERAL THEORY OF β-DECAY

The β-decay can be explained only by the use of fairly advanced quantum-mechanical methods. It is assumed that the matrix element of beta decay contains four wave functions, corresponding to the four interacting particles : neutron, proton, electron and neutrino. The two separate processes $n \rightarrow p + e^- + \bar{\nu}$ and $p \rightarrow n + e^+ + \nu$ may be combined into a generalized symmetric form

$$n + \nu \rightarrow p + e^-, \qquad \ldots(51)$$

which suggests that simultaneous transformation of one nucleon into another ($n \rightarrow p$) and one lepton into another ($\nu \rightarrow e$). Mathematically this transformation can be affected through the agency of an interaction operator. All particles participating in beta decay are fermions of spin 1/2, each of them are therefore represented by a four component wave function, *i.e.*, the bispinor. The basic relativistic interaction operators for fermions can be obtained by forming all possible linearly independent products of Dirac matrices γ_μ, which satisfy the relation

$$\gamma_\mu \gamma_\nu + \gamma_\nu \gamma_\mu = 2\,\delta_{\mu\nu}, \quad \text{with } \mu, \nu = 1, 2, 3, 4. \qquad \ldots(52)$$

The product of Dirac matrices give sixteen linearly independent elements which can be classified into four groups according to their transformation properties, as scalar (S), vector (V), tensor (T), axial vector (A) and pseudoscalar (P).

The relativistically invariant perturbation term is the sum of five terms, as

$$H = H_S + H_V + H_T + H_A + H_P,$$

or

$$\mathrm{H}_\beta = \sum_\lambda \mathrm{H}_\lambda, \text{ where } \lambda = S, V, T, A, P. \qquad \ldots(5$$

The coupling constants for these interactions are g_S, g_V, g_T, g_A, and g_P. The generalized Hamiltonian density for β-decay interaction

$$H_\lambda = g_\lambda(\psi_p^* O_\lambda \psi_n)(\psi_e^* O_\lambda \psi_\nu) + \textit{Hermitian conjugate}. \qquad \ldots(54)$$

The operator O_λ is taken to act in the first bracket upon the nucleon variables only and in the second bracket on the lepton parameters only. The linear combination may be written in terms of coupling constants C_λ, which defines the relative strength of each interaction species as

$$H_\beta = g \sum_\lambda C_\lambda H_\lambda, \qquad \ldots(55)$$

where $g\,C_\lambda = g_\lambda$ and $\Sigma\,|C_\lambda|^2 = 1$.

H_S and H_V are often called the Fermi interactions and H_T and H_A the Gamow-Teller interactions. The pseudoscalar term is not suitable for describing allowed transitions, since in this case the transitions for which $\Delta I = 0$ with parity change is only allowed.

In the case of a pure one class of allowed transition, such as $0^+ \rightarrow 0^+$ pure Fermi β^+-transition, the ft value is related with the overlap integral M_{if} as

$$\frac{1}{ft} = \frac{g^2}{2\pi^3}\frac{m_e^5 c^4}{\hbar^7 \log_e 2}|M_{if}|^2. \quad ...(56)$$

The most reliable value for ft of pure Fermi $0^+ \to 0^+$, β^+ transition ($^{14}O \to {}^{14}N$) yields the result

$$g_F = (1.4061 \pm 0.0034) \times 10^{-62}\ joule\ m^3. \quad ...(57)$$

Similarly one can find g_{GT}, but in the case of pure GT-transitions, the nuclear elements are not known sufficiently. A more reliable value can be derived from mixed transitions ($\Delta I = 0$, which no change in parity). For these

$$\frac{1}{ft} = \left(\frac{1}{ft}\right)_F + \left(\frac{1}{ft}\right)_{GT} = \frac{g^2}{2\pi^3}\frac{m_e^5 c^4}{\hbar^7 \log_e 2}\left[C_F^2\,|M_F|^2 + C_{GT}^2\,|M_{GT}|^2\right]$$

or

$$B = ft[(1-x)\,|M_F|^2 + x\,|M_{GT}|^2] \quad ...(58)$$

where

$$B = \frac{2\pi^3}{g^2}\frac{\hbar^7 \log_e 2}{m_e^5 c^4}\frac{1}{C_F^2 + C_{GT}^2} \text{ and } x = \frac{C_{GT}^2}{C_F^2 + C_{GT}^2}. \quad ...(59)$$

The constants in this formula can be obtained from experimental results on the decay of neutron and light nuclei, such as ^3H, ^6He, ^{14}O for which the theoretical matrix elements are known because of the simple nuclear structure. For mirror transitions, the theoretical matrix elements are

$$|M_F|^2 = 1$$

and

$$|M_{GT}|^2 = \frac{I+1}{I} \text{ for } I = l + 1/2 \text{ and } \frac{I}{I+1} \text{ for } I = l - 1/2.$$

Therefore for neutron decay $|M_F|^2 = 1$ and $|M_{GT}|^2 = 3$.

In the β^+-decay of ^{14}O, the two protons involved are both in the same quantum state, therefore $|M_{GT}|^2 = 0$ and $|M_F|^2 = 2$.

From the data for neutron and ^{14}O, the ratio of coupling strengths can be derived, the recent value being

$$|C_{GT}/C_F|^2 = 1.38 \pm 0.08 \quad ...(60)$$

and with $ft = 1211 \pm 37$ sec for neutron decay

$$|g_{GT}/g_F|^2 = 1.38 \pm 0.04. \quad ...(61)$$

Electron-Neutron Angular Correlation—The values of various coupling constants can be determined from the experiments for the angular correlation between electron and neutrino emitted simultaneously in β-decay. If θ is the angle between them, then the transition probability per unit time is given by

$$P(E_e, \theta)\, d\Omega = \xi \frac{p_e E_e}{4\pi^3 c^5 \hbar^7} F(Z, E_e)(E_0 - E_e)^2 \left(1 + a\frac{v_e}{c}\cos\theta + b\frac{2mc^2}{E_e}\right)\sin\theta\, d\theta \quad ...(62)$$

where

$$\xi = \tfrac{1}{2}\{|g_S|^2 + |g_S'|^2 + |g_V|^2 + |g_V'|^2\}\,|M_F|^2 + \tfrac{1}{2}\{|g_T|^2 + |g_T'|^2 + |g_A|^2 + |g_A'|^2\}\,|M_{GT}|^2. \quad ...(63)$$

$$a\xi = \tfrac{1}{2}\{|g_V|^2 + |g_V'|^2 - |g_S|^2 - |g_S'|^2\}\,|M_F|^2 + \tfrac{1}{6}\{|g_T|^2 + |g_T'|^2 - |g_A|^2 - |g_A'|^2\}\,|M_{GT}|^2 \quad ...(64)$$

$$b\xi = \tfrac{1}{2}R_e\{g_S g_V^* + g_S' g_V'^*\}\,|M_F|^2 + \tfrac{1}{2}Re\{g_T g_A^* + g_T' g_A'^*\}\,|M_{GT}|^2 \quad ...(65)$$

The unprimed and primed constants respectively represent the relative strengths of the parity-conserving and parity-nonconserving interactions. The angular correlation coefficient is obtained by dividing Eq. (64) by Eq. (63). Thus for a pure Fermi transition

$$a = \frac{|g_V|^2 + |g_V'|^2 - |g_S|^2 - |g_S'|^2}{|g_V|^2 + |g_V'|^2 + |g_S|^2 + |g_S'|^2} \quad ...(66)$$

The Eq. (62) can be written for the whole beta spectrum after integration over θ, as

$$P(E_e)\, dE_e = \frac{\xi}{2\pi^3 c^5 \hbar^7} p_e E_e (E_0 - E_e)^2 F(Z, E_e)\left(1 + \frac{2mc^2 b}{E_e}\right) dE_e. \quad ...(67)$$

Its integration over the range of beta decay energy gives

$$2\pi^3 c^5 \hbar^7 (ft)^{-1} \log_e 2 \;=\; \xi + b2mc^2 \xi E_e^{-1}. \qquad \ldots(68)$$

The Fermi plot of Eq. (67) is a straight line, therefore Fierz constant $b = 0$ for the allowed beta ray spectrum. Thus Eq. (68) can be written for the *F*-transition as

$$2\pi^3 c^5 \hbar^7 (ft)^{-1} \log_e 2 \;=\; \xi = \tfrac{1}{2}\left\{|g_S|^2 + |g'_S|^2 + |g_V|^2 + |g'_V|^2\right\}|M_F|^2 \qquad \ldots(69)$$

Allen *et al.* experimentally observed $a = 0.97 \pm 0.14$, which may be taken as unity. Consequently $|g_S|^2 + |g'_S|^2 = 0$ and therefore $|g_S| = |g'_S| = 0$. The experimentally observed polarization is consistent with $g_V = g'_V$ for a pure Fermi transition and $g_T = g'_T$ for a pure G-T transition.

Therefore for the *F*-transition, we get

$$2\pi^3 c^5 \hbar^7 (ft)^{-1} \log_e 2 \;=\; \tfrac{1}{2}\left\{|g_V|^2 + |g'_V|^2\right\}|M_F|^2 = |g_V|^2 |M_F|^2 \qquad \ldots(70)$$

From the theory of angular momentum, we have $|M_F|^2 = 2$. Using $ft = 3075 \pm 10$ sec for ^{14}O, obtained by Bardin *et al.*, we get

$$g_V \;=\; (1.4025 \pm 0.0022) \times 10^{-62}\ J\text{–}m^3. \qquad \ldots(71)$$

Wu found $ft = 3125 \pm 10$ sec and $g_V = (1.4029 \pm 0.0022) \times 10^{-62}\ J\text{–}m^3$.

For a pure G-T transition, the angular correlation coefficient is given by

$$\begin{aligned} a \;&=\; \frac{1}{3}\frac{|g_T|^2 + |g'_T|^2 - |g_A|^2 - |g'_A|^2}{|g_T|^2 + |g'_T|^2 + |g_A|^2 + |g'_A|^2} \qquad \ldots(7 \\ &=\; 1/3 \text{ for } g_A = g_A' = 0. \\ &=\; -1/3 \text{ for } g_T = g_T' = 0. \end{aligned}$$

The experimental results of Allen *et al.* show that in allowed transitions the tensor contribution is practically zero within the experimental error. The Ridiley obtained experimental value as

$$a \;=\; 0.35 + {}^{0.033}_{-0.053}. \qquad \ldots(73)$$

Johnson *et al.* obtained $a = -0.3343 \pm 0.0030$ in excellent agreement with the theory. These results show that the Fermi angular correlation coefficient is greater than the GT angular correlation coefficient. The interaction is of *V* type for pure Fermi and *A* type for pure GT and the interaction in β-decay is a pure *V-A interaction.*

6.8 ELECTRON CAPTURE

We have talked so far entirely about β^- and β^+ emission and have ignored the third type of β-transition, orbital electron capture. When the unstable nuclides have a high Z-value (proton number), the Coulomb barrier tends to prevent the emission of a positive electron. However, an alternative mechanism for transforming the proton into a neutron can come into operation. This is the capture of orbital electron by the nucleus and was first suggested by Yukawa and Sakata in 1935 and discovered by L. Alvarez in 1938. Thus

$$p^+ + e^- \rightarrow n + \nu.$$

The electron is usually captured from the first quantum level, *i.e.*, the *K*-level. Instances of an electron being captured from the *L*-level are also known, although they are not common. If the captured electron comes from the atomic *K*-shell, the process is called *K-capture*; if from the *L*-shell, *L*-capture; and so on. In *EC* transition all the energy is carried out by neutrino. The β^+-decay cannot occur unless at least $2m_e c^2$ energy is available, whereas electron capture often occurs when β^+-decay cannot. The kinetic energy of the emitted neutrino is given by

$$E_\nu \;=\; E_0 + m_e c^2 - E_B, \qquad \ldots(74)$$

where E_0 is the available energy corresponding to the mass difference between the parent and daughter nuclei and E_B is the binding energy of the electron in its respective atomic shell before being captured. A negligible portion of energy is given to the recoiling of the daughter nucleus. Thus line spectrum for the neutrino energy is observed if capture takes place simultaneously from more than one shell.

The theory of electron capture is similar to that ordinary beta decay, except that the electron is now in a definite energy state and the electron wave function is the atomic-wave function of *a K*-or and *an L*-electron. The transition probability per unit time corresponds directly to the decay constant for orbital electron capture. Thus we have

$$\lambda = \frac{2\pi}{\hbar} \left| \int \Psi_i^* H_{if} \Psi_f \, d\tau \right|^2 \frac{dN}{dE_\nu}, \qquad \text{...(75)}$$

where dN/dE_ν refers to the density of neutrino states only.

The interaction matrix element is the same as in β-decay. Hence for allowed transitions, we get

$$|H_{if}|^2 = g^2 |\psi_e(0)|^2 \, |\psi_\nu(0)|^2 \, |M_{if}|^2. \qquad \text{...(76)}$$

where '*g*' is the coupling constant.

The neutrino field can be expressed as a plane wave, and at $r = 0$, we have

$$|\psi_\nu(0)|^2 = 1/V. \qquad \text{...(77)}$$

The electron wave function must now characterize the bound state of the initial system. To a good approximation we may use for the K-electron the ^1S-wave function of a hydrogenic system, with the charge number of the parent nuclide and we have

$$\psi_{e,K} = \psi_s = \frac{1}{\sqrt{\pi}} \left(\frac{Z}{a_B} \right)^{3/2} \exp.\left(-\frac{Zr}{a_B} \right) \qquad \text{...(78)}$$

where a_B is the Bohr radius having value $4\pi\varepsilon_0 \hbar^2 / m_e e^2$. As the nuclear wave functions are appreciable over only a small distance, *i.e.*, smaller than a_B/Z, hence we may expand the neutrino and electron wavefunctions about $r = 0$ and retain only the constant terms. Thus equation (75) becomes

$$\lambda_K = \frac{2\pi}{\hbar} g^2 \, |\psi_e(0)|^2 |\psi_\nu(0)|^2 |M_{if}|^2 \frac{dN}{dE_\nu}.$$

$$= \frac{2}{\hbar} g^2 \left(\frac{Z}{a_B} \right)^3 \frac{1}{V} |M_{if}|^2 \frac{dN}{dE_\nu}. \qquad \text{...(79)}$$

The statistical factor dN/dE_ν, *i.e.*, the energy density of neutrino wave is determined solely by the neutrino energy, since the electron is in a definite quantum state before capture,

$$dN = dN_\nu = \frac{V 4\pi p_\nu^2 \, dp_\nu}{h^3} = \frac{4\pi V E_\nu^2 dE_\nu}{c^3 h^3}$$

or

$$dN/dE_\nu = VE_\nu^2 / 2\pi^2 c^3 \hbar^3. \qquad \text{...(80)}$$

Hence using value of dN/dE_ν, Eq. (79) reduces to

$$\lambda_K = \frac{g^2 Z^3 m_e^3 e^6}{32\pi^5 \varepsilon_0^3 \hbar^{10} c^3} |M_{if}|^2 E_\nu^2. \qquad \text{...(81)}$$

Here we have inserted a factor of 2 to take account of the presence of two electrons in the K-shell. In relativistic units, neutrino energy can be written as

$$W_\nu = \frac{E_\nu}{m_e c^2} = \frac{E_0 + m_e c^2}{m_e c^2} - \frac{E_B}{m_e c^2} = W_0 - \varepsilon_B.$$

$$\therefore \quad \lambda_K = 4\pi \left(\frac{Ze^2}{4\pi\varepsilon_0 \hbar c} \right)^3 (W_0 - \varepsilon_B)^2 \frac{|M_{if}|^2}{\tau_0}. \qquad \text{...(82)}$$

where $\tau_0 = 2\pi^3 \hbar^7 / g^2 m_e^5 c^4$ = Universal time constant. Introducing $4\pi(Ze^2/4\pi\varepsilon_0 \hbar c)^3 \, (W_0 - \varepsilon_B)^2$ as $f_K^{(EC)}$, the *Fermi integral function*, we have

$$\lambda_K = |M_{if}|^2 f_K^{(EC)} (\tau_0)^{-1}. \qquad \text{...(83)}$$

Using the term fine-structure constant $\alpha (= e^2/4\pi\varepsilon_0 \hbar c)$ and the binding energy for K-electron in relativistic units

$$\varepsilon_K = \tfrac{1}{2}(Ze^2/4\pi\varepsilon_0 \hbar c)^2 = \tfrac{1}{2}(\alpha Z)^2,$$

we have the Fermi integral formula as

$$f_K^{(EC)} = 4\pi(\alpha Z)^3[W_0 - \tfrac{1}{2}(\alpha Z)^2]^2. \qquad ...(84)$$

This relation is corrected for relativistic effects and for screening of the nuclear charge by atomic electrons. Using the screening effect, Z should be replaced by Z' which is $Z - 0.35$ for K-electrons and Z-4.15 for *L*-electrons.

The *ft* values built from the product of f' with $T_{1/2}$ is thus given by

$$ft = f' T_{1/2} = \tau_0 \log_e 2/|M_{if}|^2 \qquad ...(85)$$

The *ft*-values agree fairly well with those for the corresponding β^+-transitions. The good agreement between the *ft*-value for the electron capture and that for β-decay in the case of superallowed $^7Be \rightarrow {}^7Li$ (*ft* = 2000 sec) transition shows that the strength of the interaction must be approximately the same in both the processes. The various degrees of forbiddenness also apply to E-C transitions. But in practice only superallowed and allowed EC-transitions have been observed with log *ft* ~ 4.5 – 6.5.

In practice, several shells may contribute to a capture process. For each shell (K; L_I, L_{II}, L_{III}; M_I, M_{II} ...M_V; —) the appropriate wave function ψ_e must be inserted. For *S*-electrons in a hydrogen like atom it is found to vary inversely as the 3/2 power of principal quantum number n. Thus the decay constant falls off as n^{-3}. The contribution from the L_I shell ($n = 2$) to *K*-shell capture ($n = 1$) is about 1/8 provided the available transition energy is large compared with the *K*-shell binding energy E_K. The calculations show that L_{II} to L_I branching ratio is small. It increases from about 0.002 for Z = 20 to 0.1 for Z = 100.

The relation (82) shows that the decay constant is larger for heavy elements. The nuclear matrix element for electron capture is the same as for β^+-decay. We can, therefore, find a formula for the branching ratio $\lambda_K/\lambda_{\beta^+}$ which is independent of M_{if}. The ratio of the number of K-capture events to positron emissions is

$$\frac{N_K}{N_{\beta^+}} = \frac{\lambda_K}{\lambda_{\beta^+}} = \frac{e^6 Z^3 E_\nu^2}{16\pi^2\varepsilon_0^3 h^3 c^7 m_e^2 f(Z,E_0)} = \frac{4\pi(\alpha Z)^3}{f(W_0,Z)}[W_0 - \tfrac{1}{2}(\alpha Z)^2]^2 \qquad ...(86)$$

The experimental ratios of K-capture to positron emission tend to support this type of expression. Experimental study of the electron-capture process is not quite so convenient as β^- and β^+-spectroscopy. The neutrino is practically unobservable, so that the only way to detect electron capture in practice is to observe the atomic processes following the disappearance of a *K*-or an *L*-electron. Following electron capture there will be an orbital vacancy, which will promptly fill from outer orbits. These transitions will produce the characteristic *X*-ray spectrum of the daughter element. For *K*-capture, one will observe the *K*-lines and for *L*-capture, the *L*-lines in the *X*-ray spectrum. Following *K*-capture it is also possible to observe Auger electrons.

When the daughter nucleus is left in an excited state after electron capture, the gamma-ray is subsequently emitted. If this photon energy ejects an electron from the *K*-shell (or *L*-shell), photoelectrically, there will be an additional emission of the *X*-ray spectrum. Since this exchange of energy is not limited to the *K*-electrons, it is possible to observe discrete β^--energies. These β^--radiations must not be confused with the nuclear β^--radiations which gives a continuous spectrum.

6.9 VIOLATION OF PARITY CONSERVATION IN β-DECAY

As indicated in Chapter 1, the parity was conserved in the strong nuclear interactions and also in electromagnetic interactions. The suspicion that parity conservation might be violated in certain weak interactions was first given by T.D. Lee and C.N. Yang in 1956, after the study of certain mesons (then called τ and θ). Experimentally these mesons were found to have the same mass, half-life and spin, with different decay modes. The θ^+-meson decays into two π-mesons and the τ^+-meson decays into three π-mesons. It shows that θ^+ is *a + ve* parity state and τ^+ is *a – ve* parity state. Lee and Yang showed that these different decay modes were possible only when the parity was not conserved. Since the τ and θ decays were weak, they suspected that parity might not be conserved in weak-interactions.

According to our definition of parity conservation, all terms of an equation must have the same behaviour under reflection. Thus the interaction term (or transition probability) for non-conservation of parity must contain not only scalar quantities but also *pseudo-scalar* quantities. These latter behave like scalars under co-ordinate rotation, but, unlike scalars, change sign under coordinate reflection, and are represented as the scalar product of one polar vector and one axial vector. The vectors such as displacement, velocity, momentum, acceleration, electric field, etc., are called polar vectors. The angular momentum vector is the vector product of position and linear momentum and is also named as *pseudo-vector or axial-vector*. Torque, angular momentum, spin, magnetic field and magnetic moments are examples of pseudo-vectors. Vectors and pseudo-vectors behave in the same way for translations or rotations of the co-ordinates system, but behave differently on inversion.

In normal β-decay experiment we measure the momentum of the electron $\boldsymbol{p}_e$ and by means of the recoil of the nucleus, the momentum of neutrino $\boldsymbol{p}_\nu$. The interaction term $\boldsymbol{p}_e \boldsymbol{p}_\nu$ is a scalar. However, if the β-active nuclei are polarized, so that all their intrinsic angular momenta $\boldsymbol{I}$ point in the same direction, then we have an additional vector. $\boldsymbol{I}$ $(= \boldsymbol{L} + \boldsymbol{S} = \boldsymbol{r} \times \boldsymbol{p} + \boldsymbol{S})$ is an axial vector, as $\boldsymbol{r} \times \boldsymbol{p}$ and spin angular momentum $\boldsymbol{S}$ are axial vectors. Therefore, $\boldsymbol{I} \cdot \boldsymbol{p}_e$ is a pseudo-scalar. Since the polar vector $\boldsymbol{p}_e$ changes sign under the parity reflection operation, and $\boldsymbol{I}$ does not change sign under the parity operation, hence the observation of pseudo-scalars different from 0 implies the breakdown of parity conservation.

Prior to 1956, none of the experimental investigations of β-decay provided an indication of parity non-conservation. These were not sensitive to detect and measure pseudo scalar quantities. Cox *et al.* in 1928 obtained a non-zero value for the longitudinal polarization of electrons emitted in β-decay, but this finding was disbelieved at the time and later forgotton.

The first experiment which clearly demonstrated the violation of parity conservation in β-decay was performed by Wu, Ambler, Hayward, Hoppes and Hindson in 1957 at the National Bureau of Standards, Washington. They studied the emission probability of electrons from polarized ^{60}Co nuclei which decayed by an allowed Gamow-Teller transition to $^{60}Ni(\Delta I = 0$, no parity change, electron spin parallel to antineutrino spin). The degree of polarization of the nuclei can be measured by means of the anisotropy of the gamma rays following the β-decay [Fig. 6.16 *(b)*]. Schematic representation of a ^{60}Co nucleus undergoing β^--decay and its mirror image is shown in Fig. 6.16 *(a)*. Here the mirroring reverses the spin sense and hence inverts the spin vector but leaves the emission direction unchanged. The parity conservation would require the decay probabilities to be the same in both cases and therefore the β-intensity antiparallel to the nuclear spin direction should be the same as that along the nuclear spin direction. Any asymmetry would be due to non-conservation of parity.

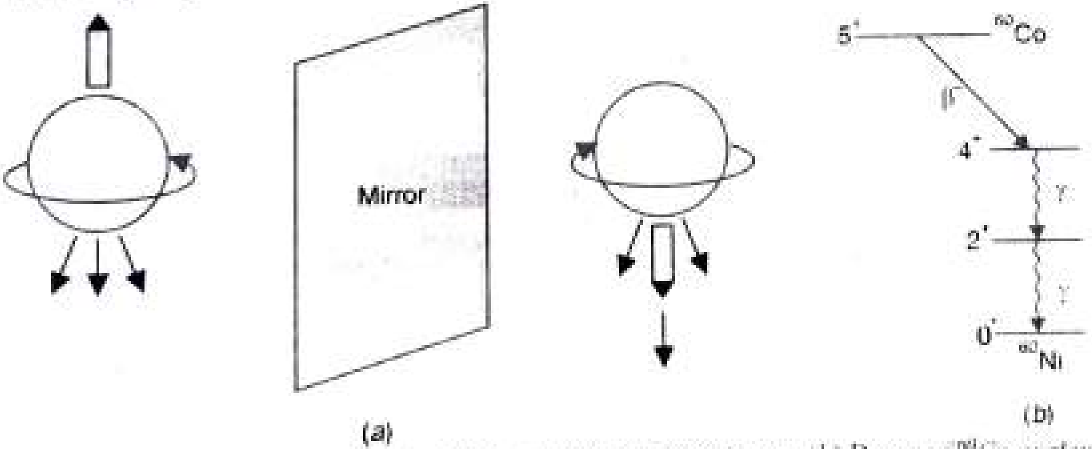

(a) (b)

Fig. 6.16. (a) ^{60}Co *nucleus undergoing* β^-*-decay and its mirror image. (b) Decay of* ^{60}Co *nucleus.*

If the spin of the nucleus is predominantly oriented in one direction, the system is called polarized. The ^{60}Co nucleus has a magnetic moment as its spin $I > 1$, so it is possible to align the nuclei by placing them in a very strong magnetic field ($\sim$ 10 Wb/m^2). To maintain this alignment or polarization, the

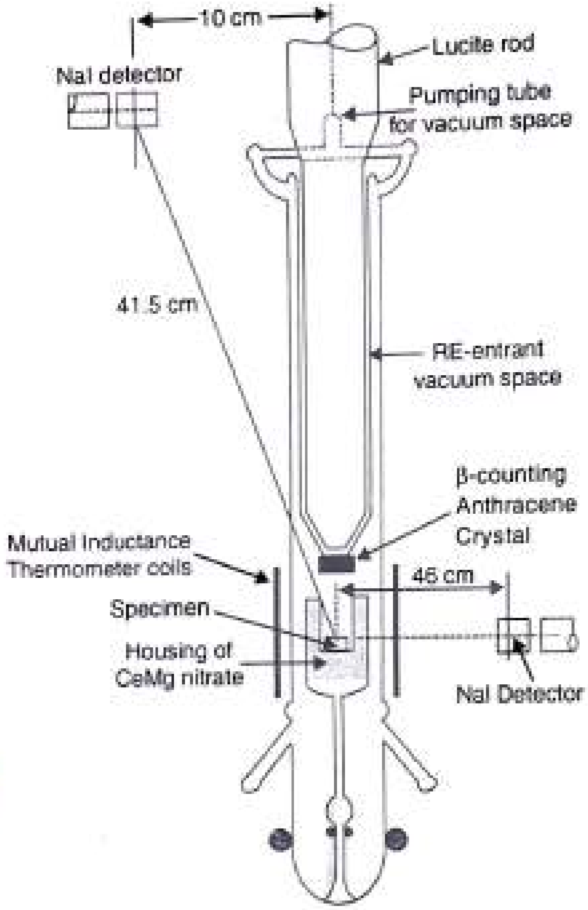

Fig. 6.17. Schematic diagram of Wu and others experiment.

temperature must be extremely low (< 0.1° K). For the polarization of ^{60}C nuclei, a method was employed by Rose and Gorter independently. A schematic diagram of the experimental arrangement used by Wu *et al.*, is shown in Fig. 6.17. A source consisted of a thin layer of ^{60}Co grown as a crystalline 0.002" layer on top of good single crystal of cerium-magnesium-nitrate $[2Ce(NO_3)_3 . 3Mg(NO_3)_2 . 24H_2O]$. It was mounted in a cryostate containing liquid hydrogen to reduce its temperature at ~1.2°K. A strong magnetic field was applied by passage of current through a solenoid, which would line up the paramagnetic ions and their tremendous fields at the nucleus in turn would orient the nuclear moments. The heat developed due to the work done was carried away to the liquid helium. The helium gas was removed by pumping, creating a very good vacuum. The magnetic field is reduced adiabatically. The demagnetization occured adiabatically thereby producing an additional cooling. Thus the temperature was further reduced well below 0.01°K. The magnetic field acting on the ^{60}Co nuclei was that due to the paramagnetic ions and was much greater than the original external field applied. The specimen eventually returned to higher temperature again, when heated by the beta and gamma rays emitted from the source, after 6–8 minutes of operation and lost its polarization through thermal agitation.

The beta-particles emitted by the polarized ^{60}Co nuclei are measured by an anthracene crystal mounted 2 cm above the source. The space between them is a vacuum. The light flashes in the scintillator, produced by the beta-rays, are transmitted through a 4 ft long lucite light pipe to a photomultiplier tube mounted outside the cryostat. Two NaI(Tl) scintillation counters are also placed outside the cryostat to measure the intensity of gamma rays emitted from ^{60}Ni, close to the axis of polarization and at right angles to it. Fig. 6.18 shows the graphs obtained with these counters. It is found that the intensity of the gamma-rays was initially much greater in the horizontal direction than in the vertical direction, but as time went on, the two intensities became equal. Here *time scale is actually a temperature scale measuring time from the instant when cooling is stopped.* Two intensities are equal when nuclei have become sufficiently warm so that their thermal motion causes the alignment to become random and the

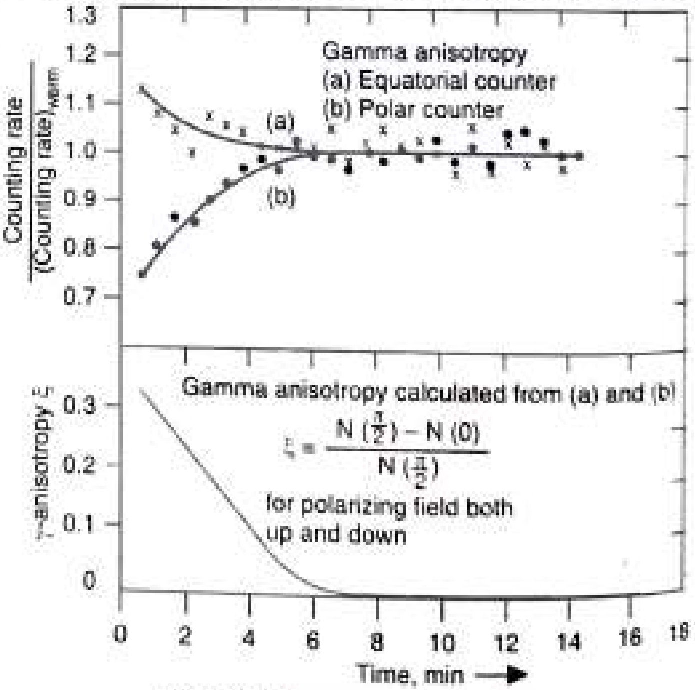

Fig. 6.18. Gamma-ray anisotropy.

gamma-anisotropy disappears. *Gamma-anisotropy is a measure of the extent of polarization* and is defined as

$$\xi = [(N_\gamma)_\perp - (N_\gamma)_\parallel]/(N_\gamma)_\perp. \qquad \ldots(87)$$

Readings of the two γ-counters showed an anisotropy which fell from its initial maximum value = 0.4, corresponding to the maximum nuclear polarization (= 65%), to zero within about 7 min. Fig. 6.18 (below). The beta rays are counted simultaneously with the γ-rays for the polarizing fields both up and down produced by the current in the solenoid. The time for the disappearance of the β-asymmetry coincided well with that of the γ-anisotropy, Fig. 6.19. The normalized asymmetry exceeded unity for B down and was less than unity for B up. It not only confirmed parity violation but showed that the emission of beta particles is favoured for electrons going in the direction opposite that of the nuclear spin.

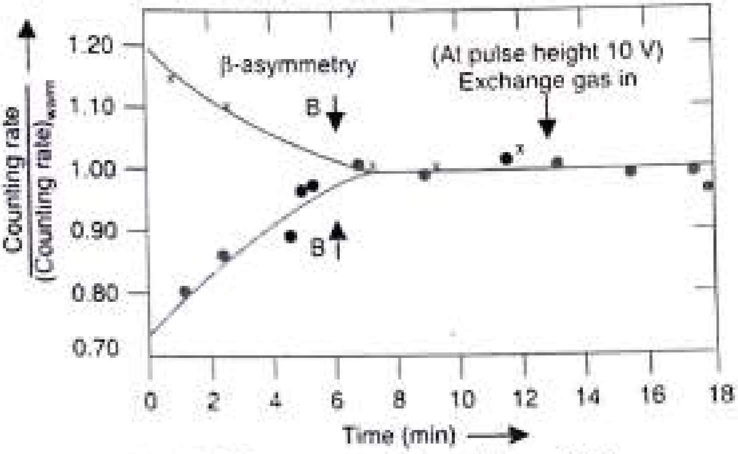

Fig. 6.19. Beta asymmetry for polarizing field.

These parity non-conserving effects are summarized as : (1) *The angular distribution of β-rays from polarized nuclei is not symmetrical about a plane through the nucleus ⊥ to the axis of polarization.* (2) *Electrons emitted in β-decay have their spins preferentially anti-parallel to their direction of travel and opposite occurs for positrons.*

6.10. HELICITY

Lee and yang suggested that the violation of parity in beta decay was a direct consequence of the longitudinal polarization of the emitted electrons and neutrinos. The state and degree of longitudinal polarization of particles and photons are represented by a term *helicity*, and is defined as

$$\mathcal{H} = \hat{\sigma} \cdot \hat{p}. \qquad \ldots(88)$$

where $\hat{\sigma}$ is a unit vector in the spin direction and $\hat{p}$ is the unit vector in the direction of the linear momentum of the particle and is the ratio of linear momentum and its magnitude. If these unit vectors are parallel, the beam is longitudinally polarized and the helicity is positive or + 1.; if they are perpendicular, the beam is transversally polarized and the helicity is negative or –1. In other words the helicity is positive or negative whether the velocity with which screw advances is parallel or anti-parallel to its angular velocity vector, or more simply, *whether the screw is right or left handed*. If the particle rotates in a clockwise sence as it recedes from the observer, it is known as right circularly polarized. The phrase *right circularly polarized* means *positive helicity* in Nuclear Physics. This is reverse of the definition in optics. Helicity is related to parity violation. If parity is a good quantum number, *i.e., the system has a definite parity either even or odd, then the helicity must be zero*. Similarly if a helicity different from zero is observed, parity must be violated in the interaction. Alternative symbols for helicity are *R* and *L*, corresponding to right circularly polarized and left circularly polarized particles.

Helicity of electron—Following the experiment of Wu and Ambler, many investigators studied the polarization of electrons of β-decay. The helicity of the electron is defined as the component of polarization along the direction of motion of the electron. Different methods have been used for the determination of electron helicities. The most widely used methods are Mott scattering, Møller scattering and bremsstrahlung, which give most accurate and reliable results.

(a) Mott scattering method—The first experiments on the helicity of electrons emitted in β-decay were based on Mott scattering, as the polarization dependence of Mott scattering had been known for a long time. Since Mott scattering is best suited for the analysis of the transverse polarization, and the electrons to be studied are longitudinally polarized, therefore *polarization transformers* are required. The polarization transformation is performed by sending the electrons through a properly chosen electromagnetic field

configuration. In the Mott scattering process, the incident electron with spin up and magnetic moment down approaching a nucleus of positive charge straight ahead are predominantly scattered to the right in a plane perpendicular to its spin. It is well suited for the analysis of the transverse polarization of electrons, but not of positrons. If $S(\theta)$ is the polarization produced when an unpolarized electron beam is scattered through an angle θ by a thin target and L/R is the ratio of intensities of electrons scattered to the left to electrons scattered to the right, then the transverse polarization P is given by

$$P = \frac{L-R}{S(\theta)(L+R)}, \qquad \ldots(89)$$

The simplest polarization transformer is a radial electric field, which acts only on the momentum but not on the spin of the electrons. In the majority of all experiments using Mott scattering, the radial electric field is produced by a cylindrical condenser. A schematic diagram of the apparatus used by Greenberg *et al.* is shown in Fig. 6.20. The electrons from the β-source S pass through a 90° deflector that acts as an energy selector and a polarization transformer. After passing through the condenser, the electrons impinge on a scatterer and the left-right asymmetry is determined using two scintillation counters. The chamber containing the scattering foil and the counters can be rotated with the help of a rotating seal and can be adjusted to the maximum left-right asymmetry. Crossed electric and magnetic fields can also be used to transform the polarization and select the electron energy. The Coulomb scattering in low Z-scatterers has also been used as polarization transformer.

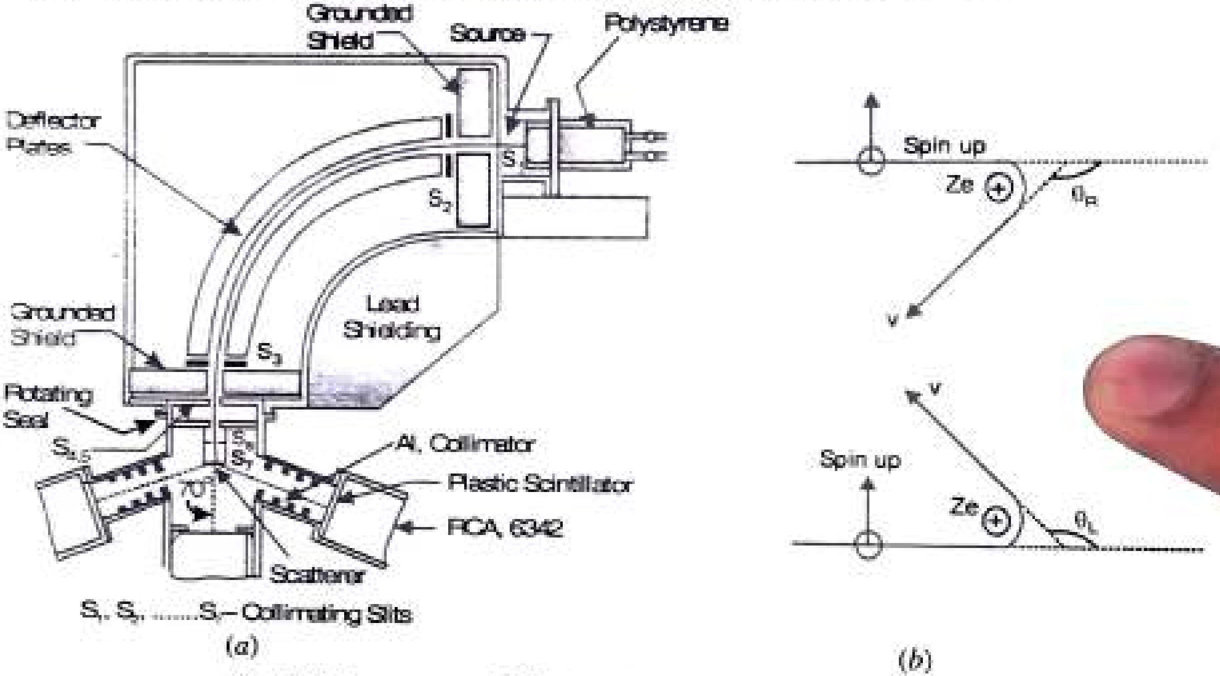

(*a*) (*b*)

Fig. 6.20. Measurement of helicity of the electron (Greenberg et al.).

In all these methods, electrons of a particular energy are selected and the intensity of scattering to the left and to the right is determined. From the ratio L/R, the polarization P is determined. The entire apparatus is built symmetric. scattering is minimized by taking large vacuum chambers. A thin and uniform scattering foil (usually gold) is placed perpendicular to the beam.

(*b*) *Electron-electron scattering (Møller scattering)*—A schematic representation of an arrangement for the determination of electron helicities using Møllar scattering is shown in Fig. 6.21. The electrons after passing through the monochromator impinge on a magnetized ferromagnetic foil. If the fractional energy transfer (w) by the incoming electron to the scattered electron is 1/2, two electrons with equal energy leave the foil. They are counted in coincidence. The pulse height analysis in the two counters further distinguishes the desired electrons from the back-ground events. Although the background events are suppressed by the angular and energy selection. If f is the fraction of electrons polarized in the scattering foil and α is the angle of inclination of the foil to the electron beam, the relative change δ of the coincidence counting rate on reversal of magnetization of the foil is given by

$$\delta = 2R\,P_i f \cos\alpha, \qquad \text{...(90)}$$

where P_i is the helicity of the incoming electrons and

$$R = (1-\sigma_{\parallel}/\sigma_{\text{ɑ}})/(1+\sigma_{\parallel}/\sigma_{\text{ɑ}}) \qquad \text{...(91)}$$

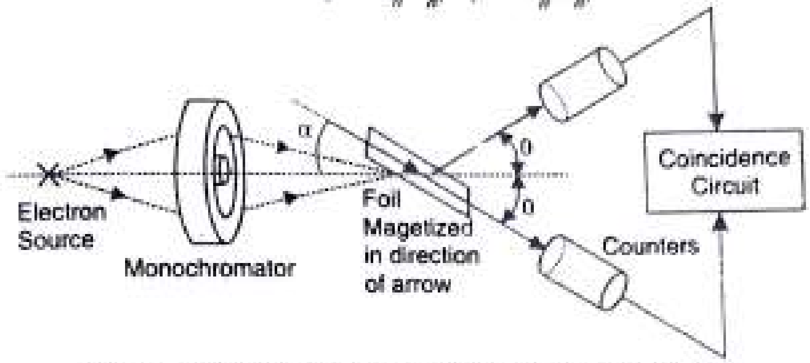
α
Electron Source
Monochromator
Foil Magetized in direction of arrow
θ
θ
Counters
Coincidence Circuit

Fig. 6.21. Schematic diagram of Mollar scattering apparatus.

The $\sigma_{\parallel}/\sigma_{\text{ɑ}}$ is the cross-section ratio for electron-electron scattering with spins parallel and antiparallel. The fraction f is related with M_s, the magnetic moment per unit volume in the material due to electron spin, N the number of electrons per unit volume and μ the Bohr magneton, as

$$f = M_s/N\mu. \qquad \text{...(92)}$$

To determine δ, the foil is first magnetized in one direction and coincidences are recorded for a known time. The magnetization is reversed and the coincidence rate is further measured.

This method has been used to determine helicity of electrons as well as of positrons. The experimental data show that electrons in β-decay are left handed, and positrons are right handed. In allowed transitions the helicity is equal to $\mp v/c$, where v is the velocity of electron, $-ve$ sign for left handed and $+ve$ for right handed.

Helicity of Neutrino—In 1958, Goldhaber, Grodzins and Sungar were able to study the polarization of the neutrino emitted in an electron capture process. The negative electron from the K-shell is captured in the isomeric 0^- excited state of ^{152}Eu, leading to the formation of ^{152}Sm in an 1^- excited state, 961 keV above its ground level. The latter decays by the emission of gamma ray photon of 961 keV and goes to the ground state 0^+, or by the emission of an 837 keV photon followed by a photon of 124 keV, Fig. 6.22 *(a)*. The entire angular momentum change (1) is carried away by the emitted photon. The K-capture process is a pure Gamow-Teller transition ($0^- \rightarrow 1^-$) and the spin of the emitted neutrino must be anti-parallel to the spin of the 961 keV ^{152}Sm state as shown in Fig. 6.22 *(b)*. There are two possibilities : the recoil nucleus and neutrino both have +1 helicity (*tensor interaction*) or they both have −1 helicity (*axial vector interaction*).

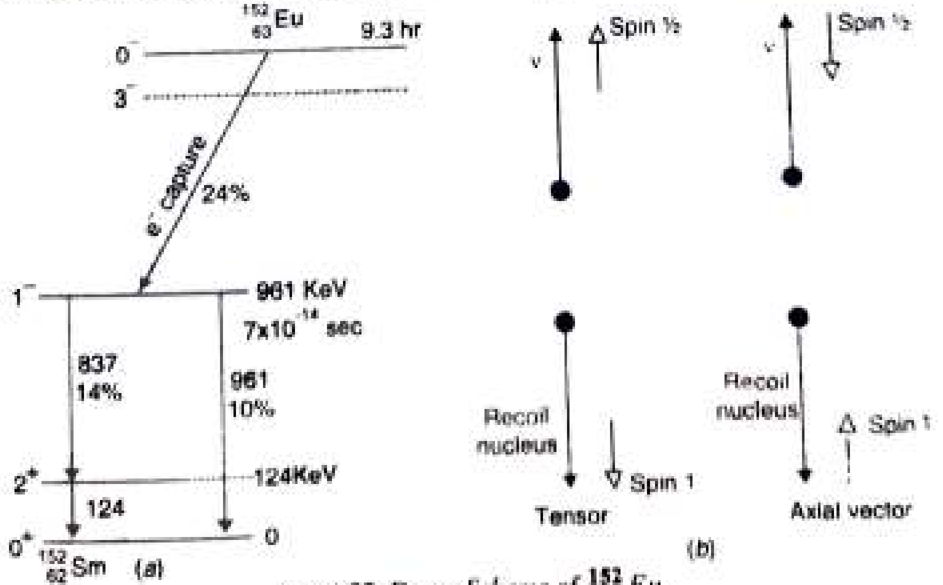
$^{152}_{63}$Eu
9.3 hr
0⁻
3⁻
e⁻ capture
24%
1⁻
961 KeV
7x10⁻¹⁴ sec
837
14%
961
10%
2⁺
124KeV
124
0⁺
0
$^{152}_{62}$Sm
(a)
v
Spin ½
v
Spin ½
Recoil nucleus
Spin 1
Tensor
Recoil nucleus
Spin 1
Axial vector
(b)

Fig. 6.22. Decay Scheme of $^{152}_{63}Eu$.

The nucleus, in excited state, must recoil with momentum equal and opposite to that of the neutrino so that the knowledge of the direction of the recoiling nucleus determines the direction of the neutrino momentum.

$$e_K(1/2) + Eu(0) \rightarrow Sm^*(1) + \nu(-1/2) \rightarrow Sm(0) + \nu(-1/2) + \gamma(1). \qquad ...(93)$$

- Furthermore, since the sum of the initial spins of captured K-electron and ^{152}Eu nucleus is one-half, the conservation of angular momentum requires that the spin of excited ^{152}Sm nucleus be opposite to that of the neutrino. Since these are moving in opposite directions, the excited nucleus must have the same helicity as the neutrino. *Thus the problem of measuring the helicity of the neutrino has been reduced to the helicity measurement of excited* ^{152}Sm *nucleus*. In the transition to the 0^+ ground state, the gamma ray takes the angular momentum with it. It is rather simple to show, by applying the laws of conservation of linear momentum and angular momentum, that the spin of the gamma rays be the same as that of excited ^{152}Sm, hence the spin of the gamma ray is opposite to that of the neutrino. Thus the *problem of measuring the neutrino helicity reduces to the measurement of the helicity of the circularly polarized gamma rays emitted opposite to the neutrino momentum.* Of course, gamma rays are emitted in all directions, but we are interested here in those that are emitted opposite to the neutrino.

The direction of polarization of these forward photons was determined by first scattering them from magnetized iron and then allowing them to be resonantly absorbed by ^{152}Sm.The 961 keV quanta have slightly less energy $(\Delta E = E_0^2/Mc^2 = 6.5 eV)$ than the excitation energy E_0 of the 1^- state because of the recoil loss in the source. Resonance scattering will only take place if extra energy equal to the energy lost is supplied to the emitted gamma ray. This may be done by the previously emitted neutrino. If v be the velocity of the recoiling of nucleus, caused by the emission of the neutrino, then

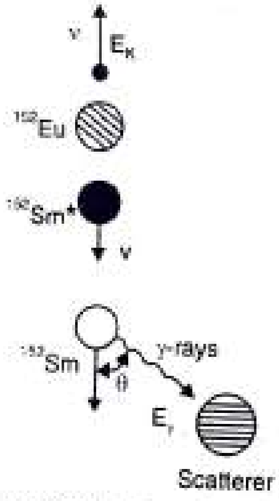

Fig. 6.23. Emission of neutrino.

Momentum of the excited nucleus Mv = Momentum of neutrino E_K/c,

or $\quad v/c = E_K/Mc^2$, ...(94)

where E_K is the energy of neutrino. If de-excitation occurs before the nucleus slows down, then the gamma ray energy E_γ is given by

$$E_\gamma = E_0 + \left(\frac{v}{c}\right)E_0 \cos\theta - \frac{E_0^2}{2Mc^2} = E_0 + \frac{E_K}{Mc^2}E_0\cos\theta - \frac{E_0^2}{2Mc^2}.$$

Thus the excitation energy which can be transferred to the absorbing nucleus ^{152}Sm is given by

$$E'_\gamma = E_0 + \frac{E_K}{Mc^2}E_0\cos\theta - \frac{E_0^2}{Mc^2}.$$

The condition for resonance is

$$E'_\gamma = E_0 \text{ or } E_K\cos\theta = E_0.$$

Thus we see that when the neutrino has same energy as the γ-ray, *resonant condition is fulfilled only for those gamma rays which are emitted opposite to the neutrino and the helicity of the neutrino can be measured by measuring the circular polarization of those γ-rays which cause resonant scattering.*

The apparatus used by Goldhaber et al. to measure the helicity of the neutrino is shown in Fig. 6.24. The radioactive europium source, produced by bombarding 10 mg of Eu_2O_3 in theBrookhaven reactor, was placed in an analyzing magnet. The circular polarization of the γ-rays was analyzed by transmission through 6.4 cm of fully magnetized iron block, as the absorption of a γ-beam on passage through the block differs slightly according as it is right-circularly or left-circularly polarized. The γ-rays scattered from a ring scatterer of 1.7 kg Sm_2O_3, were detected in a 2 × 3.5-inch $NaI(Tl)$ scintillator, which was shielded from the direct radiation by a 12 inches of conical lead absorber. The scatterer would be alternated with a lead scatterer containing an eqivalent number of electrons. The selection of the appropriate γ-direction was achieved by observing only those photons which were scattered resonantly from a Sm_2O_3 scatterer.

The pulse height spectrum of γ-rays, Fig. 6.25, shows the resonance scattering peaks superimposed on the non-resonant background. The dashed curve represents the spectrum taken with a lead scatterer. From the preceding discussion, we concluded that the two peaks (961 keV and 837 keV) in the spectrum resulted from events in which the neutrino was emitted upward. The rapid rise at lower energies was due to Compton scattering. The counting was measured with the reversal of magnetic field applied to the iron absorber. The result was a higher counting rate with the field down than with the field up, indicating that the γ-rays had left-circular polarization. The neutrino therefore has a *negative helicity.*

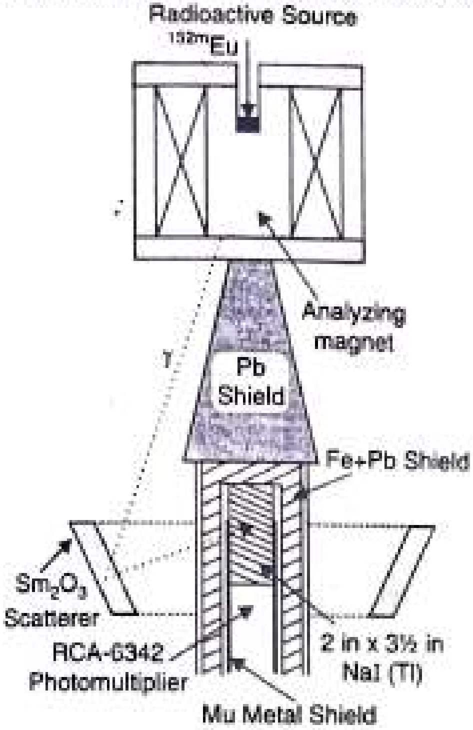

Fig. 6.24. The measurement of helicity of the neutrino.

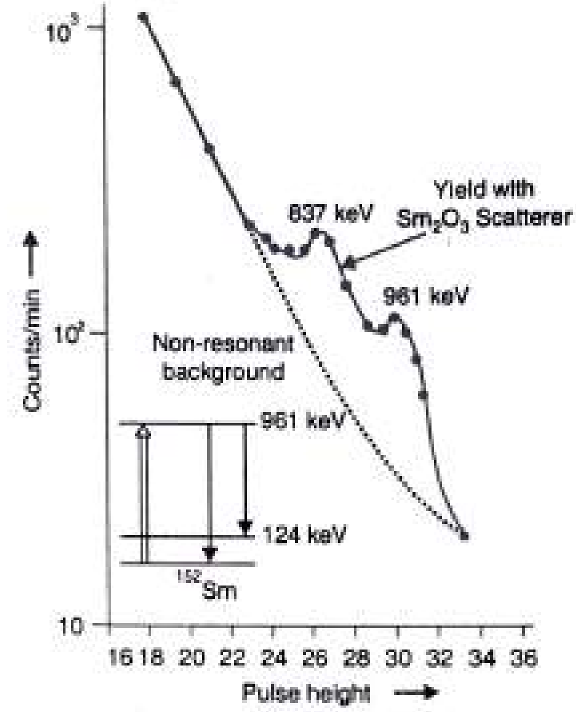

Fig. 6.25. Pulse height spectrum of γ-rays.

From the different set of measurements, it was observed that the degree of circular polarization

$$P_\gamma = 0.67 \pm 0.10,$$

was in close agreement with the theoretical expectation of 0.84, which did not include either thermal motions in the source or capture in other than the *K*-shell. The negative helicity of neutrino emitted in *K*-capture shows that in the pure GT-transition the dominant interaction mode is axial vector and not tensor in agreement with the $V - A$ interaction observed in β – ν angular correlation studies.

6.11 DOUBLE β-DECAY

Double β-decay is the second order decay involving β-interaction. In this process the nucleus (A, Z) decays spontaneously into an isobar $(A, Z \pm 2)$ with the emission of two electrons or positrons and either *(a)* two anti neutrinos or neutrinos or *(b)* no antineutrinos or neutrinos. If ν_e and $\bar{\nu}_e$ are identical, the two stages of double β-decay would combine in such a way that emission of antineutrino is compensated by absorption of neutrino and no neutrinos are emitted in the process.

$$\begin{array}{rcl} n & \rightarrow & p^+ + e^- + \bar{\nu}_e \; (\equiv \nu_e) \\ \nu_e + n & \rightarrow & p^+ + e^- \\ \hline 2n & \rightarrow & 2p^+ + 2e^- \end{array}$$

If ν_e and $\bar{\nu}_e$ are regarded as different, then two electrons are accompanied by two antineutrinos, as

$$n \rightarrow p^+ + e^- + \bar{\nu}_e$$

$$\nu_e + n \rightarrow p^+ + e^- \text{ or } n \rightarrow p^+ + e^- + \bar{\nu}_e$$

$$2n \rightarrow 2p^+ + 2e^- + 2\bar{\nu}_e$$

In this case the available transition energy is shared statistically between the two electrons and two antineutrinos and the sum of electron energies shows a broad distribution.

The half lives for both alternatives are long. The theory predicted the half lives of $10^{15} - 10^{16}$ and $10^{20} - 10^{22}$ years for the neutrinoless double β-decay and two neutrino β-decay respectively. The neutrinoless double β-decay processes are strictly forbidden if the neutrinos are Dirac particles with particles distinct from their antiparticles, and are allowed if the neutrinos are Majorana fermions with no distinction between particles and antiparticles. The experiment by R. Davis, discussed earlier, showed that the neutrinos and antineutrinos are different particles.

The recent measurements of the double β^--decay of ^{82}Se to ^{82}Kr by Elliot, Hahn and Moe show that the energy spectrum of the two electrons emitted and the half life of the decay ($\sim 4.4 \times 10^{20}$y) are consistent with the two neutrino mode. The energy spectrum of the experiment is more conclusive evidence against the neutrinoless mode than the lifetime measurements, as the nuclear transition matrix element may have differences in the values similar to single β-decays (large spread in the log ft-values).

A Brief Summary

Beta decay is the spontaneous emission of an electron (β^--decay), or a positron (β^+-decay) by the nuelcus, as well as the capture of an electron from *K*- or *L*-orbit of the atom by its nucleus. The energy of beta decay varies from 0.018 MeV to 16.6 MeV and their half lives vary between 10^{-2} *sec* and 2×10^{15} years. Unlike α-spectra which are discrete, β-spectra are continuous (0 to T_{max}). A part of this energy is carried away by the neutrino (antineutrino). The electrons and neutrinos emitted during β-decay are not contained in the nucleus, but appear just at the moment of β-decay.

The theory of β-decay, Fermi's theory, connects the lifetime of the β-radioactive nucleus and the energy of β-decay through a relation of the type $ft = const$. The ft value is also called comparative half time of a β-unstable nucleus, which is proportional to the inverse square of the matrix elements, which depends on the nuclear structure. The selection rules are used to classify the beta transitions. The ft values have a large range, therefore $\log_{10} ft$ is generally used to classify the β-transitions. The decay rate also depends strongly on the spins and parities of the nuclear states involved in the decay. The transitions are superallowed for lowest values of ft ($\sim 10^3$), allowed for $\sim 10^5$ and forbidden for 10^7 onwards. The allowed and superallowed transitions satisfy the selection rules for momentum and parity of the nucleus. The comparison of theoretical and experimental results shows that the β-interaction is extremely weak. The particle emitted with the electron is called antineutrino, which is not normally detected because of extremely weak interaction. Pauli postulated that the antineutrino $\overline{\nu}$ has zero charge, intrinsic party 1/2 and zero rest mass. In positron emission and electron capture the, particle neutrino is emitted which has the same zero charge, spin 1/2 and zero rest mass.

The theory of electron-capture is similar to that of ordinary β-decay, except that the electron is in a definite energy state and the electron wave function is the atomic wave function of a *K*-or and an *L*-electron. When the daughter nucleus is left in an excited state after electron capture, gamma rays are emitted which may produce discrete β-radiations, which are different than the continuous spectrum of β^--decay.

It has been observed experimentally that the parity is generally violated in certain weak interactions. The β-interaction constant is found to be very small, which indicates that the β-decay is extremely weak. The investigation of β^--decay in polarized nuclei confirmed the conclusion drawn by *Lee* and Yang regarding nonconservation of parity in beta decay. Wu and others in 1957 first observed the violation of parity conservation in β-decay. They studied the emission probability of electrons from polarized ^{60}Co nucleus. The parity non conserving effects are summarized as : The angular distribution of β-rays from polarized nuclei is not symmetrical about a plane through the nucleus ⊥ to the axis of polarization and the electrons emitted in β-decay have their spins preferentially antiparallel to their direction of travel (opposite occurs for positrons). The state and degree of longitudinal polarization of particles and γ-rays are represented by a term helicity. If the spin and linear momentum directions are parallel, the beam is longitudinally polarized and the helicity is (positive) +1. If they are perpendicular, the beam is transversally polarized and the helicity is negative (−1). Helicity is related to parity violation. Helicity is zero for a system of definite parity. The helicity different from zero shows the parity violation.

EXERCISES

Example 1. *A sample contains 4.00 mg of RaE. If the half-life is 5.0 days and the average energy of the β-particles emitted is 0.34 MeV, at what rate in watts does the sample emit energy?*

The rate of disintegration $dN/dt = \lambda N$.

Here $\lambda = 0.693/T = 0.693/5 \times 24 \times 60 \times 60$, *RaE* is ^{210}Bi and therefore

$$N = \frac{6.023 \times 10^{26}}{210} \times 4 \times 10^{-6}$$

$$\therefore \quad \frac{dN}{dt} = \frac{0.693}{5 \times 24 \times 60 \times 60} \times \frac{6.022137 \times 10^{26}}{210} \times 4 \times 10^{-6}.$$

$$= 1.84 \times 10^{13}.$$

This is the number of β-particles emitted per sec. Since each electron carries an average energy of 0.34 MeV, hence the rate of energy radiated

$$P = E(dN/dt) = 0.34 \times 1.60218 \times 10^{-13} \times 1.84 \times 10^{13} = 1 \text{ watt.}$$

Example 2. *The maximum energy of β-particles from* $^{32}_{15}P$ *is 1.71 MeV. What magnetic field perpendicular to the beam of β-particles from* $^{32}_{15}P$ *would bend it to give a radius of 100 mm? Given* $m = m_o(1 - v^2/c^2)^{-1/2}$.

Relativistic kinetic energy is given by

$$E = m_0c^2\left[\frac{1}{\sqrt{(1-v^2/c^2)}} - 1\right]$$

or

$$\frac{1}{\sqrt{(1-v^2/c^2)}} - 1 = \frac{E}{m_0c^2} = \frac{1.71 \times 1.60218 \times 10^{-13}}{9.10939 \times 10^{-31} \times (3 \times 10^8)^2} = 3.34.$$

∴

$$v^2/c^2 = 0.947 \text{ or } v = 2.92 \times 10^8 \text{ m./sec.}$$

We know the relation

$$Bev = mv^2/R$$

or

$$B = \frac{m_0 v}{\sqrt{(1-v^2/c^2)}eR} = \frac{9.10939 \times 10^{-31} \times 2.92 \times 10^8 \times 4.34}{1.60218 \times 10^{-19} \times 0.1}$$

$$= 0.072 \text{ web/m}^2.$$

Example 3. *The K-conversion electron from* ^{137}Cs *produces a sharp line in its β-ray spectrum whose momentum, measured with a magnetic spectrometer, yields a value of BR = 3381 gauss cm. The binding energy of this K-electron is 37.44 keV. Determine the kinetic energy of the conversion electron and the energy of the converted gamma proton.*

For relativistic mass, relation $Bev = mv^2/R$ becomes

$$\frac{m_0}{\sqrt{(1-v^2/c^2)}}v = BRe.$$

∴

$$\frac{v}{\sqrt{(1-v^2/c^2)}} = \frac{BRe}{m_0} = \frac{3381 \times 10^{-6} \times 1.60218 \times 10^{-19}}{9.10939 \times 10^{-31}}$$

$$= 5.946 \times 10^8 \text{ m./sec.}$$

From this relation, we get

$$v = 2.677 \times 10^8 \text{ m/sec.}$$

∴

$$\text{Energy } E = m_0c^2\left[\frac{1}{\sqrt{(1-v^2/c^2)}} - 1\right]$$

$$= 9.10963 \times 10^{-31} \times (2.9979 \times 10^8)^2 \times [1.221]$$

$$= 99.963 \times 10^{-15} \text{ joule} = 623.92 \text{ keV.}$$

Therefore, the energy of the converted gamma ray photon = 623.92 + 37.44 = 661.36 *keV*.

Example 4. *Show that the ratio of the average beta energy to the end point energy of a weak β-emitter* ($T_0 << m_ec^2$) *is 1/3, assuming that the Fermi function is approximately constant over the energy interval in question. Calculate the average energy carried away by neutrinos in the β-decay process which has an end point energy 18.1 keV.*

The probability of β-decay per sec for the electrons emitted with kinetic energies lying in the range T_e to $T_e + dT_e$ is given by the relation

$$P(T_e)dT_e = \frac{g^2 |M_{if}|^2}{2\pi^3 c^6 \hbar^7} F(Z, T_e)(T_e^2 + 2m_ec^2T_e)^{1/2}(T_e + m_ec^2)(T_o - T_e)^2 dT_e$$

For the beta energies with end point energy $T_o << m_ec^2$, we have $T_e << m_0c^2$ and

$$P(T_e)dT_e = \frac{g^2 |M_{if}|^2}{2\pi^3 c^6 \hbar^7} F(Z, T_e)(2m_ec^2T_e)^{1/2} m_ec^2(T_o - T_e)^2 dT_e.$$

The average energy of the emitted beta particle is thus given by

$$T_{av} = \frac{\int_0^{T_o} T_e\, P(T_e)dT_e}{\int_0^{T_o} P(T_e)dT_e} = \frac{\int_0^{T_o} T_e^{3/2}(T_o - T_e)^2\, dT_e}{\int_0^{T_o} T_e^{1/2}(T_o - T_e)^2\, dT_e}$$

$$= \frac{\int_0^{T_o} [T_o^2 T_e^{3/2} - 2T_o T_e^{5/2} + T_e^{7/2}]dT_e}{\int_0^{T_o} [T_o^2 T_e^{1/2} - 2T_o T_e^{3/2} + T_e^{5/2}]dT_e} = T_o/3 = \text{One third of the end point energy.}$$

In the present problem the average energy carried away by β-particles = 18.1/3 = 6.033 *keV*.

The rest of the energy 18.1 – 6.033 = 12.067 keV is carried out by the neutrino.

Example 5. *Calculate the maximum energy available to the electrons in the β^--decay of ^{24}Na. Why are beta particles of this energy not observed experimentally?*

$$^{24}_{11}Na \longrightarrow {}^{24}_{12}Mg + {}_{-1}\beta + \bar{\nu} \quad (4 \rightarrow 0)$$

Assuming the rocoil energy of the daughter nucleus to be negligible, the maximum energy available to the electron

$$E_o = M(^{24}Na) - M(^{24}Mg) = \Delta M(^{24}Na) - \Delta M(^{24}Mg)$$

$$= -8420.40\ keV - (-13933.50)\ keV = 5.513\ MeV.$$

Since $I_i = 4$ and $I_f = 0$ for the ground states, therefore the ground state transition is fourth forbidden and is not observed experimentally.

Example 6. *^{14}C disintegrates by β-emission with an end point energy of 0.155 MeV. A β-particle with an energy of 0.025 MeV is emitted in a direction at 135 degrees to the direction of motion of the recoil nucleus. Determine the momenta of all the three particles involved in this disintegration.*

Assuming the energy of the recoil nucleus to be negligible, the end point energy is given by

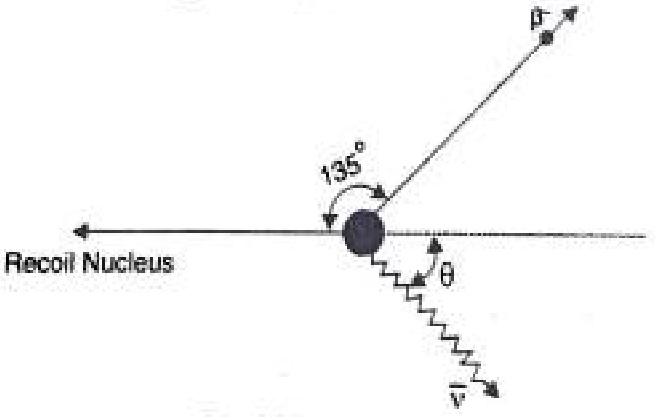

Fig. 6.26. Example 6.

$$E_0 = E_\nu + E_\beta$$

$$\therefore E_\nu = E_0 - E_\beta = 0.155 - 0.025 = 0.130\ MeV.$$

Hence the momentum of the neutrino

$$p_\nu = E_\nu/c = 0.13\ MeV/c.$$

Momentum of a β-particle can be obtained from the relation

$$p_\beta = \sqrt{(2ME_\beta)} = \sqrt{(2 \times 9.10939 \times 10^{-31} \times 0.025 \times 1.60218 \times 10^{-13})}$$

$$= 0.1598\ MeV/c.$$

Using conservation of momentum of the system, we have

$$p_\beta \sin 45^\circ = p_\nu \sin\theta \quad \text{or} \sin\theta = (p_\beta/p_\nu) \sin 45^\circ = 0.869$$

and

$$p_R = p_\beta \cos 45^\circ + p_\nu \cos\theta$$

$$= 0.1598\ (1/\sqrt{2}) + 0.13\ \sqrt{[1 - (0.869)^2]} = 0.177\ MeV/c.$$

The recoil energy of the product nucleus $E_R = p_R^2/2M$

$$= \frac{(0.177 \times 1.60218 \times 10^{-13}/2.9979 \times 10^8)^2}{2 \times 14 \times 1.66 \times 10^{-27} \times 1.60218 \times 10^{-19}} = 1.23 eV.$$

Example 7. *When a sample of 1 curie of ^{210}Bi was placed in a calorimeter, the 0.0268 cal./min heat output was observed. Calculate the mean energy of the transition and the ratio with the end point energy.*

1 curie = 3.7 × 10^{10} disintegrations/sec

∴ Number of disintegrations from the sample per minute

$$= 3.7 \times 10^{10} \times 60 = 2.22 \times 10^{12}.$$

If E is the mean energy in MeV of the emitted β^--particle, then the energy emitted per min = $2.22 \times 10^{12}\ E\ MeV = 2.22 \times 1.60218 \times 10^{-13+12}\ E$ joules

$$\therefore \quad 2.22\ E \times 1.60218 \times 10^{-1} = 0.0268\ cal = 0.0268 \times 4.186 \text{ joule}$$

or

$$E = 0.315\ MeV.$$

Since

$$^{210}_{83}Bi \rightarrow {}^{210}_{84}Po + \beta^- + \bar{\nu}.$$

Assuming the recoiling energy to be negligible, the end point energy

$$\begin{aligned} E_0 &= M(^{210}Bi) - M(^{210}Po) = \Delta M(^{210}Bi) - \Delta M(^{210}Po) \\ &= -14.815 - (-15.977) = 1.162\ MeV \end{aligned}$$

$$\therefore \quad E/E_0 = 0.315/1.162 = 0.271.$$

Example 8. *^8_3Li is an example of a β-delayed particle emitter. The ^8Li ground state has a half life of 0.85 sec and decays to the 2.9 MeV level in Be. The 2.9 MeV level then decays into 2 alpha particles with a half life of 10^{-22} sec.*

(a) What is the parity of the 2.9 MeV level in ^8Be? Give your reasoning. (b) Why is the half life of the ^8Be 2.9 MeV level so much smaller than the half life of the ^8Li ground state? (c) Where in energy with respect to the ^8Be ground state, would you expect the threshold for ^7Li neutron capture ? Why?

(a) The spin-parity of α-particle is $I^\pi = 0^+$. In $^8Be \rightarrow \alpha + \alpha$, the final state of the decay is that of two identical bosons, the wavefunction is required to be exchange-symmetric. This shows that the relative orbital angular momentum quantum number l of the α-particles is even and so the parity of the final state of the two α-particles system is

$$\pi_f = (+1)^2 (-1)^l = (+1)^2 (-1)^2 = +1.$$

As the α-decay is a strong interaction process (extremely short half life), parity is conserved. Hence the parity of the 2.9 *MeV* excited state of ^8Be is positive.

(b) The β-decay of the ^8Li ground state is a weak interaction process and the α-decay of the 2.9 *MeV* excited state of ^8Be to two alpha particles is a strong interaction process. This difference in interaction intensities is responsible for the vast difference in the lifetime.

(c) The threshold energy for ^7Li neutron capture is higher than the ^8Be ground state by

$$M(^7Li) + m_n - M(^8Be) = 18\ MeV.$$

Example 9. *Which nuclide of each pair is unstable in the following cases? Indicate its mode of decay and energy released in each case.*

(a) $^7_3Li(7.0182u), {}^7_4Be(7.0192u)$; *(b)* $^{13}_6C(13.0076u), {}^{13}_7N(13.0100u)$

(c) $^{19}_9F(19.0045u); {}^{19}_{10}Ne(19.0080u)$; *(d)* $^{34}_{15}P(33.9983u), {}^{34}_{16}S(33.9978u)$

As for each pair of isobars the atomic numbers differ by one, thus only β-decay or orbital electron capture is possible between them.

Neglecting the variation of the binding energy of the electron in different atoms and shells, the energy released in the β^--decay is given by

$$\begin{aligned} E(\beta^-) &= [M_x(Z, A) - Zm_e - M_y(Z+1, A) + (Z+1)m_e - m_e]c^2 \\ &= [M_x(Z, A) - M_y(Z+1, A)]c^2 \end{aligned}$$

where M is the mass in atomic masses. Thus β^--decay can take place if $M_x > M_y$. Similarly for β^+-decay, we have

$$E(\beta^+) = [M_x(Z, A) - M_y(Z-1, A) - 2m_e]c^2$$

Thus β^+-decay can take place only if $M_x - M_y > 2m_e = 0.0011\ u$

For orbital electron capture, we have

$$E(EC) = [M_x(Z, A) - M_y(Z-1, A]c^2 - E_{B, l}$$

where $E_{B, l}$ represents the binding energy of an electron in the *lth* atomic shell, which is about 10 *eV* or 1.1 × 10^{-8} *u* for *K*-shell.

For pair *(a)*, $\Delta m = M(Z+1, A) - M(Z, A) = 0.001\ u$ which is less than 0.0011 *u*, thus $^{7}_{4}Be$ is unstable against *K*-electron capture.

For pair *(b)*, $\Delta m = 0.0024\ u > 0.0011\ u$, thus ^{13}N is unstable against β^--decay and *K*-electron capture.

For pair *(c)*, $\Delta m = 0.0035\ u > 0.0011\ u$, thus $^{19}_{10}Ne$ is unstable against β^+-decay and *K*-electron caputre.

For pair *(d)*, $\Delta m = -0.0005\ u$ thus $^{34}_{15}P$ is unstable against β^--decay.

Example 10. *If the* β*-transition* $^3H \rightarrow {}^3He + \beta^-$ *is regarded as allowed and corresponding to an* $1/2^+ \rightarrow 1/2^+$ *transition with* $|M|^2 = 3$, *calculate the expected half period of* ^3H, *if the maximum energy for the* β*-ray spectrum is 0.018 MeV and* $\tau_0 = 7000$ *sec.*

We know that

$$ft = \frac{0.693\tau_0}{|M|^2} = \frac{0.693 \times 7000}{3} = 1617.$$

$$\log_{10} f_\beta = 4.0 \log_{10} E_0 + 0.78 + 0.02Z - 0.005\,(Z-1)\log_{10} E_0$$

$$= 4.0 \log_{10}(0.018) + 0.78 + 0.02 \times 1 = -6.1789$$

$$\log_{10} t = \log_{10} ft - \log_{10} f_\beta = 3.2087 + 6.1789 = 9.3876$$

or

$$t = 2.44 \times 10^9\ sec.$$

Example 11. *The ground state of* $^{137}_{55}Cs\,7/2^+$ *decays with a half-life of 33 years, 92% by* β^- *emission to an excited state of* $^{137}_{56}Ba$ *(which in turn decays by gamma emission with half-life 2.6 min to the ground state of* ^{137}Ba*) and 8% by* β*-emission directly to the ground state. Following quantities were measured—* $(K.E.)_{\beta, max}(92\%) = 0.51$ *MeV;* $(K.E.)_{\beta, max}(8\%) = 1.17$ *MeV.*

What is the degree of forbiddenness of each transition ?

For 92% β*-decay :*

Partial half-life (92%) β^-emission = 33/0.92 = 35.87 *years.*

$$\log_{10} f_\beta = 4.0 \log_{10} E_0 + 0.78 + 0.02\,Z - 0.005\,(Z-1)\log_{10} E_0$$

$$= 4.0 \log_{10} 0.51 + 0.78 + 0.02 \times 55 - 0.005 \times 54 \log_{10} 0.51 = 0.7893.$$

$$\therefore \quad \log_{10} ft = \log_{10} f_\beta + \log_{10} t = 0.7893 + 9.0535 = 9.8428.$$

Thus the transition is *once forbidden* $\Delta l = 1$ with parity change.

For 8% β*-decay*

Partial half life of β^--emission = 33/0.08 = 412.5 *years*

$$\log_{10} f_\beta = 4.0 \log_{10} 1.17 + 0.78 + 0.02 \times 55 - 0.005 \times 54 \log_{10} 1.17 = 2.1344$$

$$\therefore \quad \log_{10} ft = \log_{10} f_\beta + \log_{10} t = 2.1344 + 10.1142 = 12.2486$$

Thus the transition is twice forbidden, no change in parity.

Example 12. *For the following* β*-transitions deduce whether pure Fermi, pure Gamow-Teller or mixed coupling is operative.*

Transition	I_i^π	I_f^π	$\log_{10} ft$
$^1n \rightarrow {}^1H$	$1/2^+$	$1/2^+$	3.07
$^3H \rightarrow {}^3He$	$1/2^+$	$1/2^+$	3.00
$^6He \rightarrow {}^6Li$	0^+	1^+	2.92
$^{14}O \rightarrow {}^{14}N$	0^+	0^+	3.50

Calculate g_F and the ratio of coupling strengths $|C_{GT}|^2 / |C_F|^2$ with the given values $|M_F|^2 = 2$ and $|M_{GT}|^2 = 0$ for ^{14}O-decay and $|M_F|^2 = 1$ and $|M_{GT}|^2 = 3$ for ^1n-decay.

For the transition $^{14}O \rightarrow {}^{14}N$, $\Delta I = I_i \sim I_f = 0$ and $I_i = I_f = 0^+$, no change of parity. Therefore this transition is allowed by Fermi-selection rule only or it is a pure Fermi allowed transition. We know for the pure Fermi β-transition

$$\frac{1}{ft} = \frac{g_F^2}{2\pi^3} \frac{m_e^5 c^4}{\hbar^7 \log_e 2} |M_F|^2$$

or

$$g_F^2 = \frac{2\pi^3 \hbar^7 \log_e 2}{m_e^5 c^5 ft |M_F|^2} = \frac{2 \times 3.14^3 \times (1.05457 \times 10^{-34})^7 \times 0.6931}{(9.10939 \times 10^{-31})^5 \times (2.9979 \times 10^8)^4 \times 3162.28 \times 2}$$

∴

$$g_F = 1.3938 \times 10^{-62} \textit{ joule } m^3.$$

For the mixed transition ($\Delta I = 0$ with no change in parity), we have

$$\frac{1}{ft} = \frac{g^2 m_e^5 c^4}{2\pi^3 \hbar^7 \log_e 2} \left[C_F^2 |M_F|^2 + C_{GT}^2 |M_{GT}|^2 \right]$$

∴

$$\frac{ft \text{ for } {}^{14}O \text{ decay}}{ft \text{ for } {}^1n - \text{decay}} = \frac{\left[C_F^2 |M_F|^2 + G_{GT}^2 |M_{GT}|^2 \right]_{n-decay}}{\left[C_F^2 |M_F|^2 + C_{GT}^2 |M_{GT}|^2 \right]_{O-decay}}$$

$$\frac{3162.28}{1174.90} = \frac{C_F^2 \times 1 + C_{GT}^2 \times 3}{C_F^2 \times 2 + C_{GT}^2 \times 0}$$

or

$$C_{GT}^2 / C_F^2 = 1.461.$$

For transition $^3H \rightarrow {}^3He$, ($1/2^+ \rightarrow 1/2^+$), $\log ft = 3.00$, $\Delta I = I_i \sim I_f = 0$, $I_i = I_f \neq 0$; and no change in parity, therefore this transition is allowed by both Fermi and GT-selection rules or the transition is *mixed allowed*.

For transition $^6He \rightarrow {}^6Li$, $0^+ \rightarrow 1^+$, $\log ft = 2.92$. $\Delta I = I_i \sim I_f = 1$ and no change in parity. Therefore this transition is allowed by Gamow-Teller selection rule only or the transition is a pure G.T. allowed transition.

Example 13. *^{161}Ho and ^{163}Ho both decay by allowed electron capture to Dy isotopes, but the Q_{EC} values are about 850 keV and about 2.5 keV respectively. The capture rate for $3p_{1/2}$ electrons in ^{161}Ho is about 5% of the 3s capture rate. Calculate the $3p_{1/2}$ to $3s_{1/2}$ relative capture rate in ^{161}Ho. Given the binding energies of the $3s_{1/2}$ and $3p_{1/2}$ orbital electrons of Dy as 2.0 and 1.8 keV.*

Since ^{161}Ho and ^{163}Ho have the same nuclear charge Z. Their orbital electron wavefunctions are the same, their 3*s* and $3s_{1/2}$ waves differing only in phase. Thus the transition matrix elements for electron capture are also the same. The decay constant is given by

$$\lambda = A|M_{if}|^2 \rho(E),$$

where M_{if} is the transition matrix element, $\rho(E)$ is the density of states and A is a constant. For electron capture, the nucleus emits only a neutrino, so the process is a two body one. We have

$$\rho(E) \propto E_\nu^2 = (Q_{EC} - B)^2.$$

where B is the binding energy of an electron in s or p state. Since for ^{161}Ho

$$\frac{\lambda(3p_{1/2})}{\lambda(3s_{1/2})} = \frac{|M(3p_{1/2})|^2\,(Q_{EC}-B_p)^2}{|M(3s_{1/2})|^2\,(Q_{EC}-B_s)^2} = 0.05$$

$$\therefore \quad \frac{|M(3p_{1/2})|^2}{|M(3s_{1/2})|^2} = 0.05\times\left(\frac{850-2.0}{850-1.8}\right)^2 = 0.04998.$$

Hence for ^{163}Ho, we have

$$\frac{\lambda(3p_{1/2})}{\lambda(3s_{1/2})} = \frac{|M(3p_{1/2})|^2}{|M(3s_{1/2})|^2}\times\frac{(Q_{EC}-B_p)^2}{(Q_{EC}-B_s)^2} = 0.0498\times\frac{(2.5-1.8)^2}{(2.5-2.0)^2}$$

$$= 9.8\%.$$

Example 14. *The ^3H isotope undergoes β-decay with a half life of 12.5 years. An enriched sample of hydrogen gas containing 0.1 gm of tritium produces 21 calories of heat per hour. (a) calculate the average energy of the β-particles emitted (b) What specific measurements on the beta spectrum indicate that there is an additional decay product and specifically that it is light and neutral and (c) How the beta spectrum of ^3H can be used to determine the mass of the electron's neutrino ?*

(a) The decay constant $\lambda = \frac{\log_e 2}{t_{1/2}} = \frac{0.693}{12.5\times 365\times 24} = 6.33\times 10^{-6}\,hr^{-1}$.

Hence the rate of decay per hour

$$-\frac{dN}{dt} = \lambda N = 6.33\times 10^{-6}\times\frac{0.1\times 6.023\times 10^{23}}{3} = 1.27\times 10^{17}$$

∴ The average energy of the β-particles emitted

$$E = \frac{21\times 4.18}{1.27\times 10^{17}} = 6.91\times 10^{-16}\,Joule = 4.2\,keV.$$

(b) Both α- and β-decays represent transitions between two states of definite energies. However the former is a two body decay (daughter nucleus + α) and the conservation laws required the α-particles to be monoenergetic, where as β-transition is a three body decay (daughter nucleus + electron + neutrino) and so the electrons emitted have a continuous energy distribution with a definite maximum, called end point energy. In this way the measurement of the β-spectrum shows the emission of a third, neutral particle. Conservation of energy shows that it is very light.

(c) ${}^A_Z X \to {}^A_{Z+1}Y + +\beta^- + \bar{\nu}_e$.

If the end point energy, the maximum energy carried out by electrons E_m corresponds to zero kinetic energy of the antineutrino. Thus the law of conservation of energy gives

$$M({}^A_Z X) = M({}^A_{Z+1}Y) + E_m/c^2 + m_\nu.$$

If the E_m is measured precisely, the neutrino mass m_ν can be calculated with the above relation. It is found to be so small that only an upper limit can be given.

Example 15. *Discuss Fermi and Gamow—Teller selection rules for the allowed β-decays. For the expected decay of ${}^{57}_{29}Cu$ by positron emission to ${}^{57}_{28}Ni$,* estimate the ratio *Γ_F/Γ_{GT} of the two contributions to the decay rate. Does one expect appreciable β^+- decay from the copper-57 ground state to the first excited state of ^{57}Ni? Explain for the ground state, the last nucleon is in state $2p_{3/2}$, and $J^+ = 3/2^-$ in both of the mirror nuclei.*

In β^+-decay between mirror nuclei ground states $3/2^- \to 3/2^-$, as the initial and final states are similar, the transition is of a superallowed type. Such transitions can be classified into Fermi and Gamow-Teller types. For the Fermi type, the selection rules are $\Delta I = 0$, $\Delta\pi = +$, the emitted neutrino and electron have antiparallel spins.

For the Gamow-Teller type, the selection rules are $\Delta I = 0, \pm 1$, $\Delta\pi = +$, the emitted neutrino and electron have parallel spins.

For transition $3/2^- \rightarrow 3/2^-$ of the Fermi type.

$$|M_F|^2 = T(T+1) - T_{iz}T_{fz} = \frac{1}{2}\left(\frac{1}{2}+1\right) + \frac{1}{2} \times \frac{1}{2} = 1$$

For $3/2^- \rightarrow 3/2^-$ of the Gamow Teller type

$$|M_{GT}|^2 = \frac{I_f + 1}{I_f} = \frac{3/2+1}{3/2} = \frac{5}{3}.$$

The coupling constants for the two types are related roughly by $|g_{GT}| = 1.24\,|g_F|$. So the ratio of transition probabilities is

$$\frac{\lambda_F}{\lambda_{GT}} = \frac{g_F^2\,|M_F|^2}{g_{GT}^2\,|M_{GT}|^2} = \frac{1}{1.24^2 \times 5/3} = 0.39.$$

The transition from $^{57}_{29}Cu(2p_{3/2}, I^\pi = 3/2^-)$ to the first excited state of $^{57}_{28}Ni(1f_{5/2}, I^\pi = 5/2^-)$ is normal allowed transition because $\Delta I = I$, $\Delta\pi = +$. As the initial and final states are $2p_{3/2}$ and $1f_{5/2}$ and so the difference in nuclear structure is greater, the *ft* of this transition is larger than that of the superallowed one by 2 to 3 orders of magnitude.

The first excited state of ^{57}Ni is at 0.76 *MeV*. The mass difference between the mirror nuclei ^{57}Cu and ^{57}Ni is

$$\Delta E = M(Z+1,A)c^2 - M(Z,A)c^2 = \frac{3e^2}{5 \times 4\pi\varepsilon_o r}\left[(Z+1)^2 - Z^2\right] - (m_n - M_H)c^2$$

$$= \frac{3 \times (1.6023 \times 10^{-19})^2 \times 8.99 \times 10^{-9}}{5 \times 1.2 \times 57^{1/3} \times 10^{-15} \times 1.6023 \times 10^{-13}} = [29^2 - 28^2] - 0.78$$

$$= 9.87\ MeV.$$

Thus the ground state of ^{57}Cu is 9.87 MeV higher than that of ^{57}Ni. The positron end point energy for decay from the ground state of ^{57}Cu to that of ^{57}Ni is

$$E_o = \Delta E - 2m_e c^2 = 9.87 - 1.02 = 8.85\ MeV.$$

$\therefore$ Space phase factor $$\left(\frac{E_o - E_1}{E_o}\right)^2 = \left(\frac{8.85 - 0.76}{8.85}\right)^5 = 0.64$$

Hence the branching ratio is very small, rendering such a transition difficult to detect.

Oral Questions

1. The half life of a radioactive isotope is strongly dependent on the energy liberated in the decay. The energy dependence of the half life follows quite different laws for α and β-emitters, Why?

   [Alpha decay may be considered as the transmission of an α-particle through a coulomb potential barrier to exit the daughter nucleus, whereas the β-decay is the result of the disintegration of a neutron in the nucleus into a proton which remains in the nucleus and electron and an antineutrino which are emitted. Fermi has obtained the β-particle spectrum using a method similar to that for γ-emission. The transition probability per unit time is given by Fermi's golden rule No. 2. The disintegration constant for β-decays is found to vary with the end point energy of the β-particle spectrum E_o or the corresponding kinetic energy T_0 as $\lambda \sim T_0^5$ (Sargent Curve). The relation for α-decays is quite different, as $\lambda \sim e^{-const/\sqrt{E}}$.]

2. The Fermi plateau is due to *(a)* a density effect, *(b)* Lorentz contraction or *(c)* the relativistic mass increase. *(a)*

3. Mean free path for 3 MeV electron-neutrinos in matter is 10, 10^7, 10^{17} or 10^{27} *gm/cm*^{2}. (10^{17})

   [The interaction cross section between neutrino and matter is $\sigma \sim 10^{-41} cm^2$ and the atomic number density of matter $n = 10^{23}\ cm^{-3}$, density of matter $\rho = 1\ gm/cm^3$. Hence the mean free path of neutrino in matter is $\lambda = \rho/n\sigma = 10^{18}\ gm/cm^2$] *(b)*

7

GAMMA RADIATION

7.1 INTRODUCTION

A third type of radiation which could not be deflected in a magnetic field, but which nevertheless had considerable penetrating power and a marked effect on a photographic plate, was discovered in 1900 by P. Villard in France. These radiations are now called γ-rays. Gamma rays, like *X*-rays and light rays, are electromagnetic radiations, but of shorter wavelengths. Actually it is difficult to distinguish between the longest gamma rays and the shortest *X*-rays. Main difference in their behaviour is that the *X-rays result from transitions between electronic energy levels while gamma rays are associated with transitions between nuclear energy levels.*

The transition from one nuclear state to another of lower energy state by virtue of the electromagnetic field may proceed by one of the *three distinct processes; gamma ray emission, internal conversion and internal pair creation.* Electromagnetic radiation also appears in other nuclear transitions, especially those in which charged particles are emitted. The *information concerning nuclear properties*, obtained from observations of electromagnetic transitions, *fall into three main categories* :

(a) The gamma ray energies or the energies of internal conversion electrons determine the energies of the transitions, which give the energy differences between nuclear levels.

(b) The geometrical properties of the electromagnetic transition *i.e.*, the angular and radial distribution of its intensity and polarization with respect to a nuclear axis give information concerning the spins and parities of the nuclear states involved.

(c) The results, especially, for magnetic multipoles support the view that the radiation is due to the charge and magnetic moments of protons and neutrons in the nucleus rather than due to the quanta of the nuclear force field. Except in some isolated instances, there is little evidence of the predominance of a single "*radiating particle*". In some cases of electric quadrupole transitions, the large transition rates indicate that many particles must contribute to the radiating system.

There are *two categories of gamma sources,* useful in nuclear spectroscopy :

(a) Gamma rays produced by electrons in targets of *X*-ray tubes, betatrons, linear accelerators, synchrotrons, etc. These gamma-rays appear in the continuous energy spectrum.

(b) Gamma rays from excited nuclear states, either prompt [as in (n, γ), (p, γ), etc., reactions] or delayed by belonging to an isometric transition or appearing as prompt radiation following beta or alpha decay of relatively long half-life. Intense sources of gamma rays of higher energies are available from machine production. Gamma ray energies from few keV up to 20 MeV can be found among the prompt decays and upto 5 MeV in the case of delayed emission.

A very large variety of effects has been used for the qantitative detection of gamma radiation, *e.g., conductivity of gases, liquids and solids, fluorescence and phosphorescence, blackening of photographic* *emulsions, discolouration of transparent solids, changes in elastic constants of piezoelectric crystals, formation of tracks in cloud chambers by secondary electrons, etc.* The proportional counters, G.M. Counters and scintillation counters are used in most of the experiments. In all these counters gamma rays are detected by the secondary electrons they produce. We have discussed these counters in chapter 4.

7.2 MEASUREMENT OF GAMMA RAY ENERGIES

A large number of methods of measuring γ-ray energies have been used. These methods of measurement may be grouped in following four broad divisions.

1. Wavelength Measurement by Crystal Diffraction (Crystal Spectrometer). Low energy gamma ray wavelengths were first measured using crystal diffraction techniques by Rutherford and Andrade in 1914. This method was used by other workers. Frilley (1929) identified twenty three lines in the radium series, out of which seventeen were definitely nuclear gamma-rays (0.466 MeV to 0.770 MeV). Valadares (1934) extended measurements to the actinium series, where forty lines of atomic and nuclear origin were identified. In this method energy is calculated by using the relation $E_\gamma = hc/\lambda$.

Nuclear instruments such as scintillation or solid state detectors cannot of themselves give absolute energy values. DuMond and collaborators derived high precision values of the numerous γ-lines ranging upto 1.3 MeV by using the method of Bragg reflection in a bent crystal and gave the γ-energy scale. The basic geometry of the DuMond's curved crystal spectrometer is shown in Fig. 7.1. It consists of a 2mm thick slab of quartz (crystal) bent elastically in such a way that its diffracting planes, which are normal to the face of the crystal, converge when extended in a line at *B* normal to the plane of the figure. The distance *CB* is about 2*m*. This arrangement enables all γ-rays from a line shaped γ-ray source *S* to make the same angle θ with the crystal planes, thus the crystal as a whole serves as a *diffraction grating*. Source *S* has to be placed on the focusing circle passing through *C* and having radius equal to half the radius of curvature of the crystal. The γ-rays are reflected from the lattice planes when the angle θ equals the Bragg angle for the particular radiation ($2d \sin\theta = n\lambda$). After Bragg reflection, the angle of emergence of the radiation is equal to the angle of incidence, the γ-rays beam diverges and appears to be originated from a virtual focal *V*. A detector *D*, a NaI-scintillator counter, is placed on the other side of the crystal. The Bragg angle θ is 3 degrees for the diffraction of a 100 keV γ-ray from the (310) planes of quartz and 18 minutes for the 1 MeV γ-ray. Because of the close angular proximity of the direct radiation at higher energies, the divergent beam is separated from the heterogeneous radiation before reaching the detector. This is done by a diverging collimator *A* made of tapered baffles (Soller slit) constructed by lead us tungsten.

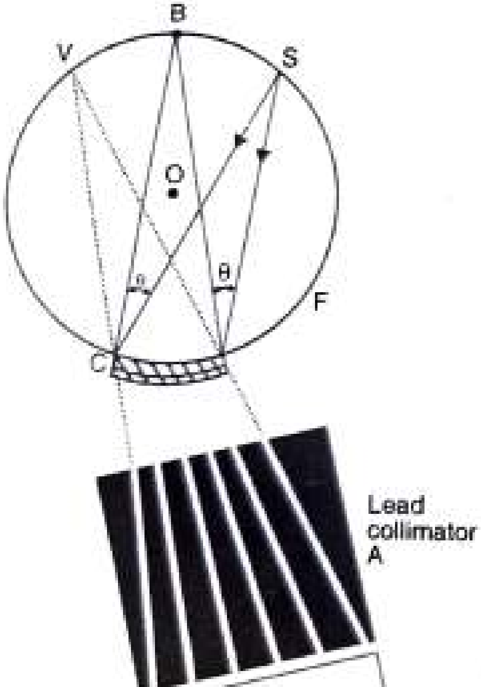

Fig. 7.1. DuMond Spectrometer.

The tapered baffle and detector are stationary, while the source and the diffracting crystal rotate. In the original DuMond spectrometer, the rotation was performed by means of a precision screw. The screw translates trolley on which spectrometer (crystal and source) is placed. The source is moved in steps of 1/50 mm along the focal circle by means of this screw. The precise rotation of the source relative to the crystal diffraction planes is made by translation of upper trolley with a precise linear screw.

The counting rate is measured as a function of the source position (angle θ). For a given gamma ray energy, a maximum is observed in a counting rate for the Bragg angle θ, given by the relation $2d \sin\theta = \lambda$. Thus the position of the source determines the wavelength and hence the energy of the γ-rays. The essential advantage of this method is that it avoids the necessity of collimating the incident gamma rays and makes full use of the whole of the aperture of the crystal. It is possible to measure γ-wavelengths as short as 0.01°A, corresponding to energies as high as 1.3 MeV. This method has two *disadvantages* : First, the measurements become more difficult and less precise as the energy of the γ-rays increases and the wavelength decreases. Second, the overall efficiency is low (10^{-8} at 0.5 MeV) and hence this method requires highly active sources which are often not available.

If the incident particle has energy too low to penetrate the Coulomb barrier of the target nucleus, the Coulomb field of the incident charged particle may excite the nucleus to a low lying state and the γ-rays are emitted. To record these Coulomb excited gamma rays, photographic quartz crystal spectrometers have been used. A high beam current, 30 mA, of 3.7 MeV protons bombards a water cooled copper target, on which a thin target layer is deposited. The majority of emitted gamma rays have an energy less than 150 keV and the wavelength determinations are of high accuracy. Heavy ion beams are needed for higher states excitation.

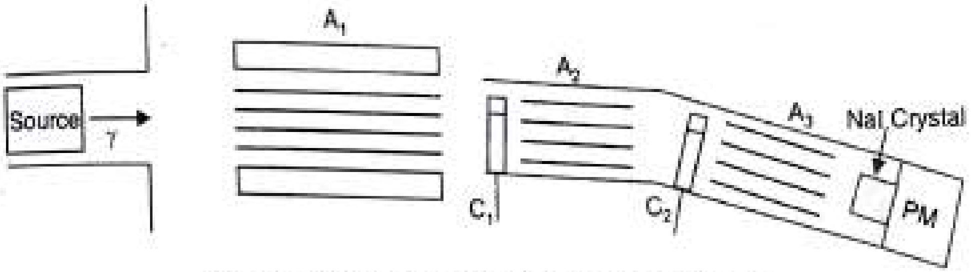

Fig. 7.2. Double flat crystal gamma ray spectrometer.

The intensity of the gamma rays diffracted by the lattice planes of a crystal increases with the thickness of the crystal. Unfortunately it is very difficult to bend a thick crystal without breaking it. This difficulty was overcomed by using thick flat crystals. Two arrangements are used employing either one or two crystals, referred to as the single and double flat crystal spectrometers respectively. In the flat double crystal spectrometer, three Soller slit baffles A_1, A_2 and A_3 constructed of very accurately parallel lead partitions, are placed between the source and the first crystal C_1 of calcite, between C_1 and second crystal C_2 and between C_2 and the scintillation counter. These crystals are rotated and controlled so that the second crystal is in the correct position to reflect the gamma radiations. If high quality crystals are used, this type of spectrometer has a very high resolving power over a wide range of energies 60 keV to 5 MeV. The double crystal spectrometer requires the Soller slit only for shielding, but the single crystal arrangement uses the Soller slit and one crystal to determine the angular setting. This has been used to measure the wavelengths of neutron capture (n, γ) gamma rays at Chalk-River.

2. Absorption Measurements. Many determinations of gamma rays energies are based on the measurement of the linear absorption coefficient of the radiation, usually in lead for energetic radiation.

The counting rate I in the counter is measured as a function of absorber thickness t. The dependence of I on t for monoenergetic gamma radiations is given by the relation

$$I = I_0 e^{-\mu t}. \qquad \ldots(1)$$

where I_0 is the counting rate in the absence of absorber and μ is the linear absorption coefficient, which is the characteristic of the absorber material and the gamma ray energy E_γ. It is more convenient to express the absorption in terms of the mass absorption coefficient μ_m (in units of cm^2/gm). If ρ is the density of the absorber (= gm/cm^3), then

$$I = I_0 e^{-\mu_m \rho t} \qquad \ldots(2)$$

Here μ_m is only a function of the atomic number Z and E_γ, and not of the physical or chemical state of the absorber except at very low energies, where coherence effects appear.

It is important to note that μ is smaller than the total linear attenuation coefficient μ_0, which includes a scattering coefficient, the energy content of all the secondary photons. The rate of energy absorption per gm is called *dose rate R*.

$$\therefore \qquad R = I\,\mu/\rho \ \text{MeV/gm sec.} \qquad \ldots(3)$$

Experimental arrangements designed to minimize the effects of secondary radiations use heavy collimation at source and counter and narrow apertures. The scintillation spectrometer has been used in recent years to discriminate against scattered radiation. A schematic diagram of the experimental arrangement using a high collimation system is shown in Fig. 7.3. Thick lead shielding blocks, separatetd by a narrow space act as the collimator. The counter is surrounded by a lead shield to absorb extraneous γ-rays and electrons. The protons are removed from the beam of γ-rays either by absorption or by scattering. To minimize the effects of scattering, some investigators favour suspending the source, absorber and detector high above the ground and at a great distance from all scattering materials.

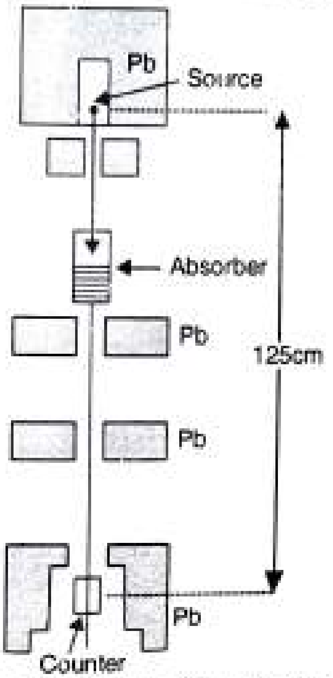

Fig. 7.3. Schematic diagram of absorption experiment.

Glendenin has tabulated the half value thickness *i.e.*, the thickness which reduces the initial intensity by a factor of 2, in aluminium and lead as a function of gamma ray energy. The energy may be obtained from a half thickness curve of known absorber. This method yields fairly accurate energy value below 1 MeV.

The absorption curve obtained with monoenergetic γ-rays is generally not a pure exponential because of the effect of secondary radiations due to background counts, *X*-rays of the absorber, annihilation quanta and compton scattered quanta.

The gamma ray energies below 80 keV can be accurately determined by the absorption in two neighbouring elements. Since the absorption coefficient at the *K*-ionization energy of the lighter of the two elements is larger while for all other energies it is slightly smaller than that of the heavier element, the gamma energies between the two *K*-edges can be identified.

3. Secondary Electron Methods. The most common methods for the determination of gamma ray spectra are based on measurements of the energy distribution of secondary electrons produced in some material. When a gamma ray is absorbed in matter all its energy is transferred into K.E. of several electrons. This energy is in turn dissipated in collisions as ionization, heat or light. The instruments used for this purpose are known as gamma ray spectrometers, in which gamma ray energy is converted into electron energy by one of the three processes : *photo electric effect, Compton effect and pair production*. We have seen in chapter 3 that the relative importance of these three processes depends on the gamma ray energy and the atomic number of the absorber in which the conversion of gamma rays takes place. The total absorption coefficient is the sum of the absorption coefficients for the three different processes.

Magnetic Spectrometers have been used for the measurement of the momentum of electrons produced by different processes. The cloud chamber, with a magnetic field was one of the early methods. The heavy liquid bubble chamber and spark chamber are both used in elementary particle physics. The photoelectric effect, the Compton effect and pair production have all been made the basis of high resolution magnetic spectrometers for photon measurements. Such β-spectrometers may be used for γ-ray measurements.

(a) Photo-electric conversion. At low energies (~ 100 keV) gamma rays, the photo-electric process is dominant, in particular for radiator materials with high *Z*. *Beta spectrometers* are used for measuring the energies of electrons ejected by photo-electric process from a thin high *Z* radiator foil. Lines appear corresponding to electrons from the *K*-shell and *L*-shell and with the high resolution spectrometers even *M*-electrons may be resolved. The energy of the electrons in a given line can be determined from its position and the gamma ray energy is obtained by adding the binding energy of the electron in the shell from which it was ejected to the above measured electron energy.

(b) Compton spectrometer. With the help of Compton spectrograph it is possible to disinguish a Compton process from the other two by detecting the electron and the scattered gamma rays simultaneously. The energy of the emitted electron is measured through deflection in a magnetic field. Between 0.2 MeV and 10 MeV, virtually all secondary electrons produced in a light element such as beryllium or carbon arise from the Compton process. The contribution due to either pair production or photoemission is extremely small. Rasmussen *et al.* were able to develop Compton lines having widths of about 5% at 6 MeV γ-ray energy. The source is enclosed in an absorber of material of low atomic number such as aluminium, thick enough to stop all the primary electrons or other charged particles but not the gamma radiation. The relationship between the energy of the incident γ-ray and the K.E. of the Compton electron is

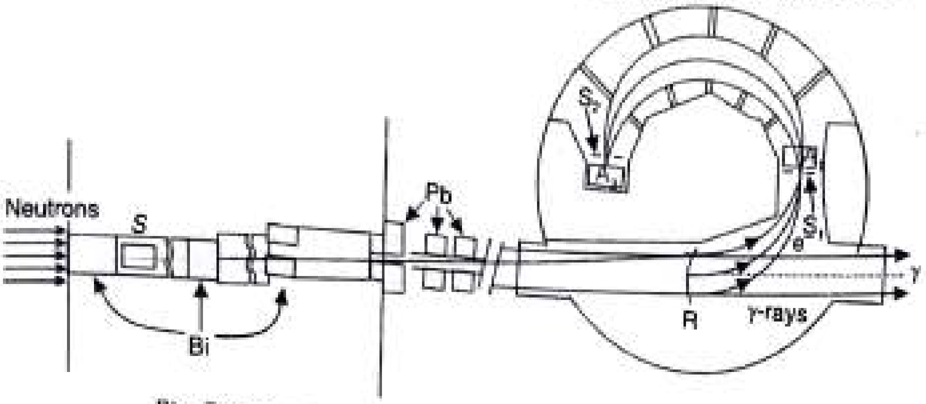

Fig. 7.4. Compton spectrometer used by Groshev and others.

$$T = h(\nu - \nu') = h\nu \frac{h\nu/m_e c^2(1-\cos\theta)}{1 + h\nu/m_e c^2(1-\cos\theta)}$$

which is zero for $\theta = 0$ and is maximum for the Compton scattered photons at $\theta = 180°$.

$$\therefore \quad T_{\text{max}} = \frac{h\nu}{1 + m_e c^2/2h\nu}. \qquad \ldots(4)$$

L.V. Groshev, and others utilized a special type of Compton spectrometer for measuring the energies of gamma rays emitted from various materials after slow neutron capture. Its principle of operation is shown in Fig. 7.4. A well collimated gamma ray beam emitted from the source *S* falls on the radiator *R*(100 microns thick sheet of polystyrene). The radiator is inside the field of a large electromagnet and the electrons of a particular momentum emitted in the forward direction within about 1° of initial direction of γ-rays will, after deflection and focusing in the magnetic field, pass through a slit S_1. Behind S_1, they pass through a thin window G.M. Counter A_1. After deflecting through 180° they arrive at the slit S_2 and coutner A_2. Only events that trigger both counters are recorded. This will cut the background counts from counter A_2 alone.

The energy of the electrons that gives rise to coincidence counts is varied with magnetic field. Fig. 7.5 shows the spectrum of Compton electrons resulting from

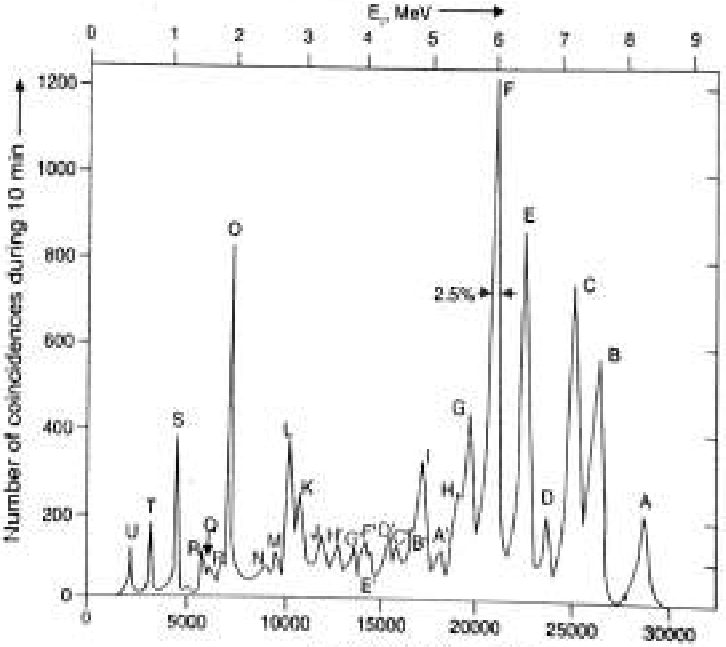

Fig. 7.5. Coincidence gamma ray spectrum.

gamma rays produced due to the capture of slow neutrons in chlorine. The bottom horizontal scale gives the magnetic rigidity $B\rho$ of the recorded electrons and the top horizontal scale gives the corresponding energy of the γ-rays in MeV. The resolving power of the instruments is $E_\gamma/\Delta E_\gamma$ (– 40), where ΔE_γ is the full width at half amplitude. To improve the resolution, the thickness of the radiator must be reduced in proportion to the line width.

(c) Pair spectrometer. At higher energies (> 3 MeV) gamma rays are best studied with a pair spectrometer, because the probability of the pair formation increases with gamma ray energy, while the Compton and photoelectric cross-sections decrease. The pair spectrometer invented by Walker and Mc Daniel is shown in Fig. 7.6. This spectrometer operates on the principle of simultaneously detecting the electron and the positron created in a pair production process. The gamma rays produced in a nuclear reaction are first collimated and allowed to impinge normally on a thin metal foil, the radiator. The electrons and positrons created in radiatior are predominantly emitted in the forward direction and leave the radiator approximately along the normal to its surface. Thereafter they are deflected in the magnetic field, one to the left and one to the right because of their different charges. After describing a semi-circle they pass through slits, Al windows, into detectors. Each detector consists of four Geiger counters labelled *L* and *R* for left and right counters. The left and right counters are connected to a coincidence circuit, which will register a count when they are simultaneously triggered.

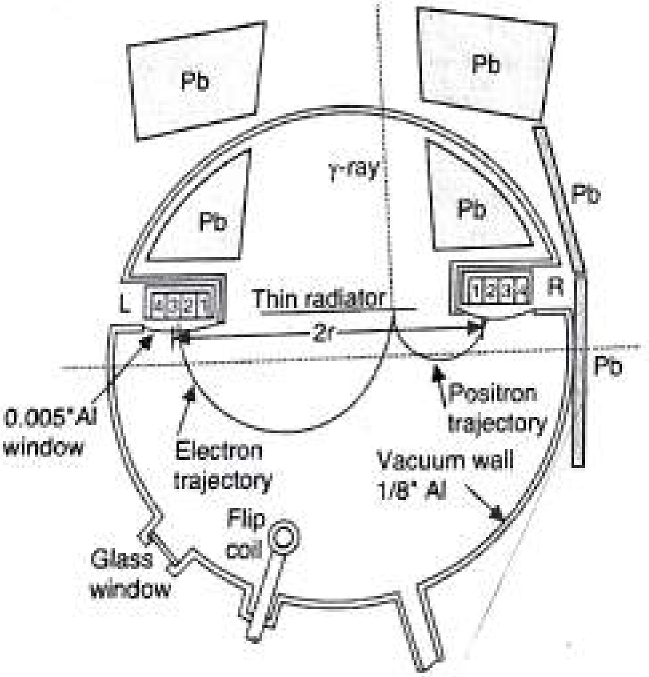

Fig. 7.6. Pair spectrometer.

Since 1.022 MeV is the threshold energy for the pair production process, hence the total kinetic energy shared by the pair is equal to $E_\gamma - 1.022$ *MeV*. Usually this energy is not equally shared between the electron and positron. If these particles are created with relativistic kinetic energies, their energies are given by

$$E_e = p_e \cdot c \text{ and } E_p = p_p \cdot c, \qquad \ldots(5)$$

where p_e and p_p are the momenta of the electron and the positron. In a uniform magnetic field *B*, directed normal to the plane containing the paths of the particles, the radii of curvature of the paths of the pair of particles are given by $r_e = p_e/B_e$ and $r_p = p_p/B_e$

$$\therefore \quad r_e + r_p = 2r = \frac{E_e + E_p}{Bec} = \frac{E_\gamma - 1.022}{Bec} \qquad \ldots(6)$$

This relation indicates that the sum of the radii of trajectories is a function of E_γ and *B*. Keeping distance $2r$ constant, the field *B* is varied until a peak coincidence rate is recorded corresponding to a group of monoenergetic gamma rays. A number of corrections is necessary for accurate determinations of E_γ. Since scattering of the electrons and the positrons in the converter is improtant hence converters of low *Z* are used. Divergence of the incident gamma beam and the finite width of slits in front of the detectors also contribute to the error of the energy determination. Pair spectrometers have been used with gamma energies as high as 100 MeV. Unfortunately they have a low detection efficiency. Their counting efficiencies fall off very sharply at the low energy and $E_\gamma < 6$ MeV. In the above experiment, the resolution was 6%. The efficiency of the instrument is low, 1 coincidence count per 10^7 photons at 7 MeV. The γ-ray energies obtained with magnetic spectrographs may require correction because of Doppler shifts due to recoil motion of the radiating source.

The proportional counters used for the measurement of secondary electron energies are of two types: gas filled ionization devices and scintillation counters. The gas ionization proportional counters are useful below about 100 keV, because the absorption and therefore the conversion efficiency of the counter gas becomes too low at higher energies. The range may be extended a little toward higher energies by increasing pressure of the gas filled. The *NaI(Tl)* is now used almost exclusively for gamma-ray scintillation counters. Its high average atomic number permits the measurement of lines due to photoelectrons and pairs. The large crystals are better for high energy γ-spectroscopy. The large crystals also have the disadvantages of expense and somewhat poor energy resolution. The very useful alternative to the totally absorbing crystal is a somewhat smaller crystal with an anticoincidence mantle surrounding it.

The two crystal spectrometer was developed by Hofstadter and McIntyre, which selects Compton events by establishing a coincidence requirement between the two crystals (one crystal detecting the recoil electron and the other the scattered photons). A second type of coincidence arrangement was developed by Johnnson and others to analyse the complex spectrum. This device consists of three crystals with a three coincidence requirement between them. The incident radiation produces a pair in the central crystal and the positron and electron both stop in this crystal. The two oppositely directed annihilation quanta from the positron at the central crystal are detected by one in each side crystal. The triple coincidence counts are taken between the crystals and the output is used to gate a pulse analyzer recording the pulses from the central crystal. This is several hundred times better than the magnetic pair spectrometer. The three crystal arrangements with germanium center have been used at lower energies and offer advantages in resolution at the expense of efficiency. Because of the sensitivity of the Compton effect to the direction of the incident electron vector, the two crystal Compton spectrometers can be used as gamma ray polarimeters. These are most suitable at intermediate energies while the three crystal pair spectrometers may be used at high energies.

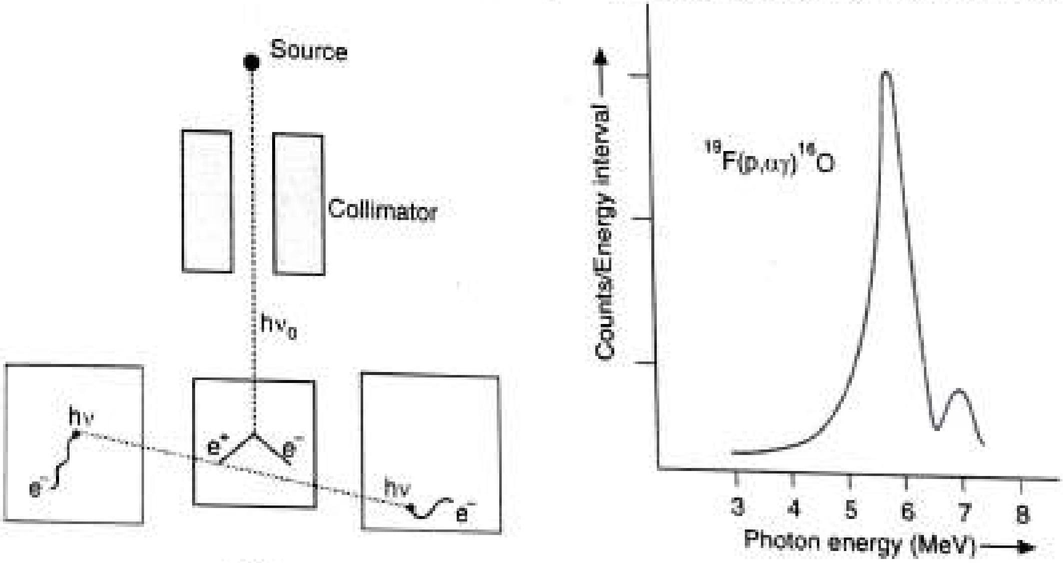

(a)

(b)

Fig. 7.7. Schematic diagram of (a) three crystal pair spectrometer and (b) Energy spectrum of radiation from $^{19}F(p, \alpha\ \gamma)\ ^{16}O$ *reaction.*

The two crystal coincidence method particularly useful in cascade γ-rays studies, has been devised by Hoogenboom. Two crystals are used with a summing circuit and a multichannel analyzer. The spectrum from crystal 1 is analyzed, but only for those events for which the sum of the pulse heights from the two crystals corresponds to the full energy $E_1 + E_2$. All Compton and pair production events for which the full energy is not delivered to the crystals are eliminated. Thus by adjustment of the single channel on the summed energy the decay schemes of each successive nuclear level can be studied.

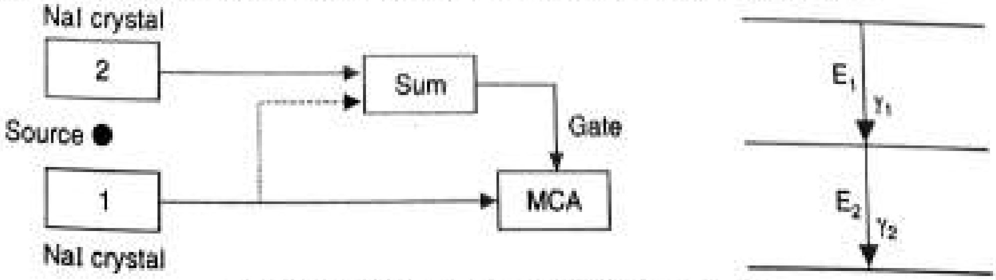

Fig. 7.8. Coincidence circuit for cascade γ-rays.

4. Energy Measurement by Photodisintegration. Sometimes photonuclear reactions are used for the detection of high energy gamma rays. The most important reactions used are $^9Be\ (\gamma, n\ 2\alpha)$ with a threshold of 1.66 MeV and $^2H(\gamma, pn)$ with a threshold of 2.23 MeV. These reactions have been used to detect gamma rays of very low abundance from radioactive decays in which other, very-intense gamma radiation below 1.66 MeV is emitted. By search for photoneutrons from Be and D_2O, one can decide whether the gamma ray energy lies between the two threshold energies or above both. The study of relative neutron yields in above two cases gives some estimate of the energy above 2.23 MeV.

The observation of the energies of photo protons from deuterium is the better method for the measurement of the energy of gamma rays. This can be done by means of ionization chambers, deuterium filled cloud chambers or D_2O soaked photographic emulsions. The earliest measurement of the photodisintegration of the deuteron by ThC″ gamma rays was performed with a proportional counter. The high background of ionization due to electrons ejected by the gamma rays from the wall of counter is the main problem with deuterium counters. For gamma ray energies well above the threshold the recoil due to the momentum of the incident gamma ray causes a significant spread in pulse height because the proton energy E_p depends on the angle of emission θ with respect to the incident ray. If B is the binding energy of deuteron, the relation between E_γ and E_p is given by

$$E_\gamma - B \ = \ 2E_p - 2E_\gamma \cos\theta \sqrt{(E_p/2Mc^2)}. \qquad \ldots(7)$$

where M is the mass of the recoil nucleus.

The cloud chamber was also used for the observation of photoprotons, by range measurements in a deuterium filled chamber and by the curvature of the proton tracks in a magnetic field. Because of uncertainty in the range energy relation and difficulties in range measurements, the method has not proved very reliable. Recently nuclear track emulsions soaked in heavy water have taken the place of the cloud chamber. They have the advantage of greater sensitivity due to their higher density.

7.3 MULTIPOLE RADIATIONS

In many β-and α-transitions the daughter nucleus is formed in an excited state, which does not have enough energy to emit a nucleon and usually decays by an electromagnetic transition. This emission of γ-rays is determined by various factors, including the nuclear spins and the differences in energy of the two states. These γ-radiations can be divided into two general categories, namely, electric and magnetic, according to their origin. *Electric radiations arise from changes in the distribution of the electric charges in the nuclei, whereas magnetic radiations arise from changes in the distribution of the magnetic poles or in the current distribution in the nuclei.* A complete description of the emission and absorption of light by a quantum mechanical system requires the quantum theory of radiation. We shall make the assumptions that the wavelength λ of the emitted radiation is much larger than the nuclear radius, and that the radiating system consists of individual nucleons which contribute to the radiation due to the motion of their charges and magnetic moments. $\lambda > R$ means $c/\omega\ R > 1$, $hc/ER > 1$ or $E < hc/R$ (= 20 MeV). Thus no photons with energies above 20 MeV are expected in nuclear decays.

Let us consider the electromagnetic field in a uniform, isotropic, lossless medium (*e.g.*, the free space) *i.e.*, in a region free of sources of radiation. The Maxwell's equations for **E** and **B** vectors are

$$\nabla \cdot \mathbf{E} \ = \ 0, \nabla \cdot \mathbf{B} = 0, \nabla \times \mathbf{E} = -\partial \mathbf{B}/\partial t \text{ and } \nabla \times \mathbf{B} = \mu_0 \varepsilon_0 \partial \mathbf{E}/\partial t.$$

These electric and magnetic fields are continuous vector functions of both position and time. Since we are dealing with radiation having definite energy, hence frequency too have definite value. Thus the time dependence is sinusoidal and field can be written as

$$\mathbf{E}(\mathbf{r}, t) \ = \ \mathbf{E}(\mathbf{r})e^{-i\omega t} + \mathbf{E}^*(\mathbf{r})e^{i\omega t}$$

and

$$\mathbf{B}(\mathbf{r}, t) \ = \ \mathbf{B}(\mathbf{r})e^{-i\omega t} + \mathbf{B}^*(\mathbf{r})e^{i\omega t}, \qquad \ldots(8)$$

where ω is the angular frequency related to the magnitude of the propagation vector $k = 2\pi/\lambda = \omega/v = \omega/c$ in the free space.

The Maxwell's equations in free space are then

$$\text{curl } \mathbf{B} = -i\omega\mu_0\varepsilon_0 \mathbf{E} \quad \text{and} \quad \text{curl } \mathbf{E} = i\omega \mathbf{B} \qquad ...(9)$$

$$\therefore \quad \nabla\times\nabla\times\mathbf{E} = \omega^2\mu_0\varepsilon_0 \mathbf{E} \quad \text{or} \quad (\nabla\times\nabla\times - k^2)\mathbf{E} = 0$$

$$\text{and} \quad \nabla\times\nabla\times\mathbf{B} = \omega^2\mu_0\varepsilon_0 \mathbf{B} \quad \text{or} \quad (\nabla\times\nabla\times - k^2)\mathbf{B} = 0, \qquad ...(10)$$

where $k^2 = \omega^2\mu_0\varepsilon_0$.

It can be shown that the vector eigen-functions of the operator $(\nabla \times \nabla \times - k^2)$ have the form $a\mathbf{L}\, j_L(kr)\, Y_{L,M}(\theta, \phi)$, where a is a constant and $\mathbf{L}$ is the angular momentum operator. $(\mathbf{L} = -i\hbar\, \mathbf{r} \times \nabla)$. If we set

$$\mathbf{B}^e_{\mathrm{L,M}} = a^e \mathbf{L}\, j_L(kr)\, Y_{L,M}(\theta, \phi). \qquad ...(11)$$

then $\mathbf{B}$ has no radial component, since $L_r = 0$. *Such fields are called electric multipole fields, hence the index e is used.* The electric field strength is thus given by

$$\mathbf{E}^e_{\mathrm{L,M}} = -(1/i\omega\varepsilon_0\mu_0)\, a^e\, \nabla\times\mathbf{L}\, j_L(kr)\, Y_{L,M}(\theta, \phi). \qquad ...(12)$$

If on the other hand, we set

$$\mathbf{E}^m_{\mathrm{L,M}} = a^m \mathbf{L}\, j_L(kr)\, Y_{L,M}(\theta, \phi), \qquad ...(13)$$

then $\mathbf{E}$ has no radial component. *Such fields are called magnetic multipole fields [we use the index (m)].* The corresponding magnetic field is

$$\mathbf{B}^m_{\mathrm{L,M}} = (1/i\omega)\, a^m\, \nabla\times\mathbf{L}\, j_L(kr)\, Y_{L,M}(\theta, \phi). \qquad ...(14)$$

The fields must be normalized to determine the constants a^e and a^m. The field energy of the radiation of multipole order L and frequency ω is equal to $\hbar\omega = \hbar ck$. Since an electromagnetic wave contains on the average half of its energy in the magnetic field and half in the electric field, hence

$$\varepsilon_0 \int |\mathbf{E}|^2\, dV = \frac{1}{\mu_0}\int |\mathbf{B}|^2\, dV = \tfrac{1}{2}\hbar\omega = \tfrac{1}{2}\hbar ck. \qquad ...(15)$$

In order to obtain a discrete spectrum for the possible values of ω, the radiation field is assumed to be enclosed in a large sphere of radius R_0 such that $kR_0 >> 1$ and the field strengths vanish for $r = R_0$, *i.e.*, $j_L(kR_0) = 0$.

For electric multipole radiation, let us insert equation (15) into (11), then

$$\tfrac{1}{2}\mu_0\hbar ck = [a^e]^2 \int_0^{R_0} |j_L(kr)|^2 r^2 dr \int (\mathbf{L}Y_{L,M})^* (\mathbf{L}Y_{L,M})\, d\Omega. \qquad ...(16)$$

Since $\mathbf{L}$ is Hamiltonian operator, we obtain that the angular part of the integral is

$$\int Y^*_{L,M} L^2 Y_{L,M}\, d\Omega = L(L+1)\,\hbar^2. \qquad ...(17)$$

In the radial integral, $j_L(kr)$ can be replaced by asymptotic approximations for $r \to \infty$. Since

$$j_L(kr) = (1/kr)\cos[kr - \tfrac{1}{2}\pi(L+1)].$$

$$\therefore \quad \int_0^{R_0} |j_L(kr)|^2 r^2\, dr = \frac{1}{k^2}\int_0^{R_0} \cos^2[kr - \tfrac{1}{2}\pi(L+1)dr = R_0/2k^2. \qquad ...(18)$$

We thus obtain, from equations (16), (17) and (18)

$$(a^e)^2 = ck^3\mu_0/\hbar\, R_0 L\, (L+1). \qquad ...(19)$$

Similarly we obtain for magnetic multipole radiation

$$(a^m)^2 = ck^3/\varepsilon_0\, \hbar\, R_0 L\, (L+1). \qquad ...(20)$$

Thus the multiple expansions for electric and magnetic fields are :

$$\mathbf{E}^e_{\mathrm{L,M}} = i\left[\frac{ck}{\varepsilon_0 \hbar\, R_0 L(L+1)}\right]^{1/2} \nabla\times\mathbf{L}\, j_L(kr) Y_{L,M}(\theta,\phi)$$

$$\mathbf{B}^e_{\mathrm{L,M}} = k\left[\frac{ck\mu_0}{\hbar\, R_0 L(L+1)}\right]^{1/2} \mathbf{L}\, j_L(kr) Y_{L,m}(\theta,\phi)$$

$$\mathbf{E}^m_{\mathrm{L,M}} = k\left[\frac{ck}{\varepsilon_0 \hbar R_0 L(L+1)}\right]^{1/2} \mathbf{L}\, j_L(kr)\, Y_{L,M}(\theta,\phi) \qquad ...(21)$$

$$\mathbf{B}^{m}_{L,M} = -i\left[\frac{ck\mu_0}{\hbar R_0 L(L+1)}\right]^{1/2} \nabla\times\mathbf{L}\, j_L(kr) Y_{L,M}(\theta,\phi)$$

Since the orbital angular momentum operator **L** is given by

$$\mathbf{L} = -i\hbar\,\mathbf{r}\times\nabla$$

$$\therefore \qquad \nabla\times\mathbf{L} = \frac{\hbar}{i}\left[\mathbf{r}\nabla^2 - \nabla\left(1+r\frac{\partial}{\partial r}\right)\right], \qquad \text{...(22)}$$

We know that

$$\nabla^2[j_L(kr)\,Y_{L,M}(\theta,\phi)] = -k^2 j_L(kr)\,Y_{L,M}(\theta,\phi)$$

and

$$r\frac{\partial}{\partial r}[j_L(kr)] = kr\,j_{L-1}(kr) - (L+1)j_L(kr) = L\,j_L(kr) - kr\,j_{L+1}(kr)$$

$$\therefore \nabla\times\mathbf{L}\,j_L(kr)\,Y_{L,M}(\theta,\phi) = \frac{\hbar}{i}\left[-k^2\mathbf{r} - (L+1)\nabla\right] j_L(kr) Y_{L,M}(\theta,\phi) + \frac{\hbar}{i}\nabla\left[kr\,j_{L+1}(kr) Y_{L,M}(\theta,\phi)\right] \qquad \text{...(23)}$$

Since the functions $Y_{L,M}$ have parity $(-1)^L$, the operator **L** has parity (+1) and the operator $\nabla\times$ has parity (−1), hence we see that $\mathbf{B}^{e}_{L,M}$ and $\mathbf{E}^{m}_{L,M}$ have parity $(-1)^L$, and that $\mathbf{B}^{m}_{L,M}$ and $\mathbf{E}^{e}_{L,M}$ have parity $(-1)^{L+1}$. Since $Y_{0,0}$ is a constant, hence the multipole fields for $L = 0$ vanish identically. This is one of the consequences of the transverse nature of a light wave in free space. The electric and magnetic multipole fields form is complete set. Any arbitrary field **E** (**r**) and **B** (**r**) can be built up from multipole fields, as

$$\mathbf{E}(\mathbf{r}) = \sum_{L=1}^{\infty}\sum_{M=-L}^{L}\left[a^{e}_{L,M}\,\mathbf{E}^{e}_{L,M} + a^{m}_{L,M}\,\mathbf{E}^{m}_{L,M}\right] \qquad \text{...(24)}$$

$$\mathbf{B}(\mathbf{r}) = \sum_{L=1}^{\infty}\sum_{M=-L}^{L}\left[b^{e}_{L,M}\,\mathbf{B}^{e}_{L,M} + b^{m}_{L,M}\,\mathbf{B}^{m}_{L,M}\right], \qquad \text{...(25)}$$

where the coefficients *a* and *b* determine the amplitudes of the individual multipole orders and are determined by the sources of the fields, as these are related to the strength of the sources and the boundary conditions. The summation over *L* extends from 1 to ∞, as the monopole ($L = 0$) fields vanish identically.

Selection Rules. The selection rules for emission of electric or magnetic multipole radiation may be obtained from the angular momentum and parity of the field. Since one quantum in the mode *L*, *M* carries an angular momentum $\sqrt{[L(L+1)]}$ and *z*-component *M* (both measured in units of $\hbar$), radiation of multipolarity *L*, *M* must remove from the nucleus a total angular momentum exactly equal to $\sqrt{[L(L+1)}\,\hbar$ with *z*-component $M\hbar$. If this quantum is emitted by a nucleus in going from the state ψ_i to state ψ_f, the vector difference between the angular momenta $\mathbf{J}_i$ of the initial state and $\mathbf{J}_f$ of the final state must be $\sqrt{[L(L+1)]}$ and the *z*-component must change by $\Delta m_j = -M$. Thus we see that transitions by emission of single multipole quantum are possible only between states of total angular momentum J_i and J_f, if

$$\mathbf{J}_i - \mathbf{J}_f = \mathbf{L} \quad \text{or} \quad |J_i - J_f| \le L \le J_i + J_f \qquad \text{...(26)}$$

The quantity **M**, the *z*-component of **L**, plays the role of total magnetic quantum number of the radiation and is related to the corresponding quantum numbers $\mathbf{M}_i$ and $\mathbf{M}_f$ of the nuclear states. It follows that

$$\mathbf{M}_{J_i} - \mathbf{M}_{J_f} = \mathbf{M} \qquad \text{...(27)}$$

For even values of *L*, the spherical harmonic function is even, therefore, the product of ψ_i and ψ_f must be even. For odd values of *L*, the product of ψ_i and ψ_f must be odd. The multipole order is expressed through the rank *L*, *e.g.*, radiation represented by the rank *L* has multipolarity 2^L. Thus $L = 1$ is called dipole radiation, $L = 2$ is quadrupole, etc. For each multipole order both *electric and magnetic* waves are possible. For each value of *L*, the electric and magnetic radiations have the same angular momentum but differing in parity. The parity of an electric multipole is the same as that of a material particle having the same *L*, *i.e.*, it is even when *L* is even and is odd if *L* is odd. Magnetic multipole radiation has the opposite parity, *i.e.*, odd when *L* is even and even when *L* is odd. We, therefore, get the following rules for the combination of parities of the initial and final states.

$$\pi_i\pi_f = (-1)^L \text{ (in electric multipole transition of order } L) \qquad \text{...(28)}$$

$$\pi_i\pi_f = -(-1)^L \text{ (in magnetic multipole transition of order } L) \qquad \text{...(29)}$$

Since there does not exist any multipole radiation with $L = 0$, relation (26) shows that *radioactive transitions between two states with $J_i = J_f = 0$ are completely forbidden by single quantum emission.* The emission of electric dipole radiation ($L = 1$) is connected with a change of parity of the nucleus, while the emission of magnetic dipole radiation is possible only if the parity does not change. The rules given above for the angular momentum and parity changes resulting from a transition of a given multipolarity are summarized in Table 7.1.

Table 7.1. Selection Rules for γ-radiation

Type	*Symbol*	*Change in Angular momentum, L*	*Parity change*
Electric dipole	E_1	1	Yes
Magnetic dipole	M_1	1	No
Electric quadrupole	E_2	2	No
Magnetic quadrupole	M_2	2	Yes
Electric octupole	E_3	3	Yes
Magnetic octupole	M_3	3	No
Electric 2^L—pole	E_L	L	[No for L even. Yes for L odd]
Magnetic 2^L—pole	M_L	L	[Yes for L even. No for L odd]

In general more than one type of multipole transition is possible between two states. For instance, if the angular momenta and partities of the initial and final states are $J_i = 1^+$ and $J_f = 2^-$, the possible L-values are 1, 2 and 3. Since the parity changes, the possible transitions are E_1, M_2 and E_3. The scheme of selection rules is illustrated in Table 7.2.

Decay Constants. To calculate decay constants, we shall follow the method used by Blatt and Weisskopf. Let us first consider the source a classical system of currents, which varies periodically as

$$\mathbf{j}(\mathbf{r}, t) = \mathbf{j}(\mathbf{r})\, e^{-i\omega t} + \mathbf{j}^*(\mathbf{r})\, e^{i\omega t}. \qquad \ldots(30)$$

The charge density associated with this current distribution is

$$\rho(\mathbf{r}, t) = \rho(\mathbf{r})e^{-i\omega t} + \rho^*(\mathbf{r})e^{i\omega t}. \qquad \ldots(31)$$

We define the electric multipole moment of order L, M as

Table 7.2. Selection Rules

	$\Delta J = 0$				$\Delta J = 1$			
$\pi_i \pi_f = -1$	E_1	M_2	E_3	----	E_1	M_2	E_3	----
$\pi_i \pi_f = +1$	M_1	E_2	M_3	----	M_1	E_2	M_3	----
Forbidden	$0 \to 0$	$0 \to 0$	$0 \to 0$	----		$0 \rightleftharpoons 1$	$0 \rightleftharpoons 1$	----
		$1/2 \to 1/2$	$1/2 \to 1/2$	----			$1/2 \rightleftharpoons 3/2$	----
			$1 \to 1$	----				
	$\Delta J = 2$				$\Delta J = 3$			
$\pi_i \pi_f = -1$	M_2	E_3	M_4	----	E_3	M_4	E_5	----
$\pi_i \pi_f = +1$	E_2	M_3	E_4	----	M_3	E_4	M_5	----
Forbidden		$0 \rightleftharpoons 2$	$0 \rightleftharpoons 2$	----		$0 \rightleftharpoons 3$	$0 \rightleftharpoons 3$	----
			$1/2 \rightleftharpoons 5/2$	----			$1/2 \rightleftharpoons 7/2$	----
	$\Delta J = 4$				$\Delta J = 5$			
$\pi_i \pi_f = -1$	M_4	E_5	M_6	----	E_5	M_6	E_7	----
$\pi_i \pi_f = 1$	E_4	M_5	E_6	----	M_5	E_6	M_7	----
Forbidden		$0 \rightleftharpoons 4$	$0 \rightleftharpoons 4$	----		$0 \rightleftharpoons 5$	$0 \rightleftharpoons 5$	----
			$1/2 \rightleftharpoons 9/2$	----			$1/2 \rightleftharpoons 11/2$	----

$$Q_{LM} = \int r^{L}\, Y^{*}_{LM}(\theta, \phi)\, \rho(\mathbf{r})\, d\tau. \qquad \text{...(32)}$$

where $Y^{*}_{L,M}$ (θ, ϕ) is the complex conjugate of the spherical harmonic function of orders L and M and $d\tau$ is the volume element. The integral is taken over the region of space occupied by the charge (the whole nucleus in this case).

The amplitude of the electric radiation of order L, M is thus given by

$$a^{e}(L, M) = -\frac{4\pi}{(2L+1)!!}\left(\frac{L+1}{L}\right)^{1/2}\left(\frac{\omega}{c}\right)^{L+2} Q_{L,M} \qquad \text{...(33)}$$

Here ω is the frequency of the radiation and $(2L + 1)!! = 1 \times 3 \times 5 \times \ldots (2L + 1)$.

The magnetic multipole moment of order L, M can be defined in a manner similar to that of electric multipole moment, as

$$M_{LM} = -\int r^{L}\, Y^{*}{}_{LM}(\theta, \phi)\,\frac{div(\mathbf{r}\times\mathbf{j})}{(L+1)}\, d\tau, \qquad \text{...(34)}$$

where j is the current density inside the charge assembly.

The amplitude of the magnetic radiation of order L, M is given by

$$a^{m}(L, M) = \frac{4\pi}{(2L+1)!!}\left(\frac{L+1}{L}\right)^{1/2}\left(\frac{\omega}{c}\right)^{L+2} M_{L,M}. \qquad \text{...(35)}$$

The energy $U^{e}(L, M, \Omega)\, d\Omega$ in a pure electric multipole radiation of order L, M with amplitude $a^{e}(L, M)$, emitted per second into the solid angle element $d\Omega$ can be written as

$$U^{e}(L, M, \Omega) = \frac{1}{4\pi\varepsilon_0}\frac{c}{2\pi k^2} Z_{L,M}(\theta,\phi)\,|\,a^{e}(L,M)\,|^2,$$

where $Z_{Z,M}$ (θ, ϕ) is angular distribution function. The total energy emitted per sec

$$U^{e}(L, M) = \frac{1}{4\pi\varepsilon_0}\frac{c}{2\pi k^2}\int |\,a^{e}(L,M)\,|^2 Z_{L,M}(\theta,\phi)\,d\Omega$$

$$= \frac{1}{4\pi\varepsilon_0}\frac{c}{2\pi k^2}|\,a^{e}(L,M)\,|^2 = \frac{2(L+1)c}{\varepsilon_0 L[(2L+1)!!]^2}\left(\frac{\omega}{c}\right)^{2L+2} |\,Q_{L,M}\,|^2 \qquad \text{...(36)}$$

Here we have used the integral of the angular distribution function $Z_{L,M}$ (θ, ϕ) over the full solid angle as unity.

Similarly the energy emitted per second by a magnetic multipole radiation is given by

$$U^{m}(L, M) = \frac{\mu_0}{4\pi}\frac{c}{2\pi k^2}\int |\,a^{m}(L,M)\,|^2 Z_{L,M}(\theta,\phi)\,d\Omega$$

$$= \frac{\mu_0}{4\pi}\frac{c}{2\pi k^2}|\,a^{m}(L,M)\,|^2 = \frac{2(L+1)c\,\mu_0}{L[(2L+1)\,!!]^2}\left(\frac{\omega}{c}\right)^{2L+2} |\,M_{L,M}\,|^2. \qquad \text{...(37)}$$

It is important to note that a periodic distribution of charges and currents is not the only possible source of radiation. In view of the intrinsic magnetic moments associated with the spins of the nucleons, the periodic distribution of magnetization must also be considered.

$$\boldsymbol{M}(\boldsymbol{r}, t) = \boldsymbol{M}(\boldsymbol{r})e^{-i\omega t} + \boldsymbol{M}^{*}(\boldsymbol{r})\, e^{i\omega t}. \qquad \text{...(38)}$$

The electric multipole radiation is given by Eqn (33) provided $Q_{L,M}$ is replaced by $Q'_{L,M}$. Similarly the magnetic multipole radiation is given by Eqn (35) provided $M_{L,M}$ is replaced by $M'_{L,M}$. Here

$$Q'_{L,M} = -\frac{ik}{c}\int r^{L} Y^{*}_{L,M}(\theta,\phi)\frac{div(\boldsymbol{r}\times\boldsymbol{M})}{L+1}\, d\tau \qquad \text{...(39)}$$

and

$$M'_{L,M} = -\int r^{L} Y^{*}_{L,M}(\theta,\phi)\, div\, \boldsymbol{M}\, d\tau. \qquad \text{...(40)}$$

The decay constant λ, which is the probability for emission of a quantum ($\hbar\,\omega$) per unit time can be obtained from above equations as

$$\lambda^{e}(L, M) = \frac{U^{e}(L,M)}{\hbar\omega} = \frac{2(L+1)}{\hbar\varepsilon_0 L[2L+1)!!]^2}\left(\frac{\omega}{c}\right)^{2L+1} |Q_{L,M} + Q'_{L,M}|^2 \qquad \ldots(41)$$

$$\lambda^{m}(L, M) = \frac{U^{m}(L,M)}{\hbar\omega} = \frac{2(L+1)\mu_0}{\hbar L[(2L+1)!!]^2}\left(\frac{\omega}{c}\right)^{2L+1} |M_{L,M} + M'_{L,M}|^2 \qquad \ldots(42)$$

Here $Q'_{L,M}$ and $M'_{L,M}$ correspond to the intrinsic magnetic moments associated with the spins of the nucleons.

Reduced Transition Probability. For a given transition $J_i \to J_f$, the reduced transition rate for electric transitions of order L is defined as

$$B(EL, J_i \to J_f) = \frac{1}{2J_i+1} \sum_{M_i} \sum_{M_f} |Q_{L,M}(i \to f)|^2 \qquad \ldots(43)$$

The double sum is taken as $|M| = |M_i - M_f| \le L$. For magnetic transitions, we replace $Q_{L,M}$ with $M_{L,M}$. We thus have

$$B(ML, J_i \to J_f) = \frac{1}{2J_i+1} \sum_{M_i} \sum_{M_f} |M_{L,M}(i \to f)|^2 \qquad \ldots(44)$$

In terms of reduced transition rates, the decay constants may be written as

$$\lambda^{e}(L, J_i \to J_f) = \frac{2(L+1)}{\hbar\varepsilon_0 L(2L+1)!!]^2}\left(\frac{\omega}{c}\right)^{2L+1} B(EL, J_i \to J_f) \qquad \ldots(45)$$

$$\lambda^{m}(L, J_i \to J_f) = \frac{2(L+1)\mu_0}{\hbar L(2L+1)!!]^2}\left(\frac{\omega}{c}\right)^{2L+1} B(ML, J_i \to J_f) \qquad \ldots(46)$$

The reduced transition probability B_{ge} for the upward excitation process is related to the downward probability B_{eg} as

$$B_{ge}(L) = [(2I_e + 1)/(2I_g + 1)]\, B_{eg}(L). \qquad \ldots(47)$$

Weisskopf's Estimates of Transition Rates—It is based upon a nuclear model with the following assumptions :

(i) The coupling between the constituent nucleons is weak, such that only a single nucleon (a proton) experiences a change in its quantum state, the other nucleons form closed shells and do not contribute to the matrix element. Thus $\psi_i = R_i(r)\, Y_{L,M}(\theta, \phi)$.

(ii) The final state is assumed to be an S-state. Thus $\psi_f = R_f(r)/\sqrt{4\pi}$..

(iii) The radial wavefunctions, R_i and R_f are assumed to be constants inside the nucleus ($r < R$) and zero outside.

The charge density ρ is replaced, for a quantum mechanical system, by the unit charge times the probability density ψ_i^2. The first two assumptions show that one proton jumps from a state with orbital angular momentum L to a state with $L = 0$. The third assumption shows that the radial wavefunction is normalized, *i.e.*,

$$\int_0^R |R_i|^2 r^2 dr = \int_0^R |R_f|^2 r^2 dr = 1$$

or

$$R_i(r) = R_f(r) = \sqrt{3/R^3} \qquad \ldots(48)$$

$$\therefore \quad Q_{L,M}(i \to f) = e\int r^L Y^*_{L,M}(\theta,\phi)\,\psi_f^*\,\psi_i\, d\tau$$

$$= \frac{e}{\sqrt{4\pi}}\int r^L \frac{3}{R^3} Y^*_{L,M}(\theta,\phi) Y_{L,M}(\theta,\phi) r^2 \sin\theta\, dr\, d\theta\, d\phi = \frac{e}{\sqrt{4\pi}}\,\frac{3R^L}{L+3}. \qquad \ldots(49)$$

Inserting this value in equation (41), we get the Weisskopf estimate of the electric multipole transition probability, as

$$\lambda_W^e(L) = \frac{2(L+1)}{L[(2L+1)!!]^2}\left(\frac{3}{L+3}\right)^2 \frac{e^2R^{2L}}{4\pi\varepsilon_0 \hbar}\left(\frac{\omega}{c}\right)^{2L+1}$$

$$= \frac{4.4(L+1)10^{21}}{L[(2L+1)!!]^2}\left(\frac{3}{L+3}\right)^2\left(\frac{E_\gamma}{197}\right)^{2L+1} R^{2L}\ sec^{-1} \qquad \text{...(50)}$$

where the transition energy $E_\gamma = \hbar\omega$ is in MeV and radius R in fermi.

Similarly for a magnetic multipole transition, we get

$$\lambda_W^m(L) = \frac{20(L+1)}{L[(2L+1)!!]^2}\left(\frac{3}{L+3}\right)^2 \frac{e^2\mu_0 c\omega}{4\pi \hbar}\left(\frac{\hbar}{M_n cR}\right)^2\left(\frac{\omega R}{c}\right)^{2L}$$

$$= \frac{1.9(L+1)10^{21}}{L[(2L+1)!!]^2}\left(\frac{3}{L+3}\right)^2\left(\frac{E_\gamma}{197}\right)^{2L+1} R^{2L-2} sec^{-1} \qquad \text{...(51)}$$

Here M_n is the nucleon mass, E_γ is in MeV and R in fermi.

Using the relation $R = R_0\, A^{1/3}$ and $R_0 = 1.2\ fm$, we may define the Weisskopf single particle estimate for L^{th} multipole reduced electric transition probability, as

$$B_W(EL) = \frac{e^2}{4\pi}\left(\frac{3R^L}{L+3}\right)^2 = \frac{1}{4\pi}\left(\frac{3}{L+3}\right)^2 (1.2)^{2L} A^{2L/3}\ e^2 fm^{2L} \qquad \text{...(52)}$$

Similarly, we have

$$B_W(ML) = 10\left(\frac{\hbar}{M_n cR}\right)^2 B(EL) = \frac{10}{\pi}\left(\frac{3}{L+3}\right)^2 (1.2)^{2L-2} A^{(2L-2)/3}\ \mu_N^2 f_M^{2L-2} \qquad \text{...(53)}$$

Using the relation $R = R_0 A^{1/3}$ and gamma decay width $\Gamma = \hbar \times$ transition probability λ. Hence for different transitions, the single particle radiative widths are given directly as

$$\Gamma_\gamma(E1) = 0.0675\, A^{2/3} E_\gamma^3, \qquad \Gamma_\gamma(M1) = 0.0207\, E_\gamma^3,$$

$$\Gamma_\gamma(E2) = 4.79\times10^{-8} A^{4/3} E_\gamma^5, \qquad \Gamma_\gamma(M2) = 1.47\times10^{-8} A^{2/3} E_\gamma^5, \qquad \text{...(54)}$$

$$\Gamma_\gamma(E3) = 2.23\times10^{-14} A^2 E_\gamma^7$$

where Γ_γ is in eV and E_γ in MeV.

Since transition probability drops very quickly with increasing L, hence the chief contributions are corresponding to $L = \Delta J$. A weak admixture of transitions of multipole order $\Delta J + 1$ is to be expected mainly when the chief contribution ($L = \Delta J$) comes from a magnetic multipole. Since the ratio of the electromagnetic field due to the magnetic dipole to that due to an electric dipole, *i.e.*, M/E factor is v/c, therefore multipole mixtures of the type (M_1, E_2) or (M_2, E_3) are frequently encountered, whereas mixtures of the type (E_1, M_2) are not found. Experimentally $M1 + E2$ is found. The admixture of $L' = L + 1$ electric multipolarity in a mixed transition ($ML + EL'$) is expressed by the mixing ratio, whose square is defined as the ratio of intensities.

$$\delta^2 = I(L')/I(L). \qquad \text{...(55)}$$

It is zero for pure L-radiation and infinity for pure L'-radiation. The percentage of ML intensity is $(1+\delta^2)^{-1}$ and of EL' is $\delta^2(1+\delta^2)^{-1}$.

From the half life measurement, the multipole order of the γ-radiation can be determined, and thus statements about ΔJ and relative parities in the transition may be made. If we know the spin and parity of final state we can obtain the values for the spin and parity of the initial state.

7.4 INTERNAL CONVERSION

In 1914, E. Rutherford suggested that the nucleus is an excited state can perform a transition to a lower state not only by emitting a light quantum but also by transmitting energy directly to the electrons surrounding the nucleus. The transition to lower state is then connected with the ejection of an atomic electron, called a *conversion electron*, from a bound orbit. The kinetic energy of the ejected electron is equal to this transition energy $(E_i - E_f)$ minus the binding energy E_B of the orbital electron. As the gamma ray is internally converted into electron, the process is known is *internal conversion*. These electrons produce a series of monoenergetic lines, and not a continuous spectrum as in β^--decays.

The line with the lowest energy $E_{eK} = (E_i - E_f) - E_K$. This is followed by the line corresponding to the conversion of L electrons. $E_{eL} = (E_i - E_f) - E_L$, etc... The transition energy can be measured accurately from the spectrum of the conversion electrons. Some-times it is wrongly treated as an *internal photo-electric effect* by describing it as : a light quantum emitted by the nucleus is immediately absorbed by the electrons of the atom.

It is similar to the atomic Auger effect, where instead of emitting a photon when an atomic electron de-excites from a higher to a lower energy orbit, one of the atomic electrons is ejected. The gamma emission is caused by *transverse* electric and magnetic fields. The internal conversion is produced by the time varying Coulomb field of the nucleus, which has a radial direction. Thus the process of internal conversion is the conversion of nuclear excitation energy to kinetic energy through the direct electromagnetic interaction between the electrons and nucleons without any intermediate γ-rays. For all electromagnetic transitions, except the zero-to-zero transition, gamma ray-emission and internal conversion compete.

In 1932, Taylor and Mott suggested that for other possible modes of decay excluded the total *transition probability* λ from a nuclear state a to a nuclear state b is the sum of two terms,

$$\lambda = \lambda_e + \lambda_\gamma, \qquad \text{...(56)}$$

where λ_e and λ_γ are the partial decay constants for conversion electron emission and for gamma emission respectively. The ratio between these two decay constants is called the *conversion coefficient* and is measured as the ratio between the total number of conversion electrons emitted over a given time divided by the number of gamma rays emitted in the same transition over the same time.

Conversion coefficient $$\alpha = N_e/N_\gamma = \lambda_e/\lambda_\gamma. \qquad \text{...(57)}$$

$$\therefore \quad \lambda = \lambda_\gamma(1+\alpha),$$

α may have any value between 0 and ∞. Since the probability of decay per unit time λ is related with the width Γ as $\lambda = \Gamma/\hbar$. Thus relation (56) may be written as

$$\Gamma = \Gamma_e + \Gamma_\gamma \qquad \text{and} \qquad \alpha = \Gamma_e/\Gamma_\gamma.$$

or the radiative width $$\Gamma_\gamma = \textit{Total width}\ \Gamma/(1+\alpha)$$

or in terms of mean lives $$\tau = \tau_\gamma/(1+\alpha). \qquad \text{...(58)}$$

As a result of internal conversion, for each gamma ray there may be several conversion lines corresponding to the ejection of electrons from different atomic shells, *e.g.*, $K.$, L_1, L_{11}, L_{111}, M_1, ... therefore, *total conversion coefficient* is given by

$$\alpha = \frac{N_K + N_L + N_M + \dots}{N_\gamma} = \frac{N_K}{N_\gamma} + \frac{N_L}{N\gamma} + \frac{N_M}{N\gamma} + \dots$$

$$= \alpha_K + \alpha_L + \alpha_M + \dots = \sum_{k=K,L,M,N\dots} \alpha_k. \qquad \text{...(59)}$$

Here α_K, α_L, α_M, ... etc., are the *partial conversion coefficients*. A description of the theory of internal conversion has been given by M.E. Rose. In this theory the point nucleus picutre is adopted. The direct interaction between nucleus and electrons is expanded in the different multipole fields as done for the theory of γ-transition rates. With the simplified description of the essential points Blatt and Weisskopf gave the approximate relations for the K-conversion coefficient in transitions for which the transition energy E_0 is small with respect to electron rest mass energy ($m_e c^2 = 0.511$ *MeV*) and greater than the binding energy of the *K*-electron. At higher energies, it would have been necessary to use relativistic electron wave function, as used in the *Dancoff-Morrison* treatment. The higher-subshell coefficients involve a more complicated treatment, as described by *Tralli and Goertzel*.

Here *K*-conversion means transition of energy to electrons in the *K*-shell of the atom. The restriction to the electrostatic interaction and use of non-relativistic electron wave functions are valid only for cases in which all the electron velocities involved are small compared to the velocity of light. As the energy of the ejected electron is large compared to its binding energy in the atom, we may therefore use a plane wave approximation for the ejected electron.

Let ψ_i and ψ_f be the nuclear wavefunctions of the nuclear states *i* and *f* with $E_i > E_f$. Furthermore let u_i, u_f be the electronic wavefunctions in the *K*-shell and in the continuum after the ejection, respectively. Thus

$$u_i = (\pi a^3)^{-1/2} \exp(-r/a)$$

and

$$u_f = V^{-1/2} \exp(i\boldsymbol{k}\cdot\boldsymbol{r}), \qquad \text{...(60)}$$

where $\boldsymbol{r}$ is the position vector of the electron with respect to the nucleus, $a = a_0/Z$, a_0 = Bohr radius of the hydrogen atom, Z = atomic number of the nucleus, $\boldsymbol{k}$ is the wave vector of the electron after ejection, and V is the volume of the box in which the system in included.

The transition probability between the initial state $\Psi_i = \psi_i\, u_i$ and the final state $\Psi_f = \psi_f\, u_f$ is given by the Golden rule

$$\omega = \frac{2\pi}{\hbar} |H_{if}|^2 \frac{dN}{dE}. \qquad \text{...(61)}$$

Here H_{if} is the matrix element of the interaction energy, the electrostatic interaction between the electrons and the protons in the nucleus and dN/dE is the number of states of the ejected electrons per unit energy interval. For electrons within the solid angle $d\Omega$, we have

$$\frac{dN}{dE} = V\frac{m_e \cdot \hbar k}{(2\pi\hbar)^3} d\Omega. \qquad \text{...(62)}$$

The total transition probability between the two nuclear states ψ_i and ψ_f due to internal conversion in the *K*-shell is thus given by

$$\lambda(i \to f) = 2\cdot\frac{2\pi}{\hbar} V \frac{m_e \hbar k}{(2\pi\hbar)^3} \int |H_{if}|^2 \, d\Omega. \qquad \text{...(63)}$$

Here a factor of 2 is because there are two electrons in the *K*-shell and the integral is over all directions of electrons.

The perturbing Hamiltonian due to the electrostatic interaction between the proton in the nucleus and the electron

$$H'_{int} = -\sum_{i=1}^{Z} \frac{e^2}{4\pi\varepsilon_0 |\boldsymbol{r}-\boldsymbol{r}_i|} = -\sum_{i=1}^{Z} \frac{e^2}{4\pi\varepsilon_0} \int \frac{\rho(\boldsymbol{r}_i)}{|\boldsymbol{r}-\boldsymbol{r}_i|} d\tau, \qquad \text{...(64)}$$

where $\rho(\boldsymbol{r}_i)$ is the static average of the nuclear charge distribution and $\boldsymbol{r}_i$ is the proton position vector. The matrix element is thus given by

$$\begin{aligned} H_{if} &= \int \Psi_f^* H'_{int} \Psi_i \, d\tau \\ &= \frac{(\pi a^3 V)^{-1/2}}{4\pi\varepsilon_0} \sum_{i=1}^{Z} \int d^3r \int d\tau\, \rho(\boldsymbol{r}_i) \exp(-i\boldsymbol{k}\cdot\boldsymbol{r})\, \psi_f^* \frac{e^2}{|\boldsymbol{r}-\boldsymbol{r}_i|} \exp\left(-\frac{r}{a}\right) \psi_i \qquad \text{...(65)} \end{aligned}$$

Here the first integration extends over the coordinates of the electron and the second integration over the coordinates which occur in the nuclear wave functions. As the electrons are outside the nucleus, $r_i < r$ and we may thus expand $|\boldsymbol{r}-\boldsymbol{r}_i|^{-1}$ as

$$\frac{1}{|\boldsymbol{r}-\boldsymbol{r}_i|} = \sum_{L=0}^{L} \sum_{M=-L}^{L} \frac{4\pi}{2L+1} \frac{r_i^L}{r^{L+1}} Y_{L,M}(\theta,\phi) Y^*_{L,M}(\theta_i,\phi_i), \qquad \text{...(66)}$$

where (θ, ϕ) are the polar angles of the vector **r** and (θ_i, ϕ_i) are that of vector $\boldsymbol{r}_i$.

The electric multipole moment for the nuclear transitions from the state i to state j may be defined quantum mechanically as

$$Q_{L,M}(i \to f) = e \sum_{i=1}^{Z} r_i^L Y_{L,M}^*(\theta_i, \phi_i) \psi_j^* \psi_i d\tau. \qquad \ldots(67)$$

Thus the substitution of (66) into (65) gives

$$H_{if} = \frac{e(\pi a^3 V)^{-1/2}}{4\pi\varepsilon_0} \sum_{L=0}^{\infty} \sum_{M=-L}^{L} \frac{4\pi}{2l+1} Q_{L,M}(i \to f) I_{L,M} \qquad \ldots(68)$$

where $I_{L,M}$ is given by the integral

$$I_{L,M} = \int \exp(-r/a) \exp(-i k \cdot r) r^{-(L+1)} Y_{L,M}(\theta, \phi) d\tau \qquad \ldots(69)$$

Since we are interested in internal conversions well above the threshold for this process. Thus for outgoing electrons $\lambda << a$, the Bohr radius of the K-shell of the atom, *i.e.*, $ka >> 1$ and we can set $\exp(-r/a) = 1$. Therefore we can evaluate $I_{L,M}$ directly by the use of the addition theorem for the spherical harmonics. We thus have

$$I_{L,M} = 4\pi i^{-L} \frac{k^{L-2}}{(2L-1)!!} Y_{L,M}(\theta, \phi) \qquad \ldots(70)$$

$$\therefore \qquad H_{if} = \frac{4\pi e}{\varepsilon_0 (\pi a^3 V)^{1/2}} \sum_{l=0}^{\infty} \sum_{M=-L}^{L} \frac{i^L k^{L-2}}{(2L+1)!!} Q_{L,M}(i \to f) Y_{L,M}(\theta, \phi). \qquad \ldots(71)$$

On substituting this value of H_{if} in equation (63) and simplifying the integration by the orthogonality and normalization of the spherical harmonics, we get the relation for the transition probability per unit time associated with the internal conversion process, as

$$\lambda^{IC}(i \to f) = \frac{8 m_e e^2}{\pi \varepsilon_0^2 \hbar^3 a^3} \sum_{L=0}^{\infty} \sum_{M=-L}^{L} \frac{k^{2L-3}}{[(2L+1)!!]^2} |Q_{L,M}(i \to f)|^2 \qquad \ldots(72)$$

Because of the selection rules, only certain values of L actually occur in the above sum. Let us neglect the contribution of $Q'_{L,M}$ in the relation for the transition probability of gamma radiation between the states i and f and compare with the above result. Neglecting the binding energy B_K of K-shell electrons compared to $\hbar\omega$, we get

$$\hbar^2 k^2 / 2m_e = \hbar\omega - B_K = \hbar\omega \text{ or } \qquad k = (2m_e \omega/\hbar)^{1/2}. \qquad \ldots(73)$$

Substitution of this value of k in equation (72) and comparison with equation (41) gives the approximate value for the internal conversion coefficient $\alpha_K^E(L)$ for K-shell conversion in a parity favoured transition of electric multipolarity L, as

$$\alpha_K^E(L) = \frac{L}{L+1} Z^3 \left(\frac{e^2}{4\pi\varepsilon_0 \hbar c}\right)^4 \left(\frac{2m_e c^2}{\hbar\omega}\right)^{L+5/2} \qquad \ldots(74)$$

The exact theoretical expression for the conversion coefficient was given by *M. E.* Rose using the relativisitic theory of Dirac. The K-shell conversion coefficient for magnetic multipolarity L is given here without proof, as

$$\alpha_K^M(L) = Z^3 \left(\frac{e^2}{4\pi\varepsilon_0 \hbar c}\right)^4 \left(\frac{2m_e c^2}{\hbar\omega}\right)^{L+3/2} \qquad \ldots(75)$$

These relations are the good approximations only for $Ze^2/4\pi\varepsilon_0\hbar c << 1$ and for the transition energies much larger than the binding energy of the K-shell.

These relations show that the conversion coefficients are proportional to Z^3 and thus increase strongly with Z. As a consequence of which the conversion process often dominates in heavy nuclei, whereas in light nuclei γ-emission is relatively favoured. They decrease with increasing transition energy $\hbar\omega$. Therefore transitions corresponding to small energies are preferentially through internal conversion. For transition energies < $2m_ec^2$ (= 1.022 *MeV*), the process of internal conversion increases with the multipole order L of the transition. Under identical conditions otherwise α^M are larger than α^E.

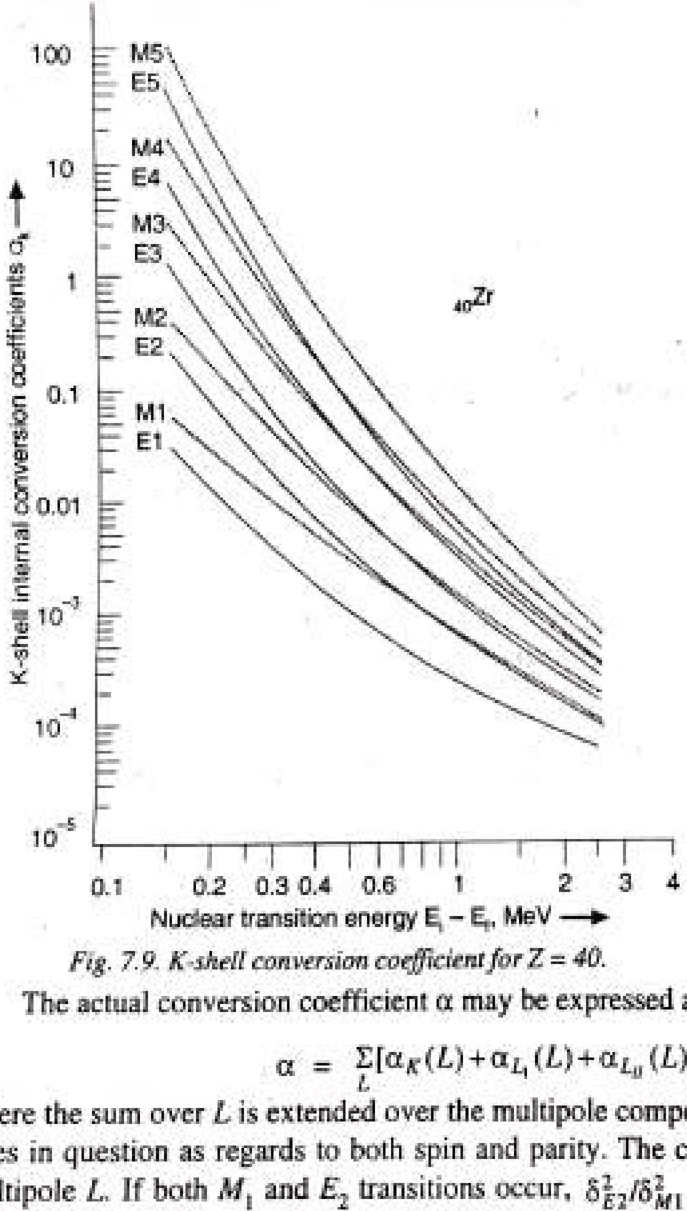

Fig. 7.9. K-shell conversion coefficient for Z = 40.

Fig. 7.9 shows the calculated values of α_K, the K-shell conversion coefficient for $Z = 40$ as a function of gamma ray energy for various multipolarities. The electric and magnetic multipole transitions are shown respectively by full and dotted lines.

Electrons can be ejected also from the L-shell of the atom. This process is in general less probable than the K-shell conversion. The ratio of K-shell to L-shell conversion decreases with increasing multipole order L, for the same value of L the ratio is larger for magnetic radiation than for electric radiation. The L-shell is divided into three subshells L_I, L_{II} and L_{III}, corresponding to $s_{1/2}$, $p_{1/2}$ and $p_{3/2}$ electrons, each with a different rate of internal conversion.

$$\lambda_e(L) = \lambda_e(L_I) + \lambda_e(L_{II}) + \lambda_e(L_{III}). \quad ...(76)$$

These subshell ratios usually differ strongly for electric and magnetic multipoles of the same order. The importance of the experimental study of internal conversion lies in the information which it may give about the multipolarity and parity change of nuclear transition. Internal conversion coefficient gives no information about nuclear structure.

The actual conversion coefficient α may be expressed as a sum of the form

$$\alpha = \sum_L [\alpha_K(L) + \alpha_{L_I}(L) + \alpha_{L_{II}}(L) + \alpha_{L_{III}}(L) + \ldots]\delta_L^2, \quad ...(77)$$

where the sum over L is extended over the multipole components which are permissible under the selection rules in question as regards to both spin and parity. The coefficient δ_L^2 is the relative contributions of the multipole L. If both M_1 and E_2 transitions occur, $\delta_{E2}^2/\delta_{M1}^2$ is called mixing ratio. Similarly, we may have mixing ratios for all other combinations.

0 → 0 transitions—If the intial and final nuclear states each have spin zero, gamma emission is impossible, as a photon must carry at least one unit of angular momentum. The 0 → 0 transition is however possible by internal conversion provided the electrons wave function does not vanish at the origin. This shows that the electron has a finite chances of being with in the nuclear volume. The 0 → 0 transitions are distinguished experimentally by the emission of conversion electrons and the complete absence of γ-ray emission. Thus the internal conversion coefficient is infinite.

The transition probability per unit time for 0 → 0 transitions is given by Blatt and Weisskopf as

$$\lambda_K = \frac{32\sqrt{2}}{9} Z^3 \left(\frac{m_e ce^2}{4\pi\varepsilon_0 \hbar^2}\right)\left(\frac{\overline{R^2}}{a_0^2}\right)^2 \left(\frac{E_0 - E_K}{m_e c^2}\right)^{1/2} \quad ...(78)$$

where $\overline{R^2}$ corresponds to the mean square nuclear radius having value $\frac{3}{5}R^2 = \frac{3}{5}(R_0 A^{1/3})^2$ and a_0 is the Bohr radius. The reciprocal of λ gives the K-conversion mean lifetime for 0 → 0 transitions between levels of the same parity. Thus we get

$$\tau_K(0 \rightarrow 0) = \frac{0.37}{Z^3 A^{4/3}} \left(\frac{m_e c^2}{E_0 - E_K} \right)^{1/2} \text{ sec.} \qquad \ldots(79)$$

Thus the internal conversion process suggests that the nuclear life-time is slightly influenced by atomic electron configuration effects. A change in the chemical environment can therefore produce a slight change in the lifetime.

Experimental determination of Internal Conversion Coefficients presupposses that the K, L, etc. lines can be separated by instrument and the number of internal conversion electrons from a given γ-ray can be compared to intensity of that γ-ray. This involves the efficiency of two different detecting arrangements which may be difficult to determine with great precision. Therefore indirect methods are prefered. The internal conversion coefficients are determined by making absolute measurements of the intensity of γ-rays and the associated converted electrons, X-rays or Augar electrons produced in radioactive decay or nuclear reactions. Magnetic spectrometer may be used or the radiations may be detected in scintillation or semiconductor detector. For a beta emitter the number of conversion electrons can be directly compared with the number of primary beta rays obtained in magnetic spectrometer. If the number of gamma transitions per beta ray is known, α can be calculated. One method is to make direct comparison between intensity of gamma rays measrured from the yield of photo electrons produced externally from a convertor foil with the number of internal conversion electrons produced by the same gamma rays. Another method is to compare the intensity of X-rays following the ejection of internal conversion electrons with the intensity of γ-rays itself.

Although the emission of K-electrons is the most probable process, the intensity of L *and* M electrons is usually easily observable with the sufficient available energy. The experiments are made difficult except for low energies and high Z.

The conversion coefficient is determined by means of magnetic spectrometer using the following procedure : The area of the conversion peak as observed in the spectrometer $N_e = N_\gamma \alpha T$, where N_γ is the number of γ-rays emitted by the source and T is the transmission of the spectrometer. The source is replaced by a thin radiatior of lead or gold. Gamma ray sources of known strength are placed one by one just behind the radiator and the number of photo-electrons is counted each time. From the relation $\mathcal{E}_{p.e.} = N_{p.e.}/N_\gamma$, the overall efficiency of the radiator-spectrometer system as a function of γ-ray energy is determined. The source under investigation is then placed behind the radiator and the number of gamma rays is determined from the number of photoelectrons. The proportional counter spectrometers may be used instead of magnetic spectrometer. In such a case no radiator is needed. The conversion coefficient is determined from the number of X-rays and gamma rays by the relation $\alpha = N_X/N_\gamma f$, where f is the fluorescent yield of the level excited.

Selection Rules—The momentum and parity selection rules for internal conversion are the same as those for γ-transitions, except some special features. The occurrence of 0 → 0 conversion transitions are strictly forbidden for γ-radiation, which cannot have an $L = 0$ component. The conversion electrons are feasible. The transition, if occurs, must be of $E0$ and not $M0$ character. The change in parity is ruled out for conversion transitions. The momentum selection rule for multipolarity

$$\Delta J = |J_i - J_f| \leq L \leq J_i + J_f \qquad \ldots(80)$$

The parity selection rule for multipole character

$$\Delta\pi = \textit{no allows } E;\ \Delta\pi = \textit{yes allows } M$$

$$0 \rightarrow 0 \textit{ transitions } E0 \textit{ allowed, } M0 \textit{ forbidden.}$$

When a transition involves a mixture of multipoles, *e.g.*, $ML + EL'$, the net conversion coefficient is

$$\alpha = I_{ML}\,\alpha(ML) + I_{EL}'\,\alpha(EL'). \qquad \ldots(81)$$

where I_{ML} and I_{EL}' are the relative intensities of the γ-rays and are related as

$$I_{ML} + I_{EL}' = 1. \qquad \ldots(82)$$

7.5 INTERNAL PAIR CREATION

If the transition energy between the nuclear states is greater than $2m_ec^2$, *i.e.*, $E_\gamma > 1.022$ *MeV* an excited nucleus may emit a positron-electron pair as an alternative to γ-ray emission and electron internal conversion. This is called internal pair creation or *internal pair production*. The theoretical formalism for this process is very similar to that of internal conversion. The only difference is that in internal conversion an electron is excited into a free state from one of the atomic electron states, whereas in pair creation the electron is excited from one of the normally filled states of the negative energy sea to a positive energy. The vacant state in this sea is seen physically as a positron. The lifting of one of these negative energy electrons into a positive energy state appears as the creation of an electron-positron pair. Pair creation thus becomes important under exactly the conditions under which internal conversion is becoming small. The ratio of pair creation events to γ-ray emissions is independent of the nuclear structure and is defined as the *coefficient of internal pair conversion* and is represented by the symbol $\pi(L)$.

The internal pair conversion coefficient is calculated by using born approximation, valid for low $Z(<< 137)$ and sufficiently high energy $(2\pi Ze^2/4\pi\varepsilon_0\,\hbar v = Z\alpha/(v/c) << 1)$. The results have been obtained by Oppenheimer and Nodelsky for E_1 and E_2 transitions and by Rose for electric and magnetic multipoles upto $L = 5$ and for energies upto $k = E/m_ec^2 = 20$. Rose calculated total internal pair conversion coefficient by numerical integration of angular distribution of the pairs over both energy and angle and presented some of the results in the graphical form as shown in Fig. 7.10.

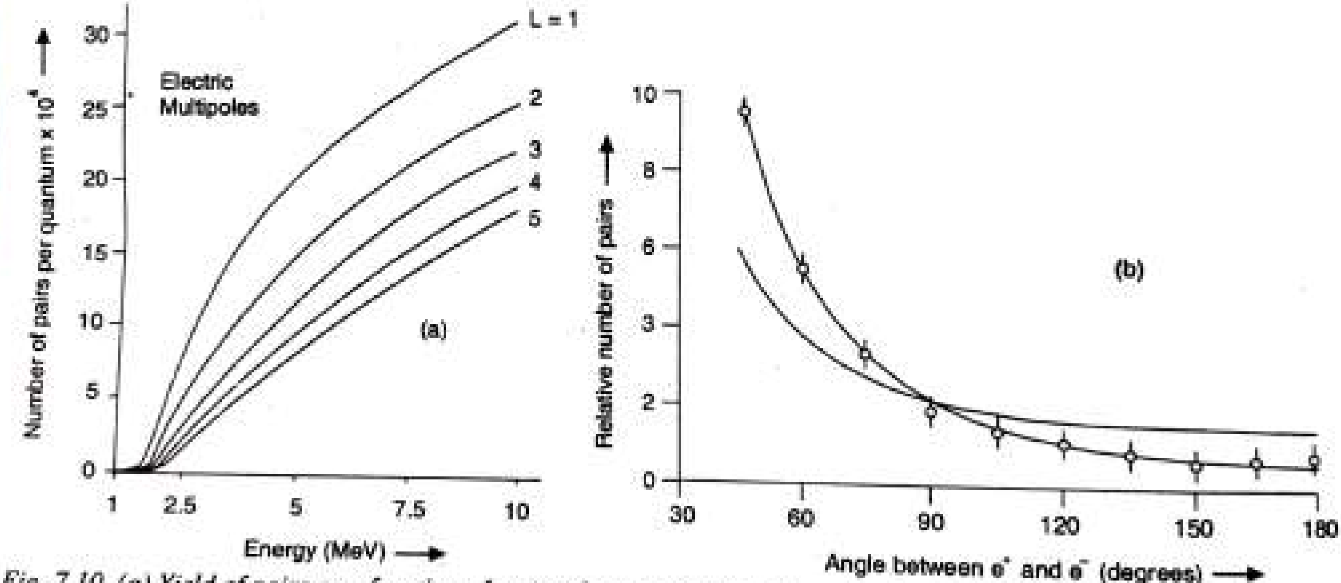

Fig. 7.10. (a) Yield of pairs as a function of energy for electric multipole radiation $(1 \le L \le 5)$. *(b) Angular correlation between* e^+ *and* e^- *for the high energy transition in the* $^7Li\,(p,\gamma)^8Be$ *reaction.*

For the low transition energies $(v/c << 1)$, Rose and Uhlenbeck have calculated the internal pair conversion coefficient using the Schrodinger approximation to the Dirac equation. It will be seen that the Schrodinger approximation is adequate to obtain a multipolarity assignment for $E/m_ec^2 < 3$ and for all Z. Thus we see that the internal pair conversion may be used as a reliable method of measuring the multipolarity of a γ-ray transition and for the specific information about the type of transition.

The internal pair creation supplements ordinary internal conversion in that the former is largest where the latter is smallest, namely in the region of low atomic number Z and high transition energies.

0 → 0 Transitions—In 0 → 0 transitions, the significant quantity is not the ratio of pair creation to γ-decay but the ratio of internal conversion to pair creation. This depends on Z and on the energy. For low Z and high energies, it reduces to $\alpha_i/\pi = 60\pi\,(\alpha Z/k)^3$. This is virtually the same as the K/β^+ ratio in allowed β-decay. The 6.04 MeV $0^+ \rightarrow 0^+$ transition in ^{16}O proceeds overwhelmingly by pair creation, while in a 1.414 MeV 0 → 0 transition in ^{214}Po only conversion electrons have been seen. The predicted values 2×10^{-5} and 170 respectively are consistent with these results.

Magnetic spectrometers of semicircular focusing type or lens type are used for the measurement of internal pair formation coefficients. Mims, Halban and Wilson measured the coefficient π of the 2.8 MeV γ-ray from $^{24}Mg^*$ by detecting the coincidences between annihilation radiations emitted in opposite directions. The triple coincidences between the beta-particle and a subsequent electron-positron pair have been counted with a counter telescopes. Cloud chambers have been used for the study of internal pair formation in meson decay.

7.6 NUCLEAR ISOMERISM

The occurrence of long lived, low-lying excited states is rather common among nuclei of intermediate and large masses. Observed life times vary over wide limits, from 10^{-10} sec to 10^8 years. These delayed transitions are called *isomeric transitions* and the states from which they originate are called *isomeric states or isomeric levels*. Nuclear species which have the same atomic and mass numbers, but have different radioactive properties, are called *nuclear isomers* and their existence is referred to as *nuclear isomerism*. Nuclides that are isomeric states of a given isotope differ from each other in energy and in angular momentum.

The phenomenon of nuclear isomerism was discovered by O. Hahn, in 1921. He found that UX_2 $({}^{234m}_{91}Pa)$ and $UZ({}^{234}_{91}Pa)$ both have the same atomic number and the same mass number but have different half lives and emit different radiations. Both grow out of $UX_1({}^{234}_{90}Th)$ by β^-decay. UX_2 has a half life of 1.18 minutes and emits three groups of electrons with end point energies of 2.31 MeV (90%), 1.50 MeV (9%) and 0.58 MeV (1%). On the other hand, UZ has a half life of 6.7 hours and emits four groups of electrons with end point energies of 0.16 MeV (28%), 0.32 MeV (32%), 0.53 MeV (27%) and 1.13 MeV (13%). About 0.15% of the UX_2 nuclei decay to ground state UZ. Both UX_2 and UZ then decay to $U_{II}({}^{234}_{92}U)$ by electron emission.

After the discovery of artificial radioactivity, indications came from several different directions that other nuclides exist in isomeric forms. When a sample containing bromine was bombarded with slow neutrons, the product was found to show three different half lives for beta decay : 18 min, 4.5 hr and 34 hr. Chemical tests showed that the radioactive elements were isotopes of bromine. This result was surprising because the reactions with slow neutrons are invariably of the (n, γ) type and since ordinary bromine consists of two isotopes only, Br^{79} and Br^{81} not more than two radioactive products ^{80}Br and ^{82}Br [$^{79}Br\ (n, \gamma)\ ^{80}Br$ and $^{81}Br\ (n, \gamma)\ ^{82}Br$] were to be expected. When bromine was bombarded with 17 MeV gamma ray two products ^{78}Br and ^{80}Br [$Br^{79}\ (\gamma, n)\ Br^{78}$, $Br^{81}\ (\gamma, n)\ Br^{80}$], with three decay periods, 6.4 min, 18 min, 4.4 hr were obtained. Two of these periods (4.4 hr and 18 min) are common to both sets of reactions and must, therefore, be assigned to the isotope that is common to both sets of reactions namely, ^{80}Br. The two half lives were attributed to two isomeric states of ^{80}Br. The difference between the nuclear isomers is attributed to a difference of nuclear energy states, one isomer represents the nucleus in its ground state, whereas the other is the same nucleus in an excited state of higher energy, or the *metastable state* (the letter *m* is sometimes written following the mass number to designate it)

Half period of isomeric transition. Most known γ-decay rates have been determined by the direct measurement of the life-times of the exited states.

Total decay rate
$$\lambda = \lambda_\gamma + \lambda_e = \lambda_\gamma (1+\alpha)$$

$\therefore$
$$T_{1/2} = (\log_e 2)/\lambda = 0.693\ \tau_\gamma/(1+\alpha). \qquad \ldots(83)$$

Since the internal conversion coefficient α can be measured or can be calculated theoretically and half life $T_{1/2}$ can be measured, hence τ_γ the average life or λ_γ the rate of photon emission can be calculated.

Classification of Nuclear Isomers. Nuclear isomers may be classified as :

(a) Isomers with independent decay—In this type, each isomer decays independently of the other with its own particular half life. The transition from the *metastable to the ground state is highly forbidden*. The transitions are shown in Fig. 7.11 *(a)* with T_1 and T_2 representing the different half-lives. One or other or

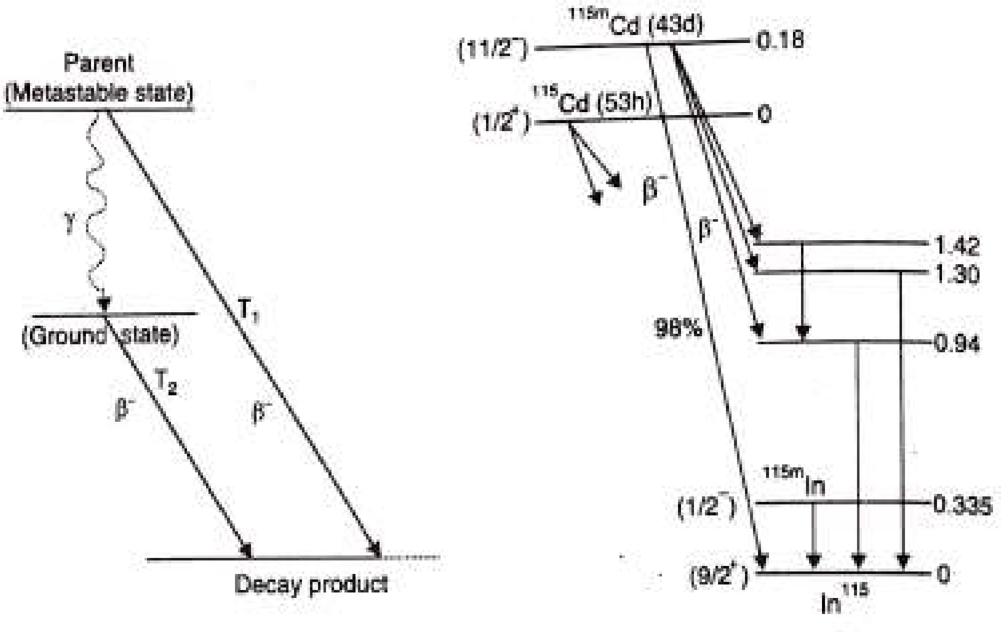
Parent
(Metastable state)
γ
(Ground state)
T₁
T₂
β⁻
β⁻
Decay product
¹¹⁵ᵐCd (43d)
(11/2⁻)
0.18
¹¹⁵Cd (53h)
(1/2⁺)
0
β⁻
β⁻
98%
1.42
1.30
0.94
¹¹⁵ᵐIn
(1/2⁻)
0.335
(9/2⁺)
0
In¹¹⁵

(a) (b)

Fig. 7.11. (a) Nuclear isomerism with independent decay, (b) Decay scheme of nuclear isomer ^{115}Cd.

both may also yield an excited state of the decay product, which will then emit the excess energy as gamma radiation. The examples of this type of nuclear isomers, together with the type of activity and half-lives are given below :

^{52}Mn(β^+, 5.7 days; β^+, 21 min); ^{71}Zn(β^-, 4.1 hr; β^-, 2.4 min.);
^{106}Ag(*EC*, 8.3 days; β^+, 24 min); ^{115}Cd(β^-, 43 days; β^-, 53 hr).

(b) Genetically related Isomers—In this type, the meta stable decays to the ground state with a definte half-life T_1. Mostly, the gamma radiation is internally converted and produces line spectrum of electrons together with characteristic *X*-rays. The ground state decays to form the product with a half-life of T_2, different from T_1. The product is not necessarily formed in its ground state and so gamma radiation may accompany the radioative change. Broken line of Fig. 7.12 (*a*) shows the possibility of direct independent decay of the excited metastable state of the parent nucleus. Some examples of genetically related isomers are given below :

^{44}Sc(IT, 2.44 days; β^+, 3.91 hr); ^{69}Zn(IT, 13.8 hr; β^- 55 min);
^{80}Br(IT, 4.4 hr; β^-, 17.6 min); ^{81}Se(IT, 57 min; β^- 18 min);
^{114}In(IT, 50 days; β^-, 72 sec); ^{131}Te(IT, 1.2 days; β^- 25 min);

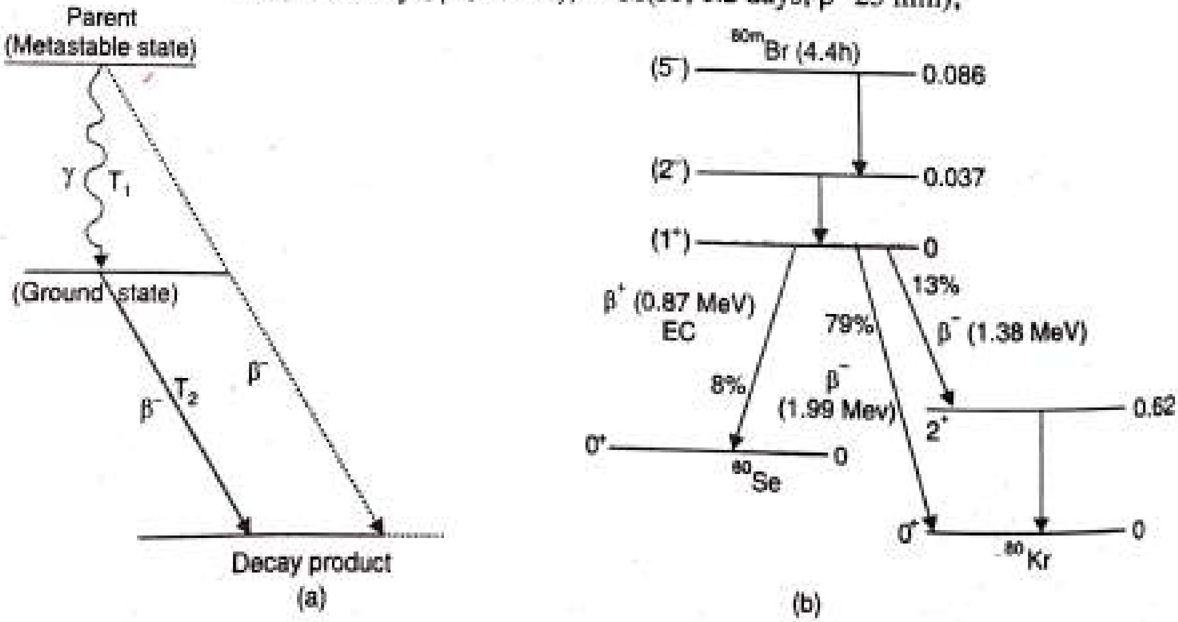
Parent
(Metastable state)
γ
T₁
(Ground state)
β⁻
T₂
β⁻
Decay product
⁸⁰ᵐBr (4.4h)
(5⁻)
0.086
(2⁻)
0.037
(1⁺)
0
β⁺ (0.87 MeV)
EC
8%
0⁺
0
⁸⁰Se
79%
β⁻
(1.99 Mev)
13%
β⁻ (1.38 MeV)
2⁺
0.62
0⁺
0
⁸⁰Kr

(a) (b)

Fig. 7.12. (a) Genetically related isomers, (b) Decay scheme of nuclear isomer ^{80}Br.

Here symbol IT implies to *isomeric transition*. From these examples it will be observed that the half-life of the internal transition process is often longer than that of the beta decay of the ground state. As a result, two groups of beta particles, corresponding to two distinct half-lives, are emitted. Sometimes isomeric transition is accompanied by the breaking of a chemical bond, which may make possible a separation of the isomeric nuclei.

(c) Isomers of Stable Nuclei—In this type of isomers, the decay process involves an isomeric transition from the metastable state to the ground state of a stable nuclide accompanied by the emission of gamma radiation. If gamma radiation is converted internally, the line spectrum of electrons, together with characteristic *X*-rays, is observed. More than 30 stable species with isomeric states are found in nature. Among them ^{83}Kr, ^{87}Sr, ^{103}Rh, ^{107}Ag, ^{117}Sn, ^{137}Ba and ^{197}Au form metastable states of appreciable life. Other number of stable nuclides form isomers of short life, *e.g.*, a millionth of a sec. or less.

Isomerism and Nuclear Spin. In 1936, C.F. von Weizsacker, a German physicist, proposed an explanation for the existence of metastable states of both stable and unstable nuclides. The probability of the transition between two excited states or an excited state and the ground state of the nucleus is dependent partly on the energy difference between these states but mainly on the multipole character of the radiation. This is determined by the spins and parities of the nuclear states involved in the transition. He suggested that an isomer is an atom whose nucleus is in an excited state and has an angular momentum which differs by several units from that of any lower energy including the ground state.

The larger spin change might result in longer and measurable half lives. The change of one or two units of spin is expected to occur in the very short half lives. Goldhaber and co-workers could classify the nuclear properties of 77 isomers, for which half-life time is between 1 sec and 8 months. About half of these are $M4$ transitions ($\Delta I = 4$, yes) and the remainder are $M3$, E_3 and E_4. The transitions accompanied by $E5$ radiations are not common. The correlation of nuclear angular momentum values with the *single particle shell model is excellent*. The shorter lived group (life times between 10^{-9} and 10^{-5} sec) is made up of M_1, M_2 and $E2$ transitions.

$E2$ transitions in heavy nuclei are 100 times faster than predicted by the single particle model. The properties of these fast $E2$ transitions are best accounted for by the *collective model*. This model predicts bands of rotational states for these spherically deformed nuclei.

7.7 COULOMB EXCITATION

When a charged projectile approaches a target, with an energy considerably less than the height of the mutual potential barrier so that the nuclear effects may be disregarded, the target nucleus gets excited through the electromagnetic interaction between the projectile and the Coulomb field of the target nucleus. Such a process is called *Coulomb excitation*. This process is important because the cross sections for this process are accurately related to electromagnetic properties of nuclei, which provide bases for nuclear models.

Coulomb excitation may be treated as the reverse process of the internal conversion, where the nuclear excitation energy is converted into the kinetic energy of charged particles (electrons) through the electromagnetic field. The very important difference is that the projectiles for Coulomb excitation are not electrons but protons and heavy ions. Secondly the relative effectiveness of magnetic interaction (between ion current and currents in the nucleus) in producing excitation is much less than in internal conversion because of the factor $(v/c)^2$. On account of this predominance of the electric force the name Coulomb excitation is given to this process of excitation.

The motion of the projectile carrying a charge ze in the Coulomb field of the nucleus with atomic number Z is characterized by the dimensionless quantity η, known as Sommerfeld number, and defined as

$$\eta = z\,Ze^2/4\pi\varepsilon_0\hbar v = \alpha z Z\, c/v. \qquad \text{...(84)}$$

where v is the velocity of the projectile at large distances and α is the fine structure constant. The Sommerfeld number may

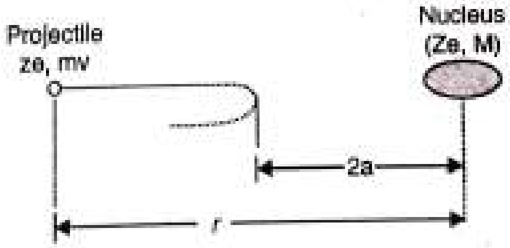

Fig. 7.13. Head on collision between a nucleus and a charged particle.

be viewed as the ratio of half of the distance of closest approach for a head on collision $a(= zZe^2/4\pi\varepsilon_0\mu v^2)$ to the reduced de Broglie wavelength of the projectile at infinity $ƛ = \hbar/p = \hbar/\mu v$). Here μ is the reduced mass of the projectile in the centre of mass [$\mu = mM/(m + M)$].

In order to observe the excitation of the target nucleus through the Coulomb field without any role of nuclear force to play, $a >> ƛ$ (or $\eta >> 1$).

$$\therefore \qquad \eta = a/ƛ = zZe^2/4\pi\varepsilon_0\hbar v = \alpha\, z\, Zc/v >> 1. \qquad \ldots(85)$$

On the other hand, $\eta << 1$, the Coulomb field produces only a small distortion of the incident wave and the collision process may be treated by the plane wave Born approximation.

Another very important aspect of the Coulomb excitation process is the time interval during which appreciable torque acts on the nucleus. The ratio of the collision time $t(= a/v)$ to the period of nuclear excitation $\tau(= 1/\omega = \hbar/\Delta E)$ is a dimensionless quantity, known as the *adiabaticity parameter* ξ. It is a measure of the extent to which the process is adiabatic.

$$\therefore \qquad \xi = \frac{a/v}{\hbar/\Delta E} = \frac{a\Delta E}{\hbar v} = \frac{zZe^2}{4\pi\varepsilon_0\,\hbar v}\cdot\frac{\Delta E}{2E}. \qquad \ldots(86)$$

where E is the kinetic energy of the projectile and ΔE is the excitation energy of the target nucleus. For Coulomb excitation process, the collision must be non-adiabatic and the parameter.

$$\xi\,[= z\,Z\,e^2\,\Delta E/4\pi\varepsilon_0\hbar v\,(2E)] << 1. \qquad \ldots(87)$$

In the classical treatment, the projectile is described by the hyperbola and the cross section for elastic scattering is given by the Rutherford expression, which for the deflection angle θ of the projectile is

$$(d\,\sigma/d\,\Omega)_{Ruth} = a^2/4\sin^4(\theta/2). \qquad \ldots(88)$$

If the trajectory is not appreciably modified by the excitation then the cross section for Coulomb excitation from the initial state i to the final state f is given by

$$(d\sigma/d\Omega)_{fi} = P(i \rightarrow f) \times (d\,\sigma/d\Omega)_{Ruth}. \qquad \ldots(89)$$

where P, the probability of excitation is determined by the transition amplitude b_{if} as

$$P = \frac{1}{2I_i + 1}\sum_{M_i, M_f}(b_{if})^2, \qquad \ldots(90)$$

where I_i is the initial spin of the target nucleus and M_i and M_f are respectively the projections of the initial and final spin on the quantization axis. The transition probability is expressed in terms of the interaction energy by the first order time dependent perturbation theory, as

$$b_{if} = \frac{1}{i\hbar}\int_{-\infty}^{\infty} <\psi_f\,|H'(t)|\,\psi_i> e^{i\omega t}\,dt, \qquad \ldots(91)$$

where ω = excitation energy $\Delta E/\hbar = (E_f - E_i)/\hbar$.

For electric transitions induced by low velocity particles ($v << c$), the main interaction energy is the Coulomb energy, therefore

$$H'(t) = H'_E(t) = \int \rho_n(r)\,\varphi\,(r, t)\,d\tau, \qquad \ldots(92)$$

where $\rho_n(r)$ is the nuclear density operator, can be described in terms of point charge protons as

$$\rho_n(r) = \sum_i e_i\,\delta(r - r_i), \qquad \ldots(93)$$

and $\varphi\,(r, t)$ is the Coulomb potential of the projectile, given as

$$\varphi\,(r, t) = \frac{1}{4\pi\varepsilon_0}\left[\frac{ze}{|r - r_p(t)|} - \frac{ze}{r_p(t)}\right]. \qquad \ldots(94)$$

Here in Eq. (93) e_i and $\mathbf{r}_i$ are the charge and position vector of the i^{th} nucleon. In Eq. (94), the projectile is considered as a point charge with its position vector $r_p(t)$ measured from the nuclear centre of mass. The second term is the contribution from the monopole. It can be eliminated since it can only deflect the projectile without taking part in excitation. In terms of spherical harmonics the factor $|r - r_p(t)|^{-1}$ may be expanded as

$$\frac{1}{\mathbf{r}-\mathbf{r}_p(t)} = \sum_{L=0}^{\infty} \sum_{M=-L}^{L} \frac{4\pi}{2L+1} \frac{r^L}{r_p^{L+1}(t)} Y_{L,M}(\theta,\phi) Y^*_{L,M}(\theta_p,\phi_p) \qquad \ldots(95)$$

Substituting these values in equation (89), the differential and total cross sections may be written in the form (as discussed by Alder *et al.*, 1956).

$$d\sigma_{E,L} = \left(\frac{ze}{4\pi\varepsilon_0 \hbar v}\right)^2 a^{-2L+2} B(EL)\, df_{EL}(\theta,\xi) \qquad \ldots(96)$$

$$\sigma_{E,L} = \left(\frac{ze}{4\pi\varepsilon_0 \hbar v}\right)^2 a^{-2L+2} B(EL, I_i \rightarrow I_f) f_{E,L}(\xi), \qquad \ldots(97)$$

where $(B(EL, I_i \rightarrow I_f)$ is the reduced transition probability defined in terms of reduced nuclear 2^L – pole matrix element of Alder *et al.* (1956).

The quantum mechanical cross sections for $L = 1$ and 2 have the same form as equations (96) and (97) except that the df_{EL} and f_{EL} depend on η_i. In the limit $\eta_i \rightarrow \infty$, the quantum mechanical cross sections reduce to the semiclassical cross sections. Alder *et al.* (1956) evaluated numerically and tabulated the semiclassical df_{EL} and f_{EL} for $L = 1, 2, 3$ and 4. The quantum functions $f_{E1}(\eta_i, \xi)$ and $f_{E2}(\eta_i, \xi)$ are also calculated and found a difference of less than 3% for $\eta_i \geq 4$.

The magnetic multipole excitations are also present in the Coulomb excitation. The form of the cross section for magnetic multipole scattering is similar to that for electric multipoles except that $B(EL)$ is replaced by the corresponding $B(ML)$, the reduced transition probability for magnetic multipole L. The f_{EL} is also replaced by f_{ML}.

Multiple Coulomb Excitation—In multiple Coulomb excitation, a particular nuclear state with high multipolarity can be populated by virtual excitation through several intermediate states. For example the probability of $E4$ excitation is reduced by about two orders of magnitude compared with $E2$ processes.

The strengths for high multipole transitions are weaker as the nuclear matrix elements involved are smaller. A succession of two $E2$ excitations may be comparable or even stronger than a single $E4$ excitation. The multiple Coulomb excitation method is best method for deducing multipole moments. The best projectiles for this process are the heavy ions with $z \geq 8$. The projectile energies are typically 25-200 *MeV*, such that $\eta_i \geq 25$.

Experimental Method—In Coulomb excitation studies thick target yields are generally observed. The thick target yield Y is given by

$$Y\left(\frac{excitation}{particle}\right) = n \int_0^x \sigma(x)dx = N \int_0^{E_p} \frac{\sigma(E)dE}{dE/dx}, \qquad \ldots(98)$$

where n is the number of target nuclei per m^3 and E_p denotes the incident projectile energy. The stopping power dE/dx of the projectile in the target material is conveniently defined as

$$S(E) = dE/d(\rho x), \textit{ in units of } MeV - m^2/kg. \qquad \ldots(99)$$

If z is the charge state of projectile, A the atomic weight of the normal target element in kg, the thick target yield is given by

$$Y(exc/\mu_C) = (3.759 \times 10^{33}/ZA) \int_0^{E_p} |\sigma(E)/S(E)|\, dE. \qquad \ldots(100)$$

Northcliffe and Schilling (1970) have tabulated $S(E)$ for various ions in 24 different material media. These are the semi-empirical results. The uncertainty in $S(E)$ for heavy ions is the primary limitation to extracting accurate values of $B(EL)$ from thick target γ-ray yields.

The thick target yield of a particular transition is experimentally measured by finding the absolute intensities of all γ-rays depopulating the given level. The intensity of the γ-ray is defined as the area under the peak divided by absolute efficiency of the detector ε at this energy. The effect of internal conversion is considered and a factor of (1 + α) is introduced for this purpose. The fractional isotope abundance a and the dead time τ_d of analysing system are also considered. Thus the yield per incident particle is given by

$$\left(\frac{Y}{I}\right)_{\exp} = \frac{1.60218\times10^{-19}\times z}{Q a \in}\left[\frac{(1+\alpha_T)N}{\varepsilon \overline{W}(1-\tau_d)}-T_C\right], \quad ...(101)$$

where Q is the charge in Coulombs collected at the target, ∈ the decay fraction of the transition, $\overline{W}$ is the angular distribution factor and T_C is the feeding from the higher levels. If f_i are the relative intensities of the various γ-transitions by which the excited state may decay and α_i are the corresponding total internal conversion coefficients, then for the detected gamma ray γ_j,

$$\in(\gamma_j) = f_j / \sum_i (1+\alpha_i) f_i. \quad ...(102)$$

The reduced transition probabilities so measured are presented in terms of Weisskop *f* single particle estimates, which are defined in equations (52) and (53).

$B(E1)$ observed in low energy spectra are of many orders of magnitude smaller than of single particle estimates. In contrast low energy $E2$-transitions are found with a strength of 10-100 times greater than of single particle estimates in most regions of the elements. Since $M1$ transitions are suppressed by a factor $(v/c)^2$, hence excitation will almost be of pure $E2$ type in the mixed de-excitations ($M1$ + $E2$). It has therefore a useful tool for studying collective quadrupole surface vibrations in nuclei as well as rotations of deformed nuclei.

7.8 ANGULAR DISTRIBUTIONS AND DIRECTIONAL CORRELATIONS

The gamma rays emitted from any assembly of nuclei have isotropic distribution as the excited states of the nuclei have randomly oriented spins. The emitted γ-rays may show an anisotropic distribution with respect to the direction of incident beam. This is called *angular distribution*. If the nuclei decay through successive emission of two γ-rays, γ_1 and γ_2. The observation of γ_1 in a fixed direction $\mathbf{k}_1$ selects an ensemble of nuclei that has a nonisotropic distribution of spin orientations. The γ_2 then shows a definite *angular correlation* with respect to $\mathbf{k}_1$. The term angular correlation comprises *of directional correlation* and *polarization correlation*. In the former only the directions of the two radiations are observed, while in the latter one determines also the linear or circular polarization of one or both the γ-rays. The measurement of the angular distribution of γ-radiation emitted from an excited nucleus or of the angular correlation between two radiations observed in coincidence can yield valuable information on multipole mixing ratio or nuclear level spins, which in turn can predict the behaviour, structure, shape and configuration of the nucleus. Both these methods are used in in-beam spectroscopy. Only the second method is useful in radioactivity experiments. There are similar angular correlations for other pairs of successive radiations, such as $\alpha-\gamma$, $\beta-\gamma$, $\beta-e^-$, $\gamma-e^-$.

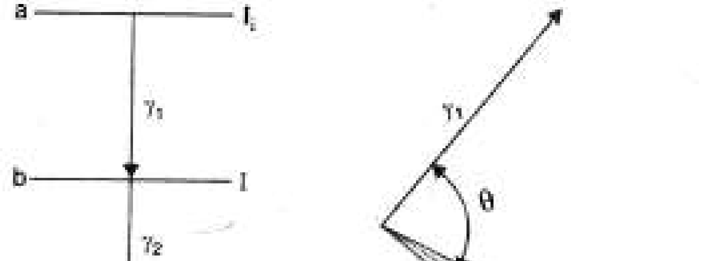

Fig. 7.14. Angular correlation for the Two successive Transitions 4(2) 2(2) 0 casade of ^{60}Ni.

Let us examine briefly the directional correlation between two successive γ-rays in the sequence shown in Fig. 7.14. The nuclear excited state (spin I_i) de-excites by a cascade or γ-rays γ_1 and γ_2 through an intermediate state (spin I) to the final state (spin I_f). The multipolarities of the γ-rays γ_1 and γ_2 are L_1 and L_2 respectively. If the intermediate state is sufficiently short-lived, coincidences between counts in the two counters (to accept signals γ_1 and γ_2) yield the angular correlation between the two radiations. The counting (coincidence) rate between γ_1 and γ_2 is measured as a function of the angle θ between the direction of emission of γ_1 and γ_2.

Dipole-Dipole Angular Correlation. Let us now consider two successive dipole γ-rays ($L_1 = L_2 = 1$) in the cascade $I_i(L_1)\ I(L_2)\ I_f$ [*i.e.*, 0(1) 1 (1) 0]. Only the intermediate level $I = 1$ is degenerate, its three magnetic substates having the quantum numbers $m = -1, 0, +1$. As the relative population of these magnetic substates is proportional to the Boltzmann factor = exp [(− μB/KT) (m/I)], which is essentially unity for all m except at the high fields and low temperatures needed to polarize nuclei. The magnetic sublevels are, therefore, equally populated under ordinary experimental conditions. Hence the transition modes $\Delta m_1 = 1, 0, -1$ as also correspondingly $\Delta m_2 = -1, 0, 1$ all occur with equal abundance.

The general expression for the emission probability of γ-rays having multipolarity L and magnetic quantum number M in a direction specified by polar angles (θ, ϕ) is given by

$$W_M(\theta)\, d\Omega = \frac{1}{2}\left[1-\frac{M(M+1)}{L(L+1)}\right]|Y_{L,M+1}|^2 + \frac{1}{2}\left[1-\frac{M(M-1)}{L(L+1)}\right]|Y_{L,M-1}|^2 + \frac{M^2}{L(L-1)}|Y_{L,M}|^2 . \quad \text{...(103)}$$

For our present case $L = 1$, hence the partial probabilities are given by

$$\begin{aligned} W_0(\theta)\, d\Omega &= (3/8\,\pi)\sin^2\theta\, d\Omega \text{ for } \Delta m = 0 \\ W_{+1}(\theta)\, d\Omega &= (3/16\,\pi)(1+\cos^2\theta)\, d\Omega \text{ for } \Delta m = +1 \\ W_{-1}(\theta)\, d\Omega &= (3/16\,\pi)(1+\cos^2\theta)\, d\Omega \text{ for } \Delta m = -1. \end{aligned} \quad \text{...(104)}$$

where θ is the angle between B and the direction of emission of the photon.

The total angular distribution is the sum of these three and is found to be constant as (3/4π) for all directions θ.

The angular distribution/correlation function may be defined as the relative probability that γ-ray 2 is emitted into an unit solid angle at an angle θ with respect to γ-ray 1 (or beam) and may be expressed as

$$W(\theta) = \sum_{k=0}^{k_{max}} b_k\, Q_k\, P_k(\cos\theta), \quad \text{...(105)}$$

where $P_k(\cos\theta)$ are the Legendre polynomials, Q_k contains the characteristics of the detector system, finite solid angle corrections, etc. $k_{\max}$ depends on the multipolarities of the transitions and the spins of the excited states and is given by

$$k_{\max} = min(2L'_1, 2L'_2, 2I), \quad \text{...(106)}$$

where

$$L'_n = L_n + 1.$$

The anisotropy is established by the occurrence of higher orders of k (*i.e.*, $k > 0$). The symmetry is established by the occurrence of only even orders $k = 0, 2, 4, \ldots$ whose range is bounded by angular momentum considerations. The directional correlation coefficients b_k for the γ − γ cascade are given by

$$b_k = A_k(\gamma_1)\, A_k(\gamma_2) \qquad k = \text{even}, \quad \text{...(107)}$$

where the coefficients A_k's are the certain combinations of Clebsch-Gordan and Racah coefficients. They have been tabulated by Biedenharn and Rose in 1953 and by Hager and Seltzer in 1968. For each cascade, $I_i(L_1)\ I\ (L_2)\ I_f$ has its own angular correlation $W(\theta)$. Thus the comparison with the experiment can give the unknown spins.

The most convenient form of describing the directional correlation $W(\theta)$ between γ_1 and γ_2 is

$$W(\theta) = 1 + A_{22}P_2(\cos\theta) + A_{44}P_4(\cos\theta) + \ldots A_{kk}P_k(\cos\theta). \quad \text{...(108)}$$

An equivalent and more common form is usually used for comparison with experiments. This is the power series in even powers of cos θ.

$$W(\theta) = 1 + a_2\cos^2\theta + a_4\cos^4\theta + \ldots a_{2L}\cos^{2L}\theta, \quad \text{...(109)}$$

where coefficients a_{2L} are functions of the angular momenta I_i, I, I_f, L_1 and L_2 but not of the relative parities of the levels. Since the highest power of cos θ that appears in the expansion is given by the smallest of the three quantities $2I$, $2L_1$ and $2L_2$, thus for quadrupole radiation, $\cos^4\theta$ is the highest power encountered. This also implies that for $I = 0$ or $\frac{1}{2}$, $a_2 = 0$, $W(\theta) = 1$ and the angular correlation distribution will be *isotropic*. *The intermediate state must, therefore, have a spin of at least 1 if an angular correlation is to be observed.*

The complexity of the angular distribution is given by the term *anisotropy*, defined as

$$Anisotropy\ A = W(180°)/W(90°) - 1 = a_2 + a_4 + \ldots a_{2L}, \quad \text{...(110)}$$

Thus we see that the angular correlation function involves only the spins of the nuclear levels concerned and not their parities.

Conditions of Validity. The relation (109) is valid under the following conditions :

1. The magnetic substates of the initial level are equally populated.

2. Each of the three levels *a*, *b* and *c* must be isolated and must have good quantum numbers of spin and parity.

3. The radiations γ_1 and γ_2 must be pure multipole radiations. Mixed radiations of opposite parity can produce interference and the angular distributions containing odd powers of cos θ.

4. The relation (109) restricts its attention to the relative directions of the two radiations, without cognizance of their states of polarization. The expression must be modified if the detectors used are able to measure the polarization.

5. The half period of the intermediate level must be short enough to permit the orientation of this level to remain undisturbed.

If a magnetic field is present, the nucleus in the intermediate state precesses about the direction of the magnetic field. This produces a change in the angular correlation, which can give the product of g_I factor of the excited state and the magnetic field strength.

Since no monopole ($L = 0$) radiation exists, hence transitions between states of angular momentum $I_i = I_f = 0$ do not occur. The transition probability diminishes rapidly with increasing order L. In fact, transitions involving higher orders than magnetic octupole ($L = 3$) have not been observed. Main contribution comes from $L = 1$ (dipole) or 2 (quadrupole).

$\gamma - \gamma$ Angular Correlation Coefficient. Angular correlation coefficients for some dipole and quadrupole $\gamma - \gamma$ cascade transitions are listed in Table 7.1.

Table 7.1

$\gamma - \gamma$ *Cascade* $I_i(L_1)\,I\,(L_2)\,I_f$	a_2	a_4	$\gamma - \gamma$ *Cascade* $I_i(L_1)\,I\,(L_2)\,I_f$	a_2	a_4
0(1) 1(1) 0	1	0	0(2)2(2) 0	−3	4
1(1) 1(1) 0	−1/3	0	1(1) 2(2) 0	−1/3	0
1(2) 1(1) 0	−1/3	0	2(1) 2(2) 0	3/7	0
2(1) 1(1) 0	1/13	0	2(2) 2(2) 0	−15/13	16/13
3(2) 1 (1) 0	−3/29	0	3(1) 2(2) 0	−3/29	0
			4(2) 2(2) 0	1/8	1/24

Here we see that there is no unique correspondence of coefficients to a given type of cascade and that the same coefficients describe either electric or magnetic multipole radiation. Thus a measurement of the angular correlation can give information only about the spins involved, but not about the parities of the corresponding levels.

In many decays, more than two radiations are emitted in cascade and one can observe the directional correlations $W(k_1, k_2)$, $W(k_1, k_3)$ and $W(k_2, k_3)$ in the triple cascade. In most cases, very little or no additional information is obtained in such a difficult measurement. The valuable additional information can be gathered if the direction of alignment of nuclei represents one of the three directions.

A complication often arises in $\gamma - \gamma$ directional correlation measurements in the cases where the radiations are not pure multipoles but are mixed. This happens with the first γ-ray of $2(L_1)\ 2(L_2)\ 0$ cascade, which is usually of mixed magnetic dipole ($L = 1$) and electric quadrupole ($L = 2$) character. In this case the A_{22} and A_{44} coefficients are functions also of the mixing ratio δ, which expresses the relative contributions of *E2* and *M1* radiation. The mixing ratio δ is established from the comparison of the normalized expansion coefficients A_{22} and A_{44} determined experimentally with those evaluated theoretically over the entire range of δ.

The experimental arrangement for measurements of angular correlation of gamma rays must consist of *fast coincident circuit. If the decay scheme is complicated*, the energies of the quanta between which the coincidences are registered must be selected with the help of a single channel and a pulse height analyzer. From the experimental data for the angular correlation, accidentals and background counts must be subtracted, corrections for coincidence loss should be applied, statistical uncertainties on each measured counts should be taken into account, and the method of least squares should be applied for the determination of coefficients A_{kk}.

The directional correlation of ^{60}Ni (obtained from the β-decay of ^{60}Co), first investigated successively by Brady and Deutsch, has become a standard cascade [4(2)2 (2) 0]. From the calculated values of the coefficients A_{22} and A_{44} for the cascade 4(2) 2(2) 0, we get the theoretical correlation as

$$
\begin{aligned}
W(\theta) &= 1 + 0.1020\, P_2 (\cos\theta) + 0.0091\, P_4 (\cos\theta) \\
&= (1 + 0.1250 \cos^2\theta + 0.0417 \cos^4\theta)\, const. \qquad \ldots(111)
\end{aligned}
$$

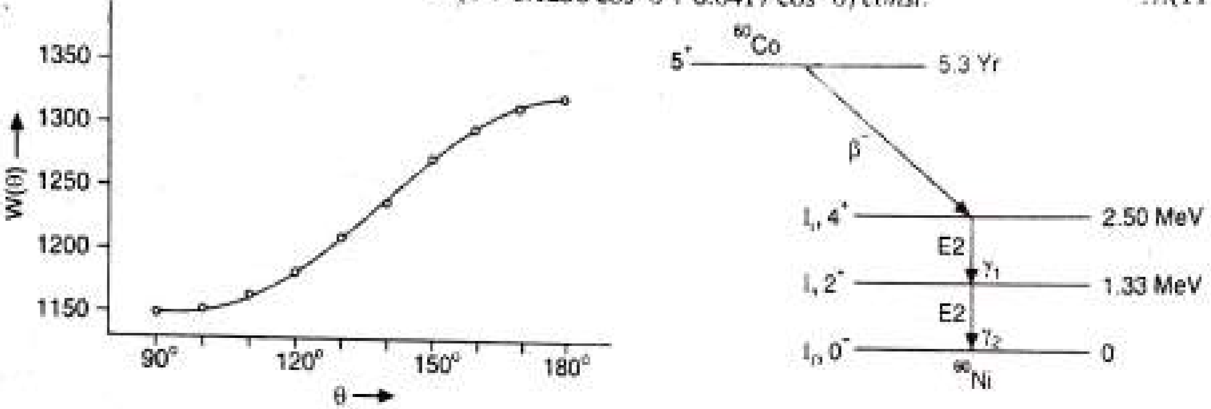

(a) (b)

Fig. 7.15. (a) Angular Correlation for the 4(2) 2(2) 0 cascade of ^{60} Ni, and (b) level scheme.

When all corrections and precautions are taken into account, the experimental values are found in excellent agreement with the theoretical curve, as can be seen from Fig. 7.15. For ^{60}Ni the theoretical asymmetry/anisotropy −0.1667 is found in excellet agreement with the experimental value − 0.167 ± 0.001.

γ − γ Polarization correlation. For the same multipole order, magnetic and electric multipoles have the same angular distribution. They differ in their parities and in the corresponding orientation of the plane of polarization of radiation. Relative parity of the nuclear levels can be measured by measuring the orientation of the polarization vector (*E*-vector) relative to the plane of the two successive-γ-rays. A detector sensitive to the linear polarization of γ-rays is called *polarimeter*.

The polarimeters are usually based on the Compton effect for low energies (< 6 *MeV*) and on nuclear photo effect for higher energies (> 3 *MeV*). The first polarization correlation experiment was successfuly performed by Metzger and Deutsch. The schematic diagram of this polarimeter is shown in Fig. 7.16. It consists of three scintillation counters *A*, *B* and *C*, which are in coincidence. One gamma ray γ_1 from the source (γ − γ cascade) is detected in counter *A*. The second gamma ray γ_2 is Compton scattered and registered in counter *B*, located at angle θ from the direction of counter *A*. The scattered gamma rays γ_c is directed toward counter *C* and produces a countable secondary electrons either by photoelectric effect or another Compton scattering. The Compton scattered photon γ_c will be preferentially directed with the electric vector $\mathfrak{E}_c$ parallel to the electric vector $\mathfrak{E}_2$ of the primary photon γ_2. Thus if $\mathfrak{E}_2$ lies normal to the plane of counters *B* and *C*, there is a maximum probability that γ_c will be directed toward counter *C*.

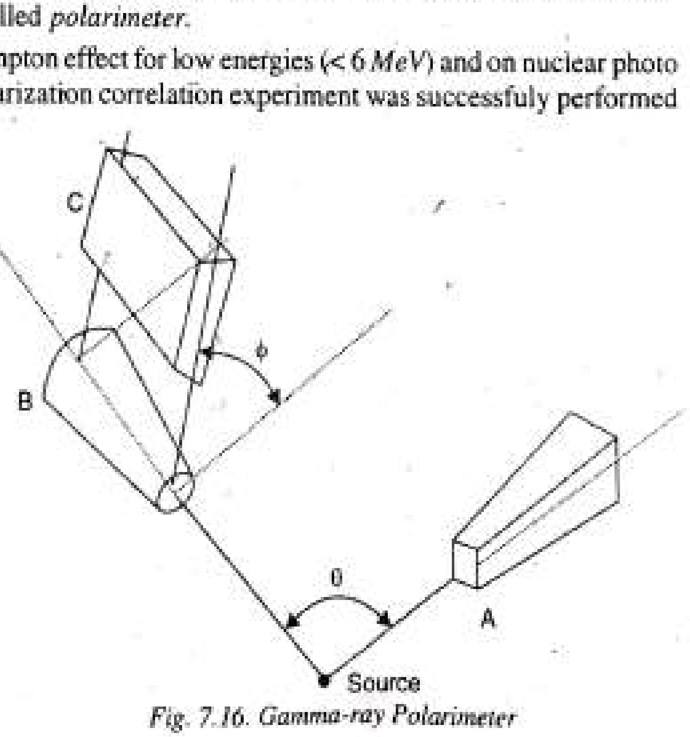

Fig. 7.16. Gamma-ray Polarimeter

The γ-γ polarization direction correlation in a quadrupole-quadrupole cascade when θ = 90° is given by

$$\mathcal{E}_{\parallel}/\mathcal{E}_{\perp} > 1 \text{ for } E2 - E2 \ (I_i \text{ and } I_f \text{ same parity})$$
$$\mathcal{E}_{\parallel}/\mathcal{E}_{\perp} < 1 \text{ for } M2 - M2 \ (I_i \text{ and } I_f \text{ same parity})$$
$$\mathcal{E}_{\parallel}/\mathcal{E}_{\perp} = 1 \text{ for } E2 - M2 \text{ or } M2 - E2 \text{ (opposite parity)}$$

Thus for two electric quadrupoles $E2 - E2$, the plane of $\mathcal{E}$ vector tends to be parallel to the plane of the two γ-rays and for two magnetic quadrupoles $M2 - M2$, it tends to be perpendicular to the plane of the two γ-rays. What θ = 180°, the ratio $\mathcal{E}_{\parallel}/\mathcal{E}_{\perp} = 1$ and is independent of the electric or magnetic character of the successive quadrupoles.

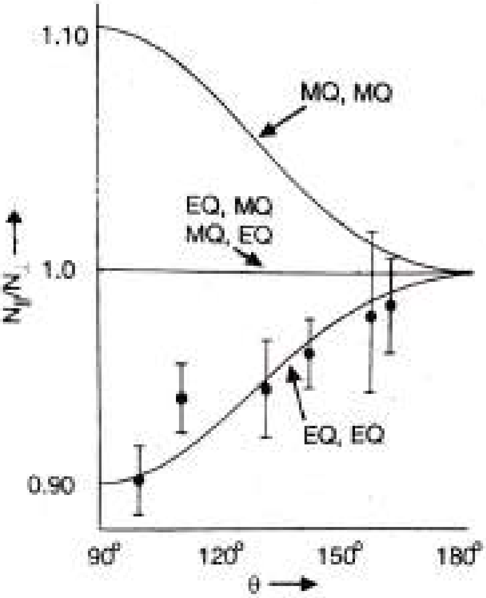

Fig. 7.17. Polarization direction correlation of two quadrupole γ-rays in ^{46}Ti.

Fig. 7.17 shows the polarization-direction correlation of ^{46}Ti, as determined by Metzger and Deutsch. The ratio $N_{\parallel}/N_{\perp}$ of the triple coincidence rates in the two extreme positions $\phi = 0$ and $\phi = \pi/2$ is plotted as a function of θ for the 1.12 MeV and 0.89 MeV cascade. These measurements are compared with the theoretical curves for both transitions magnetic ($MQ - MQ$), both transitions electric ($EQ - EQ$) and one transition electric and one magnetic ($EQ - MQ$ or $MQ - EQ$). The experimental points are found in agreement with the curve for $EQ - EQ$, which shows that both γ-rays are $E2$ transitions or the three nuclear levels of ^{46}Ti have the same parity. For the parity determination, only the values for θ = 90° and θ = 180° would have been necessary.

7.9 MEASUREMENTS OF LIFETIMES OF NUCLEAR STATES

Nuclear states produced in light element nuclear reactions have partial lifetimes for γ-ray emission in the range ~ 10^{-18} *sec* to ~ 10^{-8} *sec*. or partial widths from ~ 10^{7} eV to several hundred eV repectively ($\tau = \Delta t = \hbar/\Delta E$). The measurement of the lifetime of the excited state gives information about the width of the state (or level width and thus the matrix elements describing the mode of decay. The range of lifetimes covered by different experimental methods is shown in the chart, which is divided into direct methods (measure τ) and indirect methods (measure Γ). The widely applicable direct methods are : Electronic timing, recoil distance method (RDM) and Doppler shift attenuation method (DSAM).

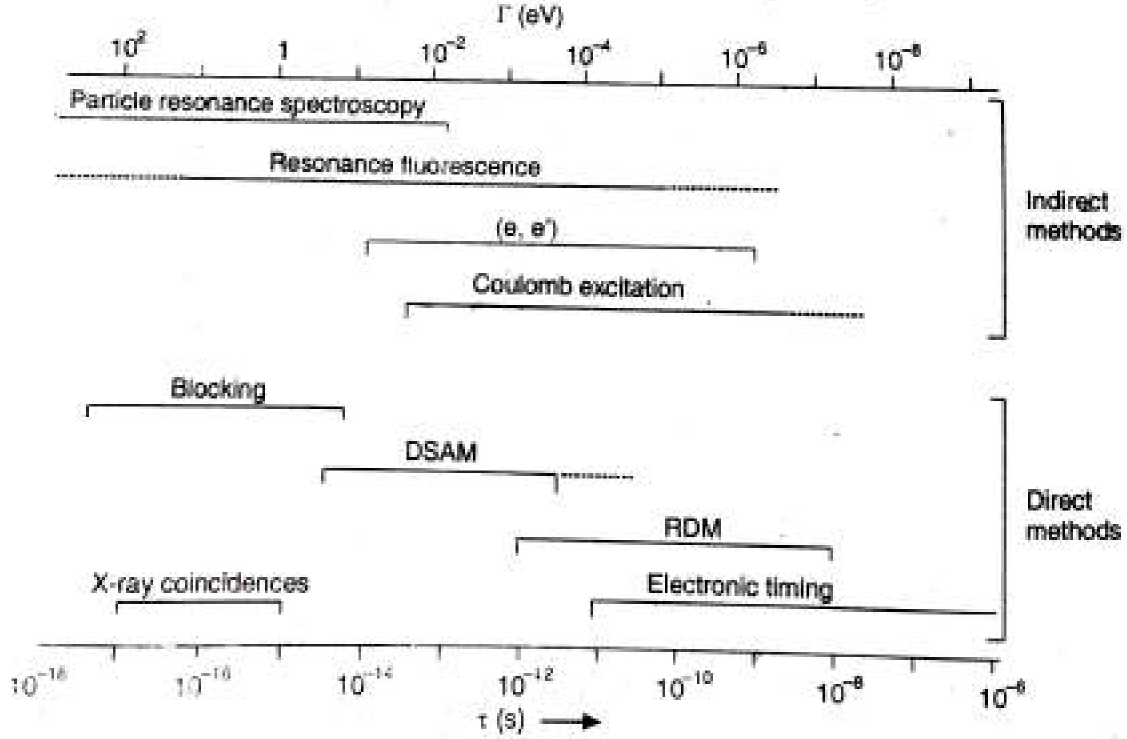

Fig. 7.18. Chart showing the range of lifetimes covered by different methods.

[A] Electronic Timing Methods—The electronic technique (or delay-coincidence technique) is widely applicable for the measurement of short nuclear lifetimes ($10^{-11} - 10^{-6}$ sec). It involves the measurement of the distribution of time delays between the formation and subsequent decay of the nuclear state of interest. The time of formation of the nuclear state is usually determined by either pulsing the beam (used in the formation of the state) or by detecting any radiation (particles or γ-rays) emitted in the formation of the state. The time of decay is marked by the detection of the decay γ-ray. The simple electronic circuit is shown in Fig. 7.19. The detectors I and II are used for the timing determination. In the case of the pulsed beam, one of the detectors is replaced with a time signal correlated with the beam pulse. The signals from the detectors are fed into the time derivation devices (TDD) which generate standard time pulses. The time intervals between these pulses are measured in a time to amplitude converter (TAC) and recorded in a multichannel analyzer. To improve the signal to background ratio and for the capability of time resolution adjustments, additional signal amplitude conditions are specified by single channel analyzer (SCA). The type of detector used depends on the experimental conditions. NaI(Tl), Ge(Li) or Si(Li) are used for γ-ray detection. Silicon surface barrier detectors are used for charged particles detection.

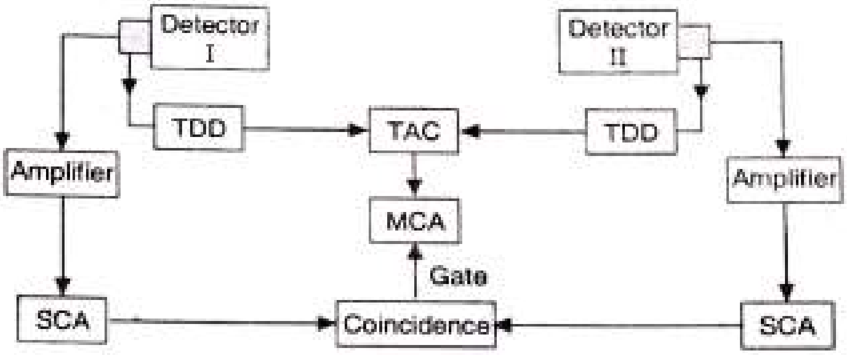

Fig. 7.19. Simple diagram of electronic timing technique.

This method should be capable of great accuracy, especially when the response time of the detectors is short compared with the life time being measured.

[B] Doppler Shift Techniques—Two different Doppler shift techniques (RDM and DSAM) for measuring nuclear lifetimes are commonly used. In both of these the Doppler shift of electromagnetic radiation emitted from a moving source is utilized. The energy of the shifted γ-ray is given to first order in β as

$$E_s = E_0(1 + \beta \cos \theta_\gamma), \qquad \ldots(112)$$

where E_0 is the energy of the γ-ray emitted by the nucleus decaying at rest, $\beta = v/c$, θ_γ is the angle between the direction of recoil of the excited nucleus (v) and that of the emitted γ-ray ($\boldsymbol{k}$). Consider the reaction of the type $X(x, y)Y^*$, where a target X is bombarded by a beam x with energy E_x producing an excited nucleus Y^* with a particle y being emitted. The recoil velocity of the centre of mass

$$\beta_{CM} = (2m_x E_x)^{1/2} (m_x + M_X), \qquad \ldots(13)$$

where the non-relativistic mass m_x, mass of the target M_X and E_x all in MeV. The recoil velocity of Y^* in the lab system (z-component of velocity) is

$$\beta_z = \beta_{CM} (1 + C \cos \phi_R), \qquad \ldots(114)$$

where ϕ_R is the recoil angle of Y^* in the *CM* system and C is the ratio of the velocity of Y^* in *CM*-system to the velocity of *CM*-system in lab system and is given by

$$C = \left\{\frac{M_X m_y}{m_x M_Y}\left[1 + \left(\frac{m_x + M_X}{M_X}\right)\left(\frac{Q}{E_x}\right)\right]\right\}^{1/2} \qquad \ldots(115)$$

where Q is the Q-value for the excited state of interest and is given by $Q_0 - \Delta E$.

Let us now discuss the methods for lifetime measurement based on Doppler shift technique.

(i) Recoil distance method—The recoil distance method (RDM), used in the range $10^{-12} - 10^{-8}$ sec, has been widely used since the availability of high resolution γ-ray detectors. Fig. 7.20 shows the basic principle of this method. In the apparatus used, the target and stopper are positioned parallel to each other. The target is thin enough to permit the residual nuclei to recoil freely into vacuum with a component of velocity v along the beam direction. The excited nuclei decay in flight. Those surviving for a time greater

than $t = d/v$ stopped quickly in the thick metal stopper and emit γ-rays. The γ-rays detected at an angle θ to the beam from nuclei that decay before reaching the stopper are Doppler shifted. Their energy to first order in v/c is given by equation (112). The γ-rays from the stopped nuclei have an energy E_0. These two γ-rays can be resolved in *Ge*(*Li*) detector. the intensities of the Doppler-shifted peak I_s and the unshifted peak I_0 corresponding to the γ-energies E_s and E_0 respectively are given by

$$I_s = N_0(1 - e^{-d/v\tau}),\ I_0 = N_0\, e^{-d/v\tau}. \qquad \ldots(116)$$

where N_0 is the total number of nuclei decaying.

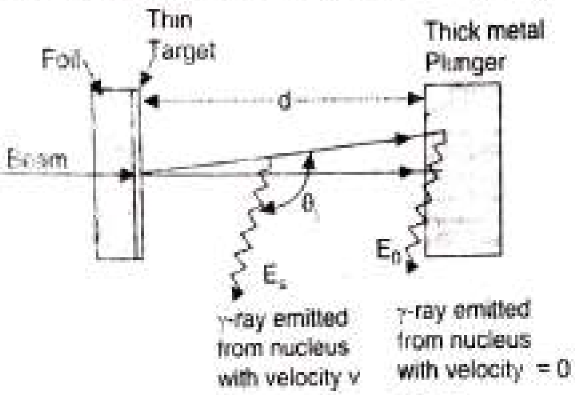

Fig. 7.20. Basic principle of RDM.

The lifetime is normally determined with the measurement of the ratio R as a function of d, where

$$R = \frac{I_0}{I_s + I_0} = \exp\left(-\frac{d}{v\tau}\right). \qquad \ldots(117)$$

The types of apparatus used today fall into two basic categories. The first are those in which micrometer drive is used to vary the separation d. The second are those which consist of two concentric cylinders which move relative to one another. The separation is measured mechanically using a calibrated screw thread. The method of capacity measurement has been used by several workers for measuring d.

Sometimes, it is necessary to use a gas target. In this case, the beam enters the gas through a thin window of metallic foil, traverses a thickness d of a gas and is stopped in or beyond the plunger. Assuming the energy loss in the gas target as negligible, the

$$\text{Ratio } R = \frac{\int_0^d e^{-x/v\tau}dx}{\int_0^d dx} = \frac{v\tau}{d}(1 - e^{-d/v\tau}) \qquad \ldots(118)$$

Several attempts have been made to use optical interferometers to both set up of the apparatus and to monitor the separation during actual measurements. Horstman *et al.* (1975) have developed a system where a laser based interferometer can continuously monitor the target during beam on periods.

(ii) Doppler Shift Attenuation Method (DSAM)—For lifetimes less than 10^{-11} sec, the recoil distance method becomes difficult because the plunger displacements are $< 10^{-5}$ *m*. Devons and his coworkers in 1955 developed Doppler shift method for measuring lifetimes ($10^{-10} - 10^{-11}$ sec). The basic method is shown in Fig. 7.21. A beam of incident particles x hit the target nucleus X. Reaction products y are emitted leaving the residual nucleus Y in excited state whose lifetime is to be measured. The recoiling nucleus Y^* slows down in the material of the target and/or target backing emitting a γ-ray with the mean lifetime τ of the excited state. The mean recoil velocity has dropped to $\bar{v}$, which is determined experimentally by measuring the average Doppler shift of the emitting γ-rays.

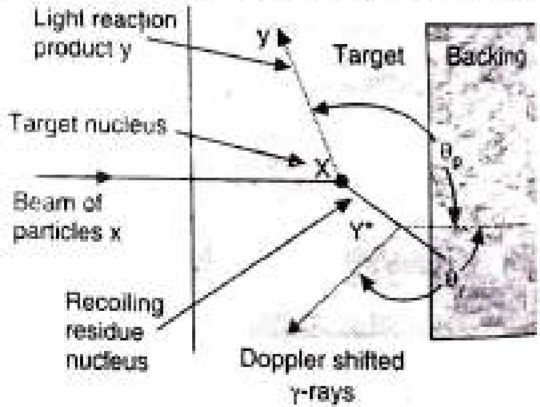

Fig. 7.21. Schematic diagram showing the principle of DSAM.

There are two basic ways of determining τ. The most widely used first method is to measure $\bar{v}$ from the equation

$$\bar{E}_s = E_0(1 + \bar{\beta}\cos\theta_\gamma), \text{ where } \bar{\beta} = \bar{v}/c. \qquad \ldots(119)$$

The variation in the centroid energy $\bar{E}_s$ of the γ-ray line is measured as a function of the angle θ_γ of observation with respect to the beam direction. The observations are expressed in terms of the factor $F =$ [illegible]. This factor is known as Doppler shift attenuation factor and this method is therefore called Doppler shift attenuation method (DSAM).The lifetime τ is obtained by comparing the measured value of F with a theoretical curve of $F(\tau)$ calculated using stopping theory. It is given by

$$F = \frac{\bar{v}}{v_0} = \frac{1}{v_0\tau}\int_0^\infty v(t)e^{-t/\tau}dt = \frac{1}{v_0\tau}\int_0^\infty \overline{v(t)\cos\theta_R(t)}e^{-t/\tau}dt. \quad \text{...(120)}$$

where θ_R is the angle through which the recoil is scattered and $\overline{v(t)\cos\theta_R(t)}$ is the average recoil velocity projected onto the beam direction.

The second method of determining τ is to compare the γ-ray line shape at an angle $\theta_\gamma \neq 90°$ (usually $\theta_\gamma = 0°$) with line shapes calculated theoretically.

The region of overlap between the RDM and DSAM is the 1–20 ps region. The lifetimes measured using both the techniques may give some information on the DSAM stopping theory. The DSAM requires a knowledge of stopping powers to find the lifetime from the observed data. A good knowledge of the composition of the target and its backing is necessary. The RDM does not need stopping theory and should be capable of great accuracy. The measurements are however difficult at short lifetime end of the range ($\leq 10^{-11}$ *sec*). The problem arises in the accurate separation of the target and stopper.

[C] Indirect Methods—These methods are called indirect as the lifetime is obtained from the measurement of the width of the level Γ or the matrix element for the transition from the ground state to the excited state. The target is excited by some form of radiation and the cross section for the excitation process is related to Γ. The Coulomb excitation, inelastic electron scattering and nuclear resonance fluorescence methods are discussed below.

(i) Coulomb excitation—It has been discussed earlier. The Coulomb excitation may be used in two ways in the measurement of lifetimes. In the first method Coulomb excitation is used as a mechanism for exciting the state whose lifetime is to be measured. Then one of the direct methods discussed previously is used. The second method involves the measurement of the yield of a particular transition. It is directly related to the matrix element for the transition or the $B(E\lambda)$. The lifetime can be obtained from the $B(E2)$ where only one multipole is involved. In this case

$$B(E2) \propto 1/\tau. \quad \text{...(121)}$$

For a mixed multipolarity transition, *e.g.*, an $E_2 + M_1$ transition. The $B(E2)$ measured is related to the lifetime τ and the mixing ratio δ as

$$B(E2) \propto \frac{1}{\tau}\frac{\delta^2}{1+\delta^2}. \quad \text{...(122)}$$

(ii) Inelastic electron scattering—The cross section for the scattering of high energy electrons from nuclei can be used for measuring the matrix elements for particular transitions. As discussed in chapter 1, this cross section can be written to first order in the plane wave Born approximation as

$$d\sigma/d\Omega = \sigma_{mott}\,\eta\,F^2(q,\theta), \quad \text{...(123)}$$

where σ_{mott} is the Mott cross section for the scattering of high energy electrons from a heavy point nucleus, η the recoil correction for finite nuclear mass and $F^2(q, \theta)$ is the nuclear form factor containing all the information regarding nuclear structure, θ is the scattering angle and q is the momentum transfer. The dependence of the form factor on the momentum transfer q allows the multipolarity of a transition to be determined. The reduced transition probability may be determined from the form factor, as

$$B(EL\uparrow) = \frac{Z^2}{4\pi}\frac{[(2L+1)!!]^2}{(\Delta E)^{2L}}F_E^2(q=\Delta E) \quad \text{...(124)}$$

$$B(ML\uparrow) = \frac{Z^2}{4\pi}\frac{[(2L+1)!!]^2}{(\Delta E)^{2L}}F_M^2(q=\Delta E), \quad \text{...(125)}$$

where the form factors are evaluated at q = excitation energy ΔE of the state. From these values the life time τ may be calculated using Eqs (121) and (122).

(iii) Nuclear resonance Fluorescence—The mean lifetime of an excited state may be determined with the help of nuclear resonance fluorescence cross section which depends on the level width of the excited state. This method will be discussed in the next section.

In the *Coulomb excitation*, the two main contributions to the error come from the statistical error in the yield measurement and the uncertainties in the stopping powers. In *inelastic electron scattering*, the uncertainty is due to its model-dependent analysis. Inelastic electron scattering method can provide a useful check on measurements made using other methods. In common with Coulomb excitation and inelastic electron scattering, lifetime measurements from *resonance fluorescence* are determined indirectly from a width measurement. One of the most important uses of the resonance fluorescence techniqe is that it can be used to determine lifetimes less than 10^{-15} sec where the number of alternative techniques available is very limited.

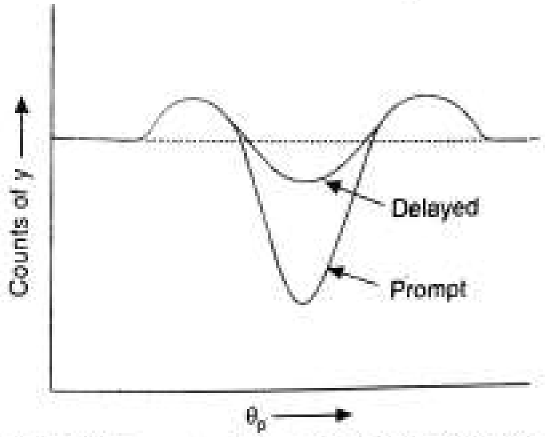

Fig. 7.22. Prompt and delayed curves for the counts of particles y.

The lifetimes in the 10^{-18} – 10^{-15} sec region can be measured using the *blocking technique*. In this a beam of particle x is incident on the target nuclei X which are on the lattice sites of a suitably aligned single crystal. An excited compound nucleus X^* is formed, which after a mean lifetime τ decays into y and Y. The light particles y are detected either in the direction of a lattice plane (planer blocking) or in the direction of a string of lattice atoms (axial blocking). If τ is such that y is scattered by the neighbouring coplaner or co-axial atoms preventing the particles from reaching the detector and producing a sharp dip in the number of counts detected. If τ is such that y is emitted between planes, then the particles can reach the detector and the characteristic blocking curve is filled in (delayed curve in Fig. 7.22). The amount by which the blocking dip is filled in will depend on τ, lattice spacing d, and orientation of lattice plane. A complex theory is needed to convert the measured filling in of the blocking dip into a lifetime.

7.10 NUCLEAR RESONANCE FLUORESCENCE

Atomic resonance fluorescence was predicted by Rayleigh and discovered by Wood in 1904 and formally explained through the quantum theory of radiation. It is a well known phenomenon in the optical wavelength region and associated with the high probability for an atom to be excited by a photon if its energy exactly coincides with one of the energy levels of the atom. If the excited atom goes back to its ground state by the re-emission of the photon, the process is called *resonance scattering*. It has been realized for a long time that the analogous effect should be expected also in the nuclei. It was first suggested by W. Kuhn in 1929, but all attempts to observe nuclear resonance fuorescence were unsuccessful for more than 20 years. The reason for this is that the nuclear absorption lines are very narrow and thus absorb very little radiation from a continuum.

The γ-rays emitted in a ground state transition are reabsorbed by another identical nuclei which are in the ground state. These absorbing nuclei thus raised to the higher energy state, which will re-radiate γ-rays of the same frequency. Such occurrences are very rare and known as *nuclear resonance absorption of the gamma rays*. The absorption and emission lines overlap for perfect resonance. In practice there is a spectral broadening of the line on account of following two reasons.

(a) Nuclear recoil effect—When the gamma ray photon is emitted with a momentum p, the nucleus of mass M recoils with equal and opposite momentum. From the considerations of energy and momentum conservation, the recoiling energy of the nucleus is given by

$$E_{re} = \frac{p^2}{2M} = \frac{E_\gamma^2}{2Mc^2} = \frac{E_0^2}{2Mc^2} \qquad \text{...(126)}$$

(E_{re} is small, therefore $E_\gamma = E_0$ = Resonance energy).

Thus the gamma ray photon will be emitted with an energy $E_0 - E_{re}$ so that the centre of the spectral line will be shifted from its expected position at E_0 to the new position at $E_0 - E_{re}$. On the other hand, when a photon of momentum E_γ/c is absorbed by an atom (or nucleus), its energy will be increased by the amount of the recoil energy, and the energy that must be absorbed from the radiation is $E_0 + E_{re}$. The effect of the recoil is thus to introduce a difference of $\Delta E = 2E_{re} = E_0^2/Mc^2$ between the energies of the emitted and absorbed photons in a resonance process.

(b) The excited state in an energy transition has a finite average life time. Heisenberg uncertainty principle implies that this finite life time τ of the excited state would cause a distribution in the energies of the emitted quanta. This energy spread, known as natural width of a γ-ray emission is given by $\Gamma = \Delta E = \hbar/\tau = 6.582 \times 10^{-16}/\tau\ eV$. If this width is large compared to $2E_{re}$ the emission line will overlap with the absorption line and so as to produce *resonance radiation*. This process is known as *resonance fluorescence*.

An excited electronic state generally has a life time of about 10^{-8} sec. Therefore, the theoretical line width Γ is given by

$$\Gamma = \hbar/\tau \approx 6.582 \times 10^{-16}/10^{-8} \approx 6.582 \times 10^{-8}\ eV.$$

For $E_0 = 5\ eV$ and $M = 100\ u$, the energy difference between the centres of the emission and absorption lines $\Delta E = E_0^2/Mc^2 = 2.68 \times 10^{-10}$ eV, which is less than a hundredth part of the line width. This means that the photon energy strongly overlaps the energy of the excited state of the resonant absorbing atom and resonance fluorescence is observed [Fig. 7.23 *(a)*].

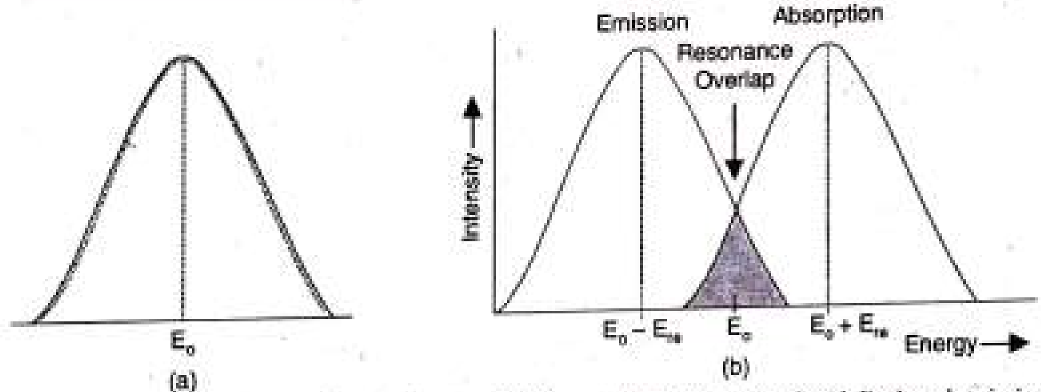

Fig. 7.23. (a) Perfect resonance as in atomic cases. (b) The overlap of broadened and displaced emission and absorption lines corresponds to nuclear resonance.

On the other hand, situation with gamma rays is quite different. Even for the fastest gamma decays, $t = 10^{-13}$ sec and $\Gamma \approx \hbar/t = 6.582 \times 10^{-3}\ eV$. For a gamma ray of energy $E = 0.5\ MeV$ emitted by a nucleus of mass number $A = 100$, $\Delta E = E_0^2/Mc^2 = 2.68$ eV, which is greater than Γ. This means that there is no overlap between the energies of the emitted and the absorbed radiations and resonant absorption cannot occur.

To increase the amount of resonance absorption, it is necessary to increase the amount of overlap between the emission and absorption curves or to reduce the recoil energy loss. Recoil energy loss can be restored and the resonance can be obtained with gamma rays by the following means :

(a) When a source of radiation of frequency ν is travelling with a velocity v in the direction of emission of the radiations, the radiations are compressed between the source and the detector. The wavelength is thus decreased and the frequency is increased to a value ν' given by

$$\nu' = \nu c/(c - v) = \nu/(1 - v/c) = \nu(1 + v/c).$$

$$\therefore \qquad \text{Doppler shift } \Delta\nu = \nu' - \nu = \nu\, v/c. \qquad \text{...(127)}$$

Thus the corresponding energy change = $\Delta E_D = h\Delta\nu = h\nu\, v/c = E_0\, v/c$. ...(128)

Consequently if the source is moving away from the detector, the radiations are spread out and frequency decreases. The magnitude of the doppler shift is equal to $E_0 v/c$ in either direction. If the Doppler shift is set equal to the recoil energy loss, the corresponding velocity of the source is E_0/Mc.

(b) Both source and absorber atoms take part in thermal motion and the lines are thus broadened by the Doppler effect. The Doppler shift due to thermal motion is given by the relation

$$\Delta = \frac{E_0}{c}\left(\frac{2kT}{M}\right)^{1/2}. \qquad ...(129)$$

Thus the recoil energy loss can be restored by heating the radio-active source so that the Doppler broadening is largely increased.

(c) It can also be done by selecting a source nuclei that emit gamma-ray photons while recoiling from a previous decay.

Nuclear resonance radiation has been observed by Moon in 1951, by using a radioactive ^{198}Au source electroplated on to the tips of a 6″ dia steel rotor which can rotate up to the peripheral speed of 800 m/sec. Tangentially emitted γ-rays thereby experienced a Doppler shift which to a large extent compensated the recoil displacement and permitted resonance absorption. For the resonant scattering of 0.411. MeV γ-quanta, the intensity attained the maximum at peripheral velocities around 700 m/sec. The ratio of scattering observed with mercury to scattering observed with lead as a function of rotor tip speed is shown in Fig. 7.24 *(b)*. It shows the increase of yield expected as the emission peak of Fig. 7.23 *(b)* moves towards the absorption line with increasing rotor speed. The thermal motion of the atoms in the source and absorber are responsible for the absence of a sharp peak in Fig. 7.24 *(b)*.

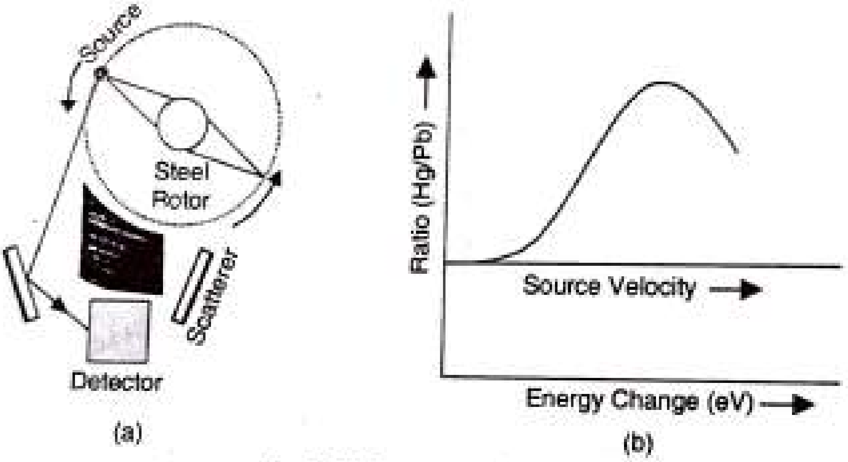

Fig. 7.24. Rotor experiment.

The mean lifetime of an excited state may be determined with the aid of the nuclear resonance fluorescence cross section which depends on the level width Γ. There are two basic types of experiments. The first is scattering experiment in which the number of γ-rays scattered from the nuclear level of interest is measured. The count rate for the transition is given by

$$R_{sc} = \pi^2\lambda^2 f n_s N(E_{re})\frac{2I_i+1}{2I_f+1}\frac{\Gamma_0^2}{\Gamma}. \qquad ...(130)$$

where factors f contains the solid angles of detector and source, the efficiency of the detector, correction for angular distribution, etc., n_s is the number of resonant nuclei per unit area, $N(E_{re})$ contains the details of the source γ-radiation, and I_i, I_f are the initial (excited) and final (ground) state spins.

The second type of experiment is the self absorption experiment which is very similar to the scattering experiment except that an absorber of the nuclei of interest is placed between the γ-ray source and the scatterer. In this case

$$R_{s.a.} = \left(\frac{\pi^3}{2}\right)^{1/2} n_A \frac{2I_i+1}{2I_f+1}\frac{\Gamma_0}{\Delta}, \qquad ...(131)$$

where n_A is the number of absorbing nuclei per unit area and $\Delta >> \Gamma$ (and (Γ_0) is the width of the γ-ray distribution in the source.

Hence the scattering experiment gives Γ_0^2/Γ and the self absorption experiment gives a value for Γ_0. Combination of the results of both experiments yields values for both Γ_0 and the ground state branching Γ_0/Γ. The nuclear resonance fluorescence technique is common for lifetimes in the atto second region to be measured. This method is limited to states which have ground state decays and especially for higher excited states where I_i is often unknown, will only yield a value of $\tau/(2I_i + 1)$. As large amounts of target material are required, this method is limited to stable nuclei of high isotopic abundance.

7.11. MÖSSBAUER EFFECT

In the preceding article, we have seen that the energy of the γ-photon emitted in a transition between two nuclear states is usually smaller than the difference in energies of the two states. This loss is due to the kinetic energy of the recoiling nucleus. It prevents the inverse process of resonance absorption in another identical nucleus. R.L. Mössbauer discovered in 1958 that some of the low energy gamma radiations (~ 10^4 eV) emitted by long lived 'isomeric' states of nuclei, with life times of the order of 10^{-8} to 10^{-7} sec., were practically recoil free. The reason for this is that the mass M is now comparable to the mass of a microcrystal of the solid. The mass to which the recoil momentum is transferred can be considered infinite in comparison with that of an atom, so that velocity of recoil is zero. This recoil free emission and resonant absorption of gamma radiation is known as the *Mössbauer effect*, in honour of its discoverer. It is thus also called *nuclear gamma resonance*.

In his original experiment, Mössbauer measured the emission of 129 keV gamma radiation from radioactive β^-–source Osmium–191. They were passed through a metallic iridium absorber (39% of ^{191}Ir) and then on to a detector. Gamma source ^{191}Ir was formed in an isomeric state in the beta decay of ^{191}Os. The natural width and life time of the 129 keV level of ^{191}Ir are 5×10^{-6} eV and 1.3×10^{-10} seconds respectively.

The recoil energy of the free nucleus for 129 keV gamma radiation would be 0.047 eV and the Doppler broadening at room temperature about 0.1 eV. Mössbauer measured the effective absorption cross section per nucleus of ^{191}Ir for radiation of 129 keV as a function of temperature by cooling the source and absorber with liquid air from about 400°K to 88°K. He found that the absorption cross-section increased sharply as the temperature was decreased.

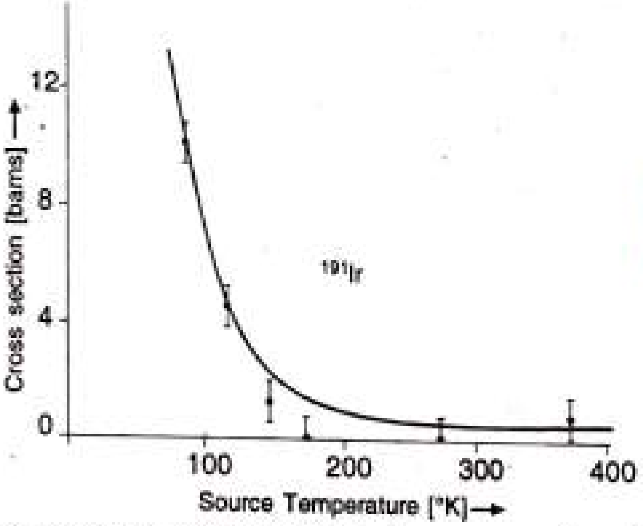

Fig. 7.25. The variation of absorption cross section with temperature in ^{191}Ir for 129 keV γ-rays.

In another experiment Mössbauer kept both the source and the absorber at 88°K and imposed a very low velocity (~ cm/sec.) on the source. It was done by mounting the source on a turn table and rotating it very slowly. The systematic diagram of the experimental arrangement is shown in Fig. 7.26. Here A is the absorber in a cryostat and S is the source at the rim of rotating cryostat and M is the region in which the source is seen from the scintillation detector. If one moves the source with respect to the absorber the frequency of the absorption line changes by an amount.

$$\Delta\omega/\omega = \Delta v/c \text{ or } \Delta E = (\Delta v/c)\, E_0, \quad \ldots(132)$$

where Δv is the relative velocity and ΔE is the Dopper-shift.

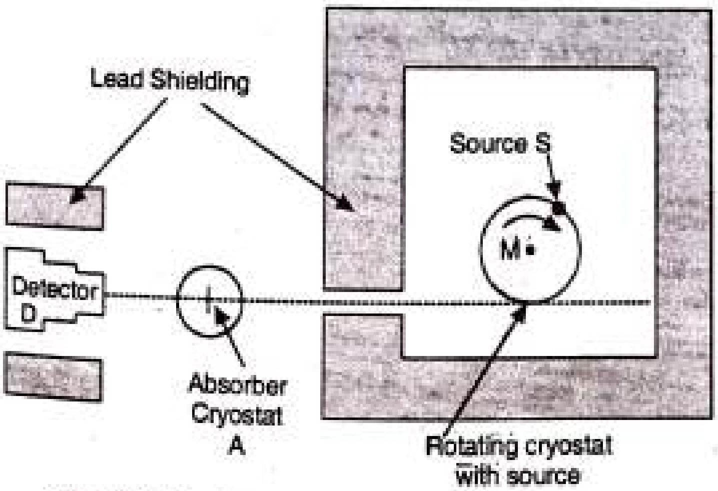

Fig. 7.26. Experimental arrangement by Mössbauer.

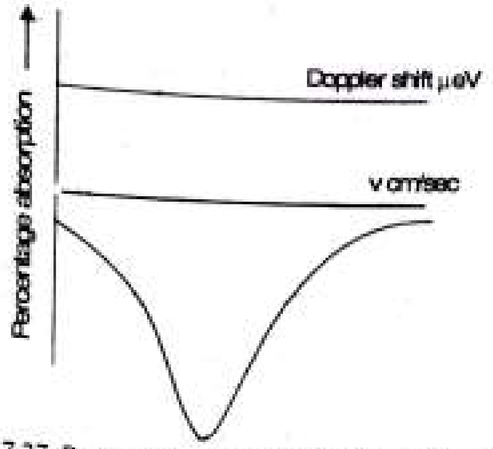

Fig. 7.27. Resonance absorption in ^{191}Ir as a function of relative velocity between source and absorbers.

The fluorescence abosrption in ^{191}Ir as a function of relative velocity v between the source and the absorber is shown in Fig. 7.27. The percentage absorption is a maximum at zero relative velocity. The curve so obtained has a width at half maximum of 2 cm/sec corresponding to an energy width of 9.2 ± 1.2 μeV. Interpreting this value as twice the natural width $\Gamma = 4.6 \pm 0.6\ \mu eV$, Mössbauer obtained the value $\tau = (1.4^{+0.2}_{-0.1}) \times 10^{-10}$ sec. for the lifetime of the 129 keV state in ^{191}Ir.

Physicists not only repeated these experiments but investigated other nuclei, suitable for Mössbauer effect. The recoilless emission of an extremely narrow 14.4 keV γ-line from the first level of ^{57}Fe was observed at several centres simultaneously. ^{57}Fe is produced by the process of orbital electron capture in ^{57}Co, which has a half-life of 270 days and is generally prepared by deuteron bombardment of an iron target in the form of a strip. Decay schemes of osmium and cobalt are given in Fig. 7.28. The positive and negative signs after the quantum numbers refer to the parity of the states.

The 14.4 keV level in ^{57}Fe has a mean life of 1.4×10^{-7} sec and the corresponding line width is 4.6×10^{-9} eV. This life time is long enough for the excited ^{57}Fe ions to occupy suitable sites in the iron crystal lattice before the decay. The 14.4 keV gamma rays can be passed through an iron absorber which can be enriched in ^{57}Fe so as to increase the probability of recoilless absorption. The gamma rays can be detected by a proportional counter or scintillation counter.

After ^{57}Fe, the substance employed most frequently is probably tin-119 and a fair amount of work has also been done with same rare earth elements. The theory of recoilless emission shows that the effect is greater when : *(a)* the gamma ray energy E is small (The best example is the 14.4 keV transition of ^{57}Fe); *(b)* the temperature of the crystal source is small; *(c)* the Debye temperature of the crystal lattice is high.

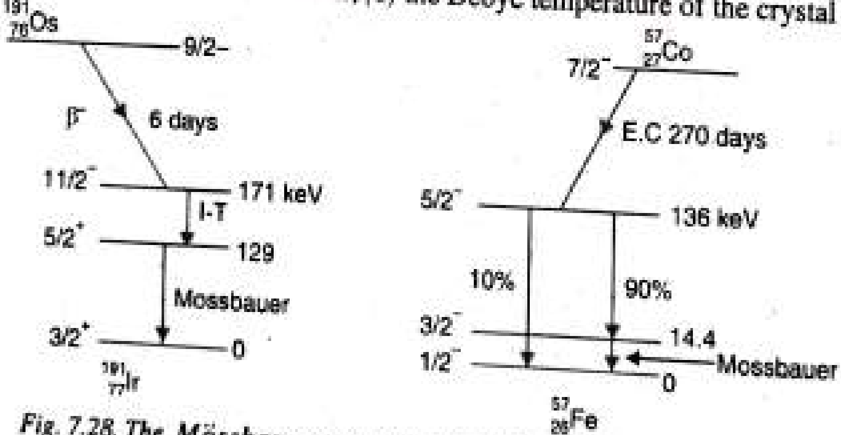

Fig. 7.28. The Mössbauer transitions of 129 keV ^{191}Ir and 14.4 keV ^{57}Fe.

The theoretical analysis, following Lamb's treatment, used Debye continuum theory to describe lattice vibration behaviour in terms of a model based on a system of independent linear oscillators with a continuous frequency distribution upto a maximum ω_D. It is related wiith Debye temp Θ, as

$$\hbar\omega_D = k\,\Theta, \qquad \ldots(133)$$

where k is the Boltzmann constant. The fraction of recoilless γ-transition, also known as *Lamb Mössbauer factor*, is given as

$$f = \exp\left[-\frac{3E_R}{2k\,\Theta}\left\{1+\frac{2}{3}\left(\frac{\pi T}{\Theta}\right)^2\right\}\right]. \qquad \ldots(134)$$

The first term is independent of temperature. It shows that even at $T = 0$, f is large only if the recoil energy of the free nucleus is small compared to $k\,\Theta$. The probability of recoilless decay decreases with increasing temperature.

In order to utilize the Mössbauer effect, one has to consider transitions in which—

(1) f is adequately large;

(2) E_0 must be fairly large for a good precision;

(3) there must be small livelihood of internal conversion;

(4) fine structure splitting should not occur, if possible.

When these requirements are satisfied, precautions should be made against undesired disturbances arising from the following :

(a) the changes in nuclear mass on emission and absorption of γ-rays, which cause the γ-ray to change by an amount $\Delta E_\gamma = (-E_\gamma/mc^2) < E_{kin} >$.

(b) the differences in the average isotopic mass number;

(c) the differences in chemical constitution of presence or lattice defects;

(d) the differences in the Debye temperature Θ between source and absorber.

(e) the differences in a absolute temperature T between source and absorber.

(f) the relative velocity between emitter and absorber.

Applications of Mössbauer Effect : *(a) Isomer Shift or Chemical Shift*—Different chemical states of an atom are associated with differences in the electron distribution around the nucleus and contribute to the energy of transition.

$$E_\gamma = \Delta E_{nuc} + \Delta E_{elec}, \qquad \ldots(135)$$

where ΔE_{nuc} is the change in nuclear binding energy and ΔE_{elec} is the change in B.E. of the atomic electrons. If the emitting nucleus (excited state) and the absorbing nucleus (ground state) are in different chemical compounds, the distributions in atomic electrons will be different, which will cause differences in ΔE_{elec} and thus in E_γ. The change in E_γ is called the *isomer* shift or *chemical shift* (as it is related to the chemical environment of the atom). The Mössbauer technique is used to show the energy shift due to the minute effects of chemical binding on the nuclear level structure.

(b) Magnetic Hyperfine Splitting—If either the emitting or the absorbing nucleus has a spin $I \geq \frac{1}{2}$, it will also have a magnetic moment. In the presence of magnetic field, the energy of the nucleus will depend on its orientation with respect to the magnetic field. The projection of spin I may take $2I + 1$ values. The absorption spectrum obtained by the Mössbauer technique will thus show a hyperfine splitting into $2I + 1$ parts. In most measurements of the nuclear hyperfine interactions the line splittings observed resulted from the interaction of the nuclear moments with internal fields. These fields are generally too weak to produce splittings larger than the natural widths of the γ-lines ($2\Gamma_0$).

Since iron is ferromagnetic, the magnetic field intensity at the nucleus of iron-57 produced by the external electrons is large enough to produce a splitting of the energy levels, depending upon the value of I. This splitting is the nuclear equivalent of a Zeeman effect. The energy separation of these levels will be given by $\Delta E = Bg\mu_N$, where μ_N is the nuclear magneton. The number of counts of components establishes the spin I and the separation ΔE at a known field B evaluates the Lande factor g. Thus the magnetic moment μ can be calculated from g and I.

In the case of ^{57}Fe, the value of I for the ground state is $1/2^-$ and for the first excited state is $3/2^-$. The selection rule $\Delta m_I = 0, \pm 1$ predicts the splitting of the γ-ray line into six components, as shown in Fig. 7.29. *(a)*. If the source is moving relative to the absorber, the change in energy of the radiation due to Doppler effect will occur $[\Delta E_D = (v/c)E]$. If both the source and absorber are ferromagnetic, there will be some velocities for which the energy change will be equal to the separations of some of the energy levels, so that the several components may overlap. Thus a non-ferromagnetic material, such as stainless steel, should be used as either the source or the absorber. The nuclear hyperfine structure of ^{57}Fe in iron metal, obtained with a stainless steel source and a natural iron absorber 0.001 inch thick, as observed by G.K. Wertheim, is shown in Fig. 7.29 *(b)*. The six components are easily resolved.

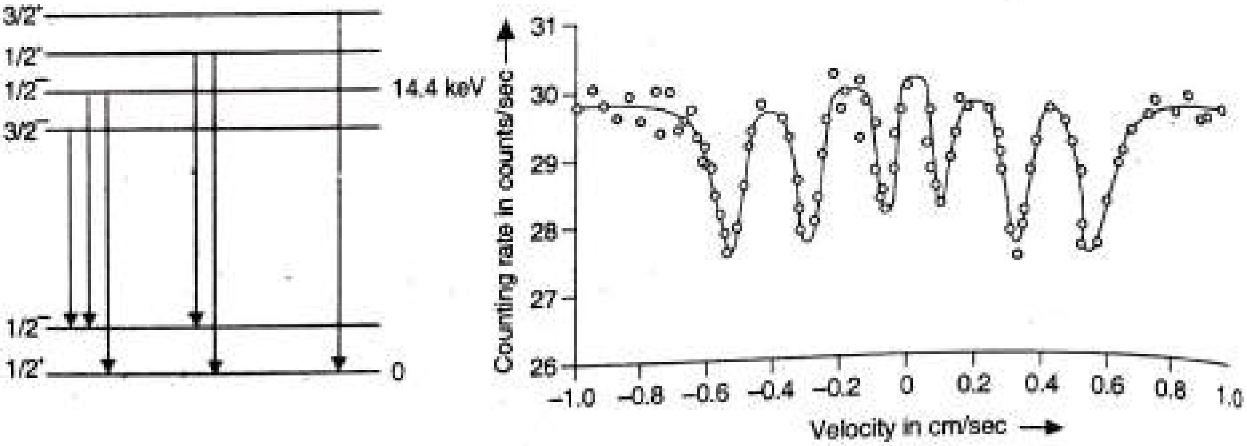

(a) (b)

Fig. 7.29. (a) Nuclear hyperfine structure of 14.4 keV transition in ^{57}Fe. (b) Hyperfine spectrum observed by G.K. Wertheim.

In the earlier experiment by Hanna *et al.* (1960), an external magnetic field was applied to both the source and the absorber and observed the nuclear hyperfine lines for ^{57}Fe. The effective value of the internal magnetic field at the ^{57}Fe nucleus was established to be $(3.33 \pm 0.10) \times 10^5$ oersteds.

(c) Quadrupole hyperfine splitting—If either the emitting or the absorbing nucleus has a spin $I \geq 1$ and is in an inhomogeneous electric field, energy may split, in several lines. It is because the interaction between the nuclear quadrupole moment and the inhomogeneous electric field causes the energy of the nucleus to depend on its orientation.

(d) Lifetime measurement—Mössbauer technique is best for the measurement of fairly short lifetimes, since when the lifetime exceeds about 10^{-10} sec, extra nuclear fields can cause line broadening. Basically the range 10^{-13} sec $\leq \tau \leq 10^{-10}$ sec seems best suited to such determinations.

(e) Gravitational shift—On the basis of the principle of equivalence, Schiff has given a simple derivation of the gravitational Doppler shift. We shall give an even more elementary derivation which is directly applicable to nuclear fluorescence experiments.

We know that the intensity I of the earth gravitational field at a distance R from an earth of mass M is the acceleration due to gravity. Hence

$$I = GM/R^2 = g \qquad \text{...(136)}$$

Similarly the gravitational potential φ at the point R due to earth is

$$\varphi = -GM/R = -gR. \qquad \text{...(137)}$$

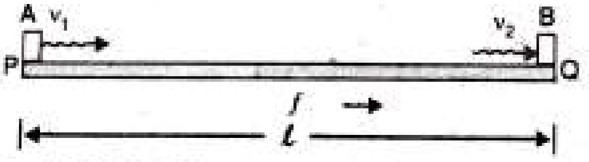

Fig. 7.30. Table PQ has constant acceleration f in inertial frame of reference.

Let us place a source nucleus A and an observer nucleus B on a horizontal table PQ, distance l apart, as shown in Fig. 7.30. Suppose that at some particular instant when the velocity of table is v_1, the nucleus A at one end emits a gamma ray photon of frequency ν_1 in the direction of its motion. The frequency of this radiation as measured by a stationary observer will be

$$\nu_{ob} = \nu_1(1 + v_1/c). \qquad \text{...(138)}$$

This photon moves towards B with a constant velocity c. It will reach an identical absorber nucleus B at a time $t(= l/c)$. The velocity of table at this time is $v_2 = v_1 + ft$. The apparent frequency of radiation, which can be absorbed by observer nucleus B, will be ν_2. The frequency of this radiation as measured by a stationary observer will be

$$\nu_{0b} = \nu_2(1 + v_2/c). \qquad \text{...(139)}$$

Clearly if the gamma ray absorbed by nucleus B is to be that one which has been emitted by nucleus A, we must have

$$\nu_1(1 + v_1/c) = \nu_2(1 + v_2/c). \qquad \ldots(140)$$

This relation indicates that absorption would take place for identical recoilless nuclei, only if $v_1 = v_2$. If we assume that $\nu_1 - \nu_2 = \Delta\nu$ and $\nu_1 = \nu_2 = \nu$, then we have

$$\Delta\nu = \frac{\nu}{c}(v_2 - v_1) = \frac{\nu}{c}\cdot f \cdot \frac{l}{c} \text{ or } \frac{\Delta\nu}{\nu} = \frac{fl}{c^2}. \qquad \ldots(141)$$

The principle of equivalence of an accelerated system tells us that the system having an acceleration f produces an effect equivalent to that of a gravitational acceleration $-f(= g)$. If $\Delta\phi$ is the potential difference between two points in a gravitational field, the difference in frequency of identical clocks at these points will be

$$\Delta\nu = \nu\,\Delta\phi/c^2. \qquad \ldots(142)$$

Thus for resonance absorption, the frequency of emission ν_1 must be larger than the frequency of absorption ν_2 by an amount $\nu\,\Delta\phi/c^2$. Hence the frequency of radiation coming from a source located below the absorber will be shifted towards the red.

Until 1960, the gravitational red shift could only be observed with light coming from stars, as $\Delta\phi$ is very large in that case. The discovery of Mössbauer technique makes it possible, for the first time to carry out a gravitational Doppler effect experiment. A series of experiments was performed independently by R.V. Pound and G.A. Rebka Jr. at Harvard and by T.E. Cranshaw and others at Harwell in 1960, using ^{57}Fe as the emiter and absorber. The Harwell group electro-deposited a ^{57}Co source on an iron disc, mounted about 40′ above a 5″ diameter foil containing 4 mg/cm^2 of iron enriched in ^{57}Fe. A proportional counter filled with krypton to about 20 cm of mercury pressure was placed underneath the absorbing iron foil to detect the transmitted 14.4 keV gamma rays. A simplified schematic diagram of their apparatus is sketched in Fig. 7.31.

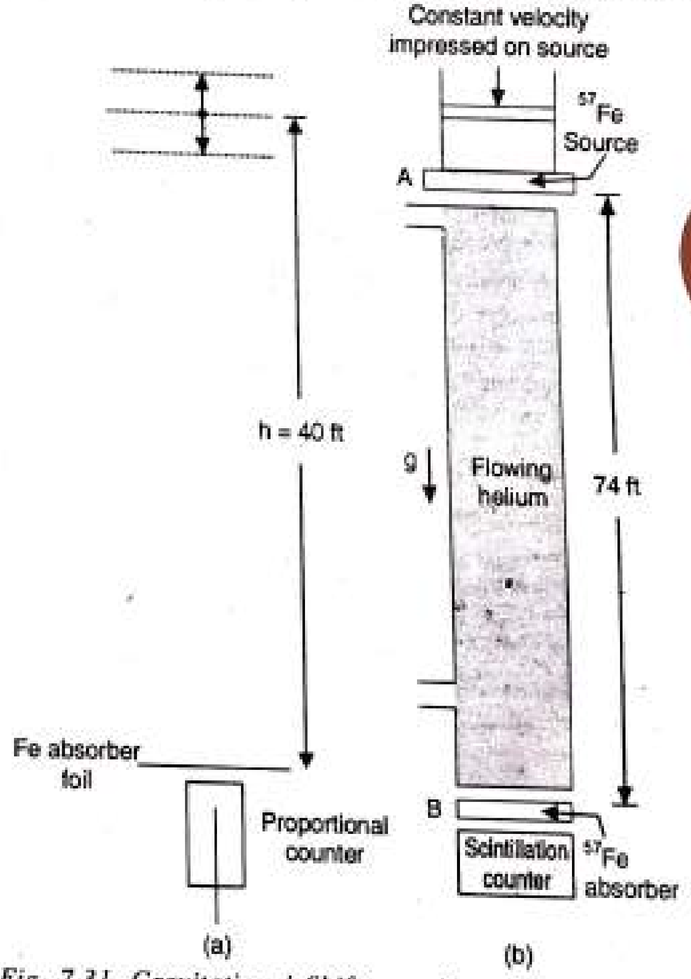

Fig. 7.31. Gravitational Shift experiment by (a) Harwell group and (b) Harvard group.

In the experiment of Harvard group, the difference in height between two positions A and B was 74 ft. The temperatures of the iron foils at A and B were measured accurately and corrections were made for the Doppler shift produced by the thermal motion of crystal lattice. A constant velocity was impressed on the emitter foil at A to provide the necessary Doppler shift to compensate for the gravitational red shift $\Delta\nu$ and to allow resonance absorption of 14.1 keV γ-ray from the source (foil at A). To reduce the absorption of these γ-rays in air cylinder containing flowing helium was placed between the source and absorber foils. To improve the accuracy, the positions of the absorber and source were inter changed, thus providing the effected height $2H = 148$ *ft*. The expected fractional frequency shift $\Delta\nu/\nu = 2gH/c^2 = 4.92 \times 10^{-15}$ was found quite in close agreement with the observed value of 5.13×10^{-15}.

In the experiment of Harwell group, the source is mounted on a transducer device and vibrated to and fro at 50 *c/s*. When the Doppler shift produced by moving the source exactly compensates the gravitational shift, maximum resonance will occur. The transmitted gamma rays are recorded by two scalars for alternate halves of the vibrating cycle. The mean counting rate is slightly different due to the asymmetry introduced by the gravitational shift. It was found that the observed red shift was (0.96 ± 0.45) times the expected shift. This source of error has to do with the Doppler shift due to the motion of the nuclei in the lattice. The emitting and absorbing nuclei are vibrating with fairly high speeds, given by the temperature of the solid. Therefore it might be expected that vibration would impart a Doppler shift.

A Brief Summary

Gamma radiation is the spontaneous transition of the nucleus from an excited state to the ground state or to a less excited state. Depending on its origin, gamma radiation is divided into electric radiation and magnetic radiation and is characterized by a definite multipolarity or the value of the angular momentum carried out by the gamma-quanta. For the nucleus with angular momenta and parities as I_i, I_f and π_i, π_f of the initial and find states, the possible values of l for allowed gamma transitions satisfy the following selection rules : $|I_i - I_f| \le l \le |I_i + I_f|$ and $\pi_i = (-1)^{l_\gamma}\pi_f$ and $\pi_i = (-1)^{l_\gamma+1}\pi_f$. The excited nuclear state has long lifetime, if $l \ge 4$ and ΔE is small. This nucleus is in metastable state and is called an isomer of the given nucleus.

Besides the gamma radiation, the nuclear excitation energy can be spent on the emission of internal conversion electrons, usually from the *K*-shell. This process is accompanied by the emission of characteristic *X*-rays and Auger electrons. Internal pair creation is also important for the excited nucleus with the transition energy between the nuclear states greater then 1.022 MeV.

The observations of electromagnetic transitions provide useful information concerning nuclear properties, such as energy levels and their spins and parities, and transition and their multipolarities and mixing ratios.

The gamma rays are measured in various ways, broadly divided into four categories : *(i)* Wavelength measurement by crystal diffraction, *(ii)* Absorption measurements, *(iii)* Secondary electron methods and *(iv)* Energy measurement by photodisintegration.

When a charged particle approaches a target with an energy considerably less than a height of the mutual potential barrier, the target nucleus gets excited through the electromagnetic interaction. Such a process is called Coulomb excitation. This process may be treated as the reverse of the internal conversion, but with a great difference. Coulomb excitation is the very important process as the cross section for this process are directly related to electromagnetic properties of the nuclei.

Angular distribution is the anisotropic distribution of emitted γ-rays with respect to the direction of the incident beam. if the nuclei decay through successive emission of two γ-rays, γ_1 and γ_2. The γ_2 shows a definite angular correlation with respect to the fixed direction of γ_1. The term angular correlation comprises of directional correlation and polarization correlation.

The experimental methods for measuring life times of nuclear states are divided into direct methods and indirect methods. The widely applicable direct methods are Electronic Timing, Recoil distance method (RDM) and Dopper shift attenuation method (DSAM). The indirect methods are : Coulomb excitation [from $B(E2)$ values], Inelastic electron scattering (from scattering cross sections), Nuclear resonance fluorescence (from measurement of level width of the excited state).

Resonance absorption of γ-radiation is a process in which the nucleus is excited under the action of γ-quanta emitted by these nuclei during the inverse transitions from the given excited state to the ground state. Mössbauer discovered that some of the low energy γ-radiations emitted by long lived isomeric states of nuclei ($T = 10^{-8}$ to 10^{-7} sec) are recoil free. This recoil free emission and resonant absorption of γ-radiation is known as Mössbauer effect, for this discovery Mössbauer was awarded, the Nobel Prize in Physics in 1961.

The materials used for investigation must have large value of the coefficient f(*i.e.*, recoil R small, low temp and high Debye Temperature). The various applications of the Mössbauer effect are : hyperfine splitting of nuclear levels, estimation of the nuclear radius in the excited state, lifetime measurement, quadrupole hyperfine splitting and gravitational shift.

EXERCISES

Example 1. *In a bent crystal spectrometer, the quartz crystal has an interplaner spacing of* 1.18×10^{-8} *cm. The radius of the focal circle is 2 meters. The source emits gamma rays of energies 1.33 and 1.17 MeV. Assuming that the source is in a position where it gives first order Bragg reflection for the 1.33 MeV gamma-ray, calculate the distance it has to be moved to obtain first order reflection for the 1.17 MeV gamma ray.*

For the first order Bragg reflection, we have $2d \sin\theta = \lambda$.

If f is the focal length and $BS = x$ (Fig. 7.1), then we have

$$2d(x/f) = hc/E$$

If x_1 and x_2 are the distances for energies E_1 and E_2, then

$$(2d/f)(x_1 - x_2) = hc(1/E_1 - 1/E_2),$$

or
$$x_1 - x_2 = \frac{hcf}{2d}\left(\frac{1}{E_1}-\frac{1}{E_2}\right)$$
$$= \frac{6.6261\times10^{-34}\times2.998\times10^{8}\times2}{2\times1.18\times10^{-10}}\times\frac{0.16}{1.33\times1.17\times1.6022\times10^{-13}}$$
$$= 1.08 \times 10^{-3} \text{ meter.}$$

Example 2. *In an experiment on the γ-rays from ^{131}Ba, the γ-rays are allowed to fall on a lead radiator and the photo-electrons ejected are analyzed in a magnetic spectrograph. The electrons fall into four groups with maximum at 1250, 1450, 2050 and 2500 gauss cm, respectively. The binding energy of the K-shell electrons in lead is 0.089 MeV. What are the energies of the γ-rays?*

We know the relation, for relativistic mass,
$$\frac{m_0}{\sqrt{(1-v^2/c^2)}}v = BRe$$
or
$$\frac{v}{\sqrt{(1-v^2/c^2)}} = \frac{BRe}{m_0} = \frac{1250\times10^{-6}\times1.6022\times10^{-19}}{9.1094\times10^{-31}} = 2.198\times10^{8}\ m/sec.$$
From this we get
$$v = 1.772 \times 10^{8}\ m/sec.$$
$$\therefore \quad \text{Energy of photoelectron } E = m_0c^2\left[\frac{1}{\sqrt{(1-v^2/c^2)}}-1\right]$$
$$= 9.1094 \times 10^{-31} \times 2.998^2 \times 10^{16} \times 0.24 = 19.655 \times 10^{-15} \text{ joule}$$
$$= 0.123\ MeV.$$
Binding energy of the K-shell electrons in lead $E_K = 0.089\ MeV$.
$$\therefore \quad \text{Energy of the γ-rays} = E_{pe} + E_K = 0.212\ MeV$$
Similar calculations can be made for other values of BR.

Example 3. *Estimate the attenuation of a 50 keV beam of X-rays in passing through a layer of human tissue (no bones) one centimeter thick.*

As the human body is mostly water, one can roughly take its density as that of water $\rho = 1\ gm/cm^3$. Generally the absorption coefficient of 50 keV X-rays is about 0.221 cm^2/gm. Then the attenuation resulting from the passage through one cm of tissue (thickness = 1 cm × 1 gm cm^{-3} = 1 gm cm^{-2}) is
$$1 - e^{-0.22\times1} = 0.20 = 20\%.$$

Example 4. *The 60-hour isomeric state of ^{195}Hg decays 65% by electron capture, 35% by isomeric transition (a 123 keV transition followed by 16.2 keV and 37.1 keV transitions in cascade). The 123 keV transition has $\alpha_K = 45$ and $\alpha_K/(\alpha_K + \alpha_L + \alpha_M) = 0.08$. What is the partial half life for γ-emission for the ^{195}Hg isomer ?*

The total decay rate λ of an excited state is given by
$$\lambda = 1/\tau = 1/60\ hr^{-1}.$$
$$\text{Probability of the isomeric transition} = \frac{35}{100}\times\frac{1}{60}hr^{-1}.$$
If λ_γ is the rate of emission of photons and λ_e is the rate of emission of conversion electrons, then
$$\lambda_e + \lambda_\gamma = 0.35/60\ hr^{-1}.$$
We know that the ratio between the two decay constants
$$\alpha = \lambda_e/\lambda_\gamma = \alpha_K + \alpha_L + \alpha_M = \frac{\alpha_K+\alpha_L+\alpha_M}{\alpha_K}\cdot\alpha_K = \frac{45}{0.08} = 562.5$$
$$\therefore \quad 562.5\,\lambda_\gamma + \lambda_\gamma = 0.35/60 \quad \text{or} \quad \lambda_\gamma = 0.35/60 \times 563.5\ hr^{-1}$$
or Paratial life time for γ-emission
$$\tau_\gamma = \frac{1}{\lambda_\gamma} = \frac{60\times563.5}{0.35\times365\times24} = 11.03\ years.$$

Example 5. *In ^{11}B, a gamma transition leads from a level at 9.28 MeV (spin-parity $5/2^+$) to a level at 4.46 MeV (spin-parity $5/2^-$). What is the dominant multipolarity of the transition ? What is the expected gamma width (in eV) on the basis of the Weisskopf model. Given the measured value as 5.4 eV.*

The angular momentum of the gamma photon emitted between the two levels I_i and I_f is restricted as

$$|I_i - I_f| \le L \le I_i + I_f$$

All the values of L contained between these two extremes are not equally probable. The most probable value is $|I_i - I_f|$ or sometimes $|I_i - I_f| + 1$.

In the present problem $I_i = 5/2$ and $I_f = 5/2$. $I_i - I_f = 5/2 - 5/2 = 0$ is not permissible as no photon transition with $L = 0$ exists. Thus the most probable transition will be with $L = 1$.

In this case parity changes. Thus the $L = 1$ with parity change transition will be of $E1$-type.

From the Weisskopf estimates, the γ-decay width in eV for the $E1$ transition of energy E_γ in MeV is given by

$$\Gamma_\gamma(E1) = 0.0675\, A^{2/3} E_\gamma^3 .$$

In this present problem $A = 11$ and $E_\gamma = 9.28 - 4.46 = 4.82$ MeV.

$$\therefore \quad \Gamma_\gamma(E1) = 0.0675 \times 11^{2/3} \times 4.82^3 = 37.39\ eV.$$

This shows that the expected value is about 7 times greater than the measured value.

Exercise 6. *What are the expected types of gamma ray transitions between the following states of odd A–nuclei; $g_{9/2} \to p_{1/2}$, $f_{5/2} \to p_{3/2}$, $h_{11/2} \to d_{5/2}$, $h_{11/2} \to d_{3/2}$?*

We know that for a transition $I_i \to I_f$, the L of the emitted γ-rays is given by

$$|I_i - I_f| \le L \le (I_i + I_f).$$

Therefore for transition $g_{9/2} \to p_{1/2}$, $I_i = \frac{9^+}{2}$ and $I_f = \frac{1^-}{2}$, hence possible L-values are 4 and 5. Since the parity changes, the possible transitions are $M4$ and $E5$.

For transition $f_{5/2} \to p_{3/2}$, $I_i = \frac{5^-}{2}$ and $I_f = \frac{3^-}{2}$, hence possible L-values are 1, 2, 3, 4. Since parity does not change, the possible transitions are $M1$, $E2$, $M3$ and $E4$.

For the transition $h_{11/2} \to d_{5/2}$, $I_i = \frac{11^-}{2}$ and $I_f = \frac{5^+}{2}$, hence possible L values 3, 4, 5, 6, 7, 8. Since parity changes, the possible transitions are $E3$, $M4$, $E5$, $M6$, $E7$ and $M8$.

For the transition $h_{11/2} \to d_{3/2}$, $I_i = \frac{11^-}{2}$ and $I_f = \frac{3^+}{2}$, hence possible L-values are 4, 5, 6, 7. Since parity changes, the possible transitions are $M4$, $E5$, $M6$, $E7$.

Since the transition probability decreases rapidly with the increase of multiple order L. Hence the predominant decay modes are $M4$, $M1$, $E3$ and $M4$ in the above transitions.

Example 7. *The following γ-lines were measured with a crystal spectrometer in ^{181}Ta obtained from the β-decay of ^{181}Hf.*

3.90 ± 0.10 keV (M1) 133.02 ± 0.02 keV (E2) 136.02 ± 0.02 (M1)
136.86 ± 0.04 (M1) 345.85 ± 0.20 (E2) 482.0 ± 0.2 (M1)
615.5 ± 0.5 (M3)

Construct the level scheme of ^{181}Ta which has a $7/2^+$ ground state, making appropriate spin and parity assignments, given that the spin-parity of the ^{181}Hf ground state is $I^\pi = 1/2^-$.

β-decay from $I^\pi = 1/2^-$ to $7/2^+$ is third forbidden, therefore the ground state of ^{181}Ta can not be $7/2^+$. It may be $1/2^+$.

Since

$$\begin{aligned} 615.5 - 482.0 &= 133.5;\ 615.5 - 345.85 = 269.65; \\ 615.5 - 136.86 &= 478.6;\ 615.5 - 133.02 = 482.5; \\ 482.0 - 345.85 &= 136.15,\ 482.0 - 136.86 = 345.14,\ 482 - 133 = 349 \\ 345.85 - 136.86 &= 209;\ 345.85 - 133 = 213 \text{ and } 136.86 - 133 = 3.84. \end{aligned}$$

Here we see that 3.90 γ-ray may be from the 137 and 133 keV levels. Since we do not observe 136 keV γ-ray from expected 616,482 and 346 levels, therefore one may consider it from the 269 keV level (269 − 133 = 136). Thus 482 and 345.85 keV γ-rays may be transitions from 616 keV level to 133 and 269 keV levels respectively.

Since 615.5 γ-ray is $M3$ transition, therefore one may assign I^π for 616 keV level as $7/2^+$. Since133 γ-ray is $E2$ transition, therefore 133 keV level may be $5/2^+$. Since 137 and 3.9 γ-rays are $M1$ transitions, therefore 137 level may be $3/2^+$.

Since 136 and 346 γ-rays are $M1$ and $E2$ transitions respectively, therefore 269 keV level may be $3/2^+$. On the basis of these observations the expected energy level diagram for ^{181}Ta is shown in Fig. 7.32.

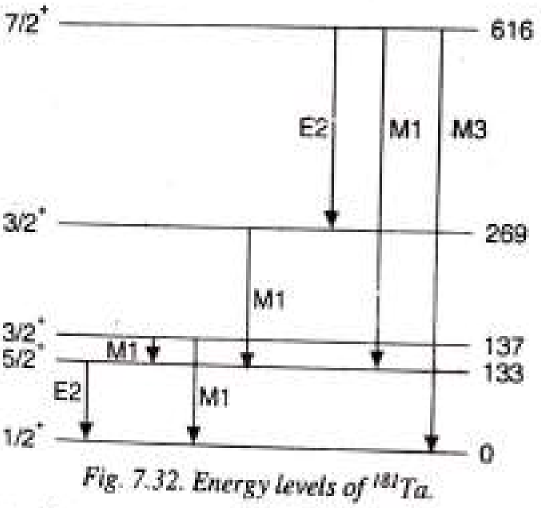

Fig. 7.32. Energy levels of ^{181}Ta.

Example 8. *The nuclide $^{113}_{49}In$ has a stable $I = 9/2^+$ ground state and an isomeric first excited state with half life $t_{1/2} = 104m$. This excited state decays to the ground state party by internal conversion. The K-conversion electrons have $BR = 2370$ gauss-cm, and the K-conversion coefficient is measured as $\alpha_K = 0.5$. The binding energy for K-electrons in indium is 28 keV. Find the excitation energy of this state, and its angular momentum and parity.*

For relativistic mass $m_0\sqrt{(1 - v^2/c^2)} = BRe/v$

or

$$\frac{v}{(1-v^2/c^2)^{1/2}} = \frac{BRe}{m_0} = \frac{2370\times10^{-6}\times1.6022\times10^{-19}}{9.1094\times10^{-31}} = 4.168\times10^{8}\ m/sec,$$

$$v = 2.435\times10^{8}\ m/sec.$$

Electron Energy $E = m_0c^2\left[\frac{1}{(1-v^2/c^2)^{1/2}}-1\right] = 0.364\ MeV.$

Hence the γ-ray energy $= E_{binding} + E_{electron} = 0.392\ MeV.$

$$K \text{ conversion coefficient } \alpha_K = (49)^3\left(\frac{1}{137}\right)^4\frac{L}{L+1}\left(\frac{2\times0.511}{0.392}\right)^{L+5/2} = 0.5$$

or

$$L = 5.3 \text{ or } 5 \text{ (approx)}.$$

The energy width at half height Γ (in eV) $= 0.46\times10^{-15}/(104\times60) = 7.37\times10^{-20}$. This suggests that the transition will be of type $M4$ or $E5$. The isomeric state thus may be a $2p_{1/2}$ level. As

$$|I_i - I_j| \le L \le |I_i + I_j|,$$

hence L may have values 4 or 5. In this way we get $I = \frac{1}{2}$, parity odd.

Example 9. *"Unlike atomic spectroscopy, electric dipole (El) transitions are not usually observed between the first few nuclear states." For light nuclei, give arguments that support this statement on the basis of the shell model. Indicate situations where exceptions might be expected. Calculate the radioactive lifetime of the lowest energy electric dipole transition expected for $^{17}_{9}F$ with your choice of suitable parameters.*

As given in the shell model, the single particle energy levels in the same shell have the same parity, especially the lowest lying levels like 1*s*, 1*p*, 1*d*, 2*s* shells, etc. For light nuclei, gamma transition occurs mainly between different single nucleon levels. The parity does not change in transitions between different energy levels of the same shell. On the other hand, electic dipole transition $E1$ follows selection rules $\Delta I = 0$ or 1, $\Delta\pi = -1$. The transitions that conserve parity can not be electric dipole in nature. However, if the ground and excited states are not in the same shell, parity may change in a transition. For example in the transition $1p_{3/2} \to 1s_{1/2}$, $\Delta I = 1$, $\Delta\pi = -1$. This is an electric dipole transition.

In the single particle model, the lowest energy electric dipole transition $E1$ of ^{17}F is $2s_{1/2} \to 1p_{1/2}$. The transition probability per unit time

$$\lambda = \frac{c}{4}\left(\frac{e^2}{4\pi\varepsilon_0 \hbar c}\right)\left(\frac{E_\gamma}{\hbar c}\right)^3 < r >^2,$$

where E_γ is the transition energy and $<r> = R = 1.4 \times 10^{-13} A^{1/3}$ *cm*. Thus

$$\lambda = \frac{3\times 10^{10} \times (1.4\times 10^{-13})^2}{4\times 137\times (197\times 10^{-13})^3} A^{2/3} E_\gamma^3 = 1.4\times 10^{14} A^{2/4} E_\gamma^3,$$

where the energy E_γ is in MeV. For ^{17}F, we may assume $E_\gamma = 5$ *MeV*, $A = 17$ and so

$$\lambda = 1.2 \times 10^{17}\ sec^{-1},$$

or

$$\tau = \lambda_r^{-1} = 9 \times 1^{-18}\ sec.$$

Example 10. *The total cross-section for the absorption of γ-rays by ^{208}Pb (I^π of ground state as 0^+) shows peaks at 1.2, 2.6 and 14.0 MeV. The peak at 2.6 MeV corresponds to a $I^\pi = 3^-$ level in ^{208}Pb which γ-decays to a 1^- level at 1.2 MeV. (a) What are the possible electric and or magnetic multipolarities of the γ-rays emitted in the transition between the 2.6 MeV and 1.2 MeV levels? Which one do you expect to dominate? (b) The width of the 2.6 MeV level is less than 1 eV, whereas the width of the level seen at 14 MeV is 1 MeV. Can you suggest a plausible reason for this large difference ?*

(a) The emitted photon in the transition $3^- \rightarrow 1^-$ may carry away an angular momentum $l = 4, 3, 2$. As there is no parity change $l = 4, 2$. Hence the possible multipolarities of the transition are *E*4, *M*3 or *E*2. Among these three the electric quadrupole transitien *E*2 is expected to dominate.

(b) The 2.6*MeV* level has a width of less than 1 *eV*. It is typical of an electromagnetic decay, where as 14 *MeV* peak is a giant dipole resonance. As the resonance energy is high, the processes are mostly strong interactions with emission of nucleons, where the single level widths are broader and many levels merge to form broad giant resonance. Thus the difference in decay mode leads to the large difference in level width.

Example 11. *^{60}Ni undergoes a cascade of γ-emissions, γ_1 and γ_2. If the I^π of the levels are 4^+, 2^+ and 0^+ (ground state). Assuming a negligible half life for the intermediate state, the measurement of the coincidence rate between the two γ-rays $I_{initial} \rightarrow I_{inter} \rightarrow I_{final}$ can give the angular correlation which may be used to determine the nuclear spins.*

If the angular correlation function is of the form $W(\theta) \sim 1+0.1248 \cos^2\theta + 0.0418 \cos^4\theta$, then discuss—

(a) Of what types are the transitions?, (b) Why are the odd powers of cos θ mission ? Why is $\cos^4\theta$ the highest power ? (c) How do you determine the coefficients in the correlation function which would prove that ^{60}Ni undergoes the transition $4 \rightarrow 2 \rightarrow 0$?

Gammarays that are emitted from an excited nuclear state frequently have non-isotopic angular distribution with respect to the spin direction of the excited nucleus. Generally the nuclear spins are not aligned, but their directions distributed in random. This anisotropy is difficult to measure.

(a) In the given problem $4^+ \rightarrow 2^+ \rightarrow 0^+$, each of the two gamma ray cascading emissions substracts 2 from the angular momentum of the excited nucleus, but does not change the parity. Hence the two emissions γ_1 and γ_2 are of electric quadrupole *E*2 type.

(c) The angular correlation function for cascading emission can be written as

$$W(\theta) = \sum_{k=0}^{k_{max}} A_{2k} P_{2k}(\cos\theta),$$

where $0 \le k_{max} \le \min(I_b, L_1, L_2)$

$$A_{2k} = F_{2k}(L_1, I_a, I_b)\, F_{2k}(L_2, I_b, I_c),$$

L_1, L_2 being the angular momenta of the two γ-rays, I_a, I_b, I_c being respectively the initial, intermediate and final nuclear spins, P_{2k} (*cos* θ) are the Legendre polynomials.

Since $W(\theta)$ depends on $P_{2k}(\cos\theta)$ only, it consists of even powers of cos θ. For the $4^+ \rightarrow 2^+ \rightarrow 0^+$ transitions of ^{60}Ni, k_{max} is 2. Hence the highest power of cos θ in $P_4(\cos\theta)$ is 4 and so in an $W(\theta)$.

The coincidence counting rate $W(\theta)$ is measured for various θ. Fitting the experimental data to the angular correlation function we can deduce the coefficients.

Example 12. *A nucleus of mass M is initially in an excited state whose energy is ΔE above the ground state of the nucleus. The nucleus emits a gamma ray of energy hν and makes a transition to its ground state. Explain why the gamma ray energy hν is not equal to the energy level difference ΔE and determine the fractional change (hν ~ ΔE)/ΔE.*

When the nucleus emits a γ-ray, it will recoil on account of the conservation of momentum. Some energy is therefore required as recoil energy from the excitation energy ΔE. This makes $h\nu$ less than ΔE.

Let the total energy of the nucleus be E and its recoil momentum be p. The conservation of momentum and energy gives

$$p = p_\gamma, E + E_\gamma = Mc^2 + \Delta E.$$

As

$$E_\gamma = p_\gamma c = h\nu, \text{ and } E = \sqrt{p^2c^2 + M^2c^4}$$

∴

$$E_\gamma = \frac{1}{2Mc^2} \cdot \frac{(\Delta E)^2 + 2Mc^2\,\Delta E}{(1 + \Delta E/Mc^2)} = \Delta E - \frac{(\Delta E)^2}{2Mc^2}.$$

or

$$\frac{\Delta E - h\nu}{\Delta E} = \frac{\Delta E}{2Mc^2}.$$

Example 13. *The 0.014 MeV gamma ray that follows electron caputre in ^{57}Co is used in a study of the Mössbauer effect. Assume that the recoil momentum is effectively distributed between 1000 neighbouring atoms in the crystal lattice, and calculate the relative source absorber velocity required to obtain resonance absorption.*

If M is the mass of the nucleus and E_γ is the energy of the emitted photon, the energy of the recoil will be given by

$$E_{re} = \frac{p_{re}^2}{2M} = \frac{p_\gamma^2}{2M} = \frac{1}{2M}\left(\frac{E_\gamma}{c}\right)^2 = \frac{E_\gamma^2}{2Mc^2} = \frac{E_0^2}{2Mc^2},$$

where E_0 = Energy difference between two levels or the resonance energy, which is nearly same as that of the emitted γ-ray ($E_\gamma = E_0 - E_{re}$).

This energy is distributed among N neighbouring atoms in the crystal lattice, then the energy imparted to each atom $\varepsilon_{re} = E_{re}/N = E_0^2/2MNc^2$. Energy difference between centers of the emission and absorption lines $\Delta E = 2\varepsilon_{re} = E_0^2/2MNc^2$.

When a source of radiation is travelling with velocity v relative to the observer, then the energy change due to Doppler effect will be given by $\Delta E_D = E_0\, v/c$.

For resonance absorption $\Delta E = \Delta E_D$

or

$$v = \frac{E_0}{MNc} = \frac{0.014 \times 1.6022 \times 10^{-13}}{57 \times 1.67 \times 10^{-27} \times 1000 \times 2.998 \times 10^8} = 0.786 \text{ meter/sec.}$$

Example 14. *Calculate the frequency shift of a photon which falls straight down through a distance at the surface of the earth. How would you measure such a small frequency shift? Estimate the number of photons you would need to detect in order to have a meaningful measurement.*

Let the original frequency of the photon be ν_o and the frequency it has after falling a distance y in the earth's gravitational field be ν. Then the equivalent masses of the photon are respectively $h\nu_o/c^2$ and $h\nu/c^2$. Suppose the earth has mass M and radius R. From conservation of energy we get

$$h\nu_0 - \frac{GM(h\nu_0/c^2)}{R+y} = h\nu - \frac{GM(h\nu/c^2)}{R},$$

where G is the gravitational constant. The above equation may be written as

$$\nu - \nu_o \simeq \nu_o \frac{GM}{c^2}\left(\frac{1}{R} - \frac{1}{R+y}\right) \approx \nu_o \frac{GMy}{R(R+y)c^2} \approx \frac{gy}{c^2}.$$

or

$$\frac{\nu - \nu_0}{\nu} = \frac{9.8}{(2.998 \times 10^8)^2} = 1.09 \times 10^{-16}\, y.$$

where y is in meters.

For $y = 20\ m$ (say), $(\nu - \nu_0)/\nu_0 = \Delta\nu/\nu_0 = 2.18 \times 10^{-15}$. To measure this frequency shift, the γ-source used must have a level of natural width Γ/E_γ less than 2.18×10^{-15}. A possible choice is ^{67}Zn which has $E_\gamma = 93$ keV, $\Gamma/E_\gamma = 5 \times 10^{-16}$. Thus crystals of ^{67}Zn must be used both as source and absorber.

At $y = 0$, both are kept fixed in the same horizontal plane and the resonant absorption curve is measured. Then the source crystal is moved up to 20 *m* above the abosrber. The frequency of the photons arriving at the fixed absorber is $\nu_0 + \Delta\nu$ and resonant absorption does not occur. If the absorber is given a downward velocity of v such that by the Doppler effect the photons have frequency ν_o as seen by the absorber, resonant absorption can take place. Thus

$$\nu_o = (\nu_o + \Delta\nu)(1 - v/c) = \nu_o + \Delta\nu - \nu_o\, v/c.$$

or

$$v = c(\Delta\nu/\nu_o) = 2.998 \times 10^8 \times 2.18 \times 10^{-15} = 6.6 \times 10^{-7}\ m/sec.$$

This is the required velocity for the absorber.

Since the natural width for γ-emission of ^{67}Zn is much smaller than $\Delta\nu/\nu_o$ there is no need for a high counting rate. A statistical error of 5% at the spectrum peak is sufficient for establishing the frequency shift. This corresponds to a photon count of 400.

Oral Questions

1. The uncharged neutron transitions can produce radiation. Explain ?

   In analogy with classical electrodynamics, we expect that only charged particles should radiate. In reality neutron transitions can also produce radiation because (i) The protons in the nucleus have to be displaced to keep the centre of mass fixed and (ii) neutrons as well as protons radiate as a result of their magnetic moments.

2. How many visible photons (~ 500 A°) does a 200 *W* bulb with 3% efficiency emit per second. (~ 1.5×10^{15})
3. Which of the following is not correct? *(a)* Gamma rays like *X*-rays and light rays are electromagnetic radiations; *(b)* It is difficult to distinguish between the longest gamma rays and the shortest *X*-rays; *(c)* Gamma rays have low penetrating power than the α-particles; *(d)* Gamma rays are associated with transitions between nuclear energy levels. *(c)*
4. What are the differences between *X*-rays and γ-rays ?
5. The most accurate technique for measuring the low energy gamma rays and based on the *X*-ray diffraction.
6. It is correct that the absorption curve obtained with monoenergetic γ-rays is generally not a pure exponential? Give the reason.
7. Gamma ray spectrometers measure *(a)* directly the γ-rays, or *(b)* the secondary electrons produced in some material. *(a)*
8. The high energy gamma rays can be detected by cloud chamber or photographic emissions. The phenomenon used is *(a)* photodisintegration, *(b)* electric ionization, or *(c)* γ-ray absorption. *(a)*
9. Which of the following is the wrong statement? *(a)* Electric radiations arise from the changes in the distribution of the electric charges in the nuclei; *(b)* electric radiations arise from the changes in the current distribution in the nuclei; *(c)* Magnetic radiations arise from the changes in the current distribution in the nuclei.
10. The maximum possible energy of the γ-rays expected in nuclear decays is… . (*hc/R* or 20 *MeV*)
11. For an atom, only electric dipole radiation is important, which is produced by oscillations in its electric dipole moment. The radiations produced by oscillations of the magnetic dipole moment are smaller than for electric dipole radiation by a factor of the order of $(v/c)^2. = 10^{-4}$. What is the ratio of transition rates for electric quadrupole radiation and for electric dipole radiation. $(r/\lambda)^2 = 10^{-6}$.
12. For a nucleus, the transition rates for magnetic dipole and electric quadrupole radiation are suppressed by the factors … $(v/c)^2 = (10^{-1})^2 = 10^{-2}$; $(r/\lambda)^2 = (10^{-14}/10^{-12})^2 = 10^{-4}$.
13. Which one of the following is not true as per gamma-decay selection rules :

    (a) The nuclear parity must change if L is odd for electric transitions. (b) The nuclear parity must change if L is even for magnetic transitions. (c) The nuclear parity must not chane if L is even for magnetic transitions. *(c)*
14. What are the predominant decay modes for the transitions $2^+ \rightarrow 0^+$, $1^+ \rightarrow 0^+ + 1/2^- \rightarrow 1/2^+$ and $9/2^+ \rightarrow 1/2^-$. (*E2, M1, E1, M4*)
15. Internal pair creation is the emission of positron-electron pair, when the transition energy between the two nuclear states is greater than 1.022 MeV. It supplements the internal conversion process. The former is largest whereas the latter is smallest in the region of low/high atomic number and high transition energies.
16. The nuclear species which have the same atomic and mass numbers, but have different radioactive properties.
17. Coulomb excitation is the process in which the target nucleus gets excited through electromagnetic interaction between the projectile and the Coulomb field of the target nucleus. The cross sections for this process are thereforeredrawing in the properties.

18. Which one of the following is not true for coulomb excitation process ?

(a) The projectiles are not electrons, but the protons and heavy ions; (b) Sommerfeld number $\eta >> 1$; *(c) The collision must be non-adiabatic and the parameter* $\xi << 1$; *(d) The lifetime can be measured directly.* (d)

19. What is difference in the atomic and nuclear resonance fluorescences ?

20. What are the applications of the Mössbauer effect in nuclear and general physics ?

Problems

1. ^{137}Ba emits a gamma-ray photon of 0.66 *MeV* during an isomeric transition. Calculate the recoil kinetic energy of the atom in eV. (1.7 eV)

2. A fictitius nuclide has a $I^\pi = 1/2^+$ ground state and evenly spaced excited states with $I^\pi = 9/2^+, 3/2^-, 1/2^+, 5/2^+, 7/2^-$ in order of ascending energy. Draw an energy level diagram for this nuclide and indicate the most likely gamma transition from each level on this diagram. Write beside the lines their multipolarity.

3. The ground state and the 0.134 *MeV* and 0.299 *MeV* excited states of ^{197}Hg have been classified as $p_{1/2}$, $f_{5/2}$ and $i_{13/2}$ states respectively. What types of transitions are expected between these states. (*E*2, *M*4, *M*6)

4. The ground state of ^{61}Ni has spin $3/2^-$. ^{61}Co decays with a half life of 1.65 hr and with the emission of a β-spectrum with end point energy of 1.22 *MeV* to an excited state of ^{61}Ni 0.068 *MeV* above the ground state. The 0.068 MeV transition has a *K*-conversion coefficient of about 0.12 and *K/L* ratio 10.3. β^--transition of ^{61}Co to the ^{61}Ni ground state takes place in less than 10^{-6} of the disintegrations. What are the spin and parities of ^{61}Co and excited ^{61}Ni. $(7/2^-, 5/2^-)$

5. Assign the excitation energies and spin-parity to the levels in ^{161}Tb, which has a ground state $3/2^+$, with the following observed γ-energies (in keV) and multipolarities (given in parentheses). 57(*M*1), 77(*M*1), 103(*E*1), 105(?), 134(*E*2?), 166(*E*1), 181(*E*2), 258(*M*1), 273(?), 284(*E*1), 315(*M*1), 361(*E*1), 481(?), 529(?.)

$[0(3/2)^+, 57(5/2)^+\ 134(7/2)^+, 315(3/2)^+, 418(5/2)^-\ 481(1/2)^-, 586(?)]$

6. In $^{11}_{5}B$ a gamma transition leads from a level at 9.28 MeV ($I^\pi = 5/2^+$) to a level at 4.46 MeV ($I^\pi = 5/2^-$). What is the dominant multipolarity of the transition ? Calculate the expected gamma width on the basis of the Weisskopf model (the measured value is 5.4 eV).

7. Show that the most probable plane angle, θ to $\theta + d\theta$, between two successive dipole γ-ray quanta in the 0(1) 1(1)0 cascade is about 55^0.

8. In γ – γ angular correlation experiment show that directional correlation will be distributed if the half period $T_{1/2}$ of the intermediate level does not satisfy the inequality $T_{1/2} << 1/2\,\pi\,\Delta\,\nu$, where $\Delta\,\nu$ is the hyperfine structure separation for an atom with $J = 1/2$. Determine the restriction on $T_{1/2}$ for the cesium nucleus. (10^{-11} sec)

9. In the recoil distance method for the determination of life time of the excited nucleus, the counting rate was found to decrease by a factor of 2 for a source displacement of 0.07 mm. If the mean lifetime of the decaying state is 7×10^{-11} s, find the velocity of recoil. (1.4×10^6 *m/sec.*)

10. A ^{14}C atom is incorporated into an organic molecule as a radioactive tracer. The bond strength is estimated from infrared spectra to be 0.97 *eV*. Compare this energy with the energy of recoil at the emission of the most energetic beta particle of 0.156 *MeV*. (8.3 eV)

11. A particle of rest mass *m* has an excited state of excitation energy ΔE, which can be reached by γ-ray absorption. Find the resonant γ-ray energy E_γ to excite the particle which is initially at rest. $\Delta E + (\Delta E)^2/2mc^2$.

12. For $^{191}_{77}Ir$ what range of emitter speeds must be used to scan the Mössbauer peak ? (–0.22 *m/sec. to*, 0.022 *m/sec.*)

13. The 14.4 *keV* γ-line of ^{57}Fe is used in a Mössbauer resonance experiment. A line shift of Γ is observed to occur when the source moves with a speed $v = 10^{-2}$ cm/sec. What is the value of Γ and of the mean life time τ of the excited state in ^{57}Fe? (4.8×10^{-9}eV, 0.137 μ sec)

14. The 14.4 keV γ-ray transition in ^{57}Fe is used in Mössbauer experiment. It is found that the ground state ($I = 1/2$) splits with an energy difference corresponding to a source velocity of 3.96 mms^{-1}. Calculate the internal magnetic field at the ^{57}Fe nucleus assuming that the ground state magnetic moment is 0.0955 μ_N. (31.5 T)

REFERENCES

1. Alder, K., A. Bohr, T. Huus, B.R. Mottelson and A. Winther, *Rev. Mod. Phys.*, **28**, 432 (1956).
2. Alzenberg-Selove F., *"Nuclear Spectroscopy"*, Academic Press, 1960.
3. Biedenharn, L.C. and M.E. Rose, *Rev. Mod. Phys.*, **25**, 729 (1953).
4. Blatt, J.M. and V.F. Weisskopf, *"Theoretical Nuclear Physics"*, John Wiley, New York, 1952.
5. Burcham, W.E. *"Nuclear Physics"* Longman 1973.

6. Buttlar, H. Von., *Nuclear Physics an Introduction"*, Academic Press, New York 1968.
7. Cerny, Joseph, *"Nuclear Spectroscopy and Reactions"*, Part C, Academic Press, New York, 1974.
8. Cooper, J.A., J.M. Hollander and J.O. Rasmussen, *Phys. Rev. Lett.*, **15**, 680 (1965).
9. Cranshaw, T.E., J.P. Schiffer and A.B. Whitehead, *Phys. Rev. letters*, **4**, 163 (1960).
10. Dancoff, S.M. and P. Morrison, *Phys. Rev.*, **55**, 122 (1939).
11. Davisson C.M. and R.D. Evans, *Rev. Mod. Phys.* **24**, 79 (1952).
12. Devons, S. and G. Goldring, *Proc. Phys. Soc.* (London) **67**, 413 (1954).
13. Du Mond, J.W.M., *Rev. Sci. Instr.*, **18**, 626 (1947). *'Ann. Revs. Nucl. Sci.'* **8**, 163 (1958).
14. Enge, H.A., *"Introduction to Nuclear Physics"*, Addison-Wesley, Reading, Mass 1966.
15. Frilley, M., *Ann. Phys.* **11**, 483 (1929).
16. Frauenfelder, H., *"The Mössbauer Effect" Benjamin Inc., New York*, 1962.
17. Groshev, L.V., B.P. Adyasevich and A.M. Demidov, *Proc. Intern. Conf. Peaceful Uses, At. Energy Geneva*, **2**, 39 (1955).
18. Hager, R.S. and E.C. Seltzer, *Nuclear Data*, **A 4**, 397 (1968).
19. Hamilton, W.D. (Editor), *"The Electromagnetic Interaction in Nuclear Spectroscopy"*, Amsterdam, North Holland, 1975.
20. Hofstadter, R. and J.A. McIntyre, *'Phys. Rev.'* **78**, 619 (1950).
21. Hoogen Boom, A.M., *'Nucl. Instr'*, **3**, 57 (1958).
22. Horstman, R.E. *et. al.*, *Nucl. Phys.* **A248**, 291 (1975).
23. Johansson, S.A.E., *'Nature'*, **166**, 794 (1950).
24. Marmier P. and E. Shelden, *"Physics of Nuclei & Particles"*, Academic Press, 1969.
25. Metzger, F. and M. Deutsch, *Phys. Rev.*, **78**, 551 (1950).
26. Mims, W., H. Halban and R. Wilson, *Nature*, **166**, 1027 (1950).
27. Mladjenovic, M. and A. Hedgran, *'Physica'*, **18**, 1242 (1952).
28. Mössbauer, R.L., *Z Physik*, **151**, 124 (1958), *Naturwissenschaften*, **45**, 538 (1958); *Z Zaturforsch*, **14**, *(a)*, 211 (1959).
29. Roy, R.R. and B.P. Nigam, *"Nuclear Physics"*, John Wiley, 1967.
30. Nolan, P.J. and J.F. Sharpey Schafer, *Rep. Prog. Phys.*, **42**, 1 (1979).
31. Northcliffe, L.C. and R.P. Schilling, *Nuclear Data Tables*, **A7**, 233 (1970).
32. Oppenheimer, J.R. and L. Nedelski, *Phys. Rev.* **44**, 948 (1933).
33. Pound, R.V. and G.A. Rebka Jr., *Phys. Rev. letters*, **4**, 33 (1960).
34. Preston, M.A. *"Physics of the Nucleus"*, Addison Wesley, 1965.
35. Rasmussen, V., W.F. Hornyak, C.C. Lauritsen and T. Lauritsen, *Phys. Rev.*, **77**, 617 (1950).
36. Rose. M.E., *Phys. Rev.*, **76**, 678 (1949), Siegbahn (α–, β-and γ spectroscopy, Vol. II, 887 (1965).
37. Rose, M.E. and G.E. Uhlenbeck, *Phys. Rev.*, **48**,211 (1935).
38. Rutherford, E. and E.N. daC, Andrade, *Phil. Mag.*, **27**, 854 (1914); **28**, 263 (1914).
39. Sakurai, J.J., *"Advanced Quantum Mechanics"*, Addison-Wesley Reading, Mass, 1973.
40. Segre, E., *"Nuclei and Particles"*, W.A. Benjamin, Inc. Amsterdam, New York, 1965.
41. Siegbahn, K. (Editor), *Alpha, Beta and Gamma Ray Spectroscopy"*, North Holland Publishing Co. Amsterdam, 1965.
42. Singru, R.M., *"Introduction to Experimental Nuclear Physics"*, Wiley Eastern, 1972.
43. Smith, C.M.H. : *"Nuclear Physics"*, Pergamon Press, Oxford, 1965.
44. Tayal, D.C., *Ph. D. Thesis*, "Nuclear Spectroscopy through Coulomb excitation with protons", Panjab University, Chandigarh 1984.
45. Taylor, T.B. and N.F. Mott, *Proc. Roy. Soc.* (London), **A 138**, 665 (1932), **A142**, 215 (1933).
46. Tralli, N, and G. Goertzel, *Phys. Rev.*, **83**, 399 (1951).
47. Walker, R.L. and B.D. Mc Daniel, *Phys. Rev.* **74**, 315 (1948).
48. Wertheim, G.K., *Journal of Applied Physics'*, Suppl to Vol. **32**, 110 S (1961).
49. Wertheim, G.K., *"Mössbauer Effect"*, Academic Press, New York, 1964.
50. Wong, Samuel S.M., *"Introductory Nuclear Physics"*, Prentice Hall of India, New Delhi, 1996.

8 NUCLEAR FORCES

8.1 INTRODUCTION

Since nuclei contain charged particles, protons, the forces acting between the protons should be forces of repulsion. If there were no other forces acting between the particles of nuclei, the latter would not be able to retain a stable state, because the repelling protons would fly out in all directions. To have a stable state of a nucleus we have to assume that some other forces act on the protons. These attractive forces exceed the forces of repulsion. Even aside from the sign of the force electrostatic forces are much too weak to account for the main effects, gravitaional forces are weaker still and offer no assistance in the problem. It is therefore necessary to postulate an entirely new type of interaction, known as *nuclear force*. Let us collect following information on nuclear forces from study of complex nuclei.

(a) Stauration Property—We know that the nuclei have the same density ($R = R_0A^{1/3}$) and the binding energy per nucleon for nuclei with $A > 40$ is constant. These facts imply that the *nuclear force saturates*. Nucleons attract each other strongly only if they are in the same orbital state.

(b) Alpha particle structure—According to the Pauli principle only two neutrons and two protons will be found in the same orbital state. Therefore it is possible to find four nucleons strongly bound or α-particle structure, also confirmed by binding energy curve.

(c) Attractive short range—Both the α-particle scattering and α-particle emission analyses showed that *there is a nuclear force*, which is *attractive* and is of *very short range*. The analyses also indicated that the nuclear force is *strong*, compared to the electrostatic force which is repulsive.

(d) Charge independence—We know that the atomic mass number A is approximately equal to twice the atomic number Z for the light and intermediate nuclei. It shows that light nuclei prefer to add nucleons in $n - p$ pairs, *i.e.*, there is a strong interaction between neutrons and protons. The neutron excess in heavy nuclei confirms that $n - n$ force is attractive, but it is sufficiently attractive to lead to a stable di-neutron. The experiments involving the scattering of protons from the neutrons also indicate that the nuclear force is charge independent. For a good approximation one can write

$n - n = p - p = n - p$ or the forces as *charge independent*.

(e) Shape of the Potential—As the nuclear interactions do not extend to very large distances beyond the nuclear rdius, and $1/r^n$ ($r >> 1$) character is not useful to solve the problem. To avoid this difficulty, the idea of cut-off in the potential is introduced. The parameters are taken to be the strength V_0 (the value of potential at the origin) and the range α (the distance beyond which potential goes to zero rapidly), which is less than nuclear dimensions.

We use the principles of wave mechanics on nuclear problems and then by comparison with experimental data, find a consistent description of the nuclear forces acting between two nucleons (*two body problem*). There are two general methods of investigation, the study of *n-p* and *p-p* scattering events over a wide range of energy and the study of deuteron (only bound state of two nucleons). Many body forces in nucleon-nucleon interactions in the nucleus also exist, but their contribution is very very small.

8.2 DEUTERON

Let us first consider deuteron in order to exhibit some of the concepts involved in discussing nuclear potentials and the quantum states of nuclei. The deuteron does possess measurable properties which might serve as a guide in the search for the correct nuclear interaction. These properties are :

1. The extraordinary stability of the alpha particle shows that the most stable nuclei are those in which number of neutrons and protons are equal. The deuteron consists of two particles of roughly equal masses M, so that the *reduced mass of the system is* $\frac{1}{2}M$.
2. The binding energy of the deuteron is very small. Its experimental value is 2.22457312 ± 22 *MeV*. Since the energy needed to pull a nucleon out of a medium mass nucleus is about 8 *MeV*, we must regard the *deuteron as loosely bound.*
3. The angular momentum quantum number, often called the *nuclear spin*, of the ground state of the deuteron determined by a number of optical, radiofrequency and micro-wave methods is one. It suggests that the spins are parallel (*triplet state*) and the orbital angular momentum of the deuteron about their common center of mass is zero. Thus the *ground state is* ^3S *state.*
4. The parity of deuteron as measured, indirectly, by studies of nuclear disintegrations and reactions for which certain rules of parity changes exist, *is even.*
5. The sum of the magnetic dipole moments of the proton ($2.792847386 \pm 63\mu_N$) and neutron ($-1.91304275 \pm 45\mu_N$), does not exactly equal to magnetic moment of the deuteron ($0.857406 \pm 1\ \mu_N$) measured by magnetic resonance absorption method.
6. A radiofrequency molecular beam method has been employed to determine the quadrupole moment of the deuteron as $Q = 0.0028590 \pm 30 \times 10^{-28}\text{cm}^2$. This shows the departure from spherical symmetry of a charge distribution. The +ve sign indicates that this *distribution is prolate* rather than oblate.

   The electric quadrupole moment and the magnetic moment discrepancy can be explained if the ground state is a mixture of the triplet states $^3S_1$ and $^3D_1$ having even parity. The percentage probability of finding the deuteron in D-state is 4 ± 2%. As deuteron spends most of the time in the spherically symmetrical state (S-state), we will for the moment ignore the D-state contribution to the deuteron wavefunction.
7. Since the neutron has no charge, the force between the neutron and proton can not be electrical. This force can not be magnetic as magnetic moments are very small. It can not be gravitational force, as the masses are very small. So we must accept the *nuclear force as a new type of force.* This force is short range, attractive and along the line joining the two particles (*central force*). Since a central force can not account for the quadrupole moment of the deuteron. As a quadrupole moment is small, the assumption will be approximately correct.
8. The *force depends only on the separation* of the nucleons not on the relative velocity or orientation of the nucleon spins with respect to the line. This force can be derived from a potential. Since the force is attractive, $V(r)$ is negative and decreases with decreasing r. Since it is short range, $V(r)$ vanishes for $r > b$, where b – 3 fermi.

The Schrodinger wave equation for the two body problem is

$$\nabla^2 \psi + (2m/\hbar^2)(E - V)\psi = 0, \qquad \text{...(1)}$$

where m is the reduced mass, E the total energy of the system equal to the binding energy of deuteron and V the potential energy describing the forces acting between the two bodies.

In terms of spherical polar coordinates, Eqn (1) becomes

$$\left[\frac{1}{r^2}\frac{\partial}{\partial r}\left(r^2\frac{\partial\psi}{\partial r}\right)+\frac{1}{r^2\sin\theta}\frac{\partial}{\partial\theta}\left(\sin\theta\frac{\partial\psi}{\partial\theta}\right)+\frac{1}{r^2\sin^2\theta}\frac{\partial^2\psi}{\partial\phi^2}\right]+\left(\frac{2m}{\hbar^2}\right)[E-V(r,\theta,\phi)]\psi = 0 \qquad \text{...(2)}$$

Let us assume that $V(r, \theta, \phi)$ actually depends on r only and not on θ and ϕ. The solution of the above equation can be written as a product of a function of r only and one of θ and ϕ only, as $\psi(r, \theta, \phi) = \psi(r)\,\psi(\theta, \phi)$. Substituting it into equation (2) we have

$$\frac{1}{\psi(r)}\frac{d}{dr}\left(r^2\frac{d\psi(r)}{dr}\right)+\frac{2mr^2}{\hbar^2}[E-V(r)] = -\frac{1}{\psi(\theta,\phi)}\left[\frac{1}{\sin\theta}\frac{\partial}{\partial\theta}\left(\sin\theta\frac{\partial\psi(\theta,\phi)}{\partial\theta}\right)+\frac{1}{\sin^2\theta}\frac{\partial^2\psi(\theta,\phi)}{\partial\phi^2}\right] \quad ...(3)$$

The left hand side of this equation depends only on r, the right hand side depends only on θ and ϕ. For all values of the variables, each side of this must separately be equal to the some constant, which comes out to be $l(l+1)$. Thus we have

$$\frac{1}{r^2}\frac{d}{dr}\left(r^2\frac{d\psi(r)}{dr}\right)+\frac{2m}{\hbar^2}\left[E-V(r)-\frac{l(l+1)\hbar^2}{2mr^2}\right]\psi(r) = 0, \quad ...(4)$$

where l is the angular momentum quantum number of the system.

The last term in the bracket appears as a straight addition to the actual potential $V(r)$ and is known as *centrifugal potential.*

The Schrodinger equation for ^3S state ($l = 0$) of the deuteron is

$$\frac{1}{r^2}\frac{d}{dr}\left(r^2\frac{d\psi(r)}{dr}\right)+\frac{2m}{\hbar^2}[E-V(r)]\psi(r) = 0. \quad ...(5)$$

In this case reduced mass $m = \frac{1}{2}M$, where M is the mass of the nucleon. We expect the ground state to be spherically symmetric (S-state), so that $\psi(r)$ depends only on r (central modified force). Substituting $\psi(r) = u(r)/r$ in equation (5), where $u(r)$ is called the radial wavefunction, we have

$$(d^2u/dr^2) + (M/\hbar^2)\,[E - V(r)]\,u = 0. \quad ...(6)$$

The wavefunction of the bound state of the deuteron is not markedly dependent on the exact shape of the potential $V(r)$ between a proton and neutron provided that a potential of short range is chosen. For simplicity, we represent $V(r)$ by a square well of depth V_0 and radius b, where b is the range of nuclear force. In it $V(r)$ has a constant negative value $-V_0$ for separations less than a certain value b and the value zero for all greater separations. The other potentials may be of

$$\begin{aligned}
\textit{Gaussian well type } V(r) &= -V_0e^{-(r/\alpha)^2}\\
\textit{Exponential well type } V(r) &= -V_0e^{-r/\alpha}\\
\textit{Yukawa well type } V(r) &= -\frac{V_0e^{-r/\alpha}}{(r/\alpha)}.\\
\textit{Hard core potential } V &= V_0' \to \infty \qquad \textit{for } r < r_c\\
&= -V_0f(r/\alpha) \qquad \textit{for } r \geq r_{c'}
\end{aligned}$$

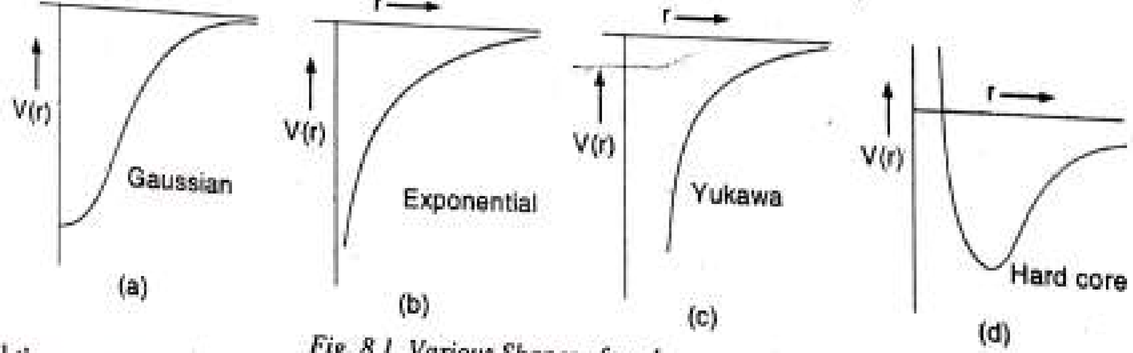

Fig. 8.1. Various Shapes of nuclear potentials.

All these potentials are central, *i.e.*, spherically symmetric. There is much evidence to indicate that the predominantly central component is admixed with a tensor force component, *i.e.*, a force that has a directional dependence. In case of the two nucleon system, both spin $\frac{1}{2}$ nucleons having anti parallel spins, they build a resultant spin zero-singlet state in which there is no distinguished spin direction and consequenty no-noncentral interaction. For both nucleons having parallel spins, the resultant spin is one-triplet state, which permits of an admixture of a noncentral interaction. The latter is the example of the deuteron. Thus we may expect to derive information on tensor forces between nucleons from the study of the deuteron's properties.

For the ground state of the deuteron, the total energy E is negative and equal to $-B$, where B(or E_B) is the binding energy of deuteron. Thus Eqn. (6) can be written as

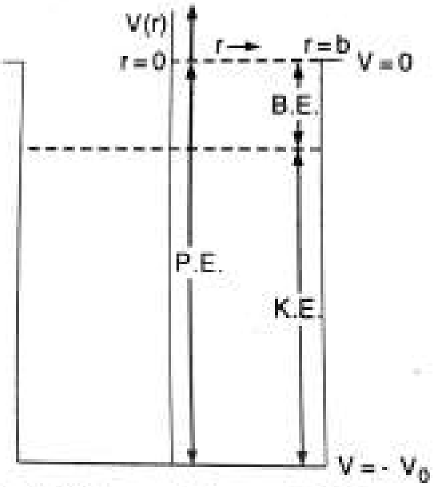

Fig. 8.2. Square well potential of deuteron.

$$\frac{d^2u}{dr^2}+\frac{M}{\hbar^2}[V_0-B]u = 0 \qquad \text{for } r<b \qquad ...(7)$$

and
$$\frac{d^2u}{dr^2}+\frac{M}{\hbar^2}(-B)u = 0 \qquad \text{for } r>b. \qquad ...(8)$$

These equations can be written as

$$d^2u/dr^2 + K^2u = 0 \qquad r<b \qquad ...(9)$$

and
$$d^2u/dr^2 - \alpha^2u = 0 \qquad r>b, \qquad ...(10)$$

where
$$K^2 = M(V_0-B)/\hbar^2 \quad \text{and} \quad \alpha^2 = MB/\hbar^2$$

General solutions of equations (9) and (10) are

$$u = A_1 \sin Kr + B_1 \cos Kr \qquad r<b \qquad ...(11)$$

and
$$u = A_2 e^{\alpha r} + B_2 e^{-\alpha r} \qquad r>b. \qquad ...(12)$$

The following boundary conditions must be imposed :

(1) $u(r \to 0) = 0$, to keep wave function ψ finite.

(2) $u(r \to \infty) = 0$, u must not diverge faster than r as $r \to \infty$.

To satisfy the conditions at zero and infinity, the solutions reduce to

$$u = A_1 \sin Kr \qquad \text{for } r<b$$
$$u = B_2 e^{-\alpha r} \qquad \text{for } r>b. \qquad ...(14)$$

Since these two solutions join smoothly at $r = b$. Hence equating the values and first derivatives of u at $r = b$, we have

$$A_1 \sin Kb = B_2 e^{-\alpha b} \qquad ...(15)$$

and
$$A_1 K \cos Kb = -B_2 \alpha e^{-\alpha b} \qquad ...(16)$$

∴
$$K \cot Kb = -\alpha. \qquad ...(17)$$

or
$$\cot Kb = -\frac{\alpha}{K} = -\left(\frac{B}{V_0-B}\right)^{1/2} = -\left(\frac{B}{V_0}\right)^{1/2}$$

As $B << V_0$, we see that cot Kb is negative and small in absolute value.

The constants A_1 and B_2 are obtained from the requirement that the integral of $|\psi^2|$ over all space must be equal to unity.

$$4\pi \int_0^\infty |\psi|^2 r^2 dr = 4\pi \int_0^\infty u^2 dr = 1$$

or
$$4\pi \int_0^b A_1^2 \sin^2 Kr dr + 4\pi \int_b^\infty B_2^2 e^{-2\alpha r} dr = 1$$

$$A_1^2[b-(1/2K)\sin 2Kb]+(B_2^2/\alpha)e^{-2\alpha b} = 1/2\pi. \qquad ...(18)$$

Thus A_1 and B_2 can be obtained from this equation with the help of equations (15) and (17). Defining $MV_0/\hbar^2 = K_0^2$, we have $K_0^2 = K^2 + \alpha^2$. Thus

$$A_1 \sin Kb = A_1(1+\cot^2 Kb)^{-1/2} = A_1K/(K^2+\alpha^2)^{1/2} = B_2e^{-\alpha b}.$$

Substituting this value in equation (18), we get

$$A_1^2\left[b-\frac{1}{2K}\frac{2K}{(\alpha^2+K^2)^{1/2}}\frac{(-\alpha)}{(\alpha^2+K^2)^{1/2}}\right]+\frac{A_1^2K^2}{\alpha(\alpha^2+K^2)}=\frac{1}{2\pi}$$

$$\text{or}\quad A_1^2\left[b+\frac{\alpha}{(\alpha^2+K^2)}+\frac{K^2}{\alpha(\alpha^2+K^2)}\right]=\frac{1}{2\pi},$$

$$\text{or}\quad A_1 = \left[\frac{1}{2\pi}\frac{\alpha}{\alpha b+1}\right]^{1/2} \qquad \text{...(19)}$$

$$\therefore\quad B_2 = A_1 \sin Kb\, e^{\alpha b}=\left[\frac{\alpha}{2\pi(\alpha b+1)}\right]^{1/2}\frac{K}{K_o}e^{\alpha b}. \qquad \text{...(20)}$$

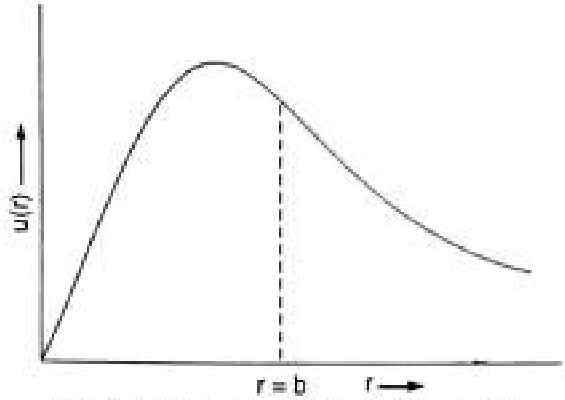

Fig. 8.3. Ground state deuteron wave function.

On Substituting $\alpha = 0.232$ fin^{-1} and $b = 1.93$ *fm*, in the above equations, we get $A_1 = 0.160$ and $B_2 = 0.247$. With these values, equation (18) shows that the second term is about twice as large as the first. Hence *the nucleons in the deuteron spend only one third of the time within the range of nuclear force and thus the deuteron is loosely bound.* This can be seen from Fig. 8.3, where $u(r)$ is plotted againt r.

No excited S-states—Equation (17) can be written as

$$x \cot x = -\alpha b, \qquad \text{...(21)}$$

where $x = Kb$. Using $B = 2.225$ MeV and $b \le 3f$ we find that $\alpha = 0.232$ and $\alpha b \le 0.7$. If we draw now curves $y = \cot x$ and $y = -\alpha b/x$, the intersections give the roots of equation (21). From Fig. 8.4 it is clear that roots are slightly greater than $\pi/2$, $3\pi/2$, $5\pi/2$, ... The correct solution is $x = Kb = \frac{1}{2}\pi$, since if Kb were greater than π, the wave function would have a radial node at $Kb = \pi$ and thus $u(r)$ and hence $\psi(r)$ would not be the wave function of the ground state—a *contradiction* of our *hypothesis*. We may thus put $Kb = \frac{1}{2}\pi+\varepsilon$ in equation (21) and get

$$\left(\tfrac{1}{2}\pi+\varepsilon\right)\cot\left(\tfrac{1}{2}\pi+\varepsilon\right) = -\alpha b. \qquad \text{...(22)}$$

As ε is small, hence $\cot\left(\frac{1}{2}\pi+\varepsilon\right) = -\varepsilon$, and $\varepsilon = 2\alpha b/\pi$.

Thus $$Kb = \pi/2 + 2\alpha b/\pi.$$

This shows that there can not be any excited *S*-states.

Range and Depth of Potential—Using $Kb = \pi/2$ and again neglecting B in the expression for K [as the depth of potential is very much greater than the binding energy *i.e.*, $K^2 >> \alpha^2$ which can be obtained from equation (21)], we get

$$MV_0b^2/\hbar^2 = \pi^2/4$$

$$\text{or}\quad V_0b^2 = \pi^2\hbar^2/4M = 1.03 \times 10^{-24}\ \text{MeV}\ cm^2. \qquad \text{...(24)}$$

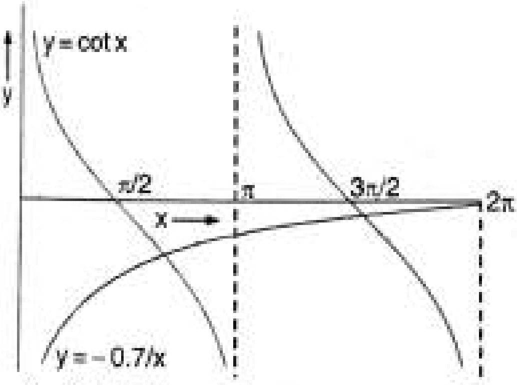

Fig. 8.4. Solution of Equation x cot x = − 0.7.

It is the relation between range b and potential depth V_0, establishes the strength of the well. Actually V_0b^2 is slightly greater than $\pi^2\hbar^2/4M$, as Kb is slightly greater than $\pi/2$. By accepting the approximate value of range $b = 2$ fermi, the value of potential depth is $V_0 = 36$ MeV, which is in close agreement with the measured values. Other types of short range potential functions give about the same results as the square well.

Another result which does not depend on the form of potential is the wavefunction outside the range of nuclear forces. In this region function $u(r)$ decreases exponentially with r and reduces to zero at infinity. The radial distance where the amplitude decreases to $1/e$ of its maximum amplitude is often called the *radius* of the deuteron.

$$\therefore\qquad \text{Radius } \rho = 1/\alpha = \hbar/\sqrt{(MB)} = 4.31 \times 10^{-15}\ m. \qquad \text{...(25)}$$

It is about twice that of the range of the internucleon force b. This explains that the *deuteron is a lossely bound system.* As $b < \rho$, hence the nuclear forces can be said to be *short range.* If we substitute $A = 2$ in the relation for radius of the deuteron nucleus. $R = r_0A^{1/3} = 1.4 \times 2^{1/3} = 1.76$ fm $= 0.4\ \rho$.

In the zero range approximation the potential acts within a short distance and must be deep, and the wave function is exponential everywhere. As the range becomes larger compared to nuclear radius, the depth of the potential decreases and the sinusoidal part becomes more and more predominant.

Excited States of the Deuteron—To see that there cannot be any bound states with higher angular momenta we first write the radial part of the Schrodinger equation for any angular momentum l

as
$$\frac{d^2u_l(r)}{dr^2}+\left[K^2-\frac{l(l+l)}{r}\right]u_l(r)=0 \qquad r\le b \qquad \ldots(26)$$

and
$$\frac{d^2u_l(r)}{dr^2}-\left[\alpha^2+\frac{l(l+l)}{r}\right]u_l(r)=0 \qquad r\ge b \qquad \ldots(27)$$

where K^2 and α^2 are having their usual values.

The general solution of the equation (26) inolves spherical Bassel function j_l and spherical Neumann functions n_l. As the latter approaches $-\infty$ as $r\to 0$, thus the solution of Eqn (26) is

$$u_l(r) = A\,j_l(Kr) \qquad r\le b \qquad \ldots(28)$$

where
$$j_l(Kr) = (\pi/2Kr)^{1/2}J_{l+1/2}(Kr). \qquad \ldots(29)$$

$J_{l+1/2}$ being the function of half odd integer order.

The solution of equation (27) outside the range of nuclear force

$$u_l(r) = Bh_l(i\alpha r) = B[j_l(i\alpha r)+in_l(i\alpha r)] \qquad r>b \qquad \ldots(30)$$

where
$$n_l(i\alpha r) = (-1)^{l+1}(\pi/2i\alpha r)^{1/2}J_{-l-1/2}(i\alpha r). \qquad \ldots(31)$$

Using boundary conditions that the function and its first derivative are continuous at the edge of the well, we get

$$\left[\frac{1}{u_l}\frac{du_l(r)}{dr}\right]_{inside} = \left[\frac{1}{u_l}\frac{du_l(r)}{dr}\right]_{outside} \qquad (r=b) \qquad \ldots(32)$$

Using the relation
$$\frac{dj_l(\rho)}{d\rho} = j_{l-1}(\rho)-\frac{l+1}{\rho}j_l(\rho), \text{ we get}$$

$$K\left[\frac{j_{l-1}(Kb)}{j_l(Kb)}-\frac{l+1}{Kb}\right] = i\alpha\left[\frac{h_{l-1}(i\alpha b)}{h_l(i\alpha b)}-\frac{l+1}{i\alpha b}\right]$$

or
$$j_{l-1}(Kb)/j_l(Kb) = (\alpha/K)\,[ih_{l-1}(i\alpha b)/h_l(i\alpha b)]. \qquad \ldots(33)$$

For $b < 1.43\times 10^{-15}$ m, $\alpha b<1$ and since $\alpha \ll K$ the expression in the bracket on R.H.S. is less than one and is approximately zero. Thus

$$j_{l-1}(Kb) \simeq 0. \qquad \ldots(34)$$

This condition holds for all angular momenta except $l=0$. We have already discussed the case $l=0$. For $l=1$, we get $j_0(Kb)=0=\sin(Kr)/Kr$. Hence $Kb=\pm\pi, \pm 3\pi, \ldots\ldots$. Thus the minimum well depth is

$$V_0 = \pi^2\hbar^2/Mb^2. \qquad \ldots(35)$$

If we choose $b = 2\times 10^{-15}$ m, we get $V_0 = 144$ MeV, which is almost four times as large as the actual well depth in the ground state. Repeating this procedure for larger and larger values of l, we find that a deeper and deeper well depth is required to produce a bound state. Thus *we conclude that no bound state exists for* $l>0$. This also confirms experimental results.

8.3 NEUTRON-PROTON SCATTERING AT LOW ENERGIES

The fact that the deuteron is a bound system, shows that attractive forces exist between neutrons and protons. Further information on the inter-nucleon forces can be obtained from a study of the scattering of free neutrons by protons. In such experiments a parallel beam of neutrons is allowed to impinge upon a target containing hydrogen atoms (hydrogenous materials like water H_2O and paraffin as targets) and the number of neutrons deflected through various angles is determined as a function of neutron energy. Since neutrons have no charge, they are uneffected by the electrostatic field and their scattering will directly reflect the operation of the nuclear forces.

Two kinds of the reactions can be involved in neutron-proton interaction : One scattering and other radiative capture. The latter has low probability and cross section for high energy neutrons, as the cross section for the competing radiative capture reaction decreases with $1/v$, where v is the neutron velocity. In practice protons are bound in molecules. The chemical binding energy of the proton in a molecule is about 0.1 eV. Thus for neutron energies > 1 eV, very much above the chemical binding energies in water or hydrogenous materials, there are no chemical effects and protons get knocked out of the molecule and thus can be assumed as free. *This sets a lower limit to the neutron energy.* If the neutron energy is less than 10 MeV, only the S-wave overlaps with the nuclear potential and is scattered. Therefore the angular distribution of the scattered neutrons is isotropic in the centre of mass system. In the centre of mass system, the Schrodigner equation for the two body (n-p system) problem is

$$\nabla^2\psi + \frac{M}{\hbar^2}[E - V(r)]\psi = 0, \qquad \text{...(36)}$$

where M = Proton or neutron mass = 2 × Reduced mass of the system.

E = Incident kinetic energy in C.M. system = $\frac{1}{2}$ (Incident K.E. in L-coordinates)

and $V(r)$ = Inter-nucleon potential energy.

At large distances from the centre of scattering the solution of this equation is expected to be of the form

$$\psi = e^{ikz} + \frac{e^{ikr}}{r} f(\theta). \qquad \text{...(37)}$$

The term e^{ikz} represents a plane wave describing a beam of particles moving in the z-direction towards the origin (scattering centre). The second term represents the scattered wave. The complex quantity $f(\theta)$ is the scattering amplitude in the direction θ and is to be evaluated in terms of k. In the case of a spherically symmetric potential the entire arrangement is axially symmetric about the incident direction and hence does not depend on the azimuthal angle ϕ. The $1/r$ dependence is necessary for the conservation of particles in the outgoing wave. The volume of a spherical shell, between r and $r + dr$ is $4\pi r^2 dr$ and hence the density of particles in it or the probability of finding one particle in the spherical shell must vary with $1/r^2$ which is proportional to the square of the amplitude of the scattered wave in the shell. Hence the amplitude of the scattered wave must vary with $1/r$.

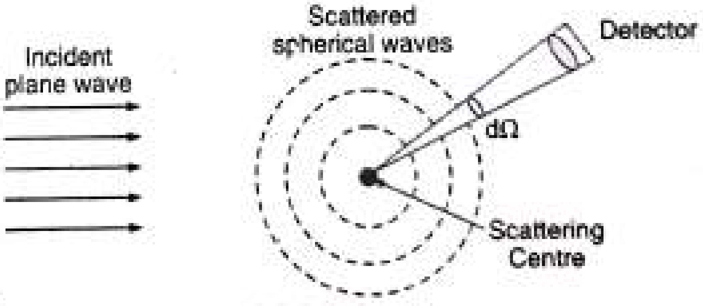

Fig. 8.5. Scattering Process.

To compute the differential scattering cross section, we must find the number of particles dN scattered in unit time by one target nucleus into a solid angle $d\Omega$ and the incident flux F. If v is the speed of an incoming particle with respect to the scatterer, then

Incoming flux of particles $F = \psi_{in}^* \psi_{in} v = v$.

Similarly dN is equal to the flux of scattered particles $\psi_{sc}^* \psi_{sc}\, v$ multiplied by the area $r^2\, d\Omega$ cut out by $d\Omega$ on a spherical surface of radius r and is given by

$$dN = \psi_{sc}^* \psi_{sc}\, v r^2\, d\Omega = |f(\theta)|^2\, v\, d\Omega.$$

∴ The differential cross section

$$d\sigma = |f(\theta)|^2\, v\, d\Omega / v = |f(\theta)|^2\, d\Omega.$$

or

$$\sigma = \int |f(\theta)|^2\, d\Omega = 2\pi \int |f(\theta)|^2 \sin\theta\, d\theta. \qquad \text{...(38)}$$

Partial wave Analysis or Phase shift Analysis : First of all let us consider the wave equation (36) in the absence of a scattering centre [$V(r) = 0$ for all values of r], *i.e.*,

$$\nabla^2\psi + (ME/\hbar^2)\psi = 0. \qquad \text{...(39)}$$

This has the solution

$$\psi = e^{ikz}. \qquad \text{...(40)}$$

where

$$k = 1/\lambda\!\!\!^- = \sqrt{(ME)}/\hbar$$

Lord Rayleigh proposed that this type of wavefunction can be expanded into a series in terms of spherical harmonic functions. Thus equation (40) can be written as an infinite series

$$\psi(r, \theta) = e^{ikz} = e^{ikr\cos\theta} = \sum_{l=0}^{\infty} R_l(r)\, Y_{l,0}(\theta). \qquad \ldots(41)$$

where l is the integer representing the number of the *partial waves*. It, as usual, signifies the orbital angular momentum of the system. The radial functions $R_l(r)$ are solutions of the radial part of equation (39).

$$\frac{1}{r^2}\frac{d}{dr}\left(r^2\frac{dR}{dr}\right)+\left(k^2-\frac{l(l+1)}{r^2}\right)R = 0. \qquad \ldots(42)$$

This equation has two solutions, one is not finite at the origin and cannot represent the plane wave.The other is finite at origin and can be represented in terms of spherical Bessel functions as

$$R_l(r) = i^l\sqrt{[4\pi\,(2l+1)]}\,j_l(kr). \qquad \ldots(43)$$

The square of this gives the r-dependence of the probability density for each partial wave in expression (41). The asymptotic form of spherical Bessel function

$$j_l(kr)\xrightarrow[r\to\infty]{}\frac{\sin(kr-l\pi/2)}{kr} = \frac{1}{2ikr}[e^{+i(kr-l\pi/2)}-e^{-i(kr-l\pi/2)}]. \qquad \ldots(44)$$

The values of first few spherical Bessel functions are

$$j_0(kr) = \frac{\sin kr}{kr}, j_1(kr) = \frac{\sin kr}{(kr)^2}-\frac{\cos kr}{kr},$$

$$j_2(kr) = \left(\frac{3}{(kr)^3}-\frac{1}{kr}\right)\sin kr-\frac{3\cos kr}{(kr)^2},$$

The spherical harmonic function

$$Y_{l,0}(\theta) = \frac{(2l+1)^{1/2}}{(4\pi)^{1/2}}P_l(\cos\theta), \qquad \ldots(45)$$

where $P_l(\cos\theta)$ is the Legendre polynominal of order l. The square of the spherical harmonic function gives the angular dependence of the probability density. The values of the first few Legendre polynomials are

$$P_0(\cos\theta) = 1, P_1(\cos\theta) = \cos\theta, P_2(\cos\theta) = \tfrac{1}{2}(3\cos^2\theta-1).$$

Thus for the field free scattering, the plane wave is given by

$$e^{ikz} = \sum_{l=0}^{\infty} i^l(2l+1)\, j_l(kr)P_l(\cos\theta). \qquad \ldots(46)$$

Substituting the value of $j_l(kr)$ from equation (44), we get

$$e^{ikz} = \sum_{l=0}^{\infty}\frac{i^l(2l+1)}{2ikr}[e^{+i(kr-l\pi/2)}-e^{-i(kr-l\pi/2)}]P_l(\cos\theta). \qquad \ldots(47)$$

The scattering amplitude $f(\theta)$ can be expanded in terms of the polynomials $P_l(\cos\theta)$, as

$$f(\theta) = \frac{i}{2k}\sum_{l=0}^{\infty} f_l(2l+1)P_l(\cos\theta), \qquad \ldots(48)$$

where the coefficients f_l are to be determined.

Substituting the values of e^{ikz} and $f(\theta)$ from equations (47) and (48) in equation (37), we get

$$\psi(r,\theta)\underset{r\to\infty}{=}\frac{1}{2ikr}\sum_{l=0}^{\infty} i^l(2l+1)[(1-f_l)e^{i(kr-l\pi/2)}-e^{-i(kr-l\pi/2)}]P_l(\cos\theta)$$

$$= \frac{1}{2ikr}\sum_{l=0}^{\infty}(2l+1)[(1-f_l)e^{ikr}-(-1)^l e^{-ikr}]P_l(\cos\theta). \qquad \ldots(49)$$

In analogy with the expression (46) of the plane wave, we can write the solution of eqn. (36) as

$$\psi(r,\theta) = \sum_{l=0}^{\infty} i^l(2l+1)\psi_l(r)\,P_l(\cos\theta),$$

where $\psi_l(r)$ is the radial part of the solution and is given by

$$\psi_l(r) = \frac{u_l(r)}{r}. \qquad \ldots(51)$$

On introducing the scattering centre, *i.e.*, the potential function $V(r)$ which scatters the incident beam, the Schrodinger equation is the same as given in equation (36). Its radial part is given by

$$\frac{d^2u_l(r)}{dr^2}+\left[\frac{M}{\hbar^2}[E-V(r)]-\frac{l(l+1)}{r^2}\right]u_l(r)=0. \quad \text{...(52)}$$

The asymptotic form of the solution of this equation for large r is given by

$$u_l(r) = C_l\sin\left(kr-\frac{l\pi}{2}+\delta_l\right). \quad \text{...(53)}$$

where δ_l is the phase shift due to scattering from the potential.

Substituting the asympotic expression, (53), for $\psi_l(r)$ in equation (50) and comparing the result with equation (49), we obtain

$$f_l = (1-e^{2i\delta_l}) \text{ and } C_l=\frac{1}{k}e^{i\delta_l}. \quad \text{...(54)}$$

From equations (54) and (48), the scattering amplitude $f(\theta)$ is given by

$$f(\theta) = \frac{1}{2ik}\sum_{l=0}^{\infty}(2l+1)(e^{2i\delta_l}-1)P_l(\cos\theta)$$

$$= \frac{1}{k}\Sigma(2l+1)e^{i\delta_l}\sin\delta_l\,P_l(\cos\theta). \quad \text{...(55)}$$

Thus the differential cross section is given by

$$d\sigma = |f(\theta)|^2\,d\Omega=\left|\frac{1}{k}\sum_l(2l+1)e^{i\delta_l}\sin\delta_l P_l(\cos\theta)\right|^2 d\Omega. \quad \text{...(56)}$$

and the total cross section

$$\sigma = \int\frac{d\sigma}{d\Omega}d\Omega=\frac{4\pi}{k^2}\sum_l(2l+1)\sin^2\delta_l. \quad \text{...(57)}$$

This is clearly a maximum for $\delta_l = \left(n+\frac{1}{2}\right)\pi, n=0, \pm1, \pm2,\ldots\ldots$

The total cross-section can be written as sum of partial cross-sections, one for each l-wave. The partial cross-sections are

$$\sigma_l = 4\pi\,\lambda\!\!\!^{-2}\,(2l+1)\sin^2\delta_l. \quad \text{...(58)}$$

In the absence of a potential, for low energies $l = 0$ is effective, and the wave function of the incoming neutron wave is given by

$$\psi_{l=0}(r) = \frac{\sin kr}{kr}=\frac{e^{ikr}-e^{-ikr}}{2ikr}. \quad \text{...(59)}$$

The first term in the last expression represents an outgoing spherical wave and the second an incoming spherical wave.

If the potential is applied, the wave function is given by

$$\psi_{l=0}(r) = \frac{u_{l=0}(r)}{r}\sim\frac{\sin(kr+\delta_0)}{r}=\frac{e^{i(kr+2\delta_0)}-e^{-ikr}}{2ikr}. \quad \text{...(60)}$$

Thus we see that the potential affects only the outgoing wave. The difference is the scattered wave

$$\therefore \quad \psi_{sc} = \frac{e^{ikr}}{2ikr}(e^{2i\delta_0}-1)=\frac{e^{ikr}e^{i\delta_0}\sin\delta_0}{kr}. \quad \text{...(61)}$$

$$\therefore \quad \text{Scattering amplitude } f(\theta) = \frac{e^{i\delta_0}\sin\delta_0}{k}. \quad \text{...(62)}$$

and

$$\sigma_{sc} = 4\pi\,\lambda\!\!\!^{-2}\sin^2\delta_0. \quad \text{...(63)}$$

The angular distribution for $l = 0$ is isotropic, as the differential scattering cross section is independent of angle. This has been experimentally verified at low energies.

Scattering length—For neutrons of very low energy scattered by free protons, λ is very large and hence k is very small. It can be seen from Eqn. (62) that as $k \to 0$, δ_0 must also approach zero, otherwise $f(\theta)$ would become infinite. Thus for low energy neutrons $f(\theta)$ can be written as

$$f_0 = \lim_{k \to 0} \frac{e^{i\delta_0} \sin \delta_0}{k} = \frac{\delta_0}{k} = -a. \quad \ldots(64)$$

where the quantity $+a$ is called the scattering length in the convention of Fermi and Marshall. Hence for low energy neutrons the wave equation outside the range of nuclear force is written as

$$u(r) = c \sin(kr + \delta_0) = c(kr + \delta_0) = ck(r - a). \quad \ldots(65)$$

This is the equation of a straight line intersecting the r-axis at $r = a$ and is obtained by extrapolating the radial wave function $u(r)$ from the point just beyond the range of the nuclear force. Scattering from a potential giving a bound state produces a positive a. If the potential gives only a virtual state, the slope of the inner wave function at $r = b$ is positive and a is negative.

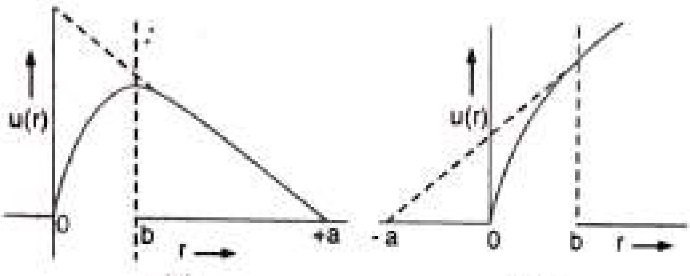

(a) (b)

Fig. 8.6. (left) Positive scattering length (bound state); (right) Negative scattering length (unbound state).

From equations (63) and (64) the zero energy scattering cross-section becomes

$$\sigma_{sc} = 4\pi \left(\frac{\sin \delta_0}{k} \right)^2 = 4\pi a^2. \quad \ldots(66)$$

This is identical with the scattering cross-section of an impenetrable sphere of radius a, in the limit of zero energy. It is four times the maximum classical area πa^2. It is due to the quantum mechanical effect, which suggests the diffraction at the boundaries giving rise to the large amount of small angle scattering. The measurement of σ_{sc} *determines the magnitude of the scattering length a but not its sign.*

Determination of the phase shift δ—We shall now attempt to determine the phase shift δ for low energy neutron-proton scattering by solving also the Schrodinger's equation in the region where the interaction between the two particles takes place. For this we make the simple assumption of a square well for the nuclear potential. Inside the well of depth V_0 and radius b the radial wave equation for particles whose total energy has the positive value E is

$$\frac{d^2 u}{dr^2} + \frac{M}{\hbar^2}[E + V_0] u(r) = 0. \quad (67)$$

Inside the square well this equation has the simple solution

$$u(r) = A \sin k_1 r,$$

where

$$k_1 = \sqrt{[M(E + V_0)]}/\hbar.$$

Outside the square well, the solution can be written as

$$u(r) = B \sin(kr + \delta). \quad \ldots(69)$$

At the edge of the rectangular well ($r = b$), the two solutions and their derivatives with respect to r must be continuous.

$$\therefore \quad A \sin k_1 b = B \sin(kb + \delta)$$

and

$$k_1 A \cos k_1 b = Bk \cos(kb + \delta).$$

Hence

$$k_1 \cot k_1 b = k \cot(kb + \delta). \quad \ldots(70)$$

This relationship is analogous in form to equation

$$K \cot Kb = -\alpha, \quad \ldots(71)$$

which describes the binding energy B of the deuteron in terms of the same rectangular well (V_0, b).

Here

$$K = \sqrt{[M(V_0 - B)]}/\hbar \quad \text{and} \quad \alpha = \sqrt{(MB)}/\hbar.$$

For low energy neutrons ($E << V_0$), we may assume $K = k_1$ (as $V_0 >> B$), hence *the wavefunction u(r) inside the well is nearly the same for the deuteron and the n-p-scattering system*. Thus for approximation we can write

$$\frac{\sqrt{(ME)}}{\hbar}\cot\left(\frac{\sqrt{(ME)}}{\hbar}b+\delta\right) = -\frac{\sqrt{(MB)}}{\hbar}.$$

As the scattering length a is much larger than the range b of the potential, thus for very low energy neutrons kb can be neglected in comparison to δ.

$$\therefore \qquad \cot\delta = -\left(\frac{B}{E}\right)^{1/2} \text{ or } \sin^2\delta = \frac{E}{E+|B|}.$$

Substituting this value of $\sin^2\delta$ in equation (63), we obtain the approximate value of total scattering cross-section as

$$\sigma_{sc} = 4\pi\lambda\!\!\!^{-2}\frac{E}{E+|B|} = \frac{4\pi\hbar^2}{M}\cdot\frac{1}{E+|B|}. \qquad \ldots(72)$$

The Spin Dependence of Nuclear Forces. At very low energies the situation is very different. Numerical substitution of $B = 2.225$ MeV in equation (72) gives a predicted value for zero energy neutrons ($E = 0$), $\sigma_0 = 2.3$ barns, which is in violent disagreement with the measured value $\sigma_0 = 20.36 \pm 0.10$ barns. This disagreement is a sign of some fundamental error in our assumptions. This point was cleared up by E.P. Wigner in 1935. He suggested that the scattering occurs not only in the triplet state (^3S), but in the singlet state (^1S) as well.

Experimentally the total angular momentum of the deuteron nucleus is unity. The spins are, therefore, correlated in the ground state of the deuteron. The situation is different in *n-p* scattering experiment. When unpolarized neutrons strike randomly oriented protons, their uncorrelated spins add up to unity in three fourths of the collisions and to zero in one fourth of the collisions. In other words we can say that the triplet state ($S = 1$) has three times the statistical weight ($2S + 1$) of a singlet ($S = 0$) state. The total *n-p* scattering cross-section will then be

$$\sigma = \tfrac{3}{4}\sigma_t + \tfrac{1}{4}\sigma_s,$$

where σ_t and σ_s indicate the cross-sections in triplet and singlet states respectively.

One test of Wigner's hypothesis is by measurement of the cross-section over the range 0 to 5 MeV. Where the theoretical expression for σ_0 should hold. We can use the calculated value $\sigma_t = 2.3$ barns and the experimental information on σ_0 (zero energy cross-section) to calculate σ_s. To fit the experimental data, we must have (in barns)

$$\begin{aligned} 20.36 &= \tfrac{3}{4}(2.3)+\tfrac{1}{4}\sigma_s \\ \sigma &= 74 \text{ barns.} \end{aligned} \qquad \ldots(73)$$

Introducing the singlet and triplet scattering lengths a_s and a_t, where $\sigma_s = 4\pi a_s^2$, and $\sigma_t = 4\pi a_t^2$, we obtain the rough estimates $a_t \sim 4.3$ fermi and $a_s \sim 24.3$ fermi.

Coherent Scattering of Slow Neutrons. Equation (66) shows that we can find the magnitude, but not the sign, of the scattering length a. A positive or negative sign of the scattering length indicates whether the system has a bound or unbound state. The most important evidence is the scattering of neutrons by diatomic hydrogen gas, which can exist in two states ortho-and para hydrogen. An experimental comparison of the coherent scattering from ortho and para hydrogen was first suggested by Teller in 1936 to test the spin dependence of the neutron proton interaction. Not only we are able to verify that the scattering is spin dependent but also will be able to show that singlet state scattering length is negative. In para-hydrogen molecules the proton spins are anti-parallel. The molecules can rotate with energies given by

$$E_J = J(J+1)\,\hbar/2\,\mathscr{I},\ (J = 0, 2, 4, \ldots\ldots),$$

where $\mathscr{I}$ is the moment of inertia. In ortho hydrogen proton spins are parallel. The rotational states are given by $J = 1, 3, 5, \ldots\ldots$ If temperature is low enough practically all the para hydrogen will be in the state $J = 0$ (singlet state) and all the ortho hydrogen will be in state $J = 1$ (triplet state).

We shall now derive an expression for the scattered intensity from a molecule of ortho or para hydrogen in terms of the singlet and triplet scattering lengths a_s and a_t when the incident neutron energy is so small that λ_n is much greater than $0.78 \times 10^{-10} m$, the distance between the atoms in hydrogen molecule. The total spin operator of the $n - p$ system is $S = \mathbf{s}_n + \mathbf{s}_p$, where the neutron spin operator $\mathbf{s}_n = \frac{1}{2}\sigma_n$ and the proton spin operator $\mathbf{s}_p = \frac{1}{2}\sigma_p$. Here σ_n and σ_p are the Pauli spin matrices. Since s_n and s_p commute being independent. Therefore

$$|S|^2 = |s_n|^2 + |s_p^2| + 2\mathbf{s}_n \cdot \mathbf{s}_p. \qquad \text{...(74)}$$

The eigenvalues of the operator S^2 are $S(S+1)$, where $S = 0$ for the singlet state and $S = 1$ for the triplet state.

$\therefore$ $|S|^2 = 0(0+1) = 0$ for singlet state and $1(1+1) = 2$ for triplet state.

$$|s_n|^2 = |s_p|^2 = \frac{1}{2}\left(\frac{1}{2}+1\right) = \frac{3}{4}.$$

Therefore equation (74) gives

$s_n \cdot s_p = \frac{1}{2}|S|^2 - \frac{3}{4} = -\frac{3}{4}$ for singlet state and $+\frac{1}{4}$ for triplet state.

We now define the two projection operators P_s and P_t as

$$P_s = \frac{1}{4} - s_n \cdot s_p = 1 \text{ for singlet and} = 0 \text{ for triplet state}$$

$$P_t = \frac{3}{4} + s_n \cdot s_p = 0 \text{ for singlet and} = 1 \text{ for triplet state.}$$

If a_1 and a_2 are the scattering lengths for scattering of neutron by protons 1 and 2 of hydrogen molecule. Which can be defined in terms of singlet and triplet $n - p$ scattering lengths and projection operators as

$$a_1 = a_s P_{s_1} + a_t P_{t_1} \text{ and } a_2 = a_s P_{s_2} + a_t P_{t_2}.$$

$\therefore$

$$a_1 = a_s\left(\frac{1}{4} - s_n \cdot s_{p_1}\right) + a_t\left(\frac{3}{4} + s_n \cdot s_{p_1}\right)$$

and

$$a_2 = a_s\left(\frac{1}{4} - s_n \cdot s_{p_2}\right) + a_t\left(\frac{3}{4} + s_n \cdot s_{p_2}\right)$$

If the separation between the two protons in the hydrogen molecule is smaller then the neutron wavelength, then the scattering length a for scattering by both protons

$$a = a_1 + a_2 = \frac{1}{2}(a_s + 3a_t) + (a_t - a_s)s_n \cdot (s_{p_1} + s_{p_2}) \qquad \text{...(75)}$$

For parahydrogen, spins are antiparallel and $S_H = s_{p_1} + s_{p_2} = 0$ and $a = \frac{1}{2}(a_s + 3a_t)$

$\therefore$ Scattering cross section σ(*para hydrogen*) $= 4\pi\left(\dfrac{a_s + 3a_t}{2}\right)^2$ ...(76)

For ortho hydrogen, spins are parallel and $S_H = s_{p_1} + s_{p_2}$.

$\therefore$ Scattering cross section σ(*ortho hydrogen*) $= 4\pi\left|\frac{1}{2}(a_s + 3a_t) + (a_t - a_s)s_n \cdot S_H\right|^2$ ...(77)

Since the neutron spin is randomly oriented and is as many times positive as negative for any given direction. Thus for the direction of S_H, we have

$$|s_n \cdot S_H|_{av} = 0.$$

Since

$$|s_n \cdot S_H|_{av}^2 = (s_{nx}^2 S_{Hx}^2 + s_{ny}^2 S_{Hy}^2 + s_{nz}^2 S_{Hz}^2)_{av} + (s_{nx} s_{ny} S_{Hx} S_{Hy} + s_{nx} s_{nz} S_{Hx} S_{Hz})_{av} + (s_{ny} s_{nx} S_{Hy} S_{Hx} + s_{ny} s_{nz} S_{Hy} S_{Hz})_{av} + (s_{nz} s_{nx} S_{Hz} S_{Hx} + s_{nz} s_{ny} S_{Hz} S_{Hy})_{av}$$

From the properties of the Pauli matrices, the average of each of the six cross terms (in the last three brackets) is zero and we therefore get

$$|s_n \cdot S_H|_{av}^2 = (s_{nx}^2 S_{Hx}^2 + s_{ny}^2 S_{Hy}^2 + s_{nz}^2 S_{Hz}^2)_{av}.$$

Since

$$s_n^2 = s_n(s_n + 1) = \frac{1}{2}\left(\frac{1}{2}+1\right) = \frac{3}{4},$$

therefore

$$(s_{nx}^2)_{av} = (s_{ny}^2)_{av} = (s_{nz}^2)_{av} = 1/4$$

and

$$(S_{Hx}^2 + S_{Hy}^2 + S_{Hz}^2)_{av} = (S_H^2)_{av} = 1(1+1) = 2.$$

$$\therefore \qquad |s_n \cdot S_H|^2_{av} = \tfrac{1}{4} \times 2 = \tfrac{1}{2}.$$

Therefore

$$\sigma_{ortho} = 4\pi\left[\left(\frac{a_s + 3a_t}{2}\right)^2 + (a_t - a_s)^2\,|s_n \cdot S_H|^2_{av}\right]$$

$$= \pi(a_s + 3a_t)^2 + 2\pi(a_t - a_s)^2. \qquad \ldots(78)$$

On combining with equation (76), we get

$$\sigma_{ortho} = \sigma_{para} + 2\pi(a_t - a_s)^2 \qquad \ldots(79)$$

and

$$\frac{\sigma_{ortho}}{\sigma_{para}} = 1 + \frac{2(a_t - a_s)^2}{(3a_t + a_s)^2} \qquad \ldots(80)$$

This theory indicates that ortho hydrogen scattering cross section is greater than that of the para hydrogen scattering cross section. These two become identical if $a_t = a_s$. In this case the nuclear forces are said to be spin independent. Thus to prove that the nuclear force is spin dependent, it is required to show that $\sigma_{ortho} > \sigma_{para}$. Several experiments have been carried out. In the experiment carried out by Sutton and others, the gaseous hydrogen target was enclosed in a tube at a temperature of liquid hydrogen. The high energy neutrons, obtained by bombarding a beryllium target with deuterons from a cyclotron, were slowed down in paraffin cooled to liquid air temperature. The range in neutron energies used for scattering varied from 10 to 30°K. The cross sections observed were $\sigma_{para} = 4$ barns and $\sigma_{ortho} = 125$ barns.

This great difference between these cross-sections indicates that the n-p force is strongly spin dependent.

$|3a_t + a_s|$ is very much smaller than $|a_t - a_s|$ when $a_s < 0$ but very much larger when $a_s > 0$. Since $\sigma_{para} < \sigma_{ortho}$ hence $|3a_t + a_s|$ is smaller than $|a_t - a_s|$ or $a_s < 0$. This –ve value of a_s indicates that the singlet state of the deuteron is virtual or unbound. We can now solve equations (76) and (78) for a_t and a_s. There are four possible pairs of a_t and a_s values. Two can be discarded because they have –ve values of a_t. A third pair can be shown to be inconsistent with $n - p$ scattering data. The remaining solution is $a_t = 0.52 \times 10^{-14}$ m. and $a_s = -2.3 \times 10^{-14}$ m. Therefore, the total cross-section will be

$$\sigma_0 = \tfrac{3}{4}\sigma_t + \tfrac{1}{4}\sigma_s = \tfrac{3}{4} \times 4\pi a_t^2 \times 4\pi + \tfrac{1}{4} 4\pi a_s^2 = 19.8 \text{ barns}.$$

Which is in fair agreement with experimental value 20.36 barns.

The presently accepted values of a_t and a_s determined from the scattering of neutrons from the ortho and para hydrogen are $a_t = 5.37 \pm 0.04$ fermi and $a_s = -23.73 \pm 0.007$ fermi.

Spin of neutron. The large observed value of $\sigma_{ortho}/\sigma_{para}$ relates to the spin of the neutron. The ground state of the deuteron has $I = 0$ and $I = 1$, if

$$S_n + S_p = \tfrac{1}{2} + \tfrac{1}{2} = 1 \qquad \text{(spin parallel)}$$

$$S_n + S_p = \tfrac{3}{2} - \tfrac{1}{2} = 1. \qquad \text{(spin anti-parallel)}.$$

In the second case the relative statistical weights for n-p collisions with free protons would change from their values of 3/4 and 1/4 to values of 5/8 and 3/8. This will change the scattering cross sections.

$$\sigma_{ortho}/\sigma_{para} = 2. \qquad \ldots(81)$$

This is against experimental results, hence the neutron has spin 1/2 not 3/2.

8.4 SHAPE-INDEPENDENT EFFECTIVE RANGE THEORY IN *n-p* SCATTERING

While defining the scattering length $a = -\delta/k$, we make the use of scattering of S-wave by using a square well potential. The phase shift method of analysis has been replaced by a general theory which gives a very good approximation for phase shift δ and at the same time does not require a specified form of potential $V(r)$. It describes the scattering at low energies in terms of the range over which the potential is especially effective along with the scattering length. This range is called *effective range* and has a dimension of length. This theory of scattering is therefore known as *shape independent effective range theory.*

In developing the effective range theory we begin by writing Schrodinger's equation for an *S*-wave and positive energy for the relative motion. Let u_1 and u_2 be the radial wavefunctions describing the scattering at energies E_1 and E_2 respectively. Then we have

$$\frac{d^2u_1}{dr^2}+\frac{M}{\hbar^2}[E_1-V]u_1=0 \qquad \text{...(82)}$$

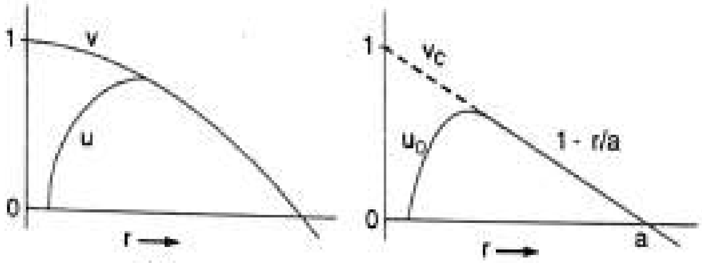

(a) (b)

Fig. 8.7. Radial wavefunction in effective range theory.

$$\frac{d^2u_2}{dr^2}+\frac{M}{\hbar^2}[E_2-V]u_2=0, \qquad \text{...(83)}$$

where V is the nuclear potential of any shape. Multiply equation (82) by u_2 and equation (83) by u_1, subtract and integrate from 0 to ∞. Then we get

$$\left[u_1u_2'-u_2u_1'\right]_0^\infty=(k_1^2-k_2^2)\int_0^\infty u_1u_2\,dr \qquad \text{...(84)}$$

where $k_1^2=ME_1/\hbar^2$ and $k_2^2=ME_2/\hbar^2$.

Consider a new function v which is identical with u outside the potential well and extra-polates the behaviour of u to the origin instead of curving over in the interior region to become zero at $r=0$. Such a function is called Ersatz function. The function is given as $v=c\sin(kr+\delta)$ and is normalized in such a way that $v\to 1$ at the origin. Thus we get

$$v = \sin(kr+\delta)/\sin\delta. \qquad \text{...(85)}$$

We get a relation like equation (84) for the wave functions v_1 and v_2. Thus

$$\left[v_1v_2'-v_2v_1'\right]_0^\infty = (k_1^2-k_2^2)\int_0^\infty v_1v_2dr. \qquad \text{...(86)}$$

We may now subtract equation (84) from equation (86). Since $v_1=u_1$ and $v_2=u_2$ outside the potential well and $u_1=u_2=0$ for $r=0$, hence

$$-(v_1v_2'-v_2v_1')_{r=0} = (k_1^2-k_2^2)\int_0^\infty (v_1v_2-u_1u_2)dr. \qquad \text{...(87)}$$

As relation (85) gives

$$v_1' = k_1\cos(k_1r+\delta_1)/\sin\delta_1$$

$\therefore$

$$(v_1')_{r=0} = k_1\cot\delta_1 \qquad \text{and} \qquad (v_1)_{r=0}=1.$$

Similarly

$$(v_2')_{r=0} = k_2\cot\delta_2 \qquad \text{and} \qquad (v_2)_{r=0}=1.$$

Substituting these values in equation (87), we have

$$-k_2\cot\delta_2+k_1\cot\delta_1 = (k_1^2-k_2^2)\int_0^\infty(v_1v_2-u_1u_2)dr. \qquad \text{...(88)}$$

Consider now the case when $k_1=k$ (for energy E) and $k_2=0$ (for zero energy). We have $u_1\to u$, and $v_1\to v$ and $u_2=u_0$ and $v_2=v_0$. By definition of scattering length $k_0\cot\delta_0=-1/a$ when $k_0\to 0$.

$\therefore$

$$v_0 = \lim_{k_0\to 0}\frac{\sin(k_0r+\delta_0)}{\sin\delta_0}=\frac{a-r}{a}=1-\frac{r}{a}.$$

Equation (88) therefore becomes

$$k\cot\delta = -1/a+\tfrac{1}{2}k^2\rho(0,E)$$

where

$$\rho(0,E) = 2\int_0^\infty(vv_0-uu_0)dr. \qquad \text{...(89)}$$

Since u and v differ only inside the range of nuclear forces, therefore, the integrand vanishes outside the nuclear force range. Inside the range, the wavefunctions are almost independent of the energy, because the depth of the potential well is much larger than the energy of the system E. We can thus write

$$v = v_0 \qquad \text{and} \qquad u=u_0$$

and

$$k\cot\delta = -1/a+k^2\int_0^\infty(v_0^2-u_0^2)dr=-1/a+\tfrac{1}{2}k^2\rho(E). \qquad \text{...(90)}$$

where $\rho(E)$ has the dimensions of a length and in general varies so slightly with energy that it can be replaced by an energy independent constant.

$$\rho(E) = 2\int_0^\infty (v_0^2 - u_0^2)\,dr = r_{eff}\,(or\ r_0). \qquad \ldots(91)$$

The quantity r_0 is constant and is known as *effective range* of nuclear potential. It is one of the average properties of the potential to be determined from the scattring. The factor 2 is included in the definition to make r_0 approximately equal to the radius at which the potential essentially vanishes (*e.g.*, for a square well potential $r_{eff} = b = r_0$). This justifies the name "*effective range*" for r_0. The *S*-wave phase shift in the shape independent approximation is valid at energies upto about 10 *MeV* and is expressed in terms of the two basic scattering parameters a (*scattering length*) and r_0 (*effective range*) as

$$k \cot \delta = -1/a + \tfrac{1}{2} r_0 k^2. \qquad \ldots(92)$$

∴ S-wave scattering cross-section $\sigma = 4\pi a^2/\{[1 - \tfrac{1}{2} a r_0 k^2]^2 + a^2 k^2\}$. ...(93)

Whatever the shape of the potential, the scattering cross section can be described by the two parameters a and r_0. The experimental values of δ and k serve to determine a and r_0. Any reasonable potential shape can be made to give matching values of a and r_0 by suitable choice of its depth V_0 and range b. Hence the two experimentally determined lengths a and r_0 do not determine the shape of the nuclear potential, but if the shape is chosen then a and r_0 fix the potential parameters, such as the depth and range of a rectangular well potential. For this reason above relation is known as the *shape independent approximation.*

Determination of scattering length and effective range. The scattering length and effective range for the *n-p* system in the low energy region can be deduced from the scattering and deuteron data. In view of the existence of triplet and singlet states, we have to derive the magnitudes of the four quantities a_t, a_s, r_{0t}, r_{0s}. A description how to find the values of a_t and a_s from $n - p$ coherent scattering data at very low energies has already been discussed earlier. The value of r_{0t} can be deduced from additional information on the triplet force involved in deuteron binding.

If $u(r)$ be the modified radial wave function for the deuteron in the external region ($r > b$) and $v(r)$ be its extrapolated Ersatz function normalized to unity at $r = 0$, we have

$$u(r) = C\,e^{-\alpha r} \quad \text{and} \quad v(r) = e^{-\alpha r} \text{ at } r > b, \qquad \ldots(94)$$

where $\alpha = [MB/\hbar^2]^{1/2}$.

We may obtain a relation similar to equation (89), as

$$-\alpha = \frac{1}{a_t} + \alpha^2 \int_0^\infty (v v_0 - u u_0)\,dr. \qquad \ldots(95)$$

As before we replace the integral by the expression

$$\int_0^\infty (v v_0 - u u_0)\,dr = \int_0^\infty (v_0^2 - u_0^2)\,dr = \tfrac{1}{2} r_{0t}.$$

$$\therefore \quad -\alpha = -\frac{1}{a_t} + \frac{1}{2}\alpha^2 r_{0t} \text{ or } r_{0t} = \frac{2}{\alpha^2}\frac{1}{a_t} - \frac{2}{\alpha}. \qquad \ldots(96)$$

On substituting the values as $\alpha = 0.232\,fm^{-1}$ and $a_t = 5.38\,fm$, we get

$$r_{0t} = 1.70\,fm.$$

Upon inserting the $n - p$ scattering data upto 10 MeV, the values of remaining parameters can be established to be

$$r_{0s} = 2.4\,fm.$$

Now inserting values of the scattering parameters as $r_{0t} = 1.70\,fm$. $r_{0s} = 2.4\,fm$, $a_t = 5.38\,fm$ and $a_s = -23.7\,fm$ into the weighted expression for cross section

$$\sigma_0 = \frac{1}{4}\left[3\frac{4\pi a_t^2}{a_t^2 k^2 + (1 - \frac{1}{2}k^2 a_t r_{0t})^2} + \frac{4\pi a_s^2}{a_s^2 k^2 + (1 - \frac{1}{2}k^2 a_s r_{0s})^2}\right] \qquad \ldots(97)$$

We obtain the relation for S-wave $n - p$ scattering cross section in terms of E_n, the neutron energy in MeV (Lab-system), as

$$\sigma_0(barn) = \frac{2.73}{0.350\,E_n - (1 - 0.0553\,E_n)^2} + \frac{17.63}{6.80\,E_n + (1 + 0.344\,E_n)^2}. \qquad ...(98)$$

This expression is found in close agreement with the experimental data upto 20 MeV.

8.5 PROTON-PROTON SCATTERING AT LOW ENERGIES

The quantitative information about the spin dependence is confirmed by analysing the scattering of low energy protons from protons. This analysis also shows that the nucleon potential is charge **independent**, *i.e.*, the same nuclear potential may be used for both $n - p$ and $p - p$ scattering. This does not mean that their cross sections are the same. There are two essential differences between $p - p$ and $n - p$ scattering. First, the $p - p$ scattering is caused not only by the nuclear forces but also by the Coulomb force. Second, the scattering and scattered particles are identical and obey the Pauli exclusion principle and, therefore, the wavefunction describing the two protons must change sign on the interchange of the two particles. Hence a symmetric space wavefunctions (*S*, *D* states, etc.) can only be associated with an antisymmeteric (singlet) spin wavefunction, whereas a symmetric (triplet) spin wavefunction is required for an anti-symmetric space wavefunction (P, F states, etc.). For incident protons of energy below 10 *MeV*, only the *S* state interaction is of any importance in the scattering, since protons in higher orbital angular momentum states stay apart from each other beyond the range of the nuclear force.

Experimentally the study of *p–p* scattering, is capable of much higher accuracy than *n–p* scattering, for the following reasons :

1. *Protons are easily available over a wide range of energies.*
2. *Protons can be made monoenergetic.*
3. *Protons can be produced in well collimated beam.*
4. *Protons can be easily detected by their ionizing properties.*
5. *Protons undergo Coulomb scattering simultaneously with nuclear scattering. This increases the sensitivity in case one of the scattering probabilities is small and also gives sign of the phase shifts resulting from nuclear scattering.*
6. *The proton combination obeys Fermi Statistics. This simplifies the analysis of proton-proton scattering.*

We are now interested in obtaining a theoretical expression for the differential elastic scattering cross-section of protons by protons. The theory is more complicated than that of *n–p* scattering because the Coulomb potential appreciably distorts the incident wave even at finite distances. For the particles incident along the *z*-axis, the total wave function is given by

$$\psi(r,\theta) = \Sigma C_l \frac{u_l(r)}{r} P_l(\cos\theta), \qquad ...(99)$$

where $u_l(r)$ is the solution of the radial wave equation for the proton-proton system given as

$$\frac{d^2u}{dr^2} + \frac{M}{\hbar^2}\left[E - V(r) - \frac{e^2}{4\pi\varepsilon_0 r} - \frac{l(l+1)\hbar^2}{Mr^2}\right]u = 0, \qquad ...(100)$$

whre $V(r)$ is the square well nuclear potential and M is the mass of the proton. For low energies, the nuclear potential will affect only to $l = 0$ partial wave, but the Coulomb potential produces higher l-value scattering state.

Phase Shift Analysis. For low energies for which $l = 0$, the *p–p* scattering can only be in the singlet state. For high energies (higher values of l), the scattering can either be a singlet state or a triplet state, depending on whether l is even or odd respectively. In the centre of mass system the probability that either proton will be scattered through an angle θ is

$$|f(\theta)|^2 + |f(\pi - \theta)|^2. \qquad ...(101)$$

Exchange of the two proton coordinates means exchanging θ with $\pi - \theta$. For identical particles, their waves interfere and instead of summing the squares of the amplitude, the amplitudes are sum up first and then we square them. Thus the eigen functions containing only spatial coordinates without spin will be

$f(\theta) \pm f(\pi - \theta)$. For plus sign this expression is symmetrical with respect to the exchange of coordinates and is antisymmetrical for minus sign. We know that the spins give a symmetrical eigenfunction in the triplet state and antisymmetrical in the singlet state. For protons the total eigen function must be anti-symmetrical, hence the resultant scattering amplitude will be

$$f(\theta) - f(\pi - \theta) \quad \text{for the triplet state}$$

$$f(\theta) + f(\pi - \theta) \quad \text{for the singlet state}$$

As the protons of target material as well as incident protons have their spins randomly oriented, the cross section for $p - p$ scattering may be obtained after taking into account the proper weights of singlet and triplet cases, as

$$\frac{d\sigma}{d\Omega} = \tfrac{1}{4}|f_s(\theta)|^2 + \tfrac{3}{4}|f_t(\theta)|^2, \qquad \ldots(102)$$

where s and t represent singlet and triplet states respectively.

$$\therefore \quad \frac{d\sigma}{d\Omega} = \tfrac{1}{4}|f(\theta) + f(\pi - \theta)|^2 + \tfrac{3}{4}|f(\theta) - f(\pi - \theta)|^2$$

$$= |f(\theta)|^2 + |f(\pi - \theta)|^2 - \text{Re}\,[f^*(\theta)\, f(\pi - \theta)] \qquad \ldots(103)$$

The first term describes scattering, second exchange scattering and the third term the interference between the direct and exchange waves.

The equation (100) shows that in p-p scattering, we have not only the Coulomb interaction which has an infinite range but also the nuclear interaction which is of finite range. Outside the range of the nuclear potential, the solution is a linear combination of two functions, one which is regular at the origin (called regular solution) and the other irregular solution and is given by

$$u(r) = \sin(kr - \eta \log_e 2kr - l\pi/2 + \xi_l + \delta_l). \qquad \ldots(104)$$

where δ_l is the change in the phase shift due to the nuclear potential $V(r)$. It is not that produced by $V(r)$ in the absence of the Coulomb force. Here $\eta = e^2/4\pi\varepsilon_0 \hbar v$ and $\xi_l = arg\,\Gamma(l + 1 + i\eta)$.

The presence of the Coulomb force complicates the problem, the plane wave is not exp (ikz), but the distorted one and is given by

$$\exp i[kz + \eta \log_e k(r - z)] = \sum_{l=0}^{\infty}(2l+1)i^l (kr)^{-1} \sin[kr - \eta \log_e 2kr - \tfrac{1}{2}l\pi] P_l(\cos\theta)$$

If we set $C_l = (2l + 1)\, k^{-1}\, i^l \exp i(\xi_l + \delta_l)$ in equation (99), we get

$$\psi(r, \theta) = \exp i[(kz + \eta \log_e k(r - z)] - f(\theta)\frac{1}{r}\exp i(kr - \eta \log_e 2kr). \qquad \ldots(106)$$

where

$$f(\theta) = -\frac{1}{2ik}\sum_{l=0}^{\infty}(2l+1)[e^{2i(\xi_l+\delta_l)} - 1] P_l(\cos\theta). \qquad \ldots(107)$$

The complete solution (106) may be written as

$$\psi(r, \theta) = I(r, \theta) + f(\theta)\, S(r), \qquad \ldots(108)$$

where

$$I(r, \theta) = \exp i[kz + \eta \log_e k(r - z)] \qquad \ldots(109)$$

and

$$S(r) = \frac{1}{r}\exp i[kr - \eta \log_e 2kr] \qquad \ldots(110)$$

For pure Coulomb scattering $\delta_l = 0$, the $f(\theta)$ can be summed to give

$$f_C(\theta) = -\frac{1}{4k^2}\cdot\frac{e^2}{4\pi\varepsilon_0}\operatorname{cosec}^2\frac{\theta}{2}\exp[-2i\eta \log_e \sin\frac{\theta}{2} + i\pi + 2i\xi_0] \qquad \ldots(111)$$

Thus $f(\theta)$ can be written as

$$f(\theta) = f_C(\theta) + f_N(\theta), \qquad \ldots(112)$$

where

$$f_C(\theta) = -\frac{1}{2ik}\sum_{l=0}^{\infty}(2l+1)[e^{2i\xi_l} - 1] P_l(\cos\theta) \qquad \ldots(113)$$

and

$$f_N(\theta) = -\frac{1}{2ik}\sum_{l=0}^{\infty}(2l+1)e^{2i\xi_l}[e^{2i\delta_l} - 1] P_l(\cos\theta). \qquad \ldots(114)$$

Substituting the value of $f(\theta)$ (for only the Coulomb force) from equation (111) in equation (103), we get

$$\frac{d\sigma}{d\Omega}=\left[\frac{e^2}{8\pi\varepsilon_0 E}\right]^2\left[cosec^4\frac{\theta}{2}+sec^4\frac{\theta}{2}-cosec^2\frac{\theta}{2}sec^2\frac{\theta}{2}\cos\left(\eta\log_e tan^2\frac{\theta}{2}\right)\right] \quad ...(115)$$

Here all quantities are measured in the center of mass system.

This is called Mott scattering cross section due to Coulomb force only.

The negative sign is because the protons obey Fermi statistics. Second and third terms drop out for unlike charged particles. For proton energies above 1 MeV, the cosine term is nearly unity as $e^2/4\pi\varepsilon_0\hbar v < 1/7$ unless $\theta/2$ is close to zero or $\pi/2$. Thus the Mott term is simplified and the above equation reduces to

$$\frac{d\sigma}{d\Omega}=\left(\frac{e^2}{8\pi\varepsilon_0 E}\right)^2\left[\frac{1}{\sin^4\theta/2}+\frac{1}{\cos^4\theta/2}-\frac{1}{\sin^2\theta/2\cos^2\theta/2}\right] \quad ...(116)$$

The first term is same as obtained by Rutherford by classical theory. Because the particles are identical (both incident and target protons), it is difficult to distinguish between these protons, therefore second term is same as obtained by replacing θ by $\pi-\theta$. The third term is the wave mechanical term which represents the interference between the wave functions of the protons.

Since the Coulomb force has a long range and even at the lowest energies high angular momenta are scattering. However at low energies the nuclear interaction effect is obtained by considering *S*-wave nuclear scattering only, which produces nuclear phase shift δ_0. Thus the total differential scattering cross section is given by

$$\frac{d\sigma}{d\Omega}=\left(\frac{e^2}{8\pi\varepsilon_0 E}\right)^2\left[\frac{1}{\sin^4\theta/2}+\frac{1}{\cos^4\theta/2}-\frac{\cos(\eta\log_e\tan^2\theta/2)}{\sin^2\theta/2\cos^2\theta/2}-\frac{2\sin\delta_o}{\eta}\left\{\frac{\cos(\delta_o+\eta\log_e\sin^2\theta/2)}{\sin^2\theta/2}\right.\right.$$

$$\left.\left.+\frac{\cos(\delta_o+\eta\log_e\cos^2\theta/2}{\cos^2\theta/2}\right\}+\frac{4}{\eta^2}\sin^2\delta_0. \quad ...(117)$$

In this equation the last term is due to nuclear scattering and the fourth term due to the interference between the Coulomb and nuclear scattering. This equation reduces to equation (116) for a Coulomb force when the nuclear phase shift δ_o is zero, *i.e.*, when there is no nuclear scattering effect. The last term would stand only, if the protons were uncharged. The fourth term is useful in determining δ_o when σ_o is small, because it is linear in $\sin\delta_o$ and is larger compared to the last term which involves $\sin^2\delta_o$. The linearity of δ_o of the interference term also permits determination of whether the nuclear potential is repulsive or attractive, as δ_0 is positive corresponding to attractive potentials and negative to repulsive potentials. For large energies the last term becomes the most important because of the v^2 coefficient.

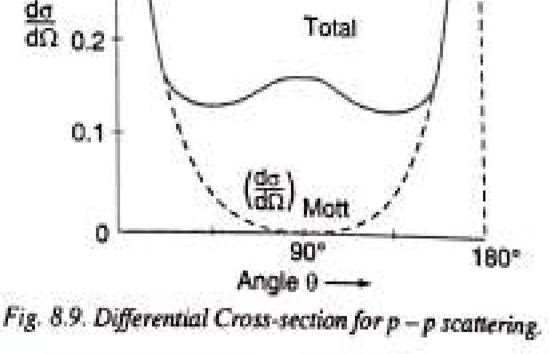

Fig. 8.9. Differential Cross-section for p – p scattering.

The differential cross section is a complicated function of the energy *E*, the angle of scattering θ and the phase shift δ_0. Differential cross section for *p* – *p* elasic scattering for 2.4 MeV protons is shown in Fig. 8.9. At small scattering angles the scattering is essentially pure Coulomb scattering. The nuclear scattering predominates in the central region of angles, near a *C.M.* angle of 90° (lab angle of 45°). At forward and backward angles, the dips are caused by interference between nuclear and Coulomb scattering.

8.6 EFFECTIVE RANGE THEORY OF p-p SCATTERING

Effective range calculations for *p-p* scattering are similar to those for *n-p* scattering, except that the Coulomb potential is included along with the nuclear potential. We consider the *S*-wave scattering for the *p-p* system and Coulomb forces (*CM*-frame) at two different energies E_1 and E_2 within the range of the nuclear force. Thus we have

$$\frac{d^2u_1}{dr^2}+\frac{2m}{\hbar^2}\left[E_1-V(r)-\frac{e^2}{4\pi\varepsilon_0 r}\right]u_1=0 \qquad \ldots(118)$$

and

$$\frac{d^2u_2}{dr^2}+\frac{2m}{\hbar^2}\left[E_2-V(r)-\frac{e^2}{4\pi\varepsilon_0 r}\right]u_2=0. \qquad \ldots(119)$$

Multiplying these equations by u_2 and u_1 respectively and subtracting, we get

$$u_1''u_2-u_2''u_1 = (k_2^2-k_1^2)u_1u_2, \qquad \ldots(120)$$

where

$$k_1^2 = 2mE_1/\hbar^2 \text{ and } k_2^2=2mE_2/\hbar^2.$$

At large distance r, $V(r)=0$ and we introduce the two Coulomb wave functions $v_1(r)$ and $v_2(r)$ which are asymptotic forms of $u_1(r)$ and $u_2(r)$ outside the range of the nuclear force. They satisfy the differential equations

$$\frac{d^2v_1}{dr^2}+\left[k_1^2-\frac{2me^2}{4\pi\varepsilon_0\hbar^2 r}\right]v_1=0 \qquad \ldots(121)$$

and

$$\frac{d^2v_2}{dr^2}+\left[k_2^2-\frac{2me^2}{4\pi\varepsilon_0\hbar^2 r}\right]v_2=0. \qquad \ldots(122)$$

Multiplying these equations by v_2 and v_1 respectively and substracting, we get

$$v_1''v_2-v_2''v_1 = (k_2^2-k_1^2)v_1v_2. \qquad \ldots(123)$$

Subtracting equation (120) from equation (123), we get

$$v_1''v_2-v_2''v_1-u_1''u_2+u_2''u_1 = (k_2^2-k_1^2)(v_1v_2-u_1u_2).$$

or

$$\left[v_1'v_2-v_2'v_1-u_1'u_2+u_2'u_1\right]_0^\infty = \int_0^\infty(k_2^2-k_1^2)(v_1v_2-u_1u_2)\,dr. \qquad \ldots(124)$$

At $r\to\infty$, u's and v's become identical. At $r=0$, the u's must vanish to keep ψ = finite. Therefore

$$[v_1'v_2-v_2'v_1]_{r=0} = (k_2^2-k_1^2)\int_0^\infty(v_1v_2-u_1u_2)\,dr. \qquad \ldots(125)$$

Because of the Coulomb interaction, $v(r)$ cannot be treated in precisely the same way as in *n-p* scattering. One can see that the solution of the Coulomb equation is made up of a linear combination of sine and cosine terms having the argument $[kr-\eta\log_e 2kr+\text{const}]$, where $\eta=e^2/4\pi\varepsilon_0\hbar v$. The constant is chosen so that sine term becomes the asymptotic form and is zero at $r=0$ and thus is the regular solution. The cosine term does not vanish at $r=0$ and thus forms the irregular solution.

The regular solution is

$$F_l(kr)\sim\sin[kr-\eta\log_e(2kr)-l\pi/2+\xi_l] \qquad \ldots(126)$$

where

$$\xi_l = \arg\Gamma(l+1+i\eta)=\xi_o+\sum_{s=1}^{l}\tan^{-1}\frac{\eta}{s}. \qquad \ldots(127)$$

For $l=0$, this reduces to

$$F_0(kr) = C_0 kr(1+\eta kr+\ldots) \qquad \ldots(128)$$

where

$$C_0^2 = 2\pi\eta/(e^{2\pi\eta}-1).$$

C_0 is the Coulomb penetration factor. At low energies < 100 keV, the Coulomb field prevents the protons from approaching close to the nuclear potential to have any effect. At higher energies (small η), $C_0\to1$ and the scattering is due to nuclear potential mainly except at small scattering angles.

The irregular solution is

$$G_l(kr) = \cos\left(kr-\eta\log_e(2kr)-\frac{l\pi}{2}+\xi_l\right) \qquad \ldots(129)$$

For $l=0$, this reduces to

$$G_0(kr) = \frac{1}{C_0}\left[1+2\eta kr\{\log_e(2\eta kr)+(2\gamma-1)+h(\eta)\}+\ldots\right], \qquad \ldots(130)$$

where γ = Euler's constant = 0.57722 and the function

$$h(\eta) = \eta^2 \sum_{n=1}^{\infty} \frac{1}{n(n^2+\eta^2)} - \log \eta - \gamma. \qquad \ldots(131)$$

For $\eta = 0$ (one particle uncharged), F_0 and G_0 reduce to the asymptotic form which corresponds to the wave function for the n-p system.

$$v_{np}(r) = \sin(kr+\delta)/\sin\delta = \cos kr + \cot\delta \sin kr. \qquad \ldots(132)$$

By analogy, the asymptotic form for the wave function of the p-p system is

$$v_{pp}(r) = C_0[G_0(kr) + \cot\delta\, F_0(kr)]$$

On differentiating, we get

$$\frac{dv}{dr} = C_0\frac{dG_0}{dr} + C_0 \cot\delta \frac{dF_0}{dr}. \qquad \ldots(133)$$

At

$$r = 0, (dF_0/dr) = C_0 k$$

and

$$\left(\frac{dG_0}{dr}\right) = \frac{1}{C_0}\left[\frac{1}{R}\log_e\frac{r}{R} + 2\frac{\gamma}{R} + \frac{1}{R}h(\eta)\right], \qquad \ldots(134)$$

where $R = 1/2\, \eta k$. Substituting these values in equation (133), we get

$$v'(0) = \frac{1}{R}\log_e\frac{r}{R} + \frac{2\gamma}{R} + \frac{1}{R}h(\eta) + C_0^2 k \cot\delta. \qquad \ldots(135)$$

As $r \to 0$, the first term is logarithmically divergent. It cancels out in the difference involved in equation (125). Thus from equations (125) and (135), we get

$$[\tfrac{1}{R}[h(\eta_2) - h(\eta_1)] + C_{02}^2 k_2 \cot\delta_2 - C_{01}^2 k_1 \cot\delta_1 = (k_2^2 - k_1^2)\int_0^\infty (v_1 v_2 - u_1 u_2)\, dr. \qquad \ldots(136)$$

Similar to the case of n-p scattering, for $k_1 \to 0$, we defnite

$$\lim_{k_1 \to 0}\left[C_{01}^2 k_1 \cot\delta_1 + \frac{1}{R}h(\eta_1)\right] = -\frac{1}{a_p}, \qquad \ldots(137)$$

where a_p is the scattering length for p-p scattering. Thus equation (136) may be written as

$$C_0^2 k \cot\delta + \frac{1}{R}h(\eta) = -\frac{1}{a_p} + k^2 \int_0^\infty (v v_0 - u u_0)\, dr. \qquad \ldots(138)$$

Similar to the case of n-p scattering, at low energies, we may write $v = v_0$ and $u = u_0$ and define

$$r_{op} = 2\int_0^\infty (v_0^2 - u_0^2)\, dr. \qquad \ldots(139)$$

where r_{op} is the effective range at about zero energy of incident protons. Thus equation (138) may be writeen as

$$C_0^2 k \cot\delta + \frac{1}{R}h(\eta) = -\frac{1}{a_p} + \frac{1}{2}k^2 r_{op}. \qquad \ldots(140)$$

This is the expression for p-p scattering in terms of the effective range r_{0p}, scattering length a_p and the Coulomb interaction $(1/R)\, h(\eta)$. At very low energies, the nuclear interaction between two protons is extremely small in comparison of the Coulomb interaction. By using extrapolation method, one can subtract the Coulomb part from the total and obtain the values of r_{op} and a_p.

For the comparison of experimental data, a nucler well shape parameter P is added and the equation (140) is modified as

$$C_0^2 k \cot\delta + \frac{1}{R}h(\eta) = -\frac{1}{a_p} + \frac{1}{2}k^2 r_{op} - P k^4 r_{op}^3. \qquad \ldots(141)$$

The parameter P is nearly zero in n-p scattering. In $l = 0$ state, the p-p system exists only in the singlet state (^1S and hence parameters to be determined are a_p and r_{op} for the singlet state. Detailed analysis of the differential and total cross section data for low energy p-p scattering has yielded the values for the parameters as

$$a_p = -7.8163 \pm 0.0048 \text{ fm}, \; r_{op} = 2.76 \pm 0.014 \text{ fm and } P = 0.028.$$

The negative value of a_p shows that *p-p* state is a unbound system. It is observed that the effective range for ${}^1S$ proton-proton system is very close to that for the ${}^1S$ neutron-proton system. This suggests that the nuclear forces in the two states may be very similar. The scattering lengths in these cases are however very different. By taking into account the Coulomb interaction as zero, the scattering length for the singlet state of *p-p* system is found to be −17.20 fm, which is quite close to the value for *n-p* scattering (−23.76 *fm*). *It further proves the charge independence of the nuclear forces.*

Experiments on p-p scattering. The experimental data are analyzed further along lines similar to those used in *n-p* scattering but are complicated considerably by the presence of the Coulomb force. In the interpretation of the *p-p* scattering results, the phase shifts δ_0 are the common meeting ground of experiment and theory. Jackson and Blatt showed that the observed variation of δ_0 with incident proton energy can be matched by any of the conventional shapes of potential well, with suitable choices of depth and range. A shape independent theory, therefore, has a natural attractiveness.

The fact that a_p is negative indicates that the ${}^1S$ state for the *p-p* system cannot be bound. Therefore the di-proton or ^{2}He can not exist. The exclusion principle prevents any ${}^3S$ state, which would be the analog of the stable deuteron. The absolute value of a_p requires further interpretation because it includes Coulomb as well as specifically nuclear effects. The latter can be isolated by treating the Coulomb force, with in the range of the nuclear force, as a small perturbation. Thus a_p is increased to the value equal to

$$a_{eq} = 17 \times 10^{-15} m.$$

We know that for neutron-proton ${}^1S$-state $a_s = -23.7 \times 10^{-15}$ m and $r_{0_s} = 2.46 \times 10^{-15}\ m$. The effective ranges do not differ significantly in view of their large experimental uncertainties. The scattering lengths are different significantly. Such a difference might arise from the magnetic moment interaction, as the intrinsic magnetic dipole moments of the neutron and proton are of opposite sign. Schwinger has evaluated a net attractive magnetic interaction in the ${}^1(np)$ force and a net attractive magnetic interaction in the ${}^1(pp)$ force. *This equality of the parameters of the (pp) and (np) singlet interactions gave rise to the hypothesis of the charge independence of the nuclear forces.* This hypothesis states that the forces between two nucleons in the same spin and orbital angular momentum state are *independent of the charge of the two nucleons.*

8.7 NEUTRON-NEUTRON SCATTERING

There is a scarcity of experimental data concerning the *n-n* system. The results for the ${}^1S_0$ scattering length are broadly falling into two distinct sets, one gives $a_{n\text{-}n} = -16$ *fm*, the value obtained for *n-p* or *p-p* scattering. The other set of values gives $a_s = 27 \pm 1.4$ fm, from a calculation making use of dispersion relations and charge symmetry for the *n-n* system. The experimental support for this prediction was provided by the values $a_s = -21.7 \pm 1.7$ *fm* obtained by Cerineo *et al.*,

$a_s = -23.6^{-1.6}_{+2.0}$ *fm* by Voitovetskii *et al.*, and $a_s = -25 \pm 3$ *fm* by Perrin *et al.* measured from the *d*(*n, p*) 2*n* reaction at about 14 MeV. The $a_s = -16.4 \pm 2.9$ *fm* is obtained by calculations of Heller *et al.* The greater diversity of experimental and theoretical evidence in favour of the second set inclines one to regard the first set as suspect. The results of Baumgartner *et al.* for the singlet *n-n* scattering parameters $a_s = 16.1 \pm 1.0$ *fm*. and $r_{eff,s} = 3.2 \pm 1.6$ *fm* are in agreement with those for the *p-p* system, but at variance with those for the *n-p* system.

To summarize the results of low energy scattering, the currently accepted scattering parameters are presented in the table 8.1.

Table 8.1. *Scattering parameters*

System	a_s *(fm)*	$r_{eff,s}$ *(fm)*	${}^1a_s$ *(fm)*	${}^1r_{eff,s}$ *(fm)*	${}^1a_t$ *(fm)*	$r_{eff,t}$ *(fm)*
$n-p$	-23.677 ± 0.029	2.46 ± 0.12	—	—	5.400 ± 0.011	1.732 ± 0.014
$p-p$	-7.8163 ± 0.0048	2.746 ± 0.014	-17.20	2.65	—	—
$n-n$	-16.1 ± 1.0	3.2 ± 1.6	—	—	—	—

Similarity Between (*nn*) and (*pp*) Forces

(*i*) Similar to diprotons, di-neutrons are not found in a stable stationary state. The scattering length for the (*nn*) interaction appears to have the same (negative) sign as that for the (*pp*) interaction.

(ii) The study of lightest pair of mirror nuclei, H^3 and He^3 provides us the direct evidence on the equivalence of $^1(nn)$ and $^1(pp)$ forces. The possible interactions between two particles in these nuclei can be written as

$$^3H \rightarrow {}^3(np) + {}^1(np) + {}^1(nn),\ {}^3He \rightarrow {}^3(np) + {}^1(np) + {}^1(pp).$$

These are all S-state interactions because orbital angular momentum is zero for each nucleus. The observed binding energy difference is 0.76 MeV. This corresponds to the Coulomb energy of two discreate protons $[\frac{3}{5}(e^2/4\pi\varepsilon_0 R)Z(Z-1) = 0.75\,\text{MeV}]$. This proves that $(nn) = (pp)$ force.

(iii) Inelastic scattering of deuteron by neutrons has given quantitative support to the similarity of (nn) and (pp) force.

(iv) The differential cross-sections at ~ 10 MeV for the $^3H\ (d, n)\ ^4He$ and $^3He\ (d, p)\ ^4He$ reactions show very similar asymmetries. These observations support the equality of (nn) and (pp) forces.

(v) Strong confirmation for equality of n-n and p-p forces comes also from the steady of heavier mirror nuclei, such as $^{31}_{16}S$ and $^{31}_{15}P$.

8.8 NON-CENTRAL FORCES

(a) Experimental evidence for the existence of non-central forces. A serious discrepancy was discovered between theory and experiment, performed by Kellogg *et al.* in 1939. The experimental results showed a fine structure in the radio frequency magnetic resonance spectrum of deuterium, but it was different from the theoretical prediction. The quadrupole moment established by this method was $2.82 \times 10^{-31}\ m^2$. It was assumed that n-p force was a central force. The ground state of deuteron must be a S-state whose quadrupole moment should be zero and the magnetic moment should be the algebraic sum of the magnetic moments μ_p and μ_n. The existence of quadrupole moments in heavier nuclei can be explained by assuming the force between neutron and proton as partly a central force and partly non-central (or *tensor*) force. From the small deviation of the deuteron wavefunction from spherical symmetry, we can calculate that the non-central part of the force is also very small compared to the central force part. The tensor force resembles a magnetic interaction between two dipoles. It results in a lower potential energy for n and p when the line joining them is ∥ to the spin direction than when it is ⊥.

***(b)* General form of the non-central force.** Let us now see whether we can construct a potential which depends not only on the relative position vector of the particles **r**, but also on their spin orientation $\boldsymbol{\sigma}_1$ and $\boldsymbol{\sigma}_2$ and which can account for the quadrupole moment. This potential must be invariant under rotations and reflections of the co-ordinate system which we use to describe the relative motion of the particles and hence must be a scalar.

Wigner and Eisenbud in 1941 has showed that, if the interactions are assumed to be invariant with respect to displacement, rotation and inversion of the observer's co-ordinate system and independent of the particle velocities, the general potential can be written as

$$V(r) = V_1(r) + V_2(r)\,\sigma_1 \cdot \sigma_2 + V_3(r)\,S_{12}. \qquad ...(142)$$

where the potentials V may depend on the orbital momentum of the two particle system as well as on the charge of the particles. The σ's being the particle spin axial vectors. The reasons of this limited choice are :

(1) The vector r changes to $-r$ under reflection and thus must occur in even powers only.

(2) Derivatives of **r** cannot occur since forces are velocity independent.

(3) Since σ_1 and σ_2 are not invariant against rotation and $\sigma_1 \cdot \sigma_2$ is invariant.

(4) $\sigma_1 \cdot r$ is invariant against rotation, but not against inversion, since $r \rightarrow -r$ and $\sigma \rightarrow \sigma$ on inversion.

Because of this, only even power of $(\sigma \cdot r)$ may occur such as $(\sigma_1 \cdot r)\,(\sigma_2 \cdot r)$.

The first term of equation (142) is corresponding to central force, the second term corresponding to a spin dependent but central force. The value of $\sigma_1 \cdot \sigma_2$ is 1 for a triplet state and –3 for a single state. The last term is corresponding to the interaction potential which depends not only on the separation between neutron and proton but also on the angle which their spins make with the line joining the two particles. The non-central character of the interaction is contained in the tensor operator, called a *tensor force operator*, and is given by

$$S_{12} = 3(\sigma_1 \cdot r)(\sigma_2 \cdot r)/r^2 - \sigma_1 \cdot \sigma_2. \qquad \text{...(143)}$$

The first term gives the dependence of the interaction upon the angle between the particle spin and the separation vector **r**. The second term has been subtracted so that the average of S_{12} over all directions **r** is zero.

(c) **Properties of the non-central force.** Since S_{12} is a scalar, the tensor force potential is a scalar. It can be shown that when $V_3(r)$ is finite, the total angular momentum **I** and the parity remain good quantum numbers but that the orbital angular momentum **L** and the spin angular momentum **S** are not constants of motion. The magnitude of the spin angular momentum S^2 is still a constant of motion for the two body systems.

The tensor operator S_{12} is defined in such a way that its average over all directions is zero. In the singlet spin state there is no preferred direction for the spin orientation hence total spin angular momentum

$$S = \tfrac{1}{2}(\sigma_1 + \sigma_2) = 0 \text{ or } \sigma_1 = -\sigma_2. \text{ Thus we get}$$

$$S_{12} = -3(\sigma_1 \cdot r)(\sigma_1 \cdot r)/r^2 + \sigma_1 \cdot \sigma_1 = -3 + 3 = 0.$$

This results that the tensor force is zero in the singlet state and all previous results for singlet states (*n-p* or *p-p* scattering) are unaffected entirely, *i.e.*, *in singlet states the nuclear forces are central forces.*

We also know that a triplet states of a given total angular momentum *I* can be written as a linear superposition of triplet states with orbital angular momenta $L = I - 1, I, I + 1$. Since parity of a wave function is $(-1)^L$, hence the state with $L = I$ has opposite parity to the two states with $L = I - 1$ and $L = I + 1$. Hence the $I = 1$ states of even parity are mixtures of $^3S_1$ and $^3D_1$ and the $I = 1$ states of odd parity are pure $^3P_1$. Proceeding this way, we have the following triplet states of the neutron-proton system with the tensor force as :

Table 8.2. *Triplet States*

I	*Even pariy*	*Odd parity*
0	—	^3P_o
1	$^3S_1, {}^3D_1$	$^3P_1$
2	$^3D_2$	$^3P_2, {}^3F_2$
3	$^3D_3, {}^3G_3$	$^3F_3$

The potential has a central force which is equal to the force between a neutron and a proton in the singlet spin state and a tensor force of somewhat longer range and of weaker strength than the central force. The central force between a neutron and a proton is spin independent. The spin dependence of the nuclear force arises entirely from the tensor force which is zero in the singlet spin state and is effective in the triplet spin state. Thus the existence of a bound triplet state of the n-p system is due to the tensor force.

(d) **The ground state of the deuteron :** The deuteron ground state wave function in the presence of a tensor force can be written as

$$\psi = \psi_S + \psi_D = \frac{u(r)}{r}\chi_S + \frac{w(r)}{r}\chi_D, \qquad \text{...(144)}$$

where χ_S and χ_D are functions of the angles describing the orientation of the neutron-proton separation vector **r** and of the spin variable of neutron and proton together. χ_S is independent of angles and symmetric in the neutron and proton spin, χ_D has a complicated dependence of angles.

The normalized spin angle wave functions Y^M_{JLS} belonging to a state of total angular momentum *J* whose z-component is *M* and which is a combination of an orbital angular momentum *L* with a spin *S* are used. Thus χ_S and χ_D are replaced by Y^M_{101} and Y^M_{121} respectively. The probability of finding the deuteron in the ^3S state is given by

$$P_S = \int_0^\infty u^2(r)\,dr, \qquad \text{...(145)}$$

and the probability of finding the deuteron in the ^3D state is given by

$$P_D = \int_0^\infty w^2(r)\,dr. \qquad \text{...(146)}$$

The radial functions are normalized so that

$$P_S + P_D = \int_0^\infty [u^2(r) + w^2(r)]dr = 1. \qquad \text{...(147)}$$

Table 8.2 shows that the tensor force operator S_{12} acting on the ${}^3S_1$ wavefunction Y_{101} can only lead to a linear combination of the ${}^3S_1$ and ${}^3D_1$ wave functions, *i.e.*,

$$S_{12}\, Y_{101}^M = a Y_{101}^M + b Y_{121}^M = b Y_{121}^M. \qquad \text{...(148)}$$

Here $a = 0$, because Y_{101}^M is independent of the direction $(l = 0)$ and the operation can not result in a spherical symmetric state $l = 0$.

$$S_{12}\, Y_{121}^M = b Y_{101}^M + c Y_{121}^M. \qquad \text{...(149)}$$

Here the constant b is same as in equation (148) because the tensor operator S_{12} is Hemitean. The calculations give $b = \sqrt{8}$ and $c = -2$.

Outside the range of nuclear forces, the deuteron ground state S-wave function, follows from the second order differential equation (Schrodinger equation) is given by

$$u(r) = N_S\, e^{-\alpha r} \qquad \text{...(150)}$$

and the D-wave function

$$w(r) = N_D\, e^{-\alpha r}\left[1 + \frac{3}{\alpha r} + \frac{3}{\alpha^2 r^2}\right]. \qquad \text{...(151)}$$

Here $1/\alpha$ is the size of the deuteron and N_S and N_D are the normalization constants.

A rough estimate of N_S can be obtained by neglecting D state probability $(p_S = 1)$, as

$$\int_0^\infty u^2(r)\, dr = 1 \text{ or } N_S^2/2\alpha = 1. \qquad \text{...(152)}$$

The value of N_D depends on the strength of the tensor force, will be determined later.

Magnetic moment of deuteron. We know that the small discrepancy between the sum of the magnetic moment of proton and neutron and the measured value for the deuteron can be interpreted as a contribution of the orbital motion of the proton in the D-state in the deuteron ground state. If nuclear forces are supposed to be central forces, the difference will be zero. This contribution can appear only with the non-central forces. The operator describing the magnetic moment of deuteron is

$$\mu = \mu_p \sigma_p + \mu_n \sigma_n + l_p, \qquad \text{...(153)}$$

where μ_n and μ_p are the magnetic moments of neutron and proton measured in nuclear magnetons, σ_n and σ_p their unitary spin operators and l_p is the orbital angular momentum of the proton about the center of mass of the bound system. The uncharged neutron cannot contribute any magnetic moment by orbital motion alone. In the centre of mass system the orbital angular momentum of the proton is half of the combined orbital angular momentum L.

Since $$\mu_n \sigma_n + \mu_p \sigma_p = \tfrac{1}{2}(\mu_n + \mu_p)(\sigma_n + \sigma_p) + \tfrac{1}{2}(\mu_n - \mu_p)(\sigma_n - \sigma_p)$$

Therefore equation (153) can be written as

$$\mu = \tfrac{1}{2}(\mu_n + \mu_p)\tfrac{1}{2}(\sigma_n + \sigma_p) + \tfrac{1}{2}(\mu_n - \mu_p)(\sigma_n - \sigma_p) + \tfrac{1}{2}L$$

Since the operator $(\sigma_n - \sigma_p)$ in the second term vanishes for a triplet state (as spins are parallel) and $\mathbf{I} = \mathbf{L} + \mathbf{S} = \mathbf{L} + \frac{1}{2}(\sigma_n + \sigma_p)$, hence the magnetic moment operator becomes

$$\mu = (\mu_n + \mu_p)\mathbf{I} - \left(\mu_n + \mu_p - \tfrac{1}{2}\right)\mathbf{L}. \qquad \text{...(154)}$$

The observed value of μ is the expectation value of this expression in the state with $I_z = I$. We therefore, can replace $\mathbf{L}$ by L_z. With the usual theory of quantum operators, we may write

$$\therefore \qquad \mathbf{L} \to L_z = \frac{\mathbf{L.I}}{I^2} I_z = \frac{I(I+1) + L(L+1) - S(S+1)}{2I(I+1)} I_z. \qquad \text{...(155)}$$

For the deuteron, $I(I + 1) = S(S + 1) = 2$ and in a mixture of S and D states, $L(L + 1)$ is 0 for the S-state and is 6 for the D-state. Therefore $[L(L + 1)]_{av} = 0 \times p_S + 6 \times p_D = 6p_D$. Here p_D and p_S represent the D-and S-state probabilities respectively. For the deuteron $I = 1$, the value of I_z in the state with $I_z = I$ is unity. Thus the expectation value of $\mathbf{L}_z$ is obtained by using eqn. (155).

$$\begin{aligned} <\psi|\mathbf{L}|\psi> &= 0 \text{ for the } S\text{-state} \\ &= 3/2 \text{ for the } D\text{-state.} \end{aligned} \qquad \ldots(156)$$

The deuteron's magnetic moment in units of the nuclear magneton is given by

$$\mu_d = P_S <\psi_S|\mu|\psi_S> + P_D <\psi_D|\mu|\psi_D> \qquad \ldots(157)$$

Substituting the values from equations (154) and (156) in the above equation, we get

$$\mu_d = P_S(\mu_n + \mu_p) + P_D\left[(\mu_n + \mu_p) - \tfrac{3}{2}\left(\mu_n + \mu_p - \tfrac{1}{2}\right)\right].$$

Since $P_S + P_D = 1$, therefore

$$\mu_d = (\mu_n + \mu_p) - \tfrac{3}{2}P_D\left(\mu_n + \mu_p - \tfrac{1}{2}\right). \qquad \ldots(158)$$

The last term gives a direct measure of the D-state probability P_D. The experimental results imply a D-state probability of about 3.93%. The above relation does not give accurate results. There are various other causes which can give corrections, especially of relativistic effects. Hence the measured magnetic moment gives only a rough estimate of the D-state probability. One may expect that the D-state probability P_D lies somewhere between 2 and 8%. Due to this reason, the n-p system is considered to be made up of 96% S-state and 4% D-state in the deuteron.

Electric Quadrupole moment. In chapter 1, the electric quadrupole moment Q was defined as the average value of $(3z^2 - r^2)$ in the state with $m = I$. When evaluating the quadrupole moment of the deuteron we must remember that only the proton contributes to the quadrupole moment and its distance from the centre of gravity is half of the proton neutron separation r. Hence the quadrupole moment operator for the deuteron is

$$Q = \tfrac{1}{4}(3z^3 - r^2) = \tfrac{1}{4}r^2(3\cos^2\theta - 1). \qquad \ldots(159)$$

Since the quadrupole moment is estimated from the S and D waves beyond the potential well, hence the expectation value of this operator $\mathbf{Q}$ is given by

$$(\psi, \mathbf{Q}\,\psi) = (\psi_S, \mathbf{Q}\,\psi_S) + (\psi_D, \mathbf{Q}\,\psi_D) + 2\,(\psi_S, \mathbf{Q}\,\psi_D). \qquad \ldots(160)$$

Since the S state is spherically symmetrical and cannot have a quadrupole moment. Therefore first term is zero. The second term is a pure D-state term and is smaller than the cross term (as $p_S >> p_D$). Hence only the cross term contributes. The measured quadrupole moment Q is the sum of the contributions of the second and third terms of equation (160), which have values.

$$(\psi_D, \mathbf{Q}\,\psi_D) = -\frac{1}{20}\int_0^\infty r^2 w^2(r)\,dr. \qquad \ldots(161)$$

and

$$2(\psi_S, \mathbf{Q}\,\psi_D) = \frac{\sqrt{2}}{10}\int_0^\infty r^2 u(r)\,w(r)\,dr. \qquad \ldots(162)$$

where the constants come from the spin sum and angular integration.

$$\therefore \quad Q = \frac{\sqrt{2}}{10}\int_0^\infty r^2 u(r)\,w(r)\,dr - \frac{1}{20}\int_0^\infty r^2 w^2(r)\,dr. \qquad \ldots(163)$$

Since the ground state of the deuteron is predominantly an S-state, the first term predominates over the second. Therefore the effective value of Q for deuteron is given by

$$Q = \frac{\sqrt{2}}{10}\int_0^\infty r^2 u(r)\,w(r)\,dr. \qquad \ldots(164)$$

$u(r)$ is the deuteron ground state S-wave function outside the range of nuclear forces and can be written as $u(r) = N_s e^{-\alpha r}$. $w(r)$ is the deuteron D-wave function at distance beyond the range of the specific potentials and can be written as

$$w(r) = N_D e^{-\alpha r}(1 + 3/\alpha r + 3/\alpha^2 r^2). \qquad \ldots(165)$$

Here N_S and N_D are normalization constants and $\alpha = \sqrt{(MB)}/\hbar^2$.

The rough estimate of N_S can be obtained by neglecting the small D-state probability compared to unity by substituting

$$P_S = \int_0^\infty u^2\,dr = 1, N_S = \sqrt{(2\alpha)}. \qquad \text{...(166)}$$

Since the weighing factor r^2 favours the contribution of the outside wave function (larger values of r), hence we can estimate the quadrupole moment by substituting the values of $u(r)$ and $w(r)$ into the equation (164). The result will be

$$Q = \frac{\sqrt{2}}{10}\int_0^\infty N_S N_D r^2 [e^{-\alpha r}]^2 \left[1 + \frac{3}{\alpha r} + \frac{3}{\alpha^2 r^2}\right] dr$$

$$= N_S N_D / \sqrt{8}\,\alpha^3. \qquad \text{...(167)}$$

This relation can be used for a good estimate of N_D. If value of N_S is taken as $\sqrt{2\alpha}$, we thus have

$$Q = N_D / 2\alpha^{5/2} \text{ or } N_D = 2Q\,\alpha^{5/2}. \qquad \text{...(168)}$$

Thus we see that the function $w(r)$ outside the range of the forces is determined completely by the quadrupole moment.

The D-state probability may be defined as

$$P_D = \int_0^\infty w^2(r)\,dr = \int_0^{R_T} w^2(r)\,dr + \int_{R_T}^\infty w^2(r)\,dr. \qquad \text{...(169)}$$

where R_T is the nuclear range of the tensor potential. If the square of the D-state radial wave function $w^2(r)$ is plotted against r. For small values of r, $w(r) = r^3$ and for large values of r, $w(r) = 1/r^2$. There is a sharp maximum at $r = r_m = R_T$, the range of the tensor forces. The behaviour of $w^2(r)$ for $r > R_T$ is determined to a first approximation by the value of the quadrupole moment of the deuteron. As a rough approximation, the total contribution of the wave function inside the potential is of the same order as outside, therefore equation (169) may be written as

$$P_D = 2\int_{R_T}^\infty w^2(r)\,dr = 2\int_{R_T}^\infty 9N_D^2 \left(\frac{1}{\alpha r}\right)^4 dr$$

$$= 6N_D^2 / R_T^3\,\alpha^4. \qquad \text{...(170)}$$

Here we have neglected first and second terms of the bracket and set the exponential equal to unity in the equation (165). Relation (170) shows that the D-state probability P_D depends strongly on the range of tensor force R_T and increases rapidly as R_T is made shorter. Substituting the value of N_D from equation (168), we get

$$P_D = 24Q^2\alpha / R_T^3. \qquad \text{...(171)}$$

This equation implies that the tensor force cannot have an arbitrarily small range otherwise the ground state would become a predominantly D state rather than predominantly S state. In that case the main contribution would have come from the direct D term instead of the term corresponding to the interference between S and D-waves. Since D term is negative. Since a high rotation will flatten the deuteron, as required by the positive quadrupole moment, the R_T can therefore not be taken as too small. The experimental value of Q is + 2.73 ($e \times 10^{-31}$ m^2).

A rough measurement of P_D is obtained from the deuteron magnetic moment (Eqn. 158). This value of P_D leads to a fair estimate of R_T, since it is in the cube of R_T which occurs in Eqn. (171). This gives that the tensor force range R_T falls near 3×10^{-15} m, which is almost independent of the range of the central force and is longer than the range of central forces.

***(e)* Neutron-Proton scattering below 10 MeV.** In principle the analysis of the scattering is very much altered by non-central forces. The separation of the various partial waves is not longer complete, since the orbital angular momentum l is not a constant of the motion. At energies below 10 MeV, it is advantageous to decompose the wave function into spherical harmonics by the use of the spin angular function. The spin S can have values 0 and 1 corresponding to the singlet and triplet states respectively. The S-scattering in the singlet state (S = 0) is unchanged by the presence of tensor forces since they do not act in that state. Therefore, we have to discuss only the triplet scattering. We know that the tensor force couples the $^3D_1$ state with the $^3S_1$ state. Thus both states contribute to the scattering even at low energies.

If the ingoing wave is a pure $^3S_1$ wave, the outgoing wave is a mixture of S and D waves owing to the action of the tensor force during the impact. Similarly an ingoing pure ${}^3D_1$ wave emerges as a mixture outgoing wave. The waves, which have the same mixture ratio of S to D states before and after the scattering event, are called *eigenstates for the scattering*. There are two such eigenstates : One is called the *α-wave* in which S wave is predominant. Other is called the *β-wave* in which D wave is predominant. Since we are dealing with the same angular momentum state $({}^3S_1 + {}^3D_1)$ as the ground state of the deuteron, the asymptotic form of perturbed $u(r)$ and $w(r)$ can be written in the form

$$\begin{aligned} u(r) &= a \sin(kr + \delta) \\ w(r) &= b \sin(kr + \delta - \pi), \end{aligned} \qquad \text{...(172)}$$

where the angle δ represents the phase shift compared to the asymptotic form of the unperturbed plane wave. The solution u, w of the wave equation is an eigen state of the scattering provided that the phase shift δ is the same for both $u(r)$ and $w(r)$. There are two (α and β) solutions satisfying this condition, with two different phase shifts (δ_α and δ_β) and two different values of the ratio b/a which determine $w(r)/u(r)$.

It can be shown that

$$b_\alpha/a_\alpha = -a_\beta/b_\beta. \qquad \text{...(173)}$$

This shows that the condition that the α-wave is predominantly an S-wave ($b_\alpha << a_\alpha$) implies automatically that the β-wave is predominatly a D-wave.

If we neglect the phase shifts of all the waves except the α-wave, the differential scattering cross-section in C-M system becomes

$$\frac{d\sigma}{d\Omega} = \frac{\sin^2 \delta_\alpha}{k^2}\left[1 + \left(1 + \frac{\tan\varepsilon}{\sqrt{8}}\right)^2 \sin^2(2\varepsilon)\, P_2(\cos\theta)\right]. \qquad \text{...(174)}$$

where P_2 (cos θ) is the second Legendre polynomial and $\varepsilon = \tan^{-1} b_\alpha/a_\alpha$, *i.e.* the asymptotic ratio of w to u, can be determined by the quadrupole moment as

$$\varepsilon = \tan\varepsilon = b_\alpha/a_\alpha = \sqrt{(2)}\, Qk^2. \qquad \text{...(175)}$$

If we substitute the numerical value of Q in this Eqn. and evaluate the angle dependent term in Eqn. (174), it gives that the coefficient of $P_2(\cos\theta)$ in the angular distribution is less than 0.01 ever. at 10 MeV. Hence this tensor effect in the scattering is much too small because in this energy region the experimental errors for angular distribution measurements are at present of the order of 10%. P-wave scattering can be expected to contribute terms with similar angle dependence of the same order of magnitude. The triplet parameters a_t and r_{ot} are not much affected by the tensor forces, if the potentials have similar shape.

(*f*) **Deuteron Photo disintegration**—Deuteron photo disintegration was first observed by Chadwick and Goldhaber in 1935. It is the interesting instance of an electromagnetic interaction of deuterons with γ-radiation. Barnes *et al.* in 1952 have carried out a set of absolute cross-section measurements with mono energetic γ-rays over the range 2.5 to 17.6 MeV. The results were found to agree with the theoretical predictions (within 5-10%) for magnetic dipole (${}^3S_1 \rightarrow$ virtual ${}^1S_0$) and electric dipole (${}^3S_1 \rightarrow$ virtual ${}^3P_{0,1,2}$) transitions, as shown in Fig. 8.10. Here *ED* means electric dipole absorption and *MD* means magnetic dipole absorption. In these experiments, the disintegration rate was measured by counting ionization pulses from the photo protons in a spherical chamber filled with gaseous deuterium.

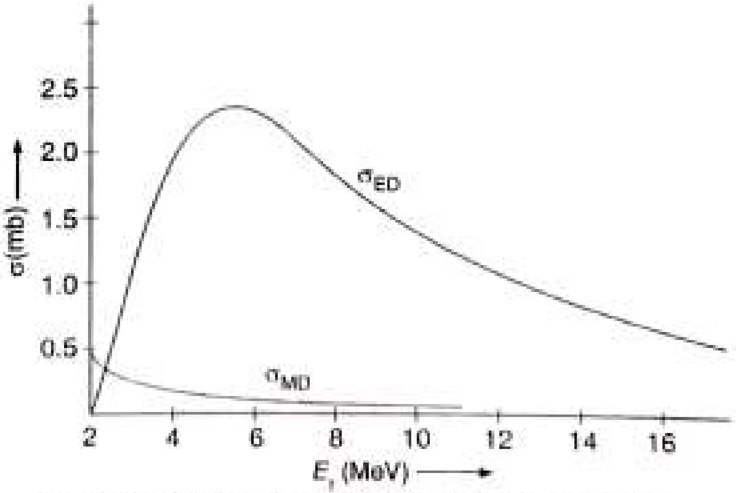

Fig. 8.10 The deuteron photo disintegration cross section.

At energies around $E_\gamma = 2.2$–4 MeV, the magnetic photo effect is not negligible and the photo nucleon distribution is more complicated, because of the interference between the outgoing S-wave from an M_1 interaction and the emergent P wave from the E_1 interaction. The angular distribution has the form

$$W(\theta) = A + B\sin\theta + C\sin^2\theta. \qquad ...(176)$$

The electric dipole distribution will be modified by the presence of an initial ^3D wave in the deuteron, giving the possible transitions $^3D_1 \rightarrow {}^3P_{0,1,2}$. The photo magnetic cross-section at low energies will be more strongly modified due to $^3D_1 \rightarrow {}^1D_2$ transitions. As it itself is very small except at the lowest energies, therefore the non-isotropic term arises due to this transition is too small to be seen.

Above 10 MeV, a forward asymmetry due to interference between outgoing waves of different parity should be observed in the photo nucleon distribution. The influence of tensor force (^3D) appears to be negligible below about 20 MeV. In general, the tensor force affects low energy processes very little except for the quadrupole moment.

8.9 SATURATION OF NUCLEAR FORCES

Thus far we have discussed mainly the character of the forces acting between pairs of nucleons. When we come to consider systems comprising more than two particles, we must except some complications to enter. We shall deal with certain quantitative aspects of nuclear forces which become important when not only the two body problem but also the properties of other nuclei are studied. There are two important facts : the density of nucleons is roughly equal for all nuclei (*saturation of density*), and the binding energy per nucleon is roughly equal for all nuclei (*saturation of binding energy*).

In the case of two body problem, following assumptions have been made about the nuclear forces :

(a) The nuclear force acts between the pairs of nucleons and is not influenced by the presence of neighbouring nucleons.

(b) The nuclear force between the nucleons is velocity independent, always attractive, independent of the type of the nucleons and is same for all relative orbital angular momenta.

(c) It is predominantly a central force.

These assumptions do not correspond to reality. The first assumption is modified. The force between two nucleons is attractive for distances $r > d$, and is repulsive otherwise. Hence d is of the order of the distance between nearest neighbours in the nuclei. For $r < d$, the force becomes highly repulsive. *Thus the force between two nucleons is attractive or repulsive depending on the state of the two nucleons with respect to each other*. Let us discuss the other explanations of the constant density and constant binding energy per nucleon.

(A) Exchange Forces. In 1932, Heisenberg proposed, in order to explain the saturation of nuclear forces, that nuclear forces were *exchange forces* which would depend explicitly on the symmetry of the wave function. At the time of Heisenberg's idea of exchange forces, mesons were known and it was known that π-meson was being exchanged between nucleons, by any of the following processes :

$$\begin{array}{llll}
n, p\ ; p, n & ; p, p & ; n, n \\
p + \pi^-, p\ ; n + \pi^+, n & ; p + \pi^\circ, p & ; n + \pi^\circ, n \\
p, \pi^- + p\ ; n, \pi^+ + n & ; p, \pi^\circ + p & ; n, \pi^\circ + n \\
p, n \quad ; n, p & ; p, p & ; n, n.
\end{array}$$

The exchange of a pion is thus equivalent to charge exchange. We can think of the nucleons as exchanging their space and spin co-ordinates. The wave equation of the two body system for an ordinary central force is

$$[(\hbar^2/M)\,\nabla^2 + E]\,\psi(\mathbf{r}_1, \mathbf{r}_2, \sigma_1, \sigma_2) = V(\mathbf{r})\,\psi(\mathbf{r}_1, \mathbf{r}_2, \sigma_1, \sigma_2). \qquad ...(177)$$

The force is known as *no exchange, ordinary or Wigner* force. The interaction does not cause any exchange between coordinates of the two particles and therefore no exchange of any particle properties. Another type of interaction in which there is an interchange of location, *viz. coordinate exchange* between the particles, is called *Majorana force*. For such interaction Schrodinger equation is written as

$$[(\hbar^2/M)\,\nabla^2 + E]\,\psi\,(\mathbf{r}_1, \mathbf{r}_2, \boldsymbol{\sigma}_1, \boldsymbol{\sigma}_2) \;=\; V(\mathbf{r})\,\psi\,(\mathbf{r}_2, \mathbf{r}_1, \boldsymbol{\sigma}_1, \boldsymbol{\sigma}_2). \qquad ...(178)$$

The interaction in which there is a *spin exchange* between the particles is called *Bartlett force.*

$$[(\hbar^2/M)\,\nabla^2 + E]\,\psi\,(\mathbf{r}_1, \mathbf{r}_2, \boldsymbol{\sigma}_1, \boldsymbol{\sigma}_2) \;=\; V(\mathbf{r})\,\psi\,(\mathbf{r}_1, \mathbf{r}_2, \boldsymbol{\sigma}_2, \boldsymbol{\sigma}_1). \qquad ...(179)$$

Another type of interaction in which the exchange of position and spin coordinates between the particles occur is called *Heisenberg force.*

$$[(\hbar^2/M)\,\nabla^2 + E]\,\psi\,(\mathbf{r}_1, \mathbf{r}_2, \boldsymbol{\sigma}_1, \boldsymbol{\sigma}_2) \;=\; V(\mathbf{r})\,\psi\,(\mathbf{r}_2, \mathbf{r}_1, \boldsymbol{\sigma}_2, \boldsymbol{\sigma}_1). \qquad ...(180)$$

Named after the investigators who first explored their characteristics, these forces have different properties and effects.

Effects of exchange forces—Exchange forces with a $V(r)$ are central forces and do not cause mixing of orbital angular momenta. If the potential includes a tensor force, this will mix different l's.

(1) Majorana Forces. The Majorana interaction is that in which it is assumed that two particles attract one another if the wave function describing the entire system does not change sign when the special co-ordinates of the two particles are interchanged and that they repel if the wave function changes sign. This interaction reflects the coordinates and replaces **r** by −**r** in the wave-function. Hence Eqn. (178) may be written as

$$[(\hbar^2/M)\,\nabla^2 + E]\,\psi\,(\mathbf{r}) \;=\; (-1)^l\,V(\mathbf{r})\,\psi\,(\mathbf{r}). \qquad ...(181)$$

This equation indicates that the force is always attractive for states of even l and always repulsive for states of odd l.

(2) Barlett Forces. The wave function of two particles is symmetric if the total spin $S = 1$ and anti-symmetric if $S = 0$. Thus equation (179) gives

$$[(\hbar^2/M)\,\nabla^2 + E]\,\psi\,(\mathbf{r}) \;=\; (-1)^{S+1}\,V(\mathbf{r})\,\psi(\mathbf{r}). \qquad ...(182)$$

This relation is equivalent to an ordinary potential which changes sign between $S = 0$ and $S = 1$. The nuclear force can not be totally of the Bartlett type because it is clear from neutron-proton scattering data that both the ^3S potentials are attractive.

(3) Heisenberg Forces. Combining the arguments of the last two cases, we see that the wave function of two particles is symmetric for $(l + S)$ even and anti-symmetric for $(l + S)$ odd, hence equation (180) may be written as

$$[(\hbar^2/M)\,\nabla^2 + E]\,\psi\,(\mathbf{r}) \;=\; (-1)^{l+S+1}\,V(\mathbf{r})\,\psi(\mathbf{r}). \qquad ...(183)$$

This relation indicates that sign of ordinary potential is positive if $(l + S)$ is odd and is negative if $(l + S)$ is even. This gives that the force is attractive for even l triplet states and odd l singlet states, but is repulsive in odd l triplet and even l singlet states. Thus for ^3S, ^1P the potential is $V(\mathbf{r})$ and is $-V(\mathbf{r})$ for ^1S and ^3P. The reversal of sign between ^3S and ^1S states indicates that the nuclear force cannot be wholly of the Heisenberg type. The difference between the *n-p* interactions in these states can be explained by assuming that the interaction is roughly 25 per cent Heisenberg or Bartlett and 75 per cent Wigner or Majorana.

These three types of exchange operators are represented by $\mathbf{P}^W$, $\mathbf{P}^M$, $\mathbf{P}^B$ and $\mathbf{P}^H$. Thus the Schrodinger equations may be written as

$$\begin{aligned}
\mathbf{P}^W\,\psi\,(\mathbf{r}_1, \mathbf{r}_2; \boldsymbol{\sigma}_1, \boldsymbol{\sigma}_2) &= \psi\,(\mathbf{r}_1, \mathbf{r}_2; \boldsymbol{\sigma}_1, \boldsymbol{\sigma}_2)\\
\mathbf{P}^M\,\psi\,(\mathbf{r}_1, \mathbf{r}_2; \boldsymbol{\sigma}_1, \boldsymbol{\sigma}_2) &= \psi\,(\mathbf{r}_2, \mathbf{r}_1; \boldsymbol{\sigma}_1, \boldsymbol{\sigma}_2)\\
\mathbf{P}^B\,\psi\,(\mathbf{r}_1, \mathbf{r}_2; \boldsymbol{\sigma}_1, \boldsymbol{\sigma}_2) &= \psi\,(\mathbf{r}_1, \mathbf{r}_2; \boldsymbol{\sigma}_2, \boldsymbol{\sigma}_1)\\
\mathbf{P}^H\,\psi\,(\mathbf{r}_1, \mathbf{r}_2; \boldsymbol{\sigma}_1, \boldsymbol{\sigma}_2) &= \psi\,(\mathbf{r}_2, \mathbf{r}_1; \boldsymbol{\sigma}_2, \boldsymbol{\sigma}_1)
\end{aligned}$$

Wigner operator is simply the identity operator. The Majorana exchange operator interchanges the positions of the two particles leaving their spin directions uneffected. The Bartlett exchange operator exchanges the spin directions of the two particles, leaving their positions uneffected. The Heisenberg exchange operator interchanges both position and spin directions. Therefore we may write

$$P^W \;=\; 1,\; P^H = P^M P^B \text{ and } (P^M)^2 = (P^B)^2 = (P^H)^2 = 1. \qquad ...(184)$$

This shows that each of the three exchange operators has only two eigenstates +1 and −1. The Majorana exchange operator is +1 for the states of even l and −1 for the states in odd l. The Bartlett exchange operator gives +1 in triplet states and −1 in singlet states, independent of l. In the various states of the two particle systems, the exchange operators have the values given below :

Table 8.3. *Exchange operators and their values*

Operator	*Even parity States*		*Odd Parity State*	
	Triplet	*Singlet*	*Triplet*	*Singlet*
$\mathbf{P}^M$	1	1	−1	−1
$\mathbf{P}^B$	1	−1	1	−1
$\mathbf{P}^H$	1	−1	−1	1

Serber in 1936 concluded from the observed constancy of E_B/A with A that n-n and p-p forces must be a combination of Wigner and Majorana components, as a pure Wigner type gives E_B/A to increase with A and a pure Majorana type gives E_B/A to decrease with A. Now one-to-one mixture is adopted, however Serber proposed originally $\frac{1}{3}$ Wigner $+\frac{2}{3}$ Majorana. Since $P^M = -1$ in states of odd parity, the Serber potential would suggest that there is no interaction between nucleons in states of odd relative orbital momentum l. The experimental evidence shows that the interaction force in P- and F-states is considerably weaker than that in the even parity S- and D-states.

The most general potential of the exchange type is written in the form

$$V = V(\mathbf{r}) = V_W(\mathbf{r}) + V_M(\mathbf{r})\,P^M + V_B(\mathbf{r})\,P^B + V_H(\mathbf{r})\,P^H, \qquad ...(185)$$

where $\mathbf{r}$ is the distance between the two particles.

The tensor force may or may not have an exchange character. The tensor operator S_{12} commutes with the Bartlett spin exchange operator P^B. Thus $P^B S_{12} = P^B = S_{12}$ and there are two types of tensor forces only, the ordinary (Wigner) tensor force and tensor force with the Majorana exchange character. Therefore the most general potential of the exchange type has the form

$$V = V_W(\mathbf{r}) + V_M(\mathbf{r})\,P^M + V_B(\mathbf{r})\,P^B + V_H(\mathbf{r})\,P^H + V_{TW}(\mathbf{r})\,S_{12} + V_{TM}(\mathbf{r})\,S_{12}\,P^M. \qquad ...(186)$$

This potential also has tensor operator S_{12} term for mixtures of Wigner and Majorana forces. More general forms of potentials have been discussed by Gillet, Green and Sanderson in 1966.

Exchange forces and Saturation—The Bartlett spin exchange force does not lead to saturation of the binding energy per nucleon. If the nuclear forces are of Bartlett type, the heavy nuclei would exist with all spins aligned where the number of interacting nucleon pairs is $A(A-1)/2$, which leads to $E_B/A \propto A$. However, the space exchange in the Majorana and the Heisenberg forces leads to saturation because the sign of potential changes between odd and even l. The space exchange part of the Heisenberg force also causes saturation. A pure Heisenberg force and a pure Bartlett force can be ruled out because either one has opposite sign in singlet and triplet states of the two particle system. Purely attractive Wigner forces are excluded by the requirement of saturation of nuclear binding energies.

Let us now consider a potential in which both Wigner and Majorana forces are present, but which does not contain Heisenberg or Bartlett forces. For the pair i, j. The potential is defined as

$$\begin{aligned} V_{ij} &= V_W + V_M\,P_{ij}^{\,M} && (\text{for } r_{ij} < b) \\ &= 0 && (\text{for } r_{ij} > b) \end{aligned} \qquad ...(187)$$

Every distance r_{ij} is necessarily smaller than b. When the exchange operator $P_{ij}^{\,M}$ operates upon a pair i, j in the same state m, the wave function remains unchanged, hence each such pair contributes +1. If the pair consists of two identical particles, the wavefunction must change its sign and these pair contribute −1. If the exclusion principle did not apply, we could put all the nucleons into the lowest space state. Then all pairs would be symmetric and we would not find any difference between Wigner and Majorana forces in the collapsed state.

The Majorana force must contribute at least four fifths of the attraction in the ground state of the deuteron. The Heisenberg forces would give special stability to the deuteron and Majorana forces to the α-particles. The Bartlett forces do not give saturation. The inclusion of the repulsive core in the nuclear force prevents the nucleus from collapsing and helps saturation.

(B) Isotopic Spin Formalism. In this formalism we are considering the proton and the neutron as different quantum states of the same particle, the nucleon. The total wave-function is written as a product of the space part, a spin part and an isospin part. The nucleus must obey Fermi-statistics in order to the consistent with the ordinary theory. Thus the total wave-function for the two or more particles

$$\psi = \psi\,(\mathit{space})\,\psi\,(\mathit{spin})\,\psi\,(\mathit{isotopic\ spin}) \qquad \text{...(188)}$$

must be anti-symmetric with respect to interchange of all co-ordinates of two nucleons. In the ground state of the deuteron, for example, ψ (space) is symmetric, as it is a mixture of an *S*-state and a *D*-state, ψ (spin) is symmetric (the two spins are parallel), so that the ψ (isotopic spin) must be anti-symmetric and thus $T = 0$ (the two isotopic spins are oppositely oriented). The lowest state of deuteron in which the two nucleon spins are opposed, ψ (spin) is then anti symmetric, and thus we have $T = 1$.

The concept of the T multiplet has been applied to β-decay, γ-decay and to nuclear reactions. *The success of these applications supplies additional support for the hypothesis of the charge independence of nuclear forces.*

In order to confirm with isospin conservation, the Hamiltonian describing the interaction between two nucleons must be rotationally invariant in isospace. Thus it must contain scalar quantities formed with the isospins τ_1 and τ_2. The product of operators $\tau_1 . \tau_2$ gives +1 when applied to isotopic spin triplet states and −3 when applied to isotopic spin singlet states. We can use $\tau_1 . \tau_2$ to define an isotopic spin operator P^τ analogous to spin operator σ.

$$P^\tau = \tfrac{1}{2}(1 + \tau_1 \cdot \tau_2). \qquad \text{...(189)}$$

The operator gives +1 when applied to the (symmetric) isotopic spin triplet states, −1 when applied to the (anti-symmetric) isotopic spin singlet states. Hence it is equivalent to simple exchange of the isotopic spin co-ordinates η_1 and η_2 of the two particles. Thus we can write

$$P^\tau \psi\,(\mathbf{r}_1, \zeta_1, \eta_1\,;\, \mathbf{r}_2, \zeta_2, \eta_2) = \psi\,(\mathbf{r}_1, \zeta_1, \eta_2;\, \mathbf{r}_2, \zeta_2, \eta_1), \qquad \text{...(190)}$$

where $\mathbf{r}_1$ denotes the position of the one particle and ζ_1 its spin direction.

We have required complete anti-symmetry under the full exchange of all the co-ordinates of the two particles. Since Heisenberg exchange operator P^H exchanges position and mechanical spin and the isotopic spin operator P^τ exchanges the isotopic spin co-ordinates, hence we can write

$$P^H P^\tau \psi = -\psi. \qquad \text{...(191)}$$

This is a condition on ψ, not an operator identity. We multiply equation (190) by P^τ on both sides and have

$$P^H \psi = -P^\tau \psi. \qquad \text{...(192)}$$

because equation (189) shows that $(P^\tau)^2 = 1$.

It is clear from equation (191) that we can replace the Heisenberg exchange operator P^H by the isotopic spin operator $-P^\tau$ in all applications with the restriction of isotopic spin wave functions obeying the Pauli principal. As the Bartlett exchange operator P^B can be written as

$$P^B = \tfrac{1}{2}(1 + \sigma_1 \cdot \sigma_2) \qquad \text{...(193)}$$

Thus we can replace the Majorana exchange operator by the combination

$$P^M = P^B P^H = \tfrac{1}{4}(1 + \sigma_1 \cdot \sigma_2)(1 + \tau_1 \cdot \tau_2) \qquad \text{...(194)}$$

Equations (192), (193) and (194) show the expressions for the three linearly independent exchange operators in terms of the mechanical and isotopic spin operators. From the point of view of the isotopic spin formalism it is more convenient to use three other linearly independent operators $(\sigma_1 \cdot \sigma_2)$, $(\tau_1 \cdot \tau_2)$ and $(\sigma_1 \cdot \sigma_2)\,(\tau_1 \cdot \tau_2)$. The values of these products in states of the two particle system are listed below :

Table 8.4 *The Values of the spin products*

Spin product	Even parity state		Odd parity state	
	triplet	singlet	triplet	singlet
$\sigma_1 \cdot \sigma_2$	1	−3	1	−3
$\tau_1 \cdot \tau_2$	−3	1	1	−3
$(\sigma_1 \cdot \sigma_2)(\tau_1 \cdot \tau_2)$	−3	−3	1	9

The most general potential of the exchange type is thus written in the form

$$V = V_d(\mathbf{r}) + V_\sigma(\mathbf{r})(\sigma_1 \cdot \sigma_2) + V_\tau(\mathbf{r})(\tau_1 \cdot \tau_2) + V_{\sigma\tau}(\mathbf{r})(\sigma_1 \cdot \sigma_2)(\tau_1 \cdot \tau_2) + V_{Td}(\mathbf{r})\, S_{12} + V_{T\tau}(\mathbf{r})\, S_{12}(\tau_1 \cdot \tau_2) \quad ...(195)$$

where

$$\begin{aligned} V_d &= V_W + \tfrac{1}{2} V_B - \tfrac{1}{2} V_H - \tfrac{1}{4} V_M,\ V_\sigma = \tfrac{1}{2} V_B - \tfrac{1}{4} V_M \\ V_\tau &= \tfrac{1}{2} V_H - \tfrac{1}{4} V_M,\ V_{\sigma\tau} = \tfrac{1}{4} V_M, \\ V_{Td} &= V_{TW} - \tfrac{1}{2} V_{TM} \text{ and } V_{T\tau} = \tfrac{1}{2} V_{TM}. \end{aligned} \quad ...(196)$$

The first form terms of equation (195) are the central force terms. Here the subscript d denotes dependence on the distance only. For non exchange or ordinary type of forces $V_d = V_W$.

Rarita and Schwinger have exployed exchange forces of two types : The *symmetry theory* and *charged theory*. In the former, isotopic spin dependence of potential is given by $\tau_1 \cdot \tau_2$ and in the latter it is given by $\tau_1 \cdot \tau_2 - \tau_{z1}\, \tau_{z2}$. In the charged theory, there is no force between two protons or between two neutrons ($\eta = 1$ for neutron and −1 for a proton), the force acts only between a proton and a neutron. These two exchange potentials are defined by

$$V_d(\mathbf{r}) = V_\sigma(\mathbf{r}) = V_{Td}(\mathbf{r}) = 0 \qquad \textit{(Symmetry theory)} \quad ...(197)$$

and other three functions $V(\mathbf{r})$ being arbitrary and

$$V_d(\mathbf{r}) = V_\tau(\mathbf{r}),\ V_\sigma(\mathbf{r}) = V_{\sigma\tau}(\mathbf{r}),\ V_{Td}(\mathbf{r}) = V_{T\tau}(\mathbf{r}) \qquad \textit{(Charged Theory)} \quad ...(198)$$

The latter conditions apply to the potential of interaction only between a proton and a neutron.

The saturation conditions can be formulated from the isotopic spin formalism as

$$\begin{aligned} & V_d = \text{value of } V_d(\mathbf{r}) \text{ inside the range } b, \text{ i.e. } V_d \geq 0 \\ & V_d + V_\sigma \geq 0,\ V_d + V_\tau \geq 0,\ V_d + V_{\sigma\tau} \geq 0 \\ & V_d + V_\sigma + V_\tau + V_{\sigma\tau} \geq 0. \end{aligned} \quad ...(199)$$

The saturation conditions for the tensor forces are

$$\begin{aligned} & -\tfrac{1}{2}(V_d + V_\tau) \leq V_{Td} \leq V_d + V_\sigma \\ & -\tfrac{1}{2}(V_d + V_{\sigma\tau}) \leq V_{T\tau} \leq V_d + V_{\sigma\tau} \\ & -\tfrac{1}{2}(V_d + V_\sigma + V_\tau + V_{\sigma\tau}) \leq V_{Td} + V_{T\tau} \leq V_d + V_\sigma + V_\tau + V_{\sigma\tau}. \end{aligned} \quad ...(20$$

These are not very important from a practical point of views.

8.10 HIGH ENERGY n-p AND p-p SCATTERING

The analysis of low energy data for nucleon-nucleon scattering and the deuteron problem has shown that the nucleon-nucleon potential has both central and tensor components and the potential is stronger in the triplet state. It can not provide the exchange character, velocity dependence, spin orbit coupling or the presence of short range repulsive core and the effects of higher angular momenta (l).

High energy scattering experiment can be used to investigate details of the potential shape and to learn about the two nucleon forces in states other than the S-state. The development of the high energy accelerators has made it possible to extend the energy range of n-p and p-p scattering to energies at which the de-Broglie wavelength of the relative motion is considerably smaller than the range of nuclear forces. At high energy, the presence of higher angular momentum states results in a large number of parameters making the data much more difficult to interpret. In the words of Blatt and Weisskopf, *the data available* *are strange and unexpected.* The analysis is still more complicated for neutrons since a mono-energetic neutron beam is not available. The cross-section, experimentally observed is an average over a rather large energy region and may consequently fail to show rapid energy dependence. The high energy *p-p* scattering data are easier to interpret than the $n - p$ scattering data, because the Pauli exclusion principle cuts the number of phase shifts in half and the experimental cross-section can be obtained with mono-energetic protons.

The observed quantities of high energy nucleon-nucleon scattering are : (*i*) total cross-section $\sigma(E)$ as a function of incident energy, (*ii*) angular distribution or differential cross-section $d\sigma/d\Omega$ or $\sigma(\theta)$ at various energies and (*iii*) polarization parameters and their related spin correlations coefficients. The high energy protons can be obtained from the accelerators and the mono energetic neutrons of high energy are generally obtained from (p, n), (d, n) or (γ, n) reactions. For obtaining very high energy neutrons heavier nuclei are also used sometimes as targets.

Although experimental data on *p-p* scattering (particularly) is available upto GeV range of energy, we confine below our attention to nucleon-nucleon scattering of laboratory energies upto about 320 MeV to avoid complications.

In absence of neutron targets, there is no direct way of deriving the high energy *n-n* data. Thus we have to depend on the indirect methods. On the assumption of charge symmetry, the *n-n* system should display the same behaviour as the *p-p* system except at comparatively low energies where the effects of the Coulomb interaction become evident. The indirect experiments consist of bombarding D_2O and H_2O with high energy neutrons and study the difference in scattering behaviour. The differential cross section for the scattering of neutrons on deuterons can be expressed in terms of *n-n* and *n-p* cross sections as

$$\sigma_{n-d}(\theta) = \theta_{n-n}(\theta) + \sigma_{n-p}(\theta) + I(\theta), \qquad \text{...(201)}$$

where $I(\theta)$ is the interference term, which is most important at low energies and small scattering angles. At 300 MeV, $I(\theta)$ is estimated to fall rapidly from 0.6 mb/sterad at 40° to one tenth this value at 90°.

1. Neutron-Proton Scattering—Data on nucleon-nucleon scattering presented here mainly based on the some what outdated review by Hess (1958).

Total cross-sections—The experimental data on total cross-sections for *n-p* scattering upto 300 MeV and beyond are shown in Fig. 8.11. The points labeled σ_{np} are from experiments in which neutrons, are incident on hydrogeneous targets. The points labeled σ_{pn} are from an experiment in which protons are incident on deuterium and the proton-proton cross section is subtracted.

$$\sigma_{pn} = \sigma_{pd} - \sigma_{pp}.$$

This is only approximation to σ_{np} since it ignores the interference terms in the deuteron scattering. As the energy increases, the approximation improves. The curve is a linear upto about 290 MeV and follows $1/E$ law. The curve flattens out beyond 290 MeV because of the production of π-mesons. The small departures from $1/E$ are due to the variation of the phase shifts of the different angular momentum states, as these become important. Between 290 MeV and 400 MeV, the curve is flat and then at still higher energies, it slopes slowly upwards because of still higher modes of meson production at these energies.

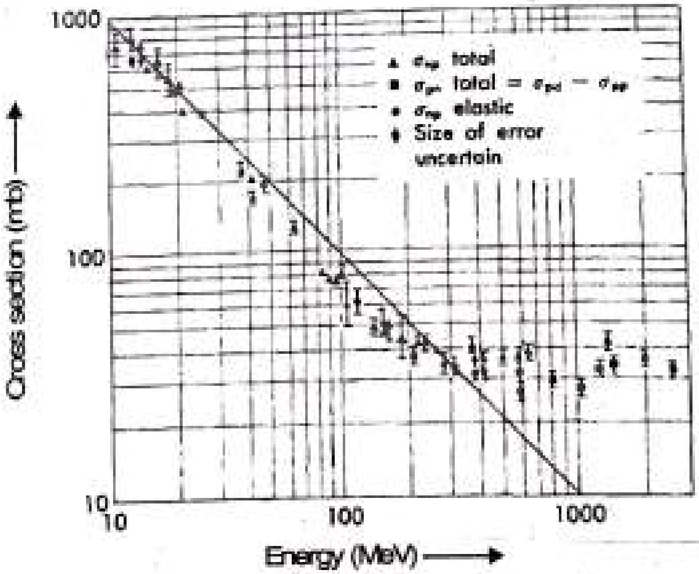

Fig. 8.11. Experimental data on n – p scattering.

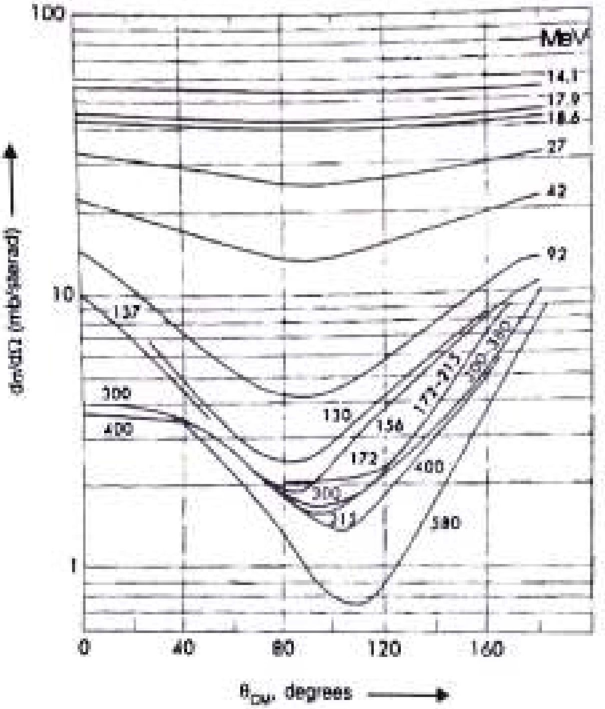

Fig. 8.12. The experimental differential n-p cross section at various energies.

Differential Cross Sections—The differential n-p cross sections at various energies from 14 MeV to 580 MeV are shown in Fig. 8.12 as a function of the angle θ_{CM}. The typical errors are of the order of 10%. This figure shows that neutrons are scattered as strongly through 0° as through 180°. Above about 100 MeV, the back scattering is the more probable. The position of the minimum cross-section or the dip in the curve varies slowly with energy and does not shift from 90° by more than about 10° for energies upto 400 MeV. The peak at 0° can be explained in terms of absorption and diffraction of neutrons in the scattering medium. The backward peak at 180° is the result of exchange forces, *i.e.*, if n- and p-interchange identity in the collision, backward scattering will be expected rather than forward scattering. Therefore equal mixture of ordinary and exchange forces would produce the observed results.

Serber force. Half and half mixture of ordinary and exchange force is known as a *Serber force* and is represented by the operator $\frac{1}{2}(1 + P^M)$. The Majorana exchange operator P^M has a value 1 for even values of l and -1 for the odd values of l. Thus the Serber force is zero for odd states (P, F, ...), and hence cannot account for the saturation. In contrast with n-p scattering below 10 MeV, the effective range for high energy scattering is dependent on the assumed shape of the potential well. Christian and Hart have used several potential shapes and found that the distribution near 90° was flat with pure central force. The addition of some tensor force makes the theoretical curve less flat near 90°.

Born approximation. The influence of exchange force and of ordinary forces on high energy scattering can be understood qualitatively by employing the Born approximation, inspite of the fact that the nucleon interactions are not weak. Born approximation can be expected to give some indication of the true behaviour at least of the less strongly interacting partial waves of higher l. The scattering amplitude as defined in Eqn. (37) is given in the Born approximation by

$$f(\theta) = -\frac{M}{4\pi\hbar^2}\int V(\mathbf{r})\, e^{i\mathbf{q}\cdot\mathbf{r}}\, d\mathbf{r}, \qquad ...(202)$$

where M is the nucleon mass, $V(\mathbf{r})$ the interaction potential and $\mathbf{q}$ the momentum transferred in scattering having a value $(\mathbf{k}_{\text{final}} - \mathbf{k}_{\text{initial}})$. For elastic collision with $E_f = E_i$, $|\mathbf{q}| = 2k \sin \theta/2$. Here θ is the angle of deflection in the C.M. system and $2\hbar^2k^2/M = E_i$. Calculation of the high energy cross-section involves the shape of the potential, and no simple general treatment of the problem can be given except at such high energies that the Born approximation is applicable. The approximation is not satisfactory for quantitative work at any energy, but it is not qualitatively wrong for energies well above the depth of the nuclear well (say 30 MeV or so). If $\mathbf{k}_f + \mathbf{k}_i = 0$, *i.e.*, when the neutron is scattered backward and the proton forward, the $f(\theta)$ due to exchange forces is large.

If the potential $V(\mathbf{r})$ vanishes outside the range R, the Born approximation predicts isotropic scattering, more or less independent of energy if $qR << 1$. The oscillations of exp. $(i\mathbf{q}.\mathbf{r})$ cause the scattering to fall of rapidly if $qR >> 1$. Near $q = 0$ (forward scattering) the cross section should stay rather large even as the energy increases. For $q = 2k$ (back scattering) the cross-section will fall rapidly with increasing energy. The general behaviour of the above equation is shown in Fig. 8.13. Eqn (202) indicates that neutrons scattered at energies in the 100 MeV range would go mostly forward and recoil protons would have mostly low energies in the neighbourhood of 10 MeV. But experimental results showed that the majority of the emergent particles were fast protons moving with nearly the energy and the direction of the incident neutrons. This can be explained if the neutron and proton change roles. It is exactly the consequence of Majorana exchange force.

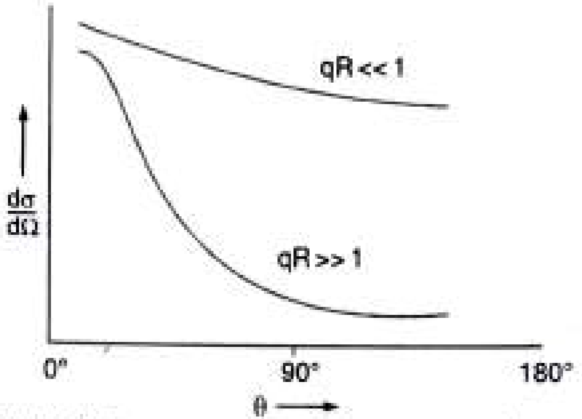

Fig. 8.13. Born approximation result for n-p scattering.

As the S wave scattering amplitude is independent of the exchange character of the nuclear force, it can be shown that, for the same radial dependence of the force and to the extent that the Born approximation for scattering in states of $l \neq 0$ is valid, a pure Majorana force gives the same scattering in the direction θ as a Wigner force does in the direction $\pi - \theta$. In other words we can say that the cross-section shows a strong maximum in the forward direction for ordinary forces and in the backward direction for Majorana exchange force. Since the recoiling proton goes forward in the latter case, the exchange potential can be said to cause an exchange of the electric charge from the proton to the neutron which then continues on its way as proton.

The exchange forces have been introduced to explain the saturation of nuclear binding energies and of nuclear densities. The Serber force is a satisfactory exchange force to fit the *n-p* scattering data at all energies, however it is unsatisfactory from the point of view of saturation. The Serber force is attractive for symmetric pairs, but zero for anti-symmetric pairs. Thus the repulsive forces are completely absent, which led to the unstability of heavy nuclei against collapse. There is no saturation with an attractive Serber force. The quantitative calculations of nuclear binding energy suggest that saturation would require a ratio of ordinary (Wigner) to exchange forces of about 1/4. Such a force is a disagreement with the experimental data. Thus we see that the *high energy n-p scattering data can be filled with an exchange force, which does not lead to saturation.*

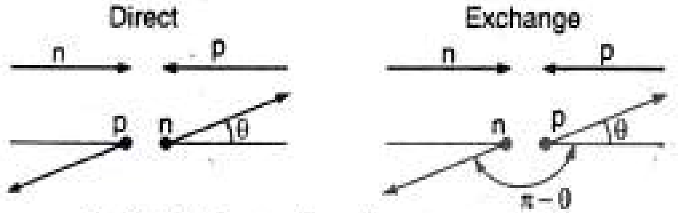

Fig. 8.14. Direct and exchange n-p scattering.

2. Proton-Proton Scattering. Just as in the case of *n-p* scattering, it is expected that more information concerning the shape and exchange character of the potential can be obtained from high energy *p-p* scattering. The Coulomb potential plays a smaller and smaller part in the scattering as the energy is increased and a direct comparison of the *n-p* and *p-p* interactions should be possible at very high energies. In the *p–p* scattering the identity of the two protons reduces considerably the number of parameters necessary to describe the scattering. As we have already noted, two protons in a singlet state have even parity while those in triplet states have odd parity. If the Serber exchange, suggested by the high energy neutron-proton data, is assumed to act between protons, no scattering occurs in states of odd parity. This result indicates that there would be no triplet scattering of one proton by another. An estimate of high energy scattering can be again made by the Born approximation. if the Coulomb scattering is ignored the differential cross-section calculated in this way for any potential with Serber exchange is just twice that for the *n-p* scattering calculated in the same approximation with the same potential. A central potential with the range for singlet and triplet states leads, in Born approximation, to the same relative angular distribution in both states. Therefore, the *p-p* angular distribution calculated in this case is the same as in the *n-p*.

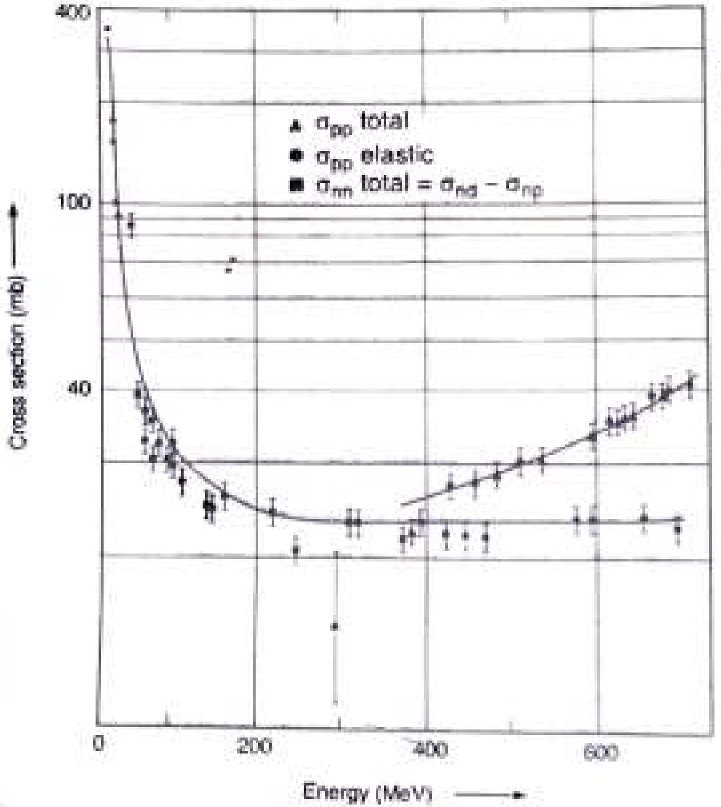

Fig. 8.15 Experimental values of the total and elastic p-p nuclear cross sections upto GeV energy range.

Total Cross Section. The total cross section together with the elastic cross section for proton-proton scattering is shown in Fig. 8.15. The total cross section σ_{pp} falls rapidly upto about 140 MeV. Beyond this energy and upto about 350 MeV, σ_{pp}, remains roughly the same ($\approx$23 mb). Beyond this energy the meson production plays a part role. σ_{pp} rises to 48 mb at 850 MeV and remains constant to about 1500 MeV. Beyond this energy, the cross section steadily diminishes. This figure shows that for *p-p* interaction upto around 300 MeV, σ_{pp} (elastic) $\approx \sigma_{pp}$ (total) $\approx \sigma_{nn}$ (total), while above this energy σ_{pp} (elastic) $\leq \sigma_{pp}$ (total) $\approx \sigma_{nn}$ (total). This shows that *p-p* and *n-n* interactions are of the same order, thus indicating *charge symmetry and charge independence of nuclear forces.* The (*p, p*) cross section has very little angular dependence at any energy except in the small angle Coulomb scattering region.

Differential Cross Sections. The experimental differential cross-sections for high energy *p-p* scattering are shown in Fig. 8.16 for various energies upto 460 MeV. We have studied earlier that as the energy increases, the effects of Coulomb scattering are confined to smaller and smaller angles. Thus the *large small angle cross section is due to Coulomb forces* and the cross section at angles above 20° to 40° is due to nuclear forces. The latter is found to be nearly flat or the differential cross section is nearly independent of angle or isotropic. The accuracy is not high at all energies, but around 150 MeV, the departure from isotropy is less than 3%. The marked flatness of the nuclear cross section allows us to calculate a total (*p, p*) cross section for nuclear forces only. If the hypothesis of charge independence is valid, *n-n* scattering cross section should be same as *p-p* scattering cross section in the angular range for which Coulomb effect are unimportant. The minimum around 10° in the angular distribution arises due to interference between Coulomb and nuclear potentials.

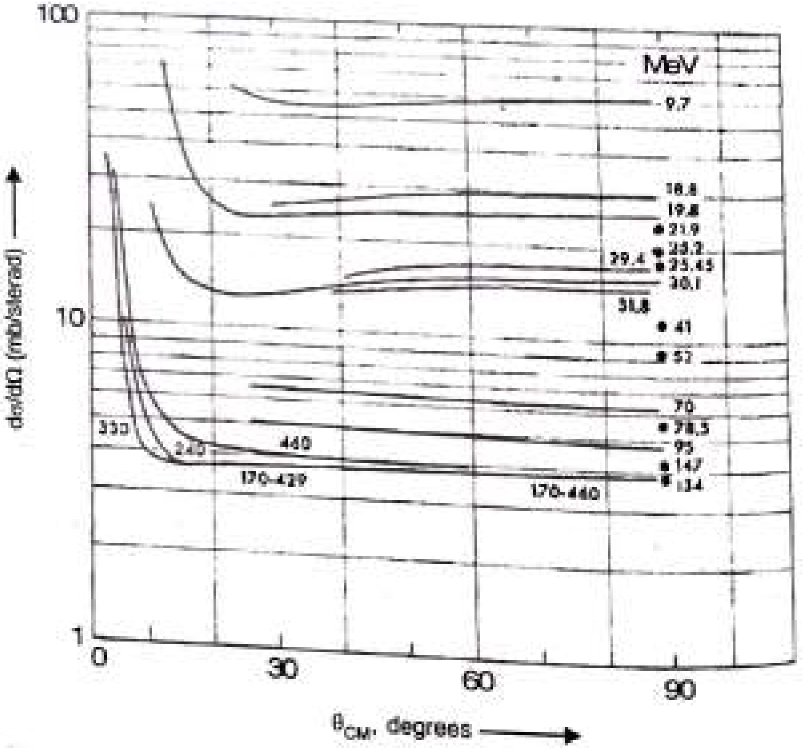

Fig. 8.16. Experimental differential cross-sections for high energy p-p scattering.

An isotropic angular disribution generally implies pure *S*-wave scattering. This is highly unlikely at incident proton energies of 100 MeV or more, as the total cross-section is almost twice as large as the maximum possible for pure *S*-wave scattering. At one particular energy, it might happen that interference between *P* and *D* wave scattering results in a nearly isotropic scattering intensity but this would not occur over a range of energies. Another puzzling result is the energy dependence of the total cross section. The total differential cross-section is nearly independent of energy for energies from 150 to 400 MeV, and has a value 3.4 ± 0.4 millibarns/steradian. Above 400 MeV, the observed cross-section begins to rise significantly as the creation of pions becomes important.

Cristian and Noyes have tried to fit the 340 MeV data with an exchange force of the Serber type and purely attractive $V(r)$. The theoretical results with the usual potential well shapes are found in qualitative disagreement with the observed cross sections at 340 MeV, as these are independent of angle in the central region of angles but too small in absolute value. This can be interpreted *as against the charge independence of nuclear forces.*

Nuclear Core. An interesting explanation of these strange results was suggested by Jastrow. For any conventional potential the *S*-phase decreases to zero with increasing energy and approximate isotropy is not possible to obtain when phases other than *S*-phase are involved. It is possible if the *S*-wave phase shift is assumed negative which corresponds to a repulsive potential. Since at high energies the *S*-wave is strongly influenced by the behaviour of the potential at very short distances hence we require a potential that is attractive at larger distances but has a strongly *repulsive core* as a *hard sphere*. The *S*-wave will have a phase shift which will depend on this central repulsive core and become repulsive over all the high enough energies. The higher *l*-values are kept away from the core by centrifugal forces. The core radius is of the order of 0.6 fermi. Another useful feature of the repulsive core hypothesis is that it helps to explain the saturation of nuclear forces.

Hard core potential of the Jastrow type is given by

$$V_t(\mathbf{r}) = -V_t S_{12} e^{(-r/r_t)} \qquad r > 0 \qquad \text{...(203)}$$

$$V_s(\mathbf{r}) = \begin{cases} \infty & r \leq r_c \\ -V_s e^{-(r-r_c)r_s} & r > r_c \end{cases} \qquad \text{...(204)}$$

where the parameters, as proposed by Jastrow are

$$\begin{aligned} V_t &= 50.8 \text{ MeV}, V_s = 375 \text{ MeV} \\ r_t &= 0.75 \text{ fm}, r_s = 0.4 \text{ fm}, r_c = 0.6 \text{ fm}. \end{aligned} \qquad \text{...(205)}$$

The theoreticians have tried to soften and diffusify the core. Beyond it, the radial interacton between two nucleons is taken to be purely static and the radii of the core and static force are adjusted to give a good fit to low energy as well as high energy characteristics of the nucleon-nucleon system, where the incoherent superposition of triplet and singlet states takes place. Thus *p-p* scattering can be described by a singlet even potential with a repulsive core surrounded by an attractive outer region and that the triplet odd potential contains a tensor force which is attractive in the $^3P_0$ state.

8.11 POLARIZATION AND SCATTERING PARAMETERS

Besides the differential and total scattering cross section determinations, the experiments on polarization yield important information about nuclear forces. Nucleon-nucleon scattering experiments are more complicated to analyze than the scattering of a nucleon on a spinless centre. One requires eleven parameters to describe the scattering completely. These are functions of energy and angle instead of the previous three. For identical nucleons this number reduces to nine. These are scattering cross section, polarization, Woftenstein parameters and the spin correlation coefficients. The different sets of measurements are required to determine these parameters. Differential scattering cross section $\sigma(\theta)$ is called the single scattering parameter and polarization $P(\theta)$ called the double scattering parameter. The triple scattering parameters are $D(\theta)$, $R(\theta)$, $A(\theta)$ etc. and the spin correlation coefficients are C_{nn}, C_{qp}, C_{pp}, C_{qq}.

(1) Polarization $P(\theta)$—Generally the spin orientation of nucleons in a beam from an accelerator are randomly distributed. If the spins are oriented in some preferred direction, the beam is then said to be polarized in that direction. If the number of particles in the beam with spin component parallel to this preferred direction is N_+ and the number with anti-parallel spin component is N_-, then the polarization P, often called the *polarizing power*, is defined for spin $\frac{1}{2}$ particles as

$$P = (N_+ - N_-)/(N_+ + N_-). \qquad ...(206)$$

The value of P varies with the scattering angle θ and is written as $P(\theta)$.

Nucleons may be polarized by elastic scattering on a spinless centre provided that the interaction producing the scattering is spin dependent. We may scatter a beam of protons on a target and select the beam scattered under angle θ_1. By scattering this beam a second time on a target under angle θ_2, we find that the scattered intensity dependes not only on θ_2 but also on angle ϕ, between the two planes of scattering and can be written as

$$I = A(\theta_2) + B(\theta_2)\cos\phi. \qquad ...(207)$$

The quantity B vanishes unless the beam incident on the second target is polarized. To define ϕ, we use vector momenta $\mathbf{k}$ of the incident and scattered particle in each scattering. The positive direction of polarization of spin $\frac{1}{2}$ particle is taken in the direction of the vector product $(\mathbf{k}_i \times \mathbf{k}_f)$.

$$\hat{n}_1 = \frac{\mathbf{k}_0 \times \mathbf{k}_1}{|\mathbf{k}_0 \times \mathbf{k}_1|} \text{ and } \hat{n}_2 = \frac{\mathbf{k}_1 \times \mathbf{k}_2}{|\mathbf{k}_1 \times \mathbf{k}_2|}$$

$$\therefore \quad \hat{n}_1 \cdot \hat{n}_2 = \cos\phi. \qquad ...(208)$$

Here $\mathbf{k}_0$, $\mathbf{k}_1$ and $\mathbf{k}_2$ represent the vector momenta of the incident particles, after first scattering and after second scattering respectively. The systematic diagram of a double scattering experiment is shown in Fig. 8.17. The degree of polarization is determined by measuring the left-right symmetry upon scattering from the second target that plays the role of an analyzer. The first target works as polarizer. It is analogous with the usual arrangements in optics, where the polarizer is followed by an analyzer. Here in nuclear physics differentially scattering targets act as analyzer.

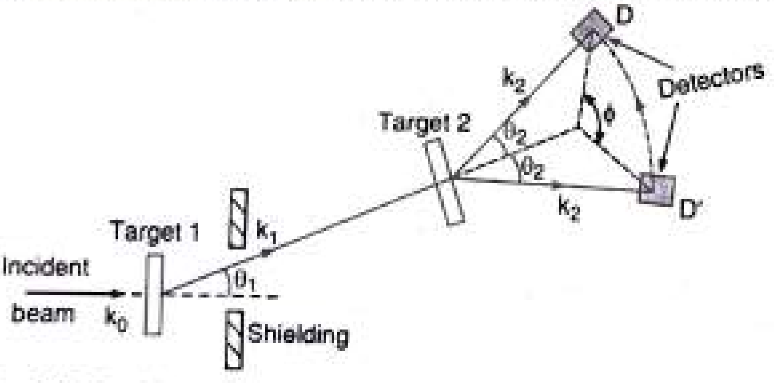

Fig. 8.17. Double scattering experiment for the detection of polarization.

Let n be the number of particles in the initial unpolarised beam. We can assume that in this beam there are $\frac{1}{2}n$ paricles with spins of each sign (+ or −). After scattering by target 1 to the left, the number of particles reaching the target 2 with polarization P_1 and spin up is $\frac{1}{2}nf_1(1 + P_1)$ and with spin down is $\frac{1}{2}nf_1(1 - P_1)$, where f_1 is the fraction of all particles reaching target 2. Similarly those particles scattered to the right by target 1, $\frac{1}{2}nf_1(1 - P_1)$ will reach target 2 with spin up and $\frac{1}{2}nf_1(1 + P_1)$ will reach target 2 with spin down. Let P_2 and f_2 be respectively the polarization with spin up and the fraction of all particles scattered by the target 2. The number scattered twice to the left with spin up $= \frac{1}{2}nf_1f_2(1 + P_1)(1 + P_2)$ and with spin down $= \frac{1}{2}nf_1f_2(1 - P_1)(1 - P_2)$. Hence the number of particles scattered twice to the left (LL) is $\frac{1}{2}nf_1f_2(2 + 2P_1P_2)$. The number of particles scattered twice, first to the left by target 1 and then to the right by target 2 with spin up is $\frac{1}{2}nf_1f_2(1 + P_1)(1 - P_2)$. Hence the number of particles scattered twice, first to the left and then to the right $(LR) = \frac{1}{2}nf_1f_2(2 - 2P_1P_2)$. Therefore the left-right asymmetry for the second scattering is given by the

$$\therefore \quad \text{Left right asymmetry ratio } A_2 = \frac{(LL) - (LR)}{(LL) + (LR)} = P_1P_2. \qquad ...(209)$$

If the second scattering is identical to the first, then $P_1 = P_2 = P$ and $A_2 = P^2$. Hence the magnitude, not the sign, of P can be easily obtained from actual experiment. The sign may be determined by studying the interference of nuclear scattering with Coulomb scattering.

The above arguments are strictly valid only for the targets with spins zero, otherwise one has to take account not only the spin orbit interaction, but also the *spin-spin interaction*. The polarization parameters $P(\theta)$ for *p-p* and *n-p* scatterings at different energies as a function of scattering angle are shown in Fig. 8.18. The magnitude of $P(\theta)$ is less than one in all cases. It is positive for *p-p* scattering for all energies from 0° to 90°. It is also positive for *n-p* scattering for these angles but for high energies it becomes negative near 90°. The change of sign in the $P(\theta)$ values shows that they do not have as good a symmetrical behaviour as in *p-p* scattering.

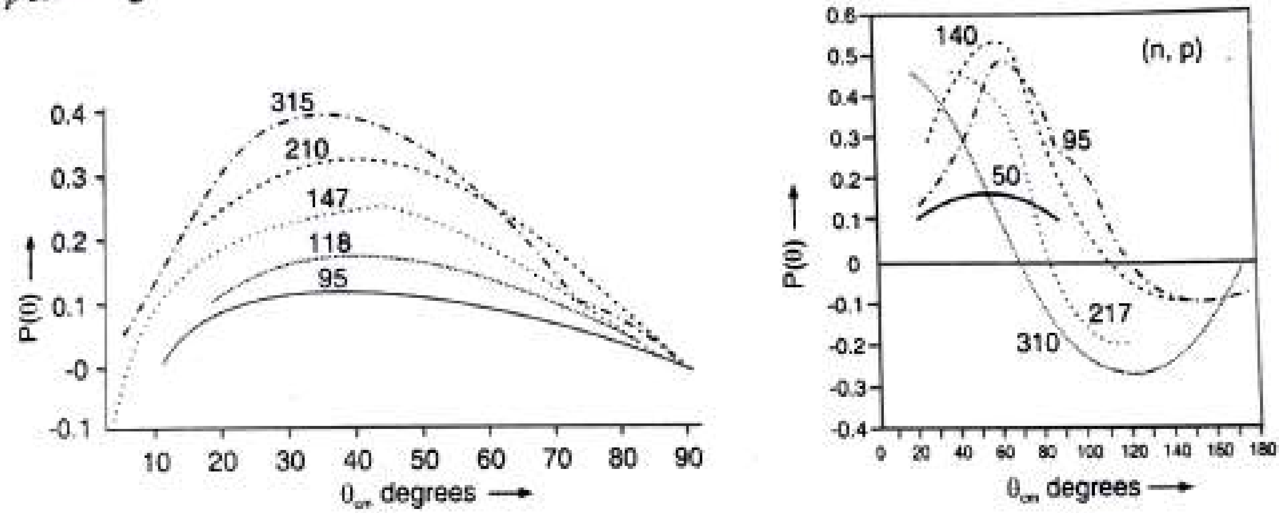

(a) (b)

Fig. 8.18 Variation of Polarization parameter P(α) with the scattering angles for (a) p – p and (b) n – p scattering at different energies.

Schwinger in 1946 proposed that the spin orbit interaction in nuclear scattering might induce polarization, which could be observed in a double scattering experiment. Later in 1948, he suggested that a tensor force could also give rise to polarization upon scattering. Wolfenstein in 1949 indicated that not only protons be polarized but neutrons emerging from a reaction might evince a large degree of polarization.

More sophisticated investigations of polarization phenomena are carried out by triple scattering techniques.

Low energy nucleon scattering cannot show any polarization, because only the *S*-wave contributes. In the energy range above 100 MeV, the scattering of protons and neutrons from heavier nuclei has been observed to polarize the nucleon beam. These scattering experiments provide valuable information concerning the spin dependence of nuclear forces. With a purely central interaction potential and an unpolarized target nucleus, the scattered particles would not show any left-right asymmetry, even with a polarized incident beam. This asymmetry can be explained, if the interaction has a tensor character with the spin-orbit coupling. The asymmetry is larger if orbital angular momentum l is large. Thus the plarization experiments become important at high energy, where high values of l contribute to the phase shift.

(2) Depolarization parameter D (θ) : This is a scatering parameter produced by the second scatterer in the coplaner *triple scattering experiment*. In this arrangement, an unpolarized beam falls on the first target T_1, which induces the polarization P_1. This beam is allowed to fall on the second target T_2, which not only causes a futher polarization P_2 but also causes depolarization D. The third target similarly introduces a polarization P_3. Then left-right asymmetry A_{23} after the third target is defined by

$$A_{23} = \frac{P_2 \pm DP_1}{1 \pm P_1 P_2} P_3, \qquad \text{...(210)}$$

where positive sign refers to the left side and negative sign to the right side in all the scattering.

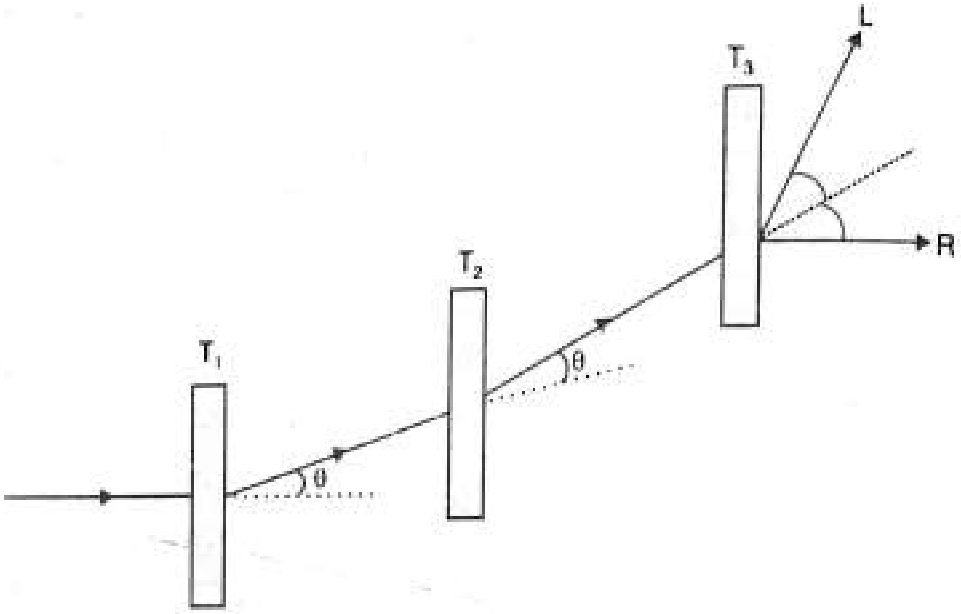

Fig. 8.19 The arrangement of the triple scattering experiment for measurement of depolarization.

For the scattering towards left in all the three targets, if the first target completely polarizes, *i.e.*, $P_1 = 1$ and if P_2 is also 1, which means that both the scatterers or targets are of the same type. Then $A_{23} = P_3$ for $D = 1$ and there is no depolarising in the second target. The depolarization parameter D determines the amount of polarization perpendicular to the scattering plane in the beam after the first scattering, which is converted into the same direction of polarization after the second scattering, or D specifies the extent to which initial polarization perpendicular to the second scattering plane is retained or modified by the second scattering. Generally $D \leq 1$. The value $D < 1$ implies that the second scatterer has converted part of the polarized beam with polarization ⊥ to the scattering plane after the first scattering in some other plane. The value $D = 1$ implies that the polarization of the beam has been completely converted by the second scatterer into its original direction. For $P_1 = 1$ and left hand scattering in all scatterers, we have

$$A_{23} = [(P_2 + D)/(1 + P_2)]P_3. \quad ...(211)$$

Equation (210) may be written as

$$D = \frac{A_{23}}{A_3}(A_2 \pm 1) \pm \frac{A_2}{A_1}, \quad ...(212)$$

where $A_1 = P_1^2$, $A_2 = P_1P_2$ and $A_3 = P_1\,P_3$.

Thus to measure D (θ), one has to measure polarization parameters P_1, P_2 and P_3 and left right asymmetry A_{23}, after the third scatterer. Note that for a spinless target, D is always 1.

(3) Transformation Parameters $A(\theta)$ and $A'(\theta)$: The parameter A refers to the degree to which polarization in the incident direction is transformed into polarization in the scattering plane, but perpendicular to the outgoing beam, while A' refers to the degree to which longitudinal polarization in the ingoing beam is converted into longitudinal polarization in the outgoing beam. If **k** represents the linear momentum of the nucleon in the C–M system and σ the spin of the nucleon, then $\mathbf{k}_i \times \mathbf{k}_s = \mathbf{n}$ and $\mathbf{n} \times \mathbf{k}_s = \mathbf{t}$. If <σ> represents the spin expectation value of the nucleon and the subscripts i and s are used for the incident and scattered beams. Then one can define

$$A = <\sigma_s> . \mathbf{t} \text{ and } A' = <\sigma_s> . \mathbf{k}_s \quad ...(213)$$

(4) Rotation Parameters $R(\theta)$ and $R'(\theta)$: The parameter R refers to extent of rotation of polarization vectors that lie in the scattering plane but are both perpendicular to their respective beams, while R' refers to conversion of ingoing transverse polarization into outgoing longitudinal polarization in the plane of second scattering. In terms of unit vectors, one can define

$$R = <\sigma_s>. \mathbf{t} \text{ and } R' = <\sigma_s>. \mathbf{k}_s \quad ...(214)$$

To observe quantities such as $<\sigma_s>$. **t** one must perform a scattering in a plane containing $\mathbf{k}_s$ and perpendicular to **t**. To observe components of $<\sigma_s>$ parallel to $\mathbf{k}_s$ one must first turn σ_s so that they become transversal to $\mathbf{k}_s$.

These definitions of Wolfenstein coefficients may be illustrated as shown in Fig. 8.20.

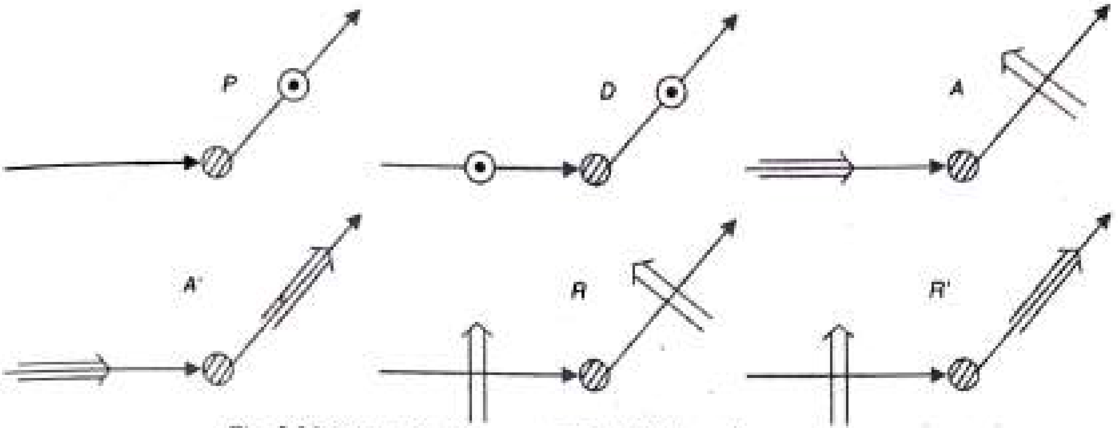

Fig. 8.20 Schematic diagram to define Wolfenstein parameters.

(5) Spin Correlation Coefficients : The spin correlation coefficients C_{nn}, C_{qp}, C_{pp} and C_{qq} constitute the another group of experimental parameters, which refer to experiments in which an unpolarized nucleon beam is scattered by target nucleons and measurements of the polarization component of the scattered nucleon are made in coincidence with that of the recoil nucleon in the directions indicated by the suffixes. For example C_{nn} gives the expectation value that the scattered projectile is polarized in direction $\hat{n}$ and recoil nucleon is also polarized in the direction $\hat{n}$ *i.e.*, $C_{nn} = \langle (\sigma_1 \cdot \hat{n})(\sigma_2 \cdot \hat{n}) \rangle$ This is obtained by measuring coincidences between the scattered particlés polarized along $\hat{n}$-direction and recoil nucleon also polarized along **n**-direction. The unit vectors **n**, **p** and **q** are defined in terms of linear momenta $\mathbf{k}_i$ and $\mathbf{k}_f$, as

$$\hat{n} = \frac{\mathbf{k}_i \times \mathbf{k}_f}{|\mathbf{k}_i \times \mathbf{k}_f|}, \hat{p} = \frac{\mathbf{k}_i + \mathbf{k}_f}{|\mathbf{k}_i + \mathbf{k}_f|} \text{ and } \hat{q} = \frac{\mathbf{k}_i - \mathbf{k}_f}{|\mathbf{k}_i - \mathbf{k}_f|} \qquad ...(215)$$

$C_{pq} = \langle (\sigma_1 \cdot \hat{p})(\sigma_2 \cdot \hat{n}) \rangle$, where $(\sigma_1 \cdot \hat{p})$ is the component of the spin of the scattered nucleon in the $\hat{p}$-direction and $(\sigma_2 \cdot \hat{n})$ is the component of the recoiling target nucleon in the $\hat{n}$-direction.

8.12 MESON THEORY OF EXCHANGE FORCES

Any attractive force between two particles is regarded as the exchange of an attractive property. The exchanged attractive property between two protons is an electron for an $(H_2)^+$ molecule and is the surrounding electric field for the Coulomb force between two charges. We may introduce similarly a new nuclear field surrounding each nucleon. The application of quantum mechanics to the electromagnetic field surrounding a charged particle leads to the conclusion that the electrical force is exerted by the transfer of a photon, which is referred to *as the field particle of the electromagnetic field*, from one charged body to another. Yukawa (1935) thought that *the strong interaction between nucleons might be accounted for in a similar manner by postulating an appropriate field particle of rest mass different from zero. This virtual particle has been given the name meson.* To show that the range of force is related to the mass of exchanged particle, assume that this meson is contained virtually in a proton, which is now called π-meson. A temporary dissociation would be allowable if it does not take a time longer than Δt, given by uncertainty principle.

$$\Delta t \approx \hbar/\Delta E. \qquad ...(216)$$

Here $\Delta E = (M_p + m_\pi)c^2 - M_p c^2 = m_\pi c^2$.

If this virtual particle travels with the velocity of light, as might be expected for a field particle, then the greatest distance the meson could travel in this time, also known as *range of the pion exchange force is given by*

$$R = c\,\Delta t \approx \hbar/m_\pi c. \qquad ...(217)$$

Based on known nuclear dimensions, Yukawa assumed that the range of the nucleon force and of the field particle would be about 2×10^{-15} m and this led to a value of m_π roughly 200 times the mass of an electron. About two years after Yukawa's theory, particles of mass about 200 m_e were discovered in cosmic radiation. These virtual particles are now known as mesons which were thought to the Yukawa field particles for more than ten years. Several different mesons with different charges and rest masses have been discovered. It was found that Yukawa particle was not the μ-meson but its parent, the shorter lived π-meson. The pion, which occurs in positive, negative and neutral forms has a mass about 270 times that of the electron and interacts very rapidly with matter. It has other properties spin and parity, which qualify it to be the field particle for nucleon forces.

The attraction between any two nucleons could arise from the transfer of a π^0-meson from one nucleon to the other. The force between a proton and a neutron could result from the transfer of a π^+-meson from the former to the latter or of a π^--meson in the opposite direction.

$$p \rightleftharpoons p+\pi^0, \quad n \rightleftharpoons n+\pi^0, \quad p \rightleftharpoons n+\pi^+ \quad n \rightleftharpoons p+\pi^-.$$

To interpret the nucleon-nucleon scattering data in terms of a potential function, let us compare the meson theory known as *one pion exchange theory* with the quantum theory of electromagnetic interactions. To obtain a pion wave equation we express the total energy E of a pion in terms of the pion rest mass energy $m_\pi c^2$ and momentum p as

$$E^2 = c^2p^2 + m_\pi^{\,2}c^2. \qquad ...(218)$$

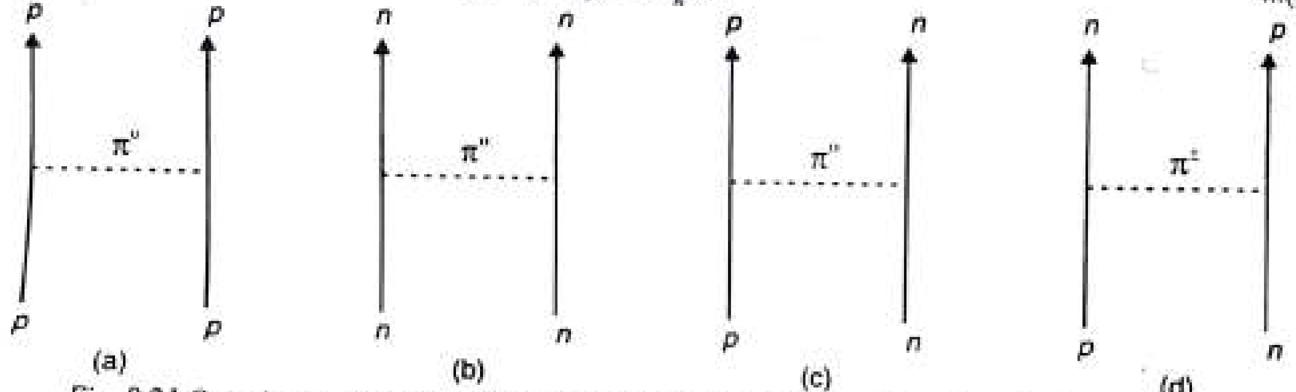

Fig. 8.21 One pion exchange diagrams, (a) p–p interaction, (b) n–n interaction, (c) direct term for n–p interaction, and (d) exchange term for n–p interaction.

The energy E and momentum component p are represented by the operators

$E = i\hbar\partial/\partial t$, $p_x = -i\hbar\partial/\partial x$, $p_y = -i\hbar\partial/\partial y$ and $p_z = -i\hbar\partial/\partial z$.

Introducing a pion wavefunction φ (a scalar), we obtain the Klein Gordon equation for a free particle of spin 0.

$$-\hbar^2\partial^2\varphi/\partial t^2 = -c^2\hbar^2\nabla^2\varphi + m_\pi^{\,2}c^4\varphi$$

or

$$\nabla^2\varphi - \frac{1}{c^2}\frac{\partial^2\varphi}{\partial t^2} - \frac{m_\pi^2c^2}{\hbar^2}\varphi = 0\,. \qquad ...(219)$$

From $m_\pi = 0$, it reduces to the well known wave-equation

$$\left(\nabla^2 - \frac{1}{c^2}\frac{\partial^2}{\partial t^2}\right)\varphi = 0 \qquad ...(220)$$

for the quanta of the electromagnetic field. The simplest type of electromagnetic field is the electrostatic field, where $\partial\varphi/\partial t = 0$. The corresponding static pion field is the analogue of Laplace's equation in the absence of electric charges. The presence of charge requires the analogue of Poisson's equation $\nabla^2\varphi = e\rho/\varepsilon_0$, where e is the magnitude of the electronic charge and ρ is the electron particle density. In our present case we have nucleon charges interacting with the pion field. For a static pion potential due to a single point nucleon at the origin, the Klein Gordon equation becomes

$$\nabla^2\varphi - (m_\pi^{\,2}c^2/\hbar^2)\,\varphi = 4\pi g\,\delta(r), \qquad ...(221)$$

where δ is the Dirac δ-function and g is a constant replacing the electronic charge in electrodynamics and called *effective nucleonic charge or coupling constant*.

The solution of this equation which vanishes at infinity is

$$\varphi(\mathbf{r}) = -\int \frac{e^{-\mu|\mathbf{r}-\mathbf{r}'|}}{|\mathbf{r}-\mathbf{r}'|} g\delta(\mathbf{r}')\,\delta\tau. \qquad ...(222)$$

Here $\mu \approx m_\pi c/\hbar$ and $d\tau'$ is the volume element. If we have a point source of strength g at $\mathbf{r}_1$, then we have,

$$\varphi(\mathbf{r}) = -g\frac{e^{-\mu|\mathbf{r}-\mathbf{r}_1|}}{|\mathbf{r}-\mathbf{r}_1|}. \qquad ...(223)$$

$\therefore$ Potenial energy of a source g at $\mathbf{r}_2$ in this field is given by $U = g\,\varphi(\mathbf{r}_2)$. If the potential φ is due to another source g at $\mathbf{r}_1$, then the interaction energy between two sources

$$U = -g^2\frac{e^{-\mu|\mathbf{r}_1-\mathbf{r}_2|}}{|\mathbf{r}_1-\mathbf{r}_2|} = -\frac{g^2e^{-\mu r}}{r}. \qquad ...(224)$$

Comparing with the relation for Coulomb potential, we see that this nuclear potential decreases more rapidly with distance from the source than the Coulomb potential by an exponential factor. At separations small compared to μ^{-1}, this potential energy varies with r just as the Coulomb energy loss. Yukawa noted that this interaction energy may account for the fact that nuclear forces act only over a short range and that the range

$$R = 1/\mu = \hbar/m_\pi c. \qquad ...(225)$$

Substitution of the value of m_π as 270 m_e, gives $R = 1.4$ fermi.

Since in this theory the nuclear particle does not change its charge, we find that according to the theory *n-n*, *n-p* and *p-p* forces are equal. However the theory does not explain the exchange nature of nuclear forces, which is established form high energy scattering experiments and is able to explain saturation of nuclear forces. The theory in its simple form cannot explain the spin dependence or the presence of non-central forces. The theory is modified by several theoretical physicists taking into account, (1) the tensoral character of the meson field wave functions, (2) the isobaric-spin character of the meson field wave functions, (3) the intrinsic nature of the source field coupling and (4) the strength of the source-coupling constant.

The interaction potential between two nucleons so calculated gives approximately $g^2/\hbar c = 17$. It may be compared with the fine structure constant $e^2/4\pi\varepsilon_0\,\hbar c = 1/137$. The large dimensionless coupling constant $g^2/\hbar c$ suggests that more than one meson is transferred simultaneously between two nucleons. For small distances, we have strong repulsive core arising from the δ function. This core prevents the nucleons from coming close together. When two nucleons collide at very high energy (~GeV), the nucleons can penetrate or disturb each other's core. Thus we see that only the exchange of a relatively small number of mesons can have an appreciable effect on the nuclear force at low and medium energies. On the one hand, we see that the meson theory is qualitatively correct, but on the other hand, not a single quantity has been calculated and measured which confirms quantitative correctness.

8.13 PHASE SHIFTS AND NUCLEON-NUCLEON SCATTERING DATA

In analysing nucleon-nucleon scattering, all available data are used to compute a set of phase shifts, as functions of energy for the different wave components. Several sets of acceptable phase shifts are available, but no unambiguous results are obtained at yet. Marmier and Sheldon considered the triple scattering parameters of *p-p* scattering data for an energy around 310 MeV obtained at Berkeley and assembled for phenomenological phase parameter analysis by Stapp *et al.* Using a least squares technique to ascertain which set of phase parameters could provide the acceptable fits to Wolfenstein parameters data, they obtained eight equally possible sets of solutions. Cziffra *et al.* on re-examination indicated that upon including explicitly the one-pion-exchange (OPE) contribution to the scattering amplitude, the most probable choice of phase shifts could be reduced to first two of the earlier eight sets. The absence of data at high angles made it impossible to distinguish them, as shown in Fig. 8.22. These not only compare theoretical and experimental results for the Wolfenstein parameters but also give the theoretical predictions for the spin correlation parameters.

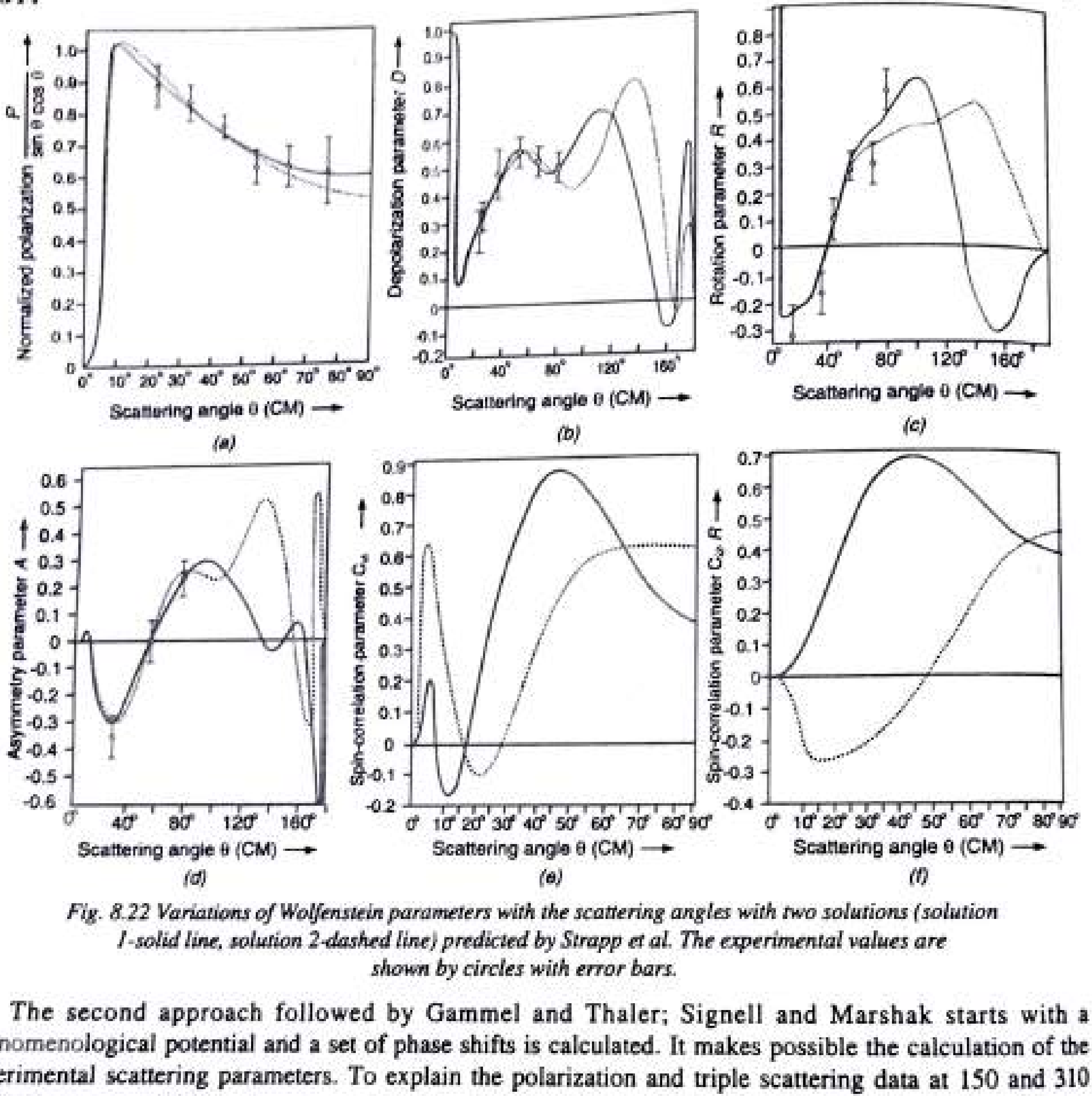

(a) (b) (c)

(d) (e) (f)

Fig. 8.22 Variations of Wolfenstein parameters with the scattering angles with two solutions (solution 1-solid line, solution 2-dashed line) predicted by Strapp et al. The experimental values are shown by circles with error bars.

The second approach followed by Gammel and Thaler; Signell and Marshak starts with a phenomenological potential and a set of phase shifts is calculated. It makes possible the calculation of the experimental scattering parameters. To explain the polarization and triple scattering data at 150 and 310 MeV, Gammel and Thaler have assumed a mixture of central, tensor and spin-orbit potentials $V_C(r)$, $V_T(r)\,\mathbf{S}_{12}$, $V_{SO}(r)\,\mathbf{L}\cdot\mathbf{S}$ with $V(r)$ in every case of the form of an infinite repulsive core inside $r = r_c$ and Yukawa shape outside.

$$\begin{aligned} V(r) &= -V e^{-\mu r}/\mu r & r > r_c \\ &= \infty & r \le r_c \qquad \text{...(226)} \end{aligned}$$

The very short range spin orbit potential parameters are : $r_c = 0.41$ fm; $V_{SO} = 0$ (L even); $V_{SO} = 7318$ MeV (L odd), $1/\mu_{SO} = 0.27$ fm (any L).

About the same time Signell and Marshak also produced a phenomenological potential by adopting Gartenhaus potential derived on the basis of the meson theory and adding to it the hard core the spin orbit potentials

$$V(r) = V(r)_{\text{Gartenhaus}} + V_{SO}(r), \qquad \text{...(227)}$$

where the short ranged attractive spin orbit component is of the form

$$V_{SO}(r) = \frac{V_0}{(r/r_0)} \frac{d}{d(r/r_0)} \left[\frac{e^{-r/r_0}}{r/r_0} \right] (\mathbf{L} \cdot \mathbf{S}) \qquad \text{for } r \geq r_{core}$$

$$= [V_{SO}(r)]_{r=r_{core}} \qquad r < r_{core} \qquad ...(228)$$

with $V_0 = 30$ MeV, $r_0 = 1.07$ fm and $r_{core} = 0.21$ fm.

It is found by Signell and Marshak to give a good fit to *p-p* and *n-p* data upto 150 MeV and a quantitative fit upto 300 MeV with variation of the core radius without changing the original Gartenhaus parameters.

The Gartenhaus potential has central parts plus the tensor parts. The interaction between two nucleons was calculated using a cut off of $6m_\pi c^2$, confining to two meson exchanges and using the static approximation which ignores the nucleon recoil. By taking into account of a two pion exchange interaction through adjustment of the spin-orbit range, Signell and Marshak have yielded still better agreement.

A study of the two nucleon phenomenological phase shifts with energy has been extensively pursued by the Yale group under Breit. This work has recieved wide spread recognition. The phase shift parameters were observed to furnish an excellent fit to *p-p* scattering data over a considerable range. Mc Donald and Hull have determined the central and spin orbit potentials from these phase shift parameters and have shown that these potentials give cross section and polarization coefficients which are in good agreement with their experimental results over the energy range 95–350 MeV. The Yale poential that reproduces the scattering results is of the form

$$V(r) = V_C(r) + V_T(r)\, \mathbf{S}_{12} + V_{SO}\, (\mathbf{L} \cdot \mathbf{S}) + V_{qSO}\, [(\mathbf{L} \cdot \mathbf{S})^2 + \mathbf{L} \cdot \mathbf{S} - L^2] \qquad ...(229)$$

The last term due to quadratic spin orbit is omitted. $V_C(r)$ is different for even and odd states and depends also on S. The $\mathbf{L} \cdot \mathbf{S}$ force is attractive for the two *i– spin* states at large distances, but becomes repulsive for $T = 0$ at about 1 fm and for $T = 1$ at about 0.4 fm. Hence the odd-parity ($T = 1$) states may have a $\mathbf{L} \cdot \mathbf{S}$ stronger effective than the even parity-states. It shows that $\mathbf{L} \cdot \mathbf{S}$ potential is meaningful.

The success of the Yale phase shift analysis incited Hamada and Johnston to make appropriate changes in the earlier potentials. The Hamada Johnston potential is able to give an excellent representation of both *p-p* and *n-p* data upto about 350 MeV. The potential has the form

$$V(r) = \infty \qquad \text{for } r < r_{core}$$

$$= V_C(r) + V_T(r)\, \mathbf{S}_{12} + V_{SO}(r)\, (\mathbf{L} \cdot \mathbf{S}) + V_{qSO}(r)\, \mathbf{L}_{12} \qquad \text{for } r \geq r_{core} \qquad ...(230)$$

where $r_{core} = 0.343\, \lambda\!\!\!^{-}_c = 0.48$ fm and the quadratic spin-orbit term $V_{qSO}(r)$ is associated with the operator

$$\mathbf{L}_{12} = (\boldsymbol{\sigma}_1 \cdot \boldsymbol{\sigma}_2)\, \mathbf{L}^2 - \tfrac{1}{2}\, [(\boldsymbol{\sigma}_1 \cdot \mathbf{L})(\boldsymbol{\sigma}_2 \cdot \mathbf{L}) + (\boldsymbol{\sigma}_2 \cdot \mathbf{L})(\boldsymbol{\sigma}_1 \cdot \mathbf{L})]$$

$$= [\delta_{LJ} + (\boldsymbol{\sigma}_1 \cdot \boldsymbol{\sigma}_2)]\, \mathbf{L}^2 - (\mathbf{L} \cdot \mathbf{S})^2 \qquad ...(231)$$

The individual terms are defined as

$$V_C(r) = 0.08\, \frac{m_\pi c^2}{3} (\boldsymbol{\tau}_1 \cdot \boldsymbol{\tau}_2)(\boldsymbol{\sigma}_1 \cdot \boldsymbol{\sigma}_2) \frac{e^{-x}}{x} \left[1 + a_C \frac{e^{-x}}{x} + b_C \frac{e^{-2x}}{x^2} \right]$$

$$V_T(r) = 0.08\, \frac{m_\pi c^2}{3} (\boldsymbol{\tau}_1 \cdot \boldsymbol{\tau}_2) \left(1 + \frac{3}{x} + \frac{3}{x^2} \right) \frac{e^{-x}}{x} \left(1 + a_T \frac{e^{-x}}{x} + b_T \frac{e^{-2x}}{x^2} \right)$$

$$V_{SO}(\mathbf{r}) = G_{SO}(m_\pi c^2) \frac{e^{-2x}}{x^2} \left(1 + b_{SO} \frac{e^{-x}}{x} \right)$$

$$V_{qSO}(\mathbf{r}) = G_{qSO}(m_\pi c^2) x^{-2} \left(1 + \frac{3}{x} + \frac{3}{x^2} \right) \frac{e^{-x}}{x} \left[1 + a_{qSO} \frac{e^{-x}}{x} + b_{qSO} \frac{e^{-2x}}{x^2} \right] \quad ...(232)$$

where m_π is the pion mass.

For sufficiently large internucleon distances x, the central and tensor potentials reduce to OPEP (one point exchange potential). The coefficients a_C, b_C, a_T and b_T denote the deviation of these potentials from

OPEP at small separations x and V_{SO} represents a short ranged linear spin orbit potential whose strength G_{SO} and deviation b_{SO} depend on the parity of the state under consideration. The quadratic spin orbit term, V_{qSO} has a strength G_{qSO} and deviation parameters a_{qSO} and b_{qSO}. The best fit values of the parameters are listed in the Table 8.5.

Table 8.5. Hamada-Johnston Potential Parameters

State	a_C	b_C	a_T	b_T	G_{SO}	b_{SO}	G_{qSO}	a_{qSO}	b_{qSO}	$r(core)$ *fm*
Triplet even	6.0	–1.0	–0.5	0.2	0.0743	–0.1	0.00267	1.8	–0.4	0.48
Triplet odd	–9.07	3.48	–1.29	0.55	0.1961	–7.12	–0.000891	–7.26	6.92	0.48
Singlet even	8.7	10.6	—	—	—	—	– 0.000791	0.2	–0.2	0.48
Singlet odd	–8.0	12.0	—	—	—	—	–0.00267	2.0	6.0	0.48

8.14 ONE BOSON EXCHANGE POTENTIAL

The nuclear force may be divided into the three parts, as shown in Fig. 8.23. The radius of the hard core is around 0.4 *f*. The long range part staring around 2*f* or so is due to the one pion exchange potential (OPEP). In the analysis of two body data, many authors (*e.g.* Breit *et al.*) included the one pion exchange potential explicitly and set up the rest of the potential phenomenologically. The potential acting between a pair of particles due to exchange of a meson has a range of the order of the meson Compton wavelength ($\lambda = \hbar/m_\pi c$). Since π-meson is the lightest boson that can be exchanged between a pair of nucleons, the OPEP determines the long range part of the two nucleons potential. Thus to get the information at medium ranges, the exchange of heaviour bosons and two, three, --- pions is used for the calculation of potential. Such a potential is called *one boson exchange potential (OBEP)*.

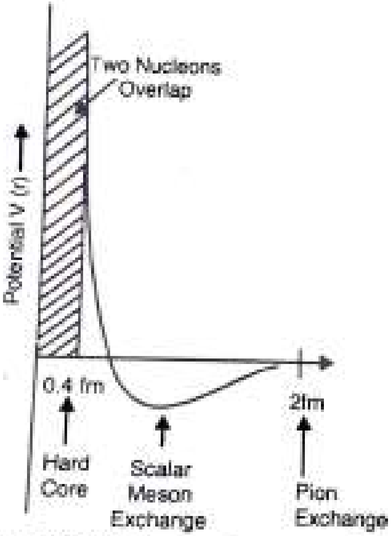

Fig. 8.23 Nuclear nucleon potential.

The pion has zero spin, odd parity and isospin $T = 1$. Thus the exchange particle must be a *p*-state to conserve parity. There are heavy mesons of spin 1 and odd parity. Their exchange between nucleons can produce a short range repulsive core and also a spin orbit force which are required. Such mesons are : (*i*) ρ-*meson* having a mass = 765 MeV is a two pion system with quantum numbers $I = 1$, parity = – 1 and isospin $T = 1$; (*ii*) ω-*meson* having mass = 784 MeV with $I = 1$, parity = – 1 and isospin $T = 0$, is a three pion resonance ; (*iii*) ϕ-*meson* having mass = 1020 MeV is a resonance of the $K\bar{K}$ system. It has same quantum numbers as that of ω-meson; (*iv*) η-*meson* having mass ~ 550 MeV with $I = 0$, parity = – 1, $T = 0$;

2π-*exchange :* The repulsive effect of the ω-meson is too large in the middle range of interaction. Thus an exchange of either two pions or of a new meson, called σ-meson ($I = 0$, Parity = 1, $T = 0$) is required to allow for this. Instead of considering one heavy meson exchange, one can consider the simultaneous emission and absorption of many mesons. If there are three nucleons, one of them emits two mesons which may be absorbed by other two nucleons. This gives rise to three body forces. Similarly we can consider four body, five body (general term) forces. These are short ranges. Out of these, three body forces are important as they contribute about 15–20% of the two body forces, to the total nuclear force.

A Brief Summary

Although the nucleus consists of a number of nucleons, the forces which act between them may be considered as two nucleon force, which is assumed as unaffected by the presence of other nucleons. Actually this force may be affected by the terms which arise only when third or fourth nucleons are present. Such forces are referred as '*many body forces*'. The two nucleon systems are the *p-p*, *n-n* and *n-p* systems. The *n-p* system can exist in a stable bound state (the deuteron). The deuteron is found mainly in ground state with the contribution of excited state as 4%. There is no direct experimental evidence on the *n-n* or *p-p* bound states. The nuclear forces are described by simple potentials, which are mainly *central*, *i.e.*, depending only on **r** and directed along the line joining two particles. We recognize nuclear forces to be (*i*) *strong* (*ii*) *short ranged*, (*iii*) *mainly attractive* and *saturable*.

The nuclear force is presumed to be mediated by an *exchange of charged* and *uncharged mesons* between nucleon cores. The $F_{p\text{-}p} = F_{n\text{-}n}$ (*charged symmetric*). $F_{n\text{-}p} = F_{nn} = F_{p\text{-}p}$ (*charge independent*). The deuteron as a mixture of S and D states, the occurrence of a magnetic dipole moment μ_d which is not exactly equal to the sum of the μ_n & μ_p and of an electric quadrupole moment can be explained by *tensor force* admixture.

A lot of experimental data is available on *n-p* and *p-p* scattering at low energies (< 10 MeV), which gives the behaviour of nuclear forces at $l = 0$. The coherent scattering of slow neutrons shows that $\sigma_{\text{ortho}} > \sigma_{\text{para}}$ and thus the nuclear force is *spin dependent*. *The shape independent theory* gives us that the scattering cross section can be described by the two parameters, the *scattering length a* and *effective range r*, whatsoever be the shape of potential. Thus four parameters a_t, a_s, r_t, r_s can be derived from the scattering data. The quantitative information about spin dependence and charge independence is confirmed by *p-p* scattering at low energies. The triplet state has statistical weight for *n-p* scattering as 3/4 while the singlet state has 1/4.

The saturation of nuclear forces could be explained by assuming these forces as *exchange forces*, where pions are being exchanged between the nucleons. The Bartlett spin exchange force does not lead to saturation of the binding energy per nucleons. The space exchange in the Majorana and the Heisenberg forces leads to saturation. The Majorana force contributes at least 4/5 of the attraction in the ground state of the deuteron. Heisenberg forces would give special stability of the deuteron and Majorana forces to the α-particles. The inclusion of the repulsive core in the nuclear force prevents the nucleus from collapsing and helps saturation.

The high energy *n-p* and *p-p* scattering data provide information about exchange character, velocity dependence, spin orbit coupling and effects of higher angular momenta (l). The observed quantities at high energy nucleon-nucleon scattering are : $\sigma(E)$, $d\sigma/d\Omega$, polarization parameters and their related spin correlations coefficients. The experimental data on *n-p* scattering show that the $\sigma(E)$ *v/s* E curve is linear follows 1/E law upto 290 MeV and flattens out beyond this energy because of the meson production. The $d\sigma/d\Omega$ *v/s* angle curves at various energies of neutrons scattered show that the differential cross section is minimum at an angle 90° with high values at 0° and 180°. The peak at 0° can be explained in terms of absorption and diffraction of neutrons. The backward peak at 180° is the result of exchange forces. The dip reduces as energy increases. These observations could be explained by Born approximation.

The *p-p* scattering cross section data at high energies show that σ_{pp} (elastic) = σ_{pp} (total) = σ_{nn} (total) or the nuclear forces are charge independence. The different cross-section data for high energy *p-p* scattering show that at small angles the cross sections are large which are due to Coulomb forces. The minimum around 10° arises due to the interference between Coulomb and nuclear potentials. The independence of angle in the central region of angles can be interpreted as against the charge independence of nuclear forces. These strange results were explained by assuming a potential that is attractive at large distances but has a strongly *repulsive core or hard sphere*.

Much information about the nuclear potential is obtained by the experiments on polarization yield. The polarization $P(\theta)$, called the double scattering parameter is obtained by measuring left-right symmetry upon scattering from the second target which works as analyzer. The depolarization can be measured with the triple scattering experiment by measuring polarization parameters of the three targets used and left-right asymmetry after the third target. The longitudinal polarization or transformation parameters, rotation parameters and the spin correlation parameters are obtained from polarization experiments. Gammel and Thaler have assumed a mixture of central, tensor and spin-orbit potential to explain the polarization and triple scattering data. Signall and Marshak also produced a potential by adopting Gartenhaus potentials derived on the basis of the meson theory and adding to it the hard core and the spin-orbit potentials. The potentials suggested by Yale group can reproduce the scattering results. Hamada and Johnston potential is able to give an excellent reproduction of both *p-p* and *n-p* data upto about 300 MeV.

Once pion exchange potential (OPEP) suggested by Yukawa was found to fit experimental data only for inter nucleon distances > 2 fm. One bosin exchange potential (OBEP) is used to explain the hard core by assuming the exchange of heavy mesons or two pions. Recently Paris group and Bonn group carried out the work for nucleon-nucleon potentials to fit the experimental data. But till date no single potential is available which satisfies the observed data.

EXERCISES

Example 1. *Recall that b~λ/4~π/2K for the ground level of the deuteron. From this, show that the radius of the deuteron, in the rectangular well model is approximately given by*

$$R = 2bV_0^{1/2}/\pi B^{1/2}.$$

From equations, (9) and (10) of the deuteron problem, we have

$$K^2 = \frac{M}{\hbar^2}(V_0 - B) \text{ and } \alpha^2 = \frac{MB}{\hbar^2}$$

$$\therefore \quad K/\alpha = [(V_0 - B)/B]^{1/2}.$$

Since $b = \pi/2K$ (given) and $R = 1/\alpha$, hence

$$\frac{\pi/2b}{1/R} = \left(\frac{V_0 - B}{B}\right)^{1/2} \text{ or } R = \frac{2b}{\pi}\left(\frac{V_0 - B}{B}\right)^{1/2}$$

As $B << V_0$, we can write for an approximation $V_0 - B \simeq V_0$.

$$\therefore \qquad R = 2b\ V_0^{1/2}/\pi B^{1/2}.$$

Example 2. *Show that for a square well of depth V_0 and range b, the scattering length a for a spinless neutron is given by the relation*

$$K \cot Kb = (b - a)^{-1}, \text{ where } K = (MV_0)^{1/2}/\hbar.$$

For a square well of depth V_0 and radius r_0, we have

$$k_1 \cot k_1 b = k \cot (kb + \delta_0)$$

where $k_1 = \sqrt{[M(E + V_0)]}/\hbar$ and $k = \sqrt{(ME)}/\hbar$.

Since $V_0 >> E$, hence we can write $k_1 = \sqrt{(MV_0)}\hbar = K$. As the phase shift $\delta_0 = -ak$.

$$\therefore \qquad K \cot Kb = k \cot (kb - ak) = k \cot k\,(b - a)$$

$$= \frac{k}{\tan k\,(b-a)} = \frac{k}{k\,(b-a)} = \frac{1}{b-a}.$$

Example 3. *If the neutron and proton in a deuteron interact through a square well potential of width $(b) = 1.9$ fm and depth $(V_0) = 40$ MeV in an $l = 0$ state. Calculate the probability that the proton moves with in the range of the neutron with the approximation $Kb = \pi/2$, where $K = \sqrt{M(V_0 - E_B)/\hbar^2}$ and E_B the binding energy of the deuteron. Find the mean square radius of the deuteron.*

For a square well potential of width b and depth V_0, the radial wavefunctions are given for easy calculations as :

$$u(r) = A \sin Kr \qquad r \le b$$

$$= Be^{-\alpha(r-b)} \qquad r > b.$$

where $K = [M(V_0 - E_B)/\hbar^2]^{1/2}$ and $\alpha = [ME_B/\hbar^2]^{1/2}$

The continuity of $u(r)$ and that of $u'(r)$ at $r = b$ gives

$$A \sin Kb = B$$

and

$$AK \cos KB = -\alpha B$$

$$\therefore \qquad \cot Kb = -\frac{\alpha}{K} = -\left[\frac{E_B}{V_0 - E_B}\right]^{1/2}$$

If we take $Kb = \pi/2$, then $A = B$ and $\cot Kb = 0$. This is equivalent to the assumption $V_0 >> E_B$, which means that there is only one bound state. To normalize, let

$$\int_0^\infty |\psi(r)|^2\, 4\pi r^2 dr = 1$$

or

$$4\pi A^2 \int_0^b \sin^2(Kr)\, dr + 4\pi B^2 \int_b^\infty e^{-2\alpha(r-b)}\, dr = 1$$

$$2\pi A^2 b\,(1 + 1/b\alpha) = 1$$

$$\therefore \qquad A = B = [2\pi b\,(1 + 1/b\alpha)]^{-1/2}.$$

The probability of the proton moving within the range of the force of the neutron is

$$P = 4\pi A^2 \int_0^b \sin^2(Kr)\, dr = (1 + 1/b\alpha)^{-1}$$

$$\text{As } Kb = b\sqrt{M(V_0 - E_B)/\hbar^2} = \pi/2,$$

$$\therefore \qquad E_B \simeq V_0 - \frac{1}{Mc^2}\left(\frac{\pi\hbar c}{2b}\right)^2 = 40 - \frac{1}{939.6}\left(\frac{\pi \times 1.97 \times 10^{-13}}{2 \times 1.9 \times 10^{-15}}\right) = 11.8 \text{ MeV}$$

and
$$\alpha = \frac{\sqrt{Mc^2 E_B}}{\hbar c} = \frac{\sqrt{939.6 \times 11.8}}{1.97 \times 10^{-13}} = 5.34 \times 10^{14}\ \text{m}^{-1}.$$

Thus we have
$$P = \left(1 + \frac{1}{5.34 \times 10^{14} \times 1.9 \times 10^{-15}}\right)^{-1} = 0.50.$$

The mean square radius of the deuteron

$$\begin{aligned}(\overline{r^2}) &= 4\pi A^2 \left[\int_0^b \sin^2(Kr)\, r^2 dr + \int_b^\infty e^{-2\alpha(r-b)} r^2 dr\right] \\ &= \frac{b^2}{1 + 1/b\alpha}\left[\left(\frac{1}{3} + \frac{4}{\pi^2}\right) + \frac{1}{b\alpha} + \frac{1}{(b\alpha)^2} + \frac{1}{2(b\alpha)^3}\right] \\ &= \frac{b^2}{2}\left(\frac{1}{3} + \frac{4}{\pi^2} + 2.5\right) = 5.85 \times 10^{-30}\ \text{m}^2 \\ (\overline{r^2})^{1/2} &= 2.42 \times 10^{-15}\ \text{m}.\end{aligned}$$

Example 4. *Calculate scattering lengths a_t and a_r. Given that $\sigma_{\text{para}} = 4.19$ and $\sigma_{\text{ortho}} = 128$ barns.*

The theoretical expressions for the total cross-sections are

$$\begin{aligned}\sigma_{\text{para}} &= 6.69\,(3a_t + a_s)^2 \\ \sigma_{\text{ortho}} &= 6.69\,[(3a_t + a_s)^2 + 2\,(a_t - a_s)^2] + 1.74\,(a_t - a_s).\end{aligned}$$

Substituting values of σ_{para} and σ_{ortho} in above relations and solving these equations, we get following four pairs :

$$\begin{array}{r|c|c|c|c|l} a_t = & 0.91 & 0.52 & -0.52 & -0.91 & \times 10^{-14}\ \text{m}. \\ a_s = & -1.95 & -2.34 & -3.38 & -3.77 & \end{array}$$

Last two pairs can be discarded immediately because they have negative a_t values. The first pair can also be discarded on the basis that it is inconsistent with the *n-p* scattering data. Thus the remaining solution is

$$a_t = 0.52 \times 10^{-14}\ \text{m}\ ;\ a_s = -2.34 \times 10^{-14}\ \text{m}.$$

Example 5. *Calculate the total cross-section for n-p scattering at neutron energy 2 MeV (lab). Given $a_t = 5.38\ F$, $a_s = -23.7\ F$, $r_{ot} = 1.70\ F$ and $r_{os} = 2.40\ F$.*

Total cross-section
$$\sigma = \tfrac{3}{4}\sigma_t + \tfrac{1}{4}\sigma_s.$$

Using equation (97), this equation can be written as

$$\sigma = \frac{1}{4}\left[3\,\frac{4\pi a_t^2}{a_t^2 k^2 + (1 - \frac{1}{2}k^2 a_t r_{ot})^2} + \frac{4\pi a_s^2}{a_s^2 k^2 + (1 - \frac{1}{2}k^2 a_s r_{os})^2}\right]$$

In C.M. System $E_{C.M.} = \frac{1}{2} E_{Lab} = 1\ MeV$

$$\therefore \quad k^2 = \frac{ME}{\hbar^2} = \frac{1.6748 \times 10^{-27} \times 1.6 \times 10^{-13}}{(1.0549 \times 10^{-34})^2} = 2.413 \times 10^{28}$$

Substituting numerical values, we get

$$\sigma = 1.83 \times 10^{-28} + 1.074 \times 10^{-28} = 2.904\ \textit{barns}.$$

Example 6. *A deuteron is formed by n-p capture reaction ($n + p \rightarrow d + \gamma$). Experimental study of this process, with the assumption that the initial nucleons are unpolarized and the centre of mass kinetic energy T in the initial state is very small, provides information on s-wave n-p scattering. Treat the deuteron as being a pure S state, (a) characterize the leading multipolarity of the reaction with reasoning, and (b) show that the capture at low energies occurs from a spin singlet rather than spin triplet initial state.*

The singlet scattering length a_s is related with the phase shift as

$$k \cot \delta \to -1/a_s \text{ as } k \to 0.$$

As the centre of mass kinetic energy of the n-p system is very small, the only reaction possible is a S-wave capture with $l = 0$. The possible initial states are ^1S_o state $(\mathbf{s}_n + \mathbf{s}_p = 0)$. As probability P of $^1S_o = 1$ and parity is + or even, we therefore have $J^\pi = 0^+$;

$^3S_1$ state $(\mathbf{s}_p + \mathbf{s}_n = 1)$. As $P(^3S_1) = 1$, therefore $J^\pi = 1^+$. The final state is a deuteron with $J^\pi = 1^+$ and thus $S = 1$, $l = 0, 2$. The initial states have $l = 0$. Hence there are two possible transitions with $\Delta l = 0, 2$ and no change of parity. Therefore the reactions are of the $M1$, $E2$ types.

Consider these two transitions $^1S_0 \to {}^3S_1$ and $^3S_1 \to {}^3S_1$. In each case the initial and final both states have $l = 0$, only those interaction terms involving spin in the Hamiltonian can cause the transition. Since

$$\text{for } {}^1S_0 \to {}^3S_1, \quad \Delta l = 0, \quad \Delta S \neq 0$$
$$\text{for } {}^3S_1 \to {}^3S_1, \quad \Delta l = 0, \quad \Delta S = 0.$$

Therefore the initial state which satisfies the transition requirement is the spin singlet $^1S_0$ state of n-p system, the deuteron.

Example 7. *In the problem given above how does the deuteron spatial wave function vary with neutron-proton separation r for large r? If the n-p force is treated as being of very short range, the cross section* σ *depends on* T, V_0, a_s, m *and the universal parameters in the form*

$\sigma = \sigma_0 (T, V_0, m) f(a_s, V_0, m)$, where $f = 1$ *for* $a_s = 0$. *Compute the factor* f *for* $a_s \neq 0$.

The radial part of the Schrodinger equation for the system for s-waves is

$$\frac{d^2u}{dr^2} + \frac{2m}{\hbar^2}(T - V)\,u = 0.$$

where $u = rR(r)$, $R(r)$ = radial spatial wave function, $m = M/2$ and V can be approximated by a rectangular potential well of depth V_0 and width b, *i.e.*,

$$\begin{aligned} V &= -V_0 && \text{for } 0 \le r \le b \\ &= 0 && \text{for } r > b \end{aligned}$$

The solution for larger r gives the deuteron spatial wave function as

$$R(r) = \frac{A}{r} \sin (kr + \delta),$$

where $k = \sqrt{mT}/\hbar$, A and δ are constants.

The solutions of the radial Schrodinger equation for s-wave are

$$\begin{aligned} u &= A \sin (kr + \delta), && \text{for } r \ge b \\ &= A' \sin Kr && \text{for } r \le b, \end{aligned}$$

where $K = \sqrt{m(T + V_0)}/\hbar$.

The continuity of the wavefunction and its first derivative at $r = b$ gives,

$$\tan (kb + \delta) = (k/K) \tan Kb.$$

$$\therefore \qquad \delta = \arctan \left(\frac{k}{K} \tan Kb \right) - kb. \qquad ...(i)$$

The scattering across section

$$\sigma = (4\pi/k^2) \sin^2\delta. \qquad ...(ii)$$

For $k \to 0$, $\delta \to \delta_0$, $K \to K_0 = \sqrt{mV_0}/\hbar$ and $a_s = -\tan \delta_0/k$. $\qquad ...(iii)$

For $k \to 0$, equation (i) gives

$$kb + \tan \delta_0 = (k/K_0) \tan K_0b\,(1 - kb \tan \delta_0) = (k/K_0) \tan K_0b$$

or

$$kb - k\,a_s = (k/K_0) \tan K_0b$$

$$\therefore \qquad a_s = -b\left(\frac{\tan K_0b}{K_0b} - 1\right)$$

If $a_s = -\dfrac{\tan \delta_0}{k} \to 0$, then $\delta_0 \to 0$ and also k is small but finite.

The corresponding scattering cross section is

$$\sigma_0 = \frac{4\pi}{k^2}\sin^2\delta_0 = \frac{4\pi}{k^2}\delta_0^2 = \frac{4\pi k^2}{k^2}a_s^2 = 4\pi b^2\left(\frac{\tan K_0 b}{K_0 b} - 1\right)^2$$

$$\therefore \qquad f(a_s, V_0, m) = \frac{\sigma}{\sigma_0} = \frac{\sin^2\left[\text{arc tan}\left(\frac{k}{K}\tan Ka\right) - ka\right]}{k^2b^2\left(\frac{\tan K_0 b}{K_0 b} - 1\right)^2}$$

$$= \frac{\sin^2\left[\text{arc tan}\left(\frac{k}{K}\tan Ka\right) - ka\right]}{k^2b^2}$$

Example 8. *The only bound state of two nucleon configuration occurs in nature is the deuteron with* $J = 1$ *and* $E_B = -2.22$ *MeV. From this information show that the n-p force must be spin dependent. Write down the possible angular momentum states for the deuterons in an LS-coupling scheme. What combinations are possible? Which of the states are ruled out by the existence of the quadrupole moment of the deuteron?*

The spin of the naturally occuring deuterons is $J = 1$. As $J = \mathbf{s}_n + \mathbf{s}_p + \mathbf{l}_p$, we may have

for $|\mathbf{s}_n + \mathbf{s}_p| = 1, l = 0, 1, 2$ possible states are ${}^3S_1, {}^3P_1, {}^3D_1$.

for $|\mathbf{s}_n + \mathbf{s}_p| = 0, l = 1$, possible state is ${}^1P_1$.

As no stable singlet state ${}^1S_o$, where n, p have antiparallel spins and $l = 0$ is found, this shows that when n- and p- interact to form $S = 1$ and $S = 0$ states, one is stable and one is not, indicating the *spin dependence of nuclear force*.

In LS-coupling, as shown above, the possible configurations are :

${}^3S_1$ and ${}^3D_1$ of even parity

${}^3P_1$ and ${}^1P_1$ of odd parity.

As the deuteron has a definite parity, only states of the same parity can be combined. Thus

$$\psi(n, p) = A_1\,{}^3S_1 + B_1\,{}^3D_1 \quad \text{or} \quad A_2\,{}^3P_1 + B_2\,{}^1P_1$$

are the possible general linear combinations.

Since $l = 1$ in the P-state corresponds to the translation of the centre of mass of the system, which does not give rise to an electric quadrupole moment. Thus the existence of an electric quadrupole moment of the deuteron rules out the combination of P-states.

Example 9. *Specify all states of a two-neutron system with total angular momentum* $J \le 2$. *Use the notation* ${}^{2S+1}X_J$, *where X gives the orbital angular momentum.*

As $\mathbf{S} = \mathbf{s}_1 + \mathbf{s}_2$ and $s_1 = s_2 = \frac{1}{2}$. Thus the quantum number S can be either 1 or 0. The possible state can be obtained by the relation $\mathbf{J} = \mathbf{s}_1 + \mathbf{s}_2 + \mathbf{l} = \mathbf{S} + \mathbf{l}$.

For $J \le 2$, we can have the states

$$\begin{aligned} S = 0, l &= 0, J = 0 \rightarrow {}^1S_o \\ l &= 1, J = 1 \rightarrow {}^1P_1 \\ l &= 2, J = 2 \rightarrow {}^1D_2 \\ S = 1, l &= 0, J = 1 \rightarrow {}^3S_1 \\ l &= 1, J = 2, 1, 0 \rightarrow {}^3P_2, {}^3P_1, {}^3P_0 \\ l &= 2, J = 2, 1 \rightarrow {}^3D_2, {}^3D_1 \\ l &= 3, J = 2 \rightarrow {}^3F_2. \end{aligned}$$

However, two neutron system must be antisymmetric with respect to particle exchange. Thus $(-1)^{(l+S+1)} = -1$ or $l + S =$ even. Hence the possible states are

$${}^1S_0, {}^1D_2, {}^3P_2, {}^3P_1, {}^3P_0, {}^3F_2.$$

Example 10. *Two nucleons interact with nuclear force of range $r = 2$ fermi in a state in which the maximum possible value of angular momentum quantum number is 1. What must be the K.E. of each nucleon in CM-frame of reference and the K.E. of the incident nucleon in the frame of reference where the nucleon with which it interacts is initially stationary? Show that the differential cross section is isotropic if the K.E. of each nucleon in CM reference frame is less than 10 MeV.*

The maximum possible value of the orbital angular momentum L for a system of two interacting nucleons of linear momenta p and maximum separation r' (at which the interaction is possible) is given by the relation

$$L = pr' = \sqrt{l(l+1)^2}\ \hbar$$

With $l_{\max} = 1$, we get $L = pr' = \sqrt{2}\,\hbar$.

or $p = L/r' = \sqrt{2}\,\hbar/r'$.

Kinetic energy of each nucleon in CM-frame of reference is

$$K = \frac{p^2}{2M} = \frac{2\hbar^2}{2Mr'^2} = \frac{(1.0546 \times 10^{-34})^2}{1.674 \times 10^{-27} \times (2 \times 10^{-15})^2} = 1.661 \times 10^{-12} \text{ joule} = 10 \text{ MeV}.$$

Therefore the total kinetic energy in the CM frame of reference is

$$K_{\text{Total, CM}} = 2K = 20 \text{ MeV}.$$

One can show that the kinetic energy of the moving particle in the frame of reference in which the other (identical) one is at rest initially is twice the total kinetic energy in the CM frame of reference.

∴ Kinetic energy of the incident nucleon = $2K_{\text{Total, CM}} = 40$ MeV.

If the K.E. of each nucleon in the C.M. frame is less than 10 MeV, then each will have a momentum p given by

$$p < \frac{\sqrt{2}\,\hbar}{r'} = \frac{h}{\sqrt{2}\pi r'} \text{ or } \frac{h}{pr'} > \sqrt{2}\pi.$$

In terms of the nucleon's wavelength λ, using de Broglie relation, we get

$$\lambda/r' > \sqrt{2}\pi \text{ or } \lambda/r' >> 1.$$

Since the separation between adjacent minima in the scattering pattern $\theta = \lambda/r'$, therefore

$$\theta = \lambda/r' >> 1.$$

This inequality means that there are no minima and the differential scattering cross section $d\sigma/d\Omega$ is isotropic.

Since $K = 10$ MeV is the condition for $l_{\max} = 1$, therefore for $K < 10$ MeV we may only have $l_{\max} = 0$. Thus $l_{\max} = 0$ is equivalent to the identity $\theta = \lambda/r' >> 1$.

Oral Questions

1. If the nuclear force is charge independent and a neutron and a proton form a bound state, then why is there no bound state for two neutrons? What information is obtained from it?
   [A system of a neutron and a proton can form either singlet or triplet spin state. The triplet state is a bound state because the energy level of the singlet state is higher. A system of two neutrons which are in the same energy level can form only singlet spin state and no bound state is therefore possible, the potential is too weak to lead to binding. This shows that the nuclear forces are spin dependent.]
2. What does the spectroscopic notation $^3D_1$ or $^3S_1$ indicates?
   [S meaning $l = 0$, D meaning $l = 2$, the subscript gives the value of total angular momentum j, and the superscript gives the value of $2s + 1$, where s is the intrinsic spin angular momentum quantum number.]
3. Show that the D-state probability in deuteron is roughly 4%.
4. The deuteron is a bound state of a proton and a neutron of total angular momentum J = 1. It is known to be an S state with a mixture of D-state. Why a P or G state can not contribute to S-state?
5. Show that the range of the tensor interaction in the deuteron having electric quadrupole moment as 2.82 mb is 2.2 $\times 10^{-15}$ m.

6. The existence of which property of deuteron shows that its probability density function is not spherically symmetric or the nuclear potential is not spherically symmetric. (Quadupole moment)
7. There are no bound deuterons with nucleon spins essentially antiparalled, why?
8. What would happen if a nucleon in a nucleus interacts with all other nucleons instead with a limited number of the many other nucleons only? ($\Delta E_B/A \propto A$)
9. Which data showed that the singlet state potential is about 40% weaker than the triplet state potential? (scattering of very low energy neutrons from ortho and para hydrogen)
10. Which information can be obtained by the scattering of the high energy nucleons only? (nucleon potential)
11. The deuteron has a magnetic moment which is approximately the sum of the proton and neutron magnetic moments. What can one infer concerning the orbital motion and spin alignment of the neutron and proton in the deuteron? ($l = 0$, $I = 1$ is $^3S_1$ state, spins parallel)
12. How might one interpret the lack of exact equality of μ_d and $\mu_n + \mu_p$? (Mixture of $^3S_1$ and $^3D_1$)
13. How can the neutron have a non zero magnetic moment on being the neutral charge? (Asymmetrical distribution of the three quarks)

Problems

1. Use the well parameters $^3a = {}^1a = 2.8$ F, $^3V_0 = 21$ MeV and $^1V_0 = 12$ MeV to compute the scattering cross-section for 2 MeV (lab) neutrons. (3.0 barns)
2. Use the parameters $a_t = 5.38$F, $r_{0t} = 1.70$ F and $a_s = -23.7$F to determine r_{0s} from the experimental observation that $\sigma = 1.69$ barns at energy 4.75 MeV (lab). (2.4 *fm*)
3. Worthington and others measured a p-p differential scattering cross section of 0.1114 barns/steradian (C.M. system) for a proton energy of 4.203 MeV (lab) and a scattering angle of 60° (C.M. system). Calculate the phase shift. (46°)
4. Prove that $(\sigma_1 \cdot \sigma_2)^2 = 3 - 2\sigma_1 \cdot \sigma_2$ and that $(\sigma_1 + \sigma_2)^2 = 0$.
5. Show that p-p scattering can take place only in ^1S, ^3P, ^1D......states. What can you say about the total isospin of the n-p system in these states?
6. Using the parameters of the shape independent approximation, calculate the absolute value of the binding energy of the singlet state of the deuteron. Given $^1a = -23.7$ fm, and $^1r_0 = 2.7$ fm and mass of nucleon $= 1.67 \times 10^{-27}$ kg. (66 keV)
7. If instead of the observed value of $J^\pi = 1^+$ the ground state of a deuteron is $J^\pi = 0^-$, what are the possible values of orbital angular momentum L, sum of intrinsic spin S and isotopic spin T in this hypothetical state? What are the implications for nuclear force in this case?
8. Show that $P_B = \frac{1}{2}(1 + \sigma_1 \cdot \sigma_2)$ and that $P_H = -P_\tau = -\frac{1}{2}(1 + \tau_1 \cdot \tau_2)$, where P_τ is an operator that exchanges only i-spin between the nuclei.
9. Show that for $E = 10$ MeV, the calculated values of scattering cross section for $n - p$ sctering agrees with experiments, but that for $E = 1$eV there is no such agreement. Explain why?
10. The scattering of epithermal neutrons from the two protons of H_2 is coherent. The cross section for scattering from parahydrogen is given by $\sigma_{para} = (16/9)4\pi\, a^2_{para}$ with a coherent scattering length $\sigma_{para} = 2\left[\frac{3}{4}a_t^2 + \frac{1}{4}a_s^2\right]$. The parahydrogen scattering cross section has been found to be $\sigma_{para} = 3.9b$, while that for free protons is $\sigma = 20.6$b. Prove that the $n - p$ singlet state is not bound.
11. A nucleon is incident on a nucleon which is initially stationary. Its kinetic energy, which is also the total kinetic energy of the system in that frame of reference, is K. Show that the total kinetic energy of the system in the frame of reference in which the centre of mass of the system is stationary is $K/2$.
12. Show that for a nucleon potential of radius $r' = 2F$, the maximum value of the orbital angular momentum quantum number is $l_{max} = 1$ unless the kinetic energy of each nucleon exceeds about 30 MeV in the centre of mass frame of reference. Also show that $l_{max} = 2$ unless the kinetic energies exceed about 60 MeV.
13. The phase analysis of triplet state $n - p$ scattering shows that δ_0 goes through zero at laboratory energy of 350 MeV. Calculate the hard core radius for a well potential (V_0, b_t) so as to give the correct deuteron binding energy, correct scattering lengh and a zero phase shift at this energy. (0.1 fm, 40.1 MeV, 1.89 fm)
14. Using the square well potential of depth $V_0 = 38.5$ MeV and width $b = 1.93$ fm, calculate the rms value of the deuteron and compare the result with the value of 2.17 fm found by electron scattering experiment.

REFERENCES

1. Benedetti, Sergio De, *"Nuclear Interactions"*, John Wiley & Sons, New York, 1967.
2. Bethe, Hans A. and Philip Morrison, *"Elementary Nuclear Theory"*, John Wiley & Sons, New York, 1956.
3. Blatt, John M. and Vector F. Weisskopf, *"Theoretical Nuclear Physics"*, John Wiley, New York, 1952.
4. Breit, G., *Rev. Mod. Phys.*, **34**, 766 (1962).
5. Brink, D.M., *"Nuclear Forces"*, Pergamon Press, 1965.
6. Brown, G.E. and A.D. Jackson, *"The Nucleon-Nucleon Interaction,"* North Halland, 1976.
7. Burhop, E.H.S. (Ed.), *High Energy Physics*, Vol I, Academic Press, New-York, 1967.
8. Christian, R.S. and H. P. Noyes, *Phys. Rev.*, **79**, 85 (1950).
9. Cziffra, P., M. H. Macgregor, M. J. Moravesik and H.P. Stapp, *Phys. Rev.*, **114**, 880 (1959).
10. Elton L.R.B., *"Introduction to Nuclear Physics"*, Sir Isaac Pitman & Sons, Ltd., 1959.
11. Enge, Harald A., *"Introduction to Nuclear Physics"*, Addison Wesley, 1966.
12. Evans Robley D., *"The Atiomic Nucleus"*, McGraw Hill., New York, 1955.
13. Flugge, S. (Ed.), *"Encyclopedia of Physics"*, Berlin Springer, 1957.
14. Gammel, J.L., and R.M. Thaler, *Phys. Rev.*, **107**, 291, 1337 (1957).
15. Gartenhaus, S., *Phys. Rev.* **100**, 900 (1955).
16. Gillet, V., A. Green and E. A. Sanderson, *"Nuclear Physics,"* **88**, 321 (1966).
17. Hess, W. N., *Rev. Mod. Phys.*, **30**, 368 (1958).
18. Jastrow, R., *Phys. Rev.*, **81**, 185 (1951), **79**, 389 (1950).
19. Machleidt, R., K. Holinde and Ch. Elster, *Phys. Rep.*, **149**, 1 (1987).
20. Marmier, P. and E. Sheldon, *"Physics of Nuclei and Particles,"* Vol II, Academic Press, N. Y. 1970.
21. Marshak, R.E. and P.S. Signell, *Phys. Rev.*, **109**, 1229 (1958).
22. Meyerhof Walter E., *"Elements of Nuclear Physics"*. McGraw Hill, 1967.
23. Moavesik, M.J., *"The Two Nucleon Interaction"*, Oxford University Press, 1963.
24. Nigam, B.P., *Rev. Mod. Phys.*, **35**, 117 (1963).
25. Preston, M.A. *"Physics of the Nucleus,"* Addison Wesley, 1962.
26. Roy, R.R. and B.P. Nigam, *"Nuclear Physics"*, John Wiley, New-York, 1967.
27. Rho, M. and D.H. Wilkinson (Ed.), *"Mesons in Nuclei"*, North Holland Amsterdam, 1979.
28. Sachs, Robert G., *"Nuclear theory"*, Addison Wesley, 1955.
29. Segre E. (Editor), *"Experimental Nuclear Physics Part IV"*, Wiley, New York, 1952.
30. Signell, P. and R.E. Marshak, *Phys. Rev.*, **106** 832 (1957).
31. Stapp, H.P., T. J. Ypsilantis, and N. Metropolis, *Phys. Rev.*, **105**, 302 (1957).
32. Wilson, R., *"Nucleon-Nucleon Interaction"*, Wiley (Interscience), NY, 1963.

13

NUCLEAR FISSION AND FUSION

13.1 NUCLEAR FISSION

When uranium was bombarded with neutrons it was found that a β-active product resulted, followed by a whole chain of β-active products such as

$$^{238}_{92}U + ^{1}_{0}n \rightarrow ^{239}_{92}U \rightarrow ^{239}_{93}X \rightarrow ^{239}_{94}Y \rightarrow \text{etc.}$$

It was recognized that more than one neutron was produced. O. Hahn and F. Strassman in 1939 proved that the product might be consisted of two large fragments, which they identified as barium and krypton. O.R. Frisch and L. Meitner in 1939 used the *word fission to describe the process which takes place when a heavy nucleus is caused to break down into two roughly equal parts, known as fission fragments.* In this process neutrons are also emitted with the release of considerable energy. This process has been also observed to occur when heavy nuclides are bombarded with protons, deuterons, α-particles and even electrons and gamma rays. Further work showed that lighter elements could also be fissioned by high energy particles, as for example in the case of copper

$$^{63}_{29}Cu + ^{1}_{1}p \rightarrow ^{24}_{11}Na + ^{39}_{19}K + ^{1}_{0}n. \qquad ...(1)$$

A-Types of Fission

(a) Thermal Fission. Since a thermal neutron adds negligible energy to the fissionable nucleus, it is clear from semi-empirical mass formula that the fission of the nuclei in which the compound nuclei are of even-even structure take place even with the thermal neutrons. Fission of ^{235}U and ^{239}Pu by thermal neutrons are the most important reactions.

(b) Fast Fission. Other isotopes of Uranium and other elements which form compound nuclei of even-odd structure enter into (n, f) reactions with fast neutrons (≥ 1 *MeV*). The example is ^{238}U.

(c) Charged-particle Fission. Elements with $Z > 90$ show fission process with protons, deuterons and α-particles. High energy charged particles induce fission in elements even in the middle of the periodic table.

(d) Photo Fission. High energy photons induce fission in the heavier elements. 5.1 *MeV-γ-rays* can produce fission with ^{238}U. The photo-fission of uranium and thorium was investigated by E.W. Titterton and coworkers in 1950 using continuous X-rays from Synchrotron with a maximum energy of 24 *MeV*. They used the photographic plate technique, and measured the ranges of the fission fragments and compared the kinetic energies of the fission fragments from thorium with those produced in slow neutron fission of ^{235}U. They found that the average kinetic energy released in the photofission of ^{232}Th was about 0.8 of that released in the slow neutron fission of ^{235}U.

(e) Ternary Fission. R. Present in 1941 using liquid drop model predicted the possibility of tripartition or ternary fission, *i.e.* the division of the excited heavy nucleus into three nuclei of comparable masses. L. Rosen and A.M. Hudson in 1949 found about 4.3 ternary fission per 10^6 binary fission of ^{235}U

bombarded with slow neutrons. K.W. Allen and J.T. Dewan in 1950 bombarded ^{233}U, ^{235}U and ^{239}Pu with slow neutron and found the third particle as a long range α-particle (~ 15 *MeV*) in about 0.2% of the fissions.

In all cases **very large** disintegration energies are released and fast neutrons are emitted. Meitner and Frisch indicated that, because of their exceptionally high neutrons to protons ratio, the fission fragments should be unstable, undergoing a chain of β^- disintegrations. For example

$$ {}^{235}_{92}U + {}^{1}_{0}n \rightarrow {}^{236}_{92}U \begin{array}{l} \nearrow {}^{98}_{40}Zr \rightarrow {}^{98}_{41}Nb \rightarrow {}^{98}_{42}Mo \\ \searrow {}^{136}_{52}Te \rightarrow {}^{136}_{53}I \rightarrow {}^{136}_{54}Xe \end{array} + 2{}^{1}_{0}n \qquad \text{...(2)} $$

A typical beta decay chain is

$$ {}^{140}_{54}Xe \rightarrow {}^{140}_{55}Cs \rightarrow {}^{140}_{56}Ba \rightarrow {}^{140}_{57}La \rightarrow {}^{140}_{58}Ce \text{ (Stable).} \qquad \text{...(3)} $$

Since the nuclei near the middle of the periodic table have binding energies E_B = 8.5 *MeV*/ nucleon, therefore the *fission process is expected to release a large amount of energy.* Assuming fission of a nucleus of mass number 240, for which E_B = 7.6, into two similar fragments with A = 120, the energy released in fission is 2 × 120 × 8.5 − 240 × 7.6 = 216 *MeV*. Assuming their separation equal to the sum of their nuclear radii, the Coulomb repulsion energy is given by

$$ E_C = \frac{Z_1Z_2e^2}{4\pi\varepsilon_0 d} = \frac{52\times 40\times(1.6023\times10^{-19})^2\times 8.9876\times10^9}{1.5\times10^{-14}\times1.6023\times10^{-13}}\,MeV. $$
$$ = 200\ MeV. $$

Thus we see that the Coulomb repulsion energy is nearly equal to the energy released in fission process. We can, therefore, regard this fission process as a result of Coulomb repulsion. The Q value of fission reaction (2) is also calculated from the exact mass difference of the two sides of the equation. The combined isotopic masses before and after fission are

$$ \Sigma m_i = m(^{235}U) + m({}^{1}_{0}n) = 235.04092 + 1.00866 = 236.04958\,u. $$

and $$ \Sigma m_f = m(^{98}Mo) + m(^{136}Xe) + m(2{}^{1}_{0}n) = 97.91189 + 135.91357 + 2.01732 = 235.84279\,u. $$

Hence $Q = \Delta mc^2 = (\Sigma m_i - \Sigma m_f)c^2$ = 193 *MeV*, which is comparable with the value calculated by the binding energy method.

B-Fission Cross-sections—Fission can be induced in some nuclides by certain incident particles of particular energy. For example, ^{235}U undergoes fission with thermal neutrons, whereas ^{238}U does not. However ^{238}U undergoes fission with fast neutrons (> 1 *MeV*).

The nucleus of the fissionable material (^{233}U, ^{235}U, ^{238}U, ^{239}Pu, etc.) may capture a thermal neutron to form the compound nucleus or the neutron may be scattered. The compound nucleus may either undergo fission or emit γ-rays and decay to the ground state, which may emit α-particles. The ratio of radiative capture cross section to the fission cross section is found to be about 0.18 for the nucleus ^{235}U and 0.39 for ^{239}Pu with thermal neutrons. The fission cross section varies with energy in a complicated way. In the thermal energy range, σ_f is found to follow $1/v$ law. At higher energies (0.28 *eV* to 20 *eV*), there are many closely spaced resonances (about 20 in ^{235}U). At high energies the fission cross section decreases and reduces to about 1 barn for ^{235}U and 2 barns for ^{233}U with 1 *MeV* neutrons.

Some heavy nuclides such as ^{234}U, ^{236}U, ^{238}U, do not undergo fission with slow neutrons. Fission is a threshold reaction in these nuclides and the fission cross section varies with energy. The threshold energies and fission cross sections have also been measured for fission induced by charged particles. For ^{235}U, the threshold for fission by deuterons is close to 8 *MeV*, the fission cross section rises to a value of 1 barn at about 20 *MeV*, increases slowly to a value 1.5-2 barns at 120-200 *MeV*. The threshold for fission of ^{235}U by alpha particles is about 21 *MeV*, the fission cross section rises to 1.5 barns at about 50 *MeV* and remains this value upto energies of about 400 *MeV*. The fission cross section of Uranium isotopes for various energies are shown in Fig. 13.1.

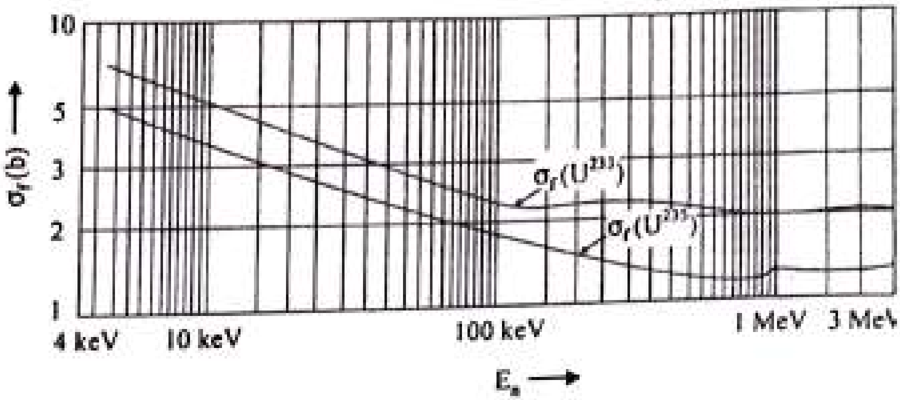

(a) Low neutron energy

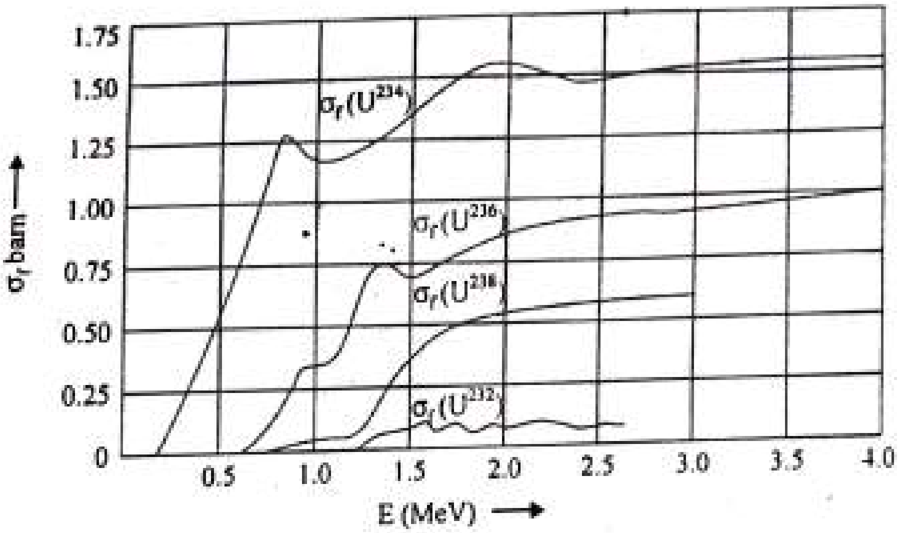

(b) Higher neutron energy

Fig. 13.1. Fission cross-sections of Uranium isotopes for neutrons of various ranges of energy.

As the energy of the incident neutron increases, various processes occur. The threshold energy is different. The lowest threshold of $^{238}U(n, f)$ reaction is ~ 2 *MeV*. As the energy reaches to ~ 6 *MeV* $(n, n'f)$ reaction starts. The $(n, 2nf)$ process can start with ~ 16 *MeV*.

Measured fission threshold energies for some nuclides are listed in the Table 13.1

Table 13.1. Measured Fission Threshold Energies

Nuclide	*Reaction*	E_{th} *(MeV)*	*Nuclide*	*Reaction*	E_{th} *(MeV)*
^{232}Th	γ, f	5.8	^{237}Np	γ, f	5.6
^{232}Pa	n, f	6.2	^{238}U	γ, f	5.8
^{233}Th	n, f	6.4	^{238}Np	n, f	6.0
^{233}U	γ, f	5.4	^{239}U	n, f	6.2
^{234}U	d, pf	5.2	^{239}Pu	γ, f	5.4
^{235}U	n, f	5.7	^{240}Pu	d, pf	4.7
^{236}U	d, pf	5.8	^{241}Pu	n, f	6.3
^{237}U	n, f	6.3	^{241}Am	γ, f	6.0

(C) Distribution of Fission Products. We have seen that a fissionable nucleus gives only two fission fragments which decay by β^--emission to a *stable end product*. Although the sum of two large fragments always adds up to 234, there is a wide distribution in possible products. The mass distribution of the fission products is shown most conveniently in the form of a *fission yield curve*, in which the percentage yields *(in log scale)* of the different products are plotted against mass number. There is a tendency for masses to concentrate respectively round 90 and round 140. Actually about 97% of the total fission products fall within the narrow range 85—104 for the lighter fragments and 130–149 for the heavier. In the case of ^{235}U the maxima lie near mass numbers 95 and 140; fission produced by slow neutrons is highly asymmetric and division into two equal fragments occurs in only about 0.01% of the fission. This feature of fission is not understood. Its explanation is possible with the detailed study of the dynamics of the fission process. It will be noted that the most probable configuration is in the region of the closed neutron shells at 50 and 82. It is not clear why such closed shells retain their influence in the nuclear fission process. Symmetric fission becomes increasingly more probable with increasing neutron energy. Single peak appears for high energy neutrons (≥ 100 *MeV*). The trough in the curve also tends to fill, when the nuclei are fissioned by the particles other than neutrons. A comparison of the ^{233}U and ^{239}Pu fission yield curves shows that the distribution of the heavier products are practically the same, whereas the portions of the curves for the lighter fragment yields are displaced by six mass units with respect to other.

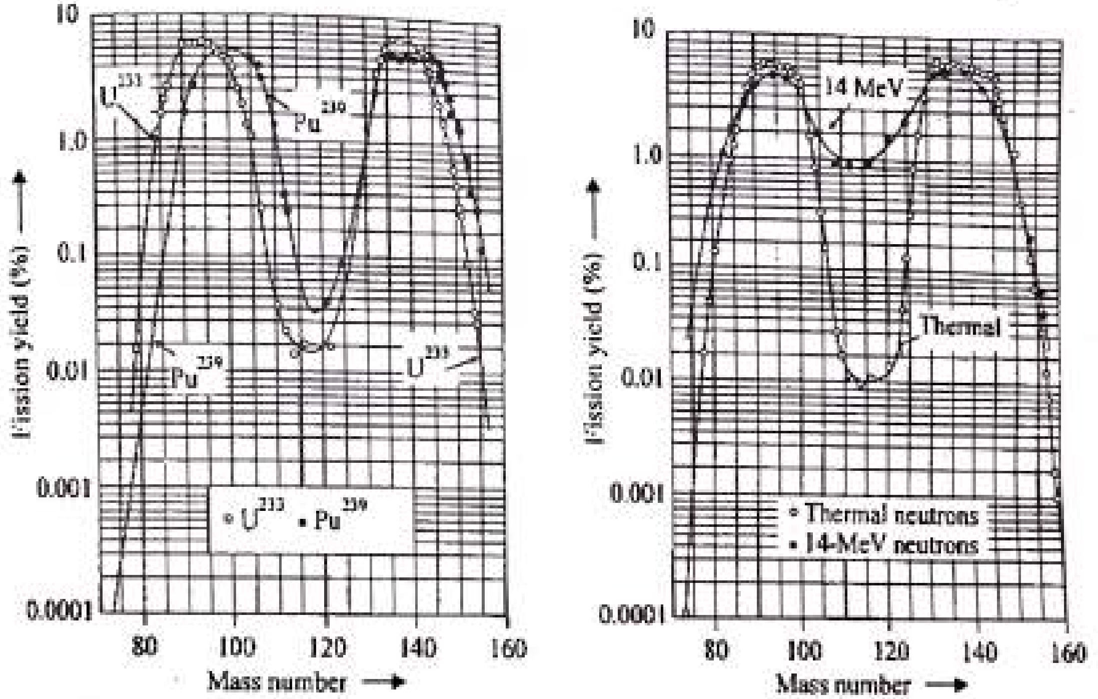

(a) (b)

Fig. 13.2. (a) Thermal fission of ^{233}U and ^{239}Pu, (b) Thermal and fast fission of ^{235}U.

The mass distribution of the fission fragments can also be obtained from the distribution of their kinetic energies. The nucleus undergoing fission can be considered to be at rest initially and, if the neutrons emitted are neglected, the law of conservation of momentum gives $M_1v_1 = M_2v_2$.

$$\frac{E_1}{E_2} = \frac{\frac{1}{2}M_1v_1^2}{\frac{1}{2}M_2v_2^2} = \frac{M_2}{M_1}. \qquad \text{...(4)}$$

Thus we see that the masses are inversely proportional to the kinetic energies. W. Jentschke and F. Prankl in Germany and Booth, Dunning and Slack in U.S.A. showed that there were two distinct groups, each group were found to have mean energies about 70 and 100 *MeV*. Later studies, based on measurement of ionization and velocities of the fission fragments, indicate that the K.E. of these fragments is 167 *MeV* in the fission of ^{235}U by slow neutrons (Fig. 13.3). There are two groups of energies, with maxima about 68 and 99 *MeV*. The difference between this quantity and the quantity released in fission process is carried out by the gamma rays, neutrons, beta particles and neutinos. From equation (4), it is clear that $M_1/M_2 = E_2/E_1 = 99/68 = 1.5$, which is in close agreement with the ratio 140/95. Such measurement on the fission fragment energies gives us a clear evidence for the asymmetry of the fission process.

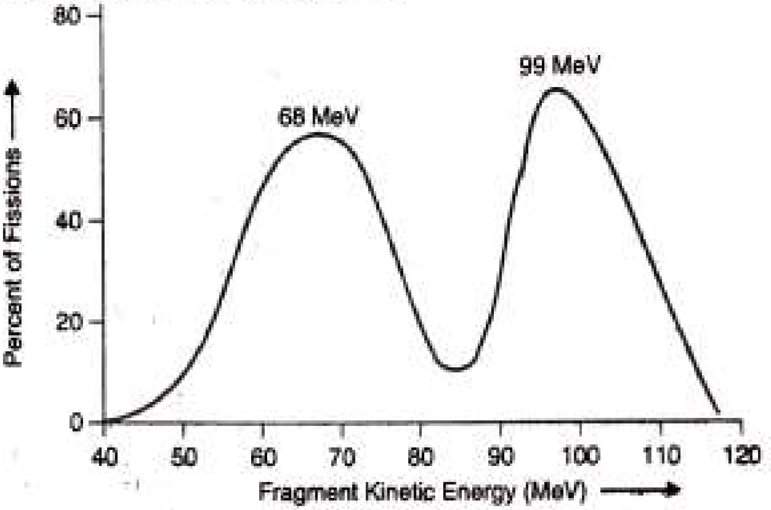

Fig. 13.3. Kinetic energy distribution of fission fragments in ^{235}U.

D-Distribution of Fission Energy—The energy released upon fission of ^{235}U by thermal neutrons is distributed among various modes as follows :

Kinetic energy of fragments	166.2 ± 1.3 *MeV*
Energy of fission neutrons	4.8 ± 0.1 *MeV*
Energy of instantaneous γ-quanta	8.0 ± 0.8 *MeV*
Energy of β-particles from the fission products	7.0 ± 0.3 *MeV*
Energy of γ-radiations from fission products	7.2 ± 1.1 *MeV*
Energy of antineutrinos from fission products	9.6 ± 0.5 *MeV*
Total Energy	202.8 ± 0.4 *MeV*

Comparing the average values of the masses and energies of fission fragments, we obtain the average kinetic energy per nucleon of the fission fragments.

For light fragments $(T_1)_{ave}/(M_1)_{ave} = 99/95 = 1 MeV/nucleon$

For heavy fragments $(T_2)_{ave}/(M_2)_{ave} = 68/140 = 0.5 MeV/nucleon.$

E—Neutron Emission in Fission—An accurate knowledge of the average number of neutrons emitted per second is of great importance to the scientists. Actually the number of neutrons released in any one fission is an integer, but average value, v_{av}, of the number of neutrons in one fission is not an integer, because the fissionable nucleus can divide in at least 30 different ways, and can be obtained by the relation

$$v_{av} = \Sigma(n\, v_0)/\Sigma n. \qquad ...(5)$$

Most of these (~ 99%) neutrons are emitted within possibly 10^{-13} sec. and are called *prompt neutrons.* A smaller number (<1%) of neutrons is also emitted with a time lag of several seconds to more than a minute after the fission. These neutrons are called *delayed neutrons.*

Measurements of the change in the number of delayed neutrons with time showed that their decrease is described by a curve which can be decomposed into several exponential curves with different half lives. About 0.65% of all ^{235}U fissions emit delayed neutrons. Six important groups of delayed neutrons are observed with half lives ranging from 0.23 to 55.7 sec. The rate of decay of each group is exponential. The same group of delayed neutrons are found in the fission of different heavy nuclides by slow or by fast neutrons, but the yields vary from nuclide to nuclide. The yield is 0.64% for ^{235}U and 0.21% for ^{239}Pu. The delay neutrons have a strong influence and play an important role in the control of fission based chain reacting system.

Table 13.2. Delayed Neutrons from Fission of ^{235}U

Half life (sec)	*Energy of neutrons MeV*	*% Yield (relative to total neutron emission)*
55	0.25	0.021
24	0.56	0.140
4.51	0.43	0.125
1.52	0.62	0.253
0.6	0.42	0.074
0.2	—	0.027

A.H. Snell and his coworkers in 1947 showed that the 55 sec delayed neutron activity came from an excited state of Krypton-87 formed by β^--decay of ^{87}Br, with a half life of 55 sec. As clear from Fig. 13.4, the ^{87}Br *emits* β^--particles forming ^{87}Kr in excited state, which emits promptly a neutron forming ^{86}Kr in ground state. ^{87}Kr may also emit γ-rays forming unstable ^{87}Kr in ground state, which further emits β^--particles forming ^{87}Rb (4.7×10^{10} *yrs*) which further emits β^--particles forming stable ^{87}Sr. An exactly analogous decay scheme was found in the β^--decay of ^{137}I (24 *sec*). The excited state of ^{137}Xe emits 24 sec delayed neutrons forming ^{136}Xe in ground state.

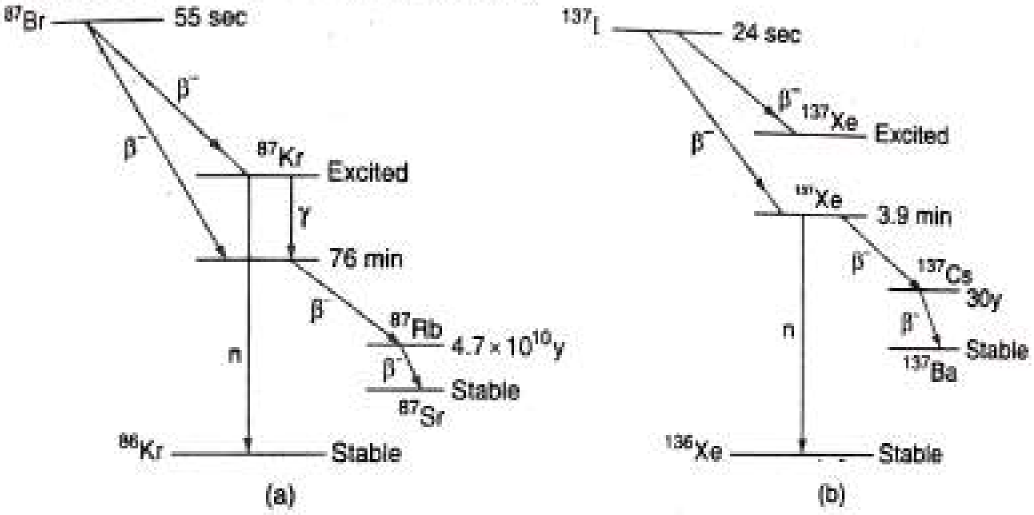

Fig. 13.4. Delay neutron emission by fission fragments.

For sufficiently large piece of fissionable substance, the neutrons that are released in a first fission process will be absorbed by the other nuclei and produce new processes which in turn emit new neutrons. Actually some of the compound nuclei decay to the ground state by gamma emission, rather than fission. The ratio of the radiative capture cross-section to the fission cross-section is usually denoted by α, given by

$$\alpha = \sigma/\sigma_f \qquad ...(6)$$

and the number of fission neutrons released per neutron absorbed in the fissionable nuclide is denoted by η and is given by

$$\eta = \nu_{av}/(1 + \alpha). \qquad ...(7)$$

The relative probability that a compound nucleus decays by fission is thus be $(1 + \alpha)^{-1}$. Values of ν_{av}, α, and η for thermal neutrons (2200 m/sec) are listed in the table 13.3.

Table 13.3. Characteristics of Fissiable Materials for 2200 m/sec neutrons

Properties	^{233}U	^{235}U	*Natural uranium*	^{239}Pu
σ_{abs}	578 ± 4	683 ± 3	7.68 ± 0.07	1028 ± 8
σ_f	525 ± 4	577 ± 5	4.18 ± 0.06	742 ± 4
σ_γ	53 ± 2	101 ± 5	3.50	286 ± 4
ν_{av}	2.51 ± 0.02	2.44 ± 0.02	2.47	2.89 ± 0.03
α	0.101 ± 0.004	0.18 ± 0.01	0.83	0.39 ± 0.03
η	2.28 ± 0.02	2.07 ± 0.01	1.34 ± 0.02	2.08 ± 0.02

F-Energy distribution of neutrons emitted in thermal fission of ^{235}U. The energies of the prompt neutrons emitted in fission vary from ~ 100 *keV* to ~ 18 *MeV*. The energy spectrum of neutrons emitted has been determined using several methods for different parts of the spectrum (energy range). In the low energy range, Bonner, Ferrell and Rinehart (1952) used a cloud chamber containing hydrogen gas and water vapour at a pressure of 1/3 atmosphere. Neutrons from thermal fission of ^{235}U entered the cloud chamber and produced recoil protons by collisions with hydrogen. The number of tracks and their lengths in the chamber were observed. The energy distribution of the recoil protons was obtained from the track lengths and thus the energy distribution of neutrons was obtained. The number of neutrons $N(E)$ per 100 *keV* energy interval were plotted against the energy from about 75 to 600 *keV*, Fig. 13.5 (a).

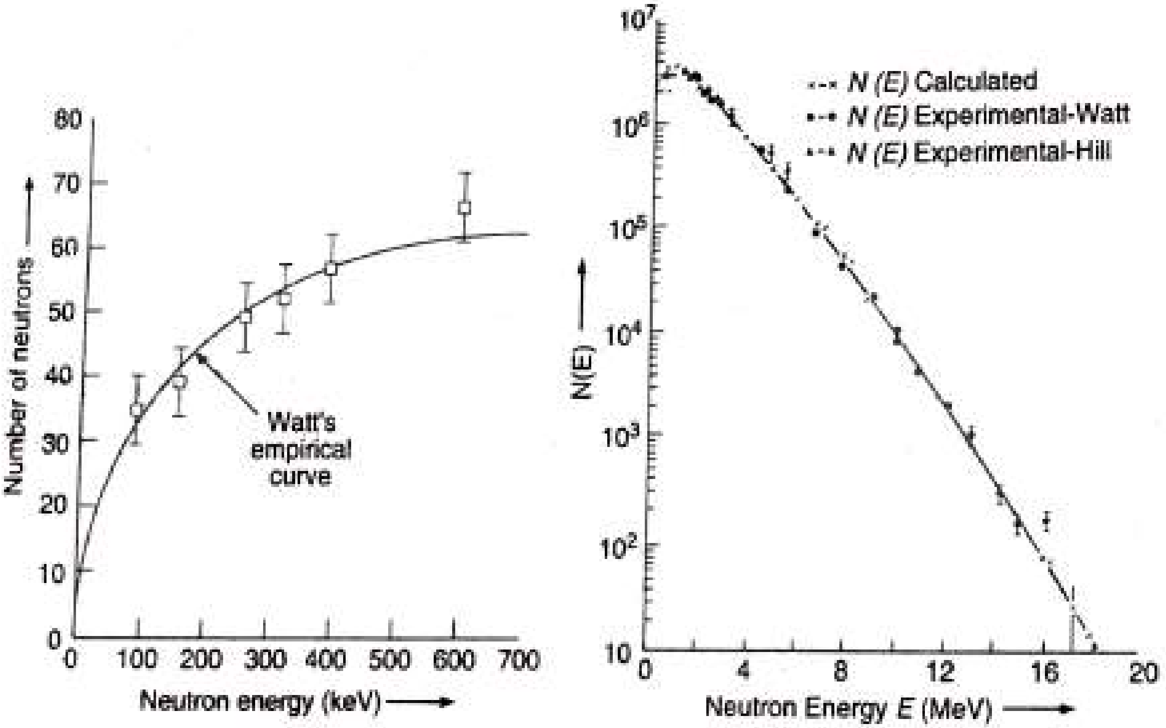

(a) Low energy range (b) High energy range

Fig. 13.5 Energy distribution of fission neutrons.

D.L. Hill in 1952 measured the spectrum of the fission neutrons in the energy range of 0.4 to 7 *MeV* by detecting the protons, ejected from a layer of paraffin due to fission neutrons, in a series of counters while passing through an absorbing material. The amount of absorbing material between the paraffin and the counters yielded the range of the protons. The energy of the protons and hence the energy of the fission neutrons could be determined from the range-energy relationship of the protons. B.E. Watt in 1952 measured the spectrum in the energy range of 3.3 to 17 *MeV* by a different technique. The fission neutrons ejected protons from a polyethylene foil and were detected by a set of counters. The different thicknesses of aluminium absorbers were placed in the path of the protons and the energy of protons and thus of neutrons were measured from the range energy relationship. These results are shown in Fig. 13.5 (b). The curve shows a maximum at 0.75 *MeV*. This distribution can be represented by a empirical formula.

$N(E) = Ce^{-E} \sinh (2E)^{1/2}$, where $N(E)$ is the number of neutrons with in a given energy interval and C is an empirically determined constant. The same empirical formula is found to be in good agreement for the low energy (as low as 0.075 *MeV*) neutrons.

G–Fissile and Fertile Materials. For a number of reasons, isotopes such as ^{238}U, which only fission with energetic neutrons; can not alone be used to fuel nuclear reactors. The only nuclide that can be fissioned with thermal neutrons is ^{235}U, which is about 0.72% of the naturally occuring uranium. The only other nuclides that can undergo fission with thermal neutrons are ^{233}U and ^{239}Pu. These do not occur in nature but can be produced by the interaction of neutrons with ^{232}Th and ^{238}U respectively and are called *fissile materials*. ^{232}Th and ^{238}U are not *fissile materials* but can be used as raw material for the production of fissile isotopes and are called fertile or fissionable materials. The nuclear reactions which convert these fertile materials into fissile materials are called *breeding reactions*. They are neutrons capture processes with subsequent β-decay.

$$\begin{aligned} {}^{238}_{92}U + {}^{1}_{0}n &\longrightarrow {}^{239}_{92}U + \gamma \\ {}^{239}_{92}U &\longrightarrow {}^{239}_{93}Np + {}^{0}_{-1}e \\ {}^{239}_{93}Np &\longrightarrow {}^{239}_{94}Pu + {}^{0}_{-1}e. \end{aligned} \qquad \text{...(8)}$$

Similarly

$$\begin{aligned} {}^{232}_{90}Th + {}^{1}_{0}n &\longrightarrow {}^{233}_{90}Th + \gamma \\ {}^{233}_{90}Th &\longrightarrow {}^{233}_{91}Pa + {}^{0}_{-1}e \\ {}^{233}_{91}Pa &\longrightarrow {}^{233}_{92}U + {}^{0}_{-1}e. \end{aligned} \qquad \text{...(9)}$$

These nuclides ^{233}U, ^{235}U and ^{239}Pu are alpha emitters, and have the following properties :

Table 13.4.

Nuclides	*Particle emitted*	*Energy (MeV)*	*Half life (years)*	*Spontaneous fission rate*
^{233}U	α	4.8	1.6×10^5	$<2 \times 10^{-4}$
^{235}U	α	4.4	7×10^8	3×10^{-4}
^{239}Pu	α	5.1	2.4×10^4	10^{-2}

H–Spontaneous Fission. Most heavy nuclides undergo spontaneous fission in competition with the α-emission. Spontaneous fission is predicted by the empirical nuclear mass equation. Consider the special case when the nucleus splits into equal parts, the *Q*-value for the fission reaction

$$E_f = [{}^{A}_{Z}M - 2({}_{z/2}M^{A/2})]c^2. \qquad \text{...(10)}$$

Consider Weizsaker's semi empirical binding energy equation and neglecting the pairing term δ, we have

$$M(Z, A) = ZM_p + (A - Z)\,M_n - a_vA + a_sA^{2/3} + a_cZ^2A^{-1/3} + a_a(A - 2Z)^2A^{-1} \qquad \text{...(11)}$$

$$M(\tfrac{1}{2}Z, \tfrac{1}{2}A) = \tfrac{1}{2}ZM_p - \tfrac{1}{2}(A - Z)M_n - a_v(\tfrac{1}{2}A) + a_s(\tfrac{1}{2}A)^{2/3} + a_c(\tfrac{1}{2}Z)^2(\tfrac{1}{2}A)^{-1/3} + \tfrac{1}{2}a_a(A - 2Z)^2A^{-1} \qquad \text{...(12)}$$

Substituting values of ${}^{A}_{Z}M$ and ${}^{A/2}_{Z/2}M$ in equation (10), we have

$$\begin{aligned} E_f &= [a_s\{A^{2/3} - 2(\tfrac{1}{2}A)^{2/3}\} + a_c\,\{Z^2/A^{1/3} - 2(\tfrac{1}{2}Z)^2/(\tfrac{1}{2}A)^{1/3}\}]\,c^2 \\ &= -\,3.42A^{2/3} + 0.22Z^2/A^{1/3}\ MeV. \end{aligned} \qquad \text{...(13)}$$

This equation shows that the splitting of a nucleus affects Coulomb energy and surface energy in such a way that the change in one and that in other tend to cancel one another partially. This is reasonable and to be expected, since the division of the nucleus increases (1) the separation between proton groups, thus reducing their Coulomb potential energy, and (2) the total nuclear surface which increases the surface energy. Thus for spontaneous fission

$$-3.42A^{2/3} + 0.22Z^2/A^{1/3} \geq 0 \quad \text{or} \quad Z^2/A \geq 15. \qquad \text{...(14)}$$

This relation shows that the fission should be energetically possible for nuclei with mass number $A \geq 85$. However, the slow neutron fission does not take place even with many of the heavy nuclei. In order to explain this discrepancy A. Bohr and J.A. Wheeler considered the Coulomb's potential barrier of the two fragments at the instant of separation. The existence of this barrier prevents the immediate breaking of these two. If we denote the height of the Coulomb barrier by E_b, we can say that the nucleus will be unstable and break apart into two fragments if $E_f > E_b$. The barrier height corresponding to the Coulomb potential between the two symmetric fragments when they are just in contact with each other is given by

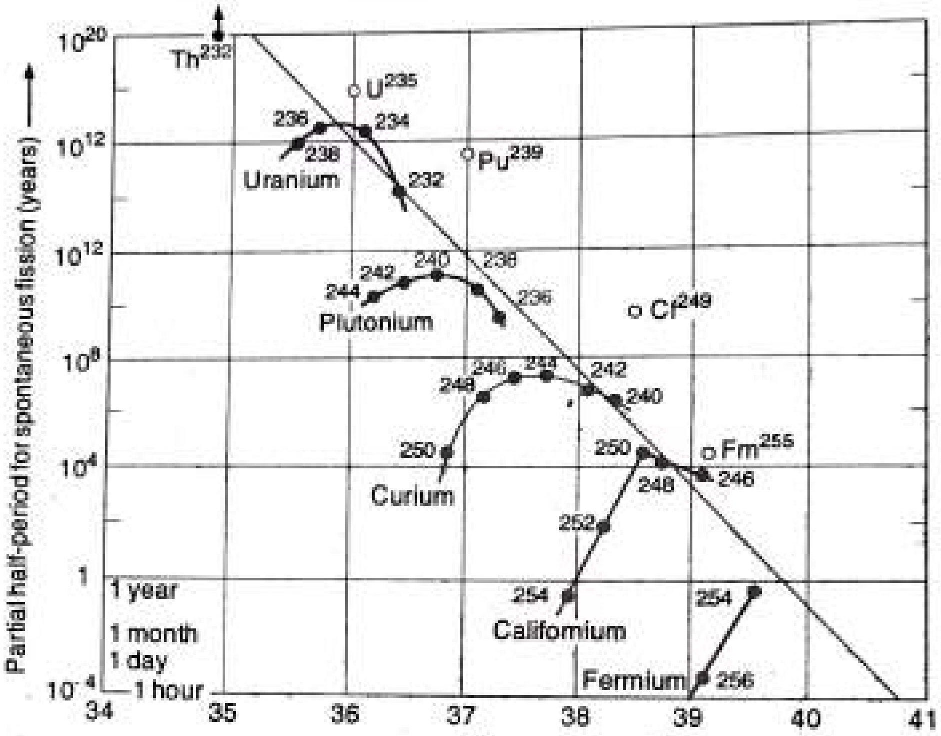

Fig. 13.6. Variation of spontaneous fission half life (Long-scale) with Z^2/A.

$$E_b = (\tfrac{1}{2}Z)^2 e^2/4\pi\varepsilon_0(2R) = Z^2e^2/32\pi\varepsilon_0 R_0(\tfrac{1}{2}A)^{1/3}$$
$$= 0.15\ Z^2/A^{1/3}\ \text{MeV}. \qquad \text{...(15)}$$

$$\therefore \quad E_b - E_f = 0.15\ Z^2/A^{1/3} - [-3.42\ A^{2/3} + 0.22\ Z^2/A^{1/3}]$$
$$= 3.42\ A^{2/3} - 0.07\ Z^2/A^{1/3}. \qquad \text{...(16)}$$

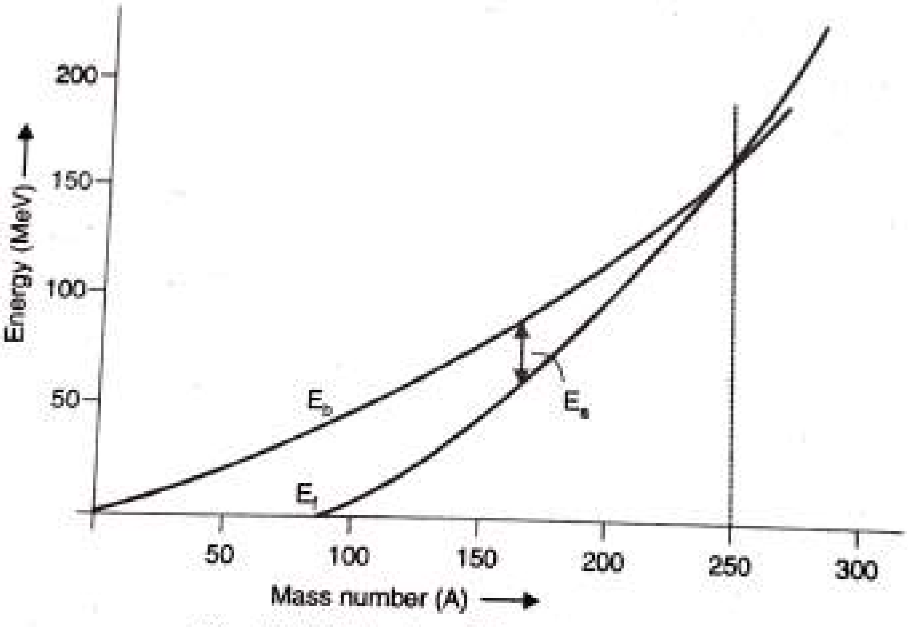

Fig. 13.7. Variation of E_b and E_f with A.

Thus the condition for stability gives

$E_b - E_f \geq 0$ or $Z^2/A \leq 49$. ...(17)

For a particular nucleus, the closer the value of Z^2/A to 50, the shorter should be the half life for spontaneous fission. It is clear that Z^2/A may have value 50 for a nucleus of mass number 250, hence a nuclide ($A > 250$) would be too unstable to exist for more than 10^{-12} sec or less. Fig. 13.6 shows the variation of half lives for spontaneous fission by a particular mode for several nuclides as a function of mass number A or Z^2/A.

Computing E_b and E_f for various values of A for symmetric fission and plotting on the same graph, we get Fig. 13.7. The graph shows that for $A \approx 250$, E_b becomes equal to E_f and $E_f > E_b$ for nuclei with $A > 250$. This indicates that we do not expect nuclei with $A > 250$ to be found in nature. This graph also shows that fission begins to become exoergic in the neighbourhood of A = 85 in agreement with the earlier occurring result.

I-Fission Isomer—In 1961, S.M. Polikanov and coworkers at Flyorov's laboratory in Dubna discovered spontaneous fission in the isomeric state (an excited state with a quite long life time). The experiment involved interaction of ^{16}O with ^{238}U. The observed period $T_{1/2}^{Sp.fission} = 0.014s$, might belong to the isomeric state of one of the product nucleus ($_{93}Np$ to $_{100}Fm$). Later experiments showed that the spontaneously fissioning isomer is the americium isotope $^{242}_{95}Am*$ whose ground state has a spontaneous fission half life $T_{1/2}^{Sp.fission} = 10^{14}$ *years*. Soon after this discovery, isomers for other isotopes of this element were discovered. More than fifty spontaneously fissioning isomers had been discovered for elements from U to La with half lives between 2×10^{-9} s and 1.4×10^{-3} s. In all these cases two astonishing results were also observed : (1) *exceptionally high probability of spontaneous fission*, about 10^{23} to 10^{26} times higher than the probability of spontaneous fission from ground state and (ii) *a very strong inhibition to gamma transitions.*

The spontaneously fissioning isomers are characterized by a large excitation energy and a small spin, which distinguishes them from ordinary isomeric nuclei. V.M. Strutinsky in 1967 explained the new class of isomers by introducing single particle corrections for the fission barrier obtained by using the liquid drop model.

Nuclear Potential Energy V = Potential energy by liquid drop model V_{ldm} + *shell correction* δ.

It was found from detailed analysis for different nuclei that the fission barrier has the form of two humps instead of one at the saddle point, Fig. 13.8. This results in the appearance of a second minimum, which corresponds to a fairly long lived excited state (isomeric state) of the nucleus. The low probability of γ-transition is due to the large potential barrier separating two potential wells. There is a very high probability of spontaneous fission in the isomeric state due to a low height and a small width $W_{fis}^{(2)}$ of the second barrier. The spontaneous fission from the ground state is determined by the parameters of the one humped barrier (dotted curve by liquid drop model). Thus the two humped fission barrier explains not only the difference in the half lives of spontaneous fission for ground and excited states, but also the strong inhibition of γ-transitions. Here E_{exc} is the excitation energy of the nucleus (in ground and excited states) at the second minimum, having value of 2-3 MeV.

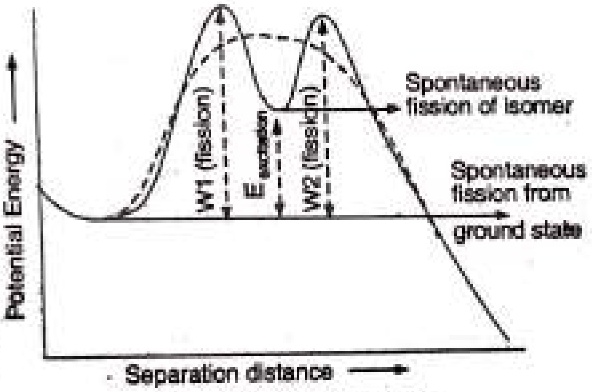

Fig. 13.8. Fission Isomers.

J-Deformation of liquid drop. The fission process can be explained with the help of liquid drop model. The incident neutron combines with the nucleus to form highly energetic compound nucleus. Its extra energy is partly the kinetic energy of the neutron but largely the added binding energy of the incident neutron. This energy appears to initiate a series of rapid oscillations in the drop, which tend to distort the spherical shape so that the drop may become ellipsoidal in shape. *The surface tension forces tend to make the drop return to its original spherical shape, while the excitation energy tends to distort the shape still further.* If the excitation energy is sufficiently large, the drop may attain the shape of a dumb-bell. If the oscillations become so violent that the critical state, stage fourth of Fig. 13.9, is reached then the final fission into stage fifth is inevitable. Thus there is a *threshold energy or a critical energy* required to produce stage fourth after which the nucleus can not return to stage first. When the distortion produced is not pronounced enough to get the nucleus beyond the critical point, the ellipsoid will return to the spherical shape with the excitation energy being liberated in the form of γ-rays and we have a *radiative capture* rather than fission.

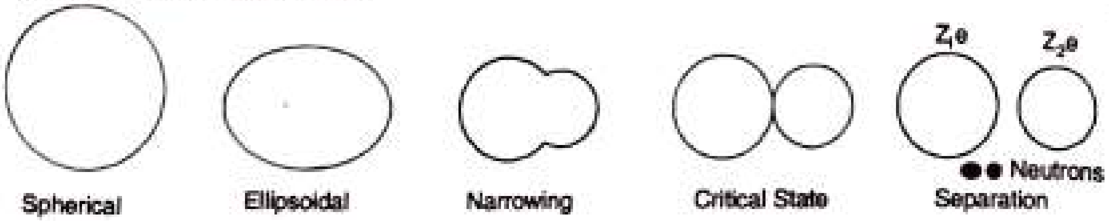

Fig. 13.9. Schematic representation of nuclear fission.

The potential energy of the drop in the different stages can be calculated as a function of the degree of deformation of the drop. It is plotted against r, the separation of the centres of two fission fragments. The curve is supposed to be divided into three regions, Fig. 13.10.

In region I, the fragments are completely separated and their potential energy E is simply the electrostatic Coulomb energy resulting from the mutual repulsion of the two positively charged nuclear fragments. If distance $r = 2R$, when the drops just touch each other, energy E at the point is less than the corresponding Coulomb potential by an amount CD. This amount is equal to the potential of the surface forces which are just beginning to come into play at this point. As we pass through region *II*, we reach the critical distance r_c, where the potential energy curve has a maximum value E_b. This corresponds to barrier height and explains why fission does not take place spontaneously in all cases where $E_f > 0$. An additional amount of energy $E_a = E_b - E_f$ the *activation energy* is required by the nuclear system before the potential barrier can be surmounted and fission can take place. In the *III* region, the fragments have coalesced and the short range nuclear forces have become predominant.

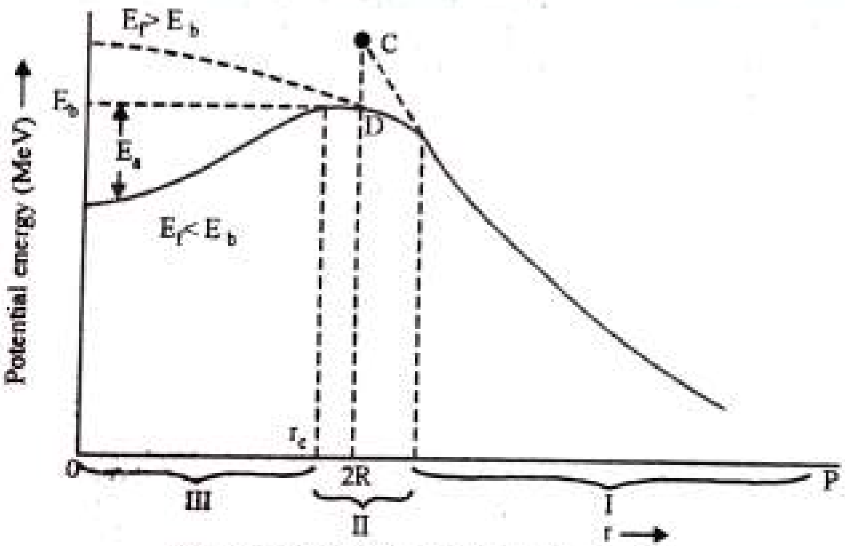

Fig. 13.10. Potential energy curve for fission.

Bohr and Wheeler's Theory of Nuclear Fission—The first thorough theoretical treatment of this process was carried out by Bohr and Wheeler in 1939. They applied a simple form of analysis (Legendre polynomial expansion) to express the radius r making angle θ with the axis of maximum deformation

$$r = R\left[1 + \sum_{l=0}^{\infty} \alpha_l P_l (\cos\theta)\right] = R\,[1 + \alpha_2 P_2 (\cos\theta) + \alpha_3 P_3 (\cos\theta) + ...]. \qquad ...(18)$$

where R is the radius of the spherical nucleus and α_2, α_3, are the deformation parameters. Here $\alpha_0 = \alpha_1 = 0$, as the centre of mass of the drop is assumed to remain unchanged.

The surface energy of a spherical drop $E^{sphere} = 4\pi R^2 T = 4\pi\,[R_0 A^{1/3}]^2 T$, where A is the mass number and T is the surface tension. Hence surface energy of the deformed drop in terms of deformation parameters is given by

$$E_s = 4\pi R_0^2 A^{2/3} T\,[1 + \alpha_2 (\tfrac{3}{2}\cos^2\theta - \tfrac{1}{2}) + ...]^2.$$
$$= 4\pi R_0^2 A^{2/3} T\,[1 + \tfrac{2}{5}\alpha_2^2 + \tfrac{5}{7}\alpha_3^2 + ...].$$

The change in surface energy of the drop due to deformation is

$$\Delta E_s = E_s^{sphere}\left[\tfrac{2}{5}\alpha_2^2 + \tfrac{5}{7}\alpha_3^2 + \dots\right]. \qquad \dots(19)$$

The Coulomb energy of a spherical drop $E_c^{sphere} = \frac{3}{5}Z^2e^2/4\pi\varepsilon_0 R$, hence that of the deformed drop

$$E_c = \frac{3}{5}\frac{Z^2e^2}{4\pi\varepsilon_0 R_0 A^{1/3}}\left[1 + \alpha_2\left(\tfrac{3}{2}\cos^2\theta - \tfrac{1}{2}\right) + \dots\right]^{-1}$$

$$\therefore \quad \Delta E_c = E_c^{sphere}\left[-\tfrac{1}{5}\alpha_2^2 - \tfrac{10}{49}\alpha_3^2 + \dots\right] = -E_c^{sphere}\left[\tfrac{1}{5}\alpha_2^2 + \tfrac{10}{49}\alpha_3^2 + \dots\right] \qquad \dots(20)$$

Thus the total energy variation, keeping only the α_2^2 term is

$$\Delta E = \Delta E_s + \Delta E_c = \tfrac{1}{5}\alpha_2^2\,[2E_s^{sphere} - E_c^{sphere}]. \qquad \dots(21)$$

If it is positive, *i.e.*, $2E_s^{sphere} > E_c^{sphere}$, the drop is stable to small distortions. Fissions may occur spontaneously if ΔE is negative or $E_s^{sphere} < \frac{1}{2}E_c^{sphere}$.

$$\therefore \quad 4\pi R_0^2\,A^{2/3}T < 3Z^2e^2/40\pi\varepsilon_0 A^{1/3}R_0 \quad or \quad Z^2/A > 45.$$

The ratio $E_c^{sphere}/2E_s^{sphere}$ is known as *critical parameter*, represented by χ. Thus when $\chi < 1$, the nucleus is stable against spontaneous fission. It is possible to estimate the degree of distortion of a nucleus in the critical state by equating the *critical or threshold energy* E_{th} to the total energy variation ΔE. From semi-empirical data $4\pi R_0^2 T = 13\ MeV$, hence for ^{238}U, $E_s^{sphere} = 520\ MeV$ and $E_c^{sphere} = 830\ MeV$ and thus $\alpha_2^2 = 1/7$.

Threshold energy or critical energy is the energy that has to be imparted to the nucleus in order to reach this critical shape when the deformed drop is about to split into two equal drops. The threshold energy is given as

$$E_{th} = 4\pi R^2 T f(\chi) = 4\pi R_0^2 A^{2/3}\,T f(\chi). \qquad \dots(22)$$

This energy can be calculated by neglecting the second order change in energy due to the neck joining the two fragments

$$E_{th} = 2\,(4\pi R_0^2)T\,(\tfrac{1}{2}A)^{2/3} - 4\pi R_0^2 A^{2/3}\,T + 2 \times \tfrac{3}{5} \times (\tfrac{1}{2}Ze)^2/4\pi\varepsilon_0 R_0 (\tfrac{1}{2}A)^{1/3}$$
$$+ (\tfrac{1}{2}Ze)^2/8\pi\varepsilon_0 R_0 (\tfrac{1}{2}A)^{1/3} - \tfrac{3}{5}(Ze)^2/4\pi\varepsilon_0 R_0 A^{1/3}.$$

$$\text{or} \quad E_{th}/4\pi R_0^2\,TA^{2/3} = f(\chi) = 0.260 - 0.215\,\chi. \qquad \dots(23)$$

For an uncharged droplet $\chi = 0$ and $f(0) = 0.260$, hence there are no electrostatic forces and the critical energy is just the work done against surface tension in separating into two drops. For $\chi = 1$, a small deformation from the spherical shape causes the drop to reach the critical shape and to separate.

If the critical energy is compared with the excitation energy, it becomes possible to predict fission probability. The excitation energy E_e, contributed to the resultant compound nucleus by the capture of a neutron, is equal to the binding energy of neutron in the compound nucleus and can be calculated by the relation

$$E_e = B(A+1, Z) - B(A, Z) = {}^{A}_{Z}M + M_n - {}^{A+1}_{Z}M.$$

The values of the excitation energy calculated in this way for a number of heavy nuclei are listed in the table 13.5 and compared with the corresponding values of the critical energy. In reviewing the results, it is seen that for ^{238}U a critical deformation energy of 6.5 *MeV* is necessary for fission, but it acquires only 5.9 *MeV* when it takes up a neutron of zero K.E. Thus no fission is possible with thermal neutrons with 0.03 *eV* energy. If the neutrons have a K.E. of 0.6 *MeV* fission becomes possible. Experiments indicate that neutrons of about 1 *MeV* energy are required. The fission cross section increases rapidly with neutron energy. The situation is quite different with ^{235}U. Here the excitation energy or the energy available by the capture of a slow neutron is greater than the threshold energy. It is evident that in this case thermal neutrons should be capable of causing fission of ^{235}U nucleus. The reason for the difference

Table 13.4. Excitation Energy and Critical Energy for Some Nuclides

Compound Nucleus	E_e *(MeV)*	E_{th} *(MeV)*	$E_e - E_{th}$ *(MeV)*
^{232}Pa	5.4	5.0	0.4
^{233}Th	5.1	6.5	–1.4
^{236}U	6.6	5.5	1.1
^{238}Np	6.0	4.2	1.8
^{239}U	5.9	6.5	–0.6
^{240}Pu	6.4	4.0	2.4

in the excitation energy for ^{236}U and ^{239}U lies in the pairing term which appears in the semi-empirical mass formula. The term makes a positive contribution of about 0.5 *MeV* to the binding energy of ^{236}U but it is zero for ^{235}U. On the other hand the contribution is zero for ^{239}U but is about 0.5 *MeV* for the ^{238}U. Thus the odd-even effect is responsible for approximately 1 *MeV* of the difference in the energies gained by these isotopes upon the addition of a neutron.

A general review of the changes in various types of nuclei, after neutron capture, shows that the liberation of energy is greater or the nuclei are likely to undergo fission with slow neutrons if the original nucleus contains an even number of protons and an odd number of neutrons or an odd numbers of both. Whereas fast neutrons would be required for the nuclei containing odd-even or even-even numbers in the same mass region.

Quantum Effects—The values shown in table 13.4 do not agree well with the measured values. This disagreement may be the result of two quantum mechanical effects.

(1) The fission may take place for excitation energies below the threshold due to the tunneling effect.

(2) The vibration of the drop in the distorted mode will have a zero point energy.

The tunneling effect is the origin of spontaneous fission. The fission problem is more difficult than the α-decay problem as it is very difficult to have a clear picture of the exact shape of the fission potential barrier. The fission barrier penetration probability

$$P \propto \exp\left[-\frac{2}{\hbar}\int_0^b (2M(V-E)^{1/2}\,dr\right], \qquad \text{...(24)}$$

where M is the reduced mass of the two fragments system, $(V - E)$ is the negative K.E. in the barrier of width b. For simplicity, let the barrier be of a parabolic form, given as

$$V = \tfrac{1}{2}K(r-R)^2, \qquad \text{...(25)}$$

where r is the separation of the two fission fragments and R is the separation at the top of the barrier. The width of the barrier b is given by the relation

$$E = \tfrac{1}{2}K(b-\tfrac{1}{2}b)^2 \quad or \quad \tfrac{1}{2}b = \sqrt{(2E/K)}. \qquad \text{...(26)}$$

Thus using parabolic function, we get

$$\begin{aligned} P &\propto \exp[-(2\pi/\hbar)(M/K)^{1/2}E]. \\ &\propto \exp[-(b\pi/2\hbar)(2ME)^{1/2}]. \end{aligned} \qquad \text{...(27)}$$

For ^{238}U, $E \sim 6$ MeV, $b = 1.5 \times 10^{-14}$ *m* and $M = 240/4 = 60$ *u*

$$\therefore \qquad P \propto \exp(-100). \qquad \text{...(28)}$$

Frankel and Metropolis obtained an expression for the life time for spontaneous fission using the idea of barrier penetration as

$$t = 10^{-21} \times 10^{7.85E_{th}} \text{ sec}. \qquad \text{...(29)}$$

Seaborg calculated E_{th} for various heavy elements and found that the fission rate could be determined by the formula

$$t = 10^{-21} \times 10^{178-3.75(Z^2/A)} \text{ sec}. \qquad \text{...(30)}$$

After comparing with equation (29), he obtained the relation

$$E_{th} = 19.0 - 0.36\, Z^2/A, \qquad \text{...(31)}$$

which is in close agreement with experiment, but applies over a small range of nuclei only.

Parity Violation in Fission—Parity violation in fission or the asymmetry of escaping fission fragments was first observed in 1978 by G.V. Danilyan and Coworkers in Moscow. A Cobalt mirror is placed in the path of the thermal neutron beam to produce about 84% polarization. It is allowed to pass through a depolarizer and spin inverter unit to invert the neutron spin s_σ. The neutron beam after passing through fission chamber enters a neutron beam monitor. The fission chamber consists of an aluminium substrate coated on both sides with a thin layer (100 $\mu g/cm^2$) of uranium oxide or plutonium oxide. The fission fragments were registered by silicon surface barrier detectors for two orientations of the neutron spin (along and opposite to the direction of motion of the fragment). The schematic diagram showing experimental set up is shown in Fig. 13.11.

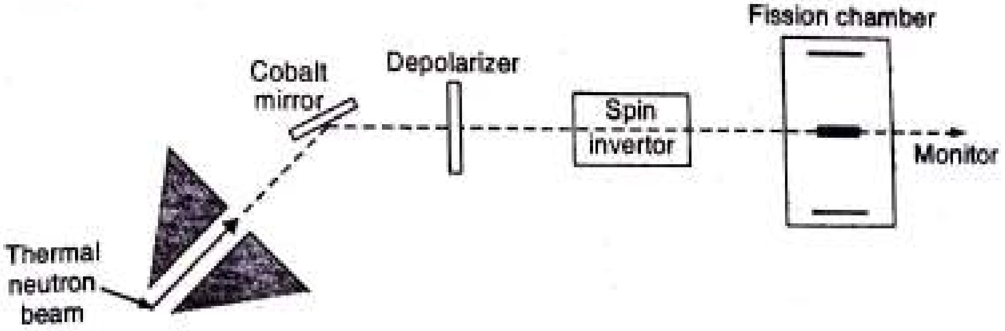

Fig. 13.11. Experimental set up by Danilyan & coworkers for studying parity violation in fission.

Asymmetry coefficient $a_{fission} = (N\uparrow - N\downarrow)/(N\uparrow + N\downarrow)$.

It is found to be $(1.37 \pm 0.35) \times 10^4$ for fissile nucleus ^{236}U, $(2.8 \pm 0.3) \times 10^4$ for ^{234}U and $(-4.8 \pm 0.8) \times 10^4$ for ^{240}Pu. The plus sign shows the excess of light fragments in the direction of neutron spin and minus the deficiency.

Fission Product Radioactivity

A plot of fission product yield against atomic number gives a double maximum curve, like the mass number distribution. The average specific charge $(Z/A)_{av}$ of light and heavy fission fragments are not identical. The fission products have neutron excess, emit β^--particles before attaining stability. The successive decays give rise to *fission chains*. On the average three decays are observed. Equal chain lengths in the two products are generally observed for low energy neutrons. The average energy emitted in radioactive decay is about 20 *MeV* per fission. Short lived nuclides drop out with time, causing the decrease in the rate of energy release. This rate is given by

$$\frac{dE}{dt} = (3.9\,t^{-1.2} + 11.7\,t^{-1.4}) \times 10^{-6}\ MeV/\sec,$$

where t is the time in days. This relation is not fit for very old fission products, since these will consist of only a long lived radioactive nuclides. The variations of energy release and decay rate as functions of time are shown in Fig. 13.12. As a rough estimate, 2/3 of the decay is carried out by beta-particles and 1/3 by the gamma rays. Average fission product gamma ray energies are 0.7 MeV and average beta particle energies are 0.4 MeV.

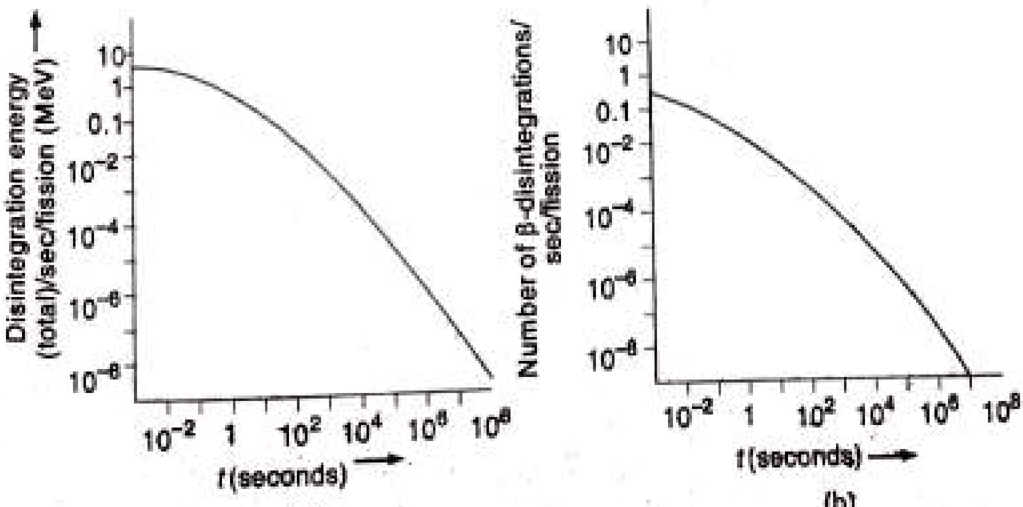

(a) (b)

Fig. 13.12. (a) Rate of energy release from fission product delay, (b) Rate of beta decay of fission products.

13.2 NUCLEAR FUSION AND THERMONUCLEAR REACTIONS

Power from nuclear fission is now a reality both on land and sea and in those countries where coal or oil is costly. An alternative to the fission reaction as a source of energy is its reverse *process* known as *fusion reaction*, in which the lighter nuclei fuse together and produce a heavier nucleus. The sum of the masses of the individual light nuclei is more than would be the mass of the nucleus formed by their fusion, and thus the fusion process should result in a liberation of energy.

Some indication of how this might be achieved can be obtained by considering the source of energy produced continuously in the stars, including the sun. It has been calculated that the sun (our nearest star) emits electromagnetic energy at a rate of about 10^{26} joules per second. Astronomical and geological evidences show that the sun has been radiating energy at about its present rate for several billion years. Chemical reactions cannot possibly be the source of this energy, because even if the sun is supposed to be consisted of pure carbon, its complete combustion would supply energy to maintain these radiations only for few thousand years. Now question arises how can the sun have maintained this energy output for so long and what is the source of all *stellar energy ?* Helmholtz, in 1853, suggested that the contraction was taking place and thus the gravitational energy was being converted into heat energy in sun. This conversion is analogous to the production of electricity from the falling of water. It has been shown that if contraction were taking place it could supply not more than 1% of the total energy output needed and it led to an estimate of the age of the sun which was much too short.

With the discovery of radioactivity at the end of the 19th century, it appeared possible that atomic energy might be contributing to the sun's energy. In 1904, J.H. Jeans suggested that the energy of the sun might be resulted from the mutual annihilation of positive and negative charges. Eddington in 1920, suggested that the stellar energy was liberated in the formation of helium from hydrogen. This theory received wide support, although there was no satisfactory mechanism to account for the formation of helium from hydrogen, because large amounts of hydrogen and helium exist in the sun. In 1929, Atkinson and Houtermans, in Germany, considered that energy might be liberated in the very high stellar temperatures. Such processes are called *thermonuclear reactions.*

In order to interact two nuclei, that must have enough kinetic energy to permit them to overcome the electrostatic repulsion barrier which tends to keep them apart. It can be shown from calculations that the energy required to make the nuclear reactions occur at a detectable rate is about 0.1 *MeV* for nuclei of the lowest atomic number (*e.g.*, isotopes of hydrogen), the larger energies are needed for nuclei of higher atomic number. This energy can be resulted from a sufficient increase in temperature (1000×10^6 °*K* if the average energy of the particles is to be 0.1 *MeV*). Such temperatures are considerably higher than those existing in stars. In stars, like sun where the central temperatures are less than 50×10^6 °*K*, the fusion reaction takes place with a finite rate and releases enough energy to keep up the heat and light of the star.

H.A. Bethe in the United States suggested in 1939 that *the production of stellar energy is by thermonuclear reactions* in which helium—4 nuclei are synthesized from four protons (the nucleus of hydrogen, the most abundant element in the universe). A few years ago, it was held that the major portion of the sun's energy was derived from the *carbon nitrogen cycle.* Recent modifications of the estimates of the central temperature of the sun now favour the *proton-proton chain.* In the *carbon-nitrogen cycle* carbon acts as a short of catalyst in facilitating the combination of four protons to form a helium nucleus. In this cycle a proton first interacts with ^{12}C nucleus with a release of fusion energy. The product nucleus ^{13}N decays in a very short time. The stable nucleus of ^{13}C, thus formed, then reacts with another proton. The more energy being liberated by this process. The stable nucleus of ^{14}N combines with a third proton. The product nucleus ^{15}O is a positive β-emitter, which decays into ^{15}N. This nucleus finally interacts with a fourth proton and regenerates ^{12}C nucleus. These reactions can be written as :

$$^{12}_{6}C + ^{1}_{1}H \rightarrow ({}_{7}N^{13})^{*} \rightarrow ^{13}_{7}N + 1.94\ MeV\ (10^{6}\ y)$$

$$^{13}_{7}N \rightarrow ^{13}_{6}C + ^{0}_{+1}e + \nu + 1.20 + 1.02\ MeV\ (9.96\ m)$$

$$
\begin{aligned}
{}^{13}_{6}C + {}^{1}_{1}H &\rightarrow ({}^{14}_{7}N)^{*} \rightarrow {}_{7}N^{14} + 7.55\ MeV\ (2 \times 10^{5}\ y)\\
{}^{14}_{7}N + {}^{1}_{1}H &\rightarrow ({}^{15}_{8}O)^{*} \rightarrow {}^{15}_{8}O + 7.29\ MeV\ (3 \times 10^{7}\ y)\\
{}^{15}_{8}O &\rightarrow {}^{15}_{7}N + {}^{0}_{+1}e + \nu + 1.74 + 1.02\ MeV\ (124\ \text{sec.})\\
{}^{15}_{7}N + {}^{1}_{1}H &\rightarrow ({}^{16}_{8}O)^{*} \rightarrow {}^{12}_{6}C + {}^{4}_{2}He + 4.96\ MeV\ (10^{4}\ y)\\
\hline
4{}^{1}_{1}H &\rightarrow {}^{4}_{2}He + 2{}^{0}_{+1}e + 2\nu + 26.7\ MeV.
\end{aligned}
$$

It will be noted that this chain of reactions can start with either carbon or nitrogen, since each one is reproduced in the reaction. The four protons are associated with four electrons to maintain electrical neutrality, whereas only two are required for the helium nucleus, and rest two electrons combine readily with positrons resulting in the formation of γ-rays.

The mass difference released as energy in this chain of reactions is simply the difference between the masses of four protons and one helium nucleus. A small amount of this energy is carried away by the neutrons that are emitted during the e^{+}-decay. Bethe estimated this to be about 1.84 *MeV* leaving rest for each α-particle formed.

In the p–p chain, two protons first fuse to produce a deuterium nucleus which combines with an another proton to yield ${}^{3}He$. Two ${}^{3}He$ nuclei interact and form ${}^{4}He$ and two protons. These reactions can be reptesented by the equations

$$
\begin{aligned}
2 \times [{}^{1}_{1}H + {}^{1}_{1}H &\rightarrow ({}^{2}_{2}He) \rightarrow {}^{2}_{1}H + {}^{0}_{+1}e + \nu + 0.42\ MeV\ (7 \times 10^{9}\ y)]\\
2 \times [{}^{2}_{1}H + {}^{1}_{1}H &\rightarrow ({}^{3}_{2}He) \rightarrow {}^{3}_{2}He + \gamma + 5.5\ MeV\ (10\ \text{sec.})]\\
{}^{3}_{2}He + {}^{3}_{2}He &\rightarrow ({}^{6}_{4}Be) \rightarrow {}^{4}_{2}He + {}^{1}_{1}H + {}^{1}_{1}H + 12.86\ MeV\ (3 \times 10^{5}\ y)\\
\hline
4{}^{1}_{1}H &\rightarrow {}^{4}_{2}He + 2{}^{0}_{+1}e + 2\nu + 2\gamma + 26.7\ MeV \qquad \text{(Path I)}
\end{aligned}
$$

With ${}^{4}He$ present in the core of the star, either generated by hydrogen burning or present in the original formation, there are other possible paths in the hydrogen burning chain after the formation of ${}^{3}He$

$${}^{3}_{2}He + {}^{4}_{2}He \rightarrow {}^{7}_{4}Be + \gamma$$

followed by either

$$
\begin{aligned}
{}^{7}_{4}Be + {}^{0}_{-1}e &\rightarrow {}^{7}_{3}Li + \nu\\
{}^{7}_{3}Li + {}^{1}_{1}H &\rightarrow + {}^{4}_{2}He + {}^{4}_{2}He \qquad \text{(Path II)}
\end{aligned}
$$

or

$$
\begin{aligned}
{}^{7}_{4}Be + {}^{1}_{1}H &\rightarrow {}^{8}_{5}B + \gamma\\
{}^{8}_{5}B &\rightarrow {}^{8}_{4}Be + {}^{0}_{+1}e + \nu\\
{}^{8}_{4}Be &\rightarrow {}^{4}_{2}He + {}^{4}_{2}He. \qquad \text{(Path III)}
\end{aligned}
$$

The positrons emitted are annihilated by free electrons with the production of gamma rays. The energy released in p–p chain is the same as in the $C-N$ cycle (26.7 *MeV* for each helium nucleus).

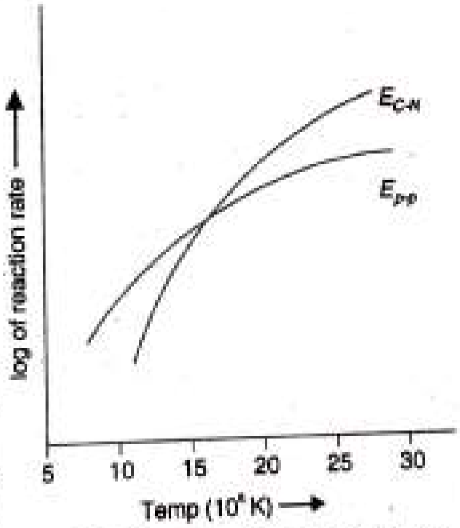

Fig. 13.13. Variation in the rate of energy produced with the central temperature.

Which of the two hydrogen-helium fusion processes plays the major role in energy production in star? The answer is based on our knowledge of the stellar temperature. H. Bondi and E.E. Salpeter (1952) developed empirical equations for the rate at which energy is liberated in each of the above chains of reaction. The p–p chain reaction rate varies more slowly with temperature, roughly as T^{4} and is much more important at lower temperatures. The carbon cycle rate predominates as the temperature is in the vicinity of 18×10^{6} °K. For the case of the sun, they estimated that the rate of generation of energy in the p–p chain was about the same as that in the carbon cycle. Actually the p–p chain predominates (96%) because the interior temperature of the sun is about 15×10^{6} °K.

Helium Burning—In contrast to the hydrogen-burning reactions of the *p–p* chains and the *CN*-cycle, the nuclear reactions consuming helium in a star are dominated by resonant processes. The first is the resonant $\alpha - \alpha$ reaction.

$$ {}^{4}_{2}He + {}^{4}_{2}He \rightleftharpoons {}^{8}_{4}Be. $$

The 0^+ ground state ${}^{8}_{4}Be$ is just unstable against breakup into two alphas, and occurs at 94 keV above the zero for the two alphas. The first phase of helium burning is completed by a second resonant reaction.

$$ {}^{8}_{4}Be + {}^{4}_{2}He \rightarrow {}^{12}_{6}C + \gamma. $$

The 0^+ excited state of ${}^{12}C$ lies 7.644 *MeV* above the ground state of ${}^{12}C$, but only 278 *keV* above the zero of ${}^{8}Be + {}^{4}He$. This state usually decays straight back to ${}^{4}He + {}^{8}Be$. The branching ratio for photon emission to the ground state of ${}^{12}C$ is only 4×10^{-4}, the 0^+ excited state decays via two $E\ 2$ -transitions going through a 2^+ excited state at 4.433 *MeV*.

The helium in the core of a star is expected to ignite at ~ 10^8 °*K*. The values of temperature and density at which helium burning maintains the equilibrium of the helium core depends on the mass of the star. The effect of the helium ignition in the central region of the helium core is to arrest the contraction of the core and expand it outwards.

The $3\alpha \rightarrow {}^{12}C$ process is very temperature sensitive and the core is an excellent thermal conductor, the helium core detonates rather than ignites. This phenomenon is called the helium flash. The helium flash raises the temperature of the core. The $3\alpha \rightarrow {}^{12}C$ reaction is backed by a series of further α-capture processes

$$ {}^{12}C + {}^{4}He \rightarrow {}^{16}O + \gamma;\ {}^{16}O + {}^{4}He \rightarrow {}^{20}Ne + \gamma $$
$$ {}^{20}Ne + {}^{4}He \rightarrow {}^{24}Mg + \gamma;\ {}^{24}Mg + {}^{4}He \rightarrow {}^{28}Si + \gamma. $$

At each stage the Coulomb barrier increases and nuclei beyond ${}^{16}O$ will only be possible in helium burning in massive stars, at relatively high temperatures.

A star in which the helium burning is going on is depleting the resources of energy (B.E. of helium is 7.1 *MeV* and of Iron is ~ 8.8 *MeV*, thus energy release beyond helium is ~ 1.7 *MeV*/nucleon only) in the central regions and is in danger of going into the red.

The Chandrasekhar limit (a star whose mass exceeds 1.45 solar masses can never be stabilized against gravitational collapse by the Pauli principle acting on degenerate electrons) and the second phenomenon the radiation of neutrinos are important in the evolution beyond the helium burning in the central regions. The Chandrasekhar limit is crucial to the evolution of massive stars beyond the helium burning phase. The accumulating Carbon-Oxygen core in a star burning helium is maintained at a temperature ~ 10^8 °*K* by the helium burning shell with energy being released as helium is converted into carbon and oxygen. As the mass of such a core rises above the Chandrasekhar limit, only the ignition of further thermonuclear processes can save the star from catastrophic collapse. However at temperatures $10^8 - 10^9$ °*K* energy is found to emit as radiation of neutrinos without any heating of the stellar material. In a carbon oxygen core the origin of neutrinos is not β-processes but rather the direct Fermi interaction between four leptons $(e^+ + e^- \rightarrow \nu + \overline{\nu})$.

Solar Future. When all the hydrogen is used up in the above thermonuclear reactions, the star will consist mostly of helium. At this stage gravitational contraction will occur once again until a temperature of about 10^8 °*K* is reached and the density of the star is about 10^7 kg/m³. Under these conditions three helium nuclei combine and form a ${}^{12}C$ nucleus with the release of about 7.3 *MeV*. Hoyle estimates that such processes provide energy for an additional 10^7 years. Further gravitational contraction of the star will occur, when all the helium is used up, and will produce a further rise in the temperature of the star. The atoms formed in this way are most stable. Any appreciable combination of these atoms to form heavier ones will lead to endothermic rather than exothermic reactions. Bondi and Salpeter suggested that the endothermic reactions might account for the sudden collapse of a star identified as the sudden appearance of a *supernova*.

13.3 CONTROLLED THERMONUCLEAR REACTIONS

In stars, nuclear fusion reactions release great amounts of energy. The rate depends upon the density and temperature of the gas and upon the cross sections or lifetimes of the reactions involved. Bearing in mind the masses of materials available on earth, it is certain that the reactions of the carbon cycle and the p-p chain would occur extremely slowly. There are thermonuclear reactions which occur much more rapidly and depend on an most abundant material. Among the nuclei of the hydrogen isotopes, ${}_1^2H$ and ${}_1^3H$ reactions are :

$$\left.\begin{aligned} {}_1^2H + {}_1^2H &\rightarrow {}_1^3H + {}_1^1H + 4.03\ MeV \\ {}_1^2H + {}_1^2H &\rightarrow {}_2^3He + {}_0^1n + 3.27\ MeV \end{aligned}\right\} \qquad D\text{–}D \text{ reaction}$$

$${}_1^2H + {}_1^3H \rightarrow {}_2^4He + {}_0^1n + 17.58\ MeV \qquad D\text{–}T \text{ reaction}$$

The *D-D* reaction can go in two equally probable ways, the first of which produces ${}_1^3H$ while the second produces ${}_2^3He$. When reactions take place in a chamber, the deuterium can react with ${}_1^3H$ to give an α-particle and neutron. 14.1 *MeV* energies are carried off by the neutron and about 3.5 *MeV* by the α-particles. In these fusion reactions the energy released is much less than that released in fission reaction but the energy yield per unit mass of material is greater slightly. Deuterium occurs in nature with an abundance of about one part in 6500 hydrogen and can be separated from the lighter isotope quite cheaply. It has been calculated that the energy equivalent of the deuterium in one gallon of water is the same as that obtained from the combustion of 300 gallons of gasoline. The more than 10^{20} gallons of water present in the oceans could thus supply the world's power requirement for several million years, if all the deuterium could be utilized to provide energy by fusion processes.

The *D-D* reactions have low cross-sections and low *Q*-values and are of most interest as a source of tritium. The *D-T* reactions has not only a large *Q*-value but also a cross-section about 200 times that of the *D-D* reactions. The reaction

$${}_1^2H + {}_2^3He \rightarrow {}_2^4He + p + 18.34\ MeV$$

is of great interest not only due to a high *Q*-value but both product nuclei are charged and can readily communicate their energy to plasma. The cross sections for these reactions as a function of the centre of mass kinetic energy are shown in Fig. 13.14.

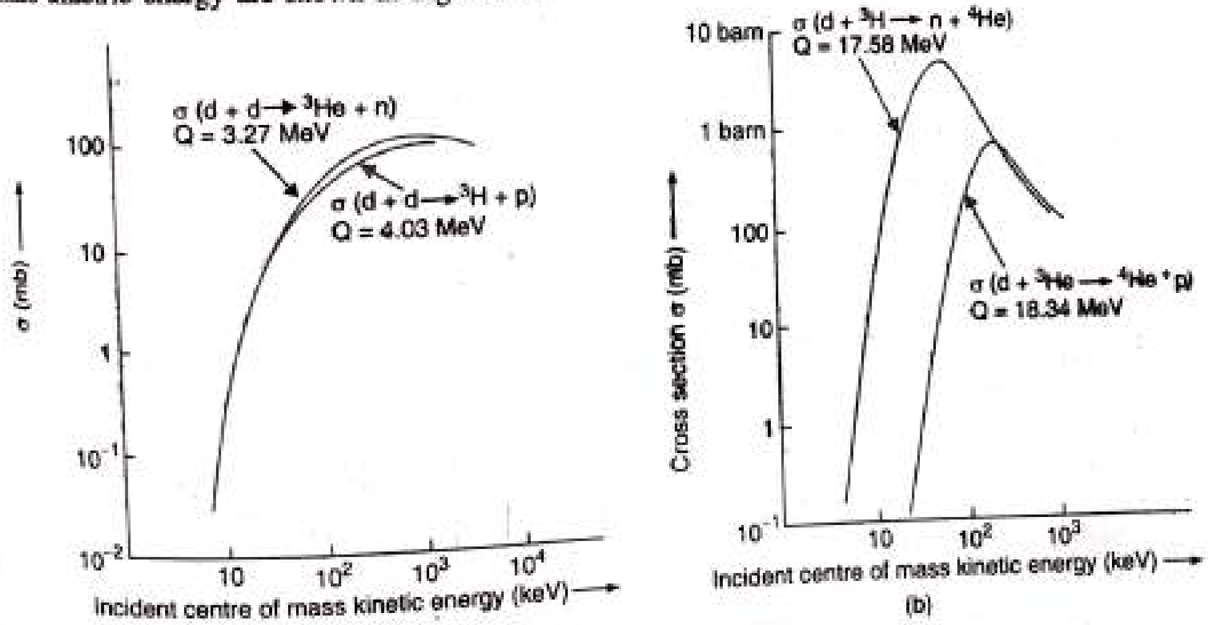

(a) (b)

Fig. 13.14. Cross-sections for thermonuclear reactions.

Thermonuclear (hydrogen) bomb—Even before the achievement of atomic bomb, it was realized by J. Robert Oppenheimer and others that the explosion of an atomic bomb might create the high temperature needed to start a thermonuclear reaction and thus an atomic bomb might serve as the *fuse* or *trigger* to set off a hydrogen bomb. Hydrogen bomb can be made with deuteron or tritium or the combination. It is possible to produce tritium (as it occurs in nature only in infinitesimal amounts) by the neutron bombardment of lithium in a nuclear reactor. Calculations show that a given weight of tritium would release 7 times as much energy as an equal weight of *Pu*. One kg of tritium would release as much energy as 140,000 tons of T.N.T. (the recognized abbreviation for the common chemical explosive 2, 4, 6-trinitrotoluene, assuming that the explosive energy of 1 ton of T.N.T. is 10^9 calories).

Fusion Reactor—The energy produced in a hydrogen bomb is in an uncontrolled manner. To control thermonuclear reactions some of the essential conditions must be satisfied. The process must be self sustaining and the balance must be obtained between the energy released in fusion and the amount lost by radiation. The temperature corresponding to this condition of balance is known as *critical ignition temperature*. The relation $E = kT$ implies that it is of the order of 10^8 °*K*. At very high temperatures the atoms are fully ionized and these ions and the free electrons are moving about very rapidly. The result is a completely ionized gas, called a *plasma*. The plasma is electrically neutral so that in the absence of electric or magnetic fields, there are no external forces acting on it except gravity. Because of the internal pressure, the plasma would expand in a vacuum to fill the container in which it is kept. When it comes in contact with the walls, it heats up the walls.

The power produced in fusion reactor will depend on the plasma density and temperature. Because of the very low density of the plasma, used in controlled thermonuclear reactions, and the relatively small volume of the system, it does not behave as a black body. The radiation should consist mainly of bremsstrahlung accompanying the deflection of the rapidly moving electrons in the plasma by the electrostatic fields of the positively charged nuclei. The amounts of energies released per unit time per unit volume in the *d-d* reactions and in the *d-t* reactions and of energy lost as radiation at various temperatures are shown in Fig. 13.15. In common practice the temperatures are expressed in *keV*, which is equivalent to 1.16×10^7 °*K*. It is clear from the figure that the bremsstrahlung loss equals to power produced at plasma temperature about 5 *keV* for a *d-t* and about 40 *keV* for *d-d* reactions. This does not necessarily mean that the plasma temperature for a *d-d* reactor has to be higher than 40 *keV* to produce a net power gain. The reason is that the bremsstrahlung is not lost but absorbed by the walls of the plasma container and converted therefore into heat in the way similar to the *K.E.* of the reaction products. The minimum operating temperature for a given reactor will therefore depend on the efficiency with which heat can be converted into other forms of energy. A part of this energy should be taken back by the plasma again to keep it at the operating voltage.

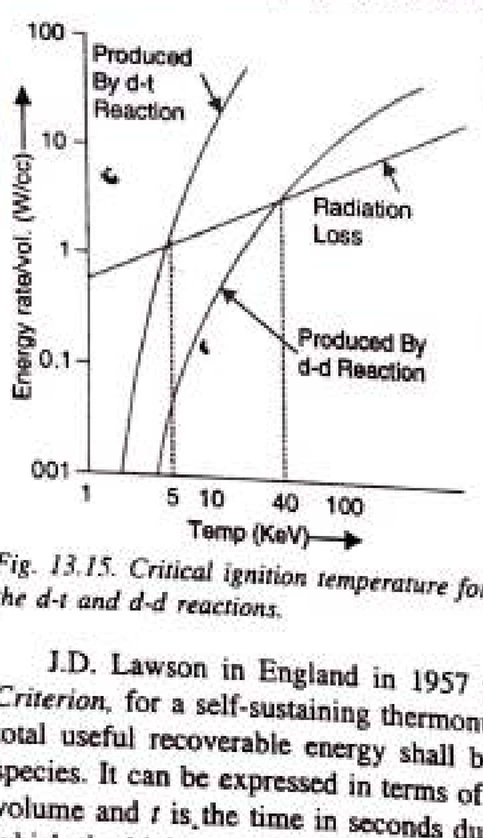

Fig. 13.15. Critical ignition temperature for the d-t and d-d reactions.

J.D. Lawson in England in 1957 pointed out another necessary condition, known as the *Lawson Criterion*, for a self-sustaining thermonuclear system. According to this criterion for a fusion reactor the total useful recoverable energy shall be at least sufficient to maintain the temperature of the reacting species. It can be expressed in terms of the product *nt*, where *n* is the number of reacting nuclei per unit volume and *t* is the time in seconds during which thermonuclear reaction takes place or the time during which the high temperature plasma can be confined. 6×10^{29} and 2×10^{21} are the calculated minimum values for *nt* for *d-t* system and *d-d* system respectively. Thus we see that critical ignition temperature and this criterion are very much favourable for *d-t* reactor than for *d-d* reactor.

Several equipments were constructed in an attempt to produce fusion reactions in a controlled manner. These are described as given below :

(a) Pinched Discharge—In principle the simplest way of heating and confinement of plasma is to make use of a phenomenon called the *pinch*, utilized in U.S.A., U.K., and in the U.S.S.R. simultaneously and independently in the early 1950. In it a very strong electric current amounting to a million amperes is passed through a deuterium like gas at low pressure. This current heats the gas and ionizes it, thus converting it into a *plasma*. At the same time the current flow produces a magnetic field with its lines of force encircling the plasma. The pressure of this field then pinches the plasma into a narrow region in the centre of the containing vessel which may be a torus or a straight tube. In this manner the plasma is not only kept away from the walls but heated also by the current itself and the current generates due to the compression produced by the magnetic field.

Several experimental machines have been built, some on quite a large scale. Two machines named *Zeta* and *Sceptre* were designed by Harwell group and by associated electrical industries respectively. An entirely different approach to the confinement and heating of plasmas is by the method of ***fast magnitude compression*** also called the *theta pinch*, originated in 1957 at the Los Alamos Scientific Laboratory. The apparatus consists of an open ended tube containing deuterium gas at low pressure surrounded by a single turn coil. An oscillating current of several million amperes is passed through the coil for a very short time by the discharge of a large bank of capacitors. A powerful oscillating axial magnetic field is thus produced. If the deuterium gas is not pre-ionized, then the first half cycle of the oscillating magnetic field produces an ionized sheath of plasma which is rapidly compressed and partially heated. Some of the magnetic lines are trapped by the plasma during this compression. In the second half cycle the direction of the magnetic field is reversed and the mutual annihilation of the oppositely directed fields releases a large amount of energy that heats the deuterium plasma. Scientists at Los Alamos were able to obtain plasmas with temperatures in excess of 5 *keV* and densities of about 4 × 10^{22} deuterons per m^3 by fast magnetic compression of low density and with pre-ionized deuterium.

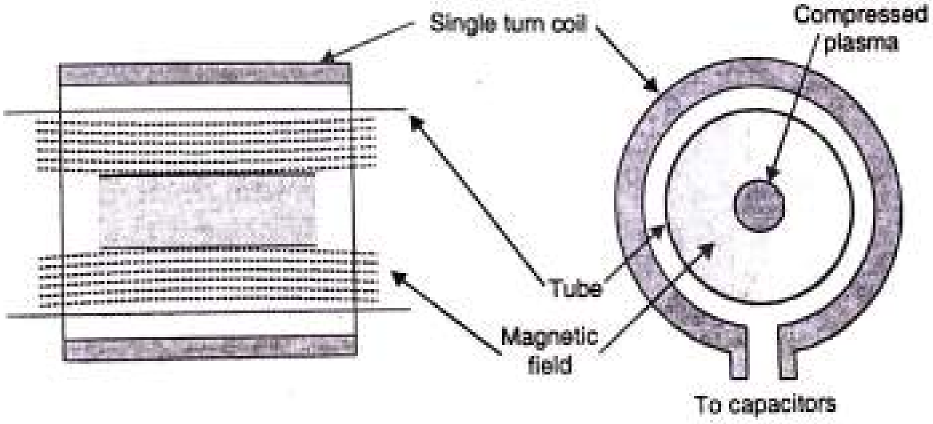

Fig. 13.16. Schematic diagram of theta pinch apparatus (fast magnetic compression system).

(b) Stellarator—In 1951, the astrophysicist L. Spitzer and Princeton University described a principle of stellarator as an another approach to plasma confinement. This name is used because controlled fusion reactions are similar to those in stars (*Stella in Latin*). Stellarators are the modified torous type machines. Here a plasma is confined in a closed ring shaped tube. The magnetic field with the lines of force parallel to the circumference of the ring is produced by winding a coil of wire

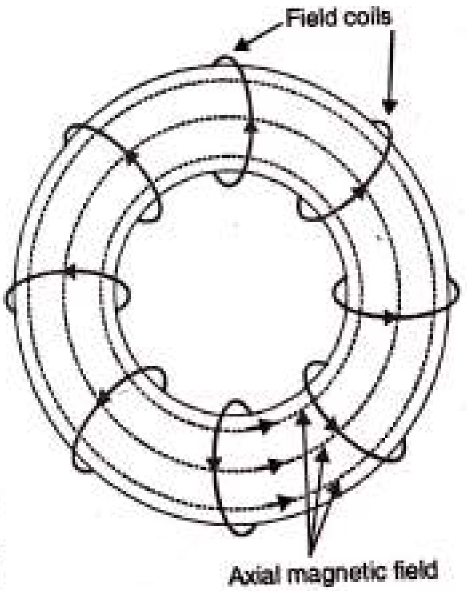

Fig. 13.17. Axial magnetic field in a toroidal tube.

around the tube and passing an electric current through it. The magnetic field is stronger at the inner perimeter of the torus than at the outer perimeter, thus causes the plasma as a whole to move to the outer walls. The stable confinement is thus impossible.

Spitzer suggested to twist the toroidal tube into a space like a figure of 8 so that tube was no longer in one plane. The difficulty of instability which causes a escape for plasma towards the walls is removed in this shape. The tendency of the plasma to drift in a particular direction in one bend of the tube is compensated by the opposite tendency in the other bend. In each circuit of the stellarator tube, a line of force is somewhat displaced from its original position. A magnetic field of this type is said to possess a *rotational transform*. Spitzer later showed that the rotational transform could be obtained with a planer recetrack tube by a combination of magnetic fields. Two sets of coils are employed : one called the confining field coils generating an axial field and the other the helical windings producing the rotational transform. The former are located around most of the tube, but the latter are used only at the ends with current flowing in opposite directions in alternate turns. The earliest stellarators were of the figure of eight type. The recent stellarator is the Model C stellarator, which was completed in 1961 at Princeton. The tube is of stainless steel with an internal diameter of 8 inches and over all length of about 40 feet. It is a large and complex but has a flexible facility for the study of plasma confinement and heating. The maximum strength of the axial magnetic field is about 5 tesla which is held constant for periods upto 1 sec or so.

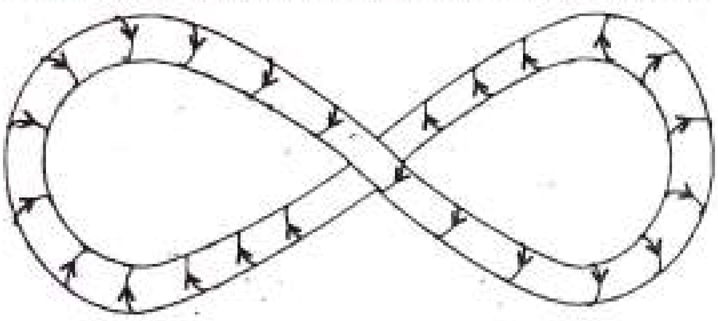
Fig. 13.18. Stellarator tube of figure eight.

In the operation of a stellarator, formation and heating of the plasma are generally accomplished in three stages : (i) A radio-frequency discharge is used to preionize the low pressure deuterium gas in the tube, (ii) The resulting weakly ionized plasma is confined by the magnetic fields and (iii) A heating current is induced from the outside by means of transformers. The temperature of the plasma is raised to ~ 0.1 *keV*. To attain the temperatures of thermonuclear interest, other heating techniques may be used—namely ion cyclotron heating, magnetic pumping using oscillating magnetic field.

(c) Magnetic Mirror System—In the stellarator and other systems using closed containing tubes, the plasma can not escape in the axial direction and so confinement is required only in radial direction. In *magnetic mirror system* the plasma is confined in a *bottle shaped magnetic field*. This system consists of a straight tube with magnetic coils wound around it in such a way as to provide a field that is considerably stronger at the ends than in the middle. The ions move in spiral orbits with radii of curvature inversely proportional to the field strength and under certain conditions are reflected when move into regions of higher field strengths. In this way the magnetic mirrors inhibit but do not prevent entirely the escape of plasma from the ends of the tube. For a particle to be reflected it must have a significant component of velocity perpendicular to the magnetic field lines in the central region between the mirrors. The greater the value of B_{max}/B_{min} the smaller the value of $v_\perp$ relative to actual velocity v for which reflection is possible. The heating of the plasma in this system is accomplished by increasing the magnetic field relatively slowly such

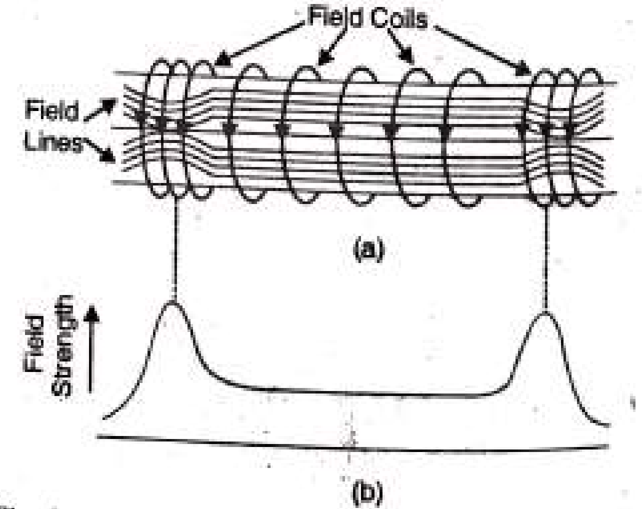

Fig. 13.19. Field coils and lines of force in a magnetic mirror system (above); (B) Variation in the magnetic field strength (lower).

that the plasma is compressed. This compression can be carried out in several stages and the compressed plasma is transferred after each stage from one magnetic bottle to a smaller one in which it is further compressed.

(d) **Beam-injection Method**—The injection of charged particles with a significant velocity component $v_\perp$ along the radial direction directly across the magnetic field lines presents a difficulty. To solve this problem, the use of electrically neutral atoms of high energy was suggested, but it was very difficult to accelerate neutral atoms to a very high energy.

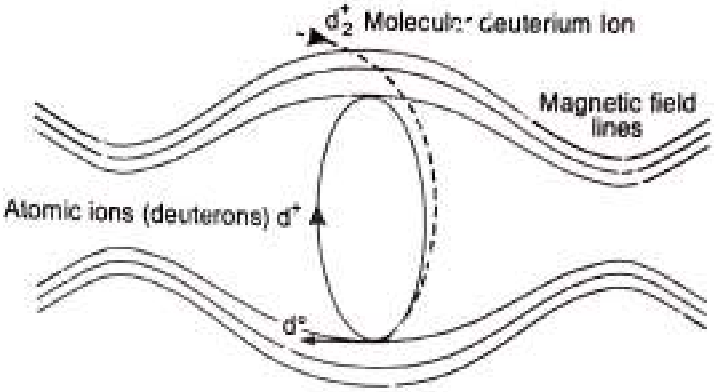
d_2^+ Molecular deuterium ion
Magnetic field lines
Atomic ions (deuterons) d^+
d^0

Fig. 13.20. Paths of molecular deuterium ions and atomic ions in a magnetic field.

indirect process is the use of deuterium ions (~ 20 *keV*) which are allowed to pass into a chamber containing neutral deuterium gas. In this chamber a charge exchange occurs and the stream of high energy neutral deuterium atoms are produced, which then enter the magnetic field where they are ionized.

$$d^+\ (\textit{high energy}) + d^0\ (\textit{low energy}) \rightarrow d^0\ (\textit{high energy}) + d^+\ (\textit{low energy}).$$

Similar injection process used at the Oak Ridge National Laboratory starts with a high energy (600 *keV*) beam of molecular deuterium ions (d_2^+). These ions dissociate as $d_2^+ \rightarrow d^+ + d^0$. Since the mass of deuterium is half that of the molecular ion, its radius of curvature in a magnetic field is also half for the same velocity. Thus for the high energy beam of d_2^+ ions, allowed to break up in a suitable magnetic field with mirrors at the ends, the resulting d^+ ions can be trapped but the undissociated d_2^+ ions are not. The neutral atoms are not affected by the magnetic field and will escape. As a result of collisions, the trapped deuterons acquire random motion equivalent to a high temperature.

A Brief Summery

The nuclear fission is an extremely complex nuclear reaction in which an atomic nucleus is divided into two nuclei of comparable mass. It is called *spontaneous* fission if takes place naturally. It is called *induced* if caused by bombardment with neutrons, charged particles, gamma rays or other carriers of energy. It is called thermal fission or fast fission corresponding to the bombarding particle as thermal neutron or fast neutron. The stability of a nucleus against fission is interpreted by liquid drop model, in which the nucleus is assumed as an incompressible charged liquid drop with a surface tension. The long range Coulomb forces between the protons will disrupt the stability of the nucleus, whereas short range nuclear forces idealized as a surface tension act to stabilize it.

The two fission fragments generally decay by β–emission to a stable end product. The distribution of fission products shows a tendency for masses to concentrate round 90 and 140. These masses are inversely proportional to the kinetic energies. Thus each group are found to have mean energies about 70 and 100 MeV. The fission of ^{235}U by thermal neutrons shows the total energy release as about 200 MeV per fission and the number of neutrons released as 2.07. The fissionable materials are those which many produce fission fragments. The material may be *fissible* or *fertile*. The former are those nuclides which can produce fission by the interaction of neutrons. The latter are those which can be used as raw material for the production of fissible isotopes. The reaction which convert fertile materials into fissible materials are called *breeding reactions*.

The theory of nuclear fission commonly used is a Bohr and Wheeler's theory, where the radius *R* of the deformed drop is expressed as a Legendre Polynomial expansion. The change in surface energy of the drop due to deformation is compared with the Coulomb energy of the deformed nucleus. The critical energy is compared with the excitation energy and the fission probability is predicted.

The *fusion* is the reverse process of *fission*. In this process the lighter nuclei fuse together and produce a heavier nucleus. The energy generated in stars is due to nuclear fusion. It will solve the power problem permanently, as our fossil fuels are limited. Nuclear fusion reactions can be self-sustaining. For light nuclei, the binding energy per nucleon increases generally with increasing mass number *A*. The nucleus formed from the fusion of two lighter nuclei have a higher binding energy per nucleon. This means a lower rest mass and a release of energy equivalent to lost rest mass. The production of stellar energy is by thermonuclear reactions in which ^4He is formed by four protons. Among the nuclei of hydrogen isotopes, $_1^2H$ and $_1^3H$ reactions are most common. They are called $d-d$ reactions and $d-t$ reactions. The $d-d$ reactions have low cross-sections and low Q-values and are of most interest as a source of tritium.

The energy produced in a hydrogen bomb is in an uncontrolled manner. The process must be self sustaining and the balanced must be obtained between the energy released in fusion and the amount lost by radiation. The atomic bomb creates the high temperature needed to start thermonuclear reaction and thus serves as the fuse or trigger to set off a hydrogen bomb. Several equipments were constructed in an attempt to produce fission reactions in a controlled manner, such as pinched discharge, stellarator, Magnetic mirror system and beam injection method.

EXERCISES

Example 1. *Calculate the fission rate for ^{235}U required to produce 2 watt and the amount of energy that is released in the complete fissioning of $\frac{1}{2}$ kg of ^{235}U.*

As we know that 200 MeV energy is released per fission of ^{235}U.

$$\therefore \quad \text{Fission rate} = 2 \text{ watt}/200\ MeV\ per\ fission = 2/200 \times 1.6023 \times 10^{-13}$$

$$= 6.25 \times 10^{10} \text{ fission/sec.}$$

Number of ^{235}U nuclei in $\frac{1}{2}$ kg. of $^{235}U = (0.5/235) \times 6.02214 \times 10^{26} = 1.28 \times 10^{24}$.

On fissioning this number of ^{235}U nuclei, the energy release will be

$$= 1.28 \times 10^{24} \times 200\ MeV = 2.56 \times 10^{26}\ MeV = 10^{10} \text{ kilocalories.}$$

Example 2. *In a fission reactor operating at a power level of 10^9 W, average time lapse between the emission of prompt neutron and its capture to induce the next generation of the chain reaction is 10^{-3} sec. Estimate the number of free neutrons present in this reactor.*

Energy E released in the fission produced by one neutron = 200 MeV

$$\therefore \quad E = 200 \times 1.6023 \times 10^{-13} = 3.2 \times 10^{-11} \text{ joule/neutron.}$$

The power produced by one free neutron

$$p = E/t = 3.2 \times 10^{-11}/10^{-3} = 3.2 \times 10^{-8}\ watt/neutron.$$

Therefore the number of free neutrons in a reactor of power level P is given by

$$N = \frac{P}{p} = \frac{10^9}{3.2 \times 10^{-8}} = 3.125 \times 10^{16}\ neutrons.$$

Example 3. *Calculate η for thermal neutron induced fission of a uranium mixture containing ^{235}U and ^{238}U isotopes in a 1 : 20 ratio. Given $\nu = 2.43$, $\sigma_a(^{235}U) = 683\ b$, $\sigma_a(^{238}U) = 2.73\ b$, $\sigma_f(^{235}U) = 583\ b$.*

Average number of fission neutrons released per absorption

$$\eta = \nu(\sigma/\sigma_a).$$

For a mixture

$$\sigma_a = \frac{N_0(235)\sigma_a(235) + N_0(238)\sigma_a(238)}{N_0(235) + N_0(238)} = \frac{683 + 20 \times 2.73}{1 + 20}$$

$$= 35.12 \text{ barns.}$$

and

$$\sigma_f = \frac{N_0(235)\sigma_f(235)}{N_0(235) + N_0(238)} = \frac{583}{1+20} = 27.76 \text{ barns.}$$

Hence

$$\eta = 2.43 \times (27.76/35.12) = 1.921.$$

Example 4. *Calculate the excitation energy for $^{236}U^*$ and for $^{239}U^*$. Estimate the rate of spontaneous fissioning of 1 gm of ^{235}U given its half life ~ 3×10^{17} years.*

The excitation energy $\quad E_e = B(Z, A+1) - B(Z, A).$

For ^{236}U

$$E_e = a_v(236 - 235) - a_s(236^{2/3} - 235^{2/3}) - a_c(92^2/236^{1/3} - 92^2/235^{1/3})$$
$$- a_a(52^2/236 - 51^2/235) + a_p(236^{-3/4} - 0)$$

$$= a_v - 0.1\ a_s - 2.2\ a_c - 0.4\ a_a + 0.0167\ a_p = 6.8\ MeV$$

Similarly for ^{239}U, $\quad E_e = 5.9$ MeV.

Rate of spontaneous fissioning $dN/dt = \lambda N$, where λN,

$$N = 6.02214 \times 10^{23}/235 \text{ and } \lambda = \log_e 2/T_{1/2} = 0.693/3 \times 10^{17} \times 3.15 \times 10^7$$

$$\therefore \quad dN/dt = 1.88 \times 10^{-4}\ sec^{-1} = 0.67\ hr^{-1}.$$

Example 5. *Calculate the amount of energy released if all the deuterium atoms in the water in the lake of area about 10^5 sq. miles and of depth $\frac{1}{20}$ th mile are used up in fusion.*

The volume of water $= 10^5 \times \frac{1}{20} = 5000$ cubic miles.

$$\therefore \quad \text{Mass of water} = 5000 \times (1.609 \times 10^3)^3 \times 10^3\ kg = 2.08 \times 10^{16}\ kg.$$

$$\text{or No. of molecules of water} = 2.08 \times 10^{16} \times 6.02214 \times 10^{26}/18 = 6.97 \times 10^{41} \text{ molecules.}$$

As the abundance of deuterium is 0.0156% so that the total number of deuterium atoms $= 6.97 \times 10^{41} \times 2 \times 0.0156 \times 10^{-2} = 2.18 \times 10^{38}$. As the fusion of 6 deuterium atoms gives an energy release of 43 MeV, hence the total energy released $= 2.18 \times 10^{38} \times (43/6)$.

$$= 1.56 \times 10^{39}\ MeV.$$

Example 6. *A thermonuclear device consists of a torus of diameter 3 m with a tube of diameter 1 m, containing deuterium gas at 10^{-2} mm mercury pressure and at room temperature. A bank of capacitors of 1200 μF is discharged through the tube at 40 kV. If only 10% of the electrical energy is transformed to plasma kinetic energy, what is the maximum temperature attained ? Assuming that the energy is equally shared between the deuterons and electrons in the plasma.*

Cross-sectional area of the torus $= \pi(1/2)^2 = 0.25\pi$ meter^2.

Circumference $= 3\pi$ meter.

$\therefore$ Volume of torus $= 0.25\,\pi \times 3\pi = 7.4\ m^3$.

Pressure of the gas $= 10^{-5} \times 13.6 \times 10^3 \times 9.81 = 1.334\ N/m^2$.

From gas equation $PV = NkT$, we have $Nk = 1.334 \times 7.4/293 = 0.0337$.

The energy obtained from the discharge

$$= \tfrac{1}{2}CV^2 = \tfrac{1}{2} \times 1200 \times 10^{-6} \times (4 \times 10^4)^2 = 9.6 \times 10^5 \text{ joules.}$$

$\therefore$ Energy transformed to plasma $K.E. = 9.6 \times 10^4$ joules.

We know that the average kinetic energy associated with the gas molecule is given as $E_{av} = \frac{3}{2}NkT_k$. Since each deuterium molecule produces two ions and two electrons, hence

$$4 \times \tfrac{3}{2}NkT_k = 9.6 \times 10^4 \quad \text{or} \quad T_k = 4.75 \times 10^5\ °K.$$

Example 7. *Calculate the energy radiated during the assembly of the sun mass into its present diameter of 1.4×10^6 km. Calculate the energy released if the diameter is suddenly shrinked by 10%. Find the temperature of the sun.*

Assuming the density of the sun as constant and equal to ρ.

Then the energy released

$$E_{released} = \int_0^{R_0} \frac{G}{r}\left(\frac{4}{3}\pi r^3 \rho\right)(4\pi r^2 \rho)\,dr = \frac{3}{5}G\frac{M_0^2}{R_0}.$$

As mass of the sun $M_\odot = 2 \times 10^{30}\ kg.$, *radius* $R_0 = 0.7 \times 10^6\ km = 7 \times 10^8\ m$,

$$\therefore \quad E_{released} = \tfrac{3}{5} \times 6.67 \times 10^{-11} \times (2 \times 10^{30})^2 / 7 \times 10^8 = 2.29 \times 10^{41}\ J.$$

Energy released if the diameter is suddenly shrinked by 10%, *i.e.*, the radius R_0 reduces to $0.9\,R_0$.

$$= \frac{3}{5}GM_0^2\left[\frac{1}{0.9R_0} - \frac{1}{R_0}\right] = \frac{3}{5}G\frac{M_0^2}{R_0}\cdot\frac{1}{9} = 2.54 \times 10^{40}\ J.$$

If the sun is pure atomic hydrogen, then sun of mass 2×10^{30} *kg* contains 2×10^{33} hydrogen moles. If the gas constant is R, and the temperature is T, then the thermal energy is the energy released in contraction, *i.e.*,

$$2 \times 10^{33}\ RT = 2.29 \times 10^{41} \text{ Joules}$$

$$\text{or} \quad T = 2.29 \times 10^{41}/2 \times 10^{33} \times 8.31 = 1.38 \times 10^7\ °K.$$

Example 8. *In the fission of a nucleus of mass number A_0 into the two nuclei A_1 and A_2, the energy released is given by*

$$Q = M_0c^2 - M_1c^2 - M_2c^2$$

Estimate Q for symmetric fission of a nucleus with $A_0 = 240$.

The mass of a nucleus of mass number A, atomic number Z is given by

$$^{A}_{Z}M = Zm_p + (A-Z)m_n - B/c^2,$$

where m_p and m_n are the proton and neutron masses respectively and B is the binding energy. For the splitting of $^{A_0}_{Z_0}M$ into M_1 and M_2 with binding energies B_1 and B_2 respectively, we have

$$A_0 = A_1 + A_2,\ Z_0 = Z_1 + Z_2$$

and

$$^{A_0}_{Z_0}M = M_1 + M_2 + (B_1 + B_2)/c^2 - B_0/c^2.$$

or

$$Q = M_0c^2 - M_1c^2 - M_2c^2 = B_1 + B_2 - B_0.$$

If $\overline{B}$ is the average binding energy per nucleon, thus $B = \overline{B} \times A$. Hence

$$Q = B_1 + B_2 - B_0 = A_1\overline{B}(A_1) + A_2\overline{B}(A_2) - A_0\overline{B}(A_0)$$

With $A_0 = 240$, $A_1 = A_2 = 120$ in a symmetric fission. From binding energy curve, we have

$$\overline{B}(120) = 8.5\,MeV \text{ and } \overline{B}(240) = (7.6)\,MeV$$

∴ Energy released in fission is

$$Q = 120(8.5) + 120(8.5) - 240(7.6) = 216\,MeV.$$

Example 9. *Use a Fermi gas model to estimate the magnitude of asymmetry term of semi-empirical mass formula, assuming $A \neq 2Z$.*

A Fermi gas of volume V at absolute temperature $T = 0$ has energy

$$E = \frac{2V}{h^3}\cdot\frac{4\pi}{5}\frac{p_0^5}{2m}$$

and particle number

$$N = \frac{2V}{h^3}\cdot\frac{4\pi}{3}\cdot p_0^3$$

∴ The limiting momentum

$$p_0 = h(3N/8\pi V)^{1/3}$$

and the corresponding energy

$$E = \frac{3}{40}\left(\frac{3}{\pi}\right)^{2/3}\frac{h^2}{m}\left(\frac{N^5}{V^2}\right)^{1/3}$$

For a nucleus (A, Z), the neutrons and protons are considered as independent gases, in the volume V. Thus the energy of the lowest state is

$$E = \frac{3}{40}\left(\frac{3}{\pi}\right)^{2/3}\frac{h^2}{m}\frac{N^{5/3}+Z^{5/3}}{V^{2/3}} = \frac{3}{40}\left(\frac{3}{\pi}\right)^{2/3}\frac{h^2}{m}\frac{N^{5/3}+Z^{5/3}}{\left(\frac{4}{3}\pi R_0^3 A\right)^{2/3}} = K\frac{N^{5/3}+Z^{5/3}}{A^{2/3}}$$

where

$$K = \frac{3}{40}\left(\frac{9}{4\pi^2}\right)^{2/3}\cdot\frac{1}{mc^2}\left(\frac{hc}{R_0}\right)^2 = 31.7\,MeV.$$

For stable nuclei

$$N + Z = A, \text{ let } N - Z = \varepsilon, \text{ therefore}$$

$$N = \tfrac{1}{2}A(1+\varepsilon/A), \text{ and } Z = \tfrac{1}{2}A(1-\varepsilon/A).$$

As $\varepsilon/A << 1$, therefore

$$\left(1+\frac{\varepsilon}{A}\right)^{5/3} = 1 + \frac{5\varepsilon}{3A} + \frac{5\varepsilon^2}{9A^2}$$

and

$$\left(1-\frac{\varepsilon}{A}\right)^{5/3} = 1 - \frac{5\varepsilon}{3A} + \frac{5\varepsilon^2}{9A^2}$$

∴
$$N^{5/3} + Z^{5/3} = 2\left(\frac{A}{2}\right)^{5/3}\left(1+\frac{5\varepsilon^2}{9A^2}\right)$$

and
$$E = 2^{-2/3}KA\left[1+\frac{5\varepsilon^2}{9A^2}\right] = 2^{-2/3}KA + \frac{5}{9}\times 2^{-2/3}K\frac{(N-Z)^2}{A}$$

The second term has the form $a_a\,(N-Z)^2/A$ of semi-empirical mass formula, therefore

$$a_a = \tfrac{5}{9}\times 2^{-2/3}K$$
$$= \tfrac{5}{9}\times 2^{-2/3}\times 31.7 = 11.1\,MeV\,.$$

Example 10. *For stable heavy nuclei, the number of neutrons is substantially greater than the number of protons. Using binding energy relations, prove that more energy is required to remove a proton than a neutron.*

The energy required to remove a protron or a neutron from a stable nucleus (Z, A) is

$$S_p = B(Z, A) - B(Z-1,\ A-1)$$

and
$$S_n = B(Z, A) - B(Z, A-1),$$

where B is the binding energy per nucleon of the nucleus. Using the semi-empirical mass relation, we get

$$S_p - S_n = -a_c(2Z-1)(A-1)^{-1/3} + 4a_a(A-2Z)/(A-1).$$

For stable nuclides $\quad \delta(B\cdot E)/\partial Z = 0$

or
$$Z = \frac{A}{2+(a_c/2a_a)A^{2/3}},$$

where
$$a_c = 0.714\text{ MeV} \quad\text{and}\quad a_a = 23.20\,MeV$$

∴
$$S_p - S_n = \frac{a_a}{A-1}\left[A^{5/3} - (A-1)^{5/3} + \frac{a_c}{4a_a}A^{5/3}(A-1)^{2/3}\right]$$

For heavy nuclei $A >> 1$, $S_p - S_n = 5.5\times 10^{-3}A^{4/3}$, which increases with A, *i.e.*, more energy is required to dissociate a proton from a heavy nucleus than to a neutron.

Oral Questions

1. Enriched uranium in nuclear reactors means (a) very pure uranium; (b) uranium in which concentration of ^{235}U is more than in the natural uranium; (c) uranium in which concentration of ^{238}U is more than in the natural uranium; (d) None of these.
2. State various types of fission processes.
3. Which isotope of uranium undergoes fission with thermal neutron and which one with fast neutrons.
4. ^{235}U is (a) fissible; (b) non-fissible; (c) used in fusion; (d) used in fission and fusion.
5. Nuclear fission process means (a) absorption of neutron by a nucleus; (b) the scattering of neutrons; (c) break up of heavy nucleus into two nearly equal halves releasing energy; (d) breakup of heavy nucleus into two nearly halves emitting 2 or 3 neutrons and releasing large amount of energy.
6. Where does the energy released in the fission of heavy elements come from ?
7. Which forces are responsible for distortion of the spherical shape of the uranium nucleus and which one beings back to its original spherical shape ?
8. Define critical energy of the fissionable nucleus.
9. Nuclear fusion process means (a) absorption of neutron by a nucleus, (b) splitting of nucleus into fragments, (c) formation of heavy nucleus with the combination of two light nuclei with the release of a large quantity of energy; (d) none of these.
10. What prevents the common elements heavier than iron but lighter than lead from fissioning spontaneously ?
11. Why is alpha decay favoured over other modes of disintegration ?

12. The fission cross sections of odd-A uranium isotopes for thermal neutrons are large in comparison to that of even-A isotopes of Uranium. Explain.
13. Estimate the ratio of the energy released when 1 gm of uranium undergoes fission to the energy released when 1 gm of TNT explodes. (1 gm of TNT is equivalent to 2.6×10^{21} eV)
14. Number of fission per second in a 100 MW reactor is ......

    Answer : 1. b; 4. a; 5. d; 6. Difference between binding energy before & after the fission; 9. (c); 13.2 × 10^{7}; 14.3 × 10^{18}.

Problems

1. In a neutron induced fission of ^{235}U two stable end products ^{98}Mo and ^{136}Xe are often found. Assuming that these isotopes have come from the original fission process, find (a) what elementary particles are released, (b) the mass defect of the reaction and (c) the equivalent energy released. ($2n$, $4\beta^-$, 0.2215 u, - 206 MeV)
2. In the fission reaction $^{118}Sn + p \rightarrow {}^{24}Na + {}^{94}Zr + n$, determine (a) the energy equivalent of the mass difference between reactants and products, (b) the excitation energy necessary for passage over the potential barrier and (c) the threshold energy for the reaction. (3.25 MeV, 71.06 MeV, 74.31 MeV)
3. What fraction of a sample of ^{235}U exposed to a thermal flux density of 2×10^{13} cm^{-2} sec^{-1} will be fissioned in one year. (29.5%)
4. How much ^{235}U and ^{238}U will be lost in 1 year from spontaneous fission in a stockpile of 1000 kg of natural uranium ? How much will be lost from α-decay ? (2.61×10^{-4}, 6.87×10^{-3}, 7.0, 15.2 μg)
5. Determine (i) the excitation energy necessary for passage over the potential barrier, (ii) the energy equivalent of the mass difference between reactants and the products and (iii) the threshold value for the reaction in the following fission reactions.

$$^{118}_{50}Sn + p \rightarrow {}^{66}_{31}\mathrm{Ga}\ {}^{49}_{20}Ca + 4n. \qquad (90.62\,MeV, -11.64\,MeV, 84.98\,MeV)$$

$$\rightarrow {}^{94}_{40}Zr + {}^{24}_{11}Na + n. \qquad (71.06\,MeV, 3.25\,MeV, 74.31\,MeV)$$

6. The energy released in a nuclear reaction is usually expressed in KT (Kilotons) of TNT, which releases 10^3 cal/gm. How many fissions are involved in 50 kT explosion ? How many gms of uranium are fissioned ? How much mass is converted. (5.14×10^{4}, 2.01 kg, 0.717 gm)
7. The total volume of water in the oceans is 1.34×10^9. What is the total mass of deuterium containted in the water ? What will be the total energy available from all of this deuterium through reaction $^2H + {}^2H \rightarrow {}^3H + p + 4.04$ MeV ? How much mass will be lost in this energy release ? (2.9×10^{40} Joules, 3.24×10^{23} kg)
8. The rate of energy delivery to the earth from the sun, 1.5×10^8 km distant, is known as the solar constant, with a value of 2.0 cal $cm^{-2}min^{-1}$. Calculate the rate at which the sun is losing mass to supply this radiated energy. What fraction of its mass of 2×10^{30} kg does the sun lose per year ? (8.27×10^{18} $kg\ yr^{-1}$, 4.13×10^{-12})
9. If all the deuterium atoms contained in a lake of 5 sq. km and 10 m deep are used for fusion reactions, how much energy will be released.? Given that lake water contains 0.1% of heavy water. (2.39×10^{33} MeV)
10. A hydrogen bomb with explosive power of 50 Megatons of TNT uses the reaction $({}^2_1H + {}^2_1H \rightarrow {}^3_2He + {}^1_0n)$. The required bomb trigger is rated at 2 Megatons (included in 50). Given that $m({}^2_1H) = 2.014102\,u$, $m({}^3_2He) = 3.016029$ u and 1 ton of TNT. = 2.6×10^{22} MeV energy. Find the energy produced per fusion and the amount of hydrogen bomb contained. (3.27 MeV, 2.53×10^3 kg)

REFERENCES

1. Allis, W.P. (Editor), *"Nuclear Fusion"* , Van Nostrand, New York, 1960.
2. Bethe, H.A., *Energy Production in Stars*, Physics Today, 21, 36 (1968).
3. Clayton, D.D., *"Principles of Stellar Evolution and Nucleosynthesis"*, McGraw-Hill, 1968.
4. Condon, E.U. and Hugh Odishaw, *"Hand Book of Physics"*, McGraw Hill Book Co., New York, 1967.
5. Enge, A. Harald, *"Introduction to Nuclear Physics"*, Addision Wesley, 1966.
6. Fraser, J.S. and J.C.D. Milton, *Ann. Rev. Nuc. Sci.*, **16**, 379 (1966).
7. Frisch, O.R. and J.A. Wheeler, *The Discovery of Fission*, Physics Today, **20,** No. 11, 43 (1967).
8. Glasstone, Samuel, *"Source Book on Atomic Energy"*, D. Van Nostrand, 1967.
9. Glasstone S. and R.H. Loveberg, *"Controlled Themonuclear Reactions"*, Van Nostrand, New York, 1960.
10. Halpern, I., *Ann. Rev. Nuc : Sci*, **9**, 245 (1959).

11. Halliday, David, "*Introductory Nuclear Physics*", Asia Publishing House, 1963.
12. Harris, M.J. *et al.*, *Ann. Rev. Astrophys.* **21**, 165 (1983).
13. Kaplan, Irving, "*Nuclear Physics*", Addision Wesley, 1969.
14. Lapp, R.E. and H.L. Andrews, "*Nuclear Radiation Physics*", Sir Isaac Pitman & Sons Ltd., 1972.
15. Lefort, Marc, "*Nuclear Chemistry*", D. Van Nostrand (1968).
16. Littlefield, T.A. and N. Thorley, "*Atomic and Nuclear Physics*", D. Van Nostrand Co., London, 1968.
17. Liverhant, S.E., "*Elementary Introduction to Nuclear Reactor Physics*", John Wiely, 1960.
18. Post, R.F., *Ann. Rev. Nucl. Sci.*, 20, 509 (1970).
19. Roy, R.R. and B.P. Nigam; "*Nuclear Physics*", John Wiley & Sons, 1977.
20. Salpeter, E.E., *Ann. Rev. Nuc. Sci.* **2**, 41 (1953).
21. Segre, E. (Editor), "*Experimental Nuclear Physics*", Vol. II, John Wiley & Sons, Inc., New York, 1953.
22. Segre, Emilio, "*Nuclei and Particles,*" W.A. Benjamin Inc. New York, 1965.
23. Semat, Henry, "*Introduction to Atomic and Nuclear Physics*", Chapman & Hall, Ltd., London, 1962.
24. Smith, C.M.H., "*A Textbook of Nuclear Physics*", Pergamon Press, Oxford, 1966.
25. Wilets, L., "*Theories of Nuclear Fission*", Clarendon Press, Oxford, 1964.
26. There is a large collection of papers on Nuclear Fission in vol. 15 of Proc. International Conference, Geneva, 1958.

18 ELEMENTARY PARTICLES

18.1 INTRODUCTION

The problems concerning the elementary particles are today the focus of interest and of research for the experimental as well as the theoretical physicists. Experimental investigations of elementary particles all involve some source of particles to study and some way of detecting those particles and measuring their behaviour. Many of the practical problems of such invetigations are caused by the fact that many elementary paticles are unstable. The classical elementary particle, the individual atom was nothing but the mass point of classical machanics. The investigaion of electromagnetic phenomena suggested that the atom had an internal structure. At that time the typical photo-type of the elementary particle was the electron. The problem of the dualistic nature of matter was resolved by the quantum theory of fields : *the elementary particles are nothing but the quanta of a corresponding field.* The study of elementary particles is the basis to the understanding of radiation phenomena, or one may regard any kind of radiation as a flux of elementary particles.

In 1932, when Chadwick identified the neutron and Heisenberg suggested that atomic nuclei consisted of neutrons and protons, it seemed as if p, n and e^- were sufficient to account for the structure of matter. Besides these, there was the photon, *the intermediary or field particle for electromagnetic forces,* which exists between the nucleus and electrons in the atom. If anti-matter exists it would then be made up of anti-electrons, *i.e.* positrons, anti-protons and antineutrons. Thus we see that seven particles could explain both matter and anti-matter. In 1935, Yukawa postulated the existence of another particle with a mass $m = 200\ m_e$ *as the field particle for the strong nuclear forces.* Recently the extensive studies made partly on high energy cosmic ray particles and even more with the help of high energy accelerators have revealed the existence of numerous new nuclear particles. Apart from a dozen or so the particles have very short lifetimes, very much less than 10^{-6} sec. They cannot therefore be regarded as normal constituents of matter. They are characterised by the parameters, mass, spin, electric charge and magnetic moment. They have been described by such adjectives, as *fundamental, strange and elementary,* but none of these is quite appropriate. The word fundamental implies that the particles are the basic building blocks of matter, but unstability of most of the particles indicates that the great majority are certainly not. It is true that their behaviour was strange in the early 1950, but it is much less now. For the want of better one the term elementary particles is now commonly used. These particles are elementary in much the same sense as are chemical elements.

According to the ancient Indian literature, the physical world is composed of *five bhutas* (basic elements); (i) *Kshiti* (earth), (ii) *Ap* (water), (iii) *Taijas* (fire), (iv) *Vayu* (air) and (v) *Akasha* (ether), or (Panch Tatvas—*Kshiti, Jal, Pawak, Gagan, Sameera*). The five elements theory of matter is based upon the fact that our senses are being affected by the bhutas in five different ways. These elements were not considered as ordinary earth, water, fire, air and ether, but as basic principles. These may represent the *solid, liquid, plasma, gaseous and field states of matter* respectively.

According to the recent studies, the fundamental constituents of matter are three generations of leptons and three generations of quarks. According to the quantum field theory, the forces between the fundmental constituents of matter arise due to the exchange of gauge bosons. The mediators of the fundamental forces are graviton, photon, bosons (W^+, W^- and Z°) and 8 coloured gluons (G). The gluons and quarks are not seen as free particles.

18.2 CLASSIFICATION OF ELEMENTARY PARTICLES

The elementary particles are separated into two general groups called bosons and fermions. These two groups have different types of spin and their behaviour is controlled respectively by a different kind of statistic (*i.e.* the Bose statistic or the Fermi statistic, hence the names). Bosons are particles with intrinsic angular momentum equal to an integral multiple of $\hbar$. Fermions are all those particles in which the spin is half integral. The most important difference between the two classes of particles is that *there is no conservation law controlling the total number of bosons in the Universe, whereas the total number of fermions is strictly conserved.*

Boson is a term, which not only includes material particles but also includes those quanta and photons which arise from interactions. Thus in the case of the simple electromagnetic field the bosons are merely the light photons or the X-ray photons. The *photon* has a mass of zero and a spin of unity and is consequently described as a massless boson. A masless boson, called a *graviton* with a probable spin of two units has been postulated as a field particle for gravity. The weak nuclear interactions are mediated by *heavy vector bosons* (W^+, W^- and Z°) also called *weak bosons.* Each carries a spin of unity and mass of the order of 90 GeV. The strong nuclear interactions are mediated by massless neutral *gluons.* Each carries a spin of unity. All these bosons are the quanta of gauge fields and are thus called the *gauge bosons.* These bosons, created by the field interactions are essentially of one kind, while the bosons formed in the strong interaction are of two distinct kinds. First there are those which are known as *pions* or *π-mesons* (π^+, π^- and π°). The second group of bosons are much heavier than that of pions, and are known as kaons or K-mesons (K^+, K^-, K° and $\bar{K}^\circ$) and η°-meson..

Table 18.1. *Classification of Elementary Particles*

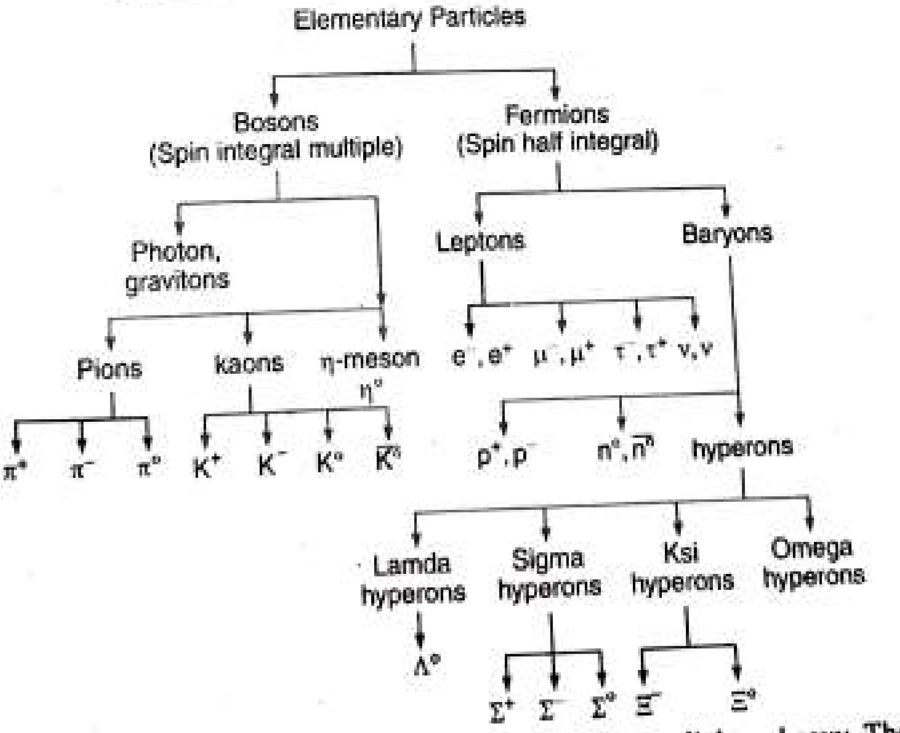

The *fermions* fall in two main classes, according to whether they are light or heavy. Those in the lighter group are often called *leptons* (after the Greek word meaning light in weight), whilst those in the heavier

According to the recent studies, the fundamental constituents of matter are three generations of leptons and three generations of quarks. According to the quantum field theory, the forces between the fundmental constituents of matter arise due to the exchange of gauge bosons. The mediators of the fundamental forces are graviton, photon, bosons (W^+, W^- and Z°) and 8 coloured gluons (G). The gluons and quarks are not seen as free particles.

18.2 CLASSIFICATION OF ELEMENTARY PARTICLES

The elementary particles are separated into two general groups called bosons and fermions. These two groups have different types of spin and their behaviour is controlled respectively by a different kind of statistic (*i.e.* the Bose statistic or the Fermi statistic, hence the names). Bosons are particles with intrinsic angular momentum equal to an integral multiple of $\hbar$. Fermions are all those particles in which the spin is half integral. The most important difference between the two classes of particles is that *there is no conservation law controlling the total number of bosons in the Universe, whereas the total number of fermions is strictly conserved.*

Boson is a term, which not only includes material particles but also includes those quanta and photons which arise from interactions. Thus in the case of the simple electromagnetic field the bosons are merely the light photons or the X-ray photons. The *photon* has a mass of zero and a spin of unity and is consequently described as a massless boson. A masless boson, called a *graviton* with a probable spin of two units has been postulated as a field particle for gravity. The weak nuclear interactions are mediated by *heavy vector bosons* (W^+, W^- and Z°) also called *weak bosons.* Each carries a spin of unity and mass of the order of 90 GeV. The strong nuclear interactions are mediated by massless neutral *gluons.* Each carries a spin of unity. All these bosons are the quanta of gauge fields and are thus called the *gauge bosons.* These bosons, created by the field interactions are essentially of one kind, while the bosons formed in the strong interaction are of two distinct kinds. First there are those which are known as *pions* or *π-mesons* (π^+, π^- and π°). The second group of bosons are much heavier than that of pions, and are known as kaons or K-mesons (K^+, K^-, K° and $\overline{K}^\circ$) and η°-meson..

Table 18.1. *Classification of Elementary Particles*

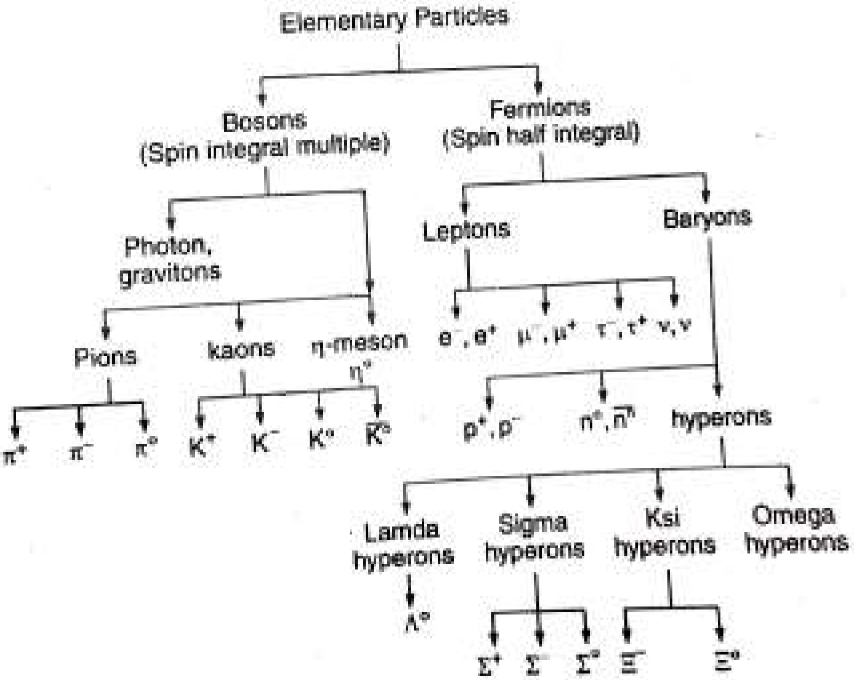

The *fermions* fall in two main classes, according to whether they are light or heavy. Those in the lighter group are often called *leptons* (after the Greek word meaning light in weight), whilst those in the heavier group are called *baryons* (after the Greek word for heavy). The leptons are the electron, muon, tau meson and respective neutrinos and their anti-particles. These are all with spin half and not made of quarks. Leptons interact weakly with other particles. The total number of leptons minus the total number of anti-leptons remains unchanged in all reactions and decay processes involving leptons and anti-leptons. The baryons consist of the two nucleons with their anti-particles (n°, $\bar{n}^\circ$; p^+, p^-) and the *hyperons.* Hyperons are the extremely unstable somewhat heavier particles and can be divided into four sub-groups, Λ°-particle (a neutral particle of mass about 1116 MeV/c^2), the Σ-particles (Σ^+, Σ° and Σ^-) with masses in the range 1189 to 1197 *MeV/c*^{2}), the Ξ-particles (Ξ^- and Ξ° with masses 1321 and 1315 *MeV/c*^{2}) and the Ω^--particle (of mass about 1672 MeV/c^2). There is no reason to doubt the existence of the anti-particles of these fermions. The total number of baryons minus the total number of anti-baryons is absolutely conserved in all interactions.

The kaons and pions together with the baryons are placed into a group of strongly interacting particles, called *hadrons*. The quarks are the basic building blocks of hadrons.

18.3 FUNDAMENTAL INTERACTIONS

The fundamental interactions may be defined as the fundamental forces that act between the elementary particles, of which all matter is assumed to be composed. They may be classified as : (i) Gravitational interaction, (ii) Electromagnetic interaction, (iii) Strong interaction and (iv) Weak interaction. All known processes in nature (from sub-nuclear to extra galactic *i.e.* microscopic to macroscopic) can be considered as a manifestation of one or more of these interactions. The gravitational forces are not significant for elementary particles and nuclear physics. Out of the rest three, weak force has a very short range ($< 10^{-17}m$) and is extremely feeble compared to strong and electromagnetic forces.

(a) The Gravitational Interactions. This interaction manifests itself as a long range force of attraction between all elementary particles. The first force that any of us discover is of gravity. It holds the moon and earth together, keeping the planets in their solar orbits and binds stars to form our galaxy. Newton gave a formula $F = Gm_1m_2/r^2$ for the interaction between two masses. The gravitational effect does not depend on the colour, size, charge, velocities, spin and angular orientation but depends on the *magnitude of the intertia.* The gravitational force between two nucleons separated by a nucleon diameter is

$$F = G\frac{m_1m_2}{r^2} = 6.67\times10^{-11}\frac{(1.67\times10^{-27})^2}{(10^{-15})^2} \approx 2\times10^{-34} \text{ newton} \qquad \ldots(1)$$

and the gravitational attraction is only about 2×10^{-49} joule. Hence we see that it plays no role in particle reactions. The dimensionless coupling constant $= Gm^2/\hbar c = 2 \times 10^{-39}$ for the gravitational interaction between two nucleons. This quantity is so small that it can be neglected in most of the nuclear effects. In the nineteenth century the forces were thought to be propagated by fields, space wraped for particular effects. In the twentieth century these fields were explained in terms of agents or messengers which actually propagate the effect. Gravitation can thus be explained in terms of the interactions of gravitons with rest mass zero and spin two. Due to zero mass their velocity must be that of light. *As the gravitational field is extremely weak, the gravitons cannot be detected in laboratory.*

(b) Electromagnetic Interactions. All of the ordinary chemical and biological effects are due to the interaction of electric charges and the fields they produce. The term electromagnetism is because the electricity and magnetism are both part of the same phenomenon. The appropriate law for the interaction of point charges bears the name of Coulomb ($F = q_1q_2/4\pi\varepsilon_0r^2$). For two protons, 10^{-15} metre apart, the repulsive force will be $9 \times 10^9 \times (1.6 \times 10^{-19})^2/(10^{-15})^2 = 230$ newtons. It is about 10^{36} times greater than the gravitational attraction caused by the mass. The energy released by the complete separation of these protons would be 2.3×10^{-13} joules.

If the particles are not at rest but are moving, the field will not only be an electric field but would be new one depending on the velocity and magnitude of the charge. When the charge is accelerated, the energy is radiated out in the form of an electric and magnetic pulses. This energy comes from the agent which accelerates the charge. The pulse is called a photon and travels with the velocity of light. If the source charge is accelerating in an oscillating fashion, the propagated signal will consist of successive waves of electric and magnetic fields or the *radio-photons*. Thus we see that the photons are emitted and reabsorbed by a charge. Interaction between two charged particles consists of an exchange of these photons. The strength of the electromagnetic interaction is given by the dimensionless coupling constant known as *fine structure constant* $\alpha = [= e^2/4\pi\varepsilon_0 \hbar c = 1/137.03604 \pm 0.00011)$ and is due to photon exchanges.

In the nucleus, the transition rates for magnetic dipole and electric quadrupole radiation are very small (10^{-2} and 10^{-4} times the electric dipole radiation respectively). As there are no oscillating electromagnetic monopoles, thus the photon has spin 1. The one photon exchange process may be represented by Feynman diagram, as shown in Fig. 18.1 (b) and by the equation

The electromagnetic interactions are of long range ($r \to \infty$).

$$e + p \to (e + \gamma) + p \to e + (p + \gamma) \to e + p.$$

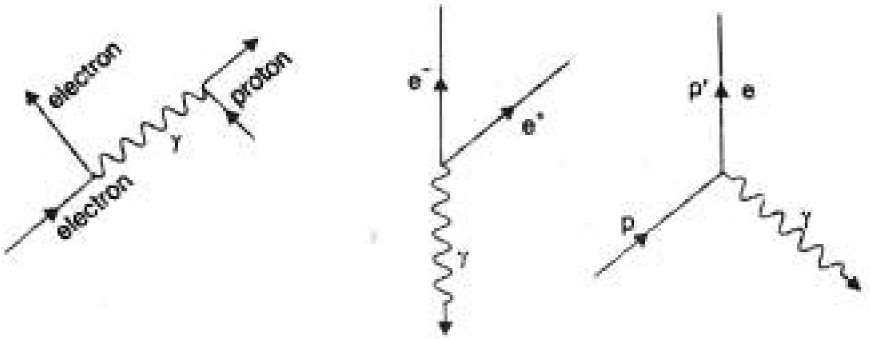

Fig. 18.1. Feynman diagrams of electromagnetic interactions.

The electromagnetic interaction is charge dependent. In terms of isobaric spin, the interaction depends on T_z or T_3 and the electromagnetic processes are governed by the isospin rule $\Delta T = 0, \pm 1$. All other quantities such as charge, baryon number, lepton number, hypercharge, parity, strangeness number are conserved. The characteristic lifetime is 10^{-15} sec and the characteristic cross-section is 10^{-4} *mb* for the electromagnetic interactions.

The capture of photon can effect the production of mesons or hyperons by an electromagnetic interaction

$$\begin{tikzcd} & \pi^\circ + p \\ \gamma + p \arrow[ur] \arrow[dr] & \\ & \Lambda^\circ + K^+. \end{tikzcd}$$

An example of a radiative capture reaction is

$$n + \gamma \to \pi^- + p.$$

Neutral particles such as π° and Σ° decay electromagnetically, since these processes involve no change of strangeness. Two photon decay of the η° is also permitted. Since the electromagnetic interaction need not conserve isospin, decay of the η° meson to $3\pi^\circ$ is permitted through this interaction.

$$\pi^\circ \to \gamma + \gamma, \Sigma^\circ \to \Lambda^\circ + \gamma,$$

$$\eta^\circ \to \pi^+ + \pi^- + \pi^\circ, \eta^\circ \to \gamma + \gamma,$$

The decay processes such as $\Sigma^+ \to p^+ + \gamma$ are forbidden because the change $\Delta S = 1$ is required. The paradox that the decay of neutral particle is by electromagnetic interaction is resolved by introducing an intermediate step in the overall reaction, the virtual production of a nucleon-antinucleon (or electron-positro pair. Thus we have

$$\pi^\circ \xrightarrow[\text{strong}]{} \underset{\text{virtual}}{(N+\bar{N})} \xrightarrow[\text{electromagnetic}]{} \gamma + \gamma.$$

The process of mutual annihilation of particle and anti-particle is an example of electromagnetic interaction.

(c) Weak Interaction. The weak interaction is responsible for the leptonic decay of strange and non-strange particles and for non-leptonic decay of strange particles. Both decay modes can be regarded as four fermion processes, such as the decay of a neutron into a proton, an electron and an antineutrino ($n \rightarrow p + e^- + \bar{\nu}_e$). The numerical constant, which is characteristic of the weak interactions, is obtained from Fermi's theory of β-decay. Its value is $g_F = 1.435 \times 10^{-62}\ Jm = 1.026 \times 10^{-5}\,(m_pc^2)\ (\hbar / m_pc)^3$. In analogy with the expression for the other interactions, the dimensionless weak interaction coupling constant is of magnitude

$$[g_F^2/(\hbar c)^2][m_\pi c/\hbar]^4 = 5 \times 10^{-14}. \quad \ldots(2)$$

The characteristic lifetime is large (= 10^{-8} *sec*) in comparison of strong and electrostatic interactions and the characteristic cross section is least (= $10^{-12} mb$). The weak force has a very short range ($< 10^{-17}\ m$) and can be distinguished from other two, strong and electromagnetic forces, by its special character. The weak interactions are classified as charged or neutral, depending on whether or not a particle participating in a weak reaction suffers a change of unit electric charge.

Consider the reactions which do not involve a change of strangeness and yet which must be due to weak interaction. The neutron decay is the proto-type of all the β-decays :

$$n \rightarrow p + e^- + \bar{\nu}_e .$$

The nature of such an equation is that the reaction can go in either direction so long as energy is conserved and that any participant can be replaced on opposite side by its anti-particle, *i.e.* $p \rightarrow n + e^+ + \nu_e$. Another variation of this four fermion interaction is the proton capture of an anti-neutrino ($\bar{\nu}_e + p \rightarrow n + e^+$). Another example of the four-fermion interaction is the muon decay ($\mu^- \rightarrow e^- + \nu_\mu + \bar{\nu}_e$.). There is also a coupling among muons, nucleons and neutrinos, thus

$$\mu^- + p \rightarrow n + \nu_\mu.$$

There are however other types of weak interactions which require coupling between other pairs of fermions.

$$\Lambda^\circ(S = -1) \rightarrow \pi^-\,(S = 0) + p\,(S = 0).$$

There is no neutrino involved here, strangeness changs by + 1 and only two fermions are involved. For four fermions one can assume this decay as through a virtual stage ($\Lambda^\circ \rightarrow \bar{p} + n^\circ + p^+$). In the first virtual step, four fermions are involved. In the next stage, the strong nuclear forces come into play. There are restrictions whether one transition is forbidden or allowed : *In a weak interaction involving change in strangeness of baryons or mesons, the change in strangeness must be equal to the change in charge.* The change in isospin T and its component T_3 may be nonzero. The strangeness and isospin are not meaningful for leptons, and are useful when hadrons are involved in the weak interactions. The lepton number is conserved in these interactions. The parity is not conserved, but CP and CPT are conserved.

Similar to the graviton for gravity, photon for electromagnetism and mesons for the strong nuclear force there is one agent for the weak interaction. It would also be a boson of mass about 80–90 GeV/c^2 and is named as the *intermediate vector Boson* (W^+, W^-, Z°). Its half life against decay into electron neutrino or muon-neutrino would be less than 10^{-17} sec.

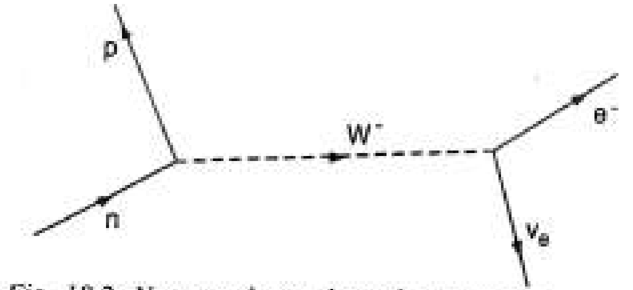

Fig. 18.2. Neutron decay through intermediate vector boson.

One associates neutrino and anti-neutrino exclusively with the weak interaction, just as one associates photons with em-interaction. One particle may respond to the different types of interactions', *e.g.*, pion scattering is effected by a strong force, pion radioactive capture by an electromagnetic interaction and decay by a weak interaction.

In the process of the neutron decay, the weak interaction transforms a neutron into a proton and at the ame time neutrino into an electron. Similar to the electromagnetism, the weak interaction is being mediated y intermediate particles, the vector boson, W^+, W^- *and* Z°.

$$p + e^- \rightarrow (n + W^+) + e^- \rightarrow n + (W^+ + e^-) \rightarrow n + \nu_e$$

$$\mu^- + \nu_e \rightarrow (\nu_\mu + W^-) + \nu_e \rightarrow \nu_\mu + (W^- + \nu_e) \rightarrow \nu_\mu + e^-.$$

The discovery at the CERN laboratory at Geneva shows in 1983 the existence of W^+ and W^- with a ass of $80.9 \pm 2.0\ GeV/c^2$. Each carries a spin of magnitude $\hbar$, just as does the photon. The mass of these articles gives the range ($\hbar/m_w c = 10^{-18} m$) of the weak interaction.

The 1983 experiments at CERN also gave evidence for the existence of an uncharged intermediate article Z°, with a mass of $93.0 \pm 2.0\ GeV/c^2$.

$$\nu_\mu + e^- \rightarrow (\nu_\mu + Z^\circ) + e^- \rightarrow \nu_\mu + (Z^\circ + e^-) \rightarrow \nu_\mu + e^-.$$

The W^+, W^- and Z° masses had been predicted by the unified theory of electromagnetic and weak teractions 16 years before the experimental discovery.

Weak processes are broadly divided into two main categories :

(A) Charged Weak Interactions. (i) *Purely leptonic*—Here only leptons are involved, such as—

$$\mu^- \rightarrow e^- + \bar{\nu}_e + \nu_\mu, \qquad \mu^+ \rightarrow e^+ + \nu_e + \bar{\nu}_\mu,$$

$$\nu_\mu + e^- \rightarrow \mu^- + \nu_e, \qquad \nu_e + e^- \rightarrow \nu_e + e^-$$

(ii) *Semi-Leptonic*—Here hadrons and a lepton pair are involved. These are further classified according to he change of flavour.

(a) *Strangeness conserving processes* ($\Delta S = 0$).

Nuclear β-decay: $n \rightarrow p + e^- + \bar{\nu}_e$

Electron capture: $e^- + p \rightarrow n + \nu_e$

μ-capture: $\mu^- + p \rightarrow n + \nu_\mu$

Neutrino reactions: $\nu_\mu + n \rightarrow p + \mu^-$, $\bar{\nu}_\mu + p \rightarrow n + \mu^+$

Pion decay: $\pi^+ \rightarrow \mu^+ + \nu_\mu$, $\pi^- \rightarrow \mu^- + \bar{\nu}_\mu$, $\pi^+ \rightarrow e^+ + \nu_e$, $\pi^- \rightarrow e^- + \bar{\nu}_e$.

Hyperon decays: $\Sigma^- \rightarrow \Lambda^\circ + e^- + \bar{\nu}_e$

(b) *Flavour change Processes*—

$$K^+ \rightarrow \mu^+ + \nu_\mu, K^+ \rightarrow \pi^\circ + \mu^+ + \nu_\mu, \Lambda^\circ \rightarrow p + e^- + \bar{\nu}_e \ (\Delta S = 1)$$

$$\Lambda_c^+ \rightarrow \Lambda^\circ + e^+ + \nu_e, D^+ \rightarrow \mu^+ + \nu_\mu \qquad [\Delta S = 0, \Delta\ Charm\ (\Delta c) = 1]$$

$$\Lambda_b \rightarrow \Lambda_c^+ + e^- + \bar{\nu}_e, \qquad [\Delta S = 1, \Delta\ \text{beauty}\ (\Delta b) = 1]$$

(iii) *Purely Non-leptonic/hadronic Processes* :

$$\Lambda^\circ \rightarrow p + \pi^-; K^- \rightarrow \pi^- + \pi^\circ; K_s^\circ \rightarrow \pi^+ + \pi^-, \qquad (\Delta S = 1)$$

$$D^\circ \rightarrow K^- + \pi^+, \Lambda_c^+ \rightarrow \Lambda + \pi^+; \Lambda_c^+ \rightarrow \Lambda + K^+ + \pi^\circ \qquad (\Delta c = 1)$$

$$\Lambda_b^* \rightarrow \Lambda_c^+ + \pi^- \qquad (\Delta b = 1)$$

(B) Neutral Weak Interactions

Neutrino-lepton scattering $\nu_\mu + e \rightarrow \nu_\mu + e$

Neutrino-nucleon scattering $\nu_\mu + N \rightarrow \nu_\mu + N$

$$\left.\begin{array}{l}\text{Lepton-lepton scattering } e^+ + e^- \rightarrow \mu^+ + \mu^- \\ \text{Electron-nucleon scattering } e + N \rightarrow e + N\end{array}\right\} \textit{competes with em - interaction}$$

Hadron-hadron interaction $N + N \rightarrow N + N$ *competes with em and strong interactions*

(d) Strong Interaction. The strong interactions act between a pair of hadrons. The hadrons include nucleons (p, n), strange baryons (Λ, Σ), mesons (π, ρ) and strange mesons (K). The strong nuclear interaction is always attractive and independent of the elecric charge. The force is same between $p-p$ and $n-n$. For this purpose the proton and neutron are one but in different electric charge states. Its range is very much shorter than that of gravitational or electromagnetic interaction. Strong interaction energy falls off rapidly when the distance between two particles increases. The interaction has a short range of about $10^{-15} m$. Yukawa in 1935 predicted the existence of heavy quanta, which played the same role in nuclear forces (or strong forces) as photons in electromagnetic ones. From estimates of the range of nuclear forces, Yukawa predicted that the new particles, called *mesons*, should have a mass of the order of 200 to 300 electron masses. The interaction for relatively large distances between nucleons is generated by the exchange of single pions. At shorter separation (*distances*) the exchange of two pion systems, such as ρ-mesons, dominates. The interaction between the strange baryons and between the strange baryons and the nucleons arises in part from the exchange of pions, but the exchange of kaons is also equally important. The range of the interaction can be calculated as $\hbar / mc$, where m is the mass of the exchanged particles. Thus for the exchange of a single pion the interaction would be 1.4×10^{-15} m and for the double pion it would be $0.7 \times 10^{-15} m$. In the chapter of nuclear forces, we outlined an elementary theory of pion-nucleon interaction and introduced the concept of an exchange nucleon charge g analogous to the electric charge e. The strength of the nuclear interaction is represented by the magnitude of the dimensional coupling constant $g^2/4\pi \hbar c$ ($\approx$ 14). It is about a thousand times the electromagnetic coupling constant α. *The strong nuclear force can now be pictured as arising through an exchange of colour quanta called gluon. It has zero rest mass and spin 1.*

Strong interactions between elementary particles are responsible for the total cross sections as a function of energy. The strong interaction is a short range force ($\approx 10^{-15}$ m), conserves baryon number B, charge Q, hypercharge Y, parity π, isospin T and its component T_z. The equivalence of cross-sections for forward and backward nuclear reactions is the evidence for invariance under time reversal T. From CPT theorem we infer invariance under charge conjugation. It is responsible for kaon production, however the decay of mesons, nucleons and hyperons proceeds by an electromagnetic or weak interactions. The characteristic life time is very small, about 10^{-24} sec, and the characteristic cross-section is very large, about 10 mb for the strong interactions.

The nuclei that consist of nucleons and one or more strange particles such as Λ particles are called hypernuclei. It has been found that the interaction between a Λ and a nucleon is not strong enough to form a stable two body system like the deuteron. It is found that the interaction between a Λ and a neutron is not same as that between a Λ and a proton, which is against the charge symmetry. Thus the concept that the strong interactions are purely charge independent is not absolute.

We can thus write these interactions as :

Table 18.2. *Comparison of the Four Basic Interactions*

Field	*Relative Magnitude*	*Associated Particles*	*Characteristic Time*	*Characteristic Range*
Strong interaction	1	Pion (gluons)	10^{-24} *sec.*	$10^{-15} m$
Electromagnetic	10^{-2}	Photon	10^{-15} *sec.*	Long
Weak interaction	10^{-13}	Intermediate boson	10^{-8} *sec.*	$10^{-18} m$
Gravitational	10^{-39}	Graviton	10^{16} *sec.*	Long

As we see that the massles photons gives the electromagnetic interaction a long range and ~ 140 MeV/c^2 pion gives the strong interaction a short range, so we see that the massive intermediate bosons give the weak interaction an extremely short range. Thus we see that the weak interaction is not intrinsically weak but appears so on account of a very large mass of quanta.

18.4 CONSERVATION LAWS

The behaviour of the elementary particles is restricted by a number of conservation laws or invariance principles. That is to say, certain properties of representative physical quantities must remain unchanged n any process. The most familiar quantities in large scale experiments that are conseved in all (strong, electromagnetic and weak, gravitation-extrememly small not considered here) interactions are :

(1) Conservation of linear momentum.

(2) Conservation of angular momemtum. The conservation of angular momentum includes both types (orbital and spin) of angular momentum together. The first is given by the motion of the object as a whole about any chosen external axis of rotation. The second is the intrinsic angular momentum of each object about an axis through its own centre of mass. Strongly interacting fermions have a half integer spin ($s = \frac{1}{2}$ for Ξ, Σ, Λ, n and p; $s = \frac{3}{2}$ for Ω), strongly interacting bosons (η, K, π) have $s = 0$, weakly inteacting fermions (leptons e, μ, τ, ν_e, ν_μ and ν_τ) have $s = \frac{1}{2}$, massless bosons (electromagnetic interacting γ-rays) have $s = 1$ and gravitons have $s = 2$.

(3) Conservation of energy. Conservation of energy on other hand seems more complicated with elementary particles because a large fraction of the total energy is oftenly interchanged between rest energy associated with mass and kinetic or potential energy. The sum of these three, the total energy is alway conserved in any reaction. For example the decay reaction $K^o \neq \pi^+ + \pi^- + \pi^o + \pi^o$ is forbidden because the rest energy of the K^o is not great enough to make four pions even if they all could be make at rest. However, the reaction $K^o \rightarrow \pi^+ + \pi^- + \pi^o$ is allowed.

(4) Conservation of charge. The most familiar of the conservation laws is the conservation of *electric charge*. The charge is conserved in all processes and no exceptions are known. It is due to conservation of charge that the electron cannot decay. The lifetime of the electron against decay into neutral particles ($e^- \rightarrow \nu_e + \nu_e + \bar{\nu}_e$) is greater than 5.3×10^{21} y and for the decay $e^- \rightarrow \nu_e + \gamma$ is greater than 1.5×10^{25} *y*. We note that all elementary charges are 1, 0, or –1; multiple charges are not found. However, the constituents of elementary particles, the quarks have fractional charges.

(5) Conservation of lepton number. The number of leptons minus the number of anti-leptons is conserved. In other words *the net leptons number in any process always remains conserved*. The ordinary electron, μ^--meson, τ^--meson and their respective neutrinos all have a lepton number +1, the corresponding anti-particles known as antileptons have a lepton number of –1. The values of L_e, L_μ and L_τ are as follows—

$L_e = 1$ for e^- and ν_e ; -1 for e^+ and $\bar{\nu}_e$ and 0 for *all other leptons*
$L_\mu = 1$ for μ^- and ν_μ ; -1 for μ^+ and $\bar{\nu}_\mu$ and 0 for *all other leptons*
$\mu_\tau = 1$ for τ^- and ν_τ ; -1 for τ^+ and $\bar{\nu}_\tau$ and 0 for *all other leptons*

The reaction $\mu^+ \rightarrow e^+ + \nu_e + \bar{\nu}_\mu$ is allowed because a lepton number of –1 is replaced by a lepton number $(-1) + (+1) + (-1) = -1$.

(6) Conservation of baryon number. The number of baryons minus the number of anti-baryons is conserved. In other words the net baryon number in any process always remains unchanged. The stability of the proton is a critical test of the exact conservation of B. Actually the law of conservation of B was introduced to forbid the decay of proton to positron and photon. The Grand Unified Theories (to be discussed latter) predict proton decay $p \rightarrow e^+ + \pi^o$ with lifetime $> 5.9 \times 10^{32}$ yrs. All normal baryons such as p^+, n^0, Λ^o, Σ^+, Σ^-, Σ^0, Ξ^-, Ξ^0 and Ω^- have a baryon number of +1, the corresponding anti-particles known as anti-baryons have a baryon number of –1. *All the mesons have a baryon number of zero.* For example, the reaction $\Lambda^o \rightarrow p^+ + \pi^-$ is allowed because the baryon Λ^0 is replaced by the baryon p^+, keeping the total number of baryons constant. The reaction $\Lambda^0 \rightarrow p^- + \pi^+$ is *forbidden* because one baryon is replaced by one anti-baryon changing the baryon number by –2.

The reaction $n \rightarrow p + e^- + \bar{\nu}$ is allowed by both conservation of leptons and conservation of baryons. No exception to the rules of conservations of leptons and baryons has been found in the many elementary particle reactions so far studied one by one. Conservation of leptons has a significance for strong interactions. There are other conservation laws which are not applicable to weak interactions. The property that is conserved in strong interactions only is known as isospin. Other properties which are not conserved for all the three interactions, but are conserved in one or two interactions only, are *strangeness, hypercharge, invariance under charge conjugation, parity and invariance under CP conjugation.*

(a) Conservation of Isospin**—**The isotopic spin or isospin is a quantum number or variable applied to the strongly interacting fundamental particles, the hadrons and their compounds, which facilitate consideration of the consequences of the charge independence of the strong nuclear forces. We know that the isospin has mathematical properties similar to those of the spin. But it has no direct physical relationship to spin. It is used to identify related energy levels or quantum states of isobars (systems with same number of nucleons).

A set of isospin T has $(2T + 1)$ states. The another quantum number T_3 or T_ζ, called the third component of isospin T, has values varying from $-T$ to $+T$. The component T_3 is related with the number of neutrons N and number of protons Z for the particular isobar, as

$$T_3 = (Z - N)/2.$$

Thus the possible values of T_3 are $\frac{1}{2}$ for the proton $(Z = 1, N = 0)$ and $-\frac{1}{2}$ for the neutron $(Z = 0, N = 1)$. T_3 is -1 for the dineutron, 0 for deuteron and $+1$ for the diproton.

The charge Q of a state and the value of T_3 for this state are connected by the Gell-Mann-Okubo relation,

$$Q = T_3 + \tfrac{1}{2} B, \qquad \text{...(3)}$$

where B is the baryon number.

B is $+1$ for baryons (the proton, neutron and hyperons) and is zero for the pions. Inserting the value of T_3 and B, one obtains :

$$\begin{aligned} Q_p &= +\tfrac{1}{2} + \tfrac{1}{2} = +1, Q_n = -\tfrac{1}{2} + \tfrac{1}{2} = 0. \\ Q_{\pi+} &= +1 + 0 = 1, Q_{\pi^\circ} = 0 + 0 = 0, Q_{\pi-} = -1 + 0 = -1. \end{aligned}$$

Isospin numbers are associated with hadrons but not with leptons. The isospin component T_3 is conserved in both strong and electromagnetic interactions but not in weak interaction.

(b) Conservation of Strangeness. The concept of strangeness has found wide application in Particle Physics. It is an additional quantum number which describes the interactions of elementary particles. It has been chosen in such a manner that it becomes zero for all the well known particles (non-strange particles). Rochester and Butler, in 1947, at the University of Manchester arranged a magnetic cloud chamber and after about a year of operation reported certain new types of forked or V shaped tracks in cloud chamber photographs of cosmic rays. These new V-particles were also investigated intensively by cloud chamber groups from various institutions for several years. By 1953, at an International Conference on Elementary Particles at Bagneres a decision was taken to name those particles of mass greater than π-mesons, but smaller than protons, *K-particles,* while those particles whose masses were greater than protons as *hyperons.*

One of the most common V-particles (Λ°) was neutral and decayed $(\Lambda^\circ \to p + \pi^-)$ in time 2.5×10^{-10} seconds. The question arised if the Λ° could interact strongly, why did not its decay go via strong interactions with a life time of $\sim 10^{-23}$ sec instead of the observed 10^{-10} sec ? To explain this, Pais suggested the *hypothesis of associated production. The V-particles can interact strongly and, therefore, are produced only in pairs, once separated each number can decay into ordinary particles only through the weak interaction. A typical example is*

$$\begin{array}{llll} \pi^- + p^+ \to \Lambda^\circ & + & K^\circ \\ \qquad\quad \hookrightarrow p^+ + \pi^- & & \hookrightarrow \pi^+ + \pi^- \end{array}$$

Both the associated creation of the strange particles and their individual stability against immediately decay were the features that earned them the title *strange.* Both features can be explained by assigning the new additive quantum number called the strangeness S and insisting that the total *strangeness* must remain constant in fast particle reactions.

If the baryons are arranged in columns according to their electric charge (plus under plus, minus under minus, neutral under neutral). The electric charge centres do not thus occur in the same vertical line. The electric charge centre of the nucleon is at $+\frac{1}{2}$, half way between p and n. The charge centre of Λ° is at 0. The triplet sigma is centred at 0, but the doublet xi is centered at $-\frac{1}{2}$. The Ω^- singlet is at charge -1. If we take the charge centre of the nucleon doublet arbitrarily to be the reference origin, then we have

For Λ° ... $\Delta Q = Q_\Lambda - Q_N = -\frac{1}{2}$; for Σ-hyperons ... $\Delta Q = Q_\Sigma - Q_N = -\frac{1}{2}$;

for Ξ doublet ... $\Delta Q = -1$ and for Ω^- ... $\Delta Q = -\frac{3}{2}$.

By defining strangeness quantum number as

$$S = 2\Delta Q. \qquad \text{...(4)}$$

We obtain $S = 0$ for the nucleons and non-zero for hyperons ($S = -1$ for Λ° and Σ's, -2 for Ξ's and -3 for Ω^-). Once a hyperon or K-meson is produced and gets beyond the influence of the collision, it can decay. As the decay products have strangeness zero hence the strangeness remains conserved in fast nuclear processes. Once produced and separated from each other, they must wait for some weaker interaction to allow them to decay. Strangeness conservation governs only the strong and electromagnetic interactions and not the weak. Even the weak interactions have some respect for strangeness. It is found experimentally that weak decays change strangeness as little as possible.

$\Delta S = \pm 1$. No example with $\Delta S = \pm 2$ has been seen.

The examples are :

$$\Sigma^+ \to \Lambda^\circ + e^+ + \nu_e, \qquad \Delta S = 0$$
$$\Sigma^- \to n + e^- + \bar{\nu}_e, \qquad \Delta S = 1$$
$$\Lambda^\circ \to p + e^- + \bar{\nu}_e, \qquad \Delta S = 1.$$

(c) Conservation of Hypercharge—Like the electric charge, the additive quantum number the strangeness is conserved in the production process. The strange particles are produced in pairs, but may decay weakly. Thus it is convenient to introduce a quantum number *hypercharge* denoted by Y, which is the sum of the baryon number B and strangeness S. It is convenient, since it treats baryons and mesons on an equal basis. Since the baryon number is always conserved, Y is a good quantum number conserved in strong interactions. Unlike the electric charge, the *hypercharge does not conserve in weak interactions.* Thus the charge is related with isospin, baryon number and strangeness as

$$Q = T_3 + \tfrac{1}{2}Y = T_3 + \tfrac{1}{2}B + \tfrac{1}{2}S. \qquad \text{...(5)}$$

This is called *Gell-Mann-Nishijima relation.* This tells us that in deciding whether strong interaction takes place we need to check only three out of four quantities Q, T_3, B and S.

For strange mesons, $B = 0$ and the above relation reduces to

$$Q = T_3 + \tfrac{1}{2}S. \qquad \text{...(6)}$$

Similarly for non-strange particles, $S = 0$ and we have

$$Q = T_3 + \tfrac{1}{2}B. \qquad \text{...(7)}$$

To cover a whole range of strongly interacting particles, the formalism has also been extended to mesons. Since all the hyperons have negative strangeness, they can be produced only in association with K-mesons of positive strangeness. On the assumption that strangeness is a conserved quantity in a reaction such as

$$p^+ + p^+ \to p^+ + \Lambda^\circ + K^+$$
$$S: \quad 0 + 0 \to 0 + (-1) + S_K.$$

It gives that the strangeness $S_K = \pm 1$. Similar argument gives strangeness $S = 1$ for neutral kaon. From the associated production reaction

$$\pi^- + p \to \Lambda^\circ + K^\circ$$
$$S: \quad S_\pi + 0 = -1 + 1.$$

It follows that $S_\pi = 0$. It also applies to π^+, π° and η° mesons. Since for mesons the baryon number $B = 0$, hence strangeness S = hypercharge Y.

Thus we see that strangeness is not an independent new quantity, but is related to a combination of Q, T_3 and B, each of which is regulated by conservation laws.

Let us now see what kinds of particle type can be formed by various choices of T, B and S.

If $S = 0$, there are three possibilities,

(a) $B = 0, T = 0$ yields $Q = 0$ *(neutral meson)*, η° *meson.*

(b) $B = 0, T = 1$ yields $Q = +1, 0, -1$ *(pions).*

(c) $B = 1, T = \frac{1}{2}$ yields $Q = +1, 0$ *(nucleons).*

If $S = 1$, the multiple charge can be avoided only when

(a) $B = 0, T = \frac{1}{2}$ and $Q = +1, 0$ (K^+, K°).

(b) $B = 1, T = 0$ and $Q = +1$ *(Baryon singlet).*

If $S = -1$, the multiple charges can be avoided only when

(a) $B = 0, T = \frac{1}{2}$ and $Q = 0, -1$ ($\bar{K}^\circ, K^-$).

(b) $B = 1, T = 0$ and $Q = 0$, *(singlet baryon Λ°).*

(c) $B = 1, T = 1$ and $Q = +1, 0 - 1$ (hyperons Σ^+, Σ° and Σ^-).

If $S = -2$, the multiple charges can be avoided only when

(a) $B = 1, T = \frac{1}{2}$ and $Q = 0, -1$ (hyperons Ξ°, Ξ^-).

If $S = -3$, the multiple charges can be avoided only when

(1) $B = 1, T = 0$ and $Q = -1$ (Ω^--hyperon).

All these results are summarised in the table 18.3.

Table 18.3. *Gell-Mann-Nishijima Scheme*

S	B	T	T_3	Q	Particle	S	B	T	T_3	Q	Particle
0	0	0	0	0	η^0	−1	0	1/2	+1/2	0	$\bar{K}^\circ$
	0	1	+1	+1	π^+				−1/2	−1	K^-
			0	0	π^0		1	0	0	0	Λ°
			−1	−1	π^-		1	1	+1	+1	Σ^+
	1	1/2	1/2	+1	p				0	0	Σ°
			−1/2	0	n				−1	−1	Σ^-
1	0	1/2	+1/2	1	K^+	−2	1	1/2	1/2	0	Ξ°
			−1/2	0	K°				−1/2	−1	Ξ^-
	1	0	0	1	Baryon	−3	1	0	0	−1	Ω^-

In the case of hadrons, the strangeness must be conserved ($\Delta S = 0$) for fast reactions. The decays of kaons and hyperons are very slow because they involve a breakdown of strangeness conservation. The decays $\Xi^- \to n + \pi^-$ and $\Xi^\circ \to p + \pi^-$, which involve $\Delta S = 2$, would be expected to be exceptionally slow, and the decays $\Xi^- \to \Lambda^\circ + \pi^-$ and $\Xi^\circ \to \Lambda^\circ + \pi^\circ$ with $\Delta S = 1$ to be slow. Since charge and baryon number are always conserved, hence for weak decay processes, equation (5) gives

$$|\Delta S| = 2\,|\Delta T_3|$$

or

$$|\Delta T_3| = \tfrac{1}{2}.$$

As T_3 is the component of total isospin along a particular direction, hence the general form of above equation for weak decays is

$$|\Delta T| = \tfrac{1}{2}.$$

Let us apply conservation laws to high energy pion-nucleon collisions which often give large quantities of kaons. Examples of possible equations are

$$\pi^+ + n^\circ \to \Lambda^\circ + K^+$$
$$\to K^\circ + K^+.$$

Using the conservation of baryons and strangeness, we see that the second reaction violates baryon conservation and therefore cannot occur. Similarly equation $\pi^- + p^+ \rightarrow \Lambda^\circ + K^\circ$ is possible, whereas $\pi^- + p^+ \rightarrow \Lambda^\circ + \pi^\circ$ is not possible due to strangeness violation.

Let us consider equation $p^- + p^+ \rightarrow 2\pi^+ + 2\pi^- + \pi^\circ$. Applying various conservation laws and remembering that the pairs of pions are ejected with opposite isospins, we have

$$Q = -1 + 1 \rightarrow 2 - 2 + 0, \quad \therefore \quad \delta Q = 0$$

$$B = -1 + 1 \rightarrow 0 + 0 + 0, \quad \therefore \quad \delta B = 0$$

$$T = 1/2 + 1/2 \rightarrow 0 + 0 + 1, \quad \therefore \quad \delta T = 0$$

$$Y = -1 + 1 \rightarrow 0 + 0 + 0, \quad \therefore \quad \delta Y = 0$$

$$S = 0 + 0 \rightarrow 0 + 0 + 0, \quad \therefore \quad \delta S = 0.$$

(d) Charge Conjugation. Charge conjugation is the operation which changes the sign of the charge of a particle without affecting any of the properties unrelated to charge. It may be defined as the transformation between a particle and its antiparticle. It has been found experimentally that the operation of both the strong and electromagnetic interactions is invariant to charge conjugation. For instance, such invariance is found experimentally in the strong interaction annihilation of a proton and an antiproton into the particle antiparticle pair K^+K^- and is also found in measurements of the electromagnetic decay of the η° meson. We thus believe that the nucleus of the antideuterium atom (strong interaction behaviour) and also the positron (electromagnetic interaction behaviour) would act in the same way. *The charge conjugation is not conserved in the weak interaction, i.e.*, the weak interaction does distinguish between a system and its charge conjugate. The charge conjugation does not simply mean a change over the opposite electric charge or magnetic moment, the sign of other charge quantum numbers [hypercharge Y, baryon number B, lepton numbers $(l_e\ l_\mu)$] is also reversed without changing mass M and spin s. Thus a unitary operator, also known as charge conjugation operator C, satisfies the following relations :

$$CQC^{-1} = -Q,\ CYC^{-1} = -Y,\ CBC^{-1} = -B,\ Cl_eC^{-1} = -l_e \text{ and } Cl_\mu C^{-1} = -l_\mu. \qquad \ldots(8)$$

Some elementary particles *e.g.*, γ, π° and η° – mesons and the positronium atom $(e^- + e^+)$ are transformed into themselves by charge conjugation. They are their own anti-particles. These are known as *self-conjugate or true neutral particles.* The neutron $(B = 1, Y = 1)$ and K°-mesons $(Y = 1, B = 0)$ are not invariant under C

A system is said to possess charge conjugation symmetry or to be invariant under charge conjugation if the system (or the process) is such that it is impossile to know that it has undergoné charge conjugation. For example, the operation C converts the negative pion decay $(\pi^- \rightarrow \mu^- + \overline{\nu}_\mu)$ into the positive pion decay $(\pi^+ \rightarrow \mu^+ + \nu_\mu)$, since the π^+ is the anti-particle of π^-. Until about four decades ago it was believed that the entire universe is invariant under C. In the end of 1956, experiments revealed that weak interactions violated it. It turned out that the μ^+ and μ^- decay electrons have angular distributions of opposite asymmetry that the π^+ and π^- decay muons have opposite polarizations and that while a free neutrino is left handed an anti-neutrino is right handed. Charge conjugation applied to a free moving neutrino then results in a process which does not exist in nature.

Positronium is a hydrogen like bound state of an electron and a positron. According to the Dirac's theory the charge conjugate, which corresponds to the wave functions of positrons, has the form

$$C = ie^{i\phi}\begin{pmatrix} 0 & \sigma_y \\ \sigma_y & 0 \end{pmatrix} = e^{i\phi} i\,\alpha_y. \qquad \ldots(9)$$

The phase ϕ is arbitrary. For zero phase $(\phi = 0)$

$$C = i\alpha_y, \qquad \ldots(10)$$

where α_y is a square matrix and σ_y is the Pauli spin matrix having value

$$\sigma_y = \begin{vmatrix} 0 & -i \\ i & 0 \end{vmatrix} \qquad ...(11)$$

For a single photon state

$$C|\gamma> \; = \; -|\gamma>. \qquad ...(12)$$

For a system of n-photons

$$C|n\gamma> \; = \; (-1)^n |n\gamma>. \qquad ...(13)$$

Thus the n-photon state is also in an eigenstate of C with the eigen value $(-1)^n$. Since π° mesons decay through electromagnetic interaction into two photons $\pi^\circ \to 2\gamma$, it follows that the π°-meson is self conjugate and that $|\pi^\circ>$ is an eigenstate of C with eigenvalue + 1, *i.e.*,

$$C|\pi^\circ> \; = \; |\pi^\circ>$$

On the other hand $|\pi^+>$ and $|\pi^->$ are not eigenstates of C as

$$C|\pi^+> \; = \; -|\pi^-> \text{ and } C|\pi^-> = -|\pi^+>$$

As the triplet spin state is symmetrical and the singlet spin state anti-symmetrical, hence to exchange an electron with a positron we must introduce a factor $(-1)^{s+1}$ as well as a factor $(-1)^l$. Thus we have

$$(-1)^{l+s+1}\,C \; = \; -1 \text{ or } C = (-1)^{l+s}. \qquad ...(14)$$

and the positronium atom is in an eigenstate of C with eigenvalue $C = (-1)^{l+s}$.

Above relation gives that the singlet ground state ($l = 0$) decays into two photons and the triplet ground state decays into three photons. Similarly a system composed of two identical bosons of opposite charges, such as π^+, π^-, is in an eigenstate of C. Since the wave function of two bosons remains unaltered under the exchange of the two particles including charge, the eigenvalue of C is given by $C = -1$.

(e) Space-inversion Invariance (parity). The parity principle says that there is a symmetry between the world and its mirror image. This may be defined as reflection of every point in space through the origin of a co-ordinate system $x \to -x$, $y \to -y$ and $z \to -z$ or $\boldsymbol{r} \to -\boldsymbol{r}$. If a system or process is such that its mirror image is impossible to obtain in nature, the system or process is said to *violate the law of parity conservation.*

Human body is a good example of mirror symmetry. The body of a car is symmetric except for the position of the steering wheel. If we were looking at the mirror image of a normal car, it seems to violate the symmetry but it is not the case as it is also possible to design a car with the steering wheel on the other side. The mirror view of a printed page looks wrong. But there is nothing impossible about it. A printer could design inverted type and produced a page. One can read the page from right to left. The type of printing is not unnatural but is unconventional and unfamiliar. The values of the physical quantities of classical physics either remain unaltered or change sign under space inversion. Thus the quantities may have either even or odd intrinsic parity. The ordinary scalars such as temperature, electric charge, energy, have even parity. The ordinary vectors such as momentum, force, electric field have odd parity. Pseudovectors such as angular momentum, magnetic field, behave as vectors under rotations but have the even parity. Similarly pseudo scalars (the product of any ordinary polar vector with a pseudovector) have the odd parity.

All phenomena involving strong and electromagnetic interactions alone do conserve parity. In these cases the systems can be classified by the eigen values of the parity operator $\mathcal{P}$. For a single particle Schrodinger wave function ψ, the result of the parity operation is

$$\mathcal{P}|\psi(x)> \; = \; e^{i\alpha}|\psi(-x)>. \qquad ...(15)$$

As α is an arbitrary real phase, hence can be set equal to zero.

$$\therefore \qquad \mathcal{P}|\psi(x)> \; = \; |\psi(-x)> \qquad ...(16)$$

and

$$P^2|\psi(x)> \; = \; |\psi(x)>. \qquad ...(17)$$

It shows that eignvalues of $\mathcal{P}$ may be + 1 *or* – 1.

The parity of the photon depends upon the mode of transition, it is due to the change of the sign of electromagnetic current **j** under the parity operation. The nucleons and electrons are assigned positive (or even) intrinsic parity. The pions have negative (or odd) parity as they involve in strong interactions with nucleons. *K*-mesons and η°-meson have negative parity. Λ°, Ξ^{-}, Σ, Ω-hyperons have positive intrinsic parity. All anti-particles of spin $\frac{1}{2}$ (the fermions) are of opposite parity to the corresponding particle, while the bosons and their anti-particles have the same parity.

The conservation of parity requires that the Hamiltonian of a free system commute with the parity operator.

$$(\mathcal{P}\mathcal{H}-\mathcal{H}\mathcal{P}) = 0. \qquad \ldots(18)$$

The transition probability must be scalar, it may contain pseudoscalar operator (**I.p**). The conservation of parity prevents the mixing of even and odd operators in the amplitude. Thus for the non-conservation of parity in β-decay, the transition probability must contain both scalar and pseudoscalar terms or *the number of electrons emitted parallel and anti-parallel to the spin of the source should be different.*

The weak decay of the *K*-mesons, which was difficult to reconcile with parity conservation and known as the $\tau - \theta$ puzzle, was explained by Lee and Yang. They suggested that *the weak interaction was not invariant to space reflection*. In 1956, Wu and others, using polarized ^{60}Co nuclei, found that the direction of emission of electrons in the transformation to ^{60}Ni was preferentially opposite to the spin direction. The value of the pseudoscalar **I.p**, where **I** is the nuclear spin and **p** the electron momentum, was measured and found to be different from 0.

(f) Combined Inversion ($\mathcal{CP}$). Landu (1956) advanced a hypothesis to the effect that any physical interaction must be invariant under simultaneous reversal of position coordinates and change over from particles to anti-particles. For example a neutrino has a definite helicity and its parity conjugate has opposite helicity. The charge conjugate of the neutrino also has opposite helicity. Thus under the combined operations $\mathcal{PC}$ *(or* $\mathcal{CP}$) the neutrino changes to anti-neutrino. The combined operation also known as combined parity (charge and space) is conserved in most of the known physical processes. Let us consider the decay of the positive pion

$$\pi^{+} \rightarrow \mu_L^{+} + \nu_{\mu_L}.$$

Here subscript *L* indicates that neutrino and positive muon fly apart with left handed spin. As the $\mathcal{C}$-inversion changes particles into anti-particles and vice-versa, whereas the $\mathcal{P}$-inverson converts left handed motion to right handed motion. Hence

$\mathcal{C}$-inverstion : $\pi^{-} \rightarrow \mu_L^{-} + \bar{\nu}_{\mu_L}$ Impossible process

$\mathcal{P}$-inversion : $\pi^{+} \rightarrow \mu_R^{+} + \nu_{\mu_R}$ Impossible process

$\mathcal{CP}$-inversion : $\pi^{-} \rightarrow \mu_R^{-} + \nu_{\mu_R}$ Possible process

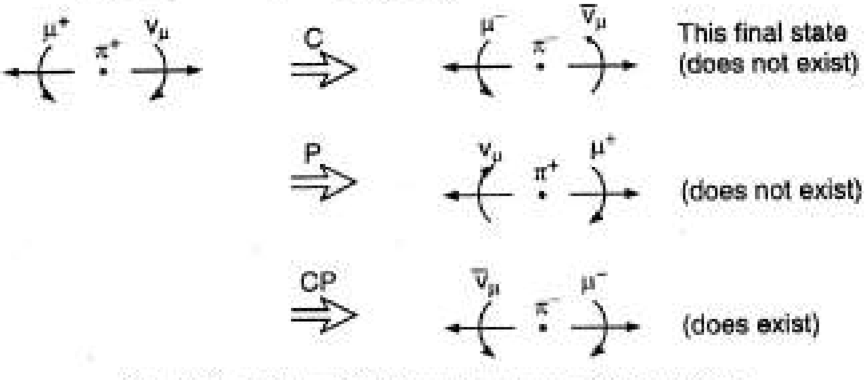

Fig. 18.3. $\mathcal{C}$- $\mathcal{P}$- and $\mathcal{CP}$ inversions in weak interactions.

Since the fermions all have intrinsic parity (+1), while the corresponding antiparticles all have intrinsic parity (−1). For bosons the corresponding antiparticle has the same parity, thus π^{+} and π^{-}-mesons have the same intrinsic parity of (−1). Thus the charge conjugation operator anticommutes with the parity operator when applied to fermions, but commutes with the parity operator when applied to bosons.

Let us consider the case of the β-decay of polarized nuclei (*e.g.*, ^{60}Co). The interpretation of the parity non-conservation, charge non-conservation and conservation under the combined operation is shown in Fig. 18.4. In this figure, ***B*** shows the direction of a magnetic field due to current loop, used for polarizing the nuclei. It represents the nuclear spin and thus *known as polarization vector.* The upper diagrams represent the result of the reflection of the process shown in the lower diagrams of Fig. 18.4. Fig 18.4 (a) shows that the space reflection creates a different system, as it changes the direction of decay arrows but not the direction of **B.** Fig. 18.4 (b) represents the charge conjugation only. This process leaves the direction of the decay unchanged, although electrons are replaced by positrons and the polarization direction is reversed. Fig. 18.4 (c) shows the combined effect of $\mathcal{CP}$ operation. This shows that under $\mathcal{CP}$ reflection, we obtain the process of decay of the antinucleus. From the above results we conclude that the reflection type of symmetry can be obtained by the combined operation of $\mathcal{C}$ and $\mathcal{P}$ only in weak interactions. Number of other examples show that the weak interactions do not grossly violate the combined $\mathcal{CP}$-invariance. Unfortunately the decay of *K*-meson is not invariant under the combined operation of $\mathcal{CP}$.

(g) Time Reversal. The time reversal operator is defined as that operator which reverses the direction of time, or the direction of all motions. Under this operation displacement, acceleration and electric fields remain invariant but momenta, angular momenta and magnetic fields invert their signs. If the time reversed process is impossible to occur in nature we can say that the process violates time reversal symmetry. Time reversal changes the direction of flow of time, like running the movie of a phenomenon backwards. The result is usually strange.

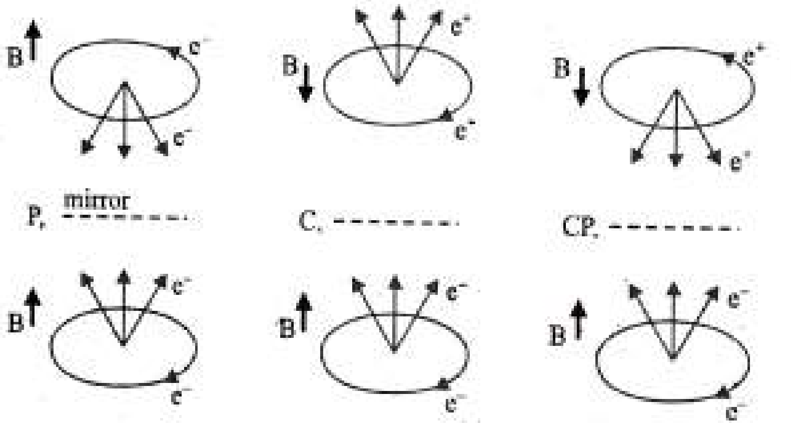

Fig. 18.4. Parity mirror, (b) Charge Conjugation mirror and (c) CP-mirror.

Time reversal invariance finds its simplest application in the world of particles, where it appears to govern the strong and electromagnetic interactions and possibly also the weak. It also shows that a particle possessing time reversal symmetry cannot have electric and magnetic dipole moments simultaneously. The time reversal process is the creation of an electron-positron pair by the collision of two photons.

If time reversal operation is applied to decaying $\pi^+ \to \mu^+ + \nu_\mu$. Under time reversal the momentum vectors are reversed and spins go around in the opposite directions. We have ν_μ and μ^+ with the proper handedness interacting to form a pion.

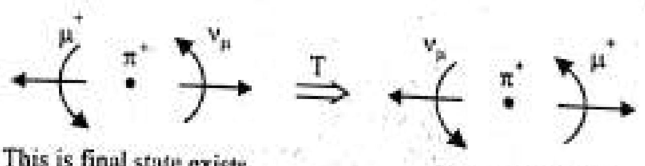

This is final state exists

This also exists

Fig. 18.5. Time reversal.

Time reversal invariance is satisfied in quantum mechanics if the Hamiltonian *H* is time independent and real. In this case $\psi^*(\mathbf{x}, -t)$ is the time reversal wave function of $\psi(\mathbf{x}, t)$. Thus time reversal operation $\mathcal{T}$ changes ψ as

$$\mathcal{T}\psi(\mathbf{x}, t) = \psi^*(\mathbf{x}, -t). \quad \ldots(11)$$

where the asterisk indicates the complex conjugate.

The motion of a particle in an external fixed magnetic field is not invariant under inversion of time. The relativistic treatment of time reversal shows that the inversion of time axis inverts the sign of the electrostatic potential. The π^0 – mesonic field, like the magnetostatic potential, is odd under time reversal in order to ensure that the interaction is time reversible.

(h) Combined Inversion of $\mathcal{CPT}$. The reflection symmetries are correlatd by the CPT theorem of G. Lüders and W. Pauli, sometimes known as *Lüders-Pauli theorem*. This theorem states that the Lorentz invariant field theory is necessarily invariant to the combined operations of particle-antiparticle interchange (charge conjugation C), reflection of the coordinate system through the origin (parity, P) and reversal of time T. In other words $\mathcal{CPT}$ operator commutes with the Hamiltonian. The strong and the electromagnetic interactions are invariant under the separate operations of $\mathcal{C}$, $\mathcal{P}$ and $\mathcal{T}$. The weak interaction does not conserve parity and also is not invariant under charge conjugation. All the interactions are invariant under the combined strong reflecton operation $\mathcal{CPT}$, irrespective of the order of the operations and so forth ($\mathcal{TCP}$, $\mathcal{TPC}$).No example of a violation of the $\mathcal{CPT}$ theorem is known. If follows that if $\mathcal{T}$ invariance is satisfied for all interactions, then these interactions will also be invariant under the combined operation of $\mathcal{CP}$. The existence of $\mathcal{CP}$ violating interactions means that the analysis is not quite accurate. The other well known consequencs of $\mathcal{CPT}$ invariance are :

(i) The equality of particle-antiparticle masses, (ii) equality of lifetimes of unstable particle and its antiparticle, (iii) the magnetic moments of particle and antiparticle are equal and opposite.

The discovery of $\mathcal{CP}$ violations in 1964 in the system of neutral K-mesons reopened the question of $\mathcal{CPT}$ invariance. Now observations show that at least 90% of the observed $\mathcal{CP}$ violation is compensated by a violation of time-reversal invariance. The less than 10% of the observed $\mathcal{CP}$ violation may be due to the violation of $\mathcal{CPT}$. This system suggests that further experimental work is required to test the validity of the $\mathcal{CPT}$ theorem.

The quantities conserved have the quantum numbers, which behave in two different ways, when one considers a system formed by the combination of two other systems. The quantum numbers, such as *angular momentum, isospin, strangeness, baryon number, lepton number, electric charge are called additive. On the other hand, quantum numbers, such as parity, invariance under charge conjugation, invariance under time reversal are called multiplicative.*

PRODUCTION AND PROPERTIES OF ELEMENTARY PARTICLES

18.5 ELECTRON–AND POSITRON

Electron—The electron is the first and best known elementary particle. It was discovered in 1897 by *J.J. Thomson* in the form of cathode rays. The mass of the electron at rest is 9.1094×10^{-31} kg. All other elementary particles have larger mass than that of the electron. Thus it is convenient to use the mass of the electron as a unit for a mass. The electron has a negative electric charge of magnitude 1.6022×10^{-19} coulomb. The electron obeys the Fermi-Dirac statistics and is therefore called *fermion*. It therefore obeys the Pauli exclusion principle. Every elementary particle possesses an intrinsic angular momentum called its spin. The spin of the electron has the magnitude $\frac{1}{2}\hbar$. Its spin can still have either one or the other of the two possible conditions, usually known as *spin up or spin down*. According to the Dirac quantum mechanical theory of the electron, the magnetic dipole moment associated with the electron spin should be exactly one Bohr magneton ($eh/4\pi m_e$). Another prediction of this theory is that the $2S_{1/2}$ and $2P_{1/2}$ atomic levels of an one electron atom should be degenerative. Both these predictions are wrong, the magnetic moment is about 0.1 per cent greater than the Dirac value and the levels have a small energy difference.

The volume of an atom is nearly all occupied by the cloud of electrons surrounding the nucleus. The electron can be regarded as having a definite radius in classical terms. It is found to be 2.818×10^{-15} *m*, one hundred-thousandth (10^{-5}) of the radius of an average atom. The electrons are emitted in radioactivity (as beta rays) and in many other decay processes. The electron is completely stable. The chemical properties of ordinary matter are determined by the electron cloud.

Positron—In 1932, C.D. Anderson of California Institute of Technology (U.S.A.), while studying cosmic rays using a cloud chamber observed a particle corresponding to the electron, but having positive charge. This particle was called positive electron or *positron*. P.M.S. Blackett and G.P.S. Occhialini in England also observed positrons in 1933. J. Thibaud in Belgium in 1934, using an arrangement of crossed magnetic and electric fields, reported that *e/m* for the positron was nearly same as that for electron. The positron is, inself, stable, but cannot exist indefinitely in the presence of matter. The positron has same spin and statistics as the electron. Positrons, like electrons, appear as decay products of many heavy particles. Neutron poor light nuclei decay with the emission of positrons. Electron-positron pairs are produced by high energy photons in matter. Just previously *P.A.M.* Dirac, in England (in 1928) has predicted the existence of a positron in his relativistic theory of the free electron. Dirac suggested that electron positron pair cannot be created by bombarding particles or photons of energy less than the threshold energy $2m_ec^2$ (1.02 *MeV*). At the time of passage through ordinary matter, the positron may join an electron to form a positron-electron system, called *positronium,* which lasts for a measurable time before combining to produce *annihilation radiation*. Because of this annihilation property, the *positron is said to be the anti-particle to the electron.*

$$e^+ + e^- = \gamma + \gamma. \qquad ...(19)$$

The positron was the first of the class known as *antiparticles* and has been given the symbol e^+.

Positronium—The lowest Bohr orbit of positronium is one for which $n = 1$ and $l = 0$ (S–state). This state has fine structure owing to the spins of the particles. The atom is in a ^1S state when the two spins are oppositely directed and in a ^3S state when the spins are parallel. Theoretical calculations by J. Pirenne (1944) and J.A. Wheeler (1946) showed that the lifetime of the singlet should be of the order of 1.3×10^{-10}. The annihilation radiation emitted by the combining of a positron-electron pair in the singlet state should consist of two gamma ray photons emitted simultaneously in opposite directions. Theoretical calculations by Ore and Powell (1949) showed that the lifetime of the triplet state should be about 1.5×10^{-7} sec. The annihilation should consist of three gamma ray photons traveling away from their origin at mutual angles of 120°. We can explain the production of two in one case and of three γ-ray photons in the other as the result of the conservation of spin in the annihilation process. In the singlet state net spin is zero, two photons (spins + 1 and −1) are expected in opposite directions in order to satisfy the law of conservation of momentum. In the triplet state (spin +1 or −1), three photons (+1, +1, −1 or −1, −1, +1) are expected. M. Deutsch (1951) measured experimentally the time between the formation of positrons and their subsequent annihilation and found the vaue 1.5×10^{-7} sec. This is the experimental evidence for the existence of the triplet state (*ortho*) of positronium.

The study of positronium (a two body system) has served as an important confirmation of theory of quantum electrodynamics. The studies of positron annihilation in solids and liquids indicate that a perturbed form of positronium exists under certain circumstances. The binding energies of positronium are one half the corresponding binding energies of the hydrogen atom. The ionization potential is 6.8 *eV*. The energy separation, often called hyperfine structure of the ground state of positronium, corresponds to a frequency difference $\Delta\nu$ of 2.0337×10^5 *MHz*. Positronium has no permanent magnetic moment, but there can be a magnetic moment induced by the external magnetic field.

18.6 PROTON AND ANTI-PROTON

Proton—E. Goldstein, in Germany in 1886 observed *positive rays* also called *canal rays*. These were the streams of positive ions produced in the gas by ionization. Thomson's studies of the positive rays from ionized hydrogen gas were the first experiments in which the second elementary particle was identified. Rutherford suggested its name as *proton*. It is the nucleus of the common hydrogen atom (singly ionized hydrogen atom). Free *protons can be easily obtained for experimental purposes by ionization (electron removal) of hydrogen atoms in an electric gas discharge.* Since the weight of the hydrogen atom is 1837

m_e hence the weight of the proton is 1836 $m_e = 1.673 \times 10^{-27}$ kg. The charge of the proton is positive and exactly equal in magnitude to that of the electron. It is a fermion of intrinsic spin half. It is useful to regard the proton as a particular charge state $T_3 = +\ 1/2$ of a single particle, the nucleon, of total isospin $T = 1/2$. Proton has a magnetic moment of 2.79285 nuclear magneton ($\mu_N = eh/4\pi m_p$). The proton is not a point, but has a radius of about 10^{-15} m.

Antiproton—Like the electron, the proton has a counter part of opposite charge with which it undergoes annihilation. Just as positron electron pairs are formed by the interaction with matter of rays or particles having sufficient energy (1.02 MeV), so it should be possible to produce proton-anti proton pairs in a similar manner, but it would require about 2000 times energy. Until 1955, the required energy was available in high energy particles in cosmic radiations and the evidence of the antiprotons could be obtained from cosmic ray events in photographic emulsions and cloud chambers. With the completion of the 6 GeV bevatron at the University of California it was possible to perform an unambiguous experiment for the production and detection of anti-protons. The first convincing evidence of the anti-proton came from the experiment performed by Chamberlain, Segre, Wiegand and Ypsilantis in 1955. However its existence was implied in 1928 by the relativistic equation of P.A.M. Dirac. The schematic diagram of their detecting apparatus, which is as a mass spectrograph, is shown in Fig. 18.6. Proton beam of 6 GeV energy from Bevatron was allowed to impinge upon a copper target T, in which it produced particles of various kinds as a result of proton-proton and proton-neutron reactions.

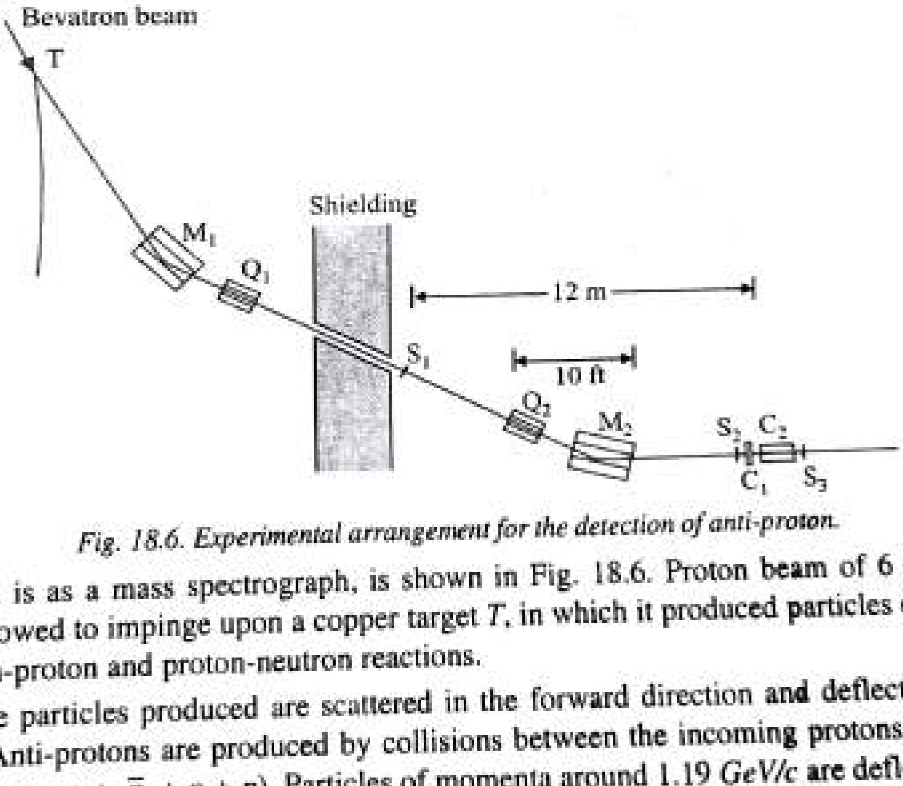

Fig. 18.6. Experimental arrangement for the detection of anti-proton.

The negative particles produced are scattered in the forward direction and deflected outward by the Bevatron field. Anti-protons are produced by collisions between the incoming protons and protons in the target nuclei ($p + p = p + \bar{p} + p + p$). Particles of momenta around 1.19 GeV/c are deflected about 21° and enter the deflecting magnet M_1. The particles with the selected momenta are deflected about 32° by M_1 and are focused by the three element quadrupole lens Q_1 at the scintillation counter S_1. The negatively charged particles reaching at S_1 have same momentum. These are not only the anti-protons, but an extremely large number of negative pions produced in the target is present in the selected beam (about 40,000 negative pions to every anti-proton). The particles of momentum 1.19 GeV/c and with a rest mass equal to the rest mass of the proton have $v/c = \beta = 0.78$. The negative pions of momentum 1.19 GeV/c have $v/c = \beta = 0.99$. Thus to separate out antiprotons from the extremely heavy background of negative pions, velocity selection mechanism is required. Chamberlain *et al.* used two methods of velocity selection : (i) time of flight of the particles between scintillation counters S_1 and S_2 and (ii) coincidence using two Čerenkov counters C_1 and C_2 and one scintillation counter S_3.

The distance between plastic scintillation counters S_1 and S_2 was 40*ft*.; the time of flight for anti-protons was 51 n sec and for pions 40 n sec. Thus we see that the pulse emitted from counter S_2 due to antiproton occurs 51 *n* sec later than that from S_1. To obtain a coincidence the signal from S_1 was delayed enough that the two signals arrived at the coincidence circuit at exactly the same time. Sometimes there would be two different mesons passing through the two counters in such a way that a pulse from the second counter would be produced just 51 *n* sec after a pulse from the first. This gave accidental coincidences appearing like anti-protons. To eliminate this difficulty the experimenters introduced the use of Čerenkov *counters*. The Čerenkov counter C_1 of chemical composition $C_8F_{16}O$ and refractive index 1.28, was designed to respond to particles with velocities greater than 0.79 c. Any pulse from C_1 cannot be due to an antiproton having velocity 0.78 c. The second Čerenkov counter C_2 of fused quartz and refractive index 1.46 was designed to respond only to particles whose velocities were between 0.75 c and 0.78 c. It was converted in anticoincidence with C_1, so that the pulses in C_2 were those produced by anti-protons only and in C_1 by negative pions only. The third scintillation counter S_3 certifies that an anti-proton has not been scattered through a large angle in C_2. The distance between S_2 and S_3 was only a few inches.

The number of counts registered by the equipment for a given exposure was measured as a function of field strength in the magnets. The field strength is converted to mass of the selected particle. A curve drawn between the number of counts and the mass of the selected particle is shown in Fig. 18.7. This curve shows that the mass of the negative particles observed corresponds to the mass of protons. The only known particle with this mass was the negative hydrogen ion. The observed particles could not be negative hydrogen ions, as the possibility that a proton with this velocity would pick up two electrons and retain them while penetrating all the counters is negligible. Thus the observed particle would be a new particle, known as *anti-proton*.

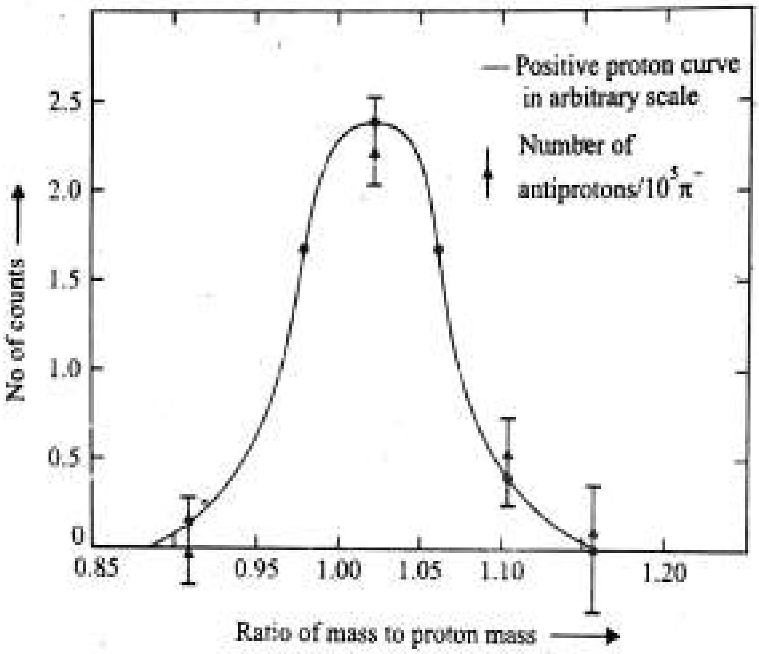

Fig. 18.7. Mass measurement of negative particles.

The mass and intrinsic angular momentum of the antiproton are equal to those of the proton, while the electric properties, charge and magnetic moment are equal in magnitude but opposite in sign. The antiproton has a structure. Massive elementary particles are produced when the accelerated antiproton collides with the equally energetic protons moving in opposite directions.

In the experiment performed by Hill, Johansson and Gardner, the beam of 6.2 GeV protons was incident on a photographic emulsion. The proton produced a star (Fig. 18.8) in a collision with a nucleus. One of the particles produced in this event was an anti-proton, which proceeded in the emulsion and found to give another star, whose several prongs were corresponding to particles appeared in this process. Measurements showed that the total energy released was greater than expected from the mass of the anti-proton alone, so that it might be annihilated by a proton.

The annihilation of an antiproton with a proton differs from that of a positron and electron in that several charged and neutral π-mesons together with protons and occasionally (if sufficient kinetic energy is supplied) deuterons and K-mesons are usually produced, rather than two or three quanta. The mass of the anti-proton has not been measured very accurately but it is presumably

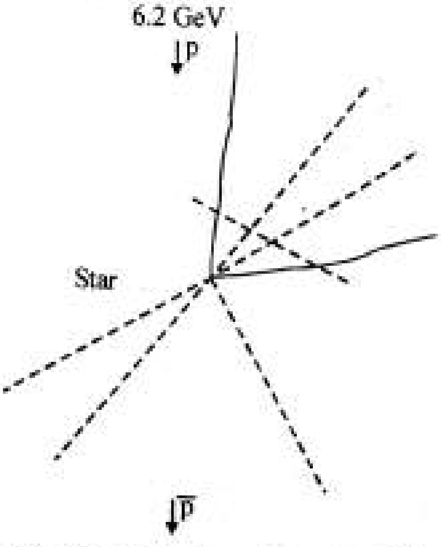

Fig. 18.8. Production of an anti-proton.

exactly equal to that of the proton. *Its electric charge is equal in magnitude, but negative in sign*, confirmed by the fact that protons annihilated with anti-protons. The energy released in proton-antiproton annihilation is 1836.12 times the energy released in electron-proton annihilation.

18.7 NEUTRON AND ANTI-NEUTRON

Neutron—Chadwick in 1932 discovered the neutron through a careful study of the kinematics of α-particle induced reactions with light nuclei. The production and properties have already been given in chapter 12.

Anti-neutron—In the series of experiments which led to the detection of the anti-proton, the anti-neutron was also found. A convincing experimental evidence for the existence of anti-neutrons was announced in September 1956 by B. Cork, G.R. Lambertson and others. When a proton and anti-proton meet, mutual annihilation generally takes place. But if these two particles come fairly close to each other, although not close enough for annihilation to occur, it is possible for an electrical charge to be transferred from the positive proton to the negative antiproton or vice-versa. As a result, both particles would become electrically neutral, the proton being converted into a neutron and the anti-proton into an anti-neutron.

$$\bar{p} + p \rightarrow \bar{n} + n. \qquad ...(20)$$

Evidence for this charge transfer process was obtained by allowing anti-protons, obtained from the Berkeley Bevatron, to enter a vessel of liquid hydrogen. About three out of every thousand antiprotons interacted with the protons in the hydrogen to form antineutrons. The latter were identified by the energy produced in the mutual annihilation of an anti-neutron and a neutron. The release of energy was accompanied by a flash of light in a detector. The recording system was designed to respond only to those associated with the correct amount of energy to be expected from neutron anti-neutron annihilation. This formation of neutron-antineutron by charge exchange was confirmed by E. Segre and W.M. Powell at Berkeley in 1958 in a more direct manner using bubble chamber. Since neither neutrons nor anti-neutrons have a net electric charge, hence the distinction of a particle from its anti-particle by its charge cannot apply to the neutron and antineutron. We do expect, however, that whatever be the internal charge distribution of the neutron, the antineutron will have the opposite internal charge distribution.

In the magnetic field free region, the masses of the neutron and antineutron are the same, the spins ($\frac{1}{2}$) are the same, the statistics (Fermi) are the same and the decay constants for β-decay are the same. The sign of the magnetic moment (μ) is inverted. In a magnetic field B, the energies differ by $2\mu B$ and the effective masses by $2\mu B/c^2$. There is a periodic transitions between the state of a neutron and the state of an anti-neutron.

18.8 NEUTRINO AND ANTI-NEUTRINO

As discussed in chapter 6, it is possible to avoid violations of the law of conservation of energy, linear and angular momenta and spin by assuming the existence of a particle, called a *neutrino*. It has charge zero, spin $\frac{1}{2}$, zero rest mass (rest mass very small in comparison with that of the electron) and magnetic moment smaller than 10^{-8} Bohr magneton or nearly zero. It also has energy and momentum.

Indeed, it has an anti-particle, the *anti-neutrino*, which is distinguishably different from it. The neutrino and anti-neutrino differ with respect to the property known as *helicity*. It is customary to call the particle accompanying a positron a neutrino, ν, while that accompanying an electron is called an anti-neutrino, $\bar{\nu}$. It is important to remember that positrons and electrons are never ejected alone. It is clear from experiments that neutrinos emitted in β-decay (positron decay and K'-capture) have a negative helicity, *i.e.* they are longitudinally polarized with their spin axes antiparallel to their direction of travel.

$$\mathcal{H} = +1 \text{ fo } \bar{\nu}; \quad \mathcal{H} = -1 \text{ for } \nu. \qquad ...(21)$$

Because of its lack of charge and magnetic moment, a neutrino has essentially no interaction with matter except that which leads to inverse β decay. This interaction is extremely weak.

The ν_e and $\bar{\nu}_e$ were postulated in 1930 to explain the β-decay. The existence of these neutinos was experimentally verified in 1953. Quantitative studies of ν interactions, undertaken in 1961 by utilizing neutrinos produced by the alternating Gradient Synchrotron at Brookhaven National Laboratory showed that there were two distinct neutrinos—the electron neutrino ν_e associated with β-decay and muon neutrino ν_μ associated with π-decay. Thus there are four neutrinos, namely ν_e, ν_μ, $\bar{\nu}_e$ and $\bar{\nu}_\mu$.

In 1975, a new heavy charged lepton (tau $\tau^{\pm}$) was discovered by Martin Perl and his collaborators. The new additional type of neutrinos ν_τ and $\bar{\nu}_\tau$ associated with this new heavy lepton are found to exist in addition to the above mentioned four neutrinos.

The neutrino is the only known particle that has only weak interactions. Thus the neutrino is a unique tool in the study of weak forces, since the interactions are free from electromagnetic and strong interactions. The scattering of neutrinos by neutrons or protons can be used to study the internal structure of the nucleons.

The neutral current interactions of neutrinos have been extensively studied in a large variety of processes, such as neutrino-electron scattering and neutrino-proton scattering. From the neutrino interaction studies, the evidence for the existence of a new class of particles called, *charmed particles,* was observed.

There are thus six distinct neutrinos, namely, ν_e, ν_μ, ν_τ, $\bar{\nu}_e$, $\bar{\nu}_\mu$ and $\bar{\nu}_\tau$. The subscripts e, μ and τ represent the neutrinos as electron-associated, muon-associated and tau-associated respectively. The rest mass and electric charge of neutrinos are assumed to be identically zero. The experimental indication and theoretical speculation suggest that some of the neutrinos have finite, although very small, mass. Astrophysicists believe that there are a very large number of neutrinos in the universe and constitutes a significant fraction of the total mass of the universe.

18.9 GRAVITON, PHOTON AND GLUON

Graviton—The field quantum for gravitational fields is called *graviton* (symbol g). Such a particle has not been detected, but it is not unreasonable to suppose its existence. It is a massless particle with a probable spin of two units. It obeys Bose-Einstein statistics and is a boson. Free gravitons would be emitted only by large masses (stars) subject to very large accelerations. The fields are stationary when the source is at rest, and free field quanta are formed only when the source is accelerated, the field is left behind as the particle is jerked away from it.

There is indirect astronomical evidence for gravitons. The spin of the graviton is known to be 2. The reason is the absence of negative gravitational mass, which prevents the existence of the oscillating dipole that would be required to radiate graviton with spin 1. The lowest possible multipolarity oscillating gravitational source is a quadrupole which emits spin 2 quantum.

The graviton plays no role in high energy particle physics, therefore not discussed in details here.

Photon—The photon is the quantum of the electromagnetic field, *i.e.*, electromagnetic interactions involve the transfer of photons from one body to another. It was first recognized by Einstein in 1905, who extended Planck's quantum hypothesis to apply to radiation in order to explain certain puzzling features of the photoelectric effect. The neutrino and the photon have a number of identical properties. The main difference in their behaviour springs from the different spin values. The spin is half for the neutrino and one for the photons. Similar to neutrino, photon has no mass and no electric charge. It is represented by a symbol γ.

The spin of the photon is associated with its polarization. Bethe measured the torque communicated to a suspended quartz disc of a torsion balance experiment illuminated with polarized light. From his measurements he was able to show that each photon polarized light carried an angular momentum of magnitude $\hbar$. Left and right circularly polarized light corresponds to opposite senses of rotation of the photon. A beam in which the electric vector at a given point rotates anti-clockwise, when viewed from the light source, is known as a *left circularly polarized light beam.* A left circularly polarized photon is the anti-particle of a right circularly polarized photon. Actually *photon and the anti-photon are one and the same, there is no distinction between them.* The above classification refers only to plane polarized light which is conveniently regarded as a mixture of left and right circular polarized components.

Gluon—Fritzsch and Gell-Mann in 1972-73 proposed that the quarks must have new quantum number called *colour* of zero rest mass. The gluon is the gauge field mediating the colour interaction. Thus the strong interactions of quarks are assumed to be mediated by eight massless, vector bosons, which are named gluons because they make up the glue, which binds quarks together. The free gluons remain undetected experimentally, as individual gluon (symbol G) cannot be isolated. The gluons are responsible for binding the quarks together to form hadrons, while photons, the gauge field mediating the electromagnetic interactions between two charged particles, have no electric charges. The gluons carry colour charges and hence interact with each other. The strong interactions of hadrons can be described by Quantum Chromodynamics in analogous with the electromagnetic interactions by the Abelian gauge field theory (the Quantum Electrodynamics). The self interaction property of gluons makes Chromodynamics different from electrodynamics.

The existence of an electrically neutral glue with in the proton came from inelastic electron-proton scattering experiments carried out at Stanford Linear Accelerator Centre (SLAC). The most unambiguous evidence for the existence of gluons was reported in 1979 at the Deutsches Elektron-Synchrotron (DESY) in Hamburg from electron-positron annihilation experiments.

MESONS

In 1937 C.D. Anderson and S.H. Neddermeyer observed few tracks, which could not be attributed to either protons or electrons, in cloud chamber cosmic ray observations. They concluded that the new particle might be ligher than a proton and heavier than an electron or positron. Almost simultaneously and independently J.C. Street and B.C. Stevenson also obtained a cloud chamber photograph and found a negatively charged particle of mass ~ 130 m_e which turns out to be ~ 175 m_e using the correct relation between specific ionization and velocity.

During 1937-38, confirmation was obtained from various sources of the existence in cosmic rays of particles lighter than a proton but about 200 times heavier than the electron. Such particles were found to carry either positive or negative charge and named *mesotrons* by Anderson and Neddermeyer, from the Greek word *meso*, meaning intermediate. Later, the name meson, suggested by the Great Indian physicist H.J. Bhaha in 1939, was adopted. The existence of this type of particle had actually been predicted by H. Yukawa in 1935. In his study of the field of the nuclear force, Yukawa predicted quantum mechanically the existence of a system of nucleon exchange forces which required the existence of a particle, with either positive or negative charge and of mass equivalent to 200 to 300 m_e, in order to give the correct distance over which the short range forces act. Before 1947 there was no evidence for the existence of more than one type of intermediate particle. In the same year C.M.G. Lattes, H. Muirhead G.P.S. Occhialini and C.F. Powell, working with Ilford Nuclear Research emulsions in England showed that two kinds of mesons with different masses existed. Upon developing photographic films with nuclear track emulsions after exposure for some time at high altitudes in the Bolivian Andes, tracks were observed indicating the presence of a meson with a mass ~ 300 m_e. It was also noted that at the end of its path in the emulsion, the heavier meson changed into a lighter particle with a mass of about 200 m_e. These two mesons were distinguished by calling the heavier one the π-meson and the lighter the μ-meson.

The μ-meson is the particle first observed by Anderson and has properties similar to the electron except the mass. The π-mesons, also called pions, are not only heavier but 100 times more stable than muons. The π-meson (primary meson as it decays to muon it $\pi^\pm \rightarrow \mu^\pm + \nu$) is identifiable as the Yukawa particle. In 1944 L. Leprince – Ringuet and M. Lheritier in France observed a particle of mass about 1000 m_e while studying a cloud chamber photograph of a collision of a positive particle with an electron. Three years later, G.D. Rochester and C.C. Butler of the university of Manchester in 1947, observed tracks in photographs of cloud chambers exposed to cosmic rays at a high altitude. These new particles are now known as *K-mesons or Kaons*. Four kaons, K^+, K^- and two neutrals K_S^0 and K_L^0 are known.

In 1961, the ω-meson of mass 783 MeV was discovered through its rapid decay to three pions in a bubble chamber investigation at Berkeley. It is highly unstable. The other known mesons are η, ρ, ϕ, J/ψ and upsilon (y).

Thus the meson is a particle that is a boson, capable of participating in strong interactions and believed to be fundamental (not composite). This definition does not say that the mass of the meson must be intermediate between that of the electron and that of the proton. Some kinds of the mesons are now found to be heavier than protons.

18.10 MUON

The muon has spin 1/2 and thus is not a boson. It is therefore incorrect to call the muon as mu-meson. The word meson should preferably be reserved for bosons. For historical reasons the meson is sometimes improperly called *mu-meson.* It is of the class *lepton.*

Production of Muons. By bombarding graphite with accelerated α-particles of energy 450 MeV it was found that mesons could be created artificially. The charge of muons is equal in magnitude to the charge of the electron. There are no neutral muons. *They are usually obtained as a decay product of the charged pions* according to the reactions :

$$\begin{aligned} \pi^+ &\rightarrow \mu^+ + \nu_\mu \\ \pi^- &\rightarrow \mu^- + \bar{\nu}_\mu . \end{aligned} \qquad \text{...(23)}$$

The π^+-meson at rest decays and the muon is emitted with a unique energy of 4.17 MeV. The π^--meson decay is not observed at rest because of the Coulomb attraction of this particle to nuclei. The decay takes place in flight. The neutrino appearing in the π-decay seems to be different from the neutrino of β-decay.

In 1958, T. Fazzini *et al.* discovered that the electron decay of the pion by the process

$$\pi^\pm \rightarrow e^\pm + \nu_e \,(or\ \bar{\nu}_e) \qquad \text{...(24)}$$

takes place at a rate about 10^4 times less than the rate of the main $\pi \rightarrow \mu$ (decay).

F. Reines and C.L. Cowan first observed electron neutrinos through the inverse beta decay process in which the anti neutrino is absorbed by a proton and changes it into a neutron.

$$\begin{aligned} \nu_e + n &\rightarrow e^- + p \\ \bar{\nu}_e + p &\rightarrow e^+ + n. \end{aligned} \qquad \text{...(25)}$$

The muon neutrinos were first observed at Brookhaven National Laboratory in 1964 with the 32 GeV accelerator. The high energy neutrinos by pion-decays in flight were allowed to pass through high shielding to remove all muons and other charged particles before entering to a very large spark chamber detector. The muons are identified in the photographs, may be produced by the processes

$$\begin{aligned} \nu_\mu + n &\rightarrow p + \mu^- \\ \bar{\nu}_\mu + p &\rightarrow n + \mu^+. \end{aligned} \qquad \text{...(26)}$$

Although, most common source of muons is the pions decay but they also appear as branchings in other decays such as

$$\begin{aligned} \Sigma^\pm &\rightarrow \mu^\pm + \nu_\mu + n \\ \Lambda^o &\rightarrow \mu^- + \bar{\nu}_\mu + p \\ K &\rightarrow \mu + \nu_\mu, \text{ etc.} \end{aligned}$$

Muons can also be generated in pairs by photo production, similar to electron pair production.

Mass of the muons. Early determinations of the mass of the muons in cosmic rays were made by utilizing the tracks in a cloud chamber in a magnetic field or in a photographic emulsion. The quantities measured were momentum and energy. From these one finds the mass. Barkas and co-workers (1956) measured the ratio of the pion-muon mass and the pion-proton mass by measuring momenta and ranges in photographic emulsion. These measurements gave the masses with an accuracy of one part in a thousand. A completely different way of obtaining the muon mass is offered by the study of relative transitions in muonic atoms. In the last few quantum jumps from one orbit to another, muonic X-rays are radiated. For high Z-absorbers, the ^1S muon orbits penetrate the nucleus and the finite size of the nucleus strongly affects the energies of the radiated X-rays. For low Z-elements, the *M* and *L* muonic X-rays have energies approximately the same as given by Bohr theory. In 1960, Devons and coworkers have determined the muon mass by measuring the mass absorption co-efficient of the $^3D_{5/2} \rightarrow {}^2P_{3/2}$ mesonic transition of phosphorus in lead. A negative muon brought to rest in the phosphorus is recorded by a coincidence between pulses from counters 1, 2, 3, 4 and an anti-coincidence in counter 5. A muonic X-rays photon is recorded by a NaI detector *D* placed behind a lead absorber. For phosphorus ($Z = 15$), the strongest line $D_{5/2} \rightarrow P_{3/2}$ has an energy

$$E({}^3D_{5/2} \rightarrow {}^2P_{3/2}) = 88{,}000 \pm 10\, eV.$$

According to the Bohr theory

$$E = hcR\left(\frac{1}{2^2}-\frac{1}{3^2}\right)Z^2(1.001163)\frac{m_\mu}{m_e}. \qquad ...(26)$$

This relation gives $m_\mu = 206.78\, m_e$. In this method we have assumed that the charge of the muon is exactly equal to that of the electron.

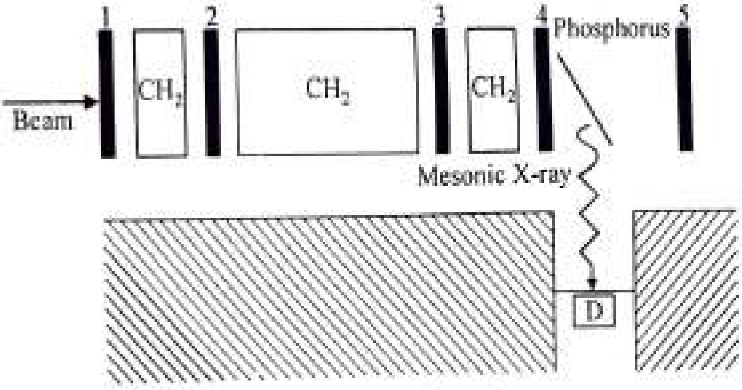

Fig. 18.8. Production of an anti-proton.

Recent accurate measurements of the gyromagnetic ratio and of the magnetic moment of the muon provide $m_\mu = (206.77 \pm 0.01)m_e$.

Muon decay and mean life. The decay of muon has been observed in cloud chamber photographs and in nuclear photographic emulsions. In 1949, Leighton, Anderson and Seriff measured the energies of the electrons and positrons produced in the decay of cosmic ray muons at sea level. They placed Geiger counter controlled cloud chamber in a magnetic field of 7200 gausses and found a range of values from 9 to 55 MeV for the decay electrons. This wide range of energies for the decay electron spectrum suggests that this decay process is accompanied by more than one invisible neutral particle to conserve energy and momentum. The form of the spectrum agrees with the predictions of reactions—

$$\mu^- \rightarrow e^- + \nu_\mu + \overline{\nu}_e$$
$$\mu^+ \rightarrow e^+ + \overline{\nu}_\mu + \nu_e.$$

Of the two neutrinos, one is believed to be of the kind found in beta decay and the other of the kind found in pion decay. Here the choice of $\nu_e + \overline{\nu}_\mu$ is preferred because it associates the e^+ with the ν_e as in beta decay. For electrons having the maximum possible energy, the neutrino pair has zero angular momentum in that direction and the electrons must have the same angular momentum as the decaying muon. The decay of μ^- would require that if e^- is defined as a particle, μ^- must likewise be a particle; $e^+$and μ^+ are then anti-particles.

The mean life of the free muons was originally informed from their disappearance in cosmic rays. The most recent work uses the signal from a muon production process $\pi^+ \rightarrow \mu^+$ in a scintillator to start a timing circuit and the subsequent decay electron pulse $\mu^+ \rightarrow e^+$ and to spot it. The lifetimes of μ^+ and μ^- have been compared and are found equal, also to 0.1 percent as predicted theoretically.

$$\tau_\mu = (2.200 \pm 0.002) \times 10^{-6}\, sec. \qquad ...(27)$$

From the lifetime and energy release, a coupling constant g can be calculated as in the case of β-decay. The value found is $g_\mu = 1.435 \times 10^{-62}\, Jm^3$ which is extremely close to β-decay value $g_\beta = 1.410 \times 10^{-62}\, Jm^3$. This result emphasises the fact that both β-and μ-decays are the examples of the basic weak interaction.

Interaction with matter. Negative muon captured into Bohr orbit surrounding nuclei may undergo nuclear capture

$$\mu^- + p \rightarrow n + \nu,$$

instead of radioactive decay, analogous to orbital electron capture. The probability of muon capture by a nucleus increases with the atomic number Z of the nucleus. The probabilities of capture and free decay becoming equal when the atomic number Z is about 12. Consequently, in matter having Z less than 12, most of the negative muons will decay with the normal muon life time, but for Z greater than this value they are captured before they can decay.

The passage of muons through matter is analogous to that of electrons, except that the decay processes decrease with Z. Cosmic rays studies show that fast muons can produce nuclear disintegration stars, which can be interpreted as an electromagnetic process. Similar to the electron scattering, muon beams of energy upto several hundred MeV have been used for nuclear scattering experiments. Slow μ^- from muonic atoms, slow μ^+ may from muonium. The μ^- may also bind two atoms to form muonic molecule. Pair production of muons (μ^+, μ^-) by high energy bremsstrahlung has also been observed.

Spin and Magnetic moment of Muons. All the direct evidences, such as decay schemes and hyperfine effects in muonic atoms support the spin quantum number $\frac{1}{2}$ to the muon.

If the muon is described by the Dirac theory of the electron, it will have a magnetic moment of one muon magneton $(= e\hbar/2m_\mu)$ corresponding to a g factor of 2 for spin 1/2. The asymmetry of the muon decay gives extremely accurate measurements of the magnetic moment.

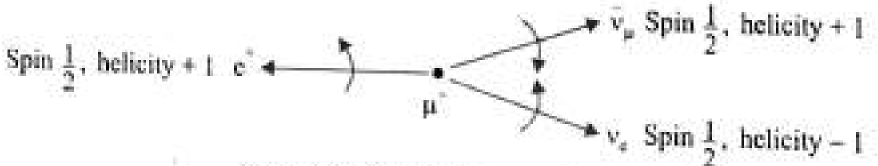
Spin $\frac{1}{2}$, helicity + 1 e^+
μ^+
$\bar{\nu}_\mu$ Spin $\frac{1}{2}$, helicity + 1
ν_e Spin $\frac{1}{2}$, helicity − 1

Fig. 18.10. Helicities in muon decay.

Parity non conservation in the muon decay requires the asymmetry in the direction of electron emission from the muon with respect to its polarization, just as in electron emission from polarized nuclei. This asymmetry was detected by Garwin. Lederman and Weinrich and established the parity nonconservation in muon decay. A 85 MeV π^+-mesons from synchrocyclotron decay during the flight. Thus a beam of pions and muons passes scintillator S_1. The pions but not the muons are stopped in the carbon absorber before reaching the scintillator S_2. The S_1 and S_2 coincidences signal the arrival of the muon which are brought to rest in a carbon target C. Since the pion has no angular momentum, therefore the muon has an angular momentum equal and opposite to that of the neutrino (ν_μ).

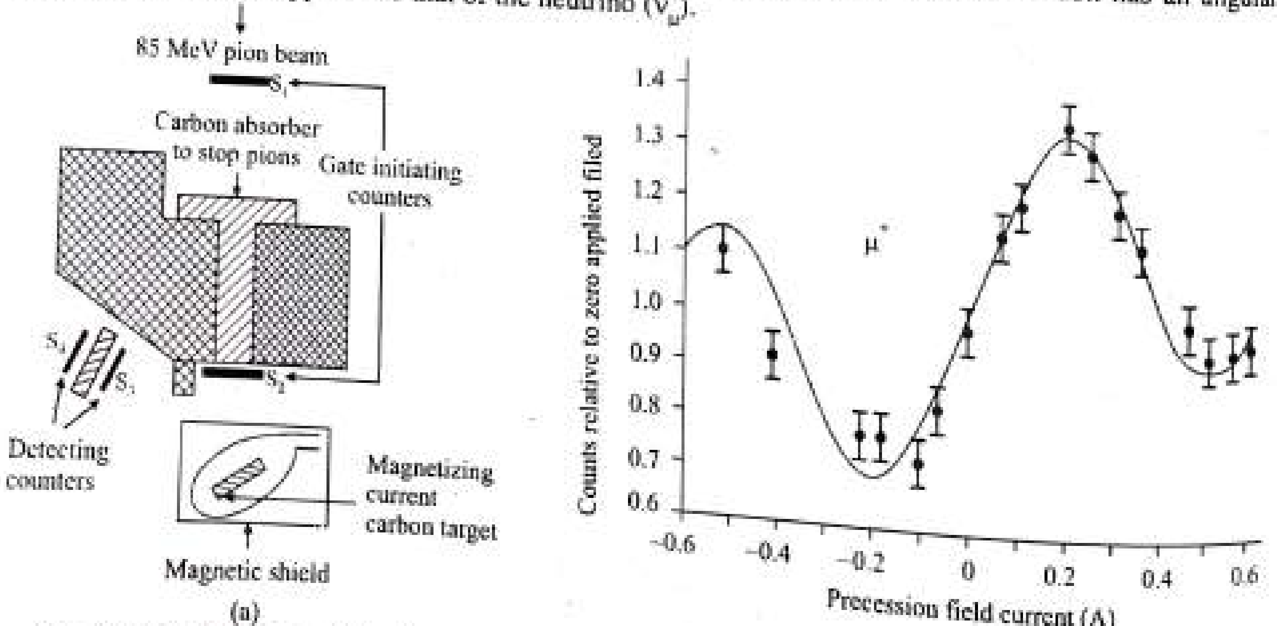

(a)

(b)

Fig. 18.11 (a) Apparatus of Garwin et al. and (b) variation of positron counting rate with magnetizing current.

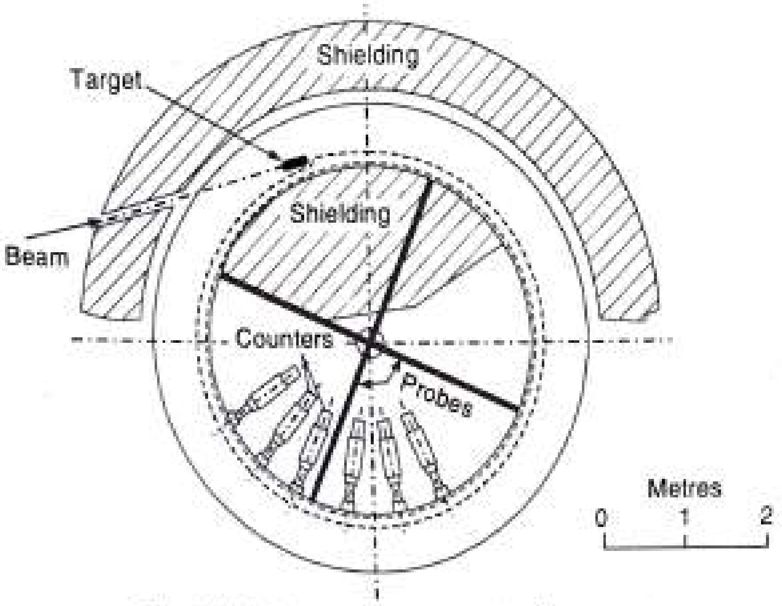

Fig. 18.11. Muon storage ring used by Bailey et al.

If the neutrino is polarized with the spin anti-parallel to the direction of motion, so is the muon. If the muons are brought to rest in a target medium, which does not seriously depolarize the muons, we have the emission of a positron (for μ^+ mesons) and two particles of zero rest mass from this polarized source. The positrons tend to travel parallel to the spin direction, thus a marked asymmetry is shown. Now if we apply magnetic field to the muon at rest, perpendicular to the plane of incidence it causes a precession of the muon moment (or spin) with the Larmor frequency $g_\mu \mu_\mu B/\hbar$ in the plane of incidence, where g_μ (= μ_μ/I) is the gyromagnetic ratio, *i.e.* the magnetic moment in natural units $e\hbar/2m_\mu$ divided by angular momentum in units of $\hbar$. The positron counting rate is found to be altered because of the non-isotropic distribution of the decay of muon. These positrons are revealed by a coincidence between S_3 and S_4. The variation of positron counting rate in fixed detector as a function of magnetic field or precesson field current is shown in Fig. 18.11(b). The precession frequency observed gave $g_\mu = 2 \times (1.0020 \pm 0.0005)$, very close to the g value of the electron. This result is a strong argument for a spin 1/2 of the muon.

The latest and most precise experiment is due to Bailey, Farley, *et al.*, at CERN. This compares the Larmor frequency of the muon in a given magnetic field with the orbital frequency of the particle in the same field. These two are equal, if $g_\mu = 2$. For a finite value of $g_\mu - 2$, a beam of longitudinally polarized muons in circular orbit will gradually build up misalignment between the spin direction and the direction of motion. The use is made of a strong ring, filled with fast muons produced by pion decay in the same orbit. The muons decay in the flight and the detector circuits are set to respond only the forward going electrons having the highest energy. Since the angular distribution of emission from muon decay is not isotropic, the observed intensity of electron emission is modulated by the muon precession due to the anomalous moment.

A 10 GeV proton beam is incident on a target placed at the injection section of a storage ring. The pions are produced, which decay in the same orbit and produce muons. Since the pion lifetime is of the order of 10^{-8} sec and for the muon is of the order of 10^{-6} sec, therefore the storage ring is filled rapidly with the muons. The relativistic transformation

$$\pi^- \to \mu^- + \bar{\nu}_\mu \text{ and } \mu^- \to e^- + \nu_e + \bar{\nu}_\mu.$$

from the rest system ensures that the forward going electrons have the highest energy. The detector circuits are set to record only the highest energy electrons emitted within a small solid angle at zero degrees to the velocity of a muon as it decays within a small segment of the ring. Since the angular distribution of emission from muon decay is not isotropic, the observed intensity is modulated by the muon precession due to anomalous moment. The electron intensity is a maximum along the muon polarization vector. The electron counters record successive maxima of intensity as the polarization vector is rotated by the magnetic field. Fig. 18.13. The time intervals between such maxima gives a measure of the magnetic moment, using the relation *angular velocity* $\omega = g(e/2\,mc)B$. The values of the anomaly (the difference from the value of unity) in intrinsic magnetons are found to be $(1.1596577 \pm .0000035) \times 10^{-3}$ and $(1.16616 \pm 0.00031) \times 10^{-3}$ for the electron and muon respectively. These are in excellent agreement with the most accurate theoretical calculations for Dirac particles using quantum electrodynamics.

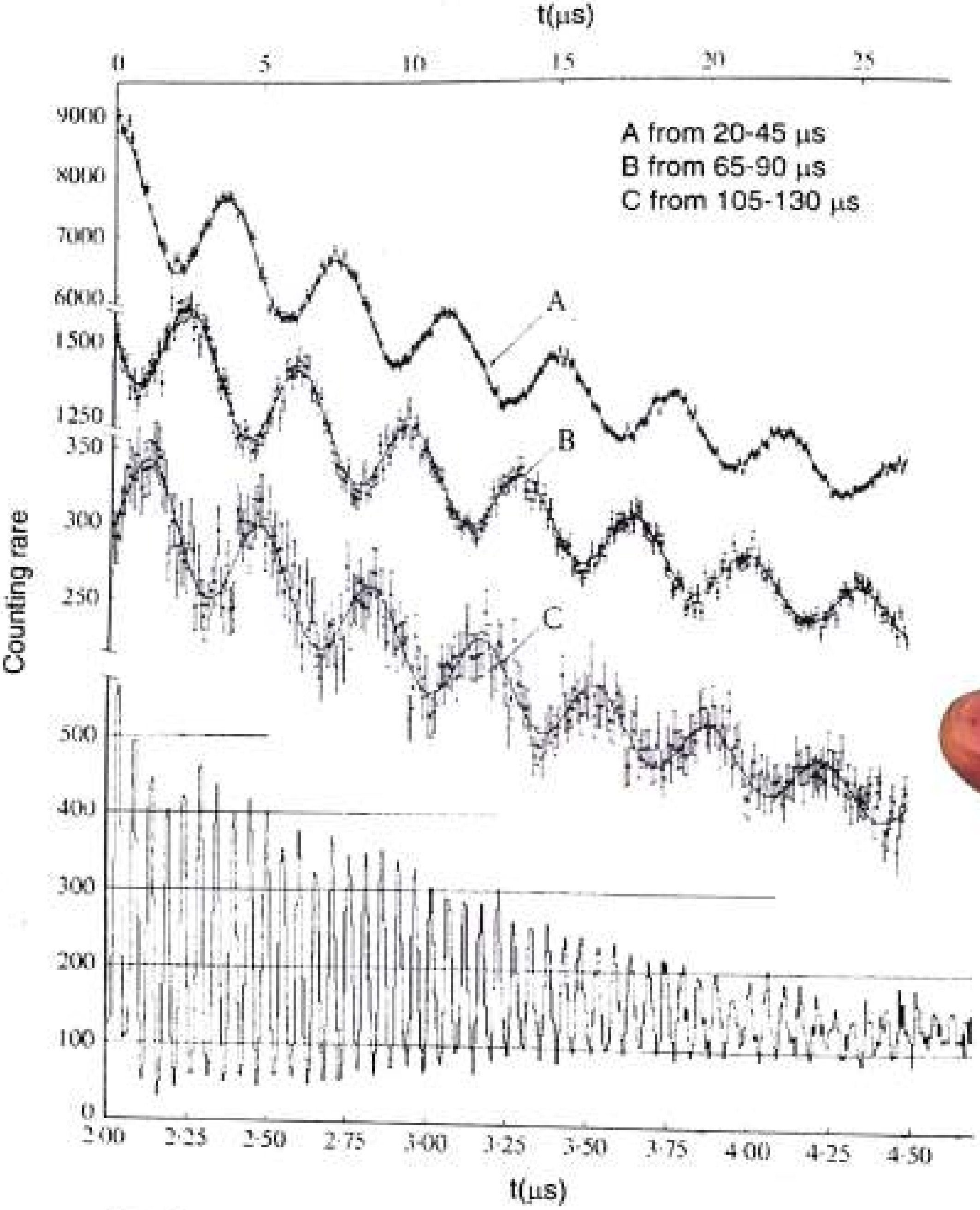

Fig. 18.13. Time distribution of the electron counts in the storage ring.

18.11 TAUONS

A new family of leptons was discovered in 1975 and named as tauons. They are quite massive having mass ~ 1784 MeV/c^2. Similar to other leptons, they are τ^+ and τ^- and accompanied by a tauonic neutrino and antineutrino (ν_τ and $\bar{\nu}_\tau$). They have all the characteristics of electron and muons, such as they are fermions (spin 1/2), they have magnetic dipole moments corresponding to a spin g factor of 2, τ^+ is the antiparticle of τ^- having charge and magnetic dipole moments of reversed signs. The respective neutrinos are also spin 1/2 fermions having no charge and magnetic dipole moment. They are distinguished physically from their antiparticles by their helicities. They participate in weak interactions.

Because of their much greater masses, the tauons can decay in variety of modes. They have purely leptonic decays as

$$\tau^+ \to e^+ + \nu_e + \bar{\nu}_\tau,\ \tau^- \to e^- + \bar{\nu}_e + \nu_\tau$$

$$\tau^+ \to \mu^+ + \nu_\mu + \bar{\nu}_\tau,\ \tau^- \to \mu^- + \bar{\nu}_\mu + \nu_\tau.$$

Tauons can also decay into leptons and strongly interacting particles, such as

$$\tau^- \rightarrow \pi^- + \nu_\tau .$$

Due to its large mass and many possible modes of decay, the tauons have quite a short lifetime ~ 10^{-13} sec. Since the fermions are created or destroyed in particle-antiparticle pairs, the number of tauons (being leptons) remain constant in an isolated system. Each tauon has lepton number L_τ which is + 1 for a particle τ^- and −1 for its antiparticle τ^+. Their respective neutrinos are also assigned lepton numbers as $L_\tau = 1$ for ν_τ and − 1 for $\bar{\nu}_\tau$.

The tautons are the weak interacting particles, have no spatial extent ($< 10^{-18}\ m$), with no internal structure and the point like leptons. The electrons, muons and tauons being of these similar properties are said to be the fundamental particles truely.

18.12 PIONS

The result of cosmic ray investigation led to the conclusion that pions are produced both in nucleon-nucleon interaction and in the interaction of high energy photons with nucleons. It is clear from this conclusion that pions can be produced in laboratory by the use of high energy particles obtained by means of an accelerator. The amount of energy which the accelerated particle must have depends on the mass of particle and the nature of the target but it will be always greater than rest mass of the pion.

Artificial Production. After the discovery in the cosmic radiations, the pions were first produced artificially by Gardner and Lattes in 1948, using a beam of 380 MeV α-particles from the 184″ Berkeley Synchrocyclotron. This beam was allowed to fall on the edge of a carbon target and the mesons emitted were detected in nuclear emulsions. For laboratory production of π-mesons, the most obvious target materials are hydrogen and deuterium or substances rich in these isotopes. At the present time strong beams of charged pions for experimental purposes with energies covering a wide range are produced by bombarding solid targets, *e.g.*, *Be*, with accelerated protons. The mesons of both signs were observed by reversing the magnetic field.

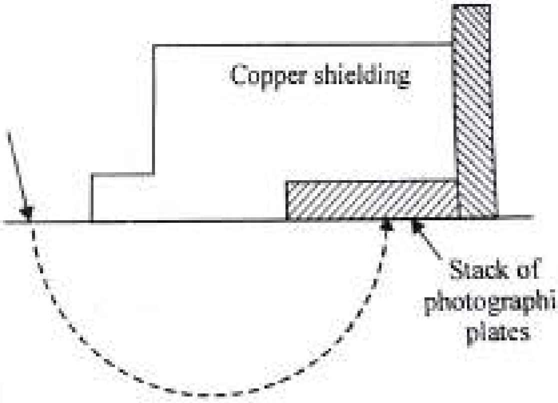

Fig. 18.14. Target meson used by Gardner and Lattes for artificial production of charged π-mesons.

The simplest nucleon-nucleon interaction involving protons as projectile and target and producing pions is evidently.

$$p + p \rightarrow \pi^+ + d$$

or

$$p + p \rightarrow \pi^+ + (n + p).$$

The interaction between a high energy proton and a deuteron may be considered as an interaction between the proton and one of the nucleons which constitute the deuteron. The possible reactions are

$$p + p\,(\text{in } d) \rightarrow \pi^+ + n + p.$$
$$p + p\,(\text{in } d) \rightarrow \pi^+ + d$$
$$p + n\,(\text{in } d) \rightarrow \pi^+ + n + n$$
$$p + n\,(\text{in } d) \rightarrow \pi^- + p + p.$$

The production of pions by gamma radiation incident on nucleons has been studied extensively in the energy range from threshold to 450 MeV and less thoroughly upto 1 GeV.

$$\gamma + p \rightarrow \pi^+ + n$$
$$\gamma + n \rightarrow \pi^- + p.$$

Besides charged pions, neutral pion has been produced by bombarding hydrogen and deuterium with high energy photons.

$$\gamma + p \rightarrow \pi^{\circ} + p; \gamma + d \rightarrow \pi^{\circ} + (n + p); \gamma + d \rightarrow \pi^{\circ} + d$$

and by proton-proton interaction as

$$p + p \rightarrow \pi^{\circ} + p + p.$$

The source of gamma rays is generally the bremsstrahlung of electrons accelerated by machines. The production of neutral pions by the interaction of high energy photons with matter was first established by Steinberger, Panofsky and Steller in 1950. In their experimental arrangement a narrow beam of 330 MeV X-rays from the synchrotron was incident on a target (beryllium or hydrogen) and the products were detected by two gamma ray counters making an angle ϕ with each other in a plane at an angle θ with the X-ray beam. Each counter consisted of three crystal scintillation counters with a thin piece of lead between the first two crystals to convert the gamma ray photons into electron-positron pairs. The measured values of the coincidence rates for different values of ϕ and θ agreed with the calculated values based on the assumption that a π°-meson was disintegrated into two gamma ray photons.

In the same year, Bjorklund, Crandall, Moyer and York produced neutral π-meson artificially using 340 MeV proton beam from a synchrocyclotron. The protons struck a beryllium or carbon target. The high energy gamma radiation from the target was analysed in a magnetic pair spectrometer.

Pions are commonly formed in the decay of kaons, hyperons and resonant states. Since there is no requirement for the conservation of pions, there is no limitation on their formation even in strong interaction.

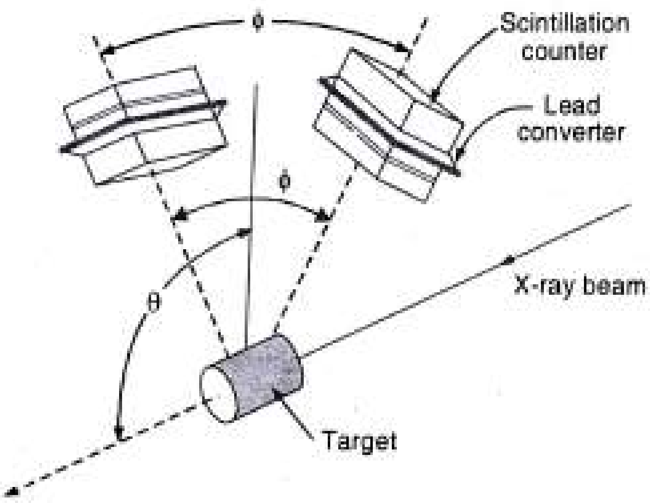

Fig. 18.15. Experimental arrangement for the production of π°-meson.

Mass of Pions. The mass of the charged pion can be determined by methods similar to those used for muons. The rest mass of the negative pions can be found by comparing the observed pionic X-ray energies for the $4f - 3d$ orbit transitions in media of low atomic number ($Z < 20$) with the theoretical expression which contains m_{π} as an unknown parameter. Apart from the reduced mass, the only important correction to the Bohr formula is the effect of vacuum polarization (~ 0.2 to 0.3%). The rest mass of the negative pion thus obtained is

$$M_{\pi^-} = (273.2 \pm 0.1)\, m_e = 139.577 \pm 0.013\ MeV/c^2. \qquad \text{...(27)}$$

The positive pions have the same mass and can be determined by the same method. The mass of the neutral pion is found by a quite different method. When very low energy negative pions are slowed down in hydrogen they are captured into orbit. These cascade down the optical levels and are ultimately captured by the proton. The reactions observed are :

$$\pi^- + p \rightarrow n + \gamma$$
$$\pi^- + p \rightarrow n + \pi^{\circ}$$
$$\pi^{\circ} \rightarrow \gamma + \gamma.$$

The first reaction gives rise to a monochromatic gamma ray whose lab energy is peaked around MeV. The second reaction is particularly important for the determination of the π°-mass. Assume that the negative pion is captured at rest, the π° and n acquire a relative kinetic energy equal to given by energy mass relation. This energy can be measured by the observation of the gamma spectrum of the decaying π°. In the co-ordinate system in which π° is at rest both gamma rays have equal and opposite momentum. In the laboratory system they appear at an angle ϕ to each other and their frequency shows the Doppler shift due to the motion of the π°. The observed photon energies in the lab system range from

$$E_\gamma(min) = \tfrac{1}{2} m_{\pi^\circ} c^2 (1-\beta)(1-\beta^2)^{-1/2} \qquad ...(28)$$

to

$$E_\gamma^{'}(max) = \tfrac{1}{2} m_{\pi^\circ} c^2 (1+\beta)(1-\beta^2)^{-1/2}. \qquad ...(29)$$

These limits are obtained from relativistic Doppler formula for a π° decaying at the instant its speed is βc. It is easy to write the rest mass energy difference as

$$(m_\pi - m_{\pi^\circ})\, c^2 = (m_n - m_p) c^2 + \frac{\alpha^2 c^2 m_{\pi^-}}{2} + \frac{\frac{1}{2}(m_p + m_{\pi^-}) \Delta E_\gamma^2}{[m_{\pi^-} - (m_n - m_p)] m_n c^2} + \dots \qquad ...(30)$$

Here the second term on the right is the pion binding energy in a ${}^1S$ Bohr orbit and the third term is the kinetic energy of the π°. In the second term α is the fine structure constant. Using known values of $\Delta E_\gamma (= E_{\gamma,\max} - E_{\gamma,\min} = p_{\pi^\circ} c)$, α, m_n, m_p and m_{π^-}, we have

$$(m_{\pi^-} - m_{\pi^\circ}) c^2 = 4.606 \pm 0.006\, MeV$$

or

$$m_{\pi^\circ} c^2 = m_{\pi^-} c^2 - 4.606\, MeV$$

$$= 139.577 \pm 0.013 - 4.606 \pm 0.006 = 134.971 \pm 0.019\, MeV. \qquad ...(31)$$

Decay. Unless they have sufficiently high energies (~ 150 MeV), positive pions do not interact to any great extent with nuclei and decay at rest according to the reaction

$$\pi^+ \to \mu^+ + \nu_\mu,$$

Since positive muon is an anti-particle, the ν_μ must be a neutrino to conserve the muonic lepton number. This decay is due to the weak interaction and the parity is not conserved. The muon is emitted with a unique energy of 4.17 MeV and is longitudinally polarized. This energy is consistent with zero mass for the muon associated neutrino. Pions may also decay according to the reactions

$$\pi^+ \to e^+ + \nu_e \qquad (1.24 \times 10^{-2}\%)$$

$$\pi^+ \to \mu^+ + \nu_\mu + \gamma \qquad (1.24 \times 10^{-2}\%)$$

$$\pi^+ \to \pi^\circ + e^+ + \nu_e \qquad (1.5 \times 10^{-6}\%)$$

The first equation requires that the helicity of the positron shall be the same as that of the neutrino. The third equation is analogous to a $0^+ \to 0^+$ Fermi transition in nuclear β-decay.

Similar decay processess are possible with negative pions.

$$\pi^- \to e^- + \bar{\nu}_e, \pi^- \to \mu^- + \bar{\nu}_\mu + \gamma, \text{ and } \pi^- \to \pi^\circ + e^- + \bar{\nu}_e.$$

Negative pion decay ($\pi^- \to \mu^-$) is not observed at rest because of the Coulomb attraction with the nuclei and strong nuclear absorption. The decay modes of the π are

$$\pi^\circ \to \gamma + \gamma \qquad (98.8\%)$$

$$\pi^\circ \to \gamma + e^+ + e^- \qquad (1.2\%)$$

$$\pi^\circ \to e^+ + e^- + e^+ + e^-. \qquad (0.003\%)$$

It is evident from the nature of the products that *π°-mesons decay by the electromagnetic interaction while charged pions decay by strong and the weak interactions both.*

Mean Life. One of the earliest determinations of the mean lifetime of charged pions was made by J.R. Richardson (1948), using the π-mesons produced by the bombardment of graphite by 380 MeV α-particles. These pions travelled in helical paths in the vertical magnetic field of the cyclotron. Those which rose upward were allowed to travel through 180° before striking a photographic plate, those which spiraled downward were allowed to travel 540° before striking a photographic plate. The number of mesons which decayed while traversing a complete cycle can be determined by the ratio of the number of mesons in the two plates. The time required to traverse a circle in a cyclotron is independent of the speed, hence the average life time of the decaying mesons could be determined. The first result for the mean life of charged pion obtained was 1.1×10^{-8} sec.

Durbin, Loar and Havens in 1952 performed an experiment of the decay in flight of positive pions. The meson beam produced in the Nevis cyclotron by the bombardment of a beryllium target with 385 MeV protons was deflected by a magnet and directed through three stilbene scintillation counters operated in coincidence. A much larger scintillation counter C_4, 8″ dia and containing xylene, was set at a distance L which could be varied from a few inches to about 8 ft. The coincidence counters C_1, C_2 and C_3 defined the beam of the π-mesons. Some of these mesons decayed in flight between C_3 and C_4, the remaining ones being detected by C_4. After suitable corrections for beam impurities, angular divergence, accidental coincidences, the difference in counts between C_1, C_2, C_3 detectors and the C_4 detector represented the number of pions decaying in the flight along the path of length L. Knowing the average velocity and determining mean free path, the mean life time could the calculated. The value so obtained as 2.54×10^{-8} sec for π^+ mesons and 2.44×10^{-8}sec for π^- mesons. Thus within the limits of experimental error, the mean lifetimes of the π^+ and π^- mesons were identical, with the average mean life = 2.5×10^{-8} sec.

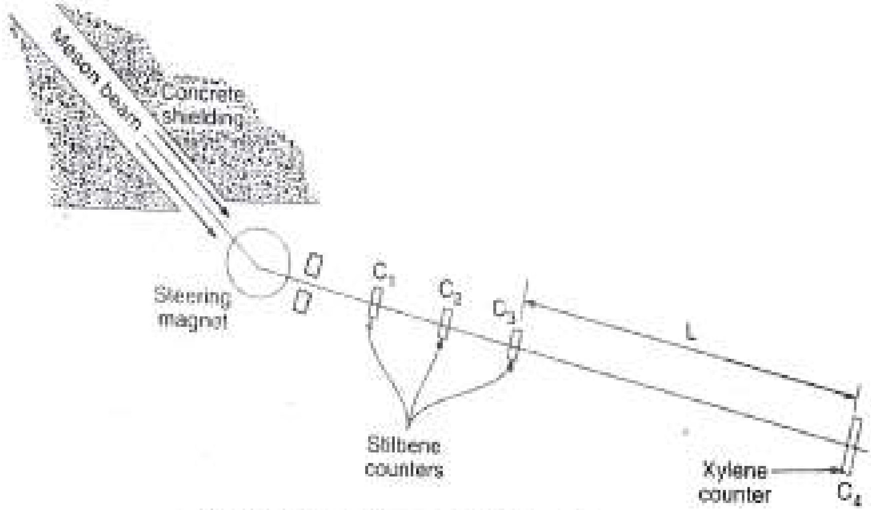

Fig. 18.16. Measurement of life time of π-mesons.

Using a beam of 34 MeV positive pions from the Rochester 130″ cyclotron, Kinsey, *et al.* (1964) found pion lifetime as $(2.640 \pm 0.008) \times 10^{-8}$ sec. By observation of decay in flight, Ayres *et al.* (1968) found that the lifetimes of the π^+ and π^- mesons are equal within standard deviations and suggested the value 2.6×10^{-8} sec.

The decay of π^0 goes through a virtual intermediate nucleon-anti-nucleon state.

$$\pi^0 \xrightarrow[\text{Strong}]{} \underset{\text{virtual}}{(n+\bar{n})} \xrightarrow[\text{EM}]{} \gamma + \gamma.$$

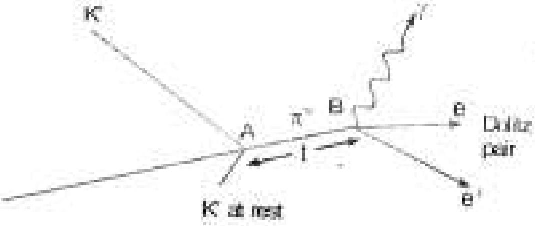

Fig. 18.17. Track in photographic emulsion for the measurement of the life time of π⁰-mesons.

This two stage decay involves both strong and electromagnetic interactions, hence suggests a short mean life of the π^0. The accurate method of measuring the mean lifetime of π^0-mesons is to measure the mean distance between the end of a track of a K^+ meson brought to rest in a photographic emulsion and the origin of a electron positron pair. The reactions are

$$K^+ \rightarrow \pi^+ + \pi^+ + 219\ MeV$$

$$\pi^0 \rightarrow \gamma + e^+ + e^- \ (1.24\%).$$

R.G. Glasser (1960) found that the mean decay distance in an Ilford $L-4$ emulsion for the flight path of π^0 was 0.122 ± 0.045 microns and hence the pion mean lifetime as $(2.3 \pm 0.8) \times 10^{-16}$ sec. P. Stamer (1966) found lifetime as $(1.0 \pm 0.5) \times 10^{-16}$ sec.

The lifetime of π^0 has also been determined from the cross-section for the photo-production of π^0 mesons in the Coulomb field of a heavy nucleus. The average of all observations is $(0.89 \pm 0.18) \times 10^{-16}$ sec.

Interaction with Matter. Because of their short life time (~ 10^{-16} *sec*.), π^0-mesons move only a few atomic diameters before they decay and thus are not affected by the matter through which they pass. Positive pions are not able to surmount the nuclear Coulomb barrier and, therefore, undergo spontaneous decay, while negative pions are captured by nuclei. All of the energy of a captured pion is transmitted to the nucleus results to a nuclear disruption, *called a star*, because of its appearance in a particle track chamber or photographic emulsion. Menon, Muirhead and Rochat in 1950 investigated the stars produced by the capture of slow π^--mesons in the nuclei of the elements composing nuclear emulsions. They studied more than 2500 stars and classified according to the number of prongs in each. About 46% of all visible stars were ascribed to the interaction of π^--mesons with light nuclei such as ^{12}C, ^{14}N, ^{16}O and about 54% were with the heavy nuclei, such as silver and bromine. All the π^--mesons absorbed in the emulsion do not produce visible stars.

By using available charged meson beams and hydrogen targets we can measure three cross-sections, corresponding to the reactions :

$$\pi^+ + p \rightarrow \pi^+ + p;\ \pi^- + p \rightarrow \pi^- + p;\ \pi^- + p \rightarrow \pi^0 + n.$$

The first two reactions are purely elastic scattering and the last reaction is known as charge exchange scattering. The first accurate measurements upto 200 MeV π-meson indicated that the total cross-sections of reactions were in the ratio of 9 : 1 : 2.

A.A. Carter, *et.al* in 1968, measured the total cross sections for pion interaction in hydrogen and deuterium. A protion beam from 7 GeV proton synchrotron at the Rutherford High Energy Lab, Chilton (USA) was deflected and allowed to fall on the copper target. The interactions due to collision lead to the production of all types of particles (π^+, π^-, p, n, K^+, K^-, etc.). The required beam of π^+ or π^- mesons was selected by means of bending magnets and passed through scintillation counters S_1, S_3 and S_2.

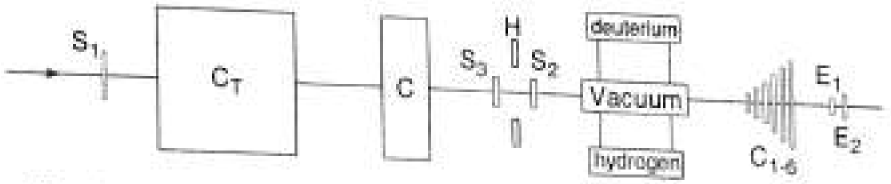

Fig. 18.18. Determination of pion cross-sections in hydrogen and deuterium.

The distance of S_1 is some tens of meters from the accelerator. During this distance, some pions and kaons in the original beam would have decayed so that at S_1 the beam will comprise for positively charged particles, protons, kaons, pions, muons and positrons. At about 500 MeV/c, the electron contamination is between 5 and 35% and muon contamination is about 4% of the beam. The pions are resolved and detected. The beam is defined by S_1, S_3 and S_2. A halo counter H, the scintillator with 2.5 inch dia hole at its centre, will velo particles which do not pass through its aperture. The only pions are selected by their Čerenkov radiation in the DISC differential counter C and the absence of Čerenkov radiation in the threshold counter C_T. Thus a pion in the beam is defined by one which gives a count in S_1, S_3 and S_2 and in the DISC counter C, but not in C_T or the halo counter H. In this way the pions are identified with great certainty. The beam then passes into the target where about 10% of the beam may interact with the atoms and nuclei of target. Coulomb scattering by the electric field of the nuclei will deflect the beam particles. The scintillation counters $C_1 \rightarrow C_6$ are placed on the exit side of the scattering equipment of such an angular acceptance that strong interactions of the pions are detected and the Coulomb scattering is discounted.The counters E_1 and E_2 are efficiency counters used to check the efficiency of counters $C_1 - C_6$.

The scattering cross-sections can be interpreted by assuming that in the strong interactions the total isospin is conserved as well as its third component. The total isospin of the π^+, p system is 3/2 and the component $T_3 = 1+\frac{1}{2} = \frac{3}{2}$. The π^-, p system has $T_3 = -1+\frac{1}{2} = -\frac{1}{2}$ and is a mixture of $T = \frac{3}{2}$ and $T = \frac{1}{2}$ states. If the scattering amplitudes corresponding to the scattering in the $T = \frac{3}{2}$ state and the $T = \frac{1}{2}$ states are a (3/2) and a(1/2) respectively, then the cross-sections are :

Elastic scattering (π^+, p)— $\sigma_{e+} \propto |a(3/2)|^2$ ...(32)

Elastic scattering (π^-, p)— $\sigma_{e-} \propto \frac{1}{9}|2a(1/2)+a(3/2)|^2$ ...(33)

Charge exchange scattering $\sigma_{re} \propto \frac{2}{9}|a(3/2)-a(1/2)|^2$ . ...(34)

If the $\pi - p$ scattering predominantly occurs in the $T=\frac{3}{2}$ state near 200 MeV, $a(3/2) >> a(1/2)$ and the cross-sections satisfy the ratios

$$\sigma_{e+} : \sigma_{e-} : \sigma_{re} = 9:1:2. \qquad ...(35)$$

From general collision theory, the maximum cross-section for elastic scattering is

$$\sigma_{\max} = 4\pi\lambda\!\!\!^{-2}\frac{2J+1}{(2s_1+1)(2s_2+1)}. \qquad ...(36)$$

In the case of $\pi^+ - p$ system, s_1 the intrinsic spin of the pion is zero, s_2 the intrinsic spin of target proton is $\frac{1}{2}$. For pions upto 300 MeV only *s*- and *p*- wave scattering is important. The *d*- wave impact parameter is beyond the range of the *pion nucleon* force. The maximum value of total cross-section scattering of π^+-mesons by protons was found 192 millibarns below approximately 200 MeV. At the peak of the resonance $\pi\lambda\!\!\!^{-2} = 24$ *mb*. These values with equation (36) give us total angular momentum of the $\pi - p$ system as $J = \frac{3}{2}$. This shows that the interaction is dominated by *p*-wave scattering $(L = J - S = \frac{3}{2} - \frac{1}{2} = 1)$.

Absorption of stopped π^--mesons. The fast charged pion slows down from an energy of about 100 MeV to about 1 keV in liquid hydrogen in 10^{-9} sec. In the further 10^{-12} sec, π^--meson loses energy and becomes bound in a 1*s* orbit to a proton. From this orbit it may decay or react with the proton as

$$\pi^- + p \to \pi^0 + n, \pi^0 \to 2\gamma \qquad ...(37)$$

or

$$\pi^- + p \to n + \gamma. \qquad ...(38)$$

Panofsky, Aamodt and Hadley studied these reactions and found peak about 130 MeV describing reaction (38) and lower peak of mean energy of 70 MeV representing the energies of photons from the π^0-meson decaying as shown by reaction (37). The initial state has spin and parity $J = \frac{1^-}{2}$, since the π^- is captured from K-shell and the pion has odd parity. In reaction (38), the neutron state has $J = \frac{1^+}{2}$, the photon must, therefore, carry odd parity and unit angular momentum.

Intrinsic Spin. The reactions $p + p = d + \pi^+$ have been used to determine the spin of the π^+-meson (and therefore presumably of the π^--meson), using the measured cross-sections of the two reactions together with the *statistical mechanical principle of detailed balance.*

*The differential cross-section for the reaction $p + p \to d + \pi^+$ given in terms of transition matrix elements is

$$\frac{d\sigma_{pp\to d\pi}}{d\Omega} = \frac{1}{(2s_p+1)(2s_p+1)}\left(\frac{1}{q_{pp}}\right)^2 \sum |T_{ab}|^2, \qquad ...(39)$$

where q_{pp} is the momentum in C.M. system of the initial state *pp*. Here T_{ba} is the matrix elements with a initial plane wave state *a* and the final state *b*.

Similarly for the reaction $d + \pi^+ \to p + p$, we have

$$\frac{d\sigma_{d\pi\to pp}}{d\Omega} = \frac{1}{(2s_d+1)(2s_\pi+1)}\left(\frac{1}{q_{d\pi}}\right)^2 \sum |T_{ab}|^2. \qquad ...(40)$$

If both cross-sections refer to the same total energy and to the same angle of scattering in C.M. system, we obtain the detailed balancing relation.

$$\frac{d\sigma_{pp\to d\pi}}{d\Omega} = \frac{(2s_d+1)(2s_\pi+1)}{(2s_p+1)(2s_p+1)}\left(\frac{q_{d\pi}}{q_{pp}}\right)^2 \frac{d\sigma_{d\pi\to pp}}{d\Omega}. \qquad ...(41)$$

Using $s_p = \frac{1}{2}$, $s_d = 1$ and the measured cross-sections and momenta in C.M. system, Cartwright, *et al.* and Durkin, *et al.* suggested spin of the π^+-meson as zero.

It is assumed that the π^--spin is the same as that of the π^+.

The spin of the neutral pion cannot be determined directly. We know that π^0-meson decays into two otons and never into three photons. This implies that the intrinsic spin must be zero. Thus we see that all ons have spin zero and have no magnetic moment.

Parity. A negative pions are slowed down and captured into Bohr orbits in deuterium gas under pressure, e get following reactions :

$$\pi^- + d \rightarrow n + n \qquad \text{...(42)}$$

$$\pi^- + d \rightarrow n + n + \gamma \qquad \text{...(43)}$$

$$\pi^- + d \rightarrow n + n + \pi^0. \qquad \text{...(44)}$$

Reaction (44) is unfavoured. Panofsky measured the cross-section ratio

$$\frac{\sigma(\pi^- + d \rightarrow n + n)}{\sigma(\pi^- + d \rightarrow n + n + \gamma)} = 2.36 \pm 0.36. \qquad \text{...(45)}$$

Slow π^- mesons are absorbed by the nuclei of hydrogen as $\pi^- + p \rightarrow \pi^0 + n^0$ and $\pi^- + p \rightarrow n + \gamma$. The ratio of hese two reactions has been determined by different workers. The latest value of this ratio is 1.53 ± 0.02.

To interpret these two ratios, there are following assumptions : *(1) The π^--mesons are absorbed by the ucleus from s-states of the mesonic atoms formed in the capture of the π^- by the atoms of deuterium and ydrogen. (2) The proton and neutron have the same parity.*

From the reactions (42) and (43), in order for the final states to be consistent with Pauli's principle, two neutrons can exist only in ${}^1S_0$; ${}^3P_{0,1,2}$; ${}^1D_2$ or ${}^3F_{2,3,4}$ etc. states. The total angular momentum of the initial state, *i.e.*, the pion and deuteron system, is just the spin of the deuteron, $J = 1$. The parity, given by $P_\pi P_d (-1)^l$ is equal to P_π since P_d is even and $l = 0$. To conserve the total angular momentum and parity, the $n + n$ system must be in a $J = 1$ state and must have same parity as that of the π^- meson. For L-even, the ucleon spins must be antiparallel ($S = 0$) and for L-odd the nucleon spins must be parallel. Thus the only state with $J = L + S = 1$ is the ${}^3P_1$ state. This corresponds to an odd parity. Thus the *intrinsic parity of π-meson is negative*. This conclusion is consistent with the suppression of reaction (44), since π^0-meson also has negative parity.

The similar reaction $\pi^+ d \rightarrow pp$ at rest cannot occur since Coulomb repulsion keeps π^+ and d apart. A detailed analysis of the cross section suggests negative parity for π^+-meson. The parity of the neutral pion is difficult to determine experimentally. It can be deduced using rare decay mode.

$$\pi^+ \rightarrow e^+ + e^- + e^+ + e^-$$

and measuring distribution of angles between the planes of the two electron pairs. It is again negative.

18.13 K-MESONS

K-mesons are also produced along with the pions when high energy protons bombard a suitable target. With increasing proton energy the fraction of K-mesons relative to pions increases. There are essentially four K-mesons, *i.e.*, two charged mesons K^+ and K^-, which are particle and anti-particle of one another, and two uncharged mesons K^0 and $\overline{K}^0$, which are also particle and anti-particle. These are obtained in laboratory by the interaction of high energy protons or pions with various atomic nuclei.

Decay and Lifetime. Both neutral and charged K-mesons decay into ordinary particles. Assuming that $\Delta S = \pm 1$ in the decay, it is necessary to assign strangeness $S = +1$ or $S = -1$ to the K-mesons. For $S = +1$, equation $Q = T_3 + B/2 + S/2$ implies that $T_3 = \pm \frac{1}{2}$, corresponding to K^+ and K^0 mesons. In addition, two corresponding anti-particles are expected for $S = -1$, these are K^- and $\overline{K}^0$ with $T_3 = -\frac{1}{2}$ and $+\frac{1}{2}$ respectively.

There are six different ways that K^+ -mesons commonly decay, in each case giving two or three less massive particles. The various decay modes of the K^+ are denoted by symbols, θ^+, τ, τ', $K_{\mu 2}$, $K_{\mu 3}$ and K_{e3}. This confusing terminology dates from the time when it seemed likely that the θ^+, τ.... decay sprang from different parent particles. The notation $K_{\mu 3}$ represents a decay into three particles one of which is a muon. The decay reactions are :

$$K^+(\theta^+) \rightarrow \pi^+ + \pi^0 + 219.3 \text{ MeV } (\sim 21.2\%)$$

$$K^+(\tau) \rightarrow \pi^+ + \pi^- + \pi^+ + 75.1\, MeV\ (\sim 5.6\%)$$

$$K^+(\tau') \rightarrow \pi^+ + \pi^0 + \pi^0 + 84.3\, MeV\ (\sim 1.7\%)$$

$$K^+(K_{\mu 2}) \to \mu^+ + \nu_\mu + 388.2\,MeV\,(\sim 63.5\%)$$
$$K^+(K_{\mu 3}) \to \mu^+ + \pi^\circ + \nu_\mu + 253.2\,MeV\,(\sim 3.2\%)$$
$$K^+(K_{e3}) \to e^+ + \pi^\circ + \nu_e + 358.3\,MeV\,(\sim 4.8\%)$$

Until 1956, it was assumed that parity was conserved in all nuclear and atomic processes. The two pion decay ($\theta^+ \to \pi^+ + \pi^\circ$) mode has even parity, but the parity of the three pion decay ($\tau^+ \to \pi^+ + \pi^+ + \pi^-$) mode is odd. There is no doubt that the theta and tau particles (may also be called $K_{\pi 2}$ and $K_{\pi 3}$ respectively) are both charged mesons with odd parity. Now difficulty is that the two identical particles end in states of different particles. This difficulty, known as "$\tau - \theta$ puzzle", not yet been resolved but it led Lee and Yang in 1956 to consider the nature of the forces between particles and to suggest that weak interactions such as those involved in β decay, parity would not be conserved.

Fitch and Motley in 1956 performed the experiment for the two predominant modes of kaon decay, $K(\theta^+)$ or $K_{\pi 2}$ and $K_{\mu 2}$. A 465 MeV beam containing predominately protons, pions and few kaons from the cosmotron at Brookhaven laboratory was produced. These particles have very different velocities on account of difference in their masses. Identification of kaons was made by the two Čerenkov counters. The materials of these counters were chosen such that the fast pions would produce pulses in both, protons in neither and kaons in the first only. These kaons were slowed down by the absorbed and stopped in the third counter. The decay products of the kaon were emitted in all directions. Two more Cerenkov counters were used to detect muon secondaries and a set of a scintillation counter and Cerenkov counter was used to detect neutral pions or their γ-rays. The time lags between the signals gave the lifetime of the kaon. The lifetimes of the two modes were shown to be equal, as

$$\tau(K^+_{\mu 2}) \;=\; 11.7^{+0.8}_{-0.7}\,ns, \quad \tau(K^+_{\pi 2}) = 12.1^{+1.1}_{-1.0}\,ns.$$

The negative kaons are also found to have same lifetimes.

M. Gell-Mann and A. Pais in 1955 predicted the different situation with the decay of the neutral K-mesons. Since K° and $\bar{K}^\circ$ have different values of the hypercharge, + 1 and – 1 respectively, hence one cannot be converted into the other by the strong interaction. However the K° can be transformed into $\bar{K}^\circ$ by the *weak interaction*, For example :

$$K^\circ \rightleftharpoons \pi^\circ + \pi^\circ \rightleftharpoons \bar{K}^\circ$$

$$\rightleftharpoons \pi^+ + \pi^- \rightleftharpoons \bar{K}^\circ \qquad K^\circ \xrightarrow[\pi^\circ + \pi^\circ]{weak} \bar{K}^\circ \text{ or } K^\circ \xrightarrow[\pi^+ + \pi^-]{weak} \bar{K}^\circ$$

The transformation is possible only when *CP* symmetry invariance is applicable to the operation Through the weak coupling between the K° and its anti-particle the $\bar{K}^\circ$, it is possible to construct two neutral K-particles (states) K_1° and K_2°, which are their own anti-particles. These states have wavefunctions

$$|K_1^\circ> = [|K^\circ> + |\bar{K}^\circ>]/\sqrt{2} \qquad ...(46)$$

$$|K_2^\circ> = [|K^\circ> - |\bar{K}^\circ>]/\sqrt{2}. \qquad ...(47)$$

Application of the *CP* operation to K_1°, *i.e.* converting K° to $\bar{K}^\circ$ and *vice versa*, changes it into K_1°, *i.e.*, K_1° is unchanged, but K_2° is changed into $- K_2^\circ$, *i.e.*, the sign of the wavefunction is changed. When the*CP* operation is applied to the decay products, it can be shown that decay of K_1° into $\pi^+ + \pi^-$ or $\pi^\circ + \pi^\circ$ is permitted. However the K_2° particle cannot decay by these two pion modes, although it can decay into three pions. The decay modes are :

$$\left.\begin{aligned} K^\circ(K_1^\circ) &\to \pi^\circ + \pi^\circ + 227.8\,MeV\,(31\%) \\ &\to \pi^+ + \pi^- + 218.6\,MeV\,(69\%) \end{aligned}\right\}\tau_1 = (0.893 \pm 0.003) \times 10^{-10}\ sec$$

$$\left.\begin{aligned} K^\circ(K_2^\circ) &\to \pi^\circ + \pi^\circ + \pi^\circ + 92.8\,MeV\,(22\%) \\ &\to \pi^+ + \pi^- + \pi^\circ + 83.6\,MeV\,(12\%) \\ &\to \pi^\pm + e^\mp + \nu_e + 229.3\,MeV\,(39\%) \\ &\to \pi^\pm + \mu^\mp + \nu_\mu + 252.5\,MeV\,(27.\%) \end{aligned}\right\}\tau_2 = (5.18 \pm 0.04) \times 10^{-8}\ sec$$

Thus $|K_1^\circ>$ and $|K_2^\circ>$ are the eigenstates of *CP* with eigenvalues +1 and –1 respectively, but not the eigenstates of strangeness S. These states $|K_1^0>$ and $|K_2^0>$ decay with definite lifetimes τ_1 and τ_2.

The decay of a neutral K-meson into two pions is accompanied by a greater decrease in mass, and hence a larger energy is released than in the three pion decays. Thus the K_1^0-particles decay rapidly and have a short life than the K_2^0. These states are also represented by K_S and K_L, where S and L indicate the shorter and longer lived respectively.

Mass of Kaons. Bristol and Brown analyzed forty seven τ^+-decay events and from all ranges and angles found $Q = 75.04 \pm 0.16\ MeV/c^2$. Using $m_\pi = 139.58 \pm 0.02\ MeV/c^2$, it was suggested that

$$m_K^+ = 493.78 \pm 0.17\ MeV/c^2.$$

Decay of neutral K^0-meson in the mode $\pi^+ + \pi^-$ provides one means for measuring its mass. The estimated mass is $498.1 \pm 0.4\ MeV/c^2$ for K^0-meson. Crawford found that close to the associated production threshold the energy balances of the reactions

$$\pi^- + p \to \Lambda + K^0$$
$$\to \Sigma^- + K^+$$

are sensitive to the mass values of the K-mesons. They found

$$m_{K^0} - m_{K^+} = 4.8 \pm 1.1\ MeV/c^2. \qquad ...(48)$$

Another approach is through the charge exchange reaction

$$K^- + p \to K^0 + n$$

Burnstein and Rubin were able to find mass difference

$$m_{K^0} - m_{K^-} = 3.90 \pm 0.25\ \text{MeV}/c^2 \qquad ...(49)$$

An earlier similar measurement by Rosenfeld *et al.* gave an estimate of $3.7 \pm 0.7\ MeV/c^2$ for this quantity. The mass of K^0-meson thus calculated is

$$m_{K^0} = 497.7 \pm 0.3\ MeV/c^2. \qquad ...(50)$$

The mass of the K^--meson has been determined by using the hyperon production reactions

$$K^- + p \to \Sigma^+ + \pi^- + Q \qquad ...(51)$$

$$K^- + p \to \Sigma^- + \pi^+ + Q'. \qquad ...(52)$$

If the Q value of the equation (51) is determined from the measured kinetic energies of the particles, the mass of the K^--meson can be found using the known mass of the Σ^+-hyperon.

$$m_{K^-} = 493.7 \pm 0.3\ MeV/c^2 \text{ (or } 965.8 \pm 1.5\ m_e\text{)}. \qquad ...(53)$$

The adopted values of the mass of the kaons are :

$$m_{K^+} \text{ or } m_{K^-} = 493.67 \pm 0.015\ MeV/c^2$$
$$m_{K^0} \text{ or } m_{\bar{K}^0} = 497.67 \pm 0.13\ MeV/c^2.$$

K-meson (K^+, K^0) are strange particles and having strangeness quantum number + 1.

Spin. The spin of the K-meson is zero, like of π-mesons. This can be obtained from any of the following arguments : (1) τ-decay does not involve a change of parity where as θ-decay does involve a parity change. This puzzle was resolved by Yang and Lee suggesting non-conservation of parity in weak interactions. The spectrum of the π^- in the 3π decay of K^+-meson agrees with the theoretically predicted for a spinless K-particle. (2) The observation of the neutral decay of the K_1^0 into two π^0-mesons is consistent only with an even spin of the neutral K-meson. (3) The longitudinal polarization of the μ^+-meson arising from the K^+-decay ($K^+ \to \mu^+ + \nu_\mu$) has been measured. It is in the same direction as the μ^+ from the decay of the π^+($\pi^+ \to \mu^+ + \nu_\mu$). This implies that the K^+ is also a spinless particle.

Parity. The decay of the K^+-meson into three pions ($K^+ \to \pi^+ + \pi^+ + \pi^-$) can give us information about the parity of K^+. The system of three pions can be divided into a dipion of the two like mesons (π^+, π^+) and the remaining π^--meson. Two like mesons $\pi^+ \pi^+$ must have even parity $P = P_\pi P_\pi (-1)^L$, hence in this ($\pi^+ \pi^+$) system L, the orbital angular momentum must be even. The intrinsic parity of the pion is negative. Hence if l is the orbital angular momentum of the π^--meson, then the parity of the three pion system is $(-1)^3 (-1)^L (-1)^l = (-1)^{l+1}$. If spin of the τ^+ particle is zero, and the parity is conserved in the τ^+ decay, then its parity will be *odd*. In the two pion decay of θ^+ particle ($\theta^+ \rightarrow \pi^+ + \pi^0$), the total parity of the system is $(-1)(-1)(-1)^l$. If parity is conserved in the θ-decay, the θ^+-paricle parity is $(-1)^l$. For a spinless θ^+-particle, the parity is thus *even*. The even and odd parities of the two states of K^+ mesons were explained by Lee and Yang, who suggested that the τ^+ and θ^+ particles were identical and the parity conservation in *K*-meson decays was violated, as in β-decay.

Dalitz Plots. The information about the spin and parity of the elementary particles which decay into three particles or which lead to final states consisting of three particles due to high energy nuclear reactions, can be obtained by the graphical method of Dalitz, known as *Dalitz plot*. Two forms of the Dalitz plot are frequently used. The first, known as *scatter plot*, is for a final state containing three particles of unequal mass among which is distributed a total energy *E* in the *C, M* system. The other in which the masses of the three particles in the final states are equal, is a *triangular plot*. If the decay occurs by strong interaction, this method will give information on both spin and parity. If the decay occurs by weak interaction, the information is limited to the spin.

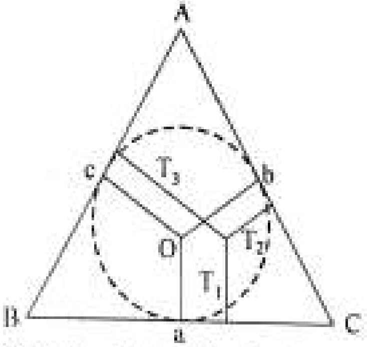

Fig. 18.19. The Dalitz plot for the three pion decay of K^+.

If the three particles have kinetic energies in the *CM* as T_1, T_2 and T_3, their sum is constant and equal to the *Q*-value of the decay. The T_1, T_2 and T_3 are represented as the perpendicular distances of a point *F* from the sides of an equilateral triangle (*ABC*) of sides $2Q/\sqrt{3}$ and the height *Q*. Thus a single point *F* in the triangle represents the decay. Conservation of energy restricts the points to the inside of the triangle. In the non-relativistic approximation, conservation of momentum restricts the allowed zone of points to the inside of the circle, inscribed within the triangle. With unequal masses *m* for the three particles, the allowed domain becomes an inscribed ellipse. For relativistic energies, the circle is distorted. The symmetry axes *Aa*, *Bb* and *Cc* divide the allowed region into six sectors, thus the configurations in each sector can be obtained from those corresponding to one chosen sector. If the process is energy independent, a uniform distribution of points corresponding to different partitions of energy is expected over these six sectors. The plot may in effect be folded on itself, so that all points lie within one sector. Particular regions of the triangular Dalitz plot correspond to simple energy or momentum distributions. Thus at point *O*, $T_1 = T_2 = T_3$, points along the lines *Oa*, *Ob*, *Oc* two particles have equal energy and at the boundary of the plot (on the sides *AB*, *BC* or *CA*), the particles are collinear (on being at rest in *CM*-system at points a, *b*, *c*).

The invariance under rotation or reflection may forbit the population of certain regions of the plot. Thus the inspection of the plot may provide information of spin & parity. For the ω°-meson decay, the distribution of data points is concentrated in the central region of the plot. This is the characteristic of decay of a particle of spin-parity 1^-. The distribution of data points is uniform for the K^+-meson (as shown in Fig. 18.19). Hence the spin of K^+-meson is zero. The negative and neutral kaons are assumed to have zero spin also. The parity of the kaon can only be determined in strong interactions. For example in the reaction $K^- + {}^4He \rightarrow \pi^- + {}^4_\Lambda He$, the hypernucleus ${}^4_\Lambda He$ containing Λ-hyperon as one of the nucleon and hence conserving strangeness is formed. Since the ordinary helium nuclei have spin zero. If this is the case for ${}^4_\Lambda He$, then *l*-value will be same on both sides of the reaction since all the particle and nuclear spins are zero. The parity equation is

$$P(K)P(He) \;=\; P(\pi^-)P({}^4_\Lambda He) = -P({}^4_\Lambda He) = -P(He)\,P(\Lambda).$$

Hence the parity of *K*-meson is opposite to that of Λ-hyperon. If Λ-parity is assumed to be even as with the nucleons, then K^--meson has odd parity. All kaons are assumed to have odd parity.

Interaction with Matter. Charged *K*-mesons lose energy by ionization as they pass through matter and also have certain interaction with atomic nuclei. K^+-mesons undergo relatively little nuclear scattering or absorption and if brought to rest in matter undergo spontaneous decay as it would be in the absence of matter. On the other hand, K^--mesons undergo quite strong nuclear scattering and absorption. *If they come to rest in matter, they form K-mesonic atoms and are absorbed, producing large stars. Neutral kaons do not* appear to have very strong interaction with nuclei and do not lose energy by ionization. On account of their short lives they decay in flight.

The only two body inelastic scattering of the K^+ is

$$K^+ + n \rightarrow K^0 + p.$$

For K^- energies less than 300 MeV, the reactions are many, as :

$$K^- + p \rightarrow K^- + p \ (\textit{Elastic scattering})$$
$$K^- + p \rightarrow \bar{K}^0 + n \ (\textit{Charge exchange})$$
$$K^- + p \rightarrow \Sigma^- + \pi^+ \ (\textit{Inelastic scattering})$$
$$\rightarrow \Sigma^+ + \pi^-$$
$$\rightarrow \Sigma^0 + \pi^0$$
$$\rightarrow \Lambda^0 + \pi^0.$$

Both elastic and inelastic scattering are characterized by rapidly increasing cross-sections as the K^- energy decreases to zero. A very sharp K^--p scattering resonance has been found in elastic and inelastic cross-sections at about 135 MeV.

The K^--mesons interact with the nuclear neutrons as :

$$K^- + n \rightarrow \Lambda^0 + \pi^-$$
$$\rightarrow \Sigma^0 + \pi^-.$$

K^--mesons produce hypernuclei, when interact with ^{16}O and ^4He. The resonance states of K and Λ (K^* and Λ^*) have been observed due to the interaction of K^- with protons. η^0-mesons are also produced when K^- interacts with protons.

CP Violation in Neutral K-Decay—We have seen earlier that the 2-pion mode is allowed by CP for the K_1^0, but forbidden for the K_2^0. The most sensitive test of the hypothesis of CP conservation is to look for the CP-violating decay $K_2^0 \rightarrow \pi^+ \pi^-$. J.H. Christenson, J.W. Cronin, V.L. Fitch and R. Turlay in 1964 have performed an experiment and have observed the CP-violating decay. It was found in that experiment that K_2^0 particles decayed into $\pi^+\pi^-$ with a low branching ratio, now known to be

$$\frac{\Gamma(K_2^0 \rightarrow \pi^+\pi^-)}{\Gamma(K_1^0 \rightarrow \text{all charged modes})} \cong (2.03 \pm 0.05) \times 10^{-3} \qquad \text{...(54)}$$

This indicates that the violation is small. The charged particles are detected and their momenta measured by the two spark chambers and magnet sandwiches. Most of the decays observed are the dominent K_2^0 modes ($\pi\mu\nu$ and $\pi e\nu$). The π^- decays are recognized by computing $\boldsymbol{P}_K = \boldsymbol{P}_{\pi^+} + \boldsymbol{P}_{\pi^-}$ and requiring that within experimental errors resultant momentum vector $\boldsymbol{P}_K$ lies along the beam direction and the invariant mass of two charged particles directed be equal to the K^0 mass. A second experiment has observed the same effect. A constructive interference between the free K_2^0-decay into two pions ($\pi^+\pi^-$) and the two pions ($\pi^+\pi^-$) from K_1^0's regenerated in baryllium has been also observed. This failure of CP invariance was soon confirmed by the observation of the decay mode $K_2^0 \rightarrow \pi^0\pi^0$ with branching ratio of $(0.94 \pm 0.18) \times 10^{-3}$.

This CP violation suggests that the long lived and short lived components of neutral K's, known as K_L^0 and K_S^0, are not the $|K_1^0>$, and $|K_2^0>$ combinations defined by equations (46) and (47), but the combination of these two as defined below :

$$|K_L^0> \; = \; \frac{|K_2^0> + \varepsilon|K_1^0>}{\sqrt{1+|\varepsilon|^2}} \text{ and } |K_S^0> = \frac{|K_1^0> + \varepsilon|K_2^0>}{\sqrt{1+|\varepsilon|^2}}, \qquad \text{...(55)}$$

where ε is a small complex number which measures the degree of CP-violation due to kaon state mixing. The evidence for direct CP-violation was first observed in an experiment at CERN in 1988 with $\varepsilon \approx 10^{-3}$.

The CP violation also amplies that it is possible to make an absolute distinction between matter and anti-matter. With CP violation $\overline{K}^{\circ}$ and K° which are particle and anti-particle pairs can be distinguished by their decays into two pions. These are mixtures of K_S° and K_L°. Since K_S° and K_L° are not very different from K_1° and K_2°. The relations are as shown by equations (46) and (47) . Both K_S° and K_L° decay to two pions, so the time dependence of the 2-pion decay rate will involve an interference term, which has opposite sign for $\overline{K}^{\circ}$ and K°,

18.14 η-MESON

Pevsner and his coworkers at Johns Hopkins in late 1961, studied the interactions of positive pions in a deuterium bubble chamber. The pion triplets produced in the reaction

$$\pi^+ + d \rightarrow p + p + (\pi^+ + \pi^- + \pi^{\circ})$$

were analyzed by plotting the spectrum of the mass of pion triplets. A small peak was observed at ~ 550 *MeV* and was named as eta (η)-meson. At first it was believed that the η is a resonance. The experiments with good resolution and high statistics showed that the peak was much narrower, $\Gamma = (2 \pm 3)$ *keV*, than those belonging to various resonances. The narrow peak corresponds to the long lifetime or to an almost stable particle. Hence its decay does not proceed through the strong interaction. Its formation has been confirmed at Berkeley where this particle has been observed in the bombardment of protons by K^--mesons.

$$K^- + p^+ \rightarrow \Lambda^0 + \eta^0.$$

The η-particle decays electromagnetically by the processes

$$\begin{aligned}\eta^{\circ} &= \gamma + \gamma \\ &= \pi^+ + \pi^- + \pi^{\circ} \\ &= \pi^{\circ} + \pi^{\circ} + \pi^{\circ}.\end{aligned}$$

The two photon decay is more prominent and is evidence that the η is not a resonance, since photons can not interact strongly. Like the π°-meson, the η°-meson is its own antiparticle. It is like the π°, except that it has $T = 0$ and greater mass. The 3π-decay implies that isospin is not conserved in the η-decay. Since the decay is too fast, hence can not be a weak process, this confirms that the electromagnetic interaction is involved in η-decay.

The η has a γ-width about 20 times larger than that of π°. Considering that the γ-decay mode contributes roughly one half of the width, the mean life time of η, obtained by comparison with that of π°, should be 5×10^{-18} sec. This corresponds to the width of less than 1 keV.

Bastien *et al.* measured the invariant mass of the three pions in the reaction ($K^- + p \rightarrow \Lambda + \pi^+ + \pi^- + \pi^{\circ}$) and found the mass of η°-meson as 549.9 ± 1.2 MeV/c^2. Delcourt *et al.* measured, with a quite different technique, the production of η-meson in the reaction $\gamma + p \rightarrow p + \eta$ just above threshold and estimated the mass 549.3 ± 2.9 MeV/c^2 for η-meson. The various published measurements are consistent. The best estimate derived is 548.8 ± 0.6 MeV/c^2.

As η particle decays into two gamma rays or three pions, hence, it is necessary to assume the spin as 0, 2 or larger. Spin 2 or larger is excluded because it would result in marked anisotropies in the decay which are not observed. Thus it is better to assign $J = 0$ to the η-particle. Since the parity of two pions in a $T = 0$ state is necessarily even, hence the η-particle must have odd parity.

The neutral η′ with mass ~ 957.50 ± 0.24 MeV/c^2 has also been observed. Being more massive, it has a still shorter lifetime $(\tau_{\eta'} < \tau_{\eta} < \tau_{\pi^0})$. However its large mass makes the decay into an η° and two π-mesons more favourable than the decay into photons. Its dominant decay mode (η′ → ηππ) is hadronic but slow, full width being only (0.29 ± 0.05) *MeV*. The photo emitting modes, $\rho^{\circ}\gamma$ and γγ compete quite strongly with $\eta^{\circ}\pi\pi$, their branching fractions being 30% and 2% respectively. An eta-meson with quarks $c\bar{c}$ is now also known. It is denoted as η_c, has a mass ~ 2981 MeV/c^2, with decay modes η π π, $2\pi^+ 2\pi^-$ and $K^+K^-\pi^+\pi^-$. Their relative rates and total width are not known. A similar meson η_b with quarks $b\bar{b}$ is predicted but not yet observed.

18.15 HYPERONS

Hyperons are the semistable particles, having masses greater than that of the nucleon. The name hyperon was taken from Greek word hyper, "meaning above". Hyperon is the collective name of baryons with nonzero strangeness number S. The hyperons have long lifetimes relative to 10^{-22} sec and decay by photon emission or through weaker decay interactions. The known hyperons are Λ, Σ^+, Σ^-, Σ°, Ξ^-, Ξ° and Ω^- and their anti-particles. The hyperonic particles which are unstable ($\tau < 10^{-22}$ sec) are called excited hyperons, observed as *resonances.*

Λ-hyperon—The first hyperon was found in cosmic rays in 1947 by Rochester and Butler in England. They observed the tracks of two charged particles emerging from a point in the gas of a cloud chamber. The upside down V-shaped figure could best be explained by assuming that some unstable neutral particle shooting down from the sky had decayed to form positive and negative charged particles. The charged particles seen in the decay were identified as a proton and a negative pion. This was the first evidence for the existence of the first and best known hyperon. *This neutral unstable particle was named as lambda and denoted by* Λ°, *because of the characteristic appearance of its decay in a cloud chamber.* For its production in laboratories, Fowler, Shutt, Thorndike and Whittemore allowed a π^--mesons beam of 1.5 *GeV* from the Brookhaven Cosmotron (proton synchrotron) to enter a diffusion cloud chamber containing hydrogen at a pressure of 18 atmospheres placed in a magnetic field of 1100 gausses. The track of an incident pion can be seen at the end in the chamber. This end point is the vertex of a V, formed by the tracks of the negative pion and proton. To conserve energy and momentum in the production of Λ°-hyperons, the necessity of the production of another neutral particle, probably K°-meson, was also suggested. The reaction is

$$\pi^- + p \rightarrow \Lambda^\circ + K^\circ.$$

Λ-hyperon undergoes following decay reactions :

$$\begin{aligned} \Lambda^\circ &\rightarrow p + \pi^- && (67.7\%) \\ &\rightarrow n^\circ + \pi^\circ. && (31.6\%) \end{aligned}$$

The mass of the Λ-hyperon has been obtained from the Q-value of the reaction $\Lambda^\circ \rightarrow p + \pi^-$. Both the pion and proton ranges, as well as the opening angles between the Λ-decay products were made and the Q-value so measured was 37.56 ± 0.13 *MeV*. Several other similar measurements have been made and the present best estimate of mass is

$$m_\Lambda = 1115.60 \pm 0.05 \; MeV/c^2.$$

The mean life of neutral lambda particle is $2.63 \pm 0.02 \times 10^{-10}$ sec. For such a very short lifetime the decay length is only of the order of centimeters which is too small a distance to allow the use of an array of electronic counters, used in case of pion and kaons. The visual detectors such as spark and bubble chambers can resolve such small distances and are therefore used. The spin of Λ° is $\frac{1}{2}$. The magnetic moment of Λ°, like the neutron is negative and equal to $0.613 \pm 0.004 \; \mu_N$.

The leptonic decays of the Λ°-hyperon

$$\begin{aligned} \Lambda^\circ &\rightarrow p + e^- + \bar{\nu}_e && (0.88 \times 10^{-5}\%) \\ &\rightarrow p + \mu^- + \bar{\nu}_\mu \end{aligned}$$

have been observed to occur. Because of parity non-conservation in weak decay processes it is impossible to relate the parity of the Λ-hyperon to that of the πp system. By convention Λ-particle, like the proton, is taken to have even parity. As Λ° appears only in one charge state, neutral, hence it has isospin $T = 0$. The decay modes are permitted by the rule $\Delta S = 1$.

Σ-hyperons. It is the family of hyperons with the greatest number of members. The first of these to be observed was the positive sigma hyperon denoted by the symbol Σ^+. It has two predominant decay schemes and three weak decays.

$$\begin{aligned} \Sigma^+ &\rightarrow p + \pi^\circ + 116.1 \; MeV \; (\sim 51\%) \\ &\rightarrow n + \pi^+ + 110.3 \; MeV \; (\sim 49\%) \\ &\rightarrow n + \pi^+ + \gamma \; (\sim 4 \times 10^{-7}\%) \end{aligned}$$

$$\rightarrow \Lambda^0 + e^+ + \nu_e \ (\sim 2 \times 10^{-7}\ \%) \text{ leptonic decay}$$
$$\rightarrow p + \gamma \ (\sim 3 \times 10^{-5}\%)$$

The mean life of Σ^+-hyperon is $8.0 \pm 0.04 \times 10^{-11}$ sec. The corresponding negative particle denoted by Σ^- was also observed within few months of the discovery of the Σ^+. Its decay scheme is

$$\Sigma^- \rightarrow n + \pi^- + 118.5\ MeV \text{ (Mean life time } 1.48 \times 10^{-10} \text{ sec).}$$

Soon afterwards, evidence for the existence of a neutral (Σ^0)-hyperon was also presented. Its decay scheme is

$$\Sigma^0 \rightarrow \Lambda^0 + \gamma + 80\ MeV \text{ (Mean life time } 6 \pm 1 \times 10^{-20} \text{ sec).}$$

The Σ-hyperon masses come from measurements carried out on the products of K^- and Σ^- capture by protons and on the disintegration products of the hyperons themselves. When such measurements are combined, they yield $m_{\Sigma^+} = 1189.36 \pm 0.06\ MeV/c^2$.

The π^- and Σ^+ ranges in the reaction

$$K^- + p \rightarrow \pi^- + \Sigma^+ + Q$$

indicate a momentum balance and yield a Q-value of $103.0 \pm 0.3\ MeV$. Using this value of Q and the mass of the Σ^+-particle, the mass of K^--meson is calculated. Then from relation $K^- + p \rightarrow \pi^+ + \Sigma^- + Q'$, we get the mass of Σ^- as $1197.34 \pm 0.05\ MeV/c^2$. This is considerably larger than the mass of Σ^+.

Burnstein *et al.* observed the sequence $\Sigma^- + p \rightarrow \Sigma^0 + n$ followed by the decay mode $\Sigma^0 \rightarrow \Lambda^0 + e^+ + e^-$. These events yielded a Σ^0 momentum of $60.3 \pm 0.9\ MeV/c$ and $m(\Sigma^-) - m(\Sigma^0) = 4.7 \pm 0.1\ MeV/c^2$ or $m(\Sigma^0) = 1192.46 \pm 0.08\ MeV/c^2$.

The less probable decay modes of Σ^- are :

$$\begin{aligned} \Sigma^- &\rightarrow n + e^- + \bar{\nu}_e && (1.4 \times 10^{-5}\%) \\ &\rightarrow n + \mu^- + \bar{\nu}_\mu && (6.6 \times 10^{-6}\%) \\ &\rightarrow \Lambda^0 + e^- + \bar{\nu}_e && (7.5 \times 10^{-7}\%) \end{aligned}$$

Σ^+, Σ^- and Σ^0 all have intrinsic parity even and intrinsic spin $\frac{1}{2}$, thus are fermions. They possess a magnetic moment. The experiments on the Σ^+-hyperon magnetic moment suggested the value 3.28 ± 0.58 μ_N. Because of the three charge states, Σ-hyperons have $T = 1$. The decay modes show that $\Delta S = 1$.The Σ-parity can be related to that of the Λ by the analysis of the electromagnetic decay process $\Sigma \rightarrow \Lambda\, e^+\, e^-$.

Σ^--hyperons undergo interactions with nucleons, as

$$\Sigma^- + p \rightarrow \Lambda^0 + n.$$

Ksi-hyperons. Ksi-hyperons known thus far are the Ξ^- and Ξ^0. Present theory of elementary particles predicts that there should be no positively charged Ξ-particle. The Ξ's were originally called cascade particles, because a Ξ-particle decays to produce π-meson and a Λ^0, which in turn decays into a nucleon and another π-meson. The known modes of decays of these particles can be represented by the equations

$$\Xi^- \rightarrow \Lambda^0 + \pi^- + 66.3\ MeV$$
$$\Xi^0 \rightarrow \Lambda^0 + \pi^0 + 70\ MeV.$$

The decay processes have been used most often for mass measurements, but a good check was made by Schneider who measured the mass of Ξ^- hyperon in the production reaction $(K^- + p \rightarrow K^+ + \Xi^-)$. Using beam energy of 35 MeV, he yielded $m(\Xi^-) = 1321.1 \pm 0.6\ MeV/c^2$. Rosenfeld *et al.* suggested $m(\Xi^-) = 1320.8 \pm 0.2\ MeV/c^2$ and $m(\Xi^0) = 1314.3 \pm 1.0\ MeV/c^2$.

The Ξ^--hyperon has mean lifetime of 1.3×10^{-10} sec. and the Ξ^0-hyperon has its mean lifetime as of the order of 10^{-10} sec.

These hyperons are produced by the interaction of π^- and K-mesons of sufficiently high energy with nucleons. These mesons are absorbed by the nucleus and undergo one of the following reactions

$$\begin{aligned} K^- + p^+ &\rightarrow \Lambda^0 + \pi^0 \\ &\rightarrow \Lambda^0 + \pi^+ + \pi^- \\ &\rightarrow \Lambda^0 + \pi^0 + \pi^0 \end{aligned}$$

$$\begin{aligned} K^- + n &\rightarrow \Lambda^0 + \pi^- \\ &\rightarrow \Lambda^0 + \pi^- + \pi^0 \\ &\rightarrow \Sigma^- + \pi^0 \end{aligned}$$

$$\begin{aligned} \pi^- + p &\rightarrow \Lambda^0 + K^0 \\ &\rightarrow \Sigma^0 + K^0 \\ &\rightarrow \Sigma^- + K^+ \end{aligned}$$

$$\begin{array}{ll} \rightarrow \Sigma^{+} + \pi^{-} & \\ \rightarrow \Sigma^{-} + \pi^{+} & \rightarrow \Sigma^{\circ} + \pi^{-} \\ \rightarrow \Sigma^{\circ} + \pi^{\circ} & \rightarrow \Xi^{-} + K^{\circ} \\ \rightarrow \Xi^{-} + K^{+} & \rightarrow \Xi^{\circ} + K^{-} \\ \rightarrow \Xi^{\circ} + K^{\circ} & \end{array}$$

In all of the above reactions considerable energy is released and the nucleus in which the absorption occurs, therefore, breaks up into several pieces. If one piece is a hyperfragment, the Λ°, it must eventually decay into a proton and a pion, each of which may either interact with the residual nucleus or escape with its full energy.

Ξ^{-} and Ξ° particles have spin $\frac{1}{2}$, and are thus fermions. They possess a magnetic moment. Ξ^{-} and Ξ° have been observed with $T = \frac{1}{2}$ and thus $T_3 = -\frac{1}{2}$ and $+\frac{1}{2}$. Their production and decay reactions show that the strangeness quantum number $S = -2$ for these two and $\Delta S = 0$.

Ω—Hyperon. Before the discovery of Ω^{-}-hyperon, all known particles had hypercharge values of +1, 0, or − 1. Gell-Mann predicted the existence of such a particle, with a negative charge, as required to give it a hypercharge of − 2. Furthermore, he suggested that it might be produced, as it actually was, by the interaction of a K^{-}-meson at energies greater than 3.5 GeV with a proton. The expected strong interaction would be

$$\begin{array}{lcc} & K^{-} + p^{+} \rightarrow & \Omega^{-} + K^{+} + K^{\circ} \\ \text{Hypercharge} & -1 \quad +1 & -2 + 1 + 1 \\ \text{Isospin} & \frac{1}{2} \quad \frac{1}{2} & 0 \quad \frac{1}{2} \quad \frac{1}{2} \end{array}$$

The experiment designed to produce and detect the Ω^{-}-hyperon was carried out at Brookhaven National Laboratory in 1964. In this experiment short bursts of 5 GeV K^{-}-mesons were allowed to enter a liquid hydrogen bubble chamber. The photograph obtained is shown in Fig. 18.20 and can be interpreted as : *A K^{-}-meson enters from the bottom and interacts with a proton at the point a to yield a K°-meson, a K^{+}-meson and the Ω^{-}-hyperon.* The positive kaon is deflected to the left by the magnetic field whereas the Ω^{-}-hyperon is deflected to the right. The Ω^{-}-hyperon decays at point *b*, after traveling a short distance during its lifetime, into Ξ° hyperon and π^{-}-meson. Ξ°-hyperon decays at point *c* into Λ° and π°, but latter forms two gamma ray photons immediately. These photons then produce electron-positron pairs at the points *d* and *e*. The Λ°-hyperon decays at point *f* into a proton and *a* π^{-}-meson.

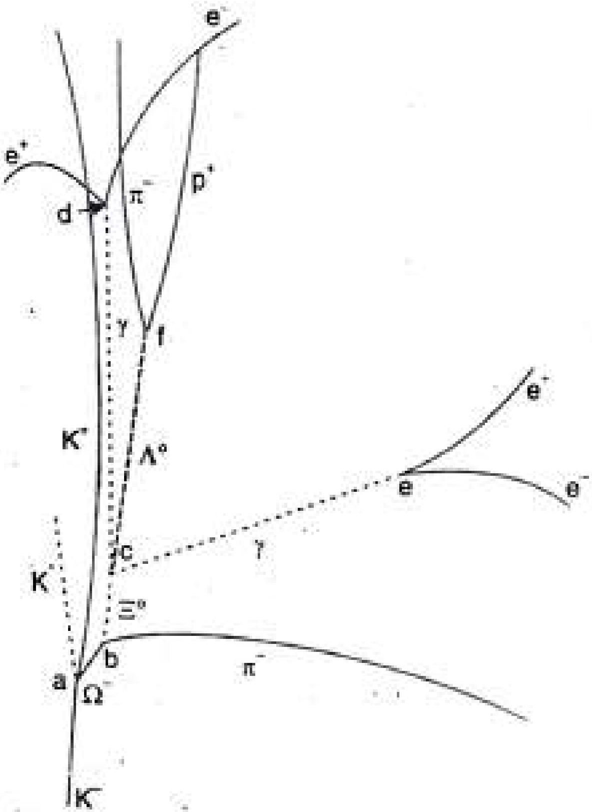

Fig. 18.20. Photograph representing the discovery of Ω^{-}-hyperon.

Gell-Mann noted that the Ω^{-}-particle should decay by the weak interaction, which it does. Its decay modes are

$$\begin{aligned} \Omega^{-} &\rightarrow \Xi^{\circ} + \pi^{-} \\ &\rightarrow \Xi^{-} + \pi^{\circ} \\ &\rightarrow \Lambda^{\circ} + K^{-} \end{aligned}$$

From the momenta of decay products (Ξ° and π^{-}), the mass of the Ω^{-} was measured to be $1686 \pm 12\ MeV/c^2$. The mass was also measured by the decay mode $\Omega^{-} \rightarrow \Lambda^{\circ} + K^{-}$. The mass was $1674 \pm 3MeV/c^2$. The mass was determined by decay mode $\Omega^{-} \rightarrow \Xi^{-} + \pi^{\circ}$. The averaged value used now is $1674 \pm 3MeV/c^2$.

Ω^--hyperon is a baryon, having strangeness quantum number – 3, hypercharge –2, spin 3/2 and parity even. It has a mean life time of 1.3×10^{-10} sec.

All these properties are summarised in Table 18.4.

18.16 HYPERNUCLEI

The lambda particle is the lightest strange baryon (hyperon) with lifetime of 2.6×10^{-10} sec. As the strangeness is conserved in strong interactions, the lifetime of the lambda particle remains essentially unchanged in the nucleus also. The is much longer than the lifetime of a typical nuclear electromagnetic transition and hence the detailed study of lambda hypernuclei can be made. The system consisting of a complex nucleus with Λ^0-particle attached in its lowest bound state will be quasi-stable. Such a quasi stable nucleus with a bound hyperon in the nucleus is called hypernucleus. The symbol ${}^{10}_{\Lambda}B$ denotes a hypernucleus which may be obtained when ${}^{9}_{4}Be$ captures a Λ^0-particle. Evidence for the existence of such *hypernuclei* was first given by Polish physicists M. Dansyz and J. Pniewski, who found a fragment stable for a time greater than 3×10^{-12} *sec*, among the products of a cosmic ray star recorded in nuclear emulsion at a height of 28,300 *m*. We shall restrict the discussion to Λ-hypernuclei. Because of the fast transformations strangeness conserving Σ- or Ξ-hypernuclei have very short lifetimes and interact with nucleons as

Table 18.4. The Elementary Particles and their Properties

Particle	*Symbol*	*Anti-particle*	*Mass (MeV)*	*Spin Parity*	*Isospin T*	*Strangeness S*	*Principal Decays*	*Lifetime (Seconds)*
Graviton	g	g itself	0	2			stable	Infinite
Photon	γ	γ itself	0	1^-			stable	Infinite
Leptons (Weakly Interacting Fermions)—								
Neutrino	ν_e	$\bar{\nu}_e$	0 (< 7.3×10^{-5})	1/2			stable	Infinite
	ν_μ	$\bar{\nu}_\mu$	0(< 0.27)	1/2			stable	Infinite
	ν_τ	$\bar{\nu}_\tau$	(< 35)	1/2			stable	Infinite
Electron	e^-	e^+	0.511066	1/2			stable	Infinite
Muon	μ^-	μ^+	105.659	1/2			$\mu^+ \to e^+ + \nu_e + \bar{\nu}_\mu$	2.2×10^{-6}
Tauon	τ^-	τ^+	1784.1	1/2			$\tau^+ \to e^+ + \nu_e + \bar{\nu}_\tau$	3.1×10^{-13}
Mesons (Strongly Interacting Bosons)—								
Pion	π^+	π^-	139.58	0^-	1	0	$\pi^+ \to \mu^+ + \nu_\mu$	2.6×10^{-8}
	π^0	π^0 itself	134.98	0^-	1	0	$\pi^0 \to \gamma + \gamma$	0.83×10^{-16}
Kaon	K^+	K^-	493.82	0^-	1/2	± 1	$K^+ \to \mu^+ + \nu_\mu$ $\to \pi^+ + \pi^0$	1.245×10^{-8}
	K^0	$\bar{K}^0$	497.67	0^-	1/2	± 1	$K_1^0 \to \pi^+ + \pi^-$ $\to \pi^0 + \pi^0$	0.89×10^{-10}
							$K_2^0 \to \pi + \nu + e(\text{or } \mu)$ $\to 3\pi^0$ or $\pi^+ \pi^- \pi^0$	5.17×10^{-8}
Eta-meson	η^0	η^0 itself	547.5	0	0^-	0	$\eta \to \gamma + \gamma$ $\to 3\pi^0$ or $\pi^0\, 2\gamma$	$\eta = 1.19$ ± 0.11 keV
Baryons (Strongly Interacting Fermions)								
Proton	p	$\bar{p}$	938.256	$1/2^+$	1/2	0	stable	infinite
Neutron	n	$\bar{n}$	939.550	$1/2^+$	1/2	0	$n \to p + e^- + \bar{\nu}$	1.01×10^3
Lambda	Λ^0	$\bar{\Lambda}^0$	1115.44	$1/2^+$	0	–1	$\Lambda^0 \to p + \pi^-$ $\to n + \pi^0$	2.6×10^{-10}
Sigma	Σ^+	$\bar{\Sigma}^-$	1189.39	$1/2^+$	1	–1	$\Sigma^+ \to p + \pi^0$ $\to n + \pi^+$	0.81×10^{-10}
	Σ^0	$\bar{\Sigma}^0$	1192.6	$1/2^+$	1	–1	$\Sigma^0 \to \Lambda + \gamma$	$< 7.4 \times 10^{-20}$
	Σ^-	$\bar{\Sigma}^+$	1197.4	$1/2^+$	1	– 1	$\Sigma^- \to n + \pi^-$	1.5×10^{-10}
Xi	Ξ^0	$\bar{\Xi}^0$	1314.9	$1/2^+$	1/2	– 2	$\Xi^0 \to \Lambda^0 + \pi^0$	2.9×10^{-10}
	Ξ^-	$\bar{\Xi}^+$	1321.3	$1/2^+$	1/2	– 2	$\Xi^- \to \Lambda^0 + \pi^-$	1.75×10^{-10}
Omega	Ω^-	$\bar{\Omega}^+$	1672.5 ± .5	$3/2^+$	0	– 3	$\Omega^- \to \Xi + \pi$ $\to \Lambda + K^-$	0.82×10^{-10}

$$\Sigma^{+}+n \rightarrow \Lambda^{0}+p$$
$$\Sigma^{-}+p \rightarrow \Lambda^{0}+n$$
$$\Xi^{-}+p \rightarrow \Lambda^{0}+\Lambda^{0}$$
$$\Xi^{0}+n \rightarrow \Lambda^{0}+\Lambda^{0}.$$

Nevertheless, sigma hypernuclei have been observed experimentally, the lifetime being $\sim 10^{-21}$ sec. There is a good chance that *Xi* and omega hypernuclei could also be experimentally observed.

Hypernuclei of all the light elements from hydrogen (${}_{\Lambda}H^{3}$) to oxygen (${}_{\Lambda}O^{16}$) have been reported. In addition from a star produced in a photographic film bombarded by K^{-} – mesons, evidence of a hypernucleus containing two Λ^{0}-hyperons was reported in 1963 at the CERN laboratory. The species formed was considered to be either ${}_{\Lambda\Lambda}Be^{10}$ or ${}_{\Lambda\Lambda}Be^{11}$. In 1966, a similar hypernucleus ${}_{\Lambda\Lambda}He^{6}$ was identified in U.S.A.

It is very difficult to obtain accurate determination of the average life-times of hypernuclei, but the average life-times are approximately slightly less than that of a free Λ^{0}-hyperon. There are usually several competing modes of decay of a given species of hypernuclei. The ${}_{\Lambda}He^{4}$ hypernucleus has the following decay modes :

$$\begin{aligned} {}_{\Lambda}He^{4} &\rightarrow \pi^{0} + \text{nucleons} \\ &\rightarrow \pi^{-}+p+{}_{2}He^{3} \\ &\rightarrow n+p+{}_{1}H^{2} \\ &\rightarrow {}_{1}H^{2}+{}_{1}H^{2}. \end{aligned}$$

The first two decay modes are called *mesonic decays*, in which hyperon may be regarded as undergoing its normal decay into $\pi^{0}+n$ or $\pi^{-}+p$. The nucleon thus produced may be expelled or it may remain in the product nucleus. Other two modes are called *non-mesonic* decays. the non-mesonic decay is equivalent to the interaction of a Λ^{0}-particle with proton or a neutron, *i.e.*

$$\Lambda^{0}+p \rightarrow (\pi^{-}+p)+p \rightarrow n+p$$
$$\Lambda^{0}+n \rightarrow (\pi^{0}+n)+n \rightarrow n+n.$$

Since a Λ^{0}-hyperon does not normally interact with a nucleon, the interaction with a nucleon is stimulated by the remainder of the nucleus and the non-mesonic decay (dominant for hyper-nuclei with $Z > 3$ or 4) is referred to as stimulated decay.

The binding energy of the Λ^{0}-particle in the hypernuclei can be calculated from the observed kinetic energies of the decay particles, which can be derived from the lengths of the tracks in a photographic emulsion. In non-mesonic decay, one or more neutrons are generally emitted, they do not produce any track in the emulsion and the kinetic energies cannot be determined. Hence the binding energy of Λ^{0}-particle is obtained from mesonic decays. The values have been found to increase fairly regularly with the atomic number of the hypernucleus. The value is 0.2 MeV in ${}_{\Lambda}He^{3}$ and about 12 MeV in ${}_{\Lambda}C^{14}$ and ${}_{\Lambda}N^{14}$. In this way it is clear that the existence of ${}_{\Lambda}H^{2}$ is not possible because in it the binding energy would be still smaller and in the heavier hypernuclei, Λ^{0}-hyperon is more strongly bound than a nucleon. Similar to with nucleon—nucleon force, the hyperon-nucleon force appears to be charge independent and dependent on the spin.

The strength of the interaction of lambda particle in the nucleus is about two-thirds that for the nucleon. The spin-orbit interaction which is strong in the case of the nucleon is negligibly small in the case of the lambda particle. Theoretically the difference of such interactions is explained as reflecting the differences in the internal quark structure of the two baryons.

18.17 RESONANCE STATES

Most resonant or unstable states result from the strong interaction of a high energy meson (π or K) with a proton. Sometimes, resonant states also result from the interaction with a neutron or a deuteron. These states can be assigned mass, charge and spin consistent with the conservation laws. The earliest evidence for the formation of resonant states, also referred to as *resonance particles or resonances*, came in 1951 from a group working with Fermi at the Chicago University. In the course of studies of the scattering of positive and negative points of various energies by protons, it was observed that the cross-sections increased rapidly at energies above about 60 MeV. In 1957, K.A. Brueckner at Indiana University suggested that a resonance interaction occurred between the proton and the pion, much as the resonance capture of a neutron by a nucleus was associated with a maximum in the cross-section. *It is for this reason that the term resonance or resonant state came into general use.* At the present time, the name is applied to a particle state of very short life (~ 10^{-23} sec) which decays into two or more particles. Because of their *extremely short lifetimes resonant states are described as unstable particles.*

In spite of their extremely short lives, two general methods have been used for detecting resonances. One is to measure the scattering cross-section as a function of energy of the incident meson. The plot of the results indicates the formation of a resonant state. The rest mass energy of this state can be calculated from the energy of the scattered particle corresponding to the maximum cross-section. The average lifetime of the resonance, equal to the uncertainty in the time, $\tau = \Delta t = \hbar/\Delta E$, where ΔE is the uncertainty in energy which is equal to the full width of the peak at half the maximum height. Suppose the peak width at half maximum is found to be 100 MeV, the mean life of the resonant state is $6.58 \times 10^{-22}/100 = 6.6 \times 10^{-24}$ sec. The scattering cross-sections of positive and negative pions by protons are shown in Fig. 18.21. The upper curve shows that the maximum of the resonant peak is at a pion energy of 195 MeV in the lab system. On converting it in the proton pion centre of mass system the rest mass energy of the resonant state is found to be 1238 MeV. The full width at half maximum is 120 MeV, corresponding to the life time of 5.5×10^{-24} sec. This short life indicates decay by the strong interaction. This particular resonance state was attributed to a state with an isospin of $\frac{3}{2}$ by K.A. Brueckner and was originally represented by the symbol $N_{3/2}{}^*$ indicating a nucleon excited state with $T = \frac{3}{2}$. It is now designated as $\Delta(1238)$. Theory predicts that in the formation of $T = \frac{3}{2}$ resonance, the maximum scattering cross-section for $\pi^+ - p$ should be three times greater than for $\pi^- - p$. It is same as indicated by Fig. 18.21.

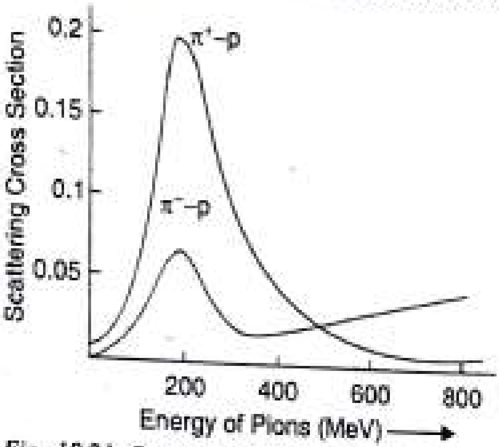

Fig. 18.21. Scattering cross-sections of π^+, π^--mesons by protons.

When the cross-sections for scattering of positive and negative pions with energies in excess of 300 MeV by protons are measured, several additional resonant states are observed. Some of these are more prominent in the π^+ interactions, whereas other are in the π^--interactions. These states can be assigned mass, charge and spin consistent with the conservation laws. The masses of some of well established resonant states are 1518, 1688, 1920 and 2360 MeV. These resonant states all have same mean lifetimes ~ 10^{-23} sec.

The second method for detecting resonances is based on a study of the energy distribution among the products, as determined from bubble chamber events. Suppose a high energy particle A interacts with a stationary particle B, in the bubble chamber to produce a particle C plus a resonant state R. The latter decays into two particles D and E in such a very short time that it leaves no track in the chamber. If all these particles are charged, the tracks obtained in the bubble chamber will be as shown in Fig. 18.22. The problem is thus to distinguish between the postulated process

$$A + B \to C + R \to C + D + E \quad \ldots(56)$$

and the direct reaction

$$A + B \to C + D + E. \quad \ldots(57)$$

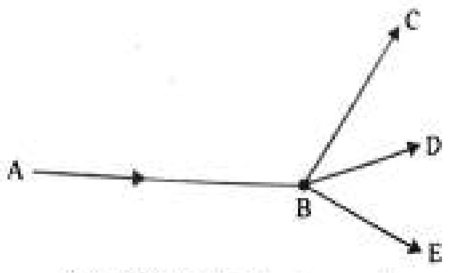

Fig. 18.22. Bubble chamber track.

The problem can be solved by a kinematic analysis of the bubble chamber event made with the aid of a computer. The available energy will be distributed among the three particles in a random manner, as given by the law of conservation of momentum, in the case in which these particles are formed by a direct reaction. If a large number of events of this type are examined, it will be found that the energy of any particle, say of C, has a spectrum of values ranging from zero to a maximum equal to the total energy available. If we consider another case in which a resonant state R is first formed together with a particle C. The available energy will be divided between them in a definite manner which depends only on the relative masses of these two. Thus in a large number of events, there will be many cases in which particle C has a specific energy value and a peak will be observed in the energy distribution curve. Energy of the resonance R can be calculated from the energy of the particle C corresponding to this peak. The mean life-time of the resonant state can be calculated by knowing the uncertainty in energy which is equal to the width of the peak at half maximum.

The problem that which of the three emergent tracks in the bubble chamber event represents particle C was solved by a group of Alston *et.al.* at the University of California, Berkeley in 1960. In the search for a hyperon-pion resonance analogous to the proton-pion resonance described earlier, the reaction was

$$K^- + p^+ \rightarrow \Lambda^\circ + \pi^+ + \pi^-.$$

Many hundreds of plates were analyzed by a computer. Some of the results suggested that the law of conservation of linear momentum was being violated and two resulting particles were indicated rather than three. Possibilities were

$$K^- + p^+ \rightarrow Y^{*+} + \pi^-$$
$$K^- + p^+ \rightarrow Y^{*-} + \pi^+,$$

where Y^* was suggested a new resonance particle showing strong decay in 10^{-23} sec into

$$Y^{*+} \rightarrow \Lambda^\circ + \pi^+$$
$$Y^{*-} \rightarrow \Lambda^\circ + \pi^-.$$

Thus we see that $\Lambda^\circ\pi^+$ and $\Lambda^\circ\pi^-$ resonances are formed, the rest mass corresponding to the pion energy of 280 MeV is calculated to be 1385 MeV. This resonance state, originally designated Y^* is now preferably indicated by the symbol Σ^* (1385). The widths at half maximum of the energy peaks at 280 MeV are both 40 MeV. This shows that the Y^* decays by the strong interaction. It is built from either $\Lambda^\circ\pi^+$ or $\Lambda^\circ\pi^-$, therefore, $S = -1$ and $T = 1$. Its baryon number is one and angular momentum is 3/2.

Evidence for an excited state of a K-particle has been obtained from hydrogen bubble chamber events

$$K^+ + p \rightarrow K^{*+} + p;\ K^* \rightarrow \overline{K}^* + \pi$$
$$K^- + p \rightarrow K^{*-} + p$$
$$K^- + p \rightarrow \overline{K}^{*\circ} + n.$$

The K^* excited state has rest mass 892.4 MeV/c^2 and isotopic spin half. It has a spin 1 and two values of strangeness $S = \pm 1$ in the two charge states as for the K-meson. In addition to these resonances, large number of others have been observed.

ω–Meson–Nambu in 1957 suggested the existence of a heavy neutral meson having zero isospin and unit angular momentum. Chew in 1960 had also shown that such a meson should exist on dynamical grounds as a 3π resonance, or bound state. The first experimental evidence for a three pion resonance, with $T = 0$ and $J = 1^-$, was found by a study of four pronged annihilation events when the 72 inch Berkeley hydrogen bubble chamber was exposed to a high energy antiproton beam. The over all process is

$$\overline{p} + p \rightarrow \pi^+ + \pi^- + \pi^\circ + \pi^+ + \pi^-.$$

In order to determine if a resonant state involving three pions are formed as an intermediate stage, three groups of pion triplets were studied, namely, singly charged $\pi^+\pi^+\pi^-$ and $\pi^-\pi^-\pi^+$, doubly charged

$\pi^+\pi^+\pi^0$ and $\pi^-\pi^-\pi^0$ and neutral $\pi^+\pi^-\pi^0$. About 800 bubble chamber events were analyzed and for each of the three groups a histogram was obtained of the number of triplets against the effective mass of the triplet. For the charged triplets, the histograms were in good agreement with the phase space distribution. The maximum is observed only in the case of neutral triplet. It follows, therefore, that a neutral resonant state is formed and that it decays into positive, negative and neutral pion. This resonant state is a **neutral meson**, known as the omega (ω)-meson. Thus the above reaction can be written as two stage process.

$$\bar{p} + p \rightarrow \omega^0 + \pi^+ + \pi^-$$

$$\omega^0 \rightarrow \pi^+ + \pi^- + \pi^0.$$

In the bubble chamber study of the four pronged proton antiproton annihilation events gave the evidence for a three pion resonance ω^0-meson. The state with charge zero shows a marked peak at a mass of 787 MeV but no such peak appears in the states with charge 1 or 2. The favoured state, therefore, has $T = 0$, $J = 1$ and parity odd. Gelfand *et al.* (1963) observed mass of 784.0 + 0.9 MeV, its decay into 3 π with width 9.5 ± 2.1 MeV and a life time of $(0.69 \pm 0.15) \times 10^{-22}$ sec. Maglic *et al.* (1961) observed mass of 787 MeV, resonance width <25 MeV and life time > 4×10^{-23} sec and the distance travelled before its decay into three pions > 13 fermis.

The ω-meson has also been observed in a liquid deuterium bubble chamber exposed to a high energy beam of π^+-mesons.

$$\pi^+ + d \rightarrow p + p + \pi^+ + \pi^- + \pi^0 \text{ or } p + p + \omega^0.$$

This experiment is accompanied by less background events than in proton-antiproton annihilation.

ρ-meson—Another quasi-particle is the rho (ρ)-meson. It is a two pions resonance particle. It can exist in three charge states ρ^+, ρ^- and ρ^0. These are produced in a fairly large fraction of high energy antiproton proton annihilations.

$$\bar{p} + p \rightarrow \rho + \pi + \pi.$$

The most frequent decay mode of the charged ρ-meson is

$$\rho^\pm \rightarrow \pi^\pm + \pi^0.$$

The most probable decay of ρ^0 is

$$\rho^0 \rightarrow \pi^+ + \pi^-.$$

Other decays have small branching ratios.

$$\rho^0 \rightarrow \pi^+ + \pi^- + \pi^0$$

$$\rho^0 \rightarrow \pi^+ + \pi^- + \pi^0 + \pi^0.$$

The observed rate of a dipion final state as a function of the total energy of the colliding beams (e^+ and e^- beams) shows a maxima at about 750 MeV. By calculating momenta of $\pi^+\pi^-$ pair by track chamber methods, the mass of ρ-meson was calculated as 765 ± 4 MeV/c^2.

The width of ρ^0-meson is 100 MeV so that its life time in sec is $\approx 10^{-23}$ sec.

As doubly charged states do not occur hence $T \neq 2$. The neutral and singly charged are observed, hence isospin $T = 1$. The assignment of $J = I$ is made by analyzing the angular distribution of the decay products of ρ-particles emitted parallel or anti-parallel to the direction of the incident pion. The decay should be spherically symmetrical for $J = 0$. The angular distribution shows $J = 1$. It follows negative parity, considering that two decay pions have zero intrinsic spin and even intrinsic parity.

η′-meson—The resonance state of η particle, named as η′ or χ^0, has mass 957.1 ± 0.6 MeV/c^2, spin 0, parity odd, isospin 0, hypercharge 0. The full width at half maximum is less that 4 MeV. Its decay modes are

$$\eta' \rightarrow \eta + \pi + \pi \; (68\%)$$

$$\rightarrow \pi^+ + \pi^- + \gamma \; (32\%).$$

There are other meson resonances few of them are listed in table 18.5.

These examples of resonance are divided into the categories of meson resonances and baryon resonances. Lepton resonances are not possible because the leptons cannot take part in the strong interactions whereby resonant states are formed and decay. The characteristics of resonances are also listed in the Table 18.5.

Table 18.5. The Hadrons (Strongly Interacting Particles)

	Symbol (mass, MeV)	J^P	*Width, MeV*	*Decay products and branching ratios %*
Mesons $Y = 0, T = 1$	$\pi(138)$	0^-	Hadronically stable	
	$\rho(775)$	1^-	160	$\pi\pi100$
	$\delta(980)$	0^+	50	$\eta\pi$, $K\bar{K}$
	$A_1(1100-1300)$	1^+	300	$\rho\ \pi100?$
	$B(1230)$	1^+	130	$\omega\ \pi100$
	$A_2(1315)$	2^+	100	$\rho\pi70$, $\eta\pi15$, $\omega\pi\pi10$, $K\bar{K}5$
	$\rho'\ (1600)$	1^-	300	$4\pi85$, $\pi\pi15$
	$A_3(1660)$	2^-	200	$f\pi60$, $\rho\pi30$
	$g(1690)$	3^-	200	$\pi\pi25$, $\omega\pi$, $A_2\pi$, $\rho\rho$....
$Y = 0, T = 0$	$\eta(549)$	0^-	Hadronically stable	
	$\omega(782)$	1^-	10	$\pi\pi\pi90$, $\pi\gamma9$, $\pi\pi1$
	$\eta'(958)$	0^-	0.3	$\eta\pi\pi66$, $\rho^0\gamma30$, $\omega\gamma^3$, $\gamma\gamma2$
	$S^*(980)$	0^+	40	$K\bar{K}$, $\pi\pi$
	$\phi(1020)$	1^-	4	K^+K^- 49, K_LK_S 35, $\rho\pi15$, $\eta\gamma2$
	$H(1190)$	1^+	300	$\rho\pi$
	$f(1275)$	2^+	180	$\pi\pi83$, $K\bar{K}$, $\pi\pi\pi\pi3$
	$\xi(1275)$	0^-	70	$\eta\pi\pi$
	$D(1285)$	1^+	30	$\eta\pi\pi50$, $\rho\pi\pi40$, $K\bar{K}10$
	$\epsilon(1300)$	0^+	200–400	$\pi\pi90$, $K\bar{K}10$
	$E(1420)$	1^+	50	$K^*\bar{K} + \bar{K}^*K$, $\delta\pi?$
	$\varepsilon(1440)$	0^-	50	$\delta\pi$
	$f'(1515)$	2^+	70	$K\bar{K}100\,?$
	$\theta(1650)$	2^+	200	$\eta\eta$
	$\omega(1665)$	3^-	165	$\rho\pi$, $B\pi$
	$h(2040)$	4^+	150	$\pi\pi$, $K\bar{K}$
	$r(2510)$	6^+	250	$\pi\pi$
	$\eta_c(2980)$	0^-	<20	$\eta\pi\pi$, $K\bar{K}\pi$, 4π, $K\bar{K}\pi\pi$, ...
	$\psi(3097) = \psi/J$	1^-	0.06	mesons 86, $\mu\bar{\mu}7$, $e\bar{e}7$
	$\chi(3415) = \chi_0$	0^+		$\pi\pi$, $K\bar{K}$, 4π, ... $J\gamma$?
	$\chi(3510) = \chi_1$	1^+		$J\gamma30$, 4π, ...
	$\chi(3556) = \chi_2$	2^+		$J\gamma15$, $\pi\pi$, $K\bar{K}$, 4π,...
	$\eta(3590) = \eta_0$	0^-		$\eta\pi\pi$, $K\bar{K}\pi$, 4π, $K\bar{K}\pi\pi$,...
	$\psi(3686) = \psi'$	1^-	0.2	$J\pi\pi50$, $\chi(3413)\gamma7$, $\chi(3508)\gamma7$, $\chi(3554)\gamma7$, $J\eta4$, $\mu\bar{\mu}1$, $e\bar{e}1$
	$\psi(3770) = \psi''$	1^-	25	$D\bar{D}100$
	$\psi(4030)$	1^-	50	hadrons
	$\psi(4160)$	1^-	80	hadrons
	$\psi(4415)$	1^-	~40	hadrons
	$\Upsilon(9460) = \Upsilon$	1^-	0.04	$\mu^+\mu^-$ 3, e^+e^- e, hadrons
	$\Upsilon(10024) = \Upsilon'$	1^-	0.02	$\mu^+\mu^-$ 2, e^+e^- 2, hadrons
	$\Upsilon(10355) = \Upsilon''$	1^-	0.01	$\mu^+\mu^-$ e^+e^-, hadrons
	$\Upsilon(10580) = \Upsilon'''$	1^-	15	$B\bar{B}100$

	Symbol (mass, MeV)	J^P	Width, MeV	Decay products and branching ratios %					
$S = 1$ $Y = 1, T = 1/2$	$K(495)$	0^-	Hadronically stable						
	$K^*(892) = K^*$	1^-	50	$K\pi$ 100					
	$Q_1(1280)$	1^+	120	$K\rho$40, $\kappa\pi$30					
	$Q_2(1400)$	1^+	150	$K^*\pi$95					
	$K^*(1435)$	2^+	100	$K\pi$49, $K^*\pi$27, $K^*\pi\pi$11, $K\rho$7, $K\omega$4, $K\eta$3					
	$\kappa(1500)$	0^+	250	$K\pi$					
	$L(1770)$	2^-	200	$K^*(1435)\pi$, $K^*\pi$, Kf					
	$K^*(1780)$	3^-	130	$K\pi\pi(l\rho, K^*\pi)$ $K\pi$20					
$T = 1/2, c = 1$	$D(1866)$	0^-	Hadronically stable						
	$D(2008) = D^*$	1^-	<2	$D\pi$, $D\gamma$					
$T = 0, S = +1, c = 1$	$F(1970) = F$	0^-?	Hadronically stable	$\phi\pi$, $\phi\pi\pi\pi$					
	$F(2140) = F^*$	1^-?		$F\gamma$					
$T = 1/2, b = +1$	$B(5275) = B$	0^-	Hadronically stable	$Dl\bar{\nu}$ or $D^*l\bar{\nu}$ [$l = e, \mu$ or τ] 80					
Baryons	$N(939) = N$	$1/2^+$	Hadronically stable	$N\pi$	$\Delta\pi$	$N\rho$	$N\epsilon$	$N\eta$	
	$N(1450)$	$1/2^+$	200	50–65	23,	7,	7,	18	
	$N(1520)$	$3/2^-$	125	55,	23,	19,	<5		
	$N(1535)$	$1/2^-$	150	40,	1,	3,	2,	55	
$Y = 1, T = 1/2$	$N(1650)$	$1/2^-$	150	60,	4–15,	7–21,	<10,	ΛK10,	ΣK2–7
Nucleons	$N(1680)$	$5/2^-$	155	40,	50,	5			
	$N(1680)$	$5/2^+$	130	60,	18,	13,	22		
	$N(1700)$	$3/2^-$	120	10,	15–40,	<5,	<40,	4	
	$N(1710)$	$1/2^+$	120	20,	10–20	40–65,	15–40,	2–20,	ΣK10
	$N(1810)$	$3/2^+$	200	17,	20,	40–70	20		
	$N(1990)$	$7/2^+$	250	5,				3	
	$N(2190)$	$7/2^-$	250	15,				2	
	$N(2200)$	$9/2^-$	250	10,				2	
	$N(2220)$	$9/2^+$	300	20,				1	
	$N(2650)$	$11/2^-$	400	5					
	$N(3030)$	?	400						
$Y = 1, T = 3/2$	$\Delta(1232) = \Delta$	$3/2^+$	115	100					
	$\Delta(1620)$	$1/2^-$	140	32,	40,	<50			
	$\Delta(1640)$	$3/2^+$	250	20,	30–45	<10			
	$\Delta(1700)$	$3/2^-$	200	15,	<50,	40			
	$\Delta(1910)$	$1/2^+$	220	20–25,	<40,		ΣK2–20		
	$\Delta(1920)$	$3/2^-$	200	4–12					
	$\Delta(1920)$	$5/2^+$	250	15,	10–30,	60			
	$\Delta(1950)$	$7/2^+$	240	40,	30,	20			
	$\Delta(2420)$	$11/2^+$	300	10					
	$\Delta(2850)$	$15/2^+$?	400						
	$\Delta(3230)$	$19/2$?	440						

	Symbol (mass, MeV)	J^P	Width, MeV	Decay products and branching ratios %			
$Y = 0, J = 0, S = -1$	$\Lambda(1116) = \Lambda$	$1/2^+$	Hadronically stable				
					$N\bar{K}$	$\Sigma\pi$	
Hyperons	$\Lambda^*(1405)$	$1/2^-$	40			100	
	$\Lambda^*(1520)$	$3/2^-$	16		46,	42,	$\Lambda\pi\pi 10$
	$\Lambda(1670)$	$1/2^-$	40		20,	20–60,	$\Lambda\eta$ 15–35
	$\Lambda(1690)$	$3/2^-$	60		25,	20–40,	$\Lambda\pi\pi 25$, $\Sigma\pi\pi 20$
	$\Lambda(1800)$	$1/2^-$	300		25–40		
	$\Lambda(1815)$	$5/2^+$	80		60,	10,	$\Sigma^*\pi$5–10
	$\Lambda(1830)$	$5/2^-$	95		<10,	35–75,	$\Sigma^*\pi > 15$
	$\Lambda(1870)$	$3/2^+$	100		15–40,	3–10	
	$\Lambda^*(2100)$	$7/2^-$	250		30,	5	
	$\Lambda(2110)$	$5/2^+$	200		5–25,	<40,	$N\bar{K}^*(892)$ 20–60
	$\Lambda(2350)$	$9/2^+$	120		12,	10	
	$\Sigma(1193) = \Sigma$	$1/2^+$	Hadronically stable				
				$N\bar{K}$	$\Lambda\pi$	$\Sigma\pi$	
	$\Sigma(1385) = \Sigma^*$	$3/2^+$	35		88,	12	
	$\Sigma(1660)$	$1/2^+$	100	<30			
	$\Sigma(1670)$	$3/2^-$	50	10,	<20,	20–60	
$Y = 0, T = 1, S = -1$	$\Sigma(1750)$	$1/2^-$	75	10–40,	5–20,	<8,	$\Sigma\eta$15–55
	$\Sigma(1765)$	$5/2^-$	120	41,	14,	1,	$\Lambda(1520)\pi 19$, $\Sigma^*\pi 9$
	$\Sigma(1915)$	$5/2^+$	100	10	15		
	$\Sigma(1940)$	$3/2^-$	220	<20			
	$\Sigma(2030)$	$7/2^+$	180	20,	20,	5–10,	$\Lambda(1520)\pi 15$, $\Sigma^*\pi 10$
	$\Sigma(2250)$	$7/2^-$?	100	<10			
	$\Sigma(2455)$	?	120				
	$\Sigma(2595)$	?	200				
$Y = 1, T = 1/2, S = -2$	$\Xi(1318) = \Xi$	$1/2^+$	Hadronically stable				
	$\Xi(1530)$	$3/2^+$	10				$\Xi\pi 100$
	$\Xi(1820)$	$3/2^-$?	20				$\Lambda\bar{K}45, \Xi(1530)\pi 45, \Sigma\bar{K}10$
	$\Xi(2030)$	?	16				$\Sigma\bar{K}80, \Lambda\bar{K}20$
$T = 0, S = -3$	$\Omega^-(1672)$	$3/2^+$	Hadronically stable				
$T = 0, c = +1$	$\Lambda_c^+(2280)$	$1/2^+$	Hadronically stable				
$= 1, c = +1$	$\Sigma_c(2440)$	$1/2^+$		$\Lambda_c^+\pi$			

18.18 ELEMENTARY PARTICLE SYMMETRIES

Mendelyeev was able to predict correctly the atomic weights and other properties of then unknown elements by means of his periodic system. Similarly, the classification of the elementary particles has also met with success in predicting new particles. The method developed for the arrangement is based on a branch of advanced mathematics, known as group theory. It has been found that, in general, *the conservation law represents an invariance which corresponds to an appropriate symmetry operation.* The set of operators that represents the symmetry constitutes the group from which the theory gets its name. The irreducible representations of a group consist of a number of states, quantities or objects to which the symmetry operations are applicable. Thus the appropriate group operation can transform any one of these states into another in the same representation. The fundamental representation is the one containing the smallest number of states for the particular group.

Linear momentum is conserved if the system is invariant with respect to displacement in space. Angular momentum is conserved if invariance is with respect to angular displacement and energy is conserved if it is with respect to time.

The simplest unitary group U (1) contains transformations which add a phase factor only to particle wave functions. The invariance under such transformations gives *conservations of charge Q, baryon number B, lepton number L and hypercharge Y.*

Unitary Symmetry [SU (2) Symmetry]. We know that proton and neutron are identical as far as the nuclear force is concerned, but differ in their electromagnetic interactions. Thus, it is possible to imagine a group of symmetry operators which could transform a neutron into a proton (or proton into a neutron) in the absence of an electromagnetic field. The proton and neutron would then form the fundamental representations of the group. The existence of such a symmetry implies that something remains constant under the strong interaction. This is known as isospin and is $\frac{1}{2}$ for proton as well as for neutron. The component of the isospin, T_3 is $+\frac{1}{2}$ for the proton and $-\frac{1}{2}$ for the neutron. The operators of the symmetry group thus change the co-ordinates of isospin in such a way as to reverse the sign of T_3. It can also be expressed as : *the strong interactions are assumed to be invariant under rotations in the isotopic spin space.*

The particular symmetry group applicable to isospin conservation is a form of *unitary symmetry known as* U (2), which can be expressed by a set of 2 × 2 matrices. This group may be reduced to a *special unitary group S U* (2), which is also written as SU_2. It is *special* because a restriction reduces by unity the number of operators in the group. The two dimensions refer to the two basic states which make up the fundamental representation in this case. The restriction of special reduces the number of operators 2 × 2 = 4 to three. The group is then said to have *three generators.*

By the use of the algebra of the SU (2) group it can be shown that all irreducible representations of the symmetry group consist of a multiplet of $2T + 1$ states. All the members of the multiplet have the same isospin T and are essentially identical except for charge. If the symmetry was exact, *i.e.* isospin is strictly conserved, the components of a multiplet would differ in charge and T_3. The SU(2) symmetry is violated by the *electromagnetic interaction for which conservation of isospin is not applicable.*

The nucleon states $|p>, |n>$ have anti-nucleon states $|\bar{p}>, |\bar{n}>$. Omitting| > brackets for clarity and separating the trace from traceless part, the combination of nucleon with an anti-nucleon may be represented as

$$\begin{pmatrix} p \\ n \end{pmatrix} \times (\bar{p}\,\bar{n}) \rightarrow \frac{p\bar{p}+n\bar{n}}{\sqrt{2}} \begin{pmatrix} 1 & 0 \\ 0 & 1 \end{pmatrix} + \begin{pmatrix} (p\bar{p}-n\bar{n})\frac{1}{2} & p\bar{n} \\ n\bar{p} & (p\bar{p}-n\bar{n})\frac{1}{2} \end{pmatrix}$$

The first term of R.H.S. represents singles (η meson, $T = 0$, $J = 0^-$) and the second term represents the triplet array (pions $T = 1$, $J = 0^-$). The second term can be written in array from with normalizing factors

$$\begin{pmatrix} \pi^0/\sqrt{2} & \pi^+ \\ \pi^- & \pi^0/\sqrt{2} \end{pmatrix}$$

Under the SU (2) group operations, the particle states transform into each other with in these multiplets :

Eightfold Way [SU (3) Symmetry].—Since SU (2) group cannot accommodate the hypercharge quantum number, the more general theory SU (3) has been used which also includes SU (2). SU (3) stands for *special unitary group in three dimensions.* The term, *three dimensions* refers to the three basic states which make up the fundamental representation in this case. In a three dimension unitary group there are, in general 3 × 3 = 9 operators, but the restriction of "special" reduces the number to eight. The group is then said to have *eight generators.* Gell-Mann has referred to the resulting group of symmetry operators as the eightfold way, named for *Buddha's Eightfold Path to Nirvana, comprising eight right actions.* Three of the generators apply to three components of isospin, as in SU (2) and a fourth is associated with hypercharge. The remaining four also involve hypercharge in a different way.

Application of the group algebra showed that the SU (3) symmetry should give rise to six supermultiplets, containing 1, 8, 8, 10, $\overline{10}$ and 27 members. The $\overline{10}$ multiplet is equivalent to the 10 but with hypercharges of opposite signs. In each of these supermultiplets the parity and intrinsic spin of members are the same, while the hypercharge and the isotopic spin are not same. Among above mentioned groups, 8 and 10 member groups are of particular interest.

In the case for $B = 0$ we may form particle anti-particle states to fill a 3 × 3 array :

$$\begin{pmatrix} p \\ n \\ \Lambda \end{pmatrix} \times (\bar{p}\,\bar{n}\,\bar{\Lambda}) \rightarrow \left\{ \begin{matrix} \frac{1}{3}(2p\bar{p} - n\bar{n} - \Lambda\bar{\Lambda}) & p\bar{n} & p\bar{\Lambda} \\ n\bar{p} & \frac{1}{3}(-p\bar{p} + 2n\bar{n} + \Lambda\bar{\Lambda}) & n\bar{\Lambda} \\ \Lambda\bar{p} & \Lambda\bar{n} & \frac{1}{3}(-p\bar{p} - n\bar{n} + 2\Lambda\bar{\Lambda} \end{matrix} \right\}$$

It can be identified with known spin zero mesons

$$\left\{ \begin{matrix} (\pi^{\circ}/\sqrt{2} + (\eta/\sqrt{6}) & \pi^{+} & K^{+} \\ \pi^{-} & (-\pi^{\circ}/\sqrt{2}) + (\eta/\sqrt{6}) & K^{\circ} \\ K^{-} & \bar{K}^{\circ} & -2\eta/\sqrt{6} \end{matrix} \right\}$$

The neutral π and η mesons are now written as

$$\pi^{\circ} = (p\bar{p} - n\bar{n})/\sqrt{2};$$

$$\eta = (p\bar{p} + n\bar{n} + 2\Lambda\bar{\Lambda})/\sqrt{6}.$$

There is in addition the symmetrical neutral combination or singlet

$$\eta' = p\bar{p} + n\bar{n} + \Lambda\bar{\Lambda}/\sqrt{3}.$$

The matrix array contains a total of eight states and is known as an *octet*. Since the mesons are formed from fermion particle-antiparticle pairs, hence have odd parity. These eight particles with $B = 0$, and $J^{\pi} = 0^{-}$ should be arranged as :

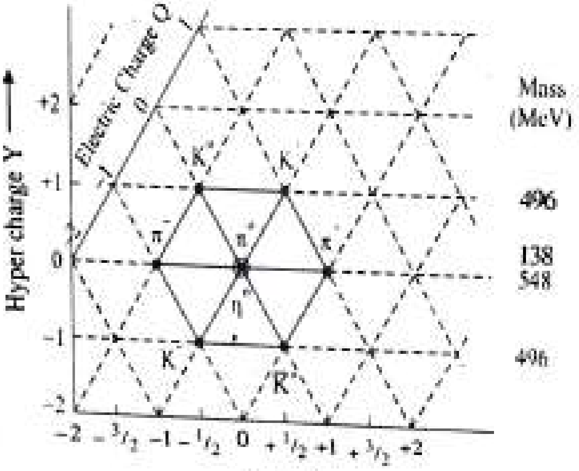

Fig. 18.23. Meson Octet ($J^{\pi} = 0^{-}$).

$$\left.\begin{matrix} \textit{one triplet with} & Y = 0, & T = 1 \\ \textit{one doublet with} & Y = 1, & T = \frac{1}{2} \\ \textit{one doublet with} & Y = -1, & T = \frac{1}{2} \\ \textit{one singlet with} & Y = 0, & T = 0 \end{matrix}\right\} \text{8 members} \quad \begin{matrix} \pi^{-}, \pi^{\circ}, \pi^{+} \\ K^{\circ}, K^{+} \\ \bar{K}^{\circ}, K^{-} \\ \eta^{\circ} \end{matrix}$$

When this was first postulated, there were seven ground state mesons. The missing meson was expected to have $Q = 0$, $Y = 0$, $T = 0$ and was predicted both by Gell-Mann and by Ne'eman. This eighth meson was named η°-meson. Octects of metastable mesons (zero intrinsic spin) is shown in Fig. 18.23.

In 1962, Gell-Mann and in 1961 Ne'eman pointed out that the baryon also formed an octet array which corresponded with the octet representation of *SU* (3). The octet array is as :

$$\left\{ \begin{matrix} (\Sigma^{\circ}/\sqrt{2} + \Lambda/\sqrt{6}) & \Sigma^{+} & p \\ \Sigma^{-} & (-\Sigma^{\circ}/\sqrt{2} + \Lambda/\sqrt{6}) & n \\ \Xi^{-} & \Xi^{\circ} & -2\Lambda/\sqrt{6}) \end{matrix} \right\}$$

These are eight in number (p, n, Λ°, Σ^{+}, Σ^{-}, Σ°, Ξ^{-}, Ξ°). For these $J^{\pi} = \frac{1}{2}^{+}$, $B = 1$. The eightfold way arrangement of this baryon octet is shown in Fig. 18.24.

Another interesting case is that of the boson octet with $J^{\pi} = 1^{-}$. The particles are :

$K^{*\circ}(T_3 = -\frac{1}{2}, Y = 1)$, $K^{*+}(T_3 = \frac{1}{2}, Y = 1)$,

$\rho^{-}(T_3 = -1, Y = 0)$, ϕ° & $\rho^{\circ}(T_3 = 0, Y = 0)$, $\rho^{+}(T_3 = 1, Y = 0)$,

$K^{*-}(T_3 = -\frac{1}{2}, Y = -1)$, $\bar{K}^{*\circ}(T_3 = \frac{1}{2}, Y = -1)$.

For $J^{\pi} = 1^{-}$, a boson singlet ω° ($T = 0$, $Y = 0$) has also been suggested. Neither the mass of ϕ° nor ω° fits with the expected value of M_0 in above relation. The masses of ω° and ϕ° are found approximately equally distant from the expected value ($M_0 = 930\ MeV/c^2$) of mass. Gell-Mann and later Sakurai explained this by assuming ω° and ϕ° approximately the following mixtures of the octet and singlet states

$$\text{Real } \omega = \sqrt{(1/3)}\,\phi - \sqrt{(2/3)}\,\omega$$

$$\text{Real } \phi = \sqrt{(2/3)}\,\phi + \sqrt{(1/3)}\,\omega. \qquad ...(58)$$

Without really knowing which particle belongs in the octet state and which in the singlet, the ϕ° has been arbitrarily placed in the octet.

Gell Mann derived a relationship among the average masses of the components of the four baryon multiplets in the intrinsic spin half octet, given as

$$2\,(M_N + M_\Xi) = 3\,M_\Lambda + M_\Sigma, \qquad ...(59)$$

where M_N is the average nucleon mass and the average masses of the hyperons are indicated by the respective subscripts.

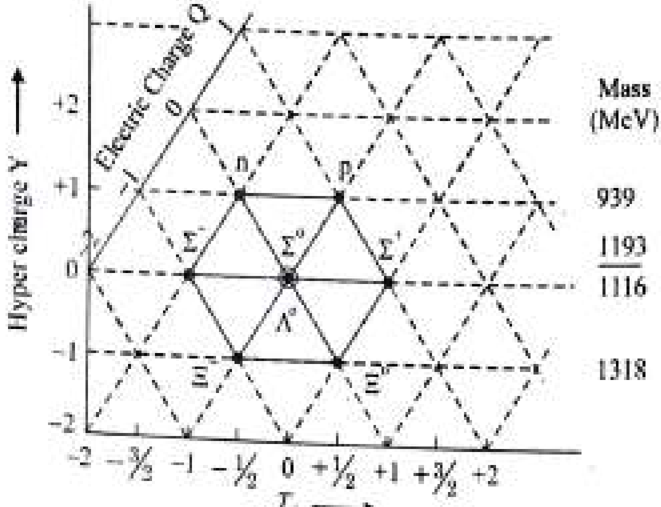

Fig. 18.24. Baryon Octet ($J^\pi = 1/2^+$).

Since the *SU* (3) couplings are the same for any octet one might expect the results for the baryon octet to apply without change to the meson octets. Thus we predict

$$2(M_{K^\circ} + M_{\overline{K}^\circ}) = M_{\pi^\circ} + 3\,M_{\eta^\circ} \qquad ...(60)$$

Since masses of the K° and $\overline{K^\circ}$ are nearly equal, thus one may expect

$$3M_{\eta^\circ} = 4\,M_{K^\circ} - M_{\pi^\circ}. \qquad ...(61)$$

The substitution of the experimental masses shows a discrepancy of about 12%. Gell-Mann-Okubo suggested that the mass formula could be better if the square of the mass was used in place of the mass, *i.e.*

$$M^2_{\eta^\circ} = \tfrac{1}{3}\left(4M^2_{K^\circ} - M^2_{\pi^\circ}\right). \qquad ...(62)$$

The above relations are special cases of the general formula, given by *M*. Gell-Mann and *S*. Okubo

$$M\,(T, Y) = M_0\,[1 + aY + b\,\{T\,(T+1) - \tfrac{1}{4}\,Y^2\}], \qquad ...(63)$$

where a and b are constants for a particular multiplet.

The baryon octet for intrinsic spin $3/2^-$ consists of one doublet ($Y = +1$; resonance states N^{*0} with $T_3 = -1/2$ and N^{*+} with $T_3 = 1/2$); one doublet ($Y = -1$; resonance states Ξ^{*-} with $T_3 = -1/2$; and Ξ^{*0} with $T_3 = 1/2$); one triplet ($Y = 0$; resonance states Y^{*-} with $T_3 = -1$, Y^{*0} with $T_3 = 0$ and Y^{*+} with $T_3 = +1$) and one singlet ($Y = 0$, $T_3 = 0$ and member is $Y^{*(0)}$).

A more remarkable prediction was the case of the ten-fold baryon group with intrinsic spin $3/2^+$. Theory predicted that there should be a group of ten members : $Y = 1$, $T = 3/2$, quartet (nucleon resonance denoted by $N_{3/2}$ and exists in four charge states), $Y = 0$, $T = 1$, triplet (hyperon resonance Y_1^* which is containing excited Σ particles), $Y = -1$, $T = 1/2$, doublet (hyperon resonance which is equivalent to excited cascade particles Ξ), $Y = -2$, $T = 0$, singlet (a particle Ω with charge−1).

In 1962, when the proposal was made to incorporate the N, Y_1, and Ξ resonances in a decuplet, the tenth particle was unknown. The existence of such a particle was predicted by Gell Mann and was named omega (Ω). The baryon decuplet for intrinsic spin $3/2^+$ is shown in Fig. 18.25.

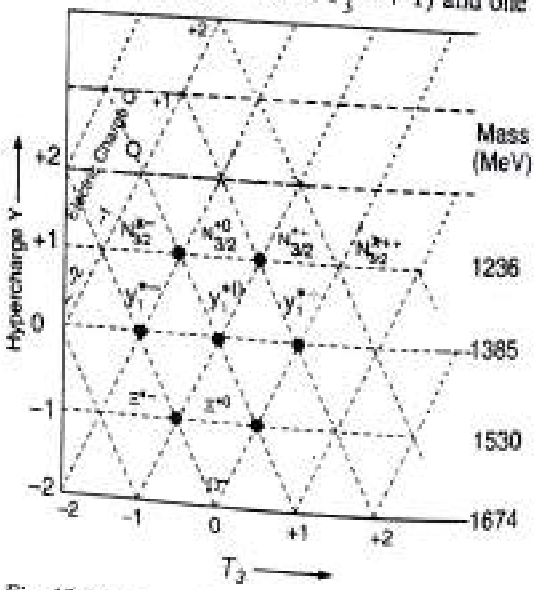

Fig. 18.25. Baryon decuplet for intrinsic spin $3/2^+$.

Before the Ω^- had been discovered, the values of a and b (Eq. 63) could be found in order to fit the $Y = 1$, 0 and -1. Thus the mass of the $Y = -2$ member was predicted as 1676 MeV, while the measured value is 1675 MeV.

Although all the other members of the baryon decuplet for intrinsic spin 3/2 are resonant states, decaying by the strong interaction, Gell-Mann noted that the Ω^--particle should decay by the weak interaction. Possible decay modes are

$$\begin{aligned}\Omega^- &\rightarrow \Xi^- + \pi^\circ\\ &\rightarrow \Xi^\circ + \pi^-\\ &\rightarrow K^- + \Lambda^\circ.\end{aligned}$$

It is clear that in these modes baryon number is conserved while isospin, hypercharge and strangeness are not conserved. These conservations only hold for strong interactions, hence the decay of Ω^- is by weak interaction.

In a recent development attempts have been made to combine ordinary spin with T and Y. The new group is described as SU (6).

18.19 QUARKS

Quarks are the basic constituent particles of which elementary particles are now believed to be composed. Many phenomena in particle physics have been predicted and explained theoretically with the concept of quarks. However the experimental observation of free quarks remains ambiguous. There were at least three factors which made a quark model plausible in the 1960s. *(i)* The classic electron-proton elastic scattering experiments which demonstrated a proton with a finite form factor. This showed a finite radial extent of the electric charge and magnetic moment distributions. *(ii)* The hadron spectroscopy revealed an order and symmetry among the states of hadronic matter that could be interpreted with the symmetry laws. *(iii)* The deep inelastic scattering of electrons on protons revealed form factors corresponding to point like quasi-free constituents (called *partons*) of the hadrons such as the proton.

Until 1974, only three flavours of quarks were known, two of very nearly equal mass, called *up quark* (u) and the *down* quark (d). The proton, neutron and pi-mesons are composed of these two quarks. The third, more massive quark is called *strange* quark (s). It is a constituent of strange particles such as K-mesons, Λ°-hyperons etc. The u and d quarks form an isospin doublet, they are alike except for T_3 and Q, while the s-quark is an isospin singlet since no other quark is found to possess strangeness. Mesons are composed of a quark and antiquark pair. The antiparticles are formed by the antiquarks of those forming the particle.

In 1974, the discovery of unusual elementary particles (J/ψ meson) with lifetimes about 1000 times longer than typical mesons which decay through the strong interaction gave the direct evidence for the new quark. The new quark has to possess a property like strangeness which was called *'Charm'* or c-quark. In 1977, at Fermi National Accelerator Lab near Chicago, L.M. Lederman and his colleagues reported a new resonance (*upsilon particle* at about 9.4 GeV and suggested it as the lowest lying state of a new quark system. This new quark was named *'b'* for *bottom* (or *beauty*). Physicists expect a similar heavier quark which has the same relationship to the b-quark that the charm quark has to the strange quark. In 1984, a CERN group reported that the observed state with a mass of 30 to 50 GeV/c^2 might be a meson containing this heavier quark named t quark. The t may stand for *top* (or *truth*).

The word *'flavour'* is used to distinguish between the quarks for convenience, not because it has anything to do with taste. Besides the flavour, quarks also come in three different *colours, e.g., red, green* and *blue*. The colour and flavour are quantum mechanical labels or quantum numbers very similar to spin and parity, that are needed to differentiate between the different states.

The *up, charm* and *top* (u, c and t) flavours each carry a positive electric charge equal in magnitude to two thirds that of the electron $\left(\frac{2}{3}e\right)$ and the *down, strange* and *bottom* (d, s and b) flavours have a negative charge one third that of the electron $\left(-\frac{1}{3}e\right)$. These two groups are also called as *up quarks* (u, c and t) with charge $\frac{2}{3}e$ and the *down quarks* (d, s and b) with charge $-\frac{1}{3}e$. The quarks have a spin angular momentum of one half unit of $\hbar$. They obey Fermi-Dirac statistics. As for interacting particles, no two quarks within a particular system can have exactly the same quantum numbers. Since the Ω-particle is made of three strange quarks, thus seems to violate the Pauli exclusion principle. O.W. Greenberg in 1964 suggested that the each quark type (u, d and s) comes in three varieties identical in all measurable qualities but different in an additional property, which is known as colour. The colour hypothesis thus triples the number of quarks. It triples the rate of decay of π^0-meson and the total production cross-section for baryons and mesons in electron-positron annihilation. The experimental result at energies between 2 GeV and 3 GeV is in reasonable agreement with this colour hypothesis.

Experimental Evidence—The quarks are not observed as free objects in high energy collisions. The reason may be their very high mass or in addition, they might be produced so rarely that the quark production cross-section might be very low. The positive evidence for quark was reported in 1969 from the cosmic rays, but the subsequent more sensitive cosmic ray experiments have failed to confirm those observations.

In an experiment at the Intersecting Storage Rings (ISR) for CERN, several telescopes of scintillation counters, Čerenkov counters and multiwire proportional chambers were assembled to search for particles of fractional charge emerging from the proton-proton intersection region. No quarks were observed with $p-p$ collisions at 52 GeV in the centre of mass among the products of 1.2×10^{10} $p-p$ interactions. Corresponding to an upper limit quark production cross-section is of $4 \times 10^{-35}\,cm^2$. This search was sensitive to quarks upto 23 GeV/c^2 rest mass. Two other experiments were carried out at the synchrotron of the Fermi National Accelerator Laboratory near Chicago. 300 GeV protons struck a beryllium target and the beams of secondary particles were detected. In the first experiment, a telescope of scintillation counters was used to search for particles of fractional charge (*quarks*). No such particle was observed among 1.4×10^9 negative particles (mesons) corresponding to an upper limit production cross section of about $10^{-36}\,cm^2$. This search was sensitive to quarks of upto 12 GeV/c^2 rest mass. The second search was with similar beams over longer period and with additional detectors. No quarks were observed with an upper limit production cross section of about $10^{-39}\,cm^2$ for 9 GeV/c^2 rest mass quarks of charge $\frac{1}{3}e$ and $10^{-38}\,\text{cm}^2$ for 11 GeV quarks of charge $-\frac{2}{3}e$.

Quark Masses—Among the six quarks, the least massive members are the u- and d- quarks, each of same mass, around 0.39 GeV/c^2. The lighest baryons, nucleons, Δ-particles, and the lightest mesons, pions must therefore be exclusively made of these two quarks. The s-quark is more massive, around 0.51 GeV/c^2. It carries a quantum number called strangeness and is therefore a necessary constituent of particles called strange particles (with non-zero strangeness), such as K-mesons, and baryon Λ. The c-quark is even more massive, having rest mass around 1.65 GeV/c^2. The b-quark has a rest mass around 5 GeV/c^2. The t-quark is even heavier, having rest mass about 30 GeV/c^2. The t-quark has been confirmed experimentally as it requires a new generation of higher energy accelerators for its creation. It is also possible to discover a fourth generation of quarks, beyond these three groups.

Quantum Numbers—The quarks have quantum numbers. The s-quark has a quantum number called strangeness. Like strangeness, the C, $\mathcal{B}$ and $\mathcal{T}$ quantum numbers are conserved in the strong and electromagnetic interactions and change by one unit in the weak interactions. This means that the number of quarks minus antiquarks for each s, c, b and t must remain constant in strong and electromagnetic interactions, whereas in the weak interaction there is a change of quark flavour with the preferred sequence $t \to b \to c \to s$. Since three of the quarks are needed to make a baryon, therefore, the baryon number is 1/3 for all the quarks. The isospin quantum number T is 1/2 and therefore T_3 = 1/2 and −1/2 for the up and down quarks respectively. The *quantum number* S of strange quark and $\mathcal{B}$ of beauty quark is −1. It is 1 for the charm and top quarks. The quark quantum numbers are summarized in table 18.6. These are related with the charge Q and isospin component T_3 with the relation

$$Q = T_3 + (\mathcal{B} + S + C + \mathcal{B} + \mathcal{T})/2$$

Thus for the up (isospin direction) or u-quark

$$Q = \tfrac{1}{2} + \left(\tfrac{1}{3} + 0 + 0 + 0 + 0 + 0\right)/2 = 2/3.$$

For the down (opposite to isospin direction) or d quark

$$Q = -\tfrac{1}{2}+\left(\tfrac{1}{3}+0+0+0+0+0\right)/2=-1/3.$$

For the strange or s-quark, $Q = 0+\frac{1}{2}\left(\frac{1}{3}-1+0+0+0\right)=-1/3.$

Table 18.6. Quark Quantum Numbers and Properties

Quantum Number	u	d	s	c	b	t
Charge	2/3	– 1/3	– 1/3	2/3	– 1/3	2/3
Mass (GeV/c^2)	0.39	0.39	0.51	1.55	~ 5	~ 30
Spin in $\hbar$	1/2	1/2	1/2	1/2	1/2	1/2
Isospin I	1/2	1/2	0	0	0	0
Isospinz Component I_3	1/2	– 1/2	0	0	0	0
Baryon number $\mathcal{B}$	1/3	1/3	1/3	1/3	1/3	1/3
Strangeness S	0	0	–1	0	0	0
Charm C	0	0	0	1	0	0
Bottom $\mathcal{B}$	0	0	0	0	–1	0
Top $\mathcal{T}$	0	0	0	0	0	1

The hypercharge is a quantum number related to quark strangeness and baryon number, whereas the isospin is a quantum number related to the $u-d$ quark difference. The colour quantum number breaks the degeneracy and allows up to three quarks of the same flavour to occupy a single quantum state.

Mesons and Baryons—All hadrons are made of six quarks and their antiquarks. The properties of the quarks is inferred from the properties of mesons and baryons. To know the masses of the quarks from the known hadron masses, we need to know the strength of the interaction between quarks in the hadron. The hadrons are subdivided into two classes, baryons and mesons. Baryons are Fermions, this implies that quarks are also the fermions. Since the quark cannot exist as a free particle, the lightest fermion in the hadron family must therefore be made of three quarks. Thus

$$|p> = |uud> \quad \text{and} \quad |n> = |u\,dd>.$$

$$\therefore \quad Q_p = \tfrac{2}{3}+\tfrac{2}{3}+\left(-\tfrac{1}{3}\right)=1;\ Q_n=\tfrac{2}{3}-\tfrac{1}{3}-\tfrac{1}{3}=0.$$

Bosons obey Bose-Einstein statistics, may be made from any even number of fermions. Thus the mesons are constructed of an even number of quarks. The mesons must be made of an equal number of quarks and antiquarks. The π-mesons, the lighest number among the mesons are made of a quark either u or d, and an anti quark, either $\bar{u}$ or $\bar{d}$.

18.20 ISOSPIN OF QUARKS

The nucleons are assigned the isospin $T = 1/2$. The proton and neutron are two states with isospin component T_z or T_3 as 1/2 and – 1/2 respectively. The nucleon may be represented as a column matrix with two components

$$N = \begin{pmatrix} p \\ n \end{pmatrix}$$

Thus the two states of the nucleon may be represented in column vector notation as

$$|p> = \begin{pmatrix} 1 \\ 0 \end{pmatrix} \text{ and } |n> = \begin{pmatrix} 0 \\ 1 \end{pmatrix}$$

If we introduce operators isospin raising τ_+ and isospin lowering τ_- that transform the neutron state to the proton state and the proton to the neutron state respectively, *i.e.*,

$$\tau_+|n> = |p> \text{ and } \tau_-|p> = |n>. \qquad \ldots(64)$$

We thus find

$$\tau_+ = \begin{pmatrix} 0 & 1 \\ 0 & 0 \end{pmatrix} \text{ and } \tau_- = \begin{pmatrix} 0 & 0 \\ 1 & 0 \end{pmatrix} \qquad \ldots(65)$$

The operators τ_+ and τ_- are not Hermitian but Hermitian matrices, and can be defined in terms of x-and y-components of the isospin operator τ as

$$\tau_+ = \tfrac{1}{2}(\tau_1+i\tau_2) = \begin{pmatrix} 0 & 1 \\ 0 & 0 \end{pmatrix} \text{ and } \tau_- = \tfrac{1}{2}(\tau_1-i\tau_2) = \begin{pmatrix} 0 & 0 \\ 1 & 0 \end{pmatrix}$$

$$\therefore \qquad \tau_1 = \begin{pmatrix} 0 & 1 \\ 1 & 0 \end{pmatrix} \text{ and } \tau_2 = \begin{pmatrix} 0 & -i \\ i & 0 \end{pmatrix} \qquad ...(66)$$

If we further define the z-component $\tau_3 = \begin{pmatrix} 1 & 0 \\ 0 & -1 \end{pmatrix}$

The eigenfunctions of the τ_3 operator for a nucleon

$$\tau_3 | p > = \begin{pmatrix} 1 & 0 \\ 0 & -1 \end{pmatrix}\begin{pmatrix} 1 \\ 0 \end{pmatrix} = \begin{pmatrix} 1 \\ 0 \end{pmatrix} = | p >$$

$$\tau_3 | n > = \begin{pmatrix} 1 & 0 \\ 0 & -1 \end{pmatrix}\begin{pmatrix} 0 \\ 1 \end{pmatrix} = -\begin{pmatrix} 0 \\ 1 \end{pmatrix} = -| n >.$$

Thus $| p >$ and $| n >$ are the eigenstates of τ_3 with eigen values + 1 and − 1 respectively.

In terms of quarks, we may write equation (64) as

$$\tau_+ | udd > = | uud > \text{ and } \tau_- (uud > = | udd > .$$

Thus we see that the only difference between a proton and neutron is the replacement of one of two u-quarks by a d-quark and the isospin raising operator τ_+ acts on the quarks, transforming a d-quark to a u-quark and the other way for the isospin lowering operator. We therefore conclude that d- and u-quarks also form an isospin doublet.

$$T_3(u) + T_3(u) + T_3(d) = T_3(p) = 1/2$$

and

$$T_3(u) + T_3(d) + T_3(d) = T_3(n) = -1/2.$$

$\therefore$ $T_3 = 1/2$ to a u-quark and $= -1/2$ to a d-quark. Thus $\tau_+ | d > = | u >$.

18.21 QUARK WAVE FUNCTIONS OF PSEUDO SCALAR MESONS

The pions are the least massive particles among mesons. Both orbital angular momentum l and intrinsic spin s are zero, thus $J = 0$ for pions. They are therefore called scalar particles. However unlike ordinary scalars, their wave functions change under a parity transformation. Therefore the pion wave function behaves like a pseudoscalar quantity—invariant under a rotation but changes sign under an inversion of the coordinate system. The pions and other $J^P = 0$ mesons are called *pseudoscalar mesons*. Three pions and one η-meson can be constructed by u, d, $\bar{u}$ and $\bar{d}$ quarks. The strange quarks s and its anti quark $\bar{s}$ are included to explain other four pseudoscalar mesons. They are listed along with their quark contents in Fig. 18.26.

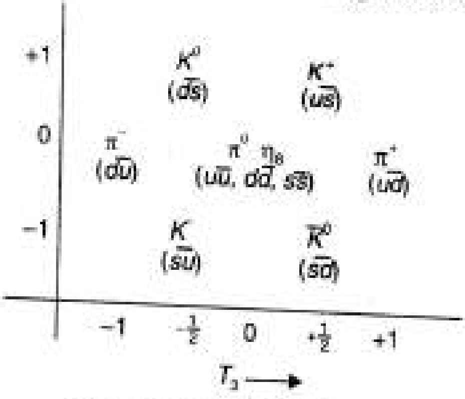

Fig. 18.26. Pseudoscalar mesons.

We know that π^--meson has isospin $T = 1$ and $T_3 = -1$. Since we cannot use any quarks other than u, d, $\bar{u}$ and $\bar{d}$. To form a system with $T_3 = -1$, we have to adopt the $\bar{u}d$ combination. Two particles with isospin − 1/2 can only be coupled to total isospin 0 and 1. The $\bar{u}d$ system cannot be $T = 0$ as it has $T_3 = -1$. Since there is no other way to form a $T = 1$ and $T_3 = -1$ state with u, d, $\bar{u}$ and $\bar{d}$, therefore

$$| \pi^- > = | \bar{u}d >.$$

One can construct the wave function of π^0 from the wave function of π^- by using the isospin raising operator

$$| \pi^0 > = N\tau_+ | \pi^- > = N\sum_{i=1}^{2} \tau_+(q_i) | \bar{u}\, d > .$$

We know that $\qquad \tau_+ | d > = | u >$, $\tau_+ | u > = 0.$

For the antiquarks $\tau_+ | \bar{u} > = -| \bar{d} >$, $\tau_+ | \bar{d} > = 0,$

where the negative sign is due to the symmetry requirement under charge conjugation.

$$\therefore \qquad N\,|\,\pi^\circ > \;=\; \tau_+(q_1)\,|\,\bar{u}\,(1)d(2) > + \tau_+\,(q_2)\,|\,\bar{u}\,(1)d(2) >$$

$$= -|\,\bar{d}\,d > + |\,\bar{u}\,u > = |\,\bar{u}\,u > - |\bar{d}\,d > \qquad \ldots(67)$$

We know that the raising and lowering operators $\tau_\pm$ changes T_3 without changing T itself

$$\tau_+\,|\,T,T_3 > \;=\; \sqrt{T(T+1)-T_3(T_3\pm 1)}\,|\,T,T_3 \pm 1 > .$$

Thus the normalization factor N in Eq. (67) may be determined using the above relation. Since $|\,\pi^- >$ is a $T = 1$ and $T_3 = -1$ system, therefore

$$\tau_+\,|\,1,-1 > \;=\; \sqrt{1(1+1)+1(-1+1)}\,|\,1,0 > = \sqrt{2}\,|\,1,0 > .$$

We thus obtain $N = \sqrt{2}$, therefore

$$|\,\pi^\circ > \;=\; \tfrac{1}{\sqrt{2}}\big[\,|\,\bar{u}\,u > - |\,\bar{d}\,d >\big] \qquad \ldots(68)$$

The wavefunction for π^+ in terms of quarks is

$$N\,|\,\pi^+ > \;=\; \tau_+\,|\,\pi^\circ > = \frac{1}{\sqrt{2}}\sum_{i=1}^{2}\tau_+(q_i)\,[\,|\,\bar{u}\,u > - |\,\bar{d}\,d >]$$

$$= \tfrac{1}{\sqrt{2}}\,[\tau_+(q_1)\,\{|\,\bar{u}(1)u\,(2) > - |\,\bar{d}(1)d(2) >\} + \tau_+(q_2)\{|\,\bar{u}(1)u(2) > - |\,\bar{d}(1)\,d(2) >\}]$$

$$= \tfrac{1}{\sqrt{2}}\,[-\,|\,\bar{d}u > -0+0-0] = -\tfrac{1}{\sqrt{2}}\,|\,\bar{d}u > .$$

Since $|\,\pi^\circ >$ is a $T = 1$ and $T_3 = 0$ system, therefore

$$\tau_+\,|1,0 > \;=\; \sqrt{1(1+1)-0(0+1)}\,|\,1,1 > = \sqrt{2}\,|\,1,1 > .$$

Therefore $N = 1/\sqrt{2}$ and we have

$$\therefore \qquad |\,\pi^+ > \;=\; -\,|\,u\,\bar{d} >. \qquad \ldots(69)$$

There are two different ways, $u\bar{u}$ and $d\bar{d}$, to form a $T_3 = 0$ state from the two quarks and two antiquarks. Besides the linear combination of these two T_3 components given in equation (68), we can also take the linear combination

$$|\,\eta_0 > \;=\; \tfrac{1}{\sqrt{2}}\,[\,|\,u\bar{u} > + |\,d\bar{d} >]. \qquad \ldots(70)$$

It is orthogonal to $|\,\pi^\circ >$ given above and must therefore describe a meson other than π°. The linear combination, given above is a different one, must correspond to an isospin zero system, and is identified as η-meson which has a rest mass $= 550\ MeV/c^2$. Thus we see that four particles π^+, π°, π^- and η are the four observed mesons which can be constructed out of u, d, $\bar{u}$ and $\bar{d}$. To obtain other mesons, we must require s-and other massive quarks.

The next particle (quark) in order of increasing mass is the s-quark. These are found in hadrons with non-zero strangeness S, *i.e.*, in the strange particle or antiparticles. The lighest strange mesons are the K-mesons or kaons, the doublet with isospin 1/2, $K^+(u\bar{s})$ and $K^\circ(d\bar{s})$ and the doublet with their antiparticles $K^-(\bar{u}s)$ and $\bar{K}^\circ(\bar{d}s)$. The s-quark is assigned the strangeness quantum number $S = -1$ and the strange antiquark $\bar{s}$ is assigned $S = 1$. The other quarks have $S = 0$. Λ-particle, a baryon, has quark structure uds. The charm quantum number $C = 1$ for a c-quark and is -1 for a $\bar{c}$-quark. $C = 0$ for all other quarks. The beauty quantum number $\mathcal{B}$ is -1 for a b-quark and is 1 for $\bar{b}$-quark. $\mathcal{B} = 0$ for all other quarks.

Relatively long lifetimes are observed for mesons made of heavy quark-antiquark pairs. ϕ-*meson* consisting of quarks $s\bar{s}$, rest mass energy 1019.41 MeV/c^2, mean life 1.49×10^{-22} *sec.*, J/ψ-meson consisting of quarks $c\bar{c}$, rest mass energy 3096.63 MeV/c^2, mean life 0.97×10^{-20} sec and Υ-meson consisting of quarks $b\bar{b}$, rest mass energy 9460.32 MeV/c^2, mean life 1.27×10^{-20} sec. Since η_0 is invariant under a transformation among the three flavors, its wave function must be a linear combination of $u\bar{u}$, $d\bar{d}$ and $s\bar{s}$ with equal weight for each quark-antiquark pair,

$$|\,\eta_0 > \;=\; \tfrac{1}{\sqrt{3}}\big[\,|\,u\bar{u} > + |\,d\bar{d} > + |\,s\bar{s} >\big] \qquad \ldots(70)$$

where the factor $1/\sqrt{3}$ comes from normalization.

18.22 QUARK WAVEFUNCTIONS OF BARYONS

The baryons are three quark states. With three flavours, we can construct a total of 3 × 3 × 3 = 27 baryons for a given set of (I, S) values. They can be classified according to their SU_3 (flavour) symmetries into four groups consisting of 10,8,8 and 1 members each. The group of ten baryons, called decuplet, is completely symmetric under a flavour transformation and the group of one baryon, called singlet, is completely antisymmetric. The remaining two groups, each of eight members thus called octets, have mixed SU_3 (flavour) symmetry. Similar to the case of mesons, one can construct the quark wave functions of baryons. The baryon wave functions are more complicated to derive than those for mesons, because we have to find a linear combination of products of three objects instead of two objects. For convenience all the quarks are treated as identical particles distinguished only by their flavour and colour lables. Since hadrons are colour neutral objects, their wavefunctions must be antisymmetric in colour. Thus the rest of the wavefunctions formed of the product of flavour, spin and spatial parts must be symmetric under a permutation of any two quarks.

Baryon Decuplet—The decuplet, the group of ten members, together with their quark contents are shown in Fig. 18.27. As we have seen-earlier, Δ is an isospin $T = 3/2$ particle with four different charge states Δ^{++}, Δ^{+}, Δ^{0} and Δ^{-}. Since it is a non strange baryon ($S = 0$), it must be made of u and d quarks only. To make a baryon of charge 2, there is only one possible combination of quarks, *i.e.*, uuu. The different colours cancel by being antisymmetric with respect to each other. In order to obtain total spin 3/2 and isospin 3/2, both the intrinsic spin and isospin parts of the Δ^{++}-particle wave function must be completely symmetric, the spatial part of the wavefunction of three u-quarks must also be symmetric. The Δ^- is made up of three d-quarks, *i.e.*, ddd and the Ω^- of three s-quarks, *i.e.*, sss. Thus Δ^{++}, Δ^- and Ω^- described as colour singlets, are called colourless, while each of their three constituent quarks possess a different colour.

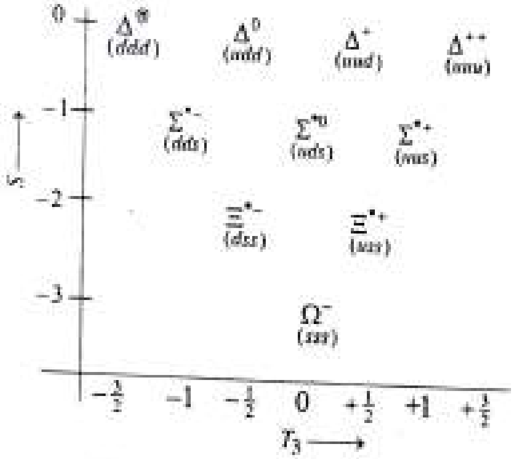

Fig. 18.27. $J^\pi = 3/2^+$ baryon decuplet.

Once the quark wavefunction of Δ^{++} is known, the wavefunctions of the other three members Δ^{+}, Δ^{0} and Δ^{-} may be obtained by using the isospin lowering operation τ_- on Δ^{++}, in the same way as done earlier while obtaining pion wavefunctions. The completely symmetric wavefunction in flavour for Δ^{++} is the symmetric product of the wavefunctions of three u-quarks, as

$$|\Delta^{++}> \;=\; |u(1)>|u(2)>|u(3)>. \qquad ...(71)$$

When τ_- is applied to $|\Delta^{++}>$ to obtain $|\Delta^{+}>$, we have a choice of changing any one of the three u-quarks into a d-quark. Thus the wavefunction of Δ^+ must be a linear combination of all three possibilities with equal weight. Thus we have the normalized and symmetrized wavefunction for Δ^+ as

$$|\Delta^{+}> = \frac{1}{\sqrt{3}}[|\,d(1)>|\,u(2)>|\,u(3)> + |\,u(1)>|\,d(2)>|\,u(3) + >|\,u(1)>|\,u(2)>|\,d(3)>|]$$

In the simplified form, we may write above two equations as

$$|\Delta^{++}> \;=\; |\,uuu> \quad\text{and}\quad |\Delta^{+}> = \frac{1}{\sqrt{3}}[|\,duu> + |\,udu> + |\,uud>] \qquad ...(72)$$

Following this procedure, the wavefunctions of Δ^0 and Δ^- can be written as

$$|\Delta^{0}> \;=\; \frac{1}{\sqrt{3}}[|\,ddu> + |\,dud> + |\,udd>] \qquad ...(73)$$

and $$|\Delta^{-}> \;=\; |\,ddd>. \qquad ...(74)$$

The wavefunctions of the different charge states of Σ^* baryons with strangeness $S = -1$ can be similarly obtained by beginning with Σ^{*+}, the $T_3 = 1$ member of the isospin triplet (Σ^{*+}, Σ^{*0} and Σ^{*-}). We can use $|\Delta^{++}>$ as the starting point and replace one of the three u-quarks with an s-quark. Instead of isospin, we are lowering the strangeness by replacing a *d*-quark with an *s*-quark. From symmetry requirements, the normalized wavefunction is

$$|\Sigma^{*+}> \; = \; \frac{1}{\sqrt{3}}\left[|\,suu> + \,|\,usu> + \,|\,uus>\right]. \qquad \text{...(75)}$$

The wavefunctions of the other members of this isospin triplet can be obtained by applying τ-operator. Since the *s*-quark is an isospin zero particle, therefore, vanishes when acted upon by τ_+ or the τ_- operator. Thus the only effect of the isospin lowering operator is to change one of the *u*-quarks to a *d*-quark. We therefore obtain

$$|\Sigma^{*0}> \; = \; \frac{1}{\sqrt{6}}\left[|\,sdu> + \,|\,sud> + \,|\,dsu> + \,|\,usd> + \,|\,dus> + \,|\,uds>\right] \qquad \text{...(76)}$$

and

$$|\Sigma^{*-}> \; = \; \frac{1}{\sqrt{3}}\left[|\,sdd> + \,|\,dsd> + \,|\,dds>\right]. \qquad \text{...(77)}$$

The wavefunctions of the isospin doublet for the strangeness $S = -2$ can be obtained in the same way as

$$|\Xi^{*+}> \; = \; \frac{1}{\sqrt{3}}\left[|\,ssu> + \,|\,uss> + \,|\,sus>\right] \qquad \text{...(78)}$$

$$|\Xi^{*-}> \; = \; \frac{1}{\sqrt{3}}\left[|\,ssd> + \,|\,dss> + \,|\,sds>\right] \qquad \text{...(79)}$$

For $S = -3$, there is only one particle possible with all the three *s*-quarks, *i.e.*,

$$|\,\Omega^-> \; = \; |\,sss>. \qquad \text{...(80)}$$

Since *s*-quark carries a charge $-\frac{1}{3}e$, therefore the particle carries one unit negative charge.

Baryon Singlet—It is easy to construct a state of three quarks *u, d* and *s* completely antisymmetric in flavour. However there are 6 choices, one can not favour anyone, therefore a linear combination of all six terms is required. This combination must be antisymmetric with respect to a permutation between any two quarks in order to obtain a singlet state. In order to satisfy the requirement of being symmetric, the three odd permutations *usd, sdu* and *dus* must be taken negative. Thus the normalized singlet quark wave function is given by

$$|\Lambda_1> \; = \; \frac{1}{\sqrt{6}}\left[|\,uds> + \,|\,dsu> + \,|\,sud> - \,|\,usd> - \,|\,sdu> - \,|\,dus>\right]$$

Since the *s*-quark is an isoscalar quantity, the isospin of the wavefunction is determined by *u*-and *d*-quarks. We can illustrate it by rewriting the above relations as

$$|\Lambda_1> = \frac{1}{\sqrt{6}}\Big[\{|\,u(1)>|\,d(2)> - \,|\,d(1)\,|>|\,u(2)>\}\,|\,s(3)> + \{|\,u(2)>|\,d(3)> - \,|\,d(2)>|\,u(3)>\}\,|\,s(1)> +$$
$$\{|\,u(3)>|\,d(1)> - \,|\,d(3)>|\,u(1)>\}\,|\,s(2)>\Big]$$

This is a $T = 0$ linear combination as the wavefunction is antisymmetric in the isospin carrying parts. Thus the particle Λ_1 is an isoscalar particle. The observed strangeness $S = -1$ isoscalar, $J^{\pi} = 1/2^+$ particle Λ is a mixture of the $|\,\Lambda_1>$ and $|\,\Lambda_8>$, the latter being a member of the $J = 1/2^+$ baryon octet.

Baryon Octet—The remaining 16 possible baryons out of total 27 that can be constructed from *u*–, *d*– and *s*-quarks have mixed symmetry in flavour. They are classified as two octets, distinguished by their symmetries under the simultaneous interchange of both flavour and spin. The octet with neutron and proton as its members is important, because the wavefunction of each member of this group is antisymmetric under the combined exchange of both flavour and intrinsic spin. The members of this octet along with their quark contents are shown in Fig. 18.28.

We can construct wavefunction for the proton with $T_z = 1/2$, intrinsic spin 1/2 and parity even in several ways. The simplest is to start with *u* and *d*

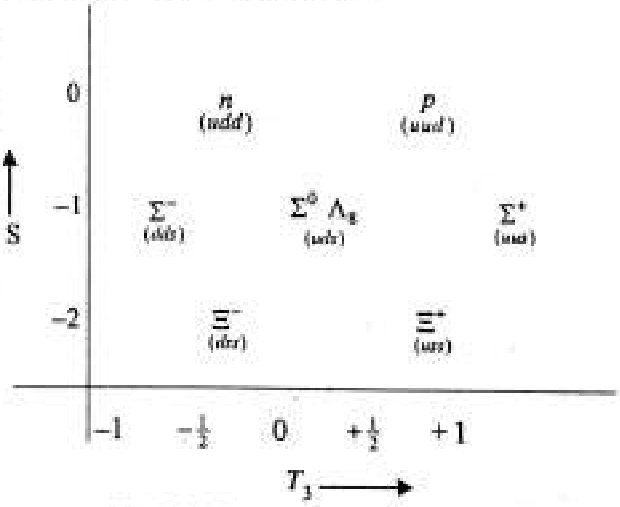

Fig. 18.28. $J^{\pi} = 1/2^+$ *baryon octet.*

quarks. This is antisymmetric in flavour of the first two quarks to form intrinsic spin as 0. This is coupled with the third one with spin up to form a system with $J = 1/2$ and $J_z = 1/2$.

$$|\tfrac{1}{2}, +\tfrac{1}{2}> \;=\; \tfrac{1}{\sqrt{2}}\left[|u(1)\uparrow>|d(2)\downarrow> - |u(1)\downarrow>|d(2)\uparrow>\right]u(3)\uparrow>$$

The combination of flavour and spin in the above equation may be symmetrized first by carrying out the process for the first two quarks with different flavours only and obtain

$$|\tfrac{1}{2}, +\tfrac{1}{2}> = \tfrac{1}{2}\left[|u(1)\uparrow>|d(2)\downarrow> - |u(1)\downarrow>|d(2)\uparrow> + |d(1)\downarrow>|u(2)\uparrow> - |d(1)\uparrow>|u(2)\downarrow>\right]u(3)\uparrow>.$$

Next we shall generate all the other terms by making the permutations P_{31} and P_{32} on each of the four terms in the above equation. This gives us 12 terms. On rearranging, the quark wavefunction for a proton with spin orientations of all the quarks indicated by the arrow, is

$$|p> = \tfrac{1}{\sqrt{18}}\left[2(|u\uparrow u\uparrow d\downarrow> + |u\uparrow d\downarrow u\uparrow> + |d\downarrow u\uparrow u\uparrow>) - (|u\uparrow u\downarrow d\uparrow> + |u\uparrow d\uparrow u\downarrow> + |d\uparrow u\uparrow u\downarrow> + |u\downarrow u\uparrow d\uparrow> + |u\downarrow d\uparrow u\uparrow> + |d\uparrow u\downarrow u\uparrow>)\right] \quad ...(81)$$

Here we have dropped the labels for quark number. This wave function for a proton is antisymmetrical under a simultaneous intercharge of flavour and spin between two quarks.

The neutron wavefunction can be obtained from the proton wavefunction by simply substituting all the *u*-quarks by *d*-quarks and vice-versa.

The wavefunctions of the strangeness $S < 0$ members of the octet can be built from that of the proton in the same way as we did for members of the decuplet.

18.23 MAGNETIC DIPOLE MOMENT OF THE BARYON OCTET

We can find static electromagnetic properties of baryons by using wave functions derived earlier. Since the hadrons are bound in relative *s*-state, the magnetic dipole moment of the hadrons is the sum of the constituent quark magnetic moments. The individual quark magnetic dipole moment may be defined as

$$\mu \;=\; gs\mu_D, \quad ...(82)$$

where *s* is the operator for intrinsic spin, μ_D is the unit of dipole moment which may be expressed in terms of the quark charge *q* and mass m_q, as $q\hbar/2m_q$. The quantity *g* is called the gyromagnetic ratio. For a Dirac particle, a particle without internal structure and having intrinsic spin $s = 1/2$, we have $g = 2$. The observed values of *g* for the electron and muon are found slightly different than 2. The small corrections to the Dirac particle value 2 may be due to the fact that these particles are not the purely Dirac particles, as they emit and absorb virtual photons. The quarks may be considered as the Dirac particles as they are the elementary particles. Assuming the masses of *u*- and *d*-quarks equal, we get

$$\mu_u/\mu_d \;=\; (2/3)/(-1/3) = -2 \quad \text{or} \quad \mu_u = -2\mu_d. \quad ...(83)$$

The contribution to the magnetic dipole moment of a baryon from quark intrinsic moments (μ_u of *u*-quark and μ_d of *d*-quark) depends also on the orientation of the spin of each quark.

For a proton, we can count the numbers of $u\uparrow$, $u\downarrow$, $d\uparrow$ and $d\downarrow$ in the wavefunction (equation 81). This may be done by calculating the expectation value (sum of the squares of the coefficients in the wave function) for each type of quark of a given spin orientation. The results are 5/3 for $u\uparrow$, 1/3 for $u\downarrow$, 1/3 for $d\uparrow$ and 2/3 for $d\downarrow$. Thus the net contribution from *u*-quarks to the proton magnetic dipole moment is 5/3 – 1/3 = 4/3 and that from *d*-quark is 1/3 – 2/3 = – 1/3. Therefore the magnetic dipole moment of the proton in terms of those for *u*-and *d*-quarks will be

$$\mu_p \;=\; \tfrac{4}{3}\mu_u - \tfrac{1}{3}\mu_d. \quad ...(84)$$

In a neutron wave function, the *u*-and *d*-quarks are interchanged, therefore

$$\mu_n \;=\; \tfrac{4}{3}\mu_d - \tfrac{1}{3}\mu_u. \quad ...(85)$$

$$\therefore \quad \frac{\mu_p}{\mu_n} \;=\; \frac{\frac{4}{3}\mu_u - \frac{1}{3}\mu_d}{\frac{4}{3}\mu_d - \frac{1}{3}\mu_u} = \frac{\frac{4}{3}\times(-2) - \frac{1}{3}}{\frac{4}{3} - \frac{1}{3}(-2)} = \frac{-9/3}{6/3} = -\frac{3}{2}. \quad ...(89)$$

This is in good agreement with the observed value of 2.793/-1.913 = −1.46. This supports the quark model.

Strange Baryons—The other six members of the baryon octet has at least one *s*-quark. Since *s*-quark is more massive than *u*-and *d*-quark, the intrinsic magnetic dipole moment of the *s*-quark can not be related to those of the *u*-and *d*-quarks. We have not calculated/obtained quark wavefunctions for the baryons with $S < 0$, as done for the proton. As shown in Fig. 18.28, the strange baryons involve two different flavours, *i.e.*, *s*-and *u*-quarks or *s*-and *d*-quarks. For example, the Σ^+ baryon is made of two *u*-quarks and one *s*-quark. Compared with the proton, made of two *u*-quarks and one *d*-quark, we see that the only difference between these two baryons Σ^+ and proton is that in place of *d*-quark in proton, Σ^+ has *s*-quark. Thus Σ^+ must have very similar quark wave functions except for the replacement of *d* with *s*. Hence the magnetic dipole moment of $\Sigma^{\pm}$ baryon is given

$$\mu_{\Sigma^+} = \tfrac{4}{3}\mu_u - \tfrac{1}{3}\mu_s. \qquad \text{...(87)}$$

Similarly the Σ^--baryon is made of two *d*-quarks and one *s*-quark. Comparing it with a neutron, we see that the magnetic dipole moment of Σ^--baryon is the same except that in place of *u*-quark in a neutron, we have *s*-quark in Σ^--baryon. Thus we have

$$\mu_{\Sigma^-} = \tfrac{4}{3}\mu_d - \tfrac{1}{3}\mu_s. \qquad \text{...(88)}$$

Similar methods are used for finding the magnetic dipole moments of the doublet corresponding to $S = -2.$, *i.e.*, $\Xi^-(dss)$ and $\Xi^\circ(uss)$. We have

$$\mu_{\Xi^\circ} = \tfrac{4}{3}\mu_s - \tfrac{1}{3}\mu_u \quad \text{and} \quad \mu_{\Xi^-} = \tfrac{4}{3}\mu_s - \tfrac{1}{3}\mu_d. \qquad \text{...(89)}$$

For the remaining members of the baryon octet, Σ° and Λ_8, the quark contents are *uds* for both. Since three different flavours are involved, the magnetic dipole moments require the intrinsic dipole moments of these three quarks. We can make use of the isospin difference of these baryons to derive their wave functions. The contributions from both *u*-and *d*-quarks are zero, as there are equal numbers of each with spin pointing up as there are with spin pointing down. Therefore the magnetic dipole moment of Λ_8 is given by

$$\mu_\Lambda = \mu_s.$$

The comparison with the experimental values gives $\mu_u = 1.852\ \mu_N$, $\mu_d = -0.972\ \mu_N$ and $\mu_s = -0.581\ \mu_N$.

All these values are summarized and compared with the observed values, as illustrated in the table 18.7.

Table 18.7. Magnetic Dipole Moment of Baryon Octet

Octet Member	μ_B	*Predicted Value* (μ_N)	*Observed Value* (μ_N)
p	$\frac{4}{3}\mu_u - \frac{1}{3}\mu_d + 0\mu_s$	2.793	2.79285
n	$\frac{4}{3}\mu_d - \frac{1}{3}\mu_u + 0\mu_s$	−1.913	−1.91304
Λ	$0\mu_u + 0\mu_d + \mu_s$	−0.581	−0.613 ± 0.004
Σ^+	$\frac{4}{3}\mu_u + 0\mu_d - \frac{1}{3}\mu_s$	2.663	2.458 ± 0.010
Σ^-	$0\mu_u + \frac{4}{3}\mu_d - \frac{1}{3}\mu_s$	−1.102	−1.157 ± 0.025
Ξ°	$-\frac{1}{3}\mu_u + 0\mu_d + \frac{4}{3}\mu_s$	−1.392	−1.250 ± 0.014
Ξ^-	$0\mu_u - \frac{1}{3}\mu_d + \frac{4}{3}\mu_s$	−0.471	−0.6507 ± .0025
Σ°	$-\frac{1}{\sqrt{3}}\mu_u + \frac{1}{\sqrt{3}}\mu_d + 0\,\mu_s$	−1.630	−1.59 ± 0.09

18.24 QUANTUM CHROMODYNAMICS

Quantum Chromodynamics (*QCD*) was developed by *H.* Fritzch and M. Gell-Mann in 1972 to describe hadrons. It is a theory in which hadrons are assumed to be composite particles with quarks as their constituents. Quantum chromodynamics explains the strong interactions among the quarks. The mediators of the strong interactions are named as *gluons* because they make up the glue which binds quarks together into hadrons. The gluons themselves carry colour. Hence the strong interactions among gluons will also occur through the exchange of gluons. However, no evidence has been reported for isolated or free gluons. Quantum chromodynamics is nearly identical in mathematical structure to quantum electrodynamics (*QED*) and to the unified theory of weak and electromagnetic interactions put forward. On account of the use of colour quantum number by non-Abelian gauge field theory to resolve certain difficulties in the quark model, the theory was named *Quantum Chromodynamics.*

The baryons are made of three quarks, each with spin 1/2. According to the Pauli principle, identical spin 1/2 particles cannot occupy the same quantum number. Thus the existence of Δ^{++} (*uuu*) and Ω^- (*sss*) would seem to be forbidden configurations. To comply with the Pauli principle, each flavour of quark is supposed to exist in three varieties, labeled by the *red, green and blue colours.* Thus a baryon can be constructed as a colourless state of red, green and blue quarks. Similarly a meson will be a colourless quark-antiquark combination. The colour could be regarded as the conserved charge of the strong interactions. It was natural to seek a gauge symmetry which would have colour conservation as its consequence. The unitary group *SU*(3) is now applied to colour rather than to flavour. The gluons are assumed to carry the *colour charge*. The colour, also called *colour quantum number*, is to the true strong interaction as the electric charge is to the electromagnetic interaction. Just as the electromagnetic interaction is the exchange of photons emitted and absorbed by electric charge, so the real strong interaction is the exchange of gluons emitted and absorbed by *colour charge*. The colour interaction is to be distinguished from the interaction between the hadrons, referred to as the nuclear strong interaction.

Like Quantum electrodynamics, we want a theory of coloured quarks to be invariant under local gauge transformations. Since there are three colours, the gauge group is *SU*(3) and the gauge transformations involve three colour degree of freedom of quarks. The generators of the group are eight Gell-Mann matrices. There are thus eight massless gauge bosons called gluons. Three coloured quarks corresponding to each quark flavour form a triplet in the fundamental representation of *SU*(3) and eight gluons form an octet in the adjoint representation. The octet of gauge fields are the gluons, each gluon possesses a colour (*r, y, b*) and an anticolour $(\bar{r}, \bar{y}, \bar{b})$. There are nine combinations of colour and anticolour, of which six are obvious $(r\bar{y}, r\bar{b}, y\bar{r}, y\bar{b}, b\bar{r}, b\bar{y})$. The remaining three $r\bar{r}, y\bar{y}$ and $b\bar{b}$ are not obvious, their mixtures form orthogonal eigenfunctions. The symmetric function $(r\bar{r} + y\bar{y} + b\bar{b})/\sqrt{3}$ has no net colour and is the singlet. The other two combinations have colour and are $(r\bar{r} - y\bar{y})/\sqrt{2}$ and $(r\bar{r} + y\bar{y} - 2b\bar{b})/\sqrt{6}$.

The octet of gluons provide local colour symmetry, which permits individual quarks to change colour but leave the hadron colourless. Baryon is colourless because it has *r, b* and *y* quarks. If the *r*-quark changes to *b* by emitting a $r\bar{b}$ gluon, the *b* quark will absorb this gluon and turn to *r* quark, leaving the baryon colourless (as it has *b, r* and *y* quarks). The gluons are generally represented by a coil like line ( ). The PETRA (at Hamburg) $e^+ e^-$ colliding 35 GeV beam accelerator has yielded a direct evidence for gluons. e^+ and e^- collide to produce a virtual photon, which then makes a quark-antiquark pair. The quark and antiquark each soon form other particles. At high incident energies, the number of particles formed are quite large and are thus close together. Thus the quark forms one jet of particles and the antiquark forms another jet. The two jet event is detected in the TASSO detector. The angular distribution of the axis of the two narrow jets with respect to the colliding beam direction is the same as for the axis of the particles (μ^+ and μ^- formed by $e^+ - e^-$ collision). Since μ has spin 1/2, this is a direct evidence that the quark also has spin 1/2.

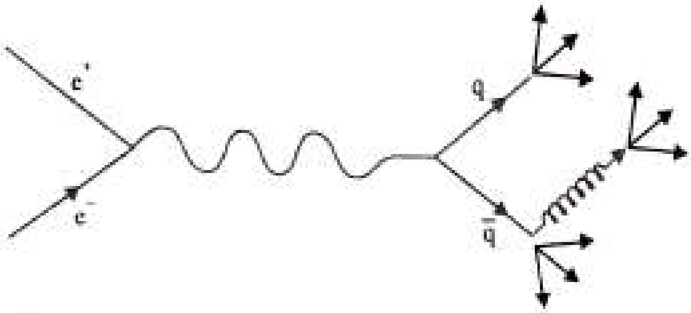

Fig. 18.29. Production of three jets of hadrons in $e^+ - e^-$ collision.

As the energy of the beam is increased, quark or antiquark radiates a gluon, from which another group of particles is formed. As the energy is further increased, the gluon induced group of particles forms its own jet, thus three jets are seen. At even higher energies two gluons often are radiated, causing four jet events. The angular distribution and energies of the jets correspond closely to *QCD* calculations, thus confirming the existence of gluons.

18.25 ELECTROWEAK INTERACTION THEORY

Gauge theories were successful for strong, electromagnetic and gravitational interactions. It was natural to suppose that such a theory might exist for the weak interaction as well. It is surprising that this theory is not just of the weak interaction but includes also the electromagnetic interaction, giving a common origin to both. The first attempt at the unification of the electromagnetic and weak interactions was made by J. Schwinger in 1956 in which he proposed to put the photon and the charged intermediate bosons W^+ and W^- in a triplet of isospin. S.L. Glashow in 1960 modified the above proposal and suggested that the electromagnetic and weak interactions might be unified in a gauge theory based on the group $SU(2)_L \times U(1)$, thus introducing an additional electrically neutral intermediate vector boson. The electroweak gauge theory was set up by Glashow in 1961, but had no way then to make the gauge bosons massive. Independently in 1967, S. Weinberg and in 1968 A. Salam applied the Higgs mechanism to give mass to the gauge bosons and produced a consistent theory. In 1971, G.T. Hooft proved that the theory was renormalizable. Thus the electromagnetic and weak interactions have been unified in the Glashow-Weinberg and Salam model. Glashow, Salam and Weinberg received the Noble prize in 1979 for their work on this topic.

This theory has four gauge fields, whose quanta are the two charged particles W^+ and W^-, a massive neutral vector boson Z^0 and the photon. The Z^0 is coupled to all particles with strengths controlled by a parameter, the single Weinberg (or weak) angle θ_W (*also called weak mixing parameter for electromagnetic and weak interactions*). The value of θ_W is found from experiment, by observation of the neutral-current weak interactions which exchange the Z^0-yields. They have been observed in high energy $e^+ - e^-$ scattering, deep inelastic $e - p$ scattering, and the low energy electron-nucleus interaction in the atom. This theory shows that the W^+, W^- and Z^0 acquire well defined masses, given by

$$m_{W^\pm} = \left(\frac{e^2\sqrt{2}}{8\beta\sin^2\theta_W}\right)^{1/2} = (37.4\ GeV/c^2)/\sin\theta_W$$

and
$$m_{Z^0} = (37.4\ GeV/c^2)/\sin\theta_W\cos\theta_W. \qquad \text{...(90)}$$

The constant $\sin^2\theta_W$ can be determined from experiments and is found to be

$$\sin^2\theta_W = 0.218 \pm 0.010. \qquad \text{...(91)}$$

The predicted theoretical mass values of W and Z-particles deduced from above equations are around 80 and 90 GeV/c^2 respectively. These are in good agreement with the experimental values found by the CERN–1983 experiments with 270 GeV proton-antiproton colliding beams.

In the electroweak theory the particles necessary for this purpose, the W^+ and W^- are a consequence of the local gauge symmetry. These particles give the standard charge-changing weak interactions, such as β-decay, *K*-decays or neutrino scattering. Quark-level diagrams for these processes are shown in Fig. 18.30 Quarks are involved here, as well as leptons. This theory predicts that the coupling the $W^{\pm}$ to both quarks and leptons is the same, *i.e.*, *the quarks and leptons have equal strengths of weak interactions.*

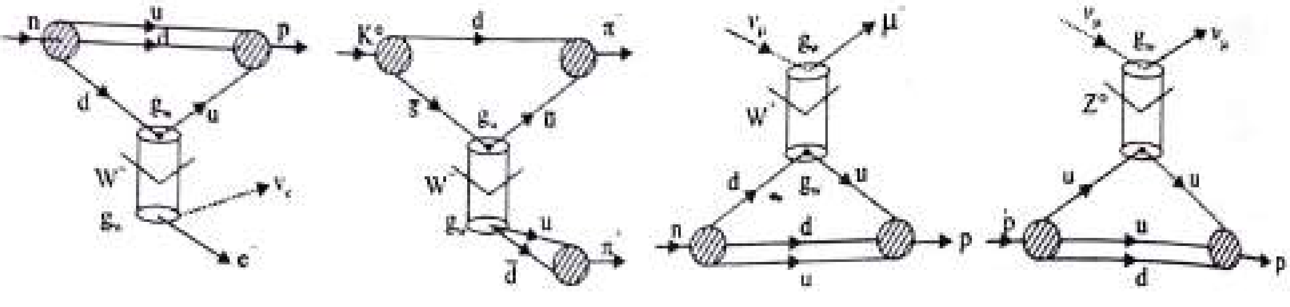

(*a*) neutron decay (*b*) $K^0 \to \pi^+ + \pi^-$ (*c*) $\nu_\mu + n \to \mu^- + p$ (*d*) $\nu_\mu + p \to \nu_\mu + p$

Fig. 18.30. Quark diagrams for weak interactions.

Comparing rates for various types of weak decay, Cabibbo in 1963 found that if the Fermi decay constant for a purely leptonic decay process like $\mu^- \to e^- + \bar{\nu}_e + \nu_\mu$ is β, then that for a non-strangeness changing process like $\pi^- \to \mu^- + \bar{\nu}_\mu$ is $\beta \cos\theta_c$ and that for one in which $\Delta S = 1$, like $K^- \to \mu^- + \bar{\nu}_\mu$ is $\beta \sin\theta_c$. Here θ_c is called Cibibbo angle. Experimentally it was found to have value 0.23 rad. Thus we see that the ratio of the decay rates for $\Delta S = 0$ to $\Delta S = 1$ decays is $\tan^2\theta_c = 0.06$. In terms of quark interactions, this shows that *the s-quark does not couple to W^+ as strongly as, say, the u-quark does.* The d_c and s_c are a mixture of *d* and *s* related by an SU_2 transformation, the Cabibbo rotation, as

$$d_c = d\cos\theta_c + s\sin\theta_c \quad \text{and} \quad s_c = -d\sin\theta_c + s\cos\theta_c.$$

With the discovery of the *b* quark, the above relation has been extended to all three $Q = -1/3$ quarks, *i.e.*, SU_3 rotation relates (d_c, s_c, b_c) and (d, s, b). The precise statement of universality is that the couplings of the $W^{\pm}$ are of the form $W\bar{U}D$ (*i.e.* $\bar{U} \to + W + D$), where the pair (U, D) stands for any of the pairs.

$$\begin{pmatrix}\nu_e\\ e\end{pmatrix}_L, \begin{pmatrix}\nu_\mu\\ \mu\end{pmatrix}_L, \begin{pmatrix}\nu_\tau\\ \tau\end{pmatrix}_L \quad \text{and} \quad \begin{pmatrix}u\\ d_c\end{pmatrix}_L, \begin{pmatrix}c\\ s_c\end{pmatrix}_L, \begin{pmatrix}t\\ b_c\end{pmatrix}_L$$

These pairs are called *weak i-spin doublets.* These are the left hand helicity components only, *i.e.*, the coupling is $V - A$. The right handed helicity components are all weak isospin singlets. Each quark doublet has charge + 2/3 and − 1/3 adding to + 1/3, but there are three colours of quark, so the total charge is 1, just cancelling the charge−1 of the corresponding lepton doublet. Each paired quark and lepton doublet is called a *generation,* and so for each generation the charges add to zero. This ties together quark-lepton symmetry, fractional quark charge and colour. Thus we may believe more and more leptons and quarks, preserving this type of symmetry.

The electric charge *e*, expressing the strength of the electromagnetic interaction and the weak charge g_W expressing the strength of the weak interaction are found to be related, as

$$e = 2\sqrt{2}\, g_W \sin\theta_W.$$

This shows that the electromagnetic and weak interactions are of about the same strength. The weak interactions are weak because of the large values of the mass m_W and m_Z, making the range of the interaction so short. The weak charge g_W is related with the Fermi weak interaction coupling constant β by the relation $\beta = \sqrt{2}g_W{}^2 / M_W{}^2$.

18.26 GRAND UNIFICATION THEORIES (GUTs)

We know that all known processes in nature from microscopic to macroscopic can be understood as a manification of one or more of the four fundamental interactions, namely strong, electromagnetic, weak and gravitation. The idea of unification of all these different interactions began, when Maxwell succeeded in unifying the then seemingly different electricity and magnetism. The success of the Glashow-Weinberg-Salam theory in unifying the electromagnetic and weak interactions, has reduced the number of interactions from three to two. The attempts were made in the recent years to develop a theory which may unify the three interactions, strong, electromagnetic and weak, if the gravitational interaction is ignored for the time being. A clear obstacle to the unification of these interactions is that at low energies the coupling constants g_s, g_{el}, g_w are all different, while in a truly unified theory, they must be equal. The symmetry should apply at some high enough energy. The renormalization group tells us that $SU(2)$ and $U(1)$ coupling constants change with momenta. The strong coupling constant also decreases as the distance decreases or the energy increases. It is interesting to find out if the strong interaction approaches the other two at high energy. These three different coupling constants come together at an energy of about 2×10^{14} *GeV*, which corresponds to a distance $\lambda = \hbar\, c/E = 10^{-30} m$. Thus at this extremely high energy or very small distance there is a strong possibility that all three interactions become the same. This energy is called *grand unification energy*.

Many methods have been employed to incorporate the symmetries $SU(3)$ of the strong colour interaction, $SU(2)$ of the weak interaction and $U(1)$ of the electromagnetic interaction into a more inclusive gauge symmetry. H. Georgi and S. Glashow in 1974 suggested $SU(5)$ model. This model is the simplest group, most economical of all the grand unified theories. The procedure in obtaining this gauge theory is simple. There are five component wave functions and gauge transformations involve 5 × 5 matrices. Thus $5 \otimes \bar{5} = 1 \oplus 24$ gauge bosons are needed to compensate for the local phase transformations. As usual, the singlet is not of interest, but of the 24, 8 are the gluons for the colour interactions, 4 others are the γ, $W^{\pm}$ and Z^0 and the remaining 12 are the so called X and Y-bosons. These additional gauge bosons are also called *lepto quarks* and have anti particles $\bar{X}$ and $\bar{Y}$. These four particles come in three colours, giving twelve particles in all. Thus the leptoquarks or diquark bosons carry both flavour and colour properties. To give an idea of the relationship among the leptons and quarks, a typical 5 representation of the group and the schematic of the reactions among the particles is shown as

$$\bar{5} = (\bar{3}, 1) + (1, 2) = \left|\begin{tikzcd}[row sep=small] \nu_e \arrow[d, bend left, "W^-"] \\ e^- \\ \bar{d}_r \arrow[u, bend right, "X"'] \\ \bar{d}_b \arrow[d, bend left, "g(b\bar{y})"] \\ \bar{d}_y \end{tikzcd}\right|_L$$

The reactions carried by gauge bosons between these 5 particles are shown by the arrows in the extreme right, as :

$$\nu_e + W^- \rightarrow e^-;\ \bar{d}_b \rightarrow \bar{d}_y + g(b\bar{y});\ \bar{d}_r + X \rightarrow e^-,$$

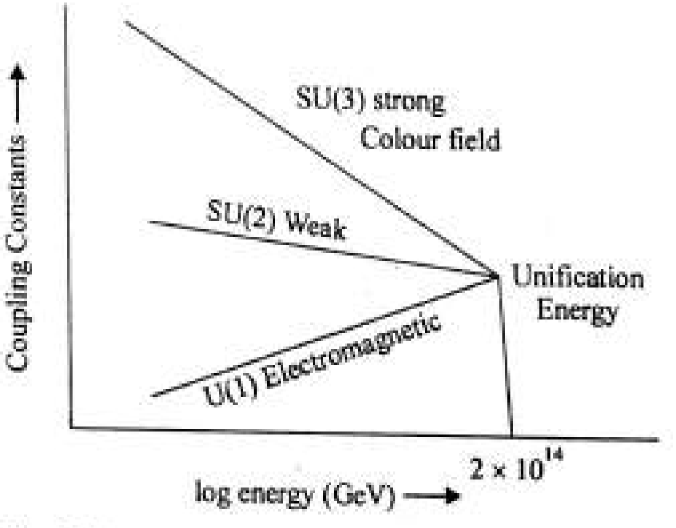

Fig. 18.31. The variation of coupling constants with energy (log scale) of different interactions.

i.e., ν_e combining with W^- to produce an e^-, a blue antidown quark emitting a blue antiyellow gluon to become a yellow antidown quark, X boson oncharge $-4/3$ is between a quark $\bar{d}_r$ of charge $+1/3$ and a lepton e^- of charge -1. This last type of reaction would cause nucleons to decay, but on account of their very large masses (about equal to the unification energy), X-and Y-bosons make this an extremely weak reaction. $M_X = M_Y = 2 \times 10^{14}\ GeV/c^2$.

$SU(5)$	12 superheavy bosons $X^{\pm 4/3}$, $Y^{\pm 1/3}$	$M = 10^{14}$ GeV
$SU(3)_c \otimes SU(2) \otimes U(1)$	$W^{\pm}$, Z^{0}, γ, gluons	$M = 10^{2}$ GeV
$SU(3)_c \otimes U(1)$	8 gluons, photon	all massless

The exchange of a leptoquark boson can result in the transformation $qqq \rightarrow l\bar{q}q$, for example $p \rightarrow e^{+}\pi^{0}$. This baryon and lepton number violating interaction is a much weaker interaction than the analogous ordinary weak interaction. Thus the proton is not stable. The lifetime predicted to be $\tau_p = 10^{30}$ *yrs*, which appears to be in conflict with experimental limits $\geq 2 \times 10^{32}$ *yrs*, as given by the University of California Irvine, University of Michigan and Brookhaven National Laboratory. Another serious difficulty in this theory is due to tremendous difference in the masses of the weak gauge bosons ($10^{2} GeV/c^{2}$) and of the leptoquarks (10^{14} GeV/c^{2}) : For long time it has been believed that lepton number and the baryon number were absolutely conserve quantities, like charge. We know that charge conservation depends upon gauge invariance and the existence of an associated massless field. There is no gauge invariance with a massless field that can be associated with the conservation of leptons or baryons. Thus if quarks and leptons are unified, leptons and baryon numbers will not be conserved. The possible existence of a neutrino mass may be the consequence of the violation of lepton number conservation.

Super Symmetry Theory—The Grand Unification theories are incomplete. A large number of features are unaccounted for. A theory which offers an escape from these difficulties is a synthesis of general relativity with supersymmetry, known as *supersymmetry theory*. In this theory every boson has a fermion partner and vice versa. Thus every fermion (quark and lepton) will have a supersymmetric spin zero partner (squark and slepton), while every boson (photon, gluon, *W*, *Z*, Higgs) will have a spin 1/2 partner (photinos, gluinos, etc.). The quantum of gravitation attraction, graviton, which has spin 2, will have a super symmetric partner the *s* graviton with spin 3/2. In the symmetric limit the particles and their supersymmetric partners should have equal masses. As supersymmetric particles have not been observed, they may be very heavy, therefore super symmetry is a hypothetical symmetry.

18.27 HEAVY QUARK EFFECTIVE THEORY

We know that the Glashow-Weinberg-Salam (GWS) model for electroweak interaction and the Quantum Chromodynamics (*QCD*) for the strong interactions form the *standard model*. Developments have been made in the theory of heavy quarks for the reliable determination of some of the parameters of the standard model. Certain properties in hadrons containing a heavy quark with spin-flavour symmetry (Isgur Wise Symmetry) are found to be independent of its mass and spin. For *N*-heavy quarks, there is an *SU*(2*N*) flavour-spin symmetry, known as the *heavy quark symmetry*, which implies that the spectrum of heavy mesons and heavy baryons is independent of the flavour and spin of the heavy quark. The effective field theory implemented with the ideas of the heavy quark is called the *Heavy Quark Effective Theory (HQET)*.

Since the heavy hadrons contain both the heavy and light quarks, both the *SU*(3) symmetry of the light quarks and *SU*(2*N*) symmetry of the heavy quarks are expected to have implications for the low energy dynamics of heavy hadrons. Comparing a simple result of the spin symmetry of the heavy quark with the experimental data, we conclude that *b* and *c* quarks may be treated as heavy and heavy flavour symmetry is thus an *SU*(2) symmetry denoted by $SU(2)_{HF}$.

It may be useful to study heavy hadrons in the heavy quarks approximation. There are many advantages of this limit–heavy quark acts as a point like probe of the light constituent quarks and the relativistic effects are simplified. *HQET*, coupled with factorization hypothesis, can be used to study nonleptonic decays of heavy hadrons. The charm baryon decay predictions show that *HQET* performs well when confronted with the experimental data. The decay $\Xi_c^{\circ} \rightarrow \Xi^{-} \pi^{+}$ provides a direct test for the factorization hypothesis. A more detailed study of the heavy to light form factors is called for. For the knowledge of the universal form factors, non perturbative *QCD* is needed. But an understanding of these functions is ultimately necessary for any quantitative analysis based on heavy quark symmetry. *QCD* sum rules have been recently employed. *HQET* with models may help in the understanding of some aspects of confinement. New data from charm and beauty factories will allow us to test heavy quark symmetry and to determine reliably some standard model parameters. Heavy quark will be a useful tool for understanding the nature of *QCD* of the light quarks.

18.28 COSMOLOGY AND PARTICLE PHYSICS

The grand unification theories cannot be confirmed experimentally because of very large energies of the order of $10^{14} - 10^{15}$ *GeV*, which seen impossible to attain with accelerators. The theoretical physicists therefore turned to cosmology and specially to the first moments of the *Big Bang*. During the last three decades, close links have been established between the particle physics and cosmology. The standard Hot Big Bang model of cosmology relates the fundamental questions in the particle physics, such as : *(i)* the universe underwent a phase transition when its temperature cooled to $10^{27} K$, which corresponds to 10^{14} GeV in energy and to the first 10^{-35} sec after the Big Bang. This was when the $SU(5)$ symmetry would have been broken, *(ii)* the phase transition caused an exponential expansion (10^{30} fold in 10^{-32} sec) of the universe which explains why the observed 3K microwave background radiation is uniform and why the universe behaves as if space is practically flat, *(iii)* the baryon number conservation at *GUT* energies to account for the dominance of matter over antimatter in the universe, *(iv)* the existence of monopole, *(v)* the existence of new species of particles and massive neutrinos. Thus the manifestations of grand unification apply not only in *particle physics* but also in *cosmology*. Let us here give a few topics/areas of great interest.

(1) *Dark Mass of the Universe*—Neutrino mass plays a role in explaining the dark mass of the universe. From the rotation rate of galaxies it is known that 80% to 90% of galactic masses are not observed. If one type of neutrino has mass betweeen 4 and 80 eV/c^2, a very large number of neutrinos available could provide most of the unobserved mass (*dark mass*) of the universe.

(2) The neutrino mass provides a mechanism of galaxy formation and its stability. If the neutrino mass has a sufficiently large value, it would eventually stop the expansion of the universe and hence close it.

(3) The antibaryon to baryon ratio in the universe is also the direct manifestation of the particle physics for cosmology. This ratio may be assumed unity at an early stage of the expansion of the universe. From observations of heavy cosmic ray nuclei and lack of *X*-ray observations from the annihilation of galactic matter, this ratio is found to be $< 10^{-4}$. This large change can be explained from theories like $SU(5)$ in which baryon nonconservation occurs. Thus more baryons rather than antibaryons have been created since universe's expansion.

(4) Both particle physics and cosmology have their standard models which have been experimentally confirmed to a reasonable degree of accuracy. The particle model is $SU(3)_C \otimes SU(2)_L \otimes U(1)_Y$ and the cosmological model is the *hot big bang*. Two key quantitative observations—the microwave background and the Big Bang Nucleosynthesis (*BBN*) and light element abundances, establish the modern physical cosmology and the hot Big Bang Model. The second of these observations is more directly connected to high energy physics.

The microwave back ground probes events at temperatures $\sim 10^4$ *K* and time $\sim 10^5$ years, while the light abundances probe the universe at $\sim 10^{10} K$ and times ~ 1 sec. Thus the nucleosynthesis results played the most significant role in leading to the particle physics cosmology merger.

18.29 ELECTROMAGNETIC STRUCTURE OF NUCLEONS

According to meson theory, the proton as well as the neutron should be surrounded by a meson cloud and consist of a distribution charge of finite extent. Electrons are used to probe the electromagnetic structure of the nucleon just as α-particles used to probe atomic structure. Owing to the small size of the proton, electrons of small wavelength (thus of high energy) are required for the experimental investigation of the charge distribution in the nucleons. After the completion of the linear accelerator at Stanford University, Hofstadter and others were able to determine nuclear radius and hence to study the structure of nucleons. Similar measurements have been carried on at Cornell University using a electron beam from a 1.3 GeV electron synchrotron.

The first observations of a finite size of the proton were made by Hofstadtor and McAllister (1955) by examining the scattering at 100 MeV electrons and found a very small effect of finite size. The experiments were further carried out at an electron energy of 236 MeV and found an rms radius of the proton to be equal to 0.78 ± 0.20 fermi. The numerical results were arrived at by assuming that the form factors corresponding to charge distribution and magnetic moment distribution .

$$F_1 = F_2 (\equiv F_p)$$

as funcions of q and effectively using the shape independent approximation

$$F = 1 - (q^2 \alpha^2/6) + \ldots,$$

where 'α' is the rms radius of the charge or magnetic moment distribution. It is related more generally to a density distribution through the Fourier transform

$$F = \frac{4\pi}{q} \int_0^\infty \rho(r) \exp(iq.r) d\tau,$$

which applies in the non-relativistic limit in which $\rho(r)$ is the static density distribution and is a function of radius. At large angles, where tan θ/2 ≥ 1 and at high energies, it becomes possible to distinguish moment scattering. Hence it becomes possible to find F_1 and F_2 separately. Chambers and Hofstadter (1956) carried out a detailed series of experiments on the proton extending to an energy of 550 MeV with scattering angles lying between 30° and 135° in the lab. frame. They found a very large deviations from point scattering. The ratio F_1/F_2 may be found independently of any model by comparing two cross sections at two different energies and different angles, such that the momentum transfer q is the same at both cross section determinations. $F_1/F_2 = 1.1 \pm 0.2$ and $q^2 = 4 \times 10^{30} m^{-2}$ found from the above experiments.

Using the fact that magnetic moment scattering falls off more slowly at large angles than charge scattering, high energy data may be analyzed to find $F_1 + kF_2$. *Since* $k = 1.79$, the data can yield F_2, if F_1 is known even approximately. At small scattering, magnetic scattering is essentially zero and hence F_1 may be investigated alone. This procedure shows that for an exponential model, the charge r.m.s. radius must be close to 0.8 fermi when the magnetic r.m.s. radius is allowed to vary from 0.60 fermi to 1.0 fermi.

Rosenbluth gave a relation for the differential cross-section as :

$$\frac{d\sigma}{d\Omega} = \left(\frac{d\sigma}{d\Omega}\right)_{Mott} \left\{ \left[F_1^2 - \frac{k^2 q^2}{4m^2} F_2^2 \right] - \frac{q^2}{2m} [F_1 + kF_2]^2 \tan^2 \frac{\theta}{2} \right\}$$

This relation, called Rosenbluth formula, contains an interference term between F_1 and F_2. Thus it is conventional to define the electric and magnetic form factors of the proton as

$$G_E = F_1 + (kq^2/4m^2) F_2 \quad \text{and} \quad G_M = F_1 + kF_2.$$

In the limit $q^2 \to 0$, $G_E(0) = 1$ and $G_M(0) = 1 + k = \mu_p$, the magnetic moment of the proton. In terms of these form factors the interference term disappears and we get the relation as :

$$\frac{d\sigma}{d\Omega} = \left(\frac{d\sigma}{d\Omega}\right)_{Mott} \left[\frac{G_E^2 - (q^2/4m^2) G_M^2}{1 - q^2/4m^2} - \frac{q^2}{2m^2} G_M^2 \tan^2\left(\frac{\theta}{2}\right) \right]$$

The form factors G_E and G_M can be determined by measuring $d\sigma/d\Omega$ as a function of θ by performing experiments at different values of q^2. The graph showing relationship between $(d\sigma/d\Omega)/(d\sigma/d\Omega)_{Mott}$ and tan² θ/2 at a fixed value of q^2 is linear. The slope of the graph gives the magnetic form factor G_M at a particular value of q^2. G_E can be determined from the intercept and G_M.

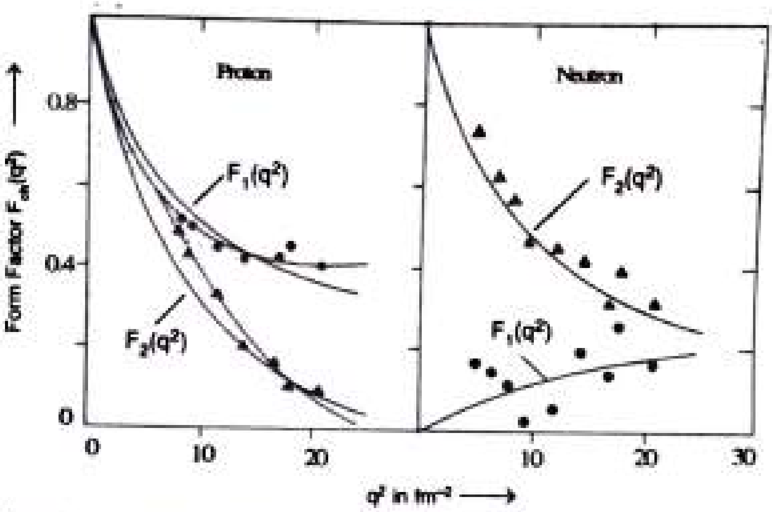

Fig. 18.32. Electric and magnetic form factors as a function of q^2 for (a) the proton and (b) the neutron.

Typical results for the form factors of the proton and neutron are shown in Fig. 18.32. They satisfy the simple law

$$G_E^p(q^2) = \frac{G_M^p(q^2)}{\mu_p} = \frac{G_M^n(q^2)}{|\mu_n|}, G_E^n(q^2) = 0.$$

The experimental results on G_E^p are consistent with the form factor. We therefore conclude that the charge distribution of the proton and the magnetic moment distribution of the neutron are both exponential roughly in space with a mean radius of about 0.8 fermi. The magnetic form factor of the proton, on average also has this behaviour, but shows deviations from the simple exponential shape in space.

From the scattering at 900 MeV and at 1.3 BeV, we find that for high four momentum transfers the charge and anomalous moment form factors differ from one another in the sense that corresponds to a wider distribution for the magnetic moment than for the charge. The equations of theoretical curves show that the proton root mean radii are given as

$$r_1 = r_{pc} = 0.88 \text{ fermi} \quad \text{and} \quad r_2 = r_{p\mu} = 0.95 \text{ fermi}.$$

Since neutron targets are not available, the information on the form factors of the neutron is obtained from the scattering of fast electrons by deuterons. Data upto 1.3 BeV have been obtained. The root mean square radii obtained from these results are :

$$r_1 = r_{nc} = 0.00 \text{ fermi} \quad \text{and} \quad r_2 = r_{n\mu} = 0.87 \text{ fermi}.$$

Charge distributions in the proton and in neutron obtained from above calculations are shown in Fig. 18.33.

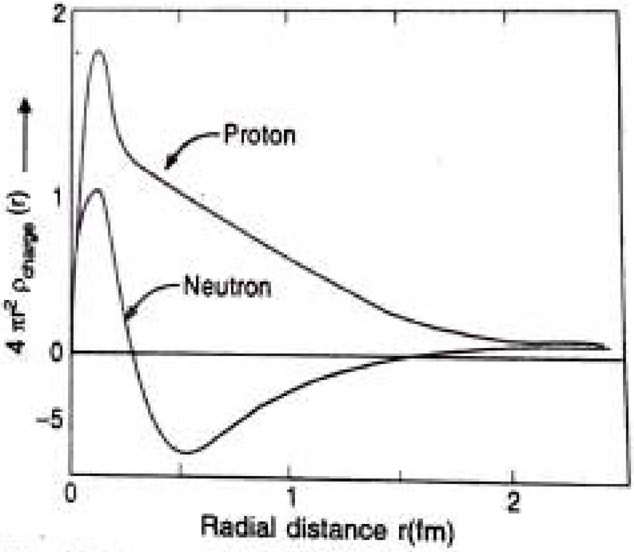

Fig. 18.33. The proton and neutron charge density distributions.

The proton has a finite extent as if there were a finite probability of finding it decomposed into a neutron and positive meson cloud. The structure of the neutron can be interpreted as due to the decomposition into a proton surrounded by a negative muon cloud, but apparently, the higher order effects may be considered that produce a positive charge density at larger distances.

A Brief Summary

The elementary particles are the fundamental constituents of the matter. More than 30 long lived particles and antiparticles have been detected experimentally. The antiparticle has the same mass and spin as its associated particle, but the electromagnetic properties such as charge and magnetic moment are opposite. In addition to long lived particles there are hundreds of resonances, called *resonance particles*. The elementary particles are broadly classified as *fermions* and *bosons* depending upon their spin values. These are grouped into four families–*bosons, leptons, mesons, and baryons*. The mesons and baryons are collectively referred to as hadrons. These groups may be subdivided into subgroups according to the types of interaction in which they participate. In addition to familiar gravitational and electromagnetic interactions, there are the strong and weak interactions. The strong interaction holds the nucleons together in a nucleus. The strong interactions occur only between hadrons. The electromagnetic interactions result from the coupling of charge to the electromagnetic field. Weak interactions explain how a neutrino interacts with nuclear matter. The neutrino does not participate in strong interactions. All leptons are fermions, they respond only to the weak interaction. The hadrons participate in the strong interactions, and contain both fermions and bosons.

The interactions responsible for the nuclear reactions fall into three groups : strong (decay rates of $10^{21}-10^{23}$ sec^{-1}), electromagnetic ($10^{16}-10^{19}$ sec^{-1}) and weak ($< 10^{13}$ sec^{-1}). All particle reactions and decays obey certain conservation laws, such as *(i)* Mass-energy, *(ii)* linear momentum, angular momentum, etc. Several other conservation laws are the conservation of lepton number, conservation of baryon number, strangeness number and isospin and parity. The particles produced by strong interactions but decayed by weak interactions are called *strange particles*. A new quantum number known as strangeness is used for such particles. The unstable hadrons are called particle resonances or excited hadrons, which have lifetimes $= \hbar / m_\pi c^2$, too short to be observed directly. The charge conjugation is the process of changing every particle of a system into its antiparticle. In the strong and electromagnetic interactions the total strangeness number is conserved. In weak interactions, it is found that $\Delta S = 0, \pm 1$. The charge independence has led to the introduction of another quantum number called isotopic spin. The parity operation or the mirror reflection shows that the linear momenta reverse direction, but the angular momenta do not because they describe circulation. Both the parity *P* and charge conjugation *C* are not conserved in weak decay. The combination of *CP*-operation is not valid for all the weak interactions. The time reversal changes the direction of flow of time, like running a motion picture backwards. In the weak interactions, the observed violation of parity requires that *C* and/or *T* be violated. As a consequence CPT theorem is correct.

Gell-Mann and Zweig proposed that the hadrons are composite objects being bound states of fermions called quarks. Three types of quarks namely up, down and strange are very common. The first two are of nearly equal mass, while the third is more massive. The antiparticles are formed by the antiquarks of those forming the particle. The other new quarks are charm, beauty (or bottom) and truth (top). The quarks are also come in three different colours-red, green and blue. The colour and flavour are quantum mechanical labels or quantum numbers very similar to spin and parity.

Quantum chromodynamics describes hadrons. It explains the strong interactions among the quarks, considering gluons as mediators. The gauge theories were not successful for weak-interaction. S.L. Glashow in 1960 suggested that the electromagnetic and weak interactions might be unified in a gauge theory. A grand unification theories have been developed in recent years to unify all the interactions.

EXERCISES

Example 1. *Calculate the energy of the neutron produced when a slow negative pion is captured by a proton. Should neutron be treated relativistically ?*

$$\pi^- + p^+ \rightarrow n^\circ + \gamma + Q.$$

$$139 + 938 \rightarrow 939 + h\nu + Q,$$

or

$$Q = 138\ MeV = \epsilon_\gamma + E_{n'}$$

From conservation of momentum $m_n v_n = E_\gamma / c$

and

$$\frac{E_n}{E_\gamma} = \frac{1}{2}\frac{m_n v_n^2}{c m_n v_n} = \frac{1}{2}\frac{v_n}{c} = \frac{1}{2}\frac{E_\gamma}{m_n c^2} = \frac{E_\gamma}{1878}$$

$$\frac{E_n}{E_\gamma + E_n} = \frac{E_\gamma}{1878 + E_\gamma} \quad \therefore \quad \frac{E_n}{138} = \frac{E_\gamma}{1878 + E_\gamma}$$

and

$$\frac{E_n}{138} = \frac{138 - E_n}{1878 + 138 - E_n} = \frac{138 - E_n}{2016 - E_n}$$

or

$$E_n = 9 \text{ MeV}.$$

Using relativistic relations

$$m_n v_n = m_{0n} v_n / (1 - \beta^2)^{1/2} = E_\gamma / c$$

and

$$E_n = m_{0n} c^2 [(1 - \beta^2)^{-1/2} - 1]$$

ve get

$$E_n = 8.8 \text{ MeV}.$$

Example 2. *Discuss the following reactions using the conservation of isotopic spin :*

(i) $p + p \rightarrow p + p + \pi^0$, *(ii)* $\pi^0 \rightarrow \gamma + \gamma$, *(iii)* $\Lambda^0 \rightarrow \pi^- + p^+$, *and (iv)* $\pi^+ + p \rightarrow \pi^+ + p$.

(i)

	p +	p →	p +	p +	π^0
T =	½	½	½	½	1
T_3 =	+½	+½	+½	+½	0

We know that in all strong and electromagnetic reactions the third component of isotopic spin is conserved. As $Q = e\,(T_3 + B/2 + S/2)$ must be conserved, hence change of T_3 will be there when strangeness changes, which happens in the weak interactions. Secondly, in combining isotopic spins, we use the same rules as for ordinary spin. Hence vector sum of T on the right hand side may be 2, 1, or 0. Again the total $T_3 = 1$, ruling out $T = 0$. The conservation law can be satisfied with the final $T = 1$.

(ii)

$\pi^0 \rightarrow \gamma + \gamma$

$T = 1$ no T

$T_3 = 0$

In this decay T_3 is conserved hence the process does not involve the weak interaction. As the total isotopic spin changes, the decay occurs through the electro-magnetic forces which do not conserve isotopic spin.

(iii)

	Λ^0 →	π^- +	p^+
T =	0	1	½
T_3 =	0	−1	+½

The decay of the Λ^0 is a weak interaction which can bypass several conservative laws. The π^- is emitted in one direction from the plane defined by the Λ^0 and the bombarding particle which produced it. Thus parity is not conserved. As T_3 does not conserve, hence the conservation of charge gives no conservation of strangeness.

(iv)

	π^+ +	p →	π^+ +	p
T =	1	½	1	½
T_3 =	+1	+½	+1	+½

In this strong reaction both T_3 and T must be conserved. In the case of π^+ reaction only one isotopic spin state is possible.

Example 3. *Allocate the isospin to the strange particles from following equations :*

(a) $\pi^- + p \rightarrow \Lambda^0 + K^0$

(b) $p + p \rightarrow \Lambda^0 + K^+ + p$

(c) $\pi^+ + n \rightarrow \Lambda^0 + K^+$

(d) $\pi^- + p \rightarrow \Sigma^- + K^+$

(e) $\pi^+ + p \rightarrow \Sigma^+ + K^+$

(f) $\pi^+ + n \rightarrow \Xi^- + K^+ + K^+$

(a)

	π^- +	p →	Λ^0 +	K^0
T	1	½	0	
T_3	−1	+½	0	

Hence T_3 must be −½ for K^0 produced with Λ^0 and T must have a value 3/2 or ½. The observed value fixes T = ½.

(b)

	p +	p →	Λ^0	+ K^+ +	p
T	½	½	0		½
T_3	+½	+½	0		+½

(c)

	π^+ +	n →	Λ^0	+ K^+
T	1	½	0	
T_3	+1	−½	0	

These reactions fix the value of T_3 for K^+ as $+\frac{1}{2}$ and T as $\frac{1}{2}$.

(d)

	$\pi^- +$	$p \rightarrow$	$\Sigma^- +$	K^+
T	1	$\frac{1}{2}$		$\frac{1}{2}$
T_3	-1	$+\frac{1}{2}$		$+\frac{1}{2}$

This fixes the value of T_3 for Σ^- as -1 and of T as 1.

(e)

	$\pi^+ +$	$p \rightarrow$	$\Sigma^+ +$	K^+
T	1	$\frac{1}{2}$		$\frac{1}{2}$
T_3	1	$+\frac{1}{2}$		$+\frac{1}{2}$

This fixes the value of T_3 for Σ^+ as $+1$ amd T as 1.

(f)

	$\pi^+ +$	$n \rightarrow$	$\Xi^- +$	$K^+ +$	K^+
T	1	$\frac{1}{2}$		$\frac{1}{2}$	$\frac{1}{2}$
T_3	$+1$	$-\frac{1}{2}$		$+\frac{1}{2}$	$+\frac{1}{2}$

This fixes the value of T_3 for Ξ^- as $-\frac{1}{2}$ and of T as $\frac{1}{2}$. The above results can also be obtained by Gell-Mann scheme.

Example 4. *Which of the following reactions are allowed and forbidden under the conservation of strangeness, conservation of baryon number and conservation of charge.*

$$\pi^+ + n \rightarrow \Lambda^\circ + K^+ \quad \text{...(i)}$$
$$\rightarrow K^\circ + K^+ \quad \text{...(ii)}$$
$$\rightarrow \bar{K}^\circ + \Sigma^+ \quad \text{...(iii)}$$
$$\rightarrow \pi^- + p \quad \text{...(iv)}$$
$$\pi^- + p \rightarrow \Lambda^\circ + K^\circ \quad \text{...(v)}$$
$$\rightarrow \pi^\circ + \Lambda^\circ. \quad \text{...(vi)}$$

Let us take one by one. Using values of charge Q, baryon number B and strangeness number S from the table 18.3, we have

	$\pi^+ +$	n	$\rightarrow$	Λ°	$+$	K^+	
Q	1	0		0		1	$\Delta Q = 0$
B	0	1		1		0	$\Delta B = 0$
S	0	0		-1		1	$\Delta S = 0.$

Hence relation *(i)* is allowed under these conservation laws.

(ii)

	$\pi^+ +$	n	$\rightarrow$	K°	$+$	K^+	
Q	1	0		0		1	$\Delta Q = 0$
B	0	1		0		0	$\Delta B \neq 0$
S	0	0		1		1	$\Delta S \neq 0.$

Hence this reaction is not allowed by baryon number and strangeness number.

(iii)

	$\pi^+ +$	n	$\rightarrow$	$\bar{K}^\circ$	$+$	Σ^+	
Q	1	0		0		1	$\Delta Q = 0$
B	0	1		0		1	$\Delta B = 0$
S	0	0		-1		-1	$\Delta S \neq 0$

Hence this reaction is not allowed by strangeness quantum number.

(iv)

	$\pi^+ +$	n	$\rightarrow$	π^-	$+$	p	
Q	1	0		-1		1	$\Delta Q \neq 0$
B	0	1		0		1	$\Delta B = 0$
S	0	0		0		0	$\Delta S = 0$

Hence this reaction is not allowed by conservation of charge

(v)

	π^- +	p	→	Λ°	+	K°	
Q	-1	1		0		0	$\Delta Q = 0$
B	0	1		1		0	$\Delta B = 0$
S	0	0		-1		1	$\Delta S = 0$

Hence this reaction is allowed under these conservation laws.

(vi)

	π^- +	p	→	π°	+	Λ°	
Q	-1	1		0		0	$\Delta Q = 0$
B	0	1		0		1	$\Delta B = 0$
S	0	0		0		-1	$\Delta S \neq 0$

Hence this reaction is not allowed by strangeness quantum number.

Example 5. *Classify the following processes in terms of the type of interactions.*

$\pi^- + p \rightarrow \Lambda^\circ + K^\circ$; $\pi^- + p \rightarrow \pi^\circ + n$; $p + \gamma \rightarrow p + \pi^\circ$; $\Sigma^\circ \rightarrow \Lambda^\circ + \gamma$; $\pi^\circ \rightarrow \gamma + \gamma$; $K^\circ \rightarrow \pi^+ + \pi^-$; $\Lambda^\circ \rightarrow p + \pi^-$; $\Xi^- \rightarrow \Lambda^\circ + \pi^-$; and $\Lambda^\circ \rightarrow p + e^- + \bar{\nu}$.

In the reactions $\pi^- + p \rightarrow \Lambda^\circ + K^\circ$ and $\pi^- + p \rightarrow \pi^\circ + n$, the inter-action is a short-range force between hadrons (π, p, n, Λ and K) corresponding to one pion-exchange. These reactions obey selection rules

$$\Delta B = 0, \Delta Q = 0, \Delta Y \ = \ 0, \Delta\pi = 0, \Delta T = 0, \Delta T_3 = 0$$

hence the interaction is strong.

In the reactions $p + \gamma \rightarrow \pi^\circ + p$, $\Sigma^\circ \rightarrow \Lambda^\circ + \gamma$ and $\pi^\circ \rightarrow \gamma + \gamma$, the interaction is electromagnetic, as the electromagnetic force arises due to the mechanical effect of the emission and absorption of virtual photons. These reactions obey all above metioned selection rules except the rule for conservation of isospin T, hence the interaction in these processes is *electromagnetic.*

In the reactions $K^\circ \rightarrow \pi^+ + \pi^-$, $\Lambda^\circ \rightarrow p + \pi^-$, $\Xi^- \rightarrow \Lambda^\circ + \pi^-$ and $\Lambda^\circ \rightarrow p + e^- + \bar{\nu}$, the interaction is weak, as the weak interaction is due to the leptonic decay of strange and non-strange particles and due to the non-leptonic decay of strange particles. These reactions do not conserve parity, strangeness, isospin and the third component of isospin, hence the interaction in these processes is *weak.*

Example 6. *Discuss the following reactions :*

(a) $\pi^- + p \rightarrow \Sigma^+ + K^-$,
(b) $K^- + p \rightarrow \Omega^- + K^+ + K^\circ$,
(c) $\Omega^- \rightarrow \Xi^\circ + \pi^-$,
(d) $\pi^+ + p \rightarrow p + p + \bar{n}$
(e) $\bar{n} \rightarrow \bar{p} + e^+ + \nu_e$,
(e) $\Lambda^\circ \rightarrow n + \gamma$.

(a) This reaction is not possible because it requires a strangeness change of 2 due to the production of two strange particles.

(b)

	K^-	+	p	→	Ω^- +	K^+	+	K°	
S	-1		0	→	-3	1	+	1	$\Delta S = 0$

$\Delta Q = 0$, $\Delta B = 0$, $\Delta T = 0$, $\Delta T_3 = 0$, angular momentum and parity are also conserved.

Therefore the reaction can proceed via *strong interaction.*

(c)

	Ω^-	→	Ξ°	+	π^-	
T	0		$\frac{1}{2}$		1	$\Delta T = \frac{1}{2}$ or $\frac{3}{2}$
T_3	0		$\frac{1}{2}$		-1	$\Delta T_3 = \frac{1}{2}$

$\Delta Q = 0$, $\Delta B = 0$, angular momentum and parity are also conserved. $\Delta T_3 = 1/2$, which is equivalent to $\Delta S = 1$. These quantum number changes do allow the decay via weak interaction, and prohibit from proceeding more rapidly by electromagnetic or strong interaction.

(d) $\pi^+ + p \rightarrow p + p + \bar{n}$.

From the table the quantum numbers of $\bar{n}$ are $Q = 0$, *spin* = 1/2, $B = -1$, *Parity* = *odd*, $T = 1/2$, $T_3 = 1/2$, $S = 0$. Thus all quantum numbers are conserved by the reaction, so it can take place by the *strong interaction.*

(*e*)

$$\bar{n} \rightarrow \bar{p} + e^+ + \nu_e.$$

Since ν_e occurs, therefore the reaction must be by the *weak interaction.* $\Delta Q = 0$, $\Delta B = 0$, electron lepton number is conserved. Angular momentum can be conserved. Parity is not definite for leptons and is also not significant for a weak interaction.

(*f*)

$$\Lambda^0 \rightarrow n + \gamma.$$

Obviously it must be *electromagnetic*, if it occurs.

It can not occur because $T_3 = 0$ for Λ^0 and γ, while it is $-1/2$ for the *n*. We know that T_3 must be conserved in the electromagnetic interaction.

Example 7. *Explain why the following decay processes are not observed.*

(*a*) $p + p \rightarrow K^+ + \Sigma^+$, (*b*) $p + n \rightarrow \Lambda^0 + \Sigma^+$, (*c*) $p + n \rightarrow \Xi^- + K^+ + \Sigma^+$

(*d*) $\Xi^0 \rightarrow \Sigma^0 + \Lambda^0$, (*e*) $\Sigma^+ \rightarrow \Lambda^0 + K^+$, (*f*) $\Lambda^0 \rightarrow K^+ + K^-$.

The first three processes (a), (b) and (c) involve only strongly interacting particles and should follow all the conservation laws. The process is forbidden or not observed if any one or some of these laws are violated in that process.

(*a*) The process $p + p \rightarrow K^+ + \Sigma^+$ is not observed because the baryon number, the isospin and its third component are not conserved.

(*b*) The process $p + n \rightarrow \Lambda^0 + \Sigma^+$ is not observed because the strangeness number and the third component of isospin are not conserved.

(*c*) The process $p + n \rightarrow \Xi^- + K^+ + \Sigma^+$ is not observed because of both reasons, as for (b).

All the processes (*d*), (*e*) and (*f*) are not leptonic decays of strange particles, where the change of strangeness quantum number *S*, isospin *T* and its third component T_3 should obey the rules $|\Delta S| = 1$, $|\Delta T| = 1/2$ and $|\Delta T_3| = 1/2$.

(*d*) The $\Xi^0 \rightarrow \Sigma^+ + \Lambda^0$ decay is not observed because the energy and the baryon number are not conserved.

(*e*) The $\Sigma^+ \rightarrow \Lambda^0 + K^+$ decay is not observed because the energy is not conserved.

(*f*) The $\Lambda^0 \rightarrow K^+ + K^-$ decay is not observed because the baryon number is not conserved.

Example 8. *Order the following decays in order of increasing lifetime. Name the interaction responsible for the decay.*

(*a*) $p \rightarrow e^+ + \pi^0$, (*b*) $\Omega^- \rightarrow \Xi^0 + K^-$, (*c*) $\rho^0 \rightarrow \pi^+ + \pi^-$,

(*d*) $\pi^0 \rightarrow \gamma + \gamma$, (*e*) $\Xi^- \rightarrow \Lambda^0 + \pi^-$, (*f*) $\mu^- \rightarrow e^- + \bar{\nu}_e + \nu_\mu$.

Using the lifetimes of the decays and the quantum numbers associated with these particles, we see that The decay (*a*) $p \rightarrow e^+ + \pi^0$ is forbidden as the lepton number and the baryon number are not conserved. The decay (*b*) $\Omega^- \rightarrow \Xi^0 + K^-$ is forbidden as the energy is not conserved.

All other decays are allowed and may be arranged in increasing order of lifetime as given below

(*c*) $\rho \rightarrow \pi^+ + \pi^-$ $(\tau = 10^{-24}\ s)$; (*d*) $\pi^0 \rightarrow \gamma + \gamma$ $(\tau = 10^{-16}\ s)$;

(*e*) $\Xi^- \rightarrow \Lambda^0 + \pi^-$ $(\tau = 10^{-10}\ s)$; (*f*) $\mu^- \rightarrow e^- + \bar{\nu}_e + \nu_\mu$ $(\tau = 10^{-6}\ s)$

Thus decay (*c*) is a strong decay, (*d*) an electro magnetic decay, (*e*) weak decay in which the strangeness number is changed, while (*f*) is the weak decay of a non-strange particle.

Example 9. *The Σ^* is an unstable hyperon with mass m = 1385 MeV and decay with Γ = 35 MeV into the channel $\Sigma^{*+} \rightarrow \pi^+ + \Lambda^0$ with a branching ratio of 88%. (a) Is this decay strong or weak ? (b) What is the isospin of Σ^*.*

The partial width of the given decay $\Sigma^{*+} \rightarrow \pi^+ + \Lambda^\circ$ is $\Gamma = 88\% \times 35 = 30.8\ MeV$.

∴ The corresponding lifetime $\tau = \dfrac{\hbar}{\Gamma} = \dfrac{6.62 \times 10^{-22}\ MeV\ sec}{30.8\ MeV} = 2.15 \times 10^{-23}\ s.$

This very short lifetime shows that this decay corresponds to the *strong interaction*.

The isospin is conserved in strong interaction. The strong decay $\Sigma^{*+} \rightarrow \pi^+ + \Lambda^\circ$ shows that

$$T(\Lambda) = T_3(\Lambda) = 0.$$

$$\therefore \quad T(\Sigma^*) = T(\pi) = 1.$$

Example 10. *The following two leptonic decays*

$$\mu^+ \rightarrow e^+ + \nu_e + \bar{\nu}_\mu \qquad \text{and} \qquad \tau^+ \rightarrow e^+ + \nu_e + \bar{\nu}_\tau\ (16\%).$$

are believed to proceed via the same interaction. Given that $m_\mu = 106\ MeV/c^2$, $m_\tau = 1784\ MeV/c^2$, $m_e = 0.5\ MeV/c^2$, $m_\nu = 0\ MeV/c^2$; *mean life time* τ *for* $\mu^+ = 2.2 \times 10^{-6}$ *s, Estimate the mean life of* τ^+.

The theory of weak interaction gives the decay probability per unit time as

$$\lambda = \tau^{-1} = G^2 m^5 / 192\, \pi^3.$$

As the interaction is same for both the given decays therefore $G_\tau = G_\mu$ and we thus get

$$\lambda_\tau / \lambda_\mu = m_\tau^5 / m_\mu^5.$$

If λ is the total decay probability per unit time of τ^+, the branching ratio $R = \lambda_\tau / \lambda$

$$\therefore \quad \tau = \lambda^{-1} = \frac{R}{\lambda_\tau} = R\left(\frac{m_\mu}{m_\tau}\right)^5 \tau_\mu$$

$$= 16\%\ (106/1784)^5 \times 2.2 \times 10^{-6} = 2.6 \times 10^{-13} s.$$

Example 11. *(A) Give the evidence supporting the quark model, (B) What is meant by the approximate SU (3) symmetry of strong interaction ? How is this broken ?*

(A) The evidence supporting the quark model includes the following : *(a)* The deep inelastic scattering data of electrons on nucleons indicate that nucleon has substructure, *(b)* the *SU* (3) symmetry of hadrons can be explained by the quark model, *(c)* The quark model gives the correct cross section relationship of hadronic reactions, and *(d)* the quark model can explain the abnormal magnetic moments of nucleons.

(B) The approximate *SU* (3) symmetry of strong interactions means that isospin multiplets with the same spin and parity, but different strangeness numbers can be transformed into each other. They are super multiplet states of the same original particle with different electric charges (T_3) and hypercharges (Y). If *SU* (3) symmetry were perfect, particles of the same supermultiplet should have the same mass. Actually the difference of their masses is not zero, but can be quite large. This shows that such a super symmetry is only approximate. The example is the supermultiplet of 0^--mesons, π° ($m_{\pi^\circ} = 135\, MeV$) and K° ($m_{K^\circ} = 498\, MeV$). The difference of masses gives the extent of breaking of the symmetry.

Example 12. *What is the evidence for another quantum number colour, under which the strong interactions are exactly symmetric ? How many colours are there ? What data are used to determine this number.*

In the quark model, a quark has spin 1/2 and thus obeys Fermi statistics. Thus for exchanging any two quarks, the wavefunction of a baryon is required to be antisymmetric. In reality, there are baryons having quark contents *uuu* or *sss* for which the wave functions are symmetric for quark exchange. This contradiction can be resolved by assuming an additional quantum number, called *colour*, which has three values. The hypothesis of colour can be tested by the measurement of R in high energy e^+e^- collisions. The ratio R is defined as

$$R = \frac{\sigma(e^+e^- \rightarrow hadrons)}{\sigma(e^+e^- \rightarrow \mu^+\mu^-)} = \sum_i Q_i^2,$$

where Q_i is the electric charge of the i^{th} quark.

If the energy of e^+e^- system is sufficient to produce all the three flavours of quarks. For the colourless quarks, this ratio

$$R = \sum_i Q_i^2 = \left(\tfrac{4}{9}+\tfrac{1}{9}+\tfrac{1}{9}\right) = \tfrac{2}{3}.$$

If each quark can have three colours

$$R = 3\Sigma Q_i^2 = 3\left(\tfrac{4}{9}+\tfrac{1}{9}+\tfrac{1}{9}\right) = 2.$$

The latter is in agreement with experiments.

Example 13. *(a) If a resonance has $I = 3/2$, $B = 1$ and $S = 0$, what are its charge states ? (b) What values of electric charge are possible for a baryon and a meson in the quark model ?*

(*a*) There are $2I + 1$ components of I with $I_3 = 3/2$, $1/2$, $-1/2$ and $-3/2$. Using the relation $Q = I_3 + (B + S)/2$, these correspond to charge states + +, +, 0 and – respectively.

(*b*) According to the quark model, a baryon is a combination of three quarks with charges $+2/3$ or $-1/3$. All possible combinations lead to charges ++, +, 0 and –.

Mesons are $q\bar{q}$ combinations with charges $2/3$, $-1/3$ and $-2/3$, $+1/3$. The possible charges are therefore +, 0 and –.

Example 14. *(i) Determine the quark contents of (a) Λ^0 the isosinglet baryon with strangeness $S = -1$ and (b) K^+, K^0 $(S = +1)$ and K^-, $\bar{K}^0$ $(S = -1)$ mesons.*

(ii) The Ξ-baryons form an isospin doublet with $S = -2$. What charge states (quark contents) are possible ?

(*i*) (*a*) Λ^0 is the singlet baryon with $S = -1$, therefore it must contain an *s*-quark with $Q = -1/3$. The other quarks necessary to give a neutral baryon are $u(Q = +2/3)$ and $d(Q = -1/3)$. Hence $\Lambda^0 = uds$.

(*b*) Mesons are $q\bar{q}$ combinations. The K^+ and K^0 with $S = 1$ must contain an $\bar{s}$-quark with $Q = 1/3$. Hence $K^+ = \bar{s}\,u$ and $K^0 = \bar{s}d$. Similarly $K^- = s\bar{u}$ and $\bar{K}^0 = s\bar{d}$.

(*ii*) The Ξ-baryons have $S = -2$ and therefore must contain two *s*-quarks. The third quark is either a *u*-quark corresponding to the Ξ^0 $(Q = 0, I_3 = 1/2)$ or a *d*-quark corresponding to the Ξ^- $(Q = -1, I_3 = -1/2)$.

Example 15. *The $\Delta(1232)$ is a resonance with $I = 3/2$. Predict the branching ratio for $(\Delta^0 \to p\pi^-)/(\Delta^0 \to n\pi^0)$. Find this ratio for a resonance with $I = 1/2$.*

The nucleon has $I = 1/2$ and the pion has $I = 1$. The Δ^0 has $I_3 = -1/2$. Clebsh-Gorden coefficients for $j_1 = 1$ and $j_2 = 1/2$ gives

$$\underset{\Delta^0}{|\tfrac{3}{2},-\tfrac{1}{2}>} = \sqrt{\tfrac{2}{3}}\,\underset{\pi^0}{|1,0>}\underset{n}{|\tfrac{1}{2},-\tfrac{1}{2}>} + \tfrac{1}{\sqrt{3}}\,\underset{\pi^-}{|1,-1>}\underset{p}{|\tfrac{1}{2},\tfrac{1}{2}>}$$

The ratio of the amplitudes for the decays $\Delta^0 \to \pi^- p$ and $\Delta^0 \to \pi^0 n$ is the ratio of the corresponding Clebsh-Gorden coefficients. Hence the branching ratio

$$\frac{\Delta^0 \to p\pi^-}{\Delta^0 \to n\pi^0} = \frac{(\sqrt{1/3})^2}{(\sqrt{2/3})^2} = \frac{1}{2}.$$

If Δ has $I = 1/2$, we will have

$$\underset{\Delta^0}{|\tfrac{1}{2},-\tfrac{1}{2}>} = \sqrt{\tfrac{1}{3}}\,\underset{\pi^0}{|1,0>}\underset{n}{|\tfrac{1}{2},-\tfrac{1}{2}>} - \sqrt{\tfrac{2}{3}}\,\underset{\pi^-}{|1,-1>}\underset{p}{|\tfrac{1}{2},\tfrac{1}{2}>}$$

and the branching ratio

$$\frac{\Delta^0 \to p\pi^-}{\Delta^0 \to n\pi^0} = \frac{(\sqrt{2/3})^2}{(\sqrt{1/3})^2} = 2.$$

Example 16. *Find the ratio of the cross-sections for the reactions $\pi^- p \to \pi^- p$ and $\pi^- p \to \pi^0 n$, given that the two I-spin amplitudes are equal in magnitude but differ in phase by 45°.*

The possible I spins of the initial and final states are $I = 1/2$ and $3/2$. We have

$$\pi^- p = \tfrac{1}{\sqrt{3}}|\tfrac{3}{2},-\tfrac{1}{2}> - \sqrt{\tfrac{2}{3}}|\tfrac{1}{2},-\tfrac{1}{2}>$$

$$\pi^0 n = \sqrt{\tfrac{2}{3}}\,|\tfrac{3}{2},-\tfrac{1}{2}> + \sqrt{\tfrac{1}{3}}\,|\tfrac{1}{2},-\tfrac{1}{2}>$$

Hence

$$<\pi^- p|H|\pi^- p> = \tfrac{1}{3}A_3 + \tfrac{2}{3}A_1$$

and

$$<\pi^0 n|H|\pi^- p> = (\sqrt{2}/3)A_3 - (\sqrt{2}/3)A_1$$

Therefore the ratio of the cross sections is

$$\frac{\sigma_1}{\sigma_2} = \left[\frac{A_3 + 2A_1}{\sqrt{2}(A_3 - A_1)}\right]^2$$

Substitution of $A_3 = A_1 e^{i\phi}$ with $\phi = \pm 45°$, gives

$$\frac{\sigma_1}{\sigma_2} = \frac{1}{2}\left|\frac{e^{i\phi}+2}{e^{i\phi}-1}\right|^2 = \frac{1}{2}\cdot\frac{5+4\cos\phi}{2-2\cos\phi} = \frac{1}{4}\left(\frac{5+4\cos 45°}{1-\cos 45°}\right) = 6.68.$$

This is independent of the sign of ϕ.

Example 17. *The product of three quark triplets is decomposed as* $3 \otimes 3 \otimes 3 = (6 \oplus \bar{3}) \otimes 3 = 10_S \oplus 8_{M_S} \oplus 8_{M_A} \oplus 1_A$. *Determine the normalized quark wavefunctions of (i) the uud and (ii) the uds states in the decuplet, the* M_A *octet and the* M_S *octet. Write the wavefunction of the unitary singlet state.*

(*i*) In *SU* (3), we have $3 \otimes 3 \otimes 3 = 10_S \oplus 8_{M_S} \oplus 8_{M_A} \oplus 1_A$, *i.e.*, the product of three flavour triplet leads to a symmetric decuplet, two octets of mixed symmetry M_S (symmetric) and M_A (antisymmetric) and an antisymmetric singlet. The decuplet states arise from the product $6 \otimes 3$. Hence to the *ud* and *uu* states in the sextet add a *u* and *d*-quark respectively to obtain, after normalization,

$$\Delta^+ = \tfrac{1}{\sqrt{3}}[uud + (ud + du)u].$$

The antisymmetric octet states arise from the product $\bar{3} \otimes 3$. Hence add a *u* quark to the $\bar{3}$ *ud* state to obtain

$$P_{M_A} = \tfrac{1}{\sqrt{2}}(ud - du)u.$$

The symmetric octet states arise from the product $6 \otimes 3$. Hence add a *u*-quark to the *ud* sextet state and a *d*-quark to the *uu* state to obtain

$$P_{M_S} = a(ud + du)u + b\,uud.$$

This state must be orthogonal to the decuplet state (Δ^+), so after normalization we get

$$P_{M_S} = \tfrac{1}{\sqrt{6}}[(ud + du)u - 2uud)]$$

(*ii*) For the decuplet states add *a u* to *ds*, *a d* to *us* and *s* to *ud* in the sextet to obtain the symmetry state

$$\Sigma^0\,(1385) = \tfrac{1}{\sqrt{6}}[sd + ds)u + (su + us)d + (du + ud)s].$$

The $I = 1$ octet states are obtained from P_{M_A} and P_{M_S} by successive application of U_- and I_-. The normalization gives

$$\Sigma^0_{M_A} = \tfrac{1}{2}[(sd - ds)u + (su - us)d]$$

$$\Sigma^0_{M_S} = \tfrac{1}{\sqrt{12}}[(sd + ds)u + (su + us)d - 2(du + ud)s]$$

The $I = 0$ states must be orthogonal to $\Sigma^0(1385)$ and $\Sigma^0_{M_A}$ and $\Sigma^0_{M_S}$ respectively. Therefore

$$\Lambda^0_{M_S} = \tfrac{1}{2}[(sd + ds)u - (su + us)d]$$

$$\Lambda^0_{M_A} = \tfrac{1}{\sqrt{12}}[(sd - ds)u + (us - su)d - 2(du - ud)s].$$

The unitary singlet state must contain the u and d-quarks in an $I = 0$ combination and contain on an equal footing the u, d and s. Hence

$$1_A = \frac{1}{\sqrt{6}}[(ud - du)s + (ds - sd)u + (su - us)d].$$

Example 18. *If the charge density distribution of the proton is given by $\rho(r) = \rho_0 e^{-mr}$ which is normalized to unity. Find the form factor and determine the root mean square radius of the charge distribution if $m^2 = 0.71$ [GeV/c^2]^2.*

We know that the form factor $F(q)$ is the Fourier transform of the electric charge density distribution and is given by

$$F(q) = \int \rho(r)\, e^{i(\mathbf{q}\cdot\mathbf{r})}\, d\tau.$$

In the spherical coordinate system, it is given as

$$F(q) = \int \rho(r)\, e^{i(q\, r \cos\theta)}\, r^2\, dr\, d\phi \sin\theta\, d\theta.$$

For normalization $\int_0^\infty \rho_0 e^{-mr} 4\pi r^2 dr = 1$ or $\rho_0 = m^3/8\pi$.

$$\therefore \quad F(q) = \frac{2\pi}{iq}\int_0^\infty \rho(r)(e^{iqr} - e^{-iqr})r\, dr = \frac{m^3}{4iq}\int_0^\infty r[e^{-(m-iq)r} - e^{-(m+iq)r}]dr$$

$$= \frac{m^4}{(m^2+q^2)^2} = \left(1 + \frac{q^2}{m^2}\right)^{-2}$$

$$<r^2> = \int_0^\infty \rho(r) r^2\, 4\pi r^2 dr = \frac{m^3}{2}\int_0^\infty r^4 e^{-mr} dr.$$

$$= \frac{m^3}{2}\frac{4!}{m^5} = \frac{12}{m^2}.$$

Substituting $m^2 = 0.71$ [GeV/c^2]^2, we get

$$r_{rms} = [<r^2>]^{1/2} = [12/m^2]^{1/2} = [12/0.71\ (\text{GeV}/c^2)^2]^{1/2}$$

$$= \sqrt{12}/(0.84 \times 5.1)\, fm = 0.81\, fm.$$

Oral Questions

1. The electrostatic force between the earth and moon can be ignored because. ...
2. Define the terms : boson, fermion, hadron and baryon.
3. The proton does have a parity while the muon does not because—*(a)* parity is not conserved in electromagnetism, *(b)* The proton is very well known, *(c)* parity is defined from reactions relative to each other.
4. Which of the following isotope one can theoretically produce from nothing except a free energy of 4.5 GeV ? *(a)* ^2D, *(b)* ^3He, *(c)* ^3T.

   [with a free energy of 4.5 GeV, one can create baryon antibaryon pair. Thus a baryon which can be created with energy 2.25 GeV, must have its rest mass < 2.25 GeV. The particle which has rest mass below 2.25 GeV out of above given three particles is ^2D only. Thus the correct answer is (a).
5. Strange particles are produced in ... interaction but decay in ... interaction.
6. Which one of the following is correct ? A particle and its antiparticle *(a)* must have same mass, *(b)* always annihilate into two photons.
7. The life time of the muon is 10^6, 10^3, 1, 10^{-3} or 10^{-6} second.
8. Given that the K and π-mesons have spin 0 show that one of the weak decay processes $K^+ \to \pi^+\pi^0$ and $K^+ \to \pi^+\pi^+\pi^-$ must violate parity conservation.
9. Discuss briefly *(a)* J/ψ particle, and *(b)* different types of neutrinos.
10. If a resonance has $I = 3/2$, $B = 1$ and $S = 0$, what are its charge states.
11. What values of electric charge are possible for *(a)* a baryon and *(b)* a meson in the quark model.
12. The Σ^0-hyperon decays to $\Lambda^0 + \gamma$ with a meanlife time of 7.4×10^{-20} s Estimate its width.
13. How many neutrino types are known to exist ? What is the spin of a neutrino ?

14. What properties of neutrinos are conserved in scattering process ?
15. What is the difference between a neutrino and an antineutrino ?

[In scattering process, the lepton number of each kind of neutrino is conserved. The difference between a neutrino and antineutrino is that *(a)* they have opposite lepton numbers. *(b)* the helicities of these are opposite, if the neutrino mass is zero.]

16. Give the quantum numbers and quark content of five hadrons (nucleons and pions).
17. Draw a Feynman diagram showing the mechanism for a μ-decay.
18. What is tachyon ?
19. Explain unitary symmetry ?
20. Define flavour, charm and colour.

nswer : (1) These are electrically neutral; 3. c; 4. (a); 5. strong, weak; 6. (a); 7. 10^{-6}*s; 10. four (++, +, 0 and – correspond to* $I_3 = 3/2, 1/2, -1/2$ *and* $-3/2$ *respectively. 11. (a) ++, + , 0 and –; (b) +, 0 and –; 12. 9 keV; 13. 6, 1/2.*

Problems

1. Which of the following reactions illustrate associated production of strange particle ?

   (i) $p + n \to p + \Sigma^- + K^+$ *(ii)* $p + \gamma \to p + \mu^+ + \mu^-$ *(iii)* $p + p \to n + \Sigma^+ + K^+ + \pi^+$.

2. Complete the following reaction formula, taking account of conservation of charge, baryon number and strangeness (more than one answer is possible and more than one particle is necessary).

$$p + p \to \Xi^- + \ldots$$

3. Which of the following reactions and decay processes conserve strangeness and which interaction is reponsible for each process ?

   (a) $\pi^0 \to \gamma + \gamma$; *(b)* $\mu^- + p \to n + \nu_\mu$ *(c)* $\Lambda^0 \to p + \pi^-$

   (d) $\Lambda^0 + p \to \Sigma^+ + n$; *(e)* $p + n \to p + p + \pi^-$.

4. Indicate for each of the following reaction, whether it is allowed, or forbidden. If allowed, tell the type of interaction.

   (a) $\pi^- + p \to \pi^0 + n$; *(b)* $\pi^0 \to \gamma + \gamma + \gamma$ *(c)* $\pi^0 \to \gamma + \gamma$

   (d) $\pi^+ \to \mu^+ + \nu_\mu$, *(e)* $\pi^+ \to \mu^+ + \bar{\nu}_\mu$ *(f)* $p + \bar{p} \to \Lambda^0 + \Lambda^0$

   (a) Allowed, strong, *(b) forbidden* $\Delta P \neq 0$, *(c) electromagnetic,*

   (d) weak, *(e) forbidden* $\Delta L \neq 0$, *(f) forbidden* $(\Delta B \neq 0)$.

5. State which of the following processes are allowed and which are forbidden. Give reasons :

   (a) $\Xi^0 \to \Sigma^0 + \gamma$, *(b)* $\mu^- + p \to \Lambda^0 + \nu_\mu$, *(c)* $\Sigma^+ \to \Lambda^0 + \mu^+ + \nu_\mu$ *(d)* $K^- + d \to \pi^+ + \Sigma^-$

   [(a)allowed-electromagnetic decay; (b) allowed weak interaction; (c) forbidden by energy conservation; (d) forbidden by baryon conservation]

6. Which of conservation law or mechanism suppresses the following decays/reactions ?

   (a) $p + n \to p + \Lambda^0$; *(b)* $\Lambda^0 \to K^0 + \pi^0$; *(c)* $K^- \to \pi^0 + e^-$; *(c)* $K^+ \to \pi^+ + \pi^+ + \pi^-$;

   (e) $\mu^+ \to e^+ + \gamma$. *(f)* $p \to n + e^+ + \nu_e$ [*(a)* S & I, *(b)* B, *(c)* L, *(d)* Q, *(e)* L, *(f)* E]

7. For each of the following decays state a conservation law that forbids it.

   (a) $n \to p + e^-$, *(b)* $n \to \pi^+ + e^-$, *(c)* $n \to p + \pi^-$,

   (d) $n \to p + \gamma$ [*(a)* I, L; *(b)* B, L; *(c)* E; *(d)* Q]

8. Explain why the following reactions are not allowed ?

   $\pi^- + p \to K^- + \Sigma^+$; $d + d \to {}^4He + \pi^0$; $\rho^0 \to \pi^0 + \pi^0$. [$\Delta T_3 \neq 0, \Delta S \neq 0, \Delta T \neq 0 : CP$]

9. Estimate the ratios of decay rates of the following.

$$\frac{\Omega^- \to \Sigma^- \pi^0}{\Omega^- \to \Xi^0 \pi^-};\ \frac{K^+ \to \pi^+ \pi^+ e^- \nu}{K^- \to \pi^+ \pi^- e^- \nu};\ \frac{\Sigma^- \to \Lambda^0 \pi^-}{\Sigma^- \to n\pi^-};$$

[All the numerators are zero, as these reactions are forbidden. Therefore the ratio is zero in each case]

10. The particle *X* has two decay modes with partial decay rates λ_1 and λ_2. *(a)* What is the inherent uncertainty in the mass of *X* ? *(b)* If *X* decays to $\pi^+ + \pi^+$ through strong interaction, estimate the isospin of *X*. [$\hbar(\lambda_1 + \lambda_2)$; 2]

11. How many of one million 1 GeV neutrinos interact when traversing the earth ? $R = 6000$ *km*, $\rho = 5$ *g/cm*^{3}, $< A > = 20$, and $\sigma = 0.7 \times 10^{-38}$ *cm*^{2}*/nucleon.* [$N = N_\nu N_n = 2R\sigma\rho N_A N_\nu = 25.2$]

12. Calculate the ratio of the cross sections for producing hadrons and for producing a muonic pair *(a)* just below the threshold for charm production, and *(b)* above that threshold but below the *b*-quark production threshold. (2, 10/3)
13. If the quark has an electric charge of – 1/3, indicate how the Gell-Mann-Nishijima formula should be modified to incorporate the new quantum number. $[Q = T_3 + \frac{1}{2}(B + S + c + b)]$
14. Given that the *K*-and π-mesons have zero spin, show that one of the weak processes $K^+ \to \pi^+\pi^0$ and $K^+ \to \pi^+\pi^+\pi^-$ must violate parity conservation. ($K^+ \to \pi^+\pi^+\pi^-$ violates)
15. Find an expression for the ratio of the cross sections for the reactions $K^-p \to \pi^-\Sigma^+$ and $K^-p \to \pi^+\Sigma^-$ in terms of the two possible *I* spin amplitudes. $[(A_1/2 + A_0/\sqrt{6})/(A_1/2 - A_0/\sqrt{6})]^2$

    (where A_0 and A_1 are the amplitudes of the resultant *I* spin 0 and 1 respectively)
16. A sextet and an antitriplet are obtained by direct product of two quark triplets (3 ⊗ 3). Determine the quark wave functions of these nine states.

    $6,|1,1\rangle = |uu\rangle$; $6,|1,0\rangle = [|ud\rangle + |du\rangle]/\sqrt{2}$, $6,|1,-1\rangle = |dd\rangle$; $6,|\frac{1}{2},\frac{1}{2}\rangle = [|us\rangle + |su\rangle]/\sqrt{2}$

    $6,|\frac{1}{2},-\frac{1}{2}\rangle = [|ds\rangle + |sd\rangle]/\sqrt{2}$; $6,|0,0\rangle = |ss\rangle$; $\bar{3},|\frac{1}{2},\frac{1}{2}\rangle = [|us\rangle - |su\rangle]/\sqrt{2}$

    $\bar{3},|\frac{1}{2},-\frac{1}{2}\rangle = [|ds\rangle - |sd\rangle]/\sqrt{2}]$.
17. Show that the direct product of three spin doublets decomposes as $2 \otimes 2 \otimes 2 = (1_A \oplus 3_S) \otimes 2 = 4s + 2_{M_S} + 2_{M_A}$.
18. Show that for arbitrary vectors **a** and **b**, we have $(\sigma \cdot a)(\sigma \cdot b) = a \cdot b + i\sigma \cdot (a \times b)$, where the components of σ are the Pauli spin matrices.
19. If the proton form factor is expressed as

$$F(q) = \int [1 + i\mathbf{q}\cdot\mathbf{r} - \frac{(\mathbf{q}\cdot\mathbf{r})^2}{2!} + \ldots]\rho(r)\,d\tau$$

and $\rho(r)$ is spherically symmetric and normalized to give $\int \rho(r)\,d\tau = 1$.

show that the mean square radius of the charge distribution is

$$\langle r^2 \rangle = -6\,\partial F(q)/\partial q^2.$$

REFERENCES

1. Adair, R.K. and E.C. Fowler, *"Strange Particles"*, John Wiley, New York, 1963.
2. Barkas, Walter H., *'Ann. Rev. of Nuc. Sci.,'* Vol. **15**, 67 (1965).
3. Bransden, B.H., D. Evans and J.V. Major, *"The Fundamental Particles"*, Van Nostrand Reinhold, 1973.
4. Bohr, A. and B.R. Motelson, *'Nuclear Structure'*, Vol. 2, Reading, Mass Benjamin, 1975.
5. Buras, A. *et al.*, *'Nucl. Phys'*, **B 135**, 66 (1978).
6. Burcham, W.E., *"Nuclear Physics an Introduction"*, Longman, 1973.
7. Clifford, E. Swartz, *"The Fundamental Particles"*, Addition-Wesley Reading, Massachusetts, 1965.
8. Condon & Odishaw, *"Hand book of Physics"*, McGraw Hill, 1967.
9. Cummins, E.D. and P.H. Bucksbaum, *"Weak Interactions of Leptons and Quarks"*, Cambridge University Press, 1983.
10. Dalitz, R.H., *'Ann. Rev. Nuc. Sci.,'* Vol. 13 (1963).
11. DeBenedetti, Sergio, *"Nuclear Interactions"*, John Wiley, 1964.
12. Emmerson, J. McL., *"Symmetry Principles in Particle Physics"*, Clarenden Press, Oxford, 1972.
13. Georgi., H. and S.L. Glashow, *'Phys. Rev. Lett.,'* **32**, 438 (1974). *'Phys. Today'*, **33**(9), 30 Sep. (1980).
14. Glashow, S.L., *'Sci. Amer.'*, **233**(4), 38, Oct. (1975).
15. Glashow, S.L., *et al.* *'Rev. Mod. Phys.'*, **52**, 515 (1980).
16. Gottfried, K. and Weisskopf, V.F., *"Concepts of Particle Physics"*, Vol. I & II, Oxford University Press, 1986.
17. Hendry, A.W. and D.B. Lichtenberg, *'Rep. Prog. Phys.'*, **41**, 1707 (1978).
18. Henley, E.M., *'Ann. Rev. Nucl. Sci.'*, **19**, 367 (1969).

19. Hofstadter, Robert, *"Nuclear and Nucleon Structure"*, W.A. Benjamin, New York, 1963.
20. Hoft, G., *Sci., Amer.'*, **242** (6), 104 (1980).
21. Hughes. I.S., *"Elementary Particles,"* 3rd Ed. Cambridge University Press, 1991.
22. Iachello, F., *'Amer. Sci.'*, **70** (3), 294, May (1982).
23. Kabir, P.K., *"The CP Puzzle"*, Academic Press, New York, 1968.
24. Kallen, G., *"Elementary Particle Physics,"* Addison Wesley, Reading Mass., 1964.
25. Kane, G., *"Modern Elementary Particle Physics'* Addison Wesley, Reading, Mass, 1987.
26. Khanna, M.P., *"Introduction to Particle Physics"*, Prentice Hall, India, 1999.
27. Lee, T.D., *"Particle Physics and Introduction to Field Theory"*, Harwood Academic Publishers, Chur Switzerland, 1984.
28. Lee, T.D., and C.S. Wu, *'Ann. Review of Nuclear Science,'* **Vol. 15,** 1965; **Vol. 16,** (1966).
29. Leighton, Robett B., *"Principles of Modern Physics"*, McGraw Hill. 1959.
30. Leon, M., *"Particle Physics An Introduction"*, Academic Press, 1973.
31. Marciano, W.J. and H. Pagels, *'Quantum Chromodynamics,' Phys. Rep.*, **36C**, 137 (1978).
32. Okun L.B., *"Weak Interaction of Elementary Particles"*, Israel Program for Scientific Translations Jerusalem, 1965.
33. Particle Data Group, *'Review of Particle Properties', Rev. Mod. Phys.* **56(2)** part 2, April 1984.
34. Puppi, G., *'Ann. Rev. Nuc. Sci.'*, **Vol. 13,** (1965).
35. Salem, A., *'Rev. Mod. Phys'*, **52** (3), 525 (1980).
36. Schwitters, R.F., *'Sci. Amer.'* **237**(4), 56 (1977).
37. Segre E., *'Nuclei and Particles'*, Benjamin, New York, 1987.
38. Smith, C.M.H., *"Nuclear Physics,"* Pergamon Press, 1966.
39. Weinberg, S., *'Sci. Amer.'* **244**(5), 64 (1981).
40. Zichichi, A. (Editor), *"Symmetries in Elementary Particle Physics"*, Academic Press, New York, 1965.